catalysts

MDPI

Review

A General Overview of Support Materials for Enzyme Immobilization: Characteristics, Properties, Practical Utility

Jakub Zdarta [1,2,*], Anne S. Meyer [2], Teofil Jesionowski [1] and Manuel Pinelo [2]

1 Institute of Chemical Technology and Engineering, Faculty of Chemical Technology, Poznan University of Technology, Berdychowo 4, PL-60965 Poznan, Poland; teofil.jesionowski@put.poznan.pl

2 Center for BioProcess Engineering, Department of Chemical and Biochemical Engineering, Technical University of Denmark, Søltofts Plads 229, DK-2800 Kgs. Lyngby, Denmark; am@kt.dtu.dk (A.S.M.); mp@kt.dtu.dk (M.P.)

* Correspondence: jakub.zdarta@put.poznan.pl; Tel.: +48-616-653-747

Received: 19 January 2018; Accepted: 21 February 2018; Published: 24 February 2018

Abstract: In recent years, enzyme immobilization has been presented as a powerful tool for the improvement of enzyme properties such as stability and reusability. However, the type of support material used plays a crucial role in the immobilization process due to the strong effect of these materials on the properties of the produced catalytic system. A large variety of inorganic and organic as well as hybrid and composite materials may be used as stable and efficient supports for biocatalysts. This review provides a general overview of the characteristics and properties of the materials applied for enzyme immobilization. For the purposes of this literature study, support materials are divided into two main groups, called *Classic* and *New materials*. The review will be useful in selection of appropriate support materials with tailored properties for the production of highly effective biocatalytic systems for use in various processes.

Keywords: enzymes; enzyme immobilization; inorganic and organic supports; hybrid materials; biocatalysts and bioprocesses

1. Introduction

Enzymes are well-known as highly effective and efficient catalysts of a wide variety of processes characterized by high selectivity and activity. Additionally, enzymes may reduce the number of reaction steps and quantities of hazardous solvents needed and thus make a process more inexpensive and environmentally friendly [1]. For these reasons enzymes have become extremely important catalysts which exhibit great potential in many practical applications in industries ranging from food to pharmaceuticals [2]. The use of enzymes in multiple catalytic processes has resulted in studies leading to significant improvement of the enzyme properties. One of the most important and widely used techniques is enzyme immobilization in which catalysts are attached to a solid support that is insoluble in the reaction mixture [3]. The greatest advantage of immobilization is that it significantly improves the stability of the biomolecules under various reaction conditions and enhances the reusability of biomolecules over successive catalytic cycles [4]. Moreover, after binding the enzyme molecules, the catalysts change from a homogeneous to a heterogeneous form, which facilitates simple separation of the biocatalytic system from the reaction mixture and results in products of higher purity [5,6]. Various immobilization techniques have been developed, including adsorption, covalent binding, entrapment, encapsulation and cross-linking [7]. These differ in the type and character of the interactions formed and in the form and type of the support materials used. Selection of the most appropriate immobilization method and support material depends strongly on the type and conditions

of the catalytic process as well as the type of the enzyme [8]. However, it should be emphasized that the selection of the support materials is the most crucial challenge due to the major impact the support material may have on the properties of the biocatalytic system.

A very broad variety of materials of various origins can be used as supports for enzyme immobilization. These materials may, in general, be divided into organic, inorganic and hybrid or composite. The support should protect the enzyme structure against harsh reaction conditions and thus help the immobilized enzyme to retain high catalytic activity [9]. Moreover, use of a suitable material, for example hydrophobic carriers in lipase immobilization, may additionally increase the activity of the biocatalyst [10,11]. However, there are some limitations in this area, because the matrix must not have a negative effect on the structure of the enzyme and should not disturb the enzyme more than is required to create stable enzyme–matrix interactions. Additionally, there should be affinity between the functional groups of the two materials to allow the formation of these enzyme–matrix interactions and effective binding of the enzyme to the support. This is particularly important in the case of covalent immobilization [12]. The carrier should expose the active sites of the catalyst for easy attachment of substrate molecules and to reduce diffusional limitations of the substrates and products [13]. The main required features of support materials for effective enzyme immobilization are summarized in Figure 1.

Figure 1. Main features of support materials used for enzyme immobilization.

Nevertheless, it should be remembered that the appropriate selection of a matrix is directly related to the type of enzyme and to the process in which the biocatalytic system will be used. For the purposes of this literature review, the materials used as supports for enzyme immobilization have been classified as *Classic materials* (Section 2), which are the most commonly used and *New materials*, which offer especially desirable properties (Section 3). The latter type is also currently used

in immobilization and not only allow effective enzyme binding but also increase the applicability of the resulting biocatalytic systems.

2. *Classic Support Materials* for Enzyme Immobilization

Since the beginning of the work to develop the immobilization techniques, there has been a need to define a group of materials to which enzymes may be attached. In general, materials have been sought which offer high stability, availability, relatively low price and high affinity to the bound enzymes. A wide variety of materials of both inorganic and organic origin have been evaluated as effective supports for biocatalysts and are classified for the purposes of this review as *Classic materials* (Figure 2). Although *Classic materials* have been less frequently applied in recent years, they remain an important group of materials used for the immobilization of enzymes.

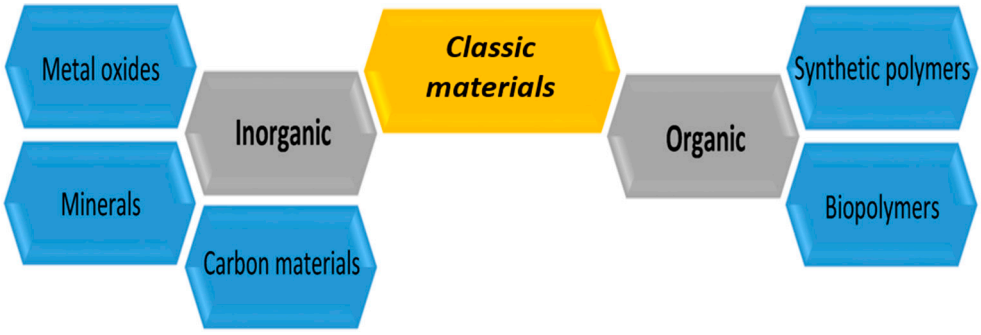

Figure 2. Selected examples of *Classic materials* of inorganic and organic origin used for enzyme immobilization.

2.1. Inorganic Materials

2.1.1. Silica and Inorganic Oxides

Silica is one of the most frequently used inorganic support materials for enzyme immobilization. Its high thermal and chemical resistance and good mechanical properties make it a suitable material for many practical applications. Silica offers good sorption properties due to its high surface area and porous structure. These properties allow effective enzyme attachment and reduce diffusional limitations [14,15]. Moreover, the presence of many hydroxyl groups on the surface of silica facilitates enzyme attachment and favours its functionalization with surface modifying agents such as glutaraldehyde or 3-aminopropyltriethoxysilane (APTES) [16]. Another advantage of this material is that it can be used in many different forms. Enzymes belonging to many catalytic classes, for example oxidoreductases, transferases, hydrolases and isomerases, have been immobilized with the use of sol-gel silica, fumed silica, colloidal silica nanoparticles and silica gel as supports [17–21]. The biocatalytic systems obtained demonstrate high catalytic activity retention and good thermal and pH resistance. For example, lipases immobilized on a silica gel matrix and on mesoporous silica retained respectively 91% and 96% of the activity of the free enzyme [22,23].

In previous studies, among other inorganic oxides, titanium, aluminium and zirconium oxides have also been used for the immobilization of many enzymes, for example lipase, cysteine, urease and α-amylase [24–27]. These supports are known for their high stability, mechanical resistance and good sorption capacity. Moreover, these materials are inert under various reaction conditions, which facilitates their application as supports for various classes of enzymes. Due to the presence of many hydroxyl groups on their surface, these materials are highly hydrophilic; this enhances enzyme immobilization and surface modification modified that favours the formation of relatively stable enzyme–matrix interactions.

2.1.2. Mineral Materials

Minerals are also used as support materials to produce recoverable biocatalytic systems with enhanced enzyme stability under reaction conditions. They are abundant in nature, are easily available, offer high biocompatibility and can be used as obtained without further advanced treatment and purification, which makes them relatively cheap [28]. Moreover, the presence of many functional groups (such as –OH, COOH, C=O, –SH, $–NH_2$) on the surface of the minerals allows the formation even of covalent bonds between the enzyme and the support and facilitates modification of the minerals. When additional functional groups are introduced, the adhesion area and hydrophobicity of the support increases while steric hindrances may be reduced [29]. The minerals used as supports for enzyme immobilization are mainly clay materials such as bentonite, halloysite, kaolinite, montmorillonite and sepiolite [30–32] though the group also includes the mineral hydroxyapatite known as calcium apatite [33,34]. In theory, enzymes belonging to many catalytic classes can be attached without limitation to the surface of mineral materials but in practice the most often immobilized are lipases, α-amylases, tyrosinases and glucose oxidases. Enzymes immobilized on minerals are used mainly in environmental engineering for waste and wastewater treatment as well as in biosensors to improve linear range and detection limit [35]. For example, according to Chrisnasari et al., glucose oxidase immobilized on bentonite modified by tetramethylammonium hydroxide retains over 50% of its initial activity after five repeated catalytic cycles [36].

2.1.3. Carbon-Based Materials

Carbon-based materials such as activated carbons and unmodified and modified charcoals have been used as effective and valuable support materials in enzyme immobilization, especially during the last two decades. The well-developed porous structure of these materials, with pores of various sizes and volumes and the high surface area (up to 1000 m^2/g) mean that these materials contain numerous contact sites on their surface for enzyme immobilization [37]. High adsorption capacity, the abundance of many functional groups and minimal release of fine particulate matter make carbon-based materials suitable carriers for the adsorption immobilization of various enzymes [38]. For example, unmodified charcoal support was used for the immobilization of amyloglucosidase. The immobilized enzyme when used for starch hydrolysis without any additional treatment retained over 90% of the free enzyme catalytic activity [39]. According to Silva et al. use of activated carbon for adsorption attachment of pancreatin allows a total immobilization yield that results in the creation of biocatalytic systems with good catalytic properties [40].

2.2. Organic Materials

It is well known that there is no universal support material suitable for all enzymes for all of their applications. Inorganic carriers have certain limitations, such as limited biocompatibility, lower affinity to biomolecules and reduced possibilities to create various geometrical shapes. Moreover, a cross-linking agent such as glutaraldehyde is usually required to create covalent bond between the enzyme and an inorganic support. Due to these reasons, some materials of organic origin are also used for the immobilization of various enzymes under different immobilization protocols. In general, organic support materials can be divided into two groups: (i) synthetic materials (mainly polymers) and (ii) renewable materials obtained from natural sources (biopolymers). Both groups have been widely used since the beginning of enzyme immobilization for the attachment of different types of biocatalysts.

2.2.1. Synthetic Polymers

The greatest advantage of synthetic polymers as support materials is that the monomers that build the polymeric chain can be selected according to the requirements of the enzyme and process in which the product of immobilization will be used [41,42]. The type and quantity of the monomers

determine the chemical structure and properties of the polymer. The composition of the monomers strongly affects the solubility, porosity, stability and mechanical properties of the polymer. A chemical feature that is directly related to the monomer structure is the presence of reactive chemical moieties in the polymeric chain. A very wide range of verified chemical functional groups may be observed in the structure of polymers. They include, for example, carbonyl, carboxyl, hydroxyl, epoxy, amine and diol groups, as well as strongly hydrophobic alkyl groups and trialkyl ammine moieties [43,44]. These groups facilitate effective enzyme binding and also functionalization of the polymer surface. The type of functional groups determines whether the enzyme is anchored to the matrix via for example adsorption or by the formation of covalent bonds, since it is mainly these two types of immobilization that take place when synthetic polymeric supports are used. Additionally, the type and quantity of functional groups determine the hydrophobic/hydrophilic character of the matrix and therefore its ability to form polar or hydrophobic interactions with the enzyme [45]. Moreover, by using polymeric supports, control of the length of the matrix–enzyme spacers has been achieved. Longer spacers allow the enzyme to retain higher conformational flexibility, while shorter spacers can protect the biomolecules against thermal inactivation and reduce leaching of the enzyme [46].

Various polymer materials can be used as effective supports and improve properties of the immobilized enzyme such as thermal stability and reusability. The polymer layers play a very important role in protecting the active sites of the enzyme from negative effects of the ingredients of the reaction mixture and the process conditions. However, it should be noted that synthesis of a polymer with the desired properties and functional groups is usually a time-consuming and costly process. Different polymers containing various functional groups have been used for enzyme immobilization. For example, α-amylase was covalently immobilized on polyaniline via –NH groups, while tyrosinase was immobilized via –NH and C=O groups on polyamide 66 (Nylon 66) without any linkers [47,48]. In another study, commercial lipase was immobilized by covalent binding on strongly hydrophobic polystyrene microspheres activated by epoxy groups [49]. In a hydrophobic environment, lipase exhibits extremely high catalytic properties which are related to the phenomenon called interfacial activation. Furthermore, polyurethane foam has been used for covalent immobilization of inulinase [50]. Bai et al. used polyvinyl alcohol modified by glutaraldehyde as a support for the immobilization of laccase via –OH groups. After immobilization, as a result of the strong interactions, the product was characterized by good storage stability and reusability which make it suitable for use in biosensors to detect bisphenol A [51]. Glucose oxidase, an antimicrobial enzyme, was immobilized on amino- and carboxyl-plasma-activated polypropylene film. The introduction of these groups enhanced the affinity of the polymer to the enzyme [52]. Commercially available ion exchange resins—for example Amberlite and Sepabeads—have also been used, respectively, for the immobilization of enzymes such as α-amylase and alcohol dehydrogenase [53,54].

2.2.2. Biopolymers

An alternative to the use of synthetic polymers as matrices for enzymes is the use of biopolymers—polymers of natural origin. Biopolymers include carbohydrates but also proteins such as albumin and gelatin [55]. Materials such as collagen, cellulose, keratins and carrageenan as well as chitin, chitosan and alginate are examples of biopolymers used for immobilization [56–59]. Biopolymers possess a unique set of properties, from biodegradability to harmless products, biocompatibility and non-toxicity, to an outstanding affinity to proteins, which make them suitable supports for enzymes [60]. Their natural origin and biocompatibility minimizes their negative impact on the structure and properties of enzymes and thus the immobilized proteins retain high catalytic activities. Furthermore, the availability of reactive functional groups in their structure—mainly hydroxyl but also amine and carbonyl moieties—enables direct reaction between the enzyme and matrix and facilitates modification of their surface [61]. Above all, however, these materials are renewable and easy to obtain; in many cases they are by-products of various industries, which makes them inexpensive and reduces the costs associated with the immobilization process [62]. Biopolymers

are used for immobilization by adsorption and covalent binding; however, their ability to create various geometrical configurations and propensity for gel formation mean that they are also used for immobilization by encapsulation and entrapment.

Chitosan on the basis of a literature survey can be considered the most frequently used biopolymer for enzyme immobilization. Chitosan can be applied in various forms and shapes. For example, Shi et al. used chitosan microspheres cross-linked by glutaraldehyde for the immobilization of nuclease, which is an important enzyme in genetic engineering [63]. In another study, glucose isomerase was adsorbed in macroporous chitosan beads prepared by chelation with various metal ions [64]. As reported by Kim et al. cellulose nanocrystals obtained from cotton linter cellulose can be used for immobilization by non-specific adsorption interactions of *Candida rugosa* lipase with high loading efficiency [65], whilst lipase was immobilized by entrapment by Tumturk et al. using κ-carrageenan hydrogels [66]. Vegetable and marine sponges characterized by an open fibrous network that reduces diffusional limitations have also been used as matrices for the immobilization of lipases, mainly via hydrogen bonds [67,68]. It may be concluded that biopolymers can be used to immobilize enzymes belonging to various catalytic classes with the retention of good catalytic properties. Moreover, the produced biocatalytic systems offer improved thermal stability and in general are noted for their good reusability.

Special attention should also be paid to alginates. Their remarkable abilities for gelation, mainly using sodium or calcium ions and for the creation of capsules in which single or multiple enzymes can be immobilized, mean that these materials are used principally for encapsulation and entrapment [69]. However, due to the relatively low mechanical stability of alginate gels and diffusional limitations in the transport of the substrates and products, their utilization in immobilization is restricted to a few applications only [70]. For example, Betigeri and Neau immobilized lipase in calcium alginate beads by entrapment, while Kocaturk and Yagar encapsulated polyphenol oxidase in copper alginate beads and obtained high immobilization yields [71,72]. The products exhibited good catalytic activity retention but their reusability was poor due to leaching of the enzyme from the matrix.

Agarose is a popular choice among biopolymers for use in enzyme immobilization. This linear heteropolysaccharide biopolymer consists of β-D-galactose and 3,6-anhydro-α-L-galactose units, linked by β-1-4 glycosidic and α-1-3 glycosidic bonds [73]. Like alginates, agarose also exhibits great ability for gelation which can occur at temperatures of agarose solution below 35 °C, without addition of any ions and results in formation of highly ordered stable and rigid structures [74]. It is worth mentioning that the 3-D architecture of this hydrophilic material remains almost unaltered in the presence of various organic solvents and does not shrink or swell under such conditions [75]. The ability of agarose gel to form various forms, such as beads, capsules or fibres, has led to this organic support material being of the great interest for industrial applications. For example, Prakash and Jaiswal used agarose beads for simple physical entrapment of thermostable α-amylase. The practical application of the resulting biocatalytic system was tested for removal of starch stains from clothes and the reusability of agarose immobilized enzyme was found to be up to five cycles [76]. In another study, a cross-linked agarose bead support highly activated with aldehyde groups was applied for multipoint covalent attachment of the commercial enzyme Depol™ 333MDP (β-1,4-endoxylanase). A high immobilization efficiency of over 85% was observed and the immobilized enzyme showed significant improvement of thermal stability compared to free protein [77].

2.3. Summary of Classic Materials

Classic materials used for enzyme immobilization of both inorganic and organic origin have been described in the above sections. Inorganic support materials, such as inorganic oxides, minerals or carbon-based materials, are characterized mainly by good thermal and chemical stability as well as by excellent mechanical resistance. These materials are also known for their good sorption properties which are a result of their well-developed porous structure and usually high surface area that ensures numerous contact sites for effective enzyme immobilization. In contrast, synthetic polymers and

biopolymers, also grouped under *Classic materials*, offer numerous functional groups that facilitate even covalent binding of enzymes without cross-linking agents. Additionally, biopolymers are usually characterized by high protein affinity as well as biocompatibility that limits negative effects of the support on the structure of enzymes. Moreover, irrespective of their origin, *Classic materials* for enzymes immobilization are usually abundant in nature (mineral, biopolymers) or are easy to synthesize (inorganic oxides, synthetic polymers) which makes them relatively cheap. These facts have meant that these support materials still play an important role as carriers for use for immobilization of enzymes.

The *Classic materials* and types of enzymes that may be immobilized using of these supports are summarized in Table 1 together with information about immobilization type, cross-linking agents and binding group.

Table 1. Summary and selected examples of *Classic materials* of both inorganic and organic origin applied for enzymes immobilization.

Support Material	Binding Groups	Cross-Linking Agent	Immobilization Type	Immobilized Enzyme	Reference
Inorganic Materials					
Sol-gel silica	–OH	–	adsorption	lipase from *Aspergillus niger*	[20]
Silica gel	–OH, C=O	glutaraldehyde	covalent binding	commercial lipase	[22]
γAl_2O_3	–OH	–	adsorption	cysteine proteinases from *Solanum granuloso-leprosum*	[25]
ZrO_2	–OH	–	adsorption	α-amylase from *Bacillus subtilis*	[26]
Montmorillonite	–OH	3-aminopropyl-triethoxysilane	covalent binding	glucoamylase from *Aspergillus niger*	[31]
Hydroxyapatite	–OH	–	adsorption	glucose oxidase from *Aspergillus niger*	[34]
Bentonite	–OH, $–NH_2$	tetramethyl ammonium hydroxide	covalent binding	glucose oxidase from *Aspergillus niger*	[36]
Commercial activated carbon	–OH, C=O	–	adsorption	cellulose from *Aspergillus niger*	[37]
Activated charcoal	–OH, C=O, COOH	–	adsorption	papain	[38]
Activated charcoal	–OH, C=O, COOH	–	adsorption	amyloglucosidase	[39]
Organic materials					
polyaniline	–N–H, C=O	glutaraldehyde	covalent binding	α-amylase	[47]
polystyrene	C=O, epoxy groups	poly(glycidyl methacrylate)	covalent binding	lipase	[49]
poly(vinyl alcohol)	–OH, C=O	glutaraldehyde	covalent binding	laccase from *Trametes versicolor*	[51]
polypropylene	–OH	plasma activated	covalent binding	Glucose oxidase	[52]
Cellulose nanocrystals	–OH	–	adsorption	lipase from *Candida rugosa*	[65]
Luffa cylindrica sponges	–OH, C=O, COOH	–	adsorption	lipase from *Aspergillus niger*	[67]
chitosan	–OH, $–NH_2$	–	entrapment	lipase from *Candida rugosa*	[71]
agarose	–OH	–	entrapment	α-amylase	[76]

3. *New Support Materials* for Enzyme Immobilization

Possibilities for practical applications of immobilized enzymes are continuing to grow. For this reason, discovery and use of *New materials* with desired properties, tailored to particular enzymes, has recently become extremely important. These materials, of both organic and inorganic origin, are characterized by exceptional thermal and chemical stability and very good mechanical properties. Moreover, these support materials are produced in various morphological shapes with controllable particle sizes, usually at nanoscale, which make them suitable for use with enzymes. Furthermore, these materials possess remarkable quantities of various functional groups, corresponding to the chemical groups of the proteins, which enhance enzyme binding and surface modification [78]. However, particularly during the last decade, scientific attention has been directed towards hybrid and composite materials, which combine properties of both composite precursor types and thus maximize their advantages [79]. Hence, with the use of *New materials* (see Figure 3) as enzyme supports, control of the technological process is improved, the immobilized enzymes exhibit enhanced catalytic efficiency

and the purity and quality of the reaction products increase compared to the processes catalysed by enzymes immobilized using the *Classic materials*.

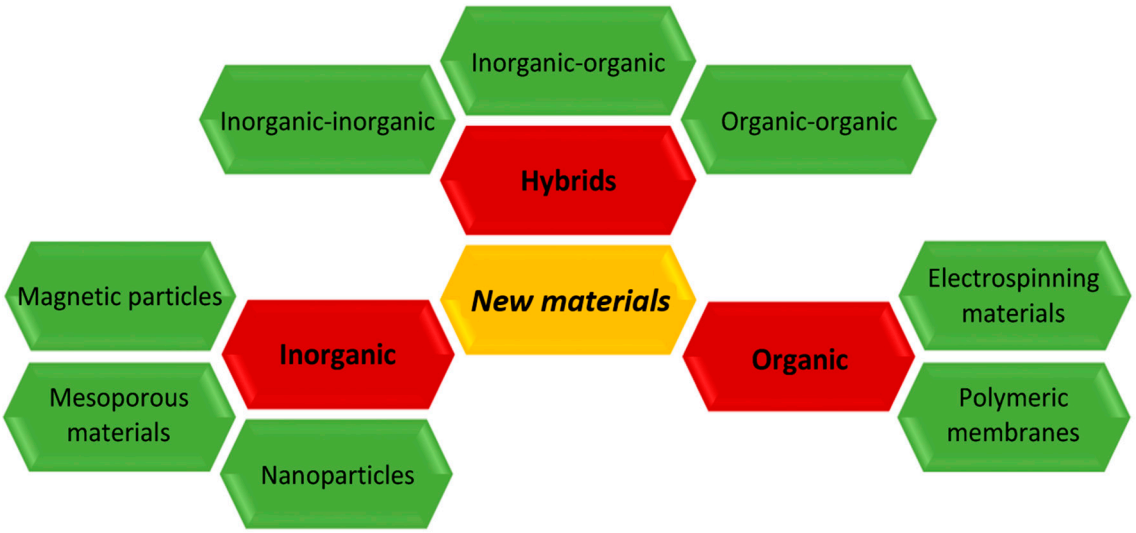

Figure 3. Selected examples of *New materials* of inorganic, organic and hybrid origin, applied for enzyme immobilization.

3.1. Inorganic Materials

3.1.1. Magnetic Particles

The separation of biocatalysts from the reaction mixture after the catalytic process is one of the crucial problems that must be solved when immobilized enzymes are used. One possible solution is attachment of the enzyme molecules to magnetic iron oxide nanoparticles (MNPs) and simple separation of the biocatalytic system with the use of an external magnetic field [80]. MNPs are also known for their large surface area and the abundance of hydroxyl groups on their surface which enables their easy modification and strong (covalent) binding of the enzyme. These are very important features. High mechanical stability and low porosity, however, which minimize steric hindrances, are also relevant for the creation of a stable enzyme–matrix biocatalytic system [81]. According to Netto et al. many enzymes grouped within the oxidoreductases, hydrolases or transferases can be immobilized on the surface of magnetic nanoparticles to create generally stable systems offering high reusability and easy separation from the reaction mixture [82]. There are several examples that demonstrate these advantages. Mehrasbi et al. immobilized lipase on magnetic nanoparticles functionalized with 3-glycidoxypropyltrimethoxysilane. The immobilized enzyme when used to catalyse the production of biodiesel from waste cooking oil, maintained 100% of its initial activity even after six reaction cycles [83]. In another study, Aber et al. immobilized glucose oxidase by adsorption on unmodified MNPs and used the resulting system for decolourization of Acid Yellow 12. After 15 catalytic cycles the immobilized glucose oxidase retained more than 90% of its initial properties [84]. Atacan et al. used magnetic nanoparticles, pre-treated with gallic acid, for the covalent immobilization of trypsin. Their results showed that the MNPs-trypsin biocatalyst can degrade bovine serum albumin with high efficiency [85].

3.1.2. Mesoporous Materials

A feature that distinguishes mesoporous supports from other materials used for enzyme immobilization is the possibility of tailoring the properties of the support to the biomolecules by adjusting the synthesis conditions and obtaining matrices with a desired pore structure [86,87].

These kinds of carriers contain mesopores with diameters of usually 2 to 50 nm, with a narrow and regular pore arrangement, surface areas as high as 1500 m^2/g and pore volumes of around 1.5 cm^3/g, which make them suitable supports for various biomolecules [88]. Enzymes can be immobilized on mesoporous materials by covalent binding or by encapsulation. In both techniques of immobilization, however, the enzyme is placed in the pores of the support, which means that the structure of the protein is protected and good catalytic properties are generally retained. When the enzyme is located in the pores of the carrier, diffusional limitations must also be taken into account because the transport of substrates and products is restricted [89]. Nevertheless, in view of their water insolubility, thermal and chemical stability, hydrophilicity and the presence of sufficient chemical groups for the binding of catalysts, mesoporous materials fulfil most of the requirements for effective enzyme matrices [90].

Materials such as zeolites, carbons and sol-gel matrices, as well as precipitated and ordered mesoporous oxides are included in the mesoporous group [91–93]. For example, various mesoporous silica materials are frequently used. Lipases from *Candida antarctica* and from *Candida rugosa* have been immobilized via non-specific interactions without any intermediate agents on SBA 15 and MCM 41 mesoporous silica, respectively and used as catalysts in organic synthesis [94,95]. The reusability of the immobilized enzymes was found to be significantly improved, because they could be reused for at least five reaction cycles without significant loss of their activity. SBA 15 and MCM 41 silicas were also used for adsorption immobilization of alkaline protease [96]. The immobilized enzyme attained its maximum loading (589.43 mg/g) when SBA 15 silica was used. The products of immobilization also had good pH and temperature stability. In another study, Mangrulkar et al. immobilized tyrosinase on the mesoporous silica MCM-41 and used the resulting biocatalytic system for the detection of phenol. The lowest concentration of phenol detectable by the immobilized tyrosinase was found to be 1 mg/L [97]. As mentioned above, mesoporous materials can also be used for enzyme encapsulation. Wang and Caruso used mesoporous silica spheres for the immobilization of catalase, protease and peroxidase and showed that after immobilization the lifetime of all tested enzymes was improved compared to their free forms [98].

3.1.3. Nanoparticles

Nanoparticles of both inorganic and organic origin with diameters of up to 30 nm have been extensively studied in recent years as potential supports for enzyme immobilization. However, for the purpose of this review, attention is focused on nanoparticles of inorganic origin as these materials are attracting growing interest due to the fact that they generally significantly improve the immobilization yield and the efficiency of the biocatalytic system obtained [99,100]. Nanoparticles provide a large surface area for enzyme binding that leads to higher loading of the enzyme on the matrix surface and increased immobilization yield. The greatest advantage, however, of nanoparticles over other inorganic materials is their ability to minimize diffusional limitations. Enzyme molecules are attached to the surface of the nonporous particles and their active sites are exposed for wide contact with substrates [101,102]. This means that biocatalytic systems based on nanoparticles usually provide high catalytic activity retention [103].

Various inorganic nanomaterials such as nanogold [104] and graphene [105] can be used as matrices for enzyme immobilization. Most frequently, however, inorganic oxide nanoparticles are used. For example, Hou et al. used titania nanoparticles for the immobilization of carbonic anhydrase by glutaraldehyde and immobilized over 160 mg of the enzyme per gram of the matrix. The product was used for biomimetic conversion of CO_2 [106]. In another study, lipase from *Rhizomucor miehei* was covalently immobilized on silica nanoparticles modified by octyltriethoxysilane and glycidoxypropyltrimethoxysilane. The immobilized lipase proved to be a very thermostable biocatalyst [107]. Notably, both biocatalytic systems achieved over 90% catalytic activity retention.

3.1.4. Ceramic Materials

Ceramic materials are known for their extremely high resistance to temperature, pressure and chemicals (organic solvents, bases, acids). These features make them very promising materials for use as supports for industrial applications of immobilized enzymes [108]. Ceramic supports also offer good mechanical stability. Hence, when the enzymes become catalytically inactive, they can be relatively easily regenerated and used for the immobilization of a new biocatalyst [109]. Hydroxyl groups are mainly present on the surface of these materials. This favours mainly adsorption immobilization of enzymes, based on non-specific interactions. For covalent attachment of biomolecules, additional surface modification is necessary. Ceramic materials such as alumina, zirconia, titania, silica, iron oxide and calcium phosphate have been used as biomolecule carriers. It should be added that these materials can also be used in the form of ceramic foam or composite (TiO_2/Al_2O_3) ceramic membranes [110,111].

Ebrahimi et al. physically immobilized β-galactosidase using a ceramic material in the form of a membrane as a support. The system was used to catalyse a transgalactosylation reaction of lactose to produce galactosyl-oligosaccharides. The immobilized enzyme was used for continuous production of oligosaccharides and its efficiency reached 40% under optimal process parameters [112]. Wang et al. immobilized horseradish peroxidase on a ceramic material (cordierite) which had been modified by *N*-β-amino-ethyl-γ-aminopropyl-trimethoxysilane for covalent attachment of the enzyme. The biocatalytic system was used to remove oil from wastewater. The highest recorded removal efficiency was close to 92% and the system exhibited good reusability [113].

3.1.5. Carbon Nanotubes

Carbon nanotubes are a new type of support material that has been more and more widely used in recent years. Both single-walled and multi-walled carbon nanotubes are characterized by an ordered, nonporous structure, large surface area and biocompatibility. Moreover, they exhibit outstanding thermal, chemical and mechanical resistance [114,115]. Carbon nanotubes are also relatively amenable to functionalization to further increase their affinity to enzymes and favour the formation of strong enzyme–matrix interactions [116]. Unlike other materials, carbon nanotubes enhance the transfer of electrons between the substrate and the immobilized enzyme. They are thus most frequently used for the immobilization of oxidoreductases and are applied in biosensors for the detection of various compounds such as phenol and its mono- and multi-substituent derivatives, bisphenols or pharmaceuticals, i.e., diclofenac or tetracycline. However, other groups of enzymes (transferases and hydrolases) have also been immobilized with the use of carbon nanotubes [117,118].

In one reported study, glucose oxidase was immobilized on carbon nanotubes and further cross-linked with chitosan. The results confirmed that the transfer rate of electrons was strongly enhanced [119]. In another study α-glucosidase was covalently immobilized on multi-walled carbon nanotubes functionalized by amine groups. The system so obtained was used in a biosensor for measuring the antidiabetic potential of medicinal plants [120]. The immobilized enzymes used in both biosensors exhibited greatly improved sensitivity and time of response and thus better detecting properties. The biosensors also offered relatively good storage stability as indicated by their activity which remained almost unaltered over 30 days.

3.1.6. Graphene and Graphene Oxide

Graphene and graphene oxide (GO) among carbon-based materials have also attracted great attention as support materials for enzymes. This interest reflects their unique features such as biodegradability, two-dimensional structure, high surface area and pore volume as well as good thermal and chemical stability [121]. Additionally, the presence of many various functional groups, such as carboxylic (COOH), hydroxyl (–OH) or epoxide groups, facilitates creation of strong enzyme-matrix interactions without linking agents or modification of the graphene surface [122]. Due to these features, enzymes like lipases [123] or peroxidases [124] can be immobilized on GO

surfaces mainly by adsorption, covalent binding or entrapment [125]. It is also worth mentioning that graphene-based materials may even enhance enzyme biocatalytic activity. Moreover, graphene-based supports are characterized by antioxidant properties and may enhance removal of free radicals (i.e., hydroxyl or dithiocyanate) from reaction mixtures [126]. This results in improved protection of enzyme molecules from inactivation.

For example, horseradish peroxidase (HRP) was covalently immobilized on reduced graphene oxide nanoparticles functionalized with glutaraldehyde. Kinetic parameters (turnover number (k_{cat}) and catalytic efficiency (k_{cat}/K_M)) of the immobilized enzyme increased after its attachment, thus demonstrating enhancement of the catalytic properties of the HRP. Moreover, reusability was also significantly improved, as indicated by immobilized enzyme which maintained over 70% of its initial activity after 10 catalytic cycles [127]. In another study, D-psicose 3-epimerase (DPEase) was immobilized on non-modified graphene oxide and applied for production of the rare sugar D-psicose, an epimer of D-fructose. After immobilization, the efficiency of biocatalytic conversion of D-fructose to D-psicose was improved. Thermal stability of immobilized DPEase was also significantly enhanced, as the graphene-bounded enzyme exhibiting a half-life of 720 min that was 180 times higher than the half-life of free D-psicose 3-epimerase (4 min) [128].

3.2. Organic Materials

As already mentioned, the properties of the immobilized enzyme are strongly dependent on the structure and characteristics of the matrix. In general, the organic materials classified here as *New materials* are mainly the same materials and containing very similar chemical groups as those described in Section 2.2. However, here these organic materials appear in completely different forms and as a result have very different properties. These materials may for example be used in the form of single particles, fibres of nanometre size, or membranes. These supports increase the performance, efficiency and stability of the immobilized biomolecules and render the latter more reusable. Moreover, control of the process is improved and processes can be carried out in a continuous manner, which makes them cost-effective [129]. Hence, biocatalytic systems based on these materials can become attractive for applications in industrial-scale processes. Selected cases of the use of *New materials* of organic origin for enzyme immobilization are discussed below.

3.2.1. Electrospun Materials

The great potential of electrospun materials as supports for enzyme immobilization results from their many functional and structural advantages. These materials are known for their length (electrospun nanofibers), uniformity of diameter and diversity of composition. They also have high porosity and surface areas, which lead to high enzyme loading [130]. The nanometre sizes of these materials provide additional benefits mainly related to low hindrance of mass transfer and reduced diffusional limitations. As a result, the efficiency of the immobilized enzyme can be increased. Electrospun support materials are also known for other useful properties, for example their biocompatibility, nontoxicity, biodegradability, high mechanical strength and hydrophilicity, which make them suitable matrices for various types of biocatalysts [131,132]. It should also be noted that due to the presence of various functional moieties on their surface, electrospun nanomaterials can be easily modified to favour enzyme attachment and increase the activity of the enzyme [133]. A very wide range of synthetic polymers such as poly(vinyl alcohol), polystyrene, polyacrylamide and polyurethane, as well as biopolymers such as chitin, chitosan, alginate and cellulose, may be used to produce electrospun carriers [134–136]. Their great advantage over other matrices is the fact that because of the variety of materials used to produce electrospun supports, they can be obtained with properties tailored to the enzyme and the process. Enzymes can be immobilized on these materials by adsorption and covalent binding (surface attachment) as well as by encapsulation carried out at the same time as the support is formed, which additionally reduces the costs of the process [137].

For example, Canbolat et al. used poly(ε-caprolactone) to immobilize catalase by encapsulation using layering methods. Moreover, to enhance the catalytic activity of the enzyme, its molecules were combined with cyclodextrin before immobilization. The results indicated that the addition of cyclic oligosaccharides had a positive effect on the catalytic properties of the biocatalyst. It should also be noted that immobilization by encapsulation results in higher stability of the catalase because the enzyme is protected from negative effects of the reaction conditions [138]. Weiser et al. used polyvinyl alcohol nanofibers for the immobilization by entrapment of five different types of lipase for the kinetic resolution of racemic secondary alcohols by acylation in inorganic media. The study proved that the activity of all tested lipases was enhanced by stabilization of the active conformation of the enzyme. Furthermore, after immobilization of the biomolecules, the turnover frequency of the reaction increased due to a reduction in mass transfer limitations, which was directly related to the structural properties of the polymeric nanofibers [139]. In another study, poly(vinyl alcohol) or polylactic acid nanofibers in the form of a membrane were used for adsorption immobilization of *Candida antarctica* lipase B. The biocatalytic system was used for the kinetic resolution of 1-phenylethanol and 1-phenyl acetate. Polyvinyl alcohol membrane with immobilized lipase may be used in both organic and water media; however, the lipase immobilized on polylactic acid fibres preserved higher activity and exhibited higher enantiomer selectivity. Nevertheless, due to the protection afforded by the nanofibers, both immobilized systems demonstrated excellent stability even over 10 reaction cycles [140].

3.2.2. Polymeric Membranes

As has been described above, polymeric materials can be used in enzyme immobilization in the form of beads, powders, fibres or foams. However, in recent years there has been growing interest in the use of commercially available polymeric membranes. This is mainly because they have easily tuneable properties which make them suitable for many groups of enzymes [141,142]. These membranes have a large surface area that allows efficient enzyme attachment. The membranes also offer good porosity as well as well-defined pore sizes and structure, which facilitate the immobilization of biomolecules not only on the surface of the support but also in its pores [143]. The reaction mixture passing through the membrane therefore has relatively easy access to the active sites of the enzyme, which reduces diffusional limitations. Moreover, membranes with tailored properties can easily be prepared in different shapes and various geometrical configurations [144]. The membranes are also generally insoluble and are known for their mechanical stability, hence they fulfil the requirements for performing as suitable carriers for enzyme immobilization.

Many types of synthetic polymers can be used for the preparation of membranes, for example poly(vinyl alcohol), polyurethane and poly(vinylidene fluoride) [145,146]. However, membranes made from biopolymers, for example from chitosan or cellulose, can also be used as enzyme support materials [147]. Depending on the type of material used, various functional groups are present in the membrane that not only favour effective enzyme immobilization but also enable modification of the membrane for covalent binding of biomolecules. It should also be noted that in addition to membranes obtained on a laboratory scale, commercially available ultra- and nanofiltration membranes can also be used for enzyme immobilization and examples such as GR51PP, NF270 and NTR7450 may be mentioned [148–150]. However, the greatest advantage of polymeric membranes as biomolecule support matrices, in comparison with other materials, is the fact that no additional separation and purification of the reaction mixture is required; the catalytic process can take place and products can be isolated from the reaction mixture in the same step [151]. It is also worth noting that polymeric membranes, as supports for enzymes, play a crucial role particularly in the case of enzymatic membrane reactors (EMR).

3.3. Hybrid and Composite Materials

In the light of the above-mentioned unique features and properties of inorganic and organic matrices, many studies have been carried out with the aim of combining them to maximize their

benefits. The possibility of selecting and combining precursors to meet the requirements of a given enzyme and the process in which it is to be used facilitates more precise control of the enzyme immobilization process. Additionally, the biocatalytic systems thus produced can be used in a wider range of practical applications [152]. Combined and reinforced materials usually exhibit properties not observed for their individual components. Hybrids and composites usually make it possible to stabilize the interactions between an enzyme and a support and make biocatalysts more mechanically resistant and stable under reaction conditions. It should be added that hybrid supports in general provide a suitable environment for biomolecules that favours the retention of high catalytic properties by the immobilized enzyme, makes the biocatalytic system reusable and protects it against conformational changes during storage [153]. An additional benefit of the use of composite supports is the fact that these materials are suitable for enzymes belonging to all catalytic classes. Hence, in the quest for support materials for enzyme immobilization, particular attention should be paid to hybrid or composite materials obtained by the conjugation of: (i) organic-organic; (ii) inorganic-inorganic, or (iii) organic-inorganic precursors.

3.3.1. Organic-Organic Hybrids

As described above, many types of polymers of synthetic and natural origin can be used as supports for enzymes. However, to increase their usability, they can be combined to obtain products with enhanced properties which are better suited to the enzyme and the technological process. Organic-organic hybrids may be synthesized by connecting together the following: (i) two synthetic materials, for example polyaniline and polyacrylonitrile, polyethyleneimine, with epoxy-activated acrylate copolymer or poly(acrylic acid) and polyvinyl alcohol [154–156]; (ii) a synthetic polymer with a biopolymer, such as poly(acrylic acid) and cellulose, polyvinyl alcohol and chitosan, or polyaniline and chitosan [157–159]; (iii) two biopolymers, such as chitosan and alginate, chitin and lignin or cellulose and dextran [160–162]. For instance, combining a synthetic polymer having good pH and thermal resistance and mechanical stability with a biopolymer known for its biocompatibility and high affinity to biocatalysts and using the resulting hybrid as an enzyme support, could result in a stable, reusable biocatalytic system with the retention of good catalytic properties [163]. Additionally, through appropriate selection of precursors, the hydrophobic/hydrophilic character of the matrix can be controlled to increase the strength of the interactions formed between the enzyme and support and to enhance the catalytic activity of the biomolecule [164]. The greatest advantage of these materials is the possibility of forming them into various shapes and sizes. The materials can be used as enzyme supports in the form of particles, fibres, tubes, beads, membranes or sheets [165–167]. The wide variety of available organic-organic hybrids makes these materials suited for immobilization of enzymes belonging to all catalytic classes by adsorption, covalent binding and also by entrapment or encapsulation [168,169]. For example, two monomers, polylactic acid and polyethylene glycol, were used to produce micro- or nanofibers by an electrospinning technique. The material thus produced had high porosity, a large surface area, the ability to incorporate functional additives, which are all excellent properties as a matrix for enzyme attachment. In the study, alkaline phosphatase was immobilized via biotin-streptavidin interactions on surface of the matrix. The bound enzyme exhibited good stability and reusability over a long storage time so this system may be a promising platform for the development of biosensors [170]. Polyvinyl alcohol–hypromellose is an example of an organic hybrid produced by merging a synthetic polymer with a semisynthetic biopolymer which is an inert derivative of methylcellulose. This material was used for the immobilization of lipase from *Burkholderia cepacia* without any cross-linkers. The resulting biocatalytic system was used for the synthesis of phenethyl butyrate in nonpolar medium and proved to be a successful catalyst, achieving 99% conversion of the phenethyl alcohol and vinyl butyrate used as substrates. The protective effect of the polymeric hybrid support resulted in the retention of high catalytic activity by the immobilized lipase and the activation energy of the reaction was found to be lower when the immobilized enzyme was used [171]. Matto and Husain employed a calcium alginate–starch hybrid gel as a carrier for

adsorption immobilization and entrapment of peroxidase. The presence of many hydroxyl groups in the starch structure enhanced the surface attachment of the enzyme, while the capacity of alginate for gelation favoured the entrapment of peroxidase. The entrapped enzyme was found to be significantly more stable against pH, temperature, solvents and inhibitors like urea or heavy metals, compared to the surface-immobilized enzyme. Moreover, this form of immobilized peroxidase retained over 70% of its original activity even after seven repeated reaction cycles [172]. In a study by Abdulla and Ravindra, equal proportions of alginate and κ-carrageenan were used to produce a novel biopolymeric hybrid for lipase immobilization by entrapment. The resulting biocatalyst was employed in biodiesel production from *Jatropha* oil and ethanol. Under optimal process conditions, total transesterification of triglycerides to fatty acid ethyl esters was achieved. This biocatalytic system also demonstrated good reusability as indicated by retention of over 75% of its initial activity after six cycles. The results suggest that lipase immobilized on an alginate–κ-carrageenan hybrid could be an efficient and environmentally friendly biocatalyst for biodiesel production [173]. Another application of a composite built from two biopolymers was reported by Nupur et al. who combined chitosan and calcium alginate and used the resulting hybrid in the form of beads for entrapment immobilization of penicillin G amidase (PGA). The immobilized PGA demonstrated high thermal and storage stability and good reusability. The enzyme entrapped in alginate–chitosan hybrid beads was found to have several advantages and could be used in the organic synthesis of 6-aminopenicillanic acid with high efficiency [174].

3.3.2. Organic-Inorganic Hybrids

A very wide range of materials of both organic and inorganic origin can be combined to create hybrid or composite supports for the immobilization of enzymes. The most frequently used inorganic precursors include silica, inorganic oxides such as zinc and titanium oxides, as well as minerals, carbon materials and magnetic nanoparticles [175–178]. They can be combined with polymers of synthetic origin, for example polyacrylonitrile, polyethyleneimine and polyvinyl alcohol [179,180], as well as with biopolymers such as chitosan, lignin and alginate [181,182]. These materials are mainly used for the adsorption or covalent immobilization of hydrolases, oxidoreductases and transferases but the encapsulation of these enzymes in carriers of this type has also been reported [183]. Organic-inorganic hybrids display great potential as support materials for enzymes; such hybrids provide good stability and mechanical resistance and very high affinity to biological molecules. The high stability and often also chemical inertness are related to features of the inorganic precursor. The good ability to bind enzymes is due to the organic components since synthetic polymers and biopolymers have many functional moieties in their structures that are able to interact with the chemical groups of biocatalysts [184]. As a result of their stability and functionality, hybrids in this group can be used for many practical applications, which is their greatest advantage. Many different combinations of organic and inorganic substances have been used to produce functional organic-inorganic composites and hybrids for enzyme immobilization. For example, Zhao et al. combined the stability and mechanical resistance of silica with the biocompatibility and gelation properties of chitosan and achieved immobilization of glucose isomerase on silica–chitosan hybrid microspheres via simple in situ encapsulation. The immobilized enzyme was further used as a catalyst for the conversion of glucose to fructose. The relative activity of the enzyme was found to be above 90% over a wide pH range of 6–8, a temperature range of 40–80 °C, a storage time of 3 months and after 15 repeated catalytic cycles [185]. In another study, a silica–dialdehyde starch (SiO_2-DAS) mixed hybrid, offering high enzyme binding capacity due to the presence of polysaccharide in the structure, was used for the immobilization of cellulose. The product maintained higher activity over broader pH and temperature ranges than the free enzyme. Moreover, the immobilized cellulase exhibited higher affinity to the substrates as well as better reusability and storage stability. This product might therefore be used as an effective biocatalyst for cellulose bioconversion [186]. Miranda et al. reported the synthesis of an eco-friendly poly-L-leucine-rehydrated hydrotalcite nanohybrid material and its effective use for tyrosinase immobilization without bifunctional linkers. They used the resulting biocatalytic system in

the asymmetric epoxidation reaction of chalcone. The nanohybrid-based biocatalyst exhibited excellent activity and enantioselectivity. The product also demonstrated good reusability, with unaltered activity after five consecutive runs. Thus, this biocatalytic system could find potential applications in protein engineering, biomedicine and catalysis [187]. Chang et al. combined natural clay composed of montmorillonite and layer silicates with chitosan, which exhibits good gelation abilities. The inorganic-organic hybrid was further cross-linked with glutaraldehyde and finally applied in the form of wet and dry beads for the immobilization of β-glucosidase. The covalently bound enzyme exhibited high stability over wide pH and temperature ranges. Additionally, the properties of wet and dry beads were compared and it was found that use of the dried materials led to higher catalytic efficiency [188]. In another study, the conductive properties of carbon nanospheres were combined with the gelation ability of sodium alginate for entrapment immobilization of glucose oxidase and its use for biosensing of glucose. Under optimal measurement conditions, the biosensor achieved very good performance for glucose over a wide linear concentration range, with a detection limit of 0.5 µM. The biosensor also exhibited satisfactory reproducibility and good long-term stability [189].

3.3.3. Inorganic-Inorganic Hybrids

Besides the types discussed above, inorganic-inorganic hybrid and composite materials also possess many features which make them interesting potential supports for enzyme immobilization. In general, inorganic hybrids exhibit good pH and thermal stability, mechanical resistance and chemical inertness. Moreover, their precursors are easily available and in many cases their synthesis is simple and hence relatively cheap [190]. A variety of functional groups such as carbonyl (C=O), carboxyl (COOH), amine ($-NH_2$) and epoxy are present on the surface of inorganic-inorganic materials, although the most frequently observed are hydroxyl (–OH) groups. These groups determine the hydrophilic character of inorganic composite supports and increase their affinity to biomolecules [191]. Additionally, the presence of many functional groups enhances immobilization efficiency and allows easy functionalization of the surface [192]. Besides simple modification, the presence of various chemical moieties allows the production of combined materials with desired technological features and high affinity for enzymes, which makes these materials promising for practical applications. For example, sol-gel derived silica was combined with multi-walled carbon nanotubes (MWCNTs) and used for the non-specific immobilization of lipase from *Candida rugosa*. The biocatalytic system thus obtained was applied in esterification reactions in organic media, with high efficiencies. The immobilized lipase also exhibited good reusability as indicated by almost unaltered initial activity after five catalytic cycles due to the protective effect of the MWCNTs [193]. In another study, Zhu et al. used carboxyl-functionalized silica-coated magnetic nanoparticles (SCMNPs) as a carrier for covalent immobilization of porcine pancreatic lipase. The addition of the magnetic nanoparticles to the composite enabled easy separation of the biocatalytic system from the reaction mixture using a magnetic field. The immobilized lipase exhibited enhanced activity compared to the free enzyme and good thermal resistance, with high catalytic efficiency at 70 °C [194].

The presence of many functional moieties enables the attachment of enzymes belonging to many catalytic classes, including hydrolases and oxidoreductases [195,196] and the potential use of all known immobilization techniques. For example, glucose oxidase was entrapped in nanozeolites combined with magnetic nanoparticles and multi-walled carbon nanotubes [197]. In another case, β-glucosidase, α-chymotrypsin and lipase B from *Candida antarctica* were successfully covalently immobilized on the surface of magnetic nanoparticles activated by *N*,*N*-disuccinimidyl carbonate [198]. In general, silica is one of the most commonly used precursors for inorganic hybrids. However, other inorganic components such as inorganic oxides, minerals, clays, noble metal nanoparticles and carbon-based materials may also act as precursors for inorganic-inorganic enzyme supports [199–202]. An interesting example of an inorganic-inorganic composite used for enzyme immobilization is a combination of calcium carbonate and gold nanoparticles ($CaCO_3$-AuNPs). This support was used by Li et al. for adsorption immobilization of horseradish peroxidase and further to produce a mediator-free hydrogen

peroxide biosensor. Due to the good electrical conductivity of the $CaCO_3$-AuNPs inorganic hybrid, as well as the favourable orientation of the enzyme molecules on the surface of the matrix, the biosensor exhibited strong activity toward H_2O_2 reduction and achieved a good linear response over a wide range of hydrogen peroxide concentrations and a relatively low limit of detection (1.0×10^{-7} M) [203]. In another study, the ability of carbon nanotubes to direct electron transfer and the high surface area of titanium dioxide were exploited to create TiO_2–carbon nanotube microparticles for adsorption immobilization of glucose oxidase by non-specific interactions. The immobilized enzyme was further used to build a biosensor for glucose detection. Electrochemical analysis showed the biosensor to have high efficiency, sensitivity and reproducibility and the capacity to detect glucose up to concentrations of 3 mM [204]. In another such system, multi-walled carbon nanotubes provided a highly porous conductive network that enhanced electrochemical transduction, while $CaCO_3$ acted as a host carrier for immobilization of tyrosinase by entrapment. This inorganic hybrid with immobilized enzyme was used as a highly effective and sensitive dopamine or catechol biosensor. The biocatalytic system was shown to be resistant to the effects of inhibitors and interferents and its parameters remained unaltered in the presence of uric and ascorbic acid [205].

3.4. Summary of New Materials

Table 2 summarizes the most important types of *New materials* and enzymes that may be immobilized by using these carriers. Moreover, information about binding groups, immobilization type or cross-linking agents are also presented.

Table 2. Summary and selected examples of *New materials* of inorganic, organic and hybrid origin applied for enzymes immobilization.

Support Material	Binding Groups	Cross-Linking Agent	Immobilization Type	Immobilized Enzyme	Reference
Inorganic Materials					
magnetic nanoparticles	epoxy groups	3-glycidoxypropyl-trimethoxylsilane	covalent binding	lipase from *Candida antarctica*	[83]
	–OH	–	adsorption	glucose oxidase from *Aspergillus niger*	[84]
silica SBA-15	–OH	–	adsorption	alkaline protease	[96]
mesoporous silica	–OH	–	encapsulation	catalase	[98]
silica mesoporous nanoparticles	epoxy groups	3-glycidoxypropyl-trimethoxylsilane	covalent binding	lipase from *Rhizomucor miehei*	[107]
TiO_2 nanoparticles	–OH	–	adsorption	carbonic anhydrase	[106]
cordierite	$–NH_2$	*N*-*β*-aminoethyl-*γ*-aminopropyl-trimethoxysilane	covalent binding	horseradish peroxidase	[113]
multi-walled carbon nanotubes	$–NH_2$	3-aminopropyl-triethoxysilane	covalent binding	α-glucosidase	[120]
reduced graphene oxide	C=O	glutaraldehyde	covalent binding	horseradish peroxidase	[127]
Organic materials					
electrospinning fibres of polycaprolactone	C=O	-	adsorption	catalase	[138]
electrospinning nanofibers of polyvinyl alcohol	–OH	-	encapsulation	lipase from *Burkholderia cepacia*	[140]
polyethersulphone membrane	-	-	adsorption	Phosphotriesterase lactonase from *Sulfolobus solfataricus*	[145]
NTR7450 membrane	-	-	adsorption	casein glycomacropeptide	[150]
Hybrid/composite materials					
polyaniline-polyacrylonitrile composite	–N–H	-	encapsulation	glucose oxidase	[154]
cellulose-poly(acrylic acid) fibres	–OH, COOH	-	covalent binding	horseradish peroxidase	[157]
chitosan-alginate beads	$–NH_2$, –OH	-	entrapment	amyloglucosidase	[160]
graphene oxide-Fe_3O_4	–OH, C=O	cyanuric chloride	covalent binding	glucoamylase	[177]
silica-lignin	–OH, C=O	-	adsorption	glucose oxidase form *Aspergillus niger*	[178]
polyacrylonitrile-multi-walled carbon nanotubes	–N–H, C=O, –OH	*N*-Hydroxy-succinimide	covalent binding	catalase	[179]
silica-graphene oxide particles	–OH, C=O	*N*-Hydroxy-succinimide	covalent binding	cholesterol oxidase	[199]
ZnO-SiO_2 nanowires	–OH	–	cross-linking	horseradish peroxidase	[202]
$CaCO_3$-gold nanoparticles	–OH, C=O	–	adsorption	horseradish peroxidase	[203]

New materials with tailored properties are increasingly frequently used as supports for enzymes both due to limitations in application of *Classic materials* and also to improve the properties of the immobilized enzymes. Materials belonging to the *New materials* group can facilitate easy separation of biocatalytic systems from reaction mixtures (magnetic nanoparticles) or enable avoidance of enzyme particles overloading on the surface of the carrier (nanoparticles and mesoporous materials). Moreover, materials such as graphene or graphene oxide enhance transfer of electrons between immobilized enzyme and substrate and result in increased catalytic activity of the biomolecules. The greatest advantage of the materials of organic origin classified as *New materials* is that they can be formed in various geometrical shapes such as fibres or membranes and reduce diffusional limitations and improve the efficiency of the biocatalytic processes. Within *New materials*, there is continuing and growing interest in hybrid materials. Hybrid supports may be synthesized through the combination of precursors of different origin and their properties can be tailored to the requirements of the biocatalysts as well as to the technological process in which the product will be used after immobilization. Hybrid supports are characterized by good thermal and chemical stability and mechanical resistance and usually ensure stable, covalent binding of the enzyme.

4. Summary

Inorganic materials such as inorganic oxides, minerals and carbon-based materials and materials of organic origin, including synthetic and natural polymers, may be classified as *Classic support materials* used for the immobilization of enzymes. These carriers are characterized by good stability under harsh reaction conditions, high availability or relatively simple synthesis and consequently low price. In general, these groups of support materials can be used for the immobilization of all classes of enzymes through the use of all immobilization techniques although adsorption immobilization is the most common. In view of the properties of these materials, the formation of highly specific interactions between the enzyme and the support is usually limited. Therefore, immobilization is based on non-specific hydrogen interactions. In some cases, however, where for example there is a high affinity of functional groups, the formation of covalent bonds cannot be excluded. The wide use of *Classic materials* as supports for enzymes is also linked to the more cost-effective immobilization process since these carriers do not require complicated preparation procedures and immobilization is usually fast and simple. *Classic materials* will continue to play a significant role as supports for the immobilization of enzymes from many catalytic classes for many practical applications ranging from the synthesis of highly pure chemical compounds to food processes and wastewater treatment.

The wide group of support materials which for the purposes of this review are called *New materials* for enzyme immobilization can offer properties designed for particular enzymes or for the requirements of a given technological process. These materials have come into use due to certain defects of the *Classic materials* and to the relatively low efficiencies of catalytic conversions carried out with biocatalysts bound to *Classic materials*. Inorganic materials in the *New materials* group include magnetic nanoparticles, which enhance fast and simple separation of the immobilized enzyme from the reaction mixture by means of an external magnetic field and mesoporous materials with a hierarchic pore structure, which ensures the uniform distribution of biomolecules in the matrix pores and thus reduces overloading of the enzymes and maintains catalytic activity at a high level. There are also materials of organic origin, such as electrospun membranes; depending on the material used for their production, these materials can significantly increase the transfer of electrons, which is a key step in many biocatalytic transformations. However, special interest particularly in recent years has been paid to applications of hybrid and composite *New materials* for enzyme immobilization. As has been described, these materials are synthesized from combinations of precursors of inorganic, organic and mixed inorganic and organic origin. They are designed to offer high stability, good affinity for enzymes and the presence of many chemical functional groups compatible with the chemical moieties present in the protein structure. Because of these features, biomolecules are attached mainly via covalent bonds and this ensures the good reusability and operational stability of the resulting biocatalytic

systems. *New materials* will be employed more and more extensively in the future for immobilization of enzymes. Their applications will not be limited to the creation of biocatalytic systems for use in synthesis; hybrids and composite materials will also be used to production of biocatalytic cells and biosensors for the detection of various compounds in medicine and in environmental monitoring, as well as for remediation of hazardous compounds.

It should be emphasized that in presented literature review the materials have been considered regardless of the type/mode of enzyme immobilization methodology employed, thus the treatise is universal with respect to this regard. However, for creation of stable and efficient biocatalytic systems, the attachment technique must be optimized individually for the specific enzyme, the specific material and the biocatalytic process to be employed.

Acknowledgments: This work was supported by research grant funds from the National Science Center, Poland, in accordance with decision no. DEC-2015/19/N/ST8/02220.

Author Contributions: Jakub Zdarta researched the literature and wrote the manuscript; Anne S. Meyer, Teofil Jesionowski and Manuel Pinelo discussed ideas and edited the manuscript.

Conflicts of Interest: The authors declare no conflict of interest. The funding sponsors had no role in the design of the study; in the collection, analysis, or interpretation of data; in the writing of the manuscript; or in the decision to publish the results.

References

1. Cowan, D.A.; Fernandez-Lafuente, R. Enhancing the functional properties of thermophilic enzymes by chemical modification and immobilization. *Enzyme Microb. Technol.* **2011**, *49*, 326–346. [CrossRef] [PubMed]
2. Wohlgemuth, R. Biocatalysis—Key to sustainable industrial chemistry. *Curr. Opin. Biotechnol.* **2010**, *21*, 713–724. [CrossRef] [PubMed]
3. Jesionowski, T.; Zdarta, J.; Krajewska, B. Enzymes immobilization by adsorption: A review. *Adsorption* **2014**, *20*, 801–821. [CrossRef]
4. Zhang, Y.; Ge, J.; Liu, Z. Enhanced activity of immobilized or chemically modified enzymes. *ACS Catal.* **2015**, *5*, 4503–4513. [CrossRef]
5. Marzadori, C.; Miletti, S.; Gessa, C.; Ciurli, S. Immobilization of jack bean urease on hydroxyapatite: Urease immobilization on alkaline soils. *Soil Biol. Biochem.* **1998**, *30*, 1485–1490. [CrossRef]
6. Mateo, C.; Palomo, J.M.; Fernandez-Lafuente, G.; Guisan, J.M.; Fernandez-Lafuente, R. Improvement of enzyme activity, stability and selectivity via immobilization techniques. *Enzyme Microb. Technol.* **2007**, *40*, 1451–1463. [CrossRef]
7. Sheldon, R.A. Enzyme immobilization: The quest for optimum performance. *Adv. Synth. Catal.* **2007**, *49*, 1289–1307. [CrossRef]
8. Guzik, U.; Hupert-Kocurek, K.; Wojcieszynska, D. Immobilization as a strategy for improving enzyme properties—Application to oxidoreductases. *Molecules* **2014**, *19*, 8995–9018. [CrossRef] [PubMed]
9. Sheldon, R.A.; van Pelt, S. Enzyme immobilisation in biocatalysis: Why, what and how? *Chem. Soc. Rev.* **2013**, *42*, 6223–6235. [CrossRef] [PubMed]
10. Rodrigues, R.C.; Berenguer-Murcia, A.; Fernandez-Lafuente, R. Coupling chemical modification and immobilization to improve the catalytic performance of enzymes. *Adv. Synth. Catal.* **2011**, *353*, 2216–2238. [CrossRef]
11. Cao, L. *Carrier-Bound Immobilized Enzymes*; Wiley-VCH: Weinheim, Germany, 2005.
12. Fernandez-Lafuente, R. Stabilization of multimeric enzymes: Strategies to prevent subunit dissociation. *Enzyme Microb. Technol.* **2009**, *45*, 405–418. [CrossRef]
13. Wong, L.S.; Khan, F.; Micklefield, J. Selective covalent protein immobilization: Strategies and applications. *Chem. Rev.* **2009**, *109*, 4025–4053. [CrossRef] [PubMed]
14. Jesionowski, T. Preparation of colloidal silica from sodium metasilicate solution and sulphuric acid in emulsion medium. *Colloids Surf. A* **2001**, *190*, 153–165. [CrossRef]
15. Jesionowski, T.; Krysztafkiewicz, A. Preparation of the hydrophilic/hydrophobic silica particles. *Colloids Surf. A* **2002**, *207*, 49–58. [CrossRef]

16. Zucca, P.; Sanjust, E. Inorganic materials as supports for covalent enzyme immobilization: Methods and mechanisms. *Molecules* **2014**, *19*, 14139–14194. [CrossRef] [PubMed]
17. Kramer, M.; Cruz, J.C.; Pfromm, P.H.; Rezac, E.; Czermak, P. Enantioselective transestrification by *Candida antarctica* lipase B immobilized on fumed silica. *J. Biotechnol.* **2010**, *150*, 80–86. [CrossRef] [PubMed]
18. Falahati, M.; Mamani, L.; Sabuory, A.A.; Shafiee, A.; Foroumadi, A.; Badiei, A.R. Aminopropyl functionalized cubic Ia3d mesoporous silica nanoparticle as an efficient support for immobilization of superoxide dismutase. *Biochim. Biophys. Acta* **2011**, *1814*, 1195–1202. [CrossRef] [PubMed]
19. Godjevargova, T.; Nenkova, R.; Konsulov, V. Immobilization of glucose oxidase by acronitrile copolymer coated silica supports. *J. Mol. Catal. B* **2006**, *38*, 59–64. [CrossRef]
20. Zdarta, J.; Sałek, K.; Kołodziejczak-Radzimska, A.; Siwińska-Stefańska, K.; Szwarc-Rzepka, K.; Norman, M.; Klapiszewski, Ł.; Bartczak, P.; Kaczorek, E.; Jesionowski, T. Immobilization of *Amano Lipase A* onto Stöber silica surface: Process characterization and kinetic studies. *Open Chem.* **2015**, *13*, 138–148. [CrossRef]
21. Kołodziejczak-Radzimska, A.; Zdarta, J.; Jesionowski, T. Physicochemical and catalytic properties of acylase I from *Aspergillus melleus* immobilized on amino- and carbonyl-grafted Stöber silica. *Biotechnol. Prog.* **2018**. [CrossRef] [PubMed]
22. Narwal, S.K.; Saun, N.K.; Gupta, R. Characterization and catalytic properties of free and silica-bound lipase: A comparative study. *J. Oleo Sci.* **2014**, *63*, 599–603. [CrossRef] [PubMed]
23. Zou, B.; Hua, Y.; Cui, F.; Jiang, L.; Yu, D.; Huang, H. Effect of surface modification of low cost mesoporous SiO_2 carriers on the properties of immobilized lipase. *J. Colloids Interface Sci.* **2014**, *417*, 210–216. [CrossRef] [PubMed]
24. Foresti, M.L.; Valle, G.; Bonetto, R.; Ferreira, M.L.; Briand, L.E. FTIR, SEM and fractal dimension characterization of lipase B from *Candida antarctica* immobilized onto titania at selected conditions. *Appl. Surf. Sci.* **2010**, *256*, 1624–1635. [CrossRef]
25. Vallés, D.; Furtado, S.; Villadóniga, C.; Cantera, A.M.B. Adsorption onto alumina and stabilization of cysteine proteinases from crude extract of solanum granuloso-leprosum fruits. *Process Biochem.* **2011**, *46*, 592–598. [CrossRef]
26. Reshmi, R.; Sanjay, G.; Sugunan, S. Immobilization of α-amylase on zirconia: A heterogeneous biocatalyst for starch hydrolysis. *Catal. Commun.* **2007**, *8*, 393–399. [CrossRef]
27. Yang, Z.; Si, S.; Zhang, C. Study on the activity and stability of urease immobilized ontonanoporous alumina membranes. *Microporous Mesoporous Mater.* **2008**, *111*, 359–366. [CrossRef]
28. Ghiaci, M.; Aghaei, H.; Soleimanian, S.; Sedaghat, M.E. Enzyme immobilization Part 1. Modified bentonite as a new and efficient support for immobilization of *Candida rugose* lipase. *Appl. Clay Sci.* **2009**, *43*, 289–295. [CrossRef]
29. Mbouguen, J.K.; Ngameni, E.; Walcarius, A. Organoclay-enzyme film electrodes. *Anal. Chim. Acta* **2006**, *578*, 145–155. [CrossRef] [PubMed]
30. An, N.; Zhou, C.H.; Zhuang, X.Y.; Tong, D.S.; Yu, W.H. Immobilization of enzymes on clay minerals for biocatalysts and biosensors. *Appl. Clay Sci.* **2015**, *114*, 283–296. [CrossRef]
31. Sanjay, G.; Sugunan, S. Acid activated montmorillonite: An efficient immobilization support for improving reusability, storage stability and operational stability of enzymes. *J. Porous Mater.* **2008**, *15*, 359–367. [CrossRef]
32. Sedaghat, M.E.; Ghiaci, M.; Aghaei, H.; Soleimanian-Zad, S. Enzyme immobilization. Part 4. Immobilization of alkaline phosphatase on Na-sepiolite and modified sepiolite. *Appl. Clay Sci.* **2009**, *46*, 131–135. [CrossRef]
33. Zdarta, J.; Budzińska, K.; Kołodziejczak-Radzimska, A.; Klapiszewski, Ł.; Siwińska-Stefańska, K.; Bartczak, P.; Piasecki, A.; Maciejewski, H.; Jesionowski, T. Hydroxyapatite as a support in protease immobilization process. *Physicochem. Probl. Miner. Process.* **2015**, *51*, 633–646.
34. Salman, S.; Soundararajan, S.; Safina, G.; Satoh, I.; Danielsson, B. Hydroxyapatite as a novel reversible in situ adsorption matrix for enzyme thermistor-based FIA. *Talanta* **2008**, *77*, 490–493. [CrossRef]
35. Zhou, C.H.; Keeling, J. Fundamental and applied research on clay minerals: From climate and environment to nanotechnology. *Appl. Clay Sci.* **2013**, *74*, 3–9. [CrossRef]
36. Chrisnasari, R.; Wuisan, Z.G.; Budhyantoro, A.; Widi, R.K. Glucose oxidase immobilization on TMAH-modified bentonite. *Indones. J. Chem.* **2015**, *15*, 22–28. [CrossRef]
37. Daoud, F.B.O.; Kaddour, S.; Sadoun, T. Adsorption of cellulose *Aspergillus niger* on a commercial activated carbon: Kinetics and equilibrium studies. *Colloids Surf. B Biointerface* **2010**, *75*, 93–99. [CrossRef] [PubMed]

38. Dutta, S.; Bhattacharyya, A.; De, P.; Ray, P.; Basu, S. Removal of mercury from its aqueous solution using charcoal-immobilized papain (CIP). *J. Hazard. Mater.* **2009**, *172*, 888–896. [CrossRef] [PubMed]
39. Rani, A.S.; Das, M.L.M.; Satyanarayana, S. Preparation and characterization of amyloglucosidase adsorbed on activated charcoal. *J. Mol. Catal. B Enzym.* **2000**, *10*, 471–476. [CrossRef]
40. Silva, V.D.M.; De Marco, L.M.; Delvivo, F.M.; Coelho, J.V.; Silvestre, M.P.C. Immobilization of pancreatin in activated carbon and in alumina for preparing whey hydrolysates. *Acta Sci. Health Sci.* **2005**, *27*, 163–169.
41. Hanefeld, U.; Gardossi, L.; Magner, E. Understanding Enzyme Immobilisation. *Chem. Soc. Rev.* **2009**, *38*, 453–468. [CrossRef] [PubMed]
42. Maksym, P.; Tarnacka, M.; Dzienia, A.; Matuszek, K.; Chrobok, A.; Kaminski, K.; Paluch, M. Enhanced polymerization rate and conductivity of ionic liquid-based epoxy resin. *Macromolecules* **2017**, *50*, 3262–3272. [CrossRef]
43. Kirk, O.; Christensen, M.W. Lipases from *Candida antarctica*: Unique biocatalysts from a unique origin. *Org. Process Res. Dev.* **2002**, *6*, 446–451. [CrossRef]
44. Ferrario, V.; Ebert, C.; Knapic, L.; Fattor, D.; Basso, A.; Spizzo, P.; Gardossi, L. Conformational changes of lipases in aqueous media: A comparative computational study and experimental implications. *Adv. Synth. Catal.* **2011**, *353*, 2466–2480. [CrossRef]
45. Basso, A.; Braiuca, P.; Cantone, S.; Ebert, C.; Linda, P.; Spizzo, P.; Caimi, P.; Hanefeld, U.; Degrassi, G.; Gardossi, L. In silico analysis of enzyme surface and glycosylation effect as a tool for efficient covalent immobilisation of CalB and PGA on Sepabeads. *Adv. Synth. Catal.* **2007**, *349*, 877–886. [CrossRef]
46. Cantone, S.; Ferrario, V.; Corici, L.; Ebert, C.; Fattor, D.; Spizzo, P.; Gardossi, L. Efficient immobilisation of industrial biocatalysts: Criteria and constraints for the selection of organic polymeric carriers and immobilisation methods. *Chem. Soc. Rev.* **2013**, *42*, 6262–6276. [CrossRef] [PubMed]
47. Ashly, P.C.; Joseph, M.J.; Mohanan, P.V. Activity of diastase α-amylase immobilized on polyanilines (PANIs). *Food Chem.* **2011**, *127*, 1808–1813. [CrossRef]
48. Jimenez Hamann, M.C.; Saville, B.A. Enhancement of tyrosinase stability by immobilization on Nylon 66. *Food Bioprod. Process Trans. Inst. Chem. Eng. C* **1996**, *74*, 47–52.
49. Wang, W.; Zhou, W.; Li, J.; Hao, D.; Su, Z.; Ma, G. Comparison of covalent and physical immobilization of lipase in gigaporous polymeric microspheres. *Bioprocess Biosys. Eng.* **2015**, *38*, 2107–2115. [CrossRef] [PubMed]
50. Silva, M.F.; Rigo, D.; Mossi, V.; Dallago, R.M.; Henrick, P.; Kuhn, G.D.O.; Rosa, C.D.; Oliveira, D.; Oliveira, J.V.; Treichel, H. Evaluation of enzymatic activity of commercial inulinase from *Aspergillus niger* immobilized in polyurethane foam. *Food Bioprod. Process.* **2013**, *91*, 54–59. [CrossRef]
51. Bai, X.; Gu, H.; Chen, W.; Shi, H.; Yang, B.; Huang, X.; Zhang, Q. Immobilized laccase on activated poly(vinyl alcohol) microspheres for enzyme thermistor application. *Appl. Biochem. Biotechnol.* **2014**, *173*, 1097–1107. [CrossRef] [PubMed]
52. Vartiainen, J.; Rättö, M.; Paulussen, S. Antimicrobial activity of glucose oxidase-immobilized plasma-activated polypropylene films. *Packag. Technol. Sci.* **2005**, *18*, 243–251. [CrossRef]
53. Kumari, A.; Kayastha, A.M. Immobilization of soybean (*Glycine max*) α-amylase onto chitosan and amberlite MB-150 beads: Optimization and characterization. *J. Mol. Catal. B Enzym.* **2011**, *69*, 8–14. [CrossRef]
54. Alsafadi, D.; Paradisi, F. Covalent immobilization of alcohol dehydrogenase (ADH2) from *Haloferaxvol canii*: How to maximize activity and optimize performance of halophilic enzymes. *Mol. Biotechnol.* **2014**, *56*, 240–247. [CrossRef] [PubMed]
55. Elnashar, M.M.M. *Biotechnology of Biopolymers*; InTech: London, UK, 2011.
56. Horchani, H.; Aissa, I.; Ouertani, S.; Zarai, Z.; Gargouri, Y.; Sayari, A. Staphylococcal lipases: Biotechnological applications. *J. Mol. Catal. B Enzyme* **2012**, *76*, 125–132. [CrossRef]
57. Vijayaraghavan, K.; Yamini, D.; Ambika, V.; Sravya Sowdamini, N. Trends in inulinase production—A review. *Crit. Rev. Biotechnol.* **2009**, *29*, 67–77. [CrossRef] [PubMed]
58. Homaei, A.A.; Sariri, R.; Vianello, F.; Stevanato, R. Enzyme immobilization: An update. *J. Chem. Biol.* **2013**, *6*, 185–205. [CrossRef] [PubMed]
59. Tischer, W.; Wedekind, F. Immobilized enzymes: Methods and applications. *Top. Curr. Chem.* **1999**, *200*, 95–126.
60. Krajewska, B. Application of chitin- and chitosan-based materials for enzyme immobilizations: A review. *Enzyme Microb. Technol.* **2004**, *35*, 126–139. [CrossRef]

61. Kurita, K. Controlled functionalization of the polysaccharide chitin. *Prog. Polym. Sci.* **2001**, *26*, 1921–1971. [CrossRef]
62. Peter, M. Applications and environmental aspects of chitin and chitosan. *J. Macromol. Sci.* **1995**, *32*, 629–640. [CrossRef]
63. Shi, L.E.; Tang, Z.X.; Yi, Y.; Chen, J.S.; Xiong, W.Y.; Ying, G.Q. Immobilization of nuclease p1 on chitosan micro-spheres. *Chem. Biochem. Eng. Q.* **2011**, *25*, 83–88.
64. Cahyaningrum, S.E.; Herdyastusi, N.; Maharani, D.K. Immobilization of glucose isomerase in surface-modified chitosan gel beads. *Res. J. Pharm. Biol. Chem. Sci.* **2014**, *5*, 104–111.
65. Kim, H.J.; Park, S.; Kim, S.H.; Kim, J.H.; Yu, H.; Kim, H.J.; Yang, Y.H.; Kan, E.; Kim, Y.H.; Lee, S.H. Biocompatible cellulose nanocrystals as supports to immobilize. *J. Mol. Catal. B Enzym.* **2015**, *12*, 170–178. [CrossRef]
66. Tumturk, H.; Karaca, N.; Demirel, G.; Sahin, F. Preparation and application of poly(*N*,*N*-dimethylacrylamide-co-acrylamide) and poly(*N*-isopropylacrylamide-co-acrylamide)/κ-Carrageenan hydrogels for immobilization of lipase. *Int. J. Biol. Macromol.* **2007**, *40*, 281–285. [CrossRef] [PubMed]
67. Zdarta, J.; Jesionowski, T. *Luffa cylindrica* sponges as a thermally and chemically stable support for *Aspergillus niger* lipase. *Biotechnol. Prog.* **2016**, *32*, 657–665. [CrossRef] [PubMed]
68. Zdarta, J.; Norman, M.; Smułek, W.; Moszyński, D.; Kaczorek, E.; Stelling, A.L.; Ehrlich, H.; Jesionowski, T. Spongin-based scaffolds from *Hippospongia communis* demosponge as an effective support for lipase immobilization. *Catalysts* **2017**, *7*, 147. [CrossRef]
69. Hwang, E.T.; Gu, M.B. Enzyme stabilization by nano/microsized hybrid materials. *Eng. Life Sci.* **2013**, *13*, 49–61. [CrossRef]
70. Coradin, T.; Nassif, N.; Livage, J. Silica-alginate composites for microencapsulation. *Appl. Microbiol. Biotechnol.* **2003**, *61*, 429–434. [CrossRef] [PubMed]
71. Betigeri, S.S.; Neau, S.H. Immobilization of lipase using hydrophilic polymers in the form of hydrogel beads. *Biomaterials* **2002**, *51*, 3627–3636. [CrossRef]
72. Kocaturk, S.; Yagar, H. Optimization of polyphenol oxidase immobilization in copper alginate beads. *Artif. Cells Blood Substit. Biotechnol.* **2010**, *38*, 157–163. [CrossRef] [PubMed]
73. Sin Ball, S.G.; Morell, M.K. From bacterial glycogen to starch: Understanding the biogenesis of the plant starch granule. *Annu. Rev. Plant Biol.* **2003**, *54*, 207–233. [CrossRef] [PubMed]
74. Delattre, C.; Fenoradosoa, T.A.; Michaud, P. Galactans: An overview of their most important sourcing and applications as natural polysaccharides. *Braz. Arch. Biol. Technol.* **2011**, *54*, 1075–1092. [CrossRef]
75. Porath, J.; Axén, R. Immobilization of enzymes to agar, agarose, and sephadex support. *Methods Enzymol.* **1976**, *44*, 19–45. [PubMed]
76. Prakash, O.; Jaiswal, N. Immobilization of a thermostable α-amylase on agarose and agar matrices and its application in starch stain removal. *World Appl. Sci. J.* **2011**, *13*, 572–577.
77. De Oliveira, S.M.; Moreno-Perez, S.; Romero-Fernandez, M.; Fernandez-Lorente, G.; Rocha-Martin, J.; Guisan, J.M. Immobilization and stabilization of commercial β-1,4-endoxylanase Depol™ 333MDP by multipoint covalent attachment for xylan hydrolysis: Production of prebiotics (xylo-oligosaccharides). *Biocatal. Biotransform.* **2018**, *36*, 141–150. [CrossRef]
78. Singh, V.; Srivastava, P.; Singh, A.; Singh, D.; Malviya, T. Polysaccharide-silica hybrids: Design and applications. *Polym. Rev.* **2016**, *56*, 113–136. [CrossRef]
79. Grigoras, A.G. Catalase immobilization—A review. *Biochem. Eng. J.* **2017**, *117*, 1–20. [CrossRef]
80. Cao, M.; Li, Z.; Wang, J.; Ge, W.; Yue, T.; Li, R.; Colvin, V.L.; Yu, W.W. Food related applications of magnetic iron oxide nanoparticles: Enzyme immobilization, protein purification, and food analysis. *Trends Food Sci. Technol.* **2012**, *27*, 47–56. [CrossRef]
81. Li, X.S.; Zhu, G.T.; Luo, Y.B.; Yuan, B.F.; Feng, Y.Q. Synthesis and applications of functionalized magnetic materials in sample preparation. *TrAC Trends Anal. Chem.* **2013**, *45*, 233–247. [CrossRef]
82. Netto, C.G.C.M.; Toma, H.E.; Andrade, L.H. Superparamagnetic nanoparticles as versatile carriers and supporting materials for enzymes. *J. Mol. Catal. B Enzym.* **2013**, *85–86*, 71–92. [CrossRef]
83. Mehrasbi, M.R.; Mohammadi, J.; Peyda, M.; Mohammadi, M. Covalent immobilization of *Candida antarctica* lipase on core-shell magnetic nanoparticles for production of biodiesel from waste cooking oil. *Renew. Energy* **2017**, *101*, 593–602. [CrossRef]

84. Aber, S.; Mahmoudikia, E.; Karimi, A.; Mahdizadeh, F. Immobilization of glucose oxidase on Fe_3O_4 magnetic nanoparticles and its application in the removal of Acid Yellow 12. *Water Air Soil Pollut.* **2016**, *227*, 93–104. [CrossRef]
85. Atacan, K.; Cakiroglu, B.; Ozacar, M. Improvement of the stability and activity of immobilized trypsin on modified Fe_3O_4 magnetic nanoparticles for hydrolysis of bovine serum albumin and its application in the bovine milk. *Food Chem.* **2016**, *212*, 460–468. [CrossRef] [PubMed]
86. Schuth, F. Endo- and exotemplating to create high-surface-area inorganic materials. *Angew. Chem. Int. Ed.* **2003**, *42*, 3604–3622. [CrossRef] [PubMed]
87. Matuszek, K.; Chrobok, A.; Latos, P.; Markiton, M.; Szymańska, K.; Jarzębski, A.; Swadźba-Kwaśny, M. Silica-supported chlorometallate(III) ionic liquids as recyclable catalysts for Diels-Alder reaction under solventless conditions. *Catal. Sci. Technol.* **2016**, *6*, 8129–8137. [CrossRef]
88. Hartmann, M. Ordered mesoporous materials for bioadsorption and biocatalysis. *Chem. Mater.* **2005**, *17*, 4577–4593. [CrossRef]
89. Fan, J.; Lei, J.; Wang, L.; Yu, C.; Tu, B.; Zhao, D. Rapid and high-capacity immobilization of enzymes based on mesoporous silicas with controlled morphologies. *Chem. Commun.* **2003**, *17*, 2140–2141. [CrossRef]
90. Yiu, H.H.P.; Wright, P.A.; Botting, N.P. Enzyme immobilisation using siliceous mesoporous molecular sieves. *Microporous Mesoporous Mater.* **2001**, *44–45*, 763–765. [CrossRef]
91. Schuth, F. Non-siliceous mesostructured and mesoporous materials. *Chem. Mater.* **2001**, *13*, 3184–3195. [CrossRef]
92. Moritz, M.; Geszke-Moritz, M. Mesoporous materials as multifunctional tools in biosciences: Principles and applications. *Mater. Sci. Eng. C* **2015**, *49*, 114–151. [CrossRef] [PubMed]
93. Catalano, P.N.; Wolosiuk, A.; Soler-Illia, G.J.A.A.; Bellino, M.G. Wired enzymes in mesoporous materials: A benchmark for fabricating biofuel cells. *Bioelectrochemistry* **2015**, *106*, 14–21. [CrossRef] [PubMed]
94. Cai, C.; Gao, Y.; Liu, Y.; Zhong, N.; Liu, N. Immobilization of *Candida antarctica* lipase B onto SBA-15 and their application in glycerolysis for diacylglycerols synthesis. *Food Chem.* **2012**, *212*, 205–212. [CrossRef] [PubMed]
95. Chen, Y.; Xu, Y.; Wu, X.M. Efficient improving the activity and enantioselectivity of *Candida rugosa* lipase for the resolution of naproxen by enzyme immobilization on MCM-41 mesoporous molecular sieve. *Int. J. Bioautom.* **2015**, *19*, 325–334.
96. Zhuang, H.; Dong, S.; Zhang, T.; Tang, N.; Xu, N.; Sun, B.; Liu, J.; Zhang, M.; Yuan, Y. Study on alkaline protease immobilized on mesoporous materials. *Asian J. Chem.* **2014**, *26*, 1139–1144.
97. Mangrulkar, P.A.; Yadav, R.; Meshram, J.S.; Labhsetwar, N.K.; Rayalu, S.S. Tyrosinase-immobilized MCM-41 for the detection of phenol. *Water Air Soil Pollut.* **2012**, *223*, 819–825. [CrossRef]
98. Wang, Y.; Caruso, F. Mesoporous silica spheres as supports for enzyme immobilization and encapsulation. *Chem. Mater.* **2005**, *17*, 953–961. [CrossRef]
99. Jia, H.; Zhu, G.; Wang, P. Catalytic behaviors of enzymes attached to nanoparticles: The effect of particle mobility. *Biotechnol. Bioeng.* **2003**, *84*, 406–414. [CrossRef] [PubMed]
100. Kim, J.; Grate, J.W.; Wang, P. Nanostructures for enzyme stabilization. *Chem. Eng. Sci.* **2006**, *61*, 1017–1026. [CrossRef]
101. Cipolatti, E.P.; Valerio, A.; Henriques, R.A.; Moritz, D.E.; Ninow, J.L.; Freire, D.M.G.; Manoel, E.A.; Fernandez-Lafuente, R.; de Oliveira, D. Nanomaterials for biocatalyst immobilization—State of the art and future trends. *RSC Adv.* **2016**, *6*, 104675–104692. [CrossRef]
102. Hu, C.; Wang, N.; Zhang, W.; Zhang, S.; Meng, Y.; Yu, X. Immobilization of *Aspergillus terreus* lipase in self-assembled hollow nanospheres for enantioselective hydrolysis of ketoprofen vinyl ester. *J. Biotechnol.* **2015**, *194*, 12–18. [CrossRef] [PubMed]
103. Wang, X.; Shi, J.; Li, Z.; Zhang, S.; Wu, H.; Jiang, Z.; Yang, C.; Tian, C. Facile one-pot preparation of chitosan/calcium pyrophosphate hybrid microflowers. *ACS Appl. Mater. Interface* **2014**, *6*, 14522–14532. [CrossRef] [PubMed]
104. Kotal, M.; Srivastava, S.K.; Matiti, T.K. Fabrication of gold nanoparticle assembled polyurethane microsphere template in trypsin immobilization. *J. Nanosci. Nanotechnol.* **2011**, *11*, 10149–10157. [CrossRef] [PubMed]
105. Bolibok, P.; Wiśniewski, M.; Roszek, K.; Terzyk, A.P. Controlling enzymatic activity by immobilization on graphene oxide. *Sci. Nat.* **2017**, *104*, 36. [CrossRef] [PubMed]

106. Hou, J.; Dong, G.; Xiao, B.; Malassigne, C.; Chen, V. Preparation of titania based biocatalytic nanoparticles and membranes for CO_2 conversion. *J. Mater. Chem. A* **2015**, *3*, 3332–3342. [CrossRef]
107. Garmroodi, M.; Mohammadi, M.; Ramazani, A.; Ashjari, M.; Mohammadi, J.; Sabour, B.; Yousefi, M. Covalent binding of hyper-activated *Rhizomucor miehei* lipase (RML) on hetero-functionalized siliceous supports. *Int. J. Biol. Macromol.* **2016**, *86*, 208–215. [CrossRef] [PubMed]
108. Ota, S.; Miyazaki, S.; Matsuoka, H.; Morisato, K.; Shintani, Y.; Nakanishi, K. High-throughput protein digestion by trypsin-immobilized monolithic silica with pipette-tip formula. *J. Biochem. Biophys. Meth.* **2007**, *70*, 57–62. [CrossRef] [PubMed]
109. de Cazes, M.; Belleville, P.; Mougel, M.; Kellner, H.; Sanchez-Marcano, J. Characterization of laccase-grafted ceramic membranes for pharmaceuticals degradation. *J. Membr. Sci.* **2015**, *476*, 384–393. [CrossRef]
110. Caldas, E.M.; Novatzky, D.; Deon, M.; de Menezes, E.W.; Hertz, P.F.; Costa, T.M.H.; Arenas, L.T.; Benvenutt, E.V. Pore size effect in the amount of immobilized enzyme for manufacturing carbon ceramic biosensor. *Microporous Mesoporous Mater.* **2017**, *247*, 95–102. [CrossRef]
111. Pazouki, M.; Zamani, F.; Khalili, M. Development of clay foam ceramic as a support for fungi immobilization for biodiesel production. *Int. J. Eng. Trans. B Appl.* **2014**, *27*, 1691–1696.
112. Ebrahimi, M.; Placido, L.; Engel, L.; Shams Ashaghi, K.; Czermak, P. A novel ceramic membrane reactor system for the continuous enzymatic synthesis of oligosaccharides. *Desalination* **2010**, *250*, 1105–1108. [CrossRef]
113. Wang, W.; Li, Z.; Li, W.; Wu, J. Horseradish peroxidase immobilized on the silane-modified ceramics for the catalytic oxidation of simulated oily water. *Sep. Purif. Technol.* **2012**, *89*, 206–211. [CrossRef]
114. Titirici, M.M.; White, R.J.; Brun, N.; Budarin, V.L.; Su, D.S.; Del Monte, F.; Clark, J.H.; MacLachlan, M.J. Sustainable carbon materials. *Chem. Soc. Rev.* **2015**, *44*, 250–290. [CrossRef] [PubMed]
115. Hong, G.; Diao, S.; Antaris, A.L.; Dai, H. Carbon nanomaterials for biological imaging and nanomedicinal therapy. *Chem. Rev.* **2015**, *115*, 10816–10906. [CrossRef] [PubMed]
116. Pedrosa, V.A.; Paliwal, S.; Balasubramanian, S.; Nepal, D.; Davis, V.; Wild, J.; Ramanculov, E.; Simonian, A. Enhanced stability of enzyme organophosphate hydrolase interfaced on the carbon nanotubes. *Colloids Surf. B Biointerface* **2010**, *77*, 69–74. [CrossRef] [PubMed]
117. Wan, X.; Zhang, C.; Yu, D.; Huang, H.; Hu, Y. Enzyme immobilized on carbon nanotubes. *Prog. Chem.* **2015**, *27*, 1251–1259.
118. Markiton, M.; Boncel, S.; Janas, D.; Chrobok, A. Highly active nanobiocatalyst from lipase noncovalently immobilized on multiwalled carbon nanotubes for Baeyer-Villiger synthesis of lactones. *ACS Sustain. Chem. Eng.* **2017**, *8*, 1685–1691. [CrossRef]
119. Liu, Y.; Wang, M.; Zhao, F.; Xu, Z.; Dong, S. The direct electron transfer of glucose oxidase and glucose biosensor based on carbon nanotubes/chitosan matrix. *Biosens. Bioelectron.* **2005**, *21*, 984–988. [CrossRef] [PubMed]
120. Mohiuddin, M.; Arbain, D.; Islam, A.K.M.S.; Ahmad, M.S.; Ahmad, M.N. Alpha-glucosidase enzyme biosensor for the electrochemical measurement of antidiabetic potential of medicinal plants. *Nanoscale Res. Lett.* **2016**, *95*, 1–12. [CrossRef] [PubMed]
121. Zhang, Y.; Wu, C.; Guo, S.; Zhang, J. Interactions of graphene and graphene oxide with proteins and peptides. *Nanotechnol. Rev.* **2013**, *2*, 27–45. [CrossRef]
122. Zhang, C.; Chen, S.; Alvarez, P.J.J.; Chen, W. Reduced graphene oxide enhances horseradish peroxidase stability by serving as radical scavenger and redox mediator. *Carbon* **2018**, *94*, 531–538. [CrossRef]
123. Pavlidis, I.V.; Vorhaben, T.; Tsoufis, T.; Rudolf, P.; Bornscheuer, U.T.; Gournis, D.; Stamatis, H. Development of effective nanobiocatalytic systems through the im mobilization of hydrolases on functionalized carbon-based nanomaterials. *Bioresour. Technol.* **2012**, *115*, 164–171. [CrossRef] [PubMed]
124. Zhang, J.; Zhang, J.; Zhang, F.; Yang, H.; Huang, X.; Liu, H.; Guo, S. Graphene oxide as a matrix for enzyme immobilization. *Langmuir* **2010**, *26*, 6083–6085. [CrossRef] [PubMed]
125. Tseng, C.; Liao, C.; Sun, Y.; Peng, C.; Tzen, J.T.C.; Guo, R.; Liu, J. Immobilization of *Clostridium cellulolyticum*. *J. Agric. Food Chem.* **2014**, *62*, 6771–6776. [CrossRef] [PubMed]
126. Lee, K.H.; Lee, B.; Hwang, S.J.; Lee, J.U.; Cheong, H.; Shin, K.; Hur, N.H. Large scale production of highly conductive reduced graphene oxide sheets by a solvent-free low temperature reduction. *Carbon* **2014**, *69*, 327–335. [CrossRef]

127. Vineh, M.B.; Saboury, A.A.; Poostchi, A.A.; Rashidi, A.M.; Parivar, K. Stability and activity improvement of horseradish peroxidase by covalent immobilization on functionalized reduced graphene oxide and biodegradation of high phenol concentration. *Int. J. Biol. Macromol.* **2018**, *106*, 1314–1322. [CrossRef] [PubMed]
128. Dedania, S.R.; Patel, M.J.; Patel, D.M.; Akhani, R.C. Immobilization on graphene oxide improves the thermal stability and bioconversion efficiency of D-psicose 3-epimerase for rare sugar production. *Enzyme Microb. Technol.* **2017**, *107*, 49–56. [CrossRef] [PubMed]
129. Bhushani, J.A.; Anandharamakrishnan, V. Electrospinning and electrospraying techniques: Potential food based applications. *Trends Food Sci. Technol.* **2014**, *38*, 21–33. [CrossRef]
130. Wang, Z.G.; Wan, L.S.; Liu, Z.M.; Huang, X.J.; Xu, Z.K. Enzyme immobilization on electrospun polymer nanofibers: An overview. *J. Mol. Catal. B Enzym.* **2009**, *56*, 189–195. [CrossRef]
131. Dai, Y.; Yao, J.; Song, Y.; Liu, X.; Wang, S.; Yuan, Y. Enhanced performance of immobilized laccase in electrospun fibrous membranes by carbon nanotubes modification and its application for bisphenol A removal from water. *J. Hazard. Mater.* **2016**, *317*, 485–493. [CrossRef] [PubMed]
132. Liang, D.; Hsiao, B.S.; Chu, B. Functional electrospun nanofibrous scaffolds for biomedical applications. *Adv. Drug Deliv. Rev.* **2007**, *59*, 1392–1412. [CrossRef] [PubMed]
133. Bhardwaj, N.; Kundu, S.C. Electrospinning: A fascinating fiber fabrication technique. *Biotechnol. Adv.* **2010**, *28*, 325–347. [CrossRef] [PubMed]
134. Wong, D.E.; Dai, M.; Talbert, J.N.; Nugen, S.R.; Goddard, J.M. Biocatalytic polymer nanofibers for stabilization and delivery of enzymes. *J. Mol. Catal. B Enzym.* **2014**, *110*, 16–22. [CrossRef]
135. Lee, K.Y.; Jeong, L.; Kang, Y.O.; Lee, S.J.; Park, W.H. Electrospinning of polysaccharides for regenerative medicine. *Adv. Drug Deliv. Rev.* **2009**, *61*, 1020–1032. [CrossRef] [PubMed]
136. Yoo, H.S.; Kim, J.; Park, T.G. Surface-functionalized electrospun nanofibers for tissue engineering and drug delivery. *Adv. Drug Deliv. Rev.* **2009**, *61*, 1033–1042. [CrossRef] [PubMed]
137. Kim, J.; Grate, J.W.; Wang, P. Nanobiocatalysis and its potential applications. *Trends Biotechnol.* **2008**, *26*, 639–646. [CrossRef] [PubMed]
138. Canbolat, M.F.; Savas, H.B.; Gultekin, F. Improved catalytic activity by catalase immobilization using γ-cyclodextrin and electrospun PCL nanofibers. *J. Appl. Sci.* **2017**, *134*, 318–326. [CrossRef]
139. Weiser, D.; Soti, P.L.; Banoczi, G.; Bodai, V.; Kiss, B.; Gellert, A.; Nagy, Z.K.; Koczka, B.; Szilagyi, A.; Marosi, G.; et al. Bioimprinted lipases in PVA nanofibers as efficient immobilized biocatalysts. *Tetrahedron* **2016**, *72*, 7335–7342. [CrossRef]
140. Soti, P.L.; Weiser, D.; Vigh, T.; Nagy, Z.K.; Poppe, L.; Maros, G. Electrospun polylactic acid and polyvinyl alcohol fibers as efficient and stable nanomaterials for immobilization of lipases. *Bioprocess. Biosyst. Eng.* **2016**, *39*, 449–459. [CrossRef] [PubMed]
141. Handayani, N.; Loos, K.; Wahyuningrum, D.; Buchari, M.; Zulfikar, M.A. Immobilization of *Mucor miehei* lipase onto macroporous aminated polyethersulfone membrane for enzymatic reactions. *Membranes* **2012**, *2*, 198–213. [CrossRef] [PubMed]
142. Orregoa, C.E.; Salgadoa, N.; Valenciab, J.S.; Giraldoc, G.I.; Giraldod, O.H.; Cardonae, C.A. Novel chitosan membranes as support for lipases immobilization: Characterization aspects. *Carbohydr. Polym.* **2010**, *79*, 9–16. [CrossRef]
143. Kuo, C.H.; Chen, G.J.; Kuo, T.Y.; Liu, Y.C.; Shieh, C.J. Optimum lipase immobilized on diamine-grafted PVDF membrane and its characterization. *Ind. Eng. Chem. Res.* **2012**, *51*, 5141–5147. [CrossRef]
144. Gupta, S.; Bhattacharya, A.; Murthy, C.N. Tune to immobilize lipases on polymer membranes: Techniques, factors and prospects. *Biocatal. Agricultur. Biotechnol.* **2013**, *2*, 171–190. [CrossRef]
145. Vitola, G.; Mazzei, R.; Fontananova, E.; Porzio, E.; Manco, G.; Gaeta, S.N.; Giorno, L. Polymeric biocatalytic membranes with immobilized thermostable phosphotriesterase. *J. Membr. Sci.* **2016**, *516*, 144–151. [CrossRef]
146. Donato, L.; Algieri, C.; Rizzi, A.; Giorno, L. Kinetic study of tyrosinase immobilized on polymeric membrane. *J. Membr. Sci.* **2014**, *454*, 346–350. [CrossRef]
147. Konovalova, V.; Guzikevich, K.; Burban, A.; Kujawski, W.; Jarzynka, K.; Kujawa, J. Enhanced starch hydrolysis using α-amylase immobilized on cellulose ultrafiltration affinity membrane. *Carbohydr. Polym.* **2016**, *152*, 710–717. [CrossRef] [PubMed]
148. Luo, J.; Meyer, A.S.; Jonsson, G.; Pinelo, M. Fouling-induced enzyme immobilization for membrane reactors. *Bioresour. Technol.* **2013**, *147*, 260–268. [CrossRef] [PubMed]

149. Luo, J.; Marpani, F.; Brites, R.; Frederiksen, L.; Meyer, A.S.; Jonsson, G.; Pinelo, M. Directing filtration to optimize enzyme immobilization in reactive membranes. *J. Membr. Sci.* **2014**, *459*, 1–11. [CrossRef]
150. Luo, J.; Nordvang, R.T.; Morthensen, S.T.; Zeuner, B.; Meyer, A.S.; Mikkelsen, J.D.; Pinelo, M. An integrated membrane system for the biocatalytic production of 3′-sialyllactose from dairy by-products. *Bioresour. Technol.* **2014**, *166*, 9–16. [CrossRef] [PubMed]
151. Morthensen, S.T.; Luo, J.; Meyer, A.S.; Jørgensen, H.; Pinelo, M. High performance separation of xylose and glucose by enzyme assisted nanofiltration. *J. Membr. Sci.* **2015**, *492*, 107–115. [CrossRef]
152. Liu, W.F.; Wei, L.N. Research progress on carbonic anhydrase immobilization. *J. Mol. Catal.* **2016**, *30*, 182–197.
153. Yang, X.-Y.; Tian, G.; Jiang, N.; Su, B.L. Immobilization technology: A sustainable solution for biofuel cell design. *Energy Environ. Sci.* **2012**, *5*, 5540–5563. [CrossRef]
154. Xue, H.; Shen, Z.; Li, C. Improved selectivity and stability of glucose biosensor based on in situ electropolymerized polyaniline–polyacrylonitrile composite film. *Biosens. Bioelectron.* **2005**, *20*, 2330–2334. [CrossRef] [PubMed]
155. Rajdeo, K.; Harini, T.; Lavanya, K.; Fadnavis, N.W. Immobilization of pectinase on reusable polymer support for clarification of apple juice. *Food Bioprod. Process.* **2016**, *99*, 12–19. [CrossRef]
156. Sui, C.-H.; Wang, Z.-Y.; Wei, Y.-Q.; Wang, C. Immobilization of glucoamylase onto electrospun PAA/PVA microfibrous membrane by active ester method. *Chin. J. Process Eng.* **2016**, *16*, 494–499.
157. Riccardi, C.M.; Kasi, R.M.; Kumar, C.V. Nanoarmoring of enzymes by interlocking in cellulose fibers with poly(acrylic acid). *Method. Enzymol.* **2017**, *590*, 475–500.
158. Badgujar, K.C.; Bhanage, B.M. Investigation of deactivation thermodynamics of lipase immobilized on polymeric carrier. *Bioprocess Biosyst. Eng.* **2017**, *40*, 717–757. [CrossRef] [PubMed]
159. Yavuz, A.G.; Uygun, A.; Bhethanabotla, V.R. Preparation of substituted polyaniline/chitosan composites by in situ electropolymerization and their application to glucose sensing. *Carbohydr. Polym.* **2010**, *81*, 712–719. [CrossRef]
160. Pervez, S.; Aman, A.; Qader, S.A. Role of two polysaccharide matrices on activity, stability and recycling efficiency of immobilized fungal amyloglucosidase of GH15 family. *Int. J. Biol. Macromol.* **2017**, *96*, 70–77. [CrossRef] [PubMed]
161. Zdarta, J.; Klapiszewski, Ł.; Wysokowski, M.; Norman, M.; Kołodziejczak-Radzimska, A.; Moszyński, D.; Ehrlich, H.; Maciejewski, H.; Stelling, A.L.; Jesionowski, T. Chitin-lignin material as a novel matrix for enzyme immobilization. *Mar. Drugs* **2015**, *13*, 2424–2446. [CrossRef] [PubMed]
162. De Paula, R.C.M.; Feitosa, J.P.A.; Paula, H.C.B. Polysaccharide based copolymers as supramolecular systems in biomedical applications. *Curr. Drug. Targets* **2015**, *16*, 1591–1605. [CrossRef]
163. Kara, F.; Aksoy, E.A.; Calamak, S.; Hasirci, N.; Aksoy, S. Immobilization of heparin on chitosan-grafted polyurethane films to enhance anti-adhesive and antibacterial properties. *J. Bioact. Compat. Polym.* **2016**, *31*, 72–90. [CrossRef]
164. Shen, L.; Cheng, K.C.K.; Schroeder, M.; Yang, P.; Marsh, E.N.G.; Lahann, J.; Chen, Z. Immobilization of enzyme on a polymer surface. *Surf. Sci.* **2016**, *648*, 53–59. [CrossRef]
165. Zucca, P.; Fernandez-Lafuente, R.; Sanjust, E. Agarose and its derivatives as supports for enzyme immobilization. *Molecules* **2016**, *21*, 1577. [CrossRef] [PubMed]
166. Schulze, A.; Breite, D.; Kim, Y.; Schmidt, M.; Thomas, I.; Went, M.; Fischer, K.; Prager, A. Bio-Inspired polymer membrane surface cleaning. *Polymers* **2017**, *9*, 97. [CrossRef]
167. Huang, J.; Kaner, R.B. A general chemical route to polyaniline nanofibers. *J. Am. Chem. Soc.* **2004**, *126*, 851–855. [CrossRef] [PubMed]
168. Lai, J.; Yi, Y.; Zhua, P.; Shen, J.; Wu, K.; Zhang, L.; Liu, J. Polyaniline-based glucose biosensor: A review. *J. Electroanal. Chem.* **2016**, *782*, 138–153. [CrossRef]
169. Fang, L.; Liang, B.; Yang, G.; Hu, Y.; Zhu, Q.; Ye, X. Study of glucose biosensor lifetime improvement in 37 °C serum based on PANI enzyme immobilization and PLGA biodegradable membrane. *Biosens. Bioelectron.* **2014**, *56*, 91–96. [CrossRef] [PubMed]
170. Kumar, M.; Rahikainen, R.; Unruh, D.; Hytönen, V.P.; Delbruck, C.; Sindelar, R.; Renz, F. Mixture of PLA–PEG and biotinylated albumin enables immobilization of avidins on electrospun fibers. *J. Biomed. Mater. Res. A* **2017**, *105*, 356–362. [CrossRef] [PubMed]

171. Badgujar, K.C.; Bhanage, B.M. Solvent stability study with thermodynamic analysis and superior biocatalytic activity of *Burkholderia cepacia* lipase immobilized on biocompatible hybrid matrix of poly(vinyl alcohol) and hypromellose. *J. Phys. Chem. B* **2014**, *118*, 14808–14819. [CrossRef] [PubMed]
172. Matto, M.; Husain, Q. Calcium alginate-starch hybrid support for both surface immobilization and entrapment of bitter gourd (*Momordicacharantia*) peroxidase. *J. Mol. Catal. B Enzym.* **2009**, *57*, 164–170. [CrossRef]
173. Abdulla, R.; Ravindra, P. Immobilized *Burkholderia cepacia* lipase for biodiesel production from crude *Jatropha curcas* L. oil. *Biomass Bioenergy* **2013**, *56*, 8–13. [CrossRef]
174. Nupur, N.; Ashish, M.; Mira Das, D. Preparation and biochemical property of penicillin G amidase-loaded alginate and alginate/chitosan hydrogel beads. *Recent Pat. Biotechnol.* **2016**, *10*, 121–132. [CrossRef] [PubMed]
175. Li, J.; Wu, H.; Liang, Y.; Jiang, Z.; Jiang, Y.; Zhang, L. Facile fabrication of organic-inorganic hybrid beads by aminated alginate enabled gelation and biomimetic mineralization. *J. Biomater. Sci-Polym. E* **2013**, *24*, 119–134. [CrossRef] [PubMed]
176. Li, L.; Ma, L.; Li, H. Characteristics of magnetic microspheres and its application in enzyme immobilization. *J. Clin. Reh. Tissue Eng. Res.* **2008**, *12*, 8198–8200.
177. Amirbandeh, M.; Taheri-Kafrani, A. Immobilization of glucoamylase on triazine-functionalized Fe_3O_4/graphene oxide nanocomposite: Improved stability and reusability. *Int. J. Biol. Macromol.* **2016**, *93*, 1183–1191. [CrossRef] [PubMed]
178. Jędrzak, A.; Rębiś, T.; Klapiszewski, Ł.; Zdarta, J.; Milczarek, G.; Jesionowski, T. Carbon paste electrode based on functional GO_x/silica-lignin systemto prepare an amperometric glucose biosensor. *Sens. Actuators B* **2018**, *256*, 176–185. [CrossRef]
179. Wan, L.S.; Ke, B.B.; Xu, Z.K. Electrospun nanofibrous membranes filled with carbon nanotubes for redox enzyme immobilization. *Enzyme Microb. Technol.* **2008**, *42*, 332–339. [CrossRef]
180. Barros, A.E.L.; Almeida, A.M.P.; Carvalho, L.B., Jr.; Azevedo, W.M. Polysiloxane/PVA-glutaraldehyde hybrid composite as solid phase or immunodetections by ELISA. *Braz. J. Med. Biol. Res.* **2002**, *35*, 459–463. [CrossRef]
181. Shah, N.; Ul-Islam, M.; Khattak, W.A.; Park, J.K. Overview of bacterial cellulose composites: A multipurpose advanced material. *Carbohyd. Polym.* **2013**, *98*, 1585–1598. [CrossRef] [PubMed]
182. Zdarta, J.; Klapiszewski, Ł.; Jędrzak, A.; Nowicki, M.; Moszyński, D.; Jesionowski, T. Lipase B from *Candida antarctica* immobilized on a silica-lignin matrix as a stable and reusable biocatalytic system. *Catalysts* **2017**, *7*, 14. [CrossRef]
183. Vatsyayan, P.; Bordoloi, S.; Goswami, P. Large catalase based bioelectrode for biosensor application. *Biophys. Chem.* **2010**, *153*, 36–42. [CrossRef] [PubMed]
184. Zhang, S.; Jiang, Z.; Zhang, W.; Wang, X.; Shi, J. Polymer-inorganic microcapsules fabricated by combining biomimetic adhesion and bioinspired mineralization and their use for catalase immobilization. *Biochem. Eng. J.* **2015**, *93*, 281–288. [CrossRef]
185. Zhao, H.; Cui, Q.; Shah, V.; Xu, J.; Wang, T. Enhancement of glucose isomerase activity by immobilizing on silica/chitosan hybrid microspheres. *J. Mol. Catal. B Enzym.* **2016**, *126*, 18–23. [CrossRef]
186. Guo, M.; Yao, S.S.; Gao, X.Y.; Fu, X.P. Preparation and enzymological properties of SiO_2-DAS immobilized cellulose. *J. Chem. Eng. Chin.* **2015**, *29*, 1407–1414.
187. Miranda, R.A.; Llorca, J.; Medina, F.; Sueiras, J.E.; Segarra, A.M. Asymmetric epoxidation of chalcone catalyzed by reusable poly-L-leucine immobilized on hydrotalcite. *J. Catal.* **2011**, *282*, 65–73. [CrossRef]
188. Chang, M.Y.; Kao, H.C.; Juang, R.S. Thermal inactivation and reactivity of β-glucosidase immobilized on chitosan–clay composite. *Int. J. Biol. Macromol.* **2008**, *43*, 48–53. [CrossRef] [PubMed]
189. Han, E.; Li, X.; Cai, J.R.; Cui, H.Y.; Zhang, X.A. Development of highly sensitive amperometric biosensor for glucose using carbon nanosphere/sodium alginate composite matrix for enzyme immobilization. *Anal. Sci.* **2014**, *30*, 897–902. [CrossRef] [PubMed]
190. Ambrogio, M.W.; Thomas, C.R.; Zhao, Y.-L.; Zink, J.I.; Stoddart, J.F. Mechanized silica nanoparticles: A new frontier in theranostic nanomedicine. *Acc. Chem. Res.* **2011**, *44*, 903–913. [CrossRef] [PubMed]
191. Yuce-Dursun, B.; Cigil, A.B.; Dongez, D.; Kahraman, M.V.; Ogan, A.; Demir, S. Preparation and characterization of sol-gel hybrid coating films for covalent immobilization of lipase enzyme. *J. Mol. Catal. B Enzym.* **2016**, *127*, 18–25. [CrossRef]

192. Zniszczoł, A.; Herman, A.P.; Szymańska, K.; Mrowiec-Białoń, J.; Walczak, K.Z.; Jarzębski, A.; Boncel, S. Covalently immobilized lipase on aminoalkyl-, carboxy- and hydroxy-multi-wall carbon nanotubes in the enantioselective synthesis of Solketal esters. *Enzyme Microb. Technol.* **2016**, *87*, 61–69. [CrossRef] [PubMed]
193. Lee, S.H.; Doan, T.T.N.; Won, K.; Ha, S.H.; Koo, Y.M. Immobilization of lipase within carbon nanotube–silica composites for non-aqueous reaction systems. *J. Mol. Catal. B Enzym.* **2010**, *62*, 169–172. [CrossRef]
194. Zhu, Y.T.; Ren, X.Y.; Liu, Y.M.; Wei, Y.; Qing, L.S.; Liao, X. Covalent immobilization of porcine pancreatic lipase on carboxyl-activated magnetic nanoparticles: Characterization and application for enzymatic inhibition assays. *Mater. Sci. Eng. C* **2014**, *38*, 278–285. [CrossRef] [PubMed]
195. Lei, Z.; Liu, X.; Ma, L.; Liu, D.; Zhang, H.; Wang, Z. Spheres-on-sphere silica microspheres as matrix for horseradish peroxidase immobilization and detection of hydrogen peroxide. *RSC Adv.* **2015**, *5*, 38665–38672. [CrossRef]
196. Bian, S.; Wu, H.; Jiang, X.; Long, Y.; Chen, Y. Syntheses and applications of hybrid mesoporous silica membranes. *Prog. Chem.* **2014**, *26*, 1352–1360.
197. Nenkova, R.; Wu, J.; Zhang, Y.; Godjevargova, T. Evaluation of immobilization techniques for the fabrication of nanomaterial-based amperometric glucose biosensors. *Anal. Lett.* **2015**, *48*, 1297–1310. [CrossRef]
198. Zlateski, V.; Fuhrer, R.; Koehle, F.M.; Wharry, S.; Zeltner, M.; Stark, W.J.; Moody, T.S.; Grass, R.N. Efficient magnetic recycling of covalently attached enzymes on carbon-coated metallic nanomagnets. *Bioconj. Chem.* **2014**, *25*, 677–684. [CrossRef] [PubMed]
199. Abraham, S.; Srivastava, S.; Kumar, V.; Pandey, S.; Rastogi, P.K.; Nirala, N.R.; Kashyap, S.; Srivastava, S.K.; Singh, V.N.; Ganesan, V.; et al. Enhanced electrochemical biosensing efficiency of silica particles supported on partially reduced graphene oxide for sensitive detection of cholesterol. *J. Electroanal. Chem.* **2015**, *757*, 65–72. [CrossRef]
200. Shoja, Y.; Rafati, A.A.; Ghodsi, J. Enzymatic biosensor based on entrapment of D-amino acid oxidase on gold nanofilm/MWCNTs nanocomposite modified glassy carbon electrode by sol-gel network: Analytical applications for D-alanine in human serum. *Enzyme Microb. Technol.* **2017**, *100*, 20–27. [CrossRef] [PubMed]
201. Fidal, V.T.K.P.; Inguva, S.; Krishnamurthy, S.; Marsili, E.; Mosnier, J.P.; Chandra, T.S. Mediator-free interaction of glucose oxidase, as model enzyme for immobilization, with Al-doped and undoped ZnO thin films laser-deposited on polycarbonate supports. *Enzyme Microb. Technol.* **2017**, *96*, 67–74.
202. Sun, H.; Jin, X.; Long, N.; Zhang, R. Improved biodegradation of synthetic azo dye by horseradish peroxidase cross-linked on nano-composite support. *Int. J. Biol. Macromol.* **2017**, *95*, 1049–1055. [CrossRef] [PubMed]
203. Li, F.; Feng, Y.; Wang, Z.; Yang, L.; Zhuo, L.; Tang, B. Direct electrochemistry of horseradish peroxidase immobilized on the layered calcium carbonate-gold nanoparticles inorganic hybrid composite. *Biosens. Bioelectron.* **2010**, *25*, 2244–2248. [CrossRef] [PubMed]
204. Lopes, J.H.; Colson, F.X.; Barralet, J.E.; Merle, G. Electrically wired enzyme/TiO_2 composite for glucose detection. *Mater. Sci. Eng. C* **2017**, *76*, 991–996. [CrossRef] [PubMed]
205. Bujduveanu, M.R.; Yao, W.; LeGoff, A.; Gorgy, K.; Shan, D.; Diao, G.W.; Ungureanu, E.M.; Cosnier, S. Multiwalled carbon nanotube-$CaCO_3$ nanoparticle composites for the construction of a tyrosinase-based amperometric dopamine biosensor. *Electroanalysis* **2013**, *25*, 613–619. [CrossRef]

catalysts

MDPI

Article

Immobilization of Cellulase on a Functional Inorganic–Organic Hybrid Support: Stability and Kinetic Study

Jakub Zdarta *, Artur Jędrzak, Łukasz Klapiszewski and Teofil Jesionowski *

Institute of Chemical Technology and Engineering, Faculty of Chemical Technology, Poznan University of Technology, Berdychowo 4, PL-60965 Poznan, Poland; artur.jedrzak@gmail.com (A.J.); lukasz.klapiszeswki@put.poznan.pl (Ł.K.)

* Correspondence: jakub.zdarta@put.poznan.pl (J.Z.); teofil.jesionowski@put.poznan.pl (T.J.); Tel.: +48-616-65-3747 (J.Z.); +48-616-65-3720 (T.J.)

Received: 7 November 2017; Accepted: 29 November 2017; Published: 1 December 2017

Abstract: Cellulase from *Aspergillus niger* was immobilized on a synthesized TiO_2–lignin hybrid support. The enzyme was effectively deposited on the inorganic–organic hybrid matrix, mainly via physical interactions. The optimal initial immobilization parameters, selected for the highest relative activity, were pH 5.0, 6 h process duration, and an enzyme solution concentration of 5 mg/mL. Moreover, the effects of pH, temperature, and number of consecutive catalytic cycles and the storage stability of free and immobilized cellulase were evaluated and compared. Thermal and chemical stability were significantly improved, while after 3 h at a temperature of 50 °C and pH 6.0, the immobilized cellulase retained over 80% of its initial activity. In addition, the half-life of the immobilized cellulase (307 min) was five times that of the free enzyme (63 min). After ten repeated catalytic cycles, the immobilized biocatalyst retained over 90% of its initial catalytic properties. This study presents a protocol for the production of highly stable and reusable biocatalytic systems for practical application in the hydrolysis of cellulose.

Keywords: enzyme immobilization; cellulases; titania-lignin hybrid; immobilized cellulase stability; cellulose hydrolysis

1. Introduction

Cellulases are classified as hydrolytic enzymes [1] and include at least three types of biocatalysts: endo-(1,4)-β-D-glucanase (EC 3.2.1.4), exo-(1,4)-β-D-glucanase (EC 3.2.1.91), and β-glucosidases (EC 3.2.1.21) [2–4]. They are produced by bacteria and microbes; however, the main enzyme acquisition process is based on fungi, which provide the highest production index [1,5,6]. The most frequently used for the production of cellulases are strains of cellulolytic fungi such as *Aspergillus*, *Humicola*, *Penicillium*, and *Trichoderma* [7,8]. Cellulases are responsible for the process of depolymerization of cellulose by delamination of the cell walls, which is a consequence of cellulose hydrolysis [1,6]. These biocatalysts have numerous practical applications in many fields of industry and agriculture. Commercial cellulases have been available for several decades, and have found applications in several important branches of industry, particularly in the wood and cellulose-paper industries, as well as in other branches including the conservation of thermoplastic polymers and plastics, bioconversion of cellulosic materials to organic solvents, fermentation processes, detergents, textiles, laundry, and the food and feed industries [9]. In view of the broad application of these enzymes, it is necessary to develop novel and more stable materials to enable the aforementioned processes to be carried out more efficiently.

Immobilization is a technique of confining cells or enzymes on organic, inorganic, or hybrid carriers [10]. Depending on the method of immobilization, the binding of the biocatalyst may occur

more or less permanently. This technique is intended to increase the efficiency of catalytic processes, reduce the associated costs, and improve the properties of enzymes [10], mainly its stability at harsh reaction conditions, as variable reaction parameters might affect enzymes' properties. Among others, the most important properties are pH and temperature, as protein denaturation is caused mainly by abovementioned parameters [11]. Immobilization of enzymes enables the retention of catalytic activity, which results in the possibility of reusing the biocatalytic system. Moreover, easier and faster separation of immobilized enzymes from the reaction mixture makes them more attractive for industrial applications [11,12]. The immobilization of biocatalysts also prevents protein from entering the process in a mobile phase reactor containing the reagents, resulting in cleaner products [13].

As has already been noted, immobilization processes are of great importance and are used in many branches of industry, mainly in the pharmaceutical, food, chemical, and biological industries, but also in research and implementation of new technological solutions. The use of immobilized enzymes might result in greater process efficiency compared with the use of free biocatalysts, by better utilizing the potential of raw materials [11–14]. Various enzyme immobilization methods have enabled the development of industrial technology on a larger scale, reducing the costs of production. At present, there are several well-known techniques that rely on physical or chemical interactions [11,14]. Immobilized enzymes are a subject of great interest, which will certainly grow, as the properties of many of the biocatalysts are not yet fully known. Furthermore, the possibility of their immobilization may contribute to a steady progress in their development and use in bioprocesses and in the field of biosensing [15,16].

The continuous development of technology helps obtain more effective and stable materials with targeted industrial applications. Nowadays, novel hybrid or composite material with immobilized enzymes, achieved by creating an innovative biocatalytic system, are increasingly used in many fields of industry, like pharmaceutical, chemical, and food industries. A combination of inorganic and organic components can provide advanced features such as better thermal and chemical resistance or electrokinetic and biological stability. For instance, Tao et al., used magnetic Fe_3O_4–SiO_2 nanoparticles for the selective immobilization of cellulase [17]. The novel hybrid material, due to the influence of the metallic oxides, exhibited enhanced adsorption parameters as well as biocompatibility and bioactivity. Similar findings are reported by Velmurugan et al., who confirmed that a newly developed MgO–Fe_3O_4 material was suitable for cellulose immobilization [18]. Furthermore, Hong et al., obtained a polyhedral oligomeric silsesquioxane-silica-titania (POSS–SiO_2–TiO_2) hybrid material for cellulase immobilization for biocatalytic applications [19]. In other studies laccase was successfully immobilized on TiO_2 nanoparticles and TiO_2 nanoparticle functionalized polyethersulfone (PES) membranes. The results revealed that both the immobilization procedures and the properties of the immobilization supports have significant impacts on the biocatalyst performance [20]. In addition, Hou et al. showed in [21] great potential for the application of the TiO_2 based biocatalytic nanoparticles and membranes for CO_2 conversion in a gas–liquid membrane contactor. These examples show that it is extremely important to continue research into the development of novel support materials for enzyme immobilization, which will lead to the creation of more effective and stable biocatalytic systems.

The main research goal of the present study was to evaluate a functional hybrid titanium dioxide–lignin hybrid material in terms of its suitability for the immobilization of cellulase, and to use the resulting biocatalytic system in the hydrolysis process of cellulose. The synthesized hybrid support was concisely characterized, immobilization of the enzyme was confirmed, and the effect of various operational conditions on the enzyme's stability and activity, as well as its reusability and storage stability, were examined.

2. Results

2.1. Synthesis of Titania–Lignin Hybrid Material and Cellulase Immobilization

The thermal stability of the TiO_2 modified by poly-L-lisine (PLL), lignin activated by sodium (meta)periodate and the synthesized TiO_2–lignin hybrid material was determined using thermogravimetric analysis (TGA) (Figure 1). Commercial titanium dioxide after surface modification exhibited extremely high thermal stability, losing only about 2% of its mass in the analyzed temperature range, which might be explained by the evaporation of physically bound water. The thermogravimetric curve of the activated lignin showed a significant decrease in mass of the activated biopolymer consisted in three mass loss stages, at temperatures up to 200 °C (marked in yellow) and in the temperature ranges 200–600 °C (marked in blue) and 650–1000 °C (marked in red), linked respectively to the removal of physically bound water, decomposition of the lignin structure, and elimination of carbon and hydrogen atoms [22]. The synthesized TiO_2–lignin hybrid showed relatively good thermal stability: up to a temperature of 1000 °C it lost about 10% of its mass. The high thermal stability (characteristic for TiO_2) and the shape of the TGA curve for the obtained material, similar to that recorded for lignin, also proved the effective connection of TiO_2 and lignin.

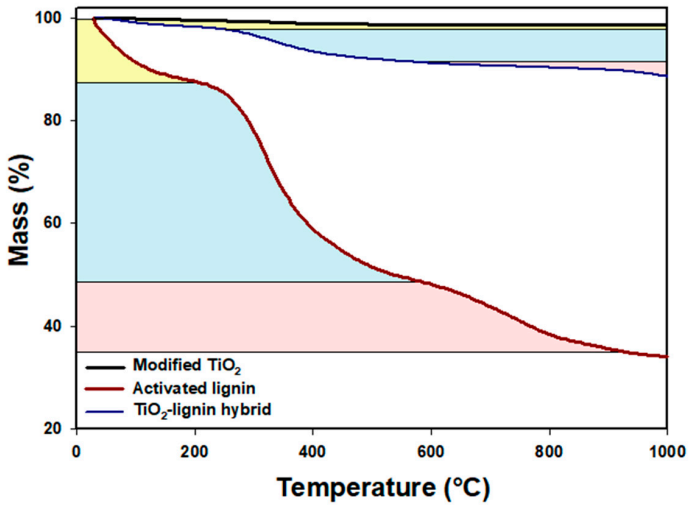

Figure 1. Results of thermogravimetric analysis of modified TiO_2, activated lignin and TiO_2–lignin hybrid.

The Fourier-transform infrared (FTIR) spectrum of the TiO_2–lignin hybrid (Figure 2) contained many signals characteristic for functional groups of both modified precursors, which indirectly confirmed the effective synthesis of the hybrid support. Among these signals, the most important are those at wavenumbers 3450 cm^{-1}, 2940 cm^{-1}, 1680 cm^{-1}, and around 1100 cm^{-1}, attributed respectively to stretching vibrations of –OH groups, C–H bonds, C=O groups, and C–O and C–O–C bonds in the lignin structure [23]. Signals were also observed in the wavenumber range 1600–1450 cm^{-1} and at 720 cm^{-1}, representing, respectively, stretching vibrations of C_{Ar}–C_{Ar} bonds in the structure of the biopolymer, and Ti–O–Ti bonds.

In the FTIR spectrum of free cellulase from *Aspergillus niger*, the most important signal is that at 3430 cm^{-1}, characteristic for amine groups, which are mainly responsible for attachment of the enzyme to the solid support, as well as peaks around 1665 cm^{-1} and 1530 cm^{-1}, generated by stretching vibrations of amide I and amide II bands. The FTIR spectrum of the produced biocatalytic system contains signals characteristic for cellulase as well as for the hybrid matrix. This suggested that the biocatalyst was successfully deposited on the surface of the support material. This is proven by the presence of a peak at 1090 cm^{-1} (C–N stretching vibrations) and changes in the intensity of signals generated by amine groups (3430 cm^{-1}), C–H bonds (2930 cm^{-1}), and amide bands, in comparison with the FTIR spectrum of the TiO_2–lignin hybrid before enzyme binding.

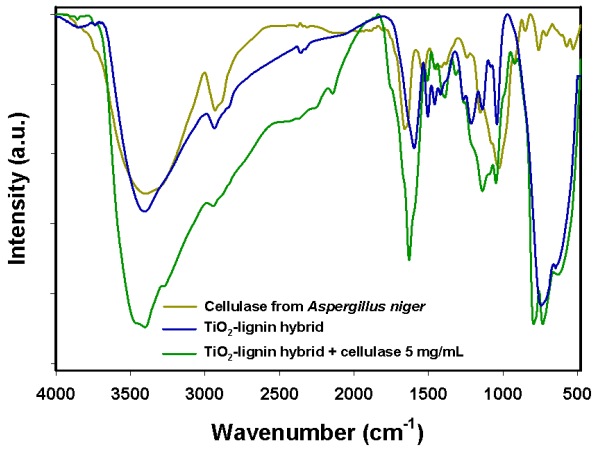

Figure 2. Results of Fourier-transform infrared (FTIR) analysis of cellulase from *Aspergillus niger*, TiO_2–lignin hybrid and the product after enzyme immobilization (immobilization conditions: pH = 7.0, T = 4 °C, t = 6 h, C_{enz} = 5 mg/mL).

Based also on the results of the analysis of the porous structure parameters of the TiO_2–lignin support material before and after immobilization, some additional conclusions can be drawn. The synthesized TiO_2–lignin hybrid before enzyme attachment had a relatively low surface area of around 10 m^2/g, while for the matrix after cellulase immobilization, this parameter decreased to about 8 m^2/g. This might suggest that effective enzyme attachment was achieved. Moreover, a decrease was recorded in the pores diameter and pores volume in the samples after immobilization. The hybrid biocomposite had pores with a mean diameter of 3.3 nm and a volume of 0.005 cm^3/g, while after cellulase immobilization these parameters fell to 1.7 nm and 0.003 cm^3/g.

2.2. Cellulase Immobilization

Besides confirmation of effective cellulase binding, the effect of initial immobilization parameters (process time and concentration of enzyme solution) on the quantity of immobilized enzyme and its relative activity was also evaluated (Figure 3).

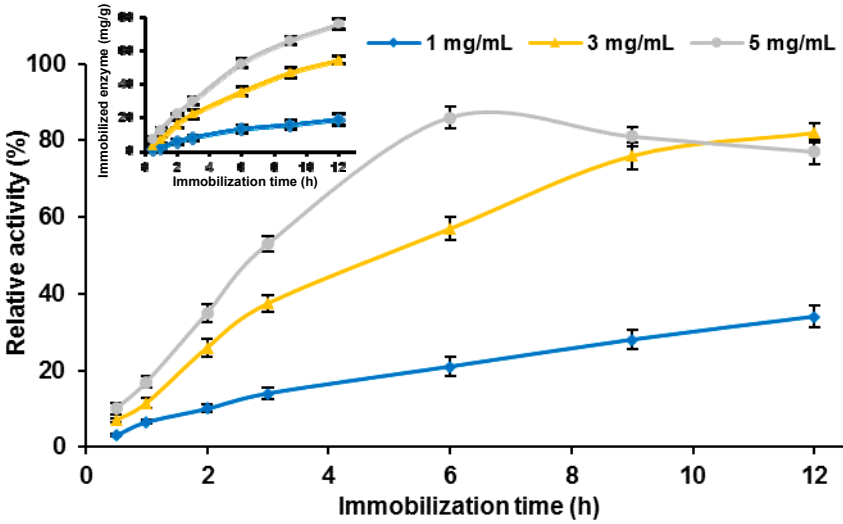

Figure 3. Effect of immobilization time on the relative activity of the immobilized cellulase. Inset: effect of immobilization time on the amount of the enzyme immobilized on the TiO_2–lignin hybrid.

As Figure 3 shows, the products after immobilization exhibited lower catalytic activity than free cellulase (relative activity up to 85%). When solution concentrations of 1 and 3 mg/mL were used, the highest relative activities, of around 30% and 80% respectively, were recorded after 12 h of the process. The amount of immobilized cellulase increased with process duration, irrespective of the concentration of the initial enzyme solution (Figure 3 inset). After 12 h of immobilization, 19, 55, and 76 mg of the biocatalyst per 1 g of the support material was deposited from solutions of 1, 3, and 5 mg/mL respectively. The results indicated that with increasing process time, the relative activity of the immobilized enzyme increased along with the amount of bounded cellulase, except in the case of the 5 mg/mL solution. When cellulase solution at this concentration was employed, the highest relative activity, about 85%, was obtained after 6 h of immobilization. Further increase in the immobilization time caused the relative activity of the bound cellulase to decrease.

As has already been mentioned, the immobilization technique used led to the attachment of cellulase molecules mainly via physical and ionic interactions, but the formation of covalent bonds cannot be excluded. Electrokinetic measurements showed that the zeta potential of the titania–lignin hybrid matrix took negative values over the whole of the analyzed pH range, which indicates that the surface of the support material was negatively charged during immobilization. Under the immobilization conditions (acetate buffer at pH 4.8), the enzyme molecules were positively charged (the IEP of cellulase is around 5). These facts imply that effective biocatalyst immobilization occurred mainly via electrostatic and ionic interactions. To verify this statement, solutions of sodium chloride at various ionic strengths were applied in cellulase desorption tests, because this salt might elute the enzyme by way of ionic exchange (Figure 4) [24].

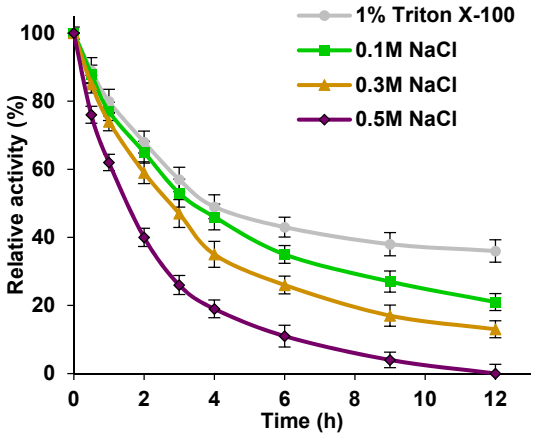

Figure 4. Effect of Triton X-100 and NaCl solution on the relative activity of free and immobilized onto TiO_2–lignin hybrid cellulase from *Aspergillus niger*.

Figure 4 shows that the relative activity of the immobilized cellulase treated with 1% Triton X-100 and NaCl solutions at various molar concentrations declined gradually during the first 6 h of treatment, which suggests elution of the enzyme from the matrix. The further decrease in relative activity is insignificant (less than 10% in all cases), which indicates that desorption occurred in the initial stages of the test and is limited in its later stages. After treatment with 1% Triton X-100 for 12 h, the immobilized cellulase retained over 40% of its relative activity. When the immobilized biocatalyst was incubated in sodium chloride solutions at molarities of 0.1; 0.3, and 0.5 M, a more significant drop in the relative activity was observed. The produced systems finally exhibited 25%, 18%, and 0% of its relative activity, respectively. Additionally, to verify if the immobilized enzyme was eluted from the support material following the treatments or was deactivated by such treatments, amount of the immobilized enzyme retained on the matrix, after 6 and 12 h of desorption process was evaluated (Table 1).

Table 1. Amount of the immobilized cellulase remained after desorption process, at different conditions.

Type of Eluent	Amount of Immobilized Enzyme (mg/g)	
	Desorption Time	
	6 h	12 h
1% Triton X-100	25.8 ± 1.3	22.4 ± 1.6
0.1 M NaCl	20.3 ± 1.5	12.6 ± 1.2
0.3 M NaCl	16.8 ± 0.6	6.9 ± 0.9
0.5 M NaCl	9.7 ± 1.0	5.1 ± 1.1

It can be seen from Table 2, that amount of the immobilized enzyme that remained on the surface of the hybrid material after desorption, irrespectively of the type and ionic strength of the eluent, is about 10–20% higher than amount of the immobilized cellulase, which corresponds to the evaluated relative activity of the biocatalytic system after desorption. The biggest differences were noticed for 0.5 M NaCl solution. After 6 and 12 h of the process, the surface of the titania–lignin hybrid retained 9.7 and 5.1 mg of the enzyme per 1 g of the support. These values corresponded to the relative activity of 18.3% and 9.7%, meanwhile, the noticed values of relative activity were 11.2% and 0%.

2.3. Stability Study of Immobilized Cellulase

Various process parameters such as pH and temperature might affect the ability of the immobilized cellulase to degrade cellulosic material. Thus, in this study, the effect of the aforementioned parameters, as well as the chemical and thermal stability of the free and immobilized enzyme, were examined and compared. Moreover, the reusability and storage stability of the free and immobilized enzyme under different conditions were tested. Kinetic parameters for both forms of the enzyme were evaluated to verify how immobilization affected the affinity of the enzyme to the substrate molecules and its catalytic efficiency.

2.3.1. Effect of pH

The effect of pH on the relative activity of free and immobilized cellulase was studied over a broad range of pH values, from 3.0 to 9.0 (Figure 5a).

The maximum relative activity was recorded at pH 5.5 for the free enzyme, and at pH 6.0 for the immobilized enzyme, as expected, since acidic cellulase was used in this study. Although the graph showed similar trends for the free and immobilized biocatalyst over the whole of the analyzed pH range, the immobilized biomolecules have higher relative activity than the free ones in the same pH conditions. The immobilized cellulase exhibited over 80% of its relative activity at pH values from 4.5 to 6.0, as the free catalyst did so only at pH values from 5.0 to 6.0. The bound enzyme also exhibited about 20% higher relative activity (76%) than the free enzyme (54%) at pH 3.0. The results also indicated a significant decrease in cellulase activity when the pH is above or below its optimum value. This was especially visible in alkaline conditions: at pH 9.0, both biocatalysts retained less than 40% of their activity. To test the chemical stability of the free and immobilized cellulase, both enzymes were incubated for 3 h under their optimal reaction conditions (Figure 5b). After 3 h, the free cellulase retained about 20% of its initial activity, as the immobilized enzymes incubated at pH 5.0 and 6.0 retained over 75% of their activity, which proved that cellulase attached to a TiO_2–lignin hybrid support has higher thermal stability than the free enzyme.

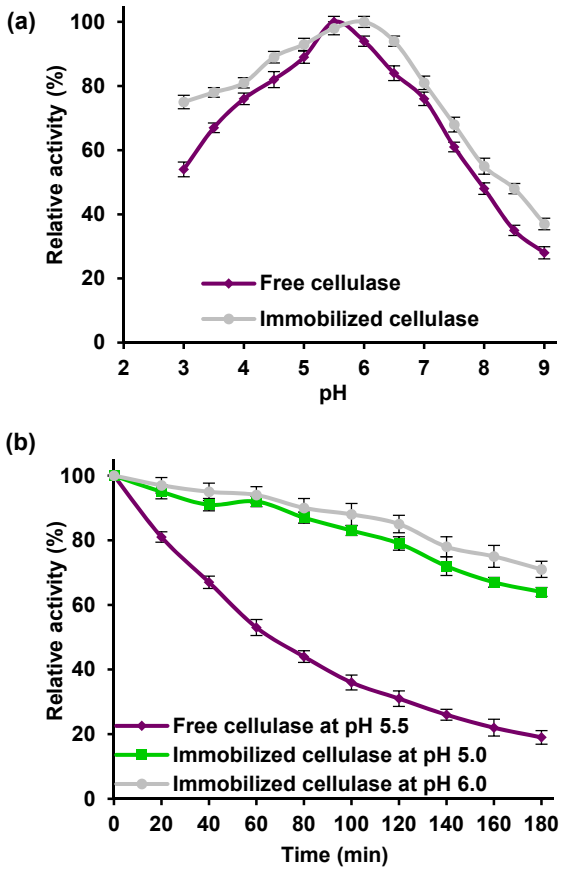

Figure 5. (**a**) Effect of pH on the relative activity of free and immobilized cellulose; (**b**) Chemical stability of free and immobilized enzyme after incubation for 3 h under optimal pH and temperature conditions.

2.3.2. Effect of Temperature

The effect of temperature on the relative activity of free and immobilized cellulase from *Aspergillus niger* was studied between 30 and 80 °C, under optimal pH conditions for free and immobilized cellulase (Figure 6a).

The free enzyme exhibited its maximum activity at 50 °C and retained 80% of its activity in a temperature range from 45 to 60 °C. At temperatures below 50 and above 60 °C the catalytic activity of the free biocatalyst significantly decreased, suggesting that the free enzyme is unstable in these conditions due to denaturation of the peptide structure [25]. By comparison, the immobilized cellulase exhibited its highest activity at temperatures of 55 and 60 °C, and retained over 80% of its maximum activity over a wide temperature range from 40 to 70 °C. In addition, the drop in relative activity above 70 °C is less significant that in the case of the free enzyme, while at 80 °C the bound cellulase exhibited over 60% of its relative activity. To determine the thermal stability of the immobilized cellulase, the free enzyme was incubated for 3 h at 50 °C and the immobilized cellulase at 50 and 60 °C (Figure 6b). After 3 h, the relative activity of the immobilized cellulase remained at a high level (over 75% and 80%, at temperatures of 50 and 60 °C, respectively). Meanwhile, there was more significant decline in the catalytic properties of the free enzyme, which after 3 h of incubation had lost almost 80% of its activity.

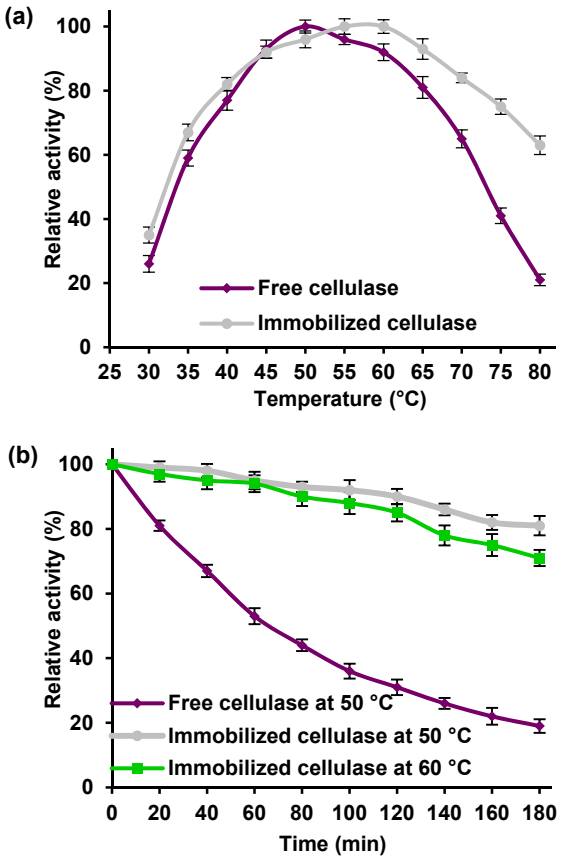

Figure 6. (**a**) Effect of temperature on the relative activity of free and immobilized cellulose; (**b**) Thermal stability of free and immobilized enzyme after incubation for 3 h under optimal temperature and pH conditions.

2.3.3. Storage Stability and Reusability

The storage stability of free and immobilized cellulase at 4 and 25 °C was evaluated by measuring the enzyme's relative activity every 5 days for 30 days (Figure 7a).

It can be seen that, irrespective of the storage temperature, the immobilized enzyme was characterized by higher activity than the free cellulase: after 30 days of storage at 4 and 25 °C, it retained over 95% and 85% of its initial activity, compared with less than 75% and less than 40% in the case of the free enzyme. These results indicated that the immobilization strategy used in this study improved the storage stability of the cellulase.

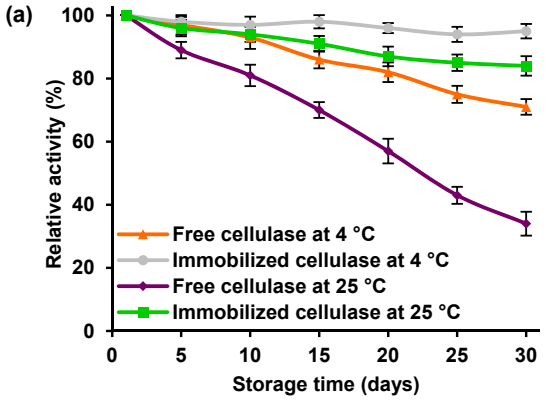

Figure 7. *Cont.*

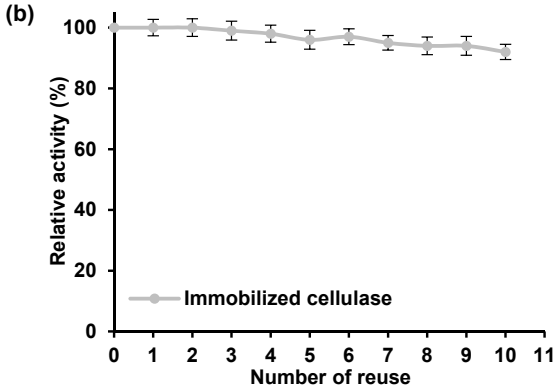

Figure 7. (**a**) Relative activity of free and immobilized cellulase stored for 30 days at 4 °C and 25 °C; (**b**) Reusability of the immobilized cellulase.

In this study, reusability of the bounded enzyme was evaluated over ten consecutive cycles of cellulose hydrolysis (Figure 7b). As can be seen, the relative activity of the immobilized cellulase remained almost unaltered during repeated catalytic cycles, and after ten cycles it retained 93% of its initial activity.

2.4. Kinetic Parameters of Free and Immobilized Cellulase

It is clear that, with changes in the three-dimensional structure of the enzyme, and its pH and temperature profiles as a result of immobilization, its kinetic parameters might also be affected. Kinetic parameters, including K_m, V_{max}, and turnover number (k_{cat}), were determined for both free and immobilized cellulase by measuring the initial reaction rates during the hydrolysis of cellulose with various initial concentrations of substrate, under optimal process conditions (Table 2).

Table 2. Kinetic parameters of cellulase from *Aspergillus niger*, free and immobilized on TiO_2–lignin hybrid.

Kinetic Parameters	Free Cellulase	Immobilized Cellulase
K_m (mM)	2.06 ± 0.85	2.63 ± 0.96
V_{max} (U/mg)	159 ± 11	125 ± 19
k_{cat} (s^{-1})	145 ± 19	114 ± 15
k_{cat}/K_m (s^{-1}·mM^{-1})	70.5 ± 3.5	43.6 ± 3.2
$t_{1/2}$ (min)	63 ± 13	307 ± 21

It can be seen that for the immobilized cellulase the value of K_m reached 2.63 mM, which is higher in comparison with free enzyme (2.06 mM), while the V_{max} value recorded for the immobilized enzyme (159 U/mg) was lower than for free cellulase. Nevertheless, higher values of the Michaelis–Menten constant and lower values of V_{max} after immobilization are typical for immobilized biocatalysts. A similar pattern was observed for turnover number (k_{cat}), which after immobilization took a value of 114 s^{-1}, and is lower than noticed for the free enzyme (145 s^{-1}). In consequence, the value of catalytic efficiency (k_{cat}/K_m) recorded for the immobilized cellulase (43.6 s^{-1}·mM^{-1}) is also significantly lower than that of the free biocatalyst (70.5 s^{-1}·mM^{-1}). This can be explained by the decrease in the affinity of the immobilized biomolecules to the substrate molecules. Nevertheless, it should be emphasized that the half-life ($t_{1/2}$) calculated for the immobilized cellulase (307 min) is almost five times as long as that of the free enzyme (63 min).

3. Discussion

3.1. Synthesis of Titania-Lignin Hybrid Material and Cellulase Immobilization

The synthesized TiO_2–lignin hybrid support was found to have relatively high thermal stability, significantly higher than that of activated kraft lignin. The improvement in thermal stability was a direct result of the incorporation of titanium dioxide particles, known to be highly thermo-resistant, into the hybrid material. The presence of various chemical moieties, such as –OH, C=O, and C–O, in the structure of the synthesized material facilitated the attachment of the cellulase molecules and the formation of relatively stable interactions. From the FTIR spectrum of the free enzyme, it can be concluded that the biocatalyst was attached mainly through the amine groups (–NH_2) present in its structure. However, particular attention should be paid to the shifts in the signals attributed to amide I bands from 1665 cm^{-1} (free enzyme) to 1645 cm^{-1} (immobilized cellulase), which suggests a mixed mechanism of interaction based mainly on the formation of physical and ionic interactions as well as covalent bonds between the enzyme and support [26]. By contrast, Tao et al. used a magnetite–silica hybrid support modified by arginine for the immobilization of cellulase. They observed that at pH above 5.0, the enzyme is negatively charged while arginine is positively charged, and in consequence, the formation of electrostatic interactions was strongly favored [17]. Moreover, after immobilization, the values of BET (Brunauer–Emmett–Teller) surface area, mean pores size, and pores volume were reduced, which suggests that the enzyme particles may be immobilized in the pores of the support as well as on its surface [27].

3.2. Cellulase Immobilization

During the study, it was also investigated how the catalytic activity of the immobilized enzyme depends on the initial immobilization parameters, namely the concentration of enzyme solution and immobilization time. The best catalytic properties were recorded for the system obtained after 6 h of immobilization from a cellulase solution with a concentration of 5 mg/mL, even though a greater amount of the enzyme was immobilized after a longer process time. This fact might be explained by the overloading of enzyme particles on the surface of the hybrid support, causing steric hindrances and diffusional limitations in transport of the reaction mixture components to the active sites of the enzyme [28]. In consequence, the relative activity of the immobilized enzyme decreased. Thus, the above parameter values were determined as the optimal immobilization conditions.

To confirm the type of interactions formed between the cellulase and hybrid support, solutions of Triton X-100 and sodium chloride at various concentrations were used to determine their effect on the activity of the immobilized enzyme. A significant decrease in relative activity might suggest that the cellulase is linked to the hybrid support mainly via hydrogen bonds and ionic interactions. The formation of these types of interactions is related to the presence of negative and positive charges on the surface of the matrix and in the structure of the enzyme, respectively in the conditions of the immobilization process. However, such interactions are unstable under the conditions of the desorption tests. In fact, the immobilized enzyme retained its catalytic properties, which indicates that covalent bonds are also present between the biomolecules and support material [29]. This is confirmed by the findings of Hirsh et al., who used polystyrene film after surface activation by plasma immersion ion implantation. They reported that, when cellulase was immobilized via covalent bonds, desorption was strongly reduced and the enzyme retained its catalytic properties [30]. Moreover, changes in the relative activity of immobilized cellulase after treatment with NaCl solutions at various concentrations indicated that the ionic strength of the solutions affected the catalytic activity of the immobilized cellulase. It also should be added that this statement is confirmed by the results of the immobilized enzyme retained on the surface of the support after desorption, which is higher than the amount of the enzyme corresponding to the measured relative activity. This could suggest that the enzyme is not only desorbed by the eluent, but partially might be also deactivated by the treatment, which is particularly noticeable in the presence of 0.5 M NaCl.

3.3. Stability Study of Immobilized Cellulase

During the immobilization process, the structure of biocatalysts may be altered, causing changes in their activity and stability. It has been shown that immobilized cellulase exhibited higher stability than the free enzyme over the analyzed pH range; however, the catalytic properties are significantly better in acidic than in alkaline conditions. This might be explained by the fact that in a basic environment, ionic groups present in the cellulase molecules form an electrostatic repulsion which influences the three-dimensional structure of the enzyme, leading to disruption and destruction of the active sites of the cellulase, and thus impairing its catalytic properties [31]. Similar observations were reported by Khorshidi et al., who cross-linked cellulase aggregates on amine-functionalized Fe_3O_4–silica core–shell magnetic nanoparticles. They recorded a large decrease in the enzyme's catalytic properties at pH values above 5.0 [32]. By comparison, in this study, the relative activity of immobilized cellulase measured at pH 7.0 was around 80%, proving that application of the titania–lignin hybrid as a support significantly improved the pH resistance of the cellulase. This may be explained by the protective effect of the hybrid support against conformational changes caused by harsh pH conditions [33] and by the fact that after immobilization, interactions between the biocatalyst and carrier are formed which stabilize the entire structure of the enzyme [34]. Results relate to the thermal stability clearly show that the stability of the cellulase was improved after immobilization on the TiO_2–lignin hybrid. This was probably because the immobilization process provided an additional external backbone and stabilization for the molecules of cellulase, as a result of the formation of interactions between the enzyme and support [35]. Moreover, as an effect of immobilization, thermal vibrations of cellulase biomolecules were reduced, which limited conformational changes caused by heat and helped to maintain the proper globular structure of the entire biomolecule [36,37]. Similar findings to those presented in this study were reported by Sanchez-Ramirez et al., who used another inorganic–organic hybrid support (chitosan-coated magnetic nanoparticles) for covalent immobilization of *Trichoderma reesei* cellulase, and found that the resulting biocatalytic system exhibited its maximum activity at 60 °C. In addition, after 3 h of incubation at that temperature, it retained about 60% of its initial activity; however, an increase in the temperature by 10 °C caused the relative activity to drop significantly, to below 40% [38]. By contrast, cellulase immobilized on the titania–lignin support retained over 80% of its activity after 3 h of incubation at 70 °C.

The storage stability of cellulase from *Aspergillus niger* was found to be significantly improved following immobilization. This can probably be attributed to a reduction in the dissociation of peptide subunits and in the enzyme denaturation rate [39]. A significant increase in the storage stability of immobilized cellulase was also reported when graphene oxide supplemented by magnesium oxide nanoparticles was used as a support. In that study, after 30 days of storage the free enzyme retained less than 20% of its initial catalytic activity, compared with over 80% for the immobilized biocatalyst [40]. It was also found that the immobilized cellulase can be used in as many as ten reaction cycles without significant loss of activity. The observed slight decrease in catalytic properties is probably related to the relatively weak strength of the interactions (mainly ionic interactions and van der Waals forces) between the enzyme and support, which causes partial leakage of the catalyst from the support. Moreover, the immobilized cellulase may undergo partial inactivation as a result of its repeated use [41]. Nevertheless, the results clearly show that immobilization is an effective tool to ensure the reusability of cellulase in the hydrolysis of cellulose. Earlier studies of cellulase immobilization have reported the retention of about 40% and 70% of initial activity after eight biocatalytic cycles, when the enzyme was attached to, respectively, magnetic nanoparticles consisting of hematite and ferrite activated by glutaraldehyde, and magnetic nanoparticles encapsulated in polymer nanospheres [34,42]. Such improvement in the operational stability and reusability of cellulase makes it more suitable for large-scale processes and greatly increases its economic viability.

3.4. Kinetic Parameters of Free and Immobilized Cellulase

The observed increase in the value of K_m and simultaneous decrease in V_{max} reflect a lower affinity to the substrate, and consequently a lower maximum reaction rate, in the case of the immobilized enzyme. These changes are probably related to the creation of diffusional limitations and changes in the structure of the enzyme caused by its attachment to the solid support, which blocks active sites of the enzyme and restricts transport of the substrates [43]. In addition, the decrease in the turnover number after immobilization suggests that the binding process has a negative effect on substrate conversion by the immobilized cellulase. However, a significant (fivefold) increase in the enzyme's half-life was recorded, indicating that cellulase attached to the TiO_2–lignin hybrid support retains its catalytic properties for a longer time than the free enzyme. These findings are in agreement with the data on thermal and chemical stability, which show a significant improvement in the stability of the cellulase after immobilization. The foregoing observations are in agreement with data published by Senyay-Oncel and Yesil-Celiktas, which showed that after the immobilization of cellulase on commercially available NaY zeolite, its substrate affinity and reaction rate also decreased [44]. Nonetheless, their study found much more significant changes in K_m (a 100% rise), V_{max} (a 30% drop), and k_{cat} (a 50% drop) than in the present study.

4. Materials and Methods

4.1. Materials

Cellulase from *Aspergillus niger* (EC 3.2.1.4, product number 22178), poly-L-lisine (PLL), kraft lignin, sodium (meta)periodate, cellulose, glucose, Whatman® qualitative filter paper (Grade 1 circles, diam. 15 mm), 3,5-dinitrosalicylic acid (3,5-DNS), sodium chloride, Triton X-100, phosphate buffer (PBS) at pH 7, acetate buffer at pH 4.8, Coomassie Brilliant Blue G-250 (CBB G-250), and bovine serum albumin (BSA) were delivered by Sigma-Aldrich (St. Louis, MO, USA). Commercially available titanium dioxide (product name Tytanpol® R-001) was supplied by Grupa Azoty SA (Tarnów, Poland). Sodium hydroxide, hydrochloric acid, dioxane, 96% ethyl alcohol, and 85% phosphoric acid were delivered by Chempur (Katowice, Poland).

4.2. Synthesis of TiO_2–Lignin Hybrid Support Material

The synthesis of a titania–lignin hybrid support was carried out in three steps, using the method described in our previous work [45,46] with some modifications. In this study, the titanium dioxide was modified with poly-L-lysine (PLL), in view of its peptide nature and to increase the amount of reactive chemical groups for the effective binding of lignin. For surface functionalization of TiO_2, it was suspended in PBS at pH 7, then a 10% (w/w) solution of PLL was added. The mixture was shaken for 12 h (KS260 Basic, IKA Werke GmbH, Staufen im Breisgau, Germany) at 4 °C and centrifuged (Eppendorf Centrifuge 5810 R, Hamburg, Germany), and washed with deionized water to remove unbound PLL and PBS. In the next step, kraft lignin was activated by sodium (meta)periodate. Finally, the activated lignin and modified titanium dioxide were linked at a mass ratio of 1:1.

4.3. Immobilization of Cellulase from Aspergillus niger

Immobilization was carried out using 0.25 g of the previously obtained TiO_2–lignin hybrid support, to which 10 mL of a solution of cellulase from *Aspergillus niger*, at concentrations of 1.0, 3.0, and 5.0 mg/mL in acetate buffer at pH 4.8, was added. The mixture was shaken for a specified period of time (1, 2, 3, 6, 9, or 12 h) in a KS 4000i Control incubator (IKA Werke GmbH, Staufen im Breisgau, Germany) at a temperature of 4 °C. Finally, the products were centrifuged (Eppendorf Centrifuge 5810 R, Hamburg, Germany) and washed several times with the acetate buffer to remove unbound enzyme.

4.4. Characterization of the Hybrid Support and Product after Immobilization

Thermogravimetric curves for the modified TiO_2, activated lignin, and synthesized TiO_2–lignin hybrid material (sample weight approximately 10 mg) were obtained using a Jupiter STA449F3 apparatus (Netzsch, Selb, Germany). Measurements were made at a heating rate of 10 °C/min over the temperature range 25–1000 °C under nitrogen flow (10 mL/min).

Porous structure parameters (BET surface area, pores diameter and pores volume) were determined using an ASAP 2020 instrument (Micromeritics Instrument Co., Norcross, GA, USA). The surface area was evaluated based on the multipoint BET (Brunauer–Emmett–Teller) method using data for nitrogen adsorption under relative pressure (p/p_0). The BJH (Barrett–Joyner–Halenda) algorithm was applied to examine the mean size and total volume of pores.

Zeta potential measurements were made on a Zetasizer Nano ZS instrument (Malvern Instruments Ltd., Malvern, UK) equipped with an autotitrator. The measurements were performed in a 0.001 M NaCl solution over the pH range 2.0–11.0. The zeta potential was computed using Henry's equation.

Fourier transform infrared (FTIR) spectra were obtained using a Vertex 70 spectrophotometer (Bruker, Billerica, MA, USA), analyzing samples in the form of KBr pellets at a resolution of 0.1 cm^{-1} over a wavenumber range of 4000–400 cm^{-1}. Pellets were made by mixing 200 mg of anhydrous potassium bromide and 2 mg of the sample.

The amount of cellulase immobilized on the hybrid support was evaluated based on the Bradford method [47]. Briefly, amount of the cellulase was measured before and after immobilization at wavelength 595 nm, using a calibration curve based on BSA solutions at known concentrations to calculate the quantity of immobilized enzyme present, in mg of cellulase per gram of support.

4.5. Activity and Stability of Free and Immobilized Cellulase

The catalytic activity of free and immobilized cellulase was evaluated by measuring the quantity of reducing sugars (glucose) during hydrolysis of the cellulose substrate. The concentration of glucose was quantified using the previously described DNS method [48]. The activity measurements were carried out as follows: 50 mg of cellulosic substrate (Whatman® paper) was placed in acetate buffer at pH 4.8, and 10 mg of free or immobilized cellulase was added to the reactor. The mixture was incubated for 60 min at 50 °C. The reaction was terminated by the addition of 2 mL of 3,5-DNS. The resulting solution was then incubated at 100 °C for 5 min in an oil bath, and after that time was immediately cooled in ice. Samples were then diluted with distilled water and centrifuged (Eppendorf Centrifuge 5810 R, Hamburg, Germany) to remove solid particles, and were subjected to spectrophotometric measurements at 540 nm using a Jasco V-750 UV–Vis spectrophotometer (Jasco, Tokyo, Japan). The calibration curve of glucose was used to determine the relation between absorbance and the quantity of reducing sugars. All measurements were made in triplicate. One enzyme activity unit (U) of free and immobilized cellulase was defined as the amount of enzyme that produced 1 μmol of glucose per minute.

The relative activity (A_R) (Equation (1)) was defined as the percentage ratio of the activity of cellulase at a specific value (A_i) to the enzyme's maximum activity (A_{max}). A_{max} is the highest activity among all values of enzymatic activity recorded in this study.

$$A_R = \frac{A_i}{A_{max}} \times 100\% \quad (1)$$

Also based on the above-mentioned reaction, the effect of pH and temperature on the activity of immobilized cellulase, as well as its thermal and chemical stability, storage stability, and reusability, were evaluated. The effect of pH was studied by incubating the reaction mixture with free or immobilized cellulase at pH values ranging from 3 to 9 (pH was adjusted by the addition of 0.1 M HCl or NaOH). The effect of temperature was evaluated over the temperature range 30–80 °C by incubating the reaction mixture under the desired temperature conditions. pH and thermal inactivation curves for free cellulase were examined after incubation of the free enzyme at pH 5.5 and a temperature

of 50 °C for 3 h. Thermal inactivation curves of immobilized cellulase were evaluated after 3 h of incubation at pH 6 at temperatures of 50 and 60 °C, while pH inactivation curves were examined after 3 h of incubation at 60 °C, at pH 5 and 6. The reusability of the immobilized cellulase was examined by measuring enzymatic activity in ten consecutive reaction cycles. After each hydrolysis cycle, the immobilized cellulase was separated from the reaction mixture by centrifugation and washed with buffer solution before the next cycle. The enzymatic activity in the first cycle was defined as 100%, and relative activity was calculated for the following cycles. Storage stability was evaluated every 5 days under optimum reaction conditions for free and immobilized cellulase stored at 4 and 25 °C, in phosphate buffer at pH 7. The initial activity was defined as 100%.

The effect of 1% Triton X-100 and sodium chloride solutions at various concentrations (0.1–0.5 M) on the relative activity of immobilized cellulase from *Aspergillus niger* was evaluated over a time of 12 h. For this purpose, the immobilized enzyme was dispersed in sodium chloride or Triton X-100 solution. After the specified period of time, the relative activity of the immobilized enzyme was evaluated based on the hydrolysis reaction of the cellulosic substrate.

4.6. Kinetic Parameters of Free and Immobilized Enzyme

The Lineweaver–Burk plots were used to evaluate the kinetic parameters: the Michaelis–Menten constant (K_m), maximum reaction rate (V_{max}), specificity constant (k_{cat}/K_m), and turnover number (k_{cat}) of free and immobilized cellulase. These parameters were evaluated based on the hydrolysis reaction of cellulose substrate at different concentrations. Initial reaction rates were evaluated under optimum reaction conditions.

5. Conclusions

The results presented in this study clearly demonstrate that cellulase, an industrially relevant enzyme, was successfully immobilized on a hybrid TiO_2–lignin support material. The immobilized cellulase exhibited significant improvement in thermal and chemical stability (with relative activity above 80% after 3 h of incubation). Furthermore, after 10 consecutive hydrolysis cycles the immobilized cellulase retained over 90% of its initial activity, which confirms its operational stability, a relevant feature for industrial applications. The approach described here provides an efficient and simple method for the synthesis of a hybrid titanium dioxide–lignin material and its application as a support material for the immobilization of cellulase. The produced biocatalytic system may be employed in industrial applications without significant loss of its properties over several cycles. Moreover, the synthesized hybrid material and the applied immobilization methodology might easily be used for the immobilization of other biocatalysts.

Acknowledgments: The scientific work was financed from budgetary resources for science in the years 2016–2019, project number IP2015 032574 (Iuventus Plus).

Author Contributions: J.Z. planned the studies, evaluated the enzyme immobilization efficiency and the immobilized enzyme's activity and stability, as well as developed results. A.J. prepared the functional hybrid material and carried out the immobilization experiments. Ł.K. interpreted the data and wrote up the results. T.J. coordinated all project tasks, planned the studies, developed the results, and participated in discussions.

Conflicts of Interest: The authors declare no conflict of interest. The funding sponsors had no role in the design of the study; in the collection, analysis, or interpretation of data; in the writing of the manuscript; or in the decision to publish the results.

References

1. Gupta, C.; Jain, P.; Kumar, D.; Dixit, A.K.; Jain, R.K. Production of cellulase enzyme from isolated fungus and its application as efficient refining aid for production of security paper. *Int. J. Appl. Microbiol. Biotechnol. Res.* **2015**, *3*, 11–19.
2. Zhang, Y.H.P.; Himmel, M.E.; Mielenz, J.R. Outlook for cellulase improvement: Screening and selection strategies. *Biotechnol. Adv.* **2006**, *24*, 452–481. [CrossRef] [PubMed]

3. Kuhad, R.C.; Singh, A.; Eriksson, K.E. Microorganisms and enzymes involved in the degradation of plant fiber cell walls. *Adv. Biochem. Eng. Biotechnol.* **1997**, *57*, 45–125. [PubMed]
4. Deswal, D.; Khasa, Y.P.; Kuhad, R.C. Optimization of cellulase production by a brown rot fungus *Fomitopsis* sp. *Bioresour. Technol.* **2011**, *102*, 6065–6072. [CrossRef] [PubMed]
5. Rana, S.; Kaur, M. Isolation and screening of cellulase-producing microorganisms from degraded wood. *Int. J. Pharm. Biol. Sci. Fundam.* **2012**, *2*, 10–15.
6. Kuhad, R.C.; Gupta, R.; Singh, A. Microbial cellulases and their industrial applications. *Enzyme Res.* **2011**, *2011*, 280696. [CrossRef] [PubMed]
7. Sun, Y.; Cheng, J. Hydrolysis of lignocellulosic materials for ethanol production: A review. *Bioresour. Technol.* **2002**, *83*, 1–11. [CrossRef]
8. Sukumaran, R.K.; Singhania, R.R.; Pandey, A. Microbial cellulases—Production, applications and challenges. *J. Sci. Ind. Res.* **2005**, *64*, 832–844.
9. Cao, L. *Carrier-Bound Immobilized Enzymes: Principles, Application and Design*; Wiley-VCh: Weinheim, Germany, 2005.
10. Rodrigues, R.C.; Ortiz, C.; Berenguer-Murcia, A.; Torres, R.; Fernandez-Lafuente, R. Modifying enzyme activity and selectivity by immobilization. *Chem. Soc. Rev.* **2013**, *42*, 6290–6307. [CrossRef] [PubMed]
11. Tischer, W.; Wedekind, F. Immobilized enzymes: Methods and applications. *Top. Curr. Chem.* **1999**, *200*, 96–126.
12. Barbosa, O.; Ortiz, C.; Berenguer-Murcia, A.; Torres, R.; Rodrigues, R.C.; Fernandez-Lafuente, R. Strategies for the one-step immobilization-purification of enzymes as industrial biocatalysts. *Biotechnol. Adv.* **2015**, *33*, 435–456. [CrossRef] [PubMed]
13. Brena, B.; González-Pombo, P.; Batista-Viera, F. Immobilization of enzymes and cells. *Methods Mol. Biol.* **2013**, *1051*, 5–31.
14. Mateo, C.; Abian, O.; Fernandez-Lorente, G.; Pedroche, J.; Fernandez-Lafuente, R.; Guisan, J.M. Epoxy sepabeads: A novel epoxy support for stabilization of industrial enzymes via very intense multipoint covalent attachment. *Biotechnol. Prog.* **2002**, *18*, 629–634. [CrossRef] [PubMed]
15. Hernandez, K.; Fernandez-Lafuente, R. Control of protein immobilization: Coupling immobilization and site-directed mutagenesis to improve biocatalyst or biosensor performance. *Enzyme Microb. Technol.* **2011**, *48*, 107–122. [CrossRef] [PubMed]
16. Jędrzak, A.; Rębiś, T.; Klapiszewski, Ł.; Zdarta, J.; Milczarek, G.; Jesionowski, T. Carbon paste electrode based on functional GOx/silica-lignin system to prepare an amperometric glucose biosensor. *Sens. Actuators B Chem.* **2018**, *256*, 176–185. [CrossRef]
17. Tao, Q.L.; Li, Y.; Shi, Y.; Liu, R.J.; Zhang, Y.W.; Guo, J. Application of molecular imprinted magnetic Fe_3O_4@SiO_2 nanoparticles for selective immobilization of cellulase. *J. Nanosci. Nanotechnol.* **2016**, *16*, 6055–6060. [CrossRef] [PubMed]
18. Velmurugan, R.; Incharoensakdi, A. MgO-Fe_3O_4 linked cellulase enzyme complex improves the hydrolysis of cellulose from *Chlorella* sp. CYB2. *Biochem. Eng. J.* **2017**, *122*, 22–30. [CrossRef]
19. Hong, G.W.; Ramesh, S.; Kim, J.H.; Kim, H.J.; Lee, H.S. Synthesis and properties of cellulose-functionalized POSS-SiO_2/TiO_2hybrid composites. *J. Nanosci. Nanotechnol.* **2015**, *15*, 8048–8054. [CrossRef] [PubMed]
20. Hou, J.; Dong, G.; Ye, Y.; Chen, V. Laccase immobilization on titania nanoparticles and titania-functionalized membranes. *J. Membr. Sci.* **2014**, *452*, 229–240. [CrossRef]
21. Hou, J.; Dong, G.; Xiao, B.; Malassigne, C.; Chen, V. Preparation of titania based biocatalytic nanoparticles and membranes for CO_2 conversion. *J. Mater. Chem. A* **2015**, *3*, 3332–3342. [CrossRef]
22. Klapiszewski, Ł.; Zdarta, J.; Antecka, K.; Synoradzki, K.; Siwińska-Stefańska, K.; Moszyński, D.; Jesionowski, T. Magnetite nanoparticles conjugated with lignin: A physicochemical and magnetic study. *Appl. Surf. Sci.* **2017**, *422*, 94–103. [CrossRef]
23. Zdarta, J.; Klapiszewski, Ł.; Jędrzak, A.; Nowicki, M.; Moszyński, D.; Jesionowski, T. Lipase B from *Candida antarctica* immobilized on a silica-lignin matrix as a stable and reusable biocatalytic system. *Catalysts* **2017**, *7*, 14. [CrossRef]
24. Hanefeld, U.; Gardossi, L.; Magner, E. Understanding enzyme immobilization. *Chem. Soc. Rev.* **2009**, *38*, 453–468. [CrossRef] [PubMed]
25. Magri, M.L.; Miranda, M.V.; Cascone, O. Immobilization of soybean seed coat peroxidase on polyaniline: Synthesis optimization and catalytic properties. *Biocatal. Biotransform.* **2005**, *22*, 339–346. [CrossRef]

26. Eslamipour, F.; Hejazi, P. Evaluating effective factors on activity and loading of immobilized α-amylase onto magnetic nanoparticles using response surface desirability approach. *RSC Adv.* **2016**, *6*, 20187–20197. [CrossRef]
27. Hou, J.; Dong, G.; Ye, Y.; Chen, V. Enzymatic degradation of bisphenol-A with immobilized laccase on TiO_2 sol–gel coated PVDF membrane. *J. Membr. Sci.* **2014**, *469*, 19–30. [CrossRef]
28. Zhang, D.H.; Zhang, Y.F.; Zhi, G.Y.; Xie, Y.L. Effect of hydrophobic/hydrophilic characteristics of magnetic microspheres on the immobilization of BSA. *Colloids Surf. B* **2011**, *82*, 302–306. [CrossRef] [PubMed]
29. Straksys, A.; Kochane, T.; Budriene, S. Catalytic properties of maltogenic α-amylase from *Bacillus stearothermophilus* immobilized onto poly(urethane urea) microparticles. *Food Chem.* **2016**, *211*, 294–299. [CrossRef] [PubMed]
30. Hirsh, S.L.; Bilek, M.M.M.; Nosworthy, N.J.; Kondyurin, A.; dos Remedios, C.G.; McKenzie, D.R. A comparison of covalent immobilization and physical adsorption of a cellulase enzyme mixture. *Langmuir* **2010**, *26*, 14380–14388. [CrossRef] [PubMed]
31. Mubarak, N.N.; Wong, J.R.; Tan, K.W.; Sahu, J.N.; Abdullah, E.C.; Jayakumar, N.S.; Ganesan, P. Immobilization of cellulase enzyme on functionalized multiwall carbon nanotubes. *J. Mol. Catal. B Enzym.* **2014**, *107*, 124–131. [CrossRef]
32. Khorshidi, K.J.; Lenjannezhadian, H.; Jamalan, M.; Zeinali, M. Preparation and characterization of nanomagnetic cross-linked cellulase aggregates for cellulose bioconversion. *J. Chem. Technol. Biotechnol.* **2016**, *91*, 539–546. [CrossRef]
33. Bohara, R.A.; Thorat, N.D.; Pawar, S.H. Immobilization of cellulase on functionalized cobalt ferrite nanoparticles. *Korean J. Chem. Eng.* **2016**, *33*, 216–222. [CrossRef]
34. Abraham, R.E.; Verma, M.L.; Barrow, C.J.; Puri, M. Suitability of magnetic nanoparticle immobilised cellulases in enhancing enzymatic saccharification of pretreated hemp biomass. *Biotechnol. Biofuels* **2014**, *7*, 1–12. [CrossRef] [PubMed]
35. Zhang, W.; Qiu, J.; Feng, H.; Zang, L.; Sakai, E. Increase in stability of cellulase immobilized on functionalized magnetic nanospheres. *J. Magn. Magn. Mater.* **2015**, *375*, 117–123. [CrossRef]
36. Sharma, S.; Kaur, P.; Jain, A.; Rajeswari, M.R.; Gupta, M.N. A smart bioconjugate of chymotrypsin. *Biomacromolecules* **2003**, *4*, 330–336. [CrossRef] [PubMed]
37. Li, Y.; Wang, X.Y.; Zhang, R.Z.; Zhang, X.Y.; Liu, W.; Xu, X.M.; Zhang, Y.W. Molecular imprinting and immobilization of cellulase onto magnetic Fe_3O_4@SiO_2 nanoparticles. *J. Nanosci. Nanotechnol.* **2014**, *14*, 2931–2936. [CrossRef] [PubMed]
38. Sanchez-Ramirez, J.; Martinez-Hernandez, J.L.; Segura-Ceniceros, P.; Lopez, G.; Saade, H.; Medina-Morales, M.A.; Ramos-Gonzalez, R.; Aguilar, C.N.; Ilyina, A. Cellulases immobilization on chitosan-coated magnetic nanoparticles: Application for *Agave atrovirens* lignocellulosic biomass hydrolysis. *Bioprocess. Biosyst. Eng.* **2017**, *40*, 9–22. [CrossRef] [PubMed]
39. Zhang, D.; Hegab, H.E.; Lvov, Y.; Snow, L.D.; Palmer, J. Immobilization of cellulase on a silica gel substrate modified using a 3-APTES self-assembled monolayer. *SpringerPlus* **2016**, *5*, 1–20. [CrossRef] [PubMed]
40. Dutta, N.; Biswas, S.; Saha, M.K. Biophysical characterization and activity analysis of nano-magnesium supplemented cellulase obtained from a psychrobacterium following graphene oxide immobilization. *Enzym. Microb. Technol.* **2016**, *95*, 248–258. [CrossRef] [PubMed]
41. Swarnalatha, V.; Esther, R.A.; Dhamodharan, R. Immobilization of α-amylase on gum acacia stabilized magnetite nanoparticles, an easily recoverable and reusable support. *J. Mol. Catal. B Enzym.* **2013**, *96*, 6–13. [CrossRef]
42. Lima, J.S.; Araujo, P.H.H.; Sayer, C.; Viegas, A.C.; de Oliveira, D. Cellulase immobilization on magnetic nanoparticles encapsulated in polymer nanospheres. *Bioprocess. Biosyst. Eng.* **2017**, *40*, 511–518. [CrossRef] [PubMed]
43. Bayramoglu, S.G.; Kiralp, S.; Yilmaz, M.; Toppare, L.; Arica, M.Y. Covalent immobilization of chloroperoxidase onto magnetic beads: Catalytic properties and stability. *Biochem. Eng. J.* **2008**, *38*, 180–188. [CrossRef]
44. Senyay-Oncel, D.; Yesil-Celiktas, O. Characterization, immobilization, and activity enhancement of cellulase treated with supercritical CO_2. *Cellulose* **2015**, *22*, 3619–3631. [CrossRef]

45. Klapiszewski, Ł.; Siwińska-Stefańska, K.; Kołodyńska, D. Preparation and characterization of novel TiO_2/lignin and TiO_2-SiO_2/lignin hybrids and their use as functional biosorbents for Pb(II). *Chem. Eng. J.* **2017**, *314*, 169–171. [CrossRef]
46. Klapiszewski, Ł.; Siwińska-Stefańska, K.; Kołodyńska, D. Development of lignin based multifunctional hybrid materials for Cu(II) and Cd(II) removal from the aqueous system. *Chem. Eng. J.* **2017**, *330*, 518–530. [CrossRef]
47. Bradford, M.M. A rapid and sensitive method for the quantitation of microgram quantities of protein utilizing the principle of protein-dye binding. *Anal. Biochem.* **1976**, *72*, 248–254. [CrossRef]
48. Miller, G.L. Use of dinitrosalicylic acid reagent for determination of reducing sugar. *Anal. Chem.* **1959**, *31*, 426–428. [CrossRef]

Heterogeneous & Homogeneous & Bio-

CHEMCATCHEM

CATALYSIS

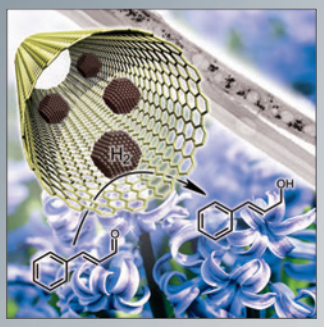

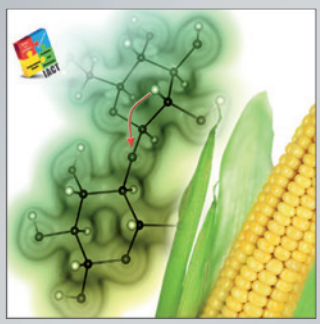

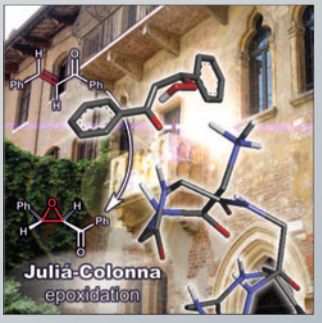

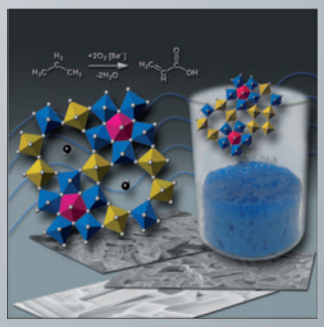

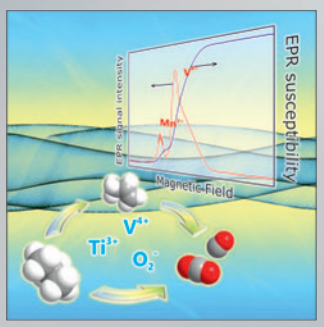

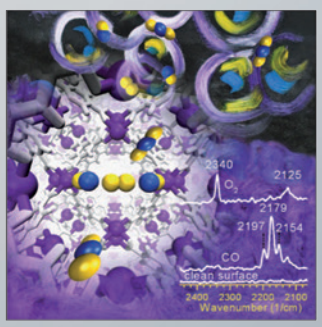

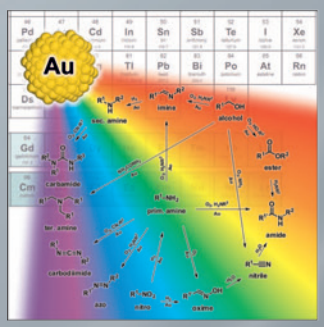

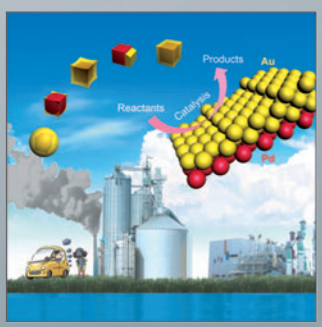

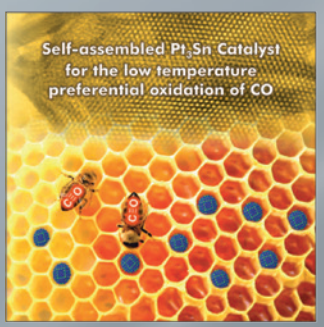

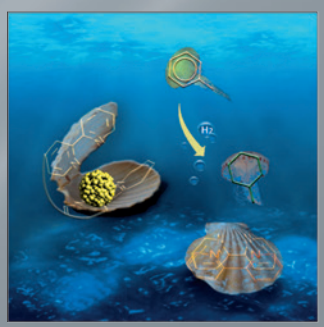

Reprint

A Journal of

ChemPubSoc Europe

WILEY-VCH

www.chemcatchem.org

ChemPubSoc Europe

DOI: 10.1002/cctc.201801335

CHEMCATCHEM Full Papers

Upgrading of Biomass Monosaccharides by Immobilized Glucose Dehydrogenase and Xylose Dehydrogenase

Jakub Zdarta,*[a, b] Manuel Pinelo,[b] Teofil Jesionowski,[a] and Anne S. Meyer[b]

Direct upgrading and separation of the monosaccharides from biomass liquors is an overlooked area. In this work we demonstrate enzymatic production of gluconic acid and xylonic acid from glucose and xylose present in pretreated birchwood liquor by glucose dehydrogenase (GDH, EC 1.1.1.47) and xylose dehydrogenase (XDH, EC 1.1.1.175), respectively. The biocatalytic conversions were compared using two different kinds of silica support materials (silica nanoparticles ($nanoSiO_2$) and porous silica particles with hexagonal pores (SBA 15 silica) for enzyme immobilization. Upon immobilization, both enzymes showed significant improvement in their thermal stability and robustness at alkaline pH and exhibited over 50% activity even at pH 10 and 60 °C on both immobilization matrices. When compared to free enzymes at 45 °C, GDH immobilized on $nanoSiO_2$ and SBA silica displayed a 4.5 and 7.25 fold increase in half-life, respectively, whilst XDH immobilized on $nanoSiO_2$ and SBA showed a 4.7 and 9.5 fold improvement in half-life, respectively. Additionally, after five reaction cycles both $nanoSiO_2$GDH and $nanoSiO_2$XDH retained more than 40% activity and GDH and XDH immobilized on SBA silica maintained around 50% of their initial activity resulting in about 1.5–1.6 fold increase in biocatalytic productivity compared to the free enzymes.

Introduction

Bio-based conversion of biomass components by soluble or immobilized enzymes has been presented as a promising and efficient approach for sustainable production of valuable chemical compounds under mild reaction conditions.[1,2] Use of glucose dehydrogenase (GDH) (EC 1.1.1.47) and xylose dehydrogenase (XDH) (EC 1.1.1.175) is of interest in this regard because these NAD+ dependent enzymes catalyze conversion of D-glucose into gluconic acid and D-xylose into xylonic acid, respectively.[3] Besides transformation of monosaccharides, the enzymatic conversion adds a charge to the products, which can facilitate separation of acid products from a mixed product stream, for instance using membrane technology.[4] Both gluconic acid and xylonic acid are classified by the US Department of Energy among the top 30 potential high-value compounds from biomass.[5] Gluconic acid is a mild organic acid that has multiple applications in the food industry but also in pharmaceuticals synthesis.[6] Xylonic acid is used as a substrate for synthesis of 1,2,4-butanetriol and 1,2,4-butanetriol trinitrate[7] and has moreover been projected for various uses in the food, pharmaceutical and agriculture industries.[8] However, the practical biocatalytic conversion of biomass components using GDH and XDH is limited due to their relatively low stability at extreme pH and temperature conditions.

A possible approach to overcome these limitations and at the same time increase the biocatalytic productivity via maximizing enzyme "reuse" is enzyme immobilization.[4,9] Enzyme immobilization may moreover reduce the complexity of enzyme separation from the products after reaction.[6,10] Various techniques and methods of immobilization such as adsorption, covalent binding, entrapment or encapsulation have been described previously.[11–13] Silica-based materials are frequently used as support materials in enzyme immobilization due to their thermal, chemical and mechanical resistance, good sorption properties, and the presence of many hydroxyl groups that facilitate enzyme binding.[14–16] Moreover, silica-based materials are easy to obtain and relatively cheap, a feature of particular significance in biomass valorization processes. Nonetheless, data related to immobilization of glucose dehydrogenase and xylose dehydrogenase on silica are limited.

As data about immobilization of glucose dehydrogenase and xylose dehydrogenase are limited, a simple protocol is required to use efficient and stable support materials for immobilization of GDH and XDH which additionally facilitating further separation of products of enzymatic conversion. Thus, in the present study, we examine immobilization, characterization and comparison of GDH and XDH on two types of silica support materials – silica nanoparticles and mesoporous silica with hexagonally ordered pores. As part of the study, we also investigate the kinetics of the enzymatic conversions of monosaccharides, and examine the effect of various pH and temperature conditions on free and immobilized GDH and XDH and evaluate the influence of these parameters on the enzyme stability. The practical application of the biocatalytic systems is validated by applying them for conversion of glucose and

[a] Dr. J. Zdarta, Prof. T. Jesionowski
Institute of Chemical Technology and Engineering
Faculty of Chemical Technology
Poznan University of Technology
Berdychowo 4
Poznan 60965 (Poland)
E-mail: jakub.zdarta@put.poznan.pl
[b] Dr. J. Zdarta, Prof. M. Pinelo, Prof. A. S. Meyer
Center for BioProcess Engineering
Department of Chemical and Biochemical Engineering
Technical University of Denmark
Soltofts Plads 229
Lyngby 2800 (Denmark)

xylose present in authentic pretreated birch wood biomass liquors.

Results and Discussion

GDH and XDH Immobilization

In this study, silica nanopowder of particle size in the range of 10–20 nm and pore diameters of around 2 nm size (nanoSiO$_2$) and mesoporous SBA 15 silica (< 150 μm particle size) with hexagonal pore morphology and pore size up to 20 nm (SBA 15) were used. It should be emphasized that type of the support material is known to affect place of enzyme binding. According to the previously published articles, using silica nanoparticles, GDH and XDH are expected to be immobilized on the particle surfaces, while in case of SBA silica, biomolecules are presumably bound mainly inside the SBA 15 silica pores, as it is schematically presented in Figure 1.[14,15]

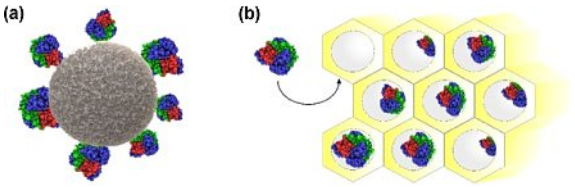

Figure 1. Schematic presentation of immobilization of glucose dehydrogenase and/or xylose dehydrogenase: (a) on silica nanoparticles and (b) in pores of hexagonal mesoporous silica.

These expectations were confirmed by the images from transmission electron microscopy and changes of the porous structure parameters of silica-based materials after GDH and XDH immobilization (Figure 2 and Table 1). After immobilization of both enzymes surface area of the nanoSiO$_2$ decreased around two times and reached about 120 m^2/g as its pore size was unaltered after enzyme binding. Surface area of SBA 15 silica was intact after immobilization, meanwhile significant changes were noticed in pore size and pore volume indicating GDH and XDH immobilization into the pores of the hexagonal silica.

Table 1. Porous structure parameters of nanoSiO$_2$ silica and hexagonal mesoporous silica SBA 15 before and after immobilization of glucose dehydrogenase or xylose dehydrogenase.

Sample name	BET surface area [m^2/g]	Pore volume [cm^3/g]	Pore size [nm]
nanoSiO$_2$	219.6	0.098	2.048
nanoSiO$_2$GDH	118.3	0.087	2.046
nanoSiO$_2$XDH	121.6	0.091	2.047
SBA 15	579.6	0.868	19.211
SBA15GDH	567.2	0.476	14.754
SBA15XDH	570.2	0.513	15.634

The different ways of immobilization were thus anticipated to produce different amounts of immobilized enzymes, highest on the nanoparticles due to their high surface area: 2.8 mg (560 U) of GDH and 534 U of XDH were immobilized on 1 g of nanoSiO$_2$, which was about 10–15% higher compared with SBA 15 (Table 2). Immobilization yield also followed this trend: when nanoSiO$_2$ was used, immobilization yield for GDH and XDH reached 94 and 82%, whereas for SBA 15 it was 89 and 75%, respectively, Hence, irrespective of the support material, a higher quantity of the immobilized enzyme was noticed in case of glucose dehydrogenase. Greater amounts of immobilized GDH, as compared to XDH, are probably related to the three-dimensional structure and amino acids composition of this enzyme.[17] A possible explanation for this is that enzymes molecules possessing more accessible amino acids in their structure, like arginine, asparagine, glutamic acid or lysine and are more effectively immobilized, as it was previously reported for glucose-6-phosphate dehydrogenase.[18] Nevertheless, both enzymes are linked to the silica by adsorption immobilization, by creation of electrostatic interactions and hydrogen bonds between mainly amino (–NH$_2$), hydroxyl (–OH) and carbonyl (–COOH) groups of the enzymes and hydroxyl groups of the silica-based support.

The specific activity of GDH and XDH was 42.2 U/mg and 46.8 U/ml, respectively, indicating that both enzymes showed similar catalytic activity in model reaction. The specific activity of the immobilized enzymes was lower and reached 30.5 and 27.3 U/mg of the enzyme, respectively, for nanoSiO$_2$GDH and SBA15GDH, which corresponded to an activity retention of 72.3 and 64.7%, respectively. For nanoSiO$_2$XDH and SBA15XDH, these values were slightly lower and reached 29.0 and 24.6 U/mg, respectively. Also noticed was a lower activity retention of 61.8% for nanoSiO$_2$XDH and 52.6% for SBA15XDH. The lower values of specific activity and activity retention noticed for enzymes immobilized onto SBA 15 compared with nanoSiO$_2$, might be explained by two factors: (i) lower amount of immobilized biocatalysts and (ii) hindered accessibility of the enzyme active sites for the substrates molecules due to immobilization of enzymes mainly into the pores of the support. Nevertheless, lower activity of immobilized XDH compared with GDH is probably related to the larger conformational changes of 3-D biomolecule structure that occur upon immobilization, as reported earlier by Li et al.[19]

Table 2. Immobilization yield and amount of immobilized enzyme in different biocatalytic systems. Specific activity and activity retention of free and immobilized GDH and XDH.

Analyzed parameter	freeGDH	nanoSiO$_2$GDH	SBA15GDH	freeXDH	nanoSiO$_2$XDH	SBA15XDH
Amount of immobilized enzyme'[mg/g]; *[U/g]	–	2.8 ± 0.1′ 560 ± 19*	2.5 ± 0.1′ 500 ± 14*	–	534 ± 16*	450 ± 12*
Immobilization yield [%]	–	94 ± 3.5	82 ± 2.8	–	89 ± 3.0	75 ± 2.7
Specific activity [U/mg]	42.2 + 0.9	30.5 ± 0.8	27.3 ± 1.1	46.8 ± 1.7[a]	29.0 ± 0.7	24.6 ± 0.8

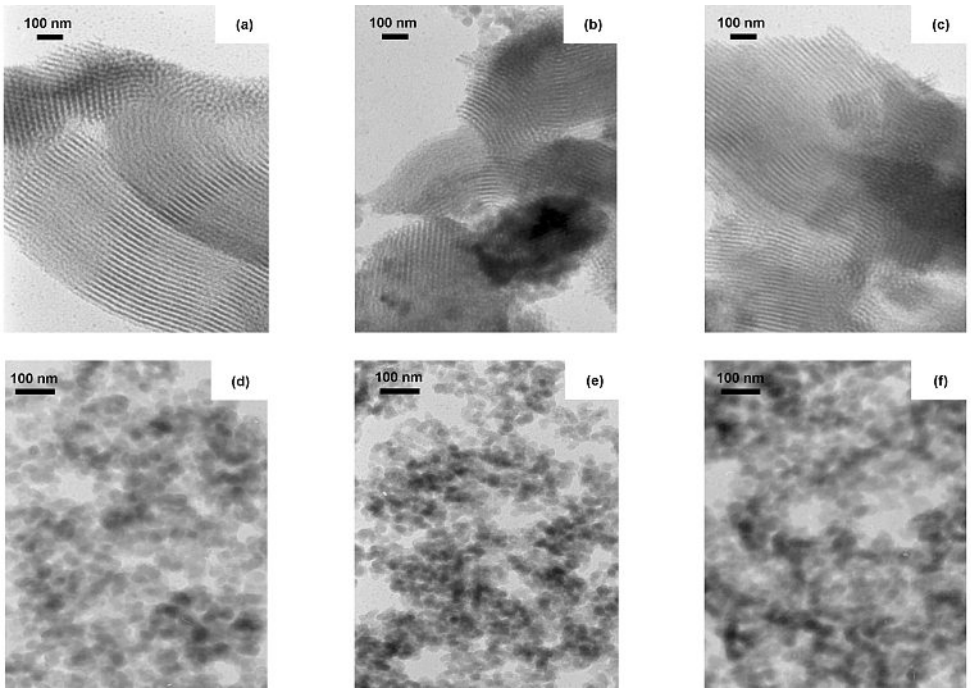

Figure 2. TEM images of the: (a) SBA 15 silica and (b) nanoSiO_2 silica before enzyme immobilization; (b) and (e) after immobilization of glucose dehydrogenase; (c) and (f) after immobilization of xylose dehydrogenase.

There is no available literature about efficient immobilization of XDH, and though there are some reports about immobilization of GDH, results presented here go further than previously published data. For example, Baron et al. used controlled pore silica with average pore size of 500 Å, as a support for *Bacillus megaterium* glucose dehydrogenase and immobilized less than 0.5 mg of enzyme per 1 g of the support,[20] whereas here we report a loading capacity of silica nanoparticles of 2.8 mg/g, probably due to higher density of hydroxyl groups on the surface of nanoSiO_2.

Effect of Temperature and pH on Activity and Stability of Free and Immobilized GDH

Free GDH as well as both of the GDH-based immobilized systems exhibited the highest activity at 45 °C (Figure 3a). At temperatures below optimum, free GDH was characterized by slightly higher, but significantly different, activity than the immobilized enzyme. But at higher temperatures (45–60 °C), immobilized GDH showed better activity than the free biocatalyst. This is particularly noticeable in the case of the mesoporous SBA 15 silica support as GDH immobilized on this material showed higher residual activity (53%) than free enzyme (29%) even at a temperature of 60 °C. GDH is known as an enzyme that exhibits catalytic activity only in multimeric form. In a previous study, it has been shown that at temperatures above 50 °C, multimers tend to dissociate, which leads to irreversible inactivation.[21] Since immobilization using silica provided enzymes multipoint attachment and improved rigidity of the enzyme, thermal dissociation of silica-bounded GDH multimers could be prevented that lead to better activity retention at higher temperatures.

Free and silica immobilized GDH showed similar pH profiles which were, however, statistically significantly different over whole analyzed pH range (6–10), as illustrated in Figure 3b. However, nanoSiO_2GDH and SBA15GDH exhibited about 10 and 15% enhancement of catalytic activity, respectively, particularly at basic conditions (8.5–10), compared to free catalysts. A shift of the pH optima from 8 (free GDH) to 8.5 (immobilized GDH) was also observed. Changes in the pH and temperature profiles could be explained by the fact that immobilization, in general, leads to conformational changes of the structure of the enzyme.[22] These changes occur mainly as a result of ionization of side chains of active site amino acids. However, type, nature and functional group of the matrix also play a significant role. These factors lead to modifications of microenvironment around the active site of the enzyme and in consequence affect the pH and temperature profile of the immobilized biocatalysts.[23]

Evaluation of the thermal stability of the immobilized enzyme is a crucial step in determining practical applications of the produced biocatalytic systems. Binding of GDH to the silica support significantly improved thermal stability of the enzyme: after 45 min of heating at 45 °C, at pH 8, free enzyme maintained 42.5% of its activity, while nanoSiO_2GDH and SBA15GDH retained 47 and 53% of catalytic activity, respectively (Figure 3c). Moreover, after 210 min of incubation under the same conditions, no catalytic activity was observed for free GDH whereas immobilized enzyme was more stable and retained about 30 and 35% of its activity when immobilized using nanoSiO_2 and SBA silica, respectively that might be

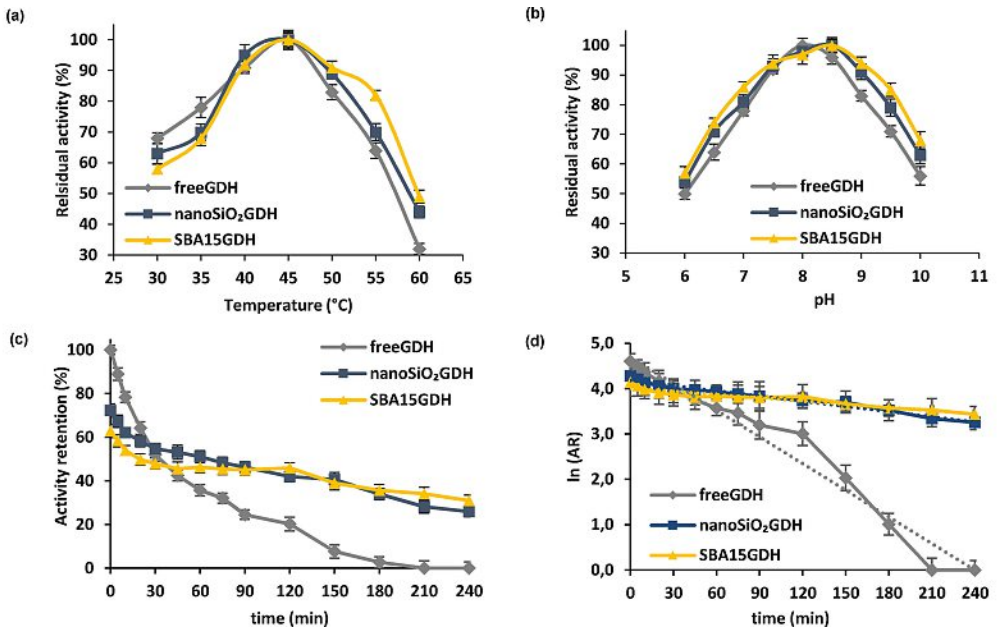

Figure 3. (a) Temperature profiles, (b) pH profiles and (c, d) Thermal stability of free and silica immobilized glucose dehydrogenase (GDH). Thermal stability of free and silica immobilized GDH was examined under optimal temperature (45 °C) and pH (8) conditions. Inactivation constants (k_D) were evaluated based on the linear regression slope. All data are presented as means ± standard deviation.

explained by creation of a more suitable microenvironment after immobilization as reported also by Li et al.[24] Since drop in the relative activity of free GDH could be explained mainly by thermal and chemical inactivation of the biocatalyst, decrease in the activity of the immobilized enzyme could also partially reflect leakage of GDH from the matrix. Nevertheless, the higher relative activity noticed for SBA15GDH, as compared to nanoSiO$_2$GDH, is related to catalyst immobilization in the hexagonal pores of the support, which ensures better protection of the enzyme molecules against harsh reaction conditions.

Significant improvement in the stability of the immobilized GDH can also be observed in values of the inactivation constant (k_D) and enzyme half-life ($t_{1/2}$) (Figure 3d). k_D and $t_{1/2}$ for free glucose dehydrogenase was found to be 0.0174 1/min and 39.8 min, respectively, whereas inactivation constants of nanoSiO$_2$GDH and SBA15GDH were, respectively, 4.5 fold and 7.2 fold (0.0038 1/min and 0.0024 1/min) lower than of those of the free enzyme. As a result, enzyme half-life was significantly improved and reached 182.4 min for nanoSiO$_2$GDH and 288.8 min for SBA15GDH. These findings are in agreement with data reported earlier by Twala et al. who immobilized GDH on functionalized ReSynTM polymer microspheres. However, in their study, immobilized enzyme half-life increased two fold after immobilization and further incubation at 45 °C compared to the free catalysts, while in the current study, enzyme half-life was improved much more (for about 4.5 fold). That is probably related to the more suitable chemical microenvironment created by the silica nanoparticles compared to polymeric support.[1]

Effect of Temperature and pH on Activity and Stability of Free and Immobilized GDH

The optimum temperature of free XDH was 40 °C, whereas for nanoSiO$_2$XDH and SBA15XDH, the optimum shifted slightly upwards (45 °C) (Figure 4). Temperature profiles of free and immobilized XDH were also statistically significantly different. At temperatures below maximum, free enzyme showed higher activity compared with immobilized enzymes. However, when temperature exceed 40 °C, activity of free enzyme dropped sharply while immobilized XDH retained significantly higher activities. At 65 °C nanoSiO$_2$XDH and SBA15XDH retained 69 and 64%, respectively, of their residual activity while free biocatalyst showed less than 50% residual activity. The higher temperature optimum recorded for immobilized XDH and the significant improvement of immobilized enzyme activity at higher temperatures are probably a result of creation of enzyme-matrix interactions that form external enzyme backbones and increase rigidity of the biocatalyst.[25] Such changes would have protected the active sites of the XDH against conformational changes and denaturation at higher temperatures, and thus help to maintain high catalytic activity.

All tested XDH systems exhibited their optimum at pH 8 (Figure 4b). Moreover, their pH profiles were significantly different, however, particularly at pH values close to neutral (6.5–8.5), they were similar. Immobilization of XDH at basic pH (9–10) resulted in nanoSiO$_2$XDH and SBA15XDH showing about 10 and 20% higher activity, respectively, compared to the free catalyst. Under strongly acidic or basic conditions, ionic groups presented in the enzyme structure might be protonated or deprotonated, respectively. These changes result in formation of electrostatic repulsion between these groups, and hence

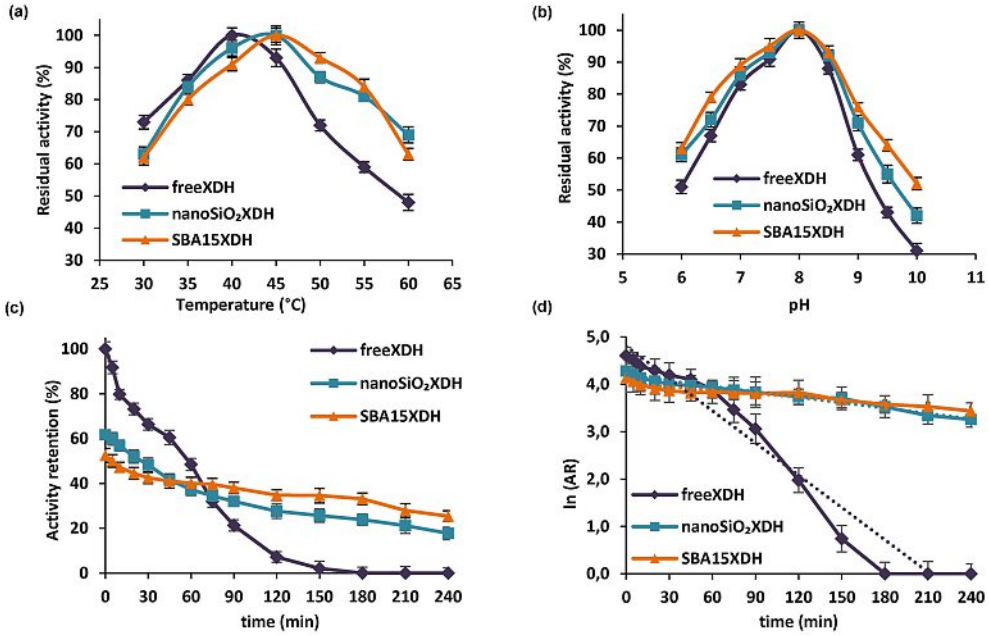

Figure 4. (a) Temperature profiles, (b) pH profiles and (c, d) Thermal stability of free and silica immobilized xylose dehydrogenase (XDH). Thermal stability of free and silica immobilized XDH was examined at optimal temperature (40 °C for free enzyme and 45 °C for immobilized enzymes) and pH (8) conditions. Inactivation constants (k_D) were evaluated based on the linear regression slope. All data are presented as means ± standard deviation.

destruction and degeneration of the enzyme active site and decrease in catalytic properties of the enzyme.[28] Creation of the enzyme-matrix interactions which limit dissociation of enzyme subunits and stiffening the structure of the biomolecule after immobilization, caused that susceptibility of the enzyme to conformational changes in pH decreases, and leads to improvements of enzyme activity under harsh pH conditions.

Additionally, thermal stability of free and both silica-immobilized XDH was studied. Although, after immobilization activity decreased (Table 2), stability of immobilized XDH was improved compared to the free enzyme (Figure 4c). After 180 min of incubation at pH 8 and 40 °C, free enzyme completely lost its activity while nanoSiO$_2$XDH and SBA15XDH retained more than 50% of their initial activity. Moreover, after 240 min of incubation at 45 °C, XDH immobilized on silica nanoparticles or in hexagonal silica retained over 25 and over 30% of activity, respectively. As stability and catalytic activity of the enzyme after immobilization were improved, inactivation constant (k_D) and enzyme half-life ($t_{1/2}$) were also enhanced (Figure 4d). k_D and $t_{1/2}$ of free enzyme reached 0.0237 1/min and 29.2 min, respectively, while after immobilization on silica nanoparticles the values were 0.005 1/min and 138.6 min, respectively. When hexagonal SBA silica was used as support, an even higher enzyme half-life (277.2 min) and lower inactivation constant (0.0025 1/min) were obtained. It might be explained by the fact that due to immobilization in the pores of the matrix, enzyme molecules are better protected compared to attachment of biocatalysts onto the surface of the matrix. Free enzyme on the other hand was subject to total inactivation due mainly to thermal and chemical denaturation caused by heating and contact with base. However, negative effect of harsh reactive conditions on GDH and XDH was strongly hampered after enzyme immobilization due mainly to stabilization of the entire biocatalyst structure.

Kinetic Parameters of Free and Immobilized Enzymes

The K_M Michaelis-Menten constant and the V_{max} for free GDH were found to be 16.1 mM and 7.7 U/mg, respectively. After immobilization K_M increased and reached 21.8 and 28.7 mM for nanoSiO$_2$GDH and SBA15GDH, respectively. Simultaneously, V_{max} dropped 35 and 45% for nanoSiO$_2$GDH and SBA15GDH, respectively, compared to free catalyst. Nevertheless, it should be underlined that turnover number of immobilized biocatalysts was maintained almost unaltered as k_{cat} of nanoSiO$_2$GDH and SBA15GDH were 97 and 94% of that of free GDH, respectively (Table 3). Since turnover numbers of free and immobilized glucose dehydrogenase are comparable, increase in K_M value could be explained by the fact that after immobilization diffusional limitations occurred. As a result, active sites of the silica-bounded GDH are less accessible to the substrate and cofactor molecules, however, additional effects of cofactor-matrix and substrate-matrix interactions cannot be excluded either.[20] Thus, as suggested earlier by Zhou et al., a higher concentration of substrates is required to enhance their interactions with immobilized catalysts.[27] Moreover, as a result of enzyme attachment to the support, some of the active sites could be blocked, which reduces reaction rate and leads to drop in the maximum reaction velocity (V_{max}).[30] Baron et al., who immobilized GDH from *Bacillus* onto DEAE-Sephadex modified by glutaraldehyde, also made similar observations. However, in their study K_M was 4-fold greater after immobiliza-

Table 3. [a] [U/mL]Table 3
Kinetic parameters for free and silica immobilized GDH and XDH.

Analyzed parameter	freeGDH	nanoSiO$_2$GDH	SBA15GDH	freeXDH	nanoSiO$_2$XDH	SBA15XDH
K_M [mM]	16.1	21.8	28.7	0.31	0.34	0.45
V_{max} [U/mg]	7.7	5.1	4.1	0.81[a]	0.70	0.64
k_{cat} [1/s]	79	77	75	27	21	19
k_{cat}/K_m [1/s*mM]	4.9	3.5	2.6	87.1	61.7	42.2

[a] [U/mL]

tion and V_{max} was simultaneously almost 4-fold lower compared to the free enzyme.[20]

The K_M and V_{max} calculated for free XDH were 0.31 mM and 0.81 U/mL, respectively, and were comparable to those reported in our previous study where V_{max} has been found to be 0.56 U/mL.[31] The K_M of nanoSiO$_2$XDH and SBA15XDH were about 10 and 50% higher, respectively, compared with K_M of free XDH. However, the increase of K_M after immobilization observed for XDH was less significant than for GDH immobilized in this study. Simultaneously, a less significant drop of V_{max} was also noticed for immobilized XDH. These results could indicate that diffusional limitations that occurred after XDH immobilization were minimalized compared to GDH immobilization. This effect is probably related to the smaller molecular weight of XDH.[17] Nevertheless, the turnover number of nanoSiO$_2$XDH and SBA15XDH were about 80 and 70%, respectively, of that of the free enzyme, which suggested that some conformational changes in the structure of active site amino acids occurred upon immobilization.[30] These results support the data related to the retention of catalytic properties by immobilized XDH presented above (Table 2). It also should be emphasized that, irrespectively of the used enzyme, higher values of K_M were noticed for enzymes immobilized using SBA silica, compared to nanoSiO$_2$, indicating lower substrate affinity to bounded GDH and XDH. It is related to the fact that using mesoporous silica (SBA 15) higher diffusional limitations occurred because biomolecules are immobilized mainly into its pores, as in case of nanoSiO$_2$ enzyme is attached onto the surface of the support, as presented in Figure 1.

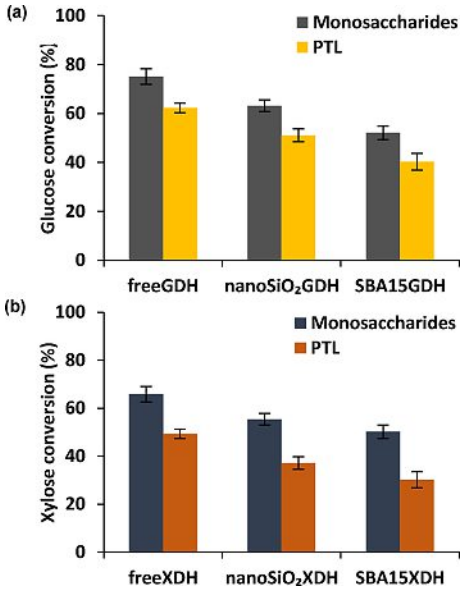

Figure 5. Conversion of (a) glucose to gluconic acid and (b) xylose to xylonic acid catalyzed by free and silica immobilized GDH and XHD, respectively, from monosaccharides solution and pretreated liquor (PTL). Dosage of enzyme: 0.5 mg of free or immobilized GDH or 200 U of free or immobilized XDH. All data are presented as means ± standard deviation.

Conversion of Biomass Liquors

Investigation of stability of free and immobilized enzymes was carried out based on model solutions of xylose and glucose. Thus, to evaluate practical applications of the biocatalytic systems produced, for conversion of glucose xylose two different real biomass solutions: (i) a stream of monosaccharides (glucose, xylose, arabinose) obtained after nanofiltration of PTL and (ii) pretreated liquor (PTL), were used.

Conversion of glucose to gluconic acid in the stream of monosaccharides by free GDH, nanoSiO$_2$GDH and SBA15GDH reached 76, 64 and 56%, respectively (Figure 5a), corresponding to biocatalytic productivity values of 17.08, 14.41 and 12.56 mg of gluconic acid per 1 mg of free, nanoSiO$_2$ or SBA 15 immobilized GDH, respectively (Table 4). By contrast, transformation of xylose from the same feed solution was lower and achieved 67, 57 and 52% for free, nanoSiO$_2$XDH and SBA15XDH, respectively (Figure 5b), corresponding to a biocatalytic productivity of 0.180, 0.155 and 0.141 mg of xylonic acid per 1 U of free, nanoSiO$_2$ or SBA 15 immobilized XDH, respectively as shown in Table 4. Higher conversion of glucose

Table 4. Biocatalytic productivity of free and immobilized GDH (mg of gluconic acid per mg of enzyme) and free and immobilized XDH (mg of xylonic acid per U of enzyme) after five consecutive catalytic cycles.

Analyzed parameter	Biocatalytic productivity (GDH in [mg/mg]) and (XDH in [mg/U])					
	freeGDH	nanoSiO$_2$GDH	SBA15GDH	freeXDH	nanoSiO$_2$XDH	SBA15XDH
Monosaccharides	32.11	52.44	45.61	0.307	0.502	0.461
PTL	31.12	51.10	39.08	0.204	0.336	0.279

to gluconic acid was mainly due to two factors. First of all, a greater amount of GDH was immobilized on silica carriers, moreover, attached GDH exhibited higher specific activity and activity retention compared to immobilized XDH. Second, concentration of glucose was about five times lower than xylose. The drop in conversion of both monosaccharides which was observed for immobilized enzymes compared to the free ones is related to decrease in enzyme activity upon immobilization, and has also been observed in other studies.[31,32]

Conversion of glucose and xylose presented in crude PTL (containing inhibitors) followed the same trend (Figure 5a,b). However, compared to the stream of monosaccharides, in case of the PTL feed solution, about 15 and 20% lower values of conversion were achieved for glucose and xylose, respectively. This is directly related to the presence of inhibitors, such as formic and acetic acids or furans, in the feed solution, which could inhibit enzyme catalytic properties. The presence of trace amounts of phenols and monovalent (K^+ or Na^+) or divalent (Mg^{2+} or Ca^{2+}) ions could also affect activity of both enzymes as reported earlier.[33] Nevertheless, the results presented clearly show that investigated biocatalytic systems demonstrated efficient conversion of monosaccharides and therefore could find practical applications in the food industry as well as in biorefinery.

Reusability of the Free and Immobilized GDH and XDH

One of the great advantages of immobilization is enhancement of enzyme reusability in sequential conversion processes, which leads to decrease in process costs. As can be seen, free GDH and XDH gradually lost their catalytic properties: GDH was inactivated after four catalytic cycles using a monosaccharides stream and after four cycles using PTL as feed solution, while XDH was inactivated after three catalytic cycles irrespective of the feed solution used (Figure 6). On the other hand, immobilized GDH retained around 70% of its initial activity and immobilized XDH maintained around 60% of its catalytic properties after three reaction cycles irrespective of the support material and feed solution. Moreover, after five reaction cycles, GDH and XDH immobilized using SBA 15 retained over 50% of their initial activity during conversion of glucose and xylose from monosaccharides solution, and over 40% of initial catalytic properties when PTL was used as feed solution. This retention of activity was higher than retention obtained when silica nanoparticles were used as carrier, as after five reaction cycles nanoSiO_2GDH and nanoSiO_2XDH maintained, respectively, only 43 and 39% of their catalytic properties with monosaccharides solution, and 38 and 33%, respectively, of their catalytic properties with PTL as feed solution.

The above results are in agreement with the data of biocatalytic productivity. After five consecutive reaction cycles, productivity of gluconic acid with the monosaccharides solution as the feed by free GDH reached 32.11 mg of gluconic acid per mg of enzyme. Productivity of nanoSiO_2GDH was about 1.6 fold higher (52.44 mg/mg), while productivity of SBA15GDH was about 1.4 fold higher (45.61 mg/mg) compared to the free enzyme (Table 4). Even higher increase in biocatalytic productivity of xylose was noticed using silica immobilized XDH and monosaccharides solution. After five reaction steps free XDH exhibited a productivity of 0.307 mg of xylonic acid per 1 unit of XDH, while productivity of nanoSiO_2XDH and SBA15XDH was 0.502 mg/U (1.7 fold) and 0.461 mg/U (1.6 fold), respectively. It should also be mentioned that lower values of biocatalytic productivity of gluconic and xylonic acid were observed using PTL as a feed solution; this result is directly related to higher concentration of glucose and xylose in PTL compared to in the stream of monosaccharides. These results

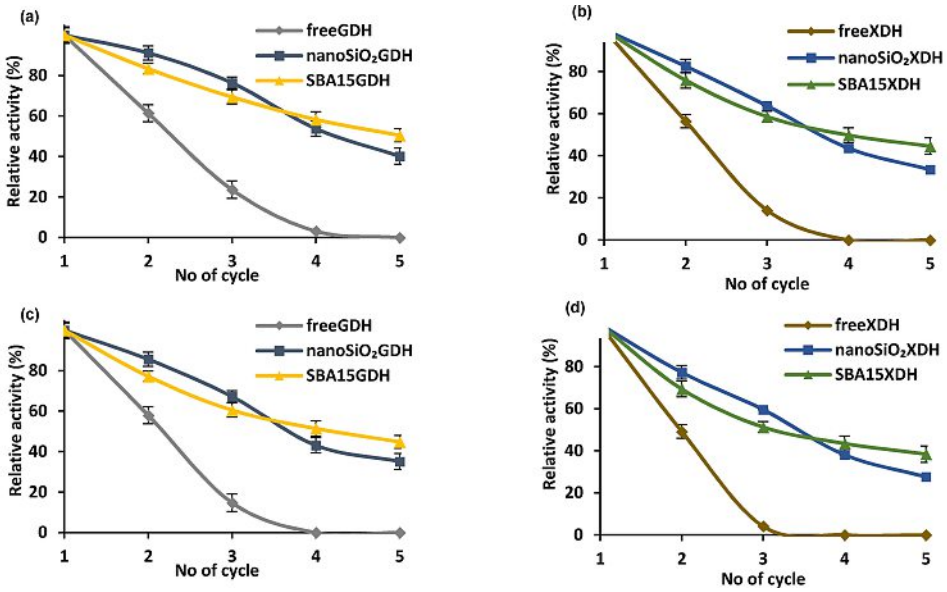

Figure 6. Reusability of the free and silica immobilized GDH and XHD evaluated based on consecutive conversion of glucose and xylose, respectively, using monosaccharides solution after nanofiltration (a) and (b) and PTL (c) and (d) as feed solution. All data are presented as means ± standard deviation.

confirm that reusability of the immobilized GDH and XDH was significantly improved. Nevertheless, it should be emphasized that irrespective of the feed solution used, during initial reaction cycles (up to third cycle), enzymes immobilized onto silica nanoparticles exhibited higher catalytic properties, but in further conversion steps, SBA 15 based systems showed higher activity. This phenomenon could be explained by the fact that enzyme immobilized in pores of hexagonal silica is better protected before inactivation and elution from the matrix, and thus its activity is less affected during the sequential conversion process. Higher retention of catalytic activity by enzymes used for conversion of both glucose and xylose from monosaccharides solution is probably related to the fact that the amount of enzyme inhibitors such as metal ions, inorganic acids and furans was significantly reduced compared to their presence in the PTL solution. Nevertheless, gradual decrease in enzyme activity after just a few catalytic cycles could be explained by several factors, such as enzyme inhibition by product, structural modification of the enzymes as well as by catalyst inactivation caused by their thermal and pH denaturation.[34] It should be also mentioned that due mainly to adsorption interactions, some enzyme leakage from the matrix (up to 30% after last cycle) also occurred as a contributory factor. Earlier studies reported that glucose-6-phosphate dehydrogenase encapsulated in silica-based hydrogels retained less than 40% of its initial activity just after one reaction cycle,[35] as in another study, 40% of activity retention was observed after seven reaction cycles when glucose-6-phosphate dehydrogenase was immobilized in alginate.[23]

Conclusions

Our study provides proof-of-concept for the immobilization of glucose dehydrogenase (GDH) and xylose dehydrogenase (XDH) on silica nanoparticles and hexagonal mesoporous SBA15 silica, and application of the obtained biocatalytic systems for effective conversion of glucose and xylose from biomass liquors. Specific activity of free GDH and XDH (assessed as NADH consumption during reduction of glucose and xylose, respectively) was comparable and reached 42.2 U/mg and 46.8 U/mL, respectively. After immobilization, both enzymes exhibited high catalytic activity retention, but better loadings and activity retention were obtained for GDH and XDH immobilized on the surface of silica nanoparticles than on the mesoporous silica particles, which confirms that type of support material affects properties of the biocatalytic systems obtained. Nevertheless, both silica-immobilized enzymes are characterized by improved thermal stability, with half-life of SBA15GDH and SBA15XDH being increased 7.25 and 9.5 fold, respectively as compared to free biocatalysts, after incubation for four hours at 45 °C. However, immobilization did not affect the pH optima of any of the two enzymes, regardless of the type of silica immobilization material, and the immobilized enzymes showed the same high activity over a broad range of pH (over 50% activity at pH range 8–10). Robustness at higher pH, above the pK_a of gluconic and xylonic acid, is of particular interest, because this feature facilitates simple separation of the gluconic and xylonic acid from reaction mixture even by a simple membrane filtration. Additionally, the immobilized enzymes exhibited improved reusability; not only was their catalytic activity retained after five consecutive reaction cycles but the biocatalytic productivity was improved about 1.6 fold by nanoSiO_2GDH and nanoSiO_2XDH compared to the free enzymes. The data thus clearly shown that immobilization of GDH and XDH is an attractive approach for efficient transformation of glucose and xylose into valuable products. Hopefully, the data may stimulate further development of the use of monosaccharide dehydrogenases in biorefining and separation of monosaccharides in genuine biomass liquors.

Experimental Section

Chemicals and Reagents

Commercially available silica nanopowder of 10–20 nm particle size (nanoSiO_2) and mesoporous SBA 15 silica (< 150 μm particle size) with hexagonal pore morphology and pore size up to 20 nm (SBA 15) used in this study were provided by Sigma-Aldrich (Steinheim, Germany). Tris-HCl buffer, phosphate buffer, β-nicotinamide adenine dinucleotide hydrate (NAD+), β-nicotinamide adenine dinucleotide, reduced disodium salt hydrate (NADH), D-glucose, D-xylose and glucose dehydrogenase from *Pseudomonas* sp. (GDH) (EC 1.1.1.47) were purchased from Sigma-Aldrich (Steinheim, Germany). Xylose dehydrogenase (XDH) (EC 1.1.1.175) was provided by Megazyme (Bray, Wicklow, Ireland). All chemicals were of analytical grade and were used as received from the suppliers without further purification.

Real Liquors

The pretreated liquor (PTL) used in this study was obtained after combined acid and hydrothermal pretreatment of the biomass. For pretreatment, diluted sulfuric acid and high temperature steam (180 °C) were injected in the reactor containing soaked wood for a 10 min. After pretreatment, the liquid fraction was separated from the solids by pressing in reactor. Prior to use, the PTL was filtered using the microfiltration membrane GR40PP (MWCO 100 kDa) at 4 bar in an Amicon 8050 (Millipore, Burlington, MA, USA) stirred cell to clarify the solution. The concentration of monosaccharides, glucose, xylose and arabinose was 13.3 g/L, 55.2 g/L, and 2.1 g/L, respectively. The stream of monosaccharides without inhibitors (inorganic acids and furans) containing glucose (10.3 g/L), xylose (48.8 g/L) and arabinose (1.9 g/L) was obtained after nanofiltration of PTL at 40 bar using a NF90 nanofiltration membrane (MWCO 200–400 Da) in a stainless steel stirred cell (HP4750, Sterlitech Corporation, Kent, WA, USA).

Immobilization of GDH and XDH

For the immobilization of GDH and XDH, 50 mg of silica nanoparticles or silica SBA 15 was immersed in 2 mL of enzyme solution in phosphate buffer at pH 7 containing 0.15 mg (30 U) of GDH or 30 U of XDH. The immobilization was carried out by incubation of the silica support (nanoSiO_2 or SBA 15) with each enzyme solution for 3 h at 4 °C in an IKA KS 4000i control incubator (IKA Werke GmbH, Germany) with mixing at 200 rpm. The immobilized enzymes (nanoSiO_2GDH, SBA15GDH, nanoSiO_2XDH, SBA15XDH) were recovered from the solution by centrifugation at 4000 rpm for

15 min (Sigma 4 K15, Sigma Laborzentrifugen GmbH). The protein content in the samples after immobilization (amount of immobilized enzyme (mg/g)) was determined by the Bradford method [Equation (1)] as the difference in the initial enzyme dosage and the concentration of protein present in the supernatant after immobilization[36] and considering mass of the support material, according to Equation 1. From the results of the Bradford method, immobilization yield (%) was calculated [Equation (2)].

$$\text{Amount of immobilized enzyme} = \frac{c_i V_i - c_s V_s}{m_{support}} \quad (1)$$

$$\text{Immobilization yield } (\%) = \frac{c_i V_i - c_s V_s}{c_i V_i} \cdot 100\,\% \quad (2)$$

where c_i and c_s denote concentration of enzyme before and after immobilization (mg/mL or U/mL), V_i and V_s denote volume of the solution (mL) before and after immobilization, and $m_{support}$ is the mass of the support material (g).

GDH and XDH Activity

Activity assays for GDH and XDH were performed spectrophotometrically during kinetic reduction of NAD+ to NADH, as presented below, using a standard calibration curve of NADH. One unit of free or immobilized enzyme activity was defined as the quantity of enzyme required to produce 1 μM of NADH per minute under the assay conditions. Specific activity values (U/mg) of free and immobilized enzymes are presented as initial enzyme activity retained per unit mass of enzyme, and per unit mass of enzyme and solid support, respectively. The activity retention (%) of immobilized enzyme was defined as the percentage activity of the immobilized GDH and XDH compared to the catalytic activity of free enzymes. All measurements were done in triplicate and error bars are presented as means ± standard deviation.

GDH Activity Assay

Catalytic activity of free and immobilized GDH was evaluated spectrophotometrically by measuring the absorbance at λ= 340 nm (Shimadzu UV1280, Shimadzu, Japan) during kinetic reduction of NAD+ to NADH. The reaction was carried out for 2 min in a styrene cuvette with a volume of 1 mL of reaction mixture containing 20 U of free or immobilized GDH, 3 mM NAD+ and 50 mM D-glucose in Tris-HCl buffer at pH 8, 45°C.

XDH Activity Assay

Activity of free and immobilized XDH was determined spectrophotometrically by following changes in the absorbance at λ=340 nm during kinetic reduction of NAD+ to NADH.[37] The reaction was carried out in a styrene cuvette with a volume of 1 mL of reaction mixture containing 30 U of free or immobilized XDH, 3 mM NAD+ and 70 mM D-xylose in Tris-HCl buffer at pH 8 for 2 min at 45°C.

pH Profiles of Free and Immobilized Enzymes

The pH profiles of free and immobilized GDH and XDH were examined using the methodology described above, at pH values ranging from 6 to 10 at 45 °C. The pH of the solution was adjusted using 0.1 M HCl and 0.1 M NaOH. All measurements were made in triplicate and error bars are presented as means ± standard deviation.

Temperature Profiles of Free and Immobilized Enzymes

The temperature profiles of free and immobilized glucose dehydrogenase and xylose dehydrogenase were evaluated based on the above-mentioned methodology at temperatures varying from 30 °C to 60 °C in steps of 5 °C, at pH 8. Prior to spectrophotometric measurements, free and immobilized enzymes were incubated at the desired temperature for 30 min. All measurements were made in triplicate and error bars are presented as means ± standard deviation.

Stability of Free and Immobilized Enzymes

Stability of both free and immobilized enzyme over time was evaluated after incubating the native and immobilized enzymes for 240 min under optimum pH and temperature conditions. For free and silica immobilized GDH, the optima were 45 °C and pH 8, while for free and silica immobilized XDH, the optima were pH 8 and 40 °C and pH 8 and 45 °C, respectively. The relative activity of free and immobilized enzyme was further determined after a specified period of time. The initial activity of free GDH and XDH was defined as 100% activity. The inactivation constant (k_D), and half-life ($t_{1/2}$) were evaluated based on the linear regression slope. All measurements were made in triplicate and error bars are presented as means ± standard deviation.

Kinetic Parameters of Free and Immobilized Enzymes

Examination of the kinetic parameters – the Michaelis-Menten constant (K_M), maximum reaction rate (V_{max}), turnover number (k_{cat}) and specificity constant (k_{cat}/K_M) – of free and immobilized GDH and XDH was performed based on the model enzymatic reactions (see section GDH and XDH activity), using various concentrations of NAD+. The kinetic parameters were calculated based on Hanes-Wolf plots under optimum assay conditions.

Glucose and Xylose Conversion

In the presented study, two biomass liquors were used which contained monosaccharides only (monosaccharides stream) and monosaccharides with inhibitors (PTL) (see section Real liquors). The reaction was performed in glass tubes. For the reaction, 1 mL of monosaccharides solution or PTL was used to which was added 0.5 mg of free or immobilized GDH or 200 U of free or immobilized XDH and 10 mM of NAD+. Prior to the reaction, the pH of mixture was adjusted to 8 and to 8.5 for GDH and XDH, respectively using 0.1 M NaOH. After 30 min of the process, the reaction was terminated by addition of 2 mL of 1 M HCl and the mixture was subjected to HPLC analysis.

Conversion of glucose to gluconic acid by GDH and xylose to xylonic acid by XDH was evaluated based on the results of High Performance Liquid Chromatography (HPLC) and calculated using Equation 3. Shimadzu Corp. (Japan) equipment was used in the HPLC-analysis (LC-20AD, DGU-20A3, SIL-20AC, SCL-10 A, CTO-10A). The column system consisted of an Aminex HPX-87H Ion Exclusion Column (300 mm × 8.7 mm) (Bio-Rad) and a security guard (H+) pre-column. The temperature was 63 °C, the eluent was 4 mM H_2SO_4 and the flow rate was 0.6 mL/min. Carbohydrates and acids were detected using a refractive index detector (RID-10 A). Samples were diluted with the eluent to obtain concentrations of monosaccharides, and acids in the range of 0.05–5 g/L and 0.025–3 g/L, respectively.

$$\text{Conversion } (\%) = \frac{C_F - C_P}{C_F} \cdot 100\,\% \quad (3)$$

where C_F and C_P denote xylose or glucose concentration (g/L) in feed solution and after enzymatic conversion, respectively.

Reusability Study of Free and Immobilized Enzymes

The reusability of the free and immobilized GDH and XDH was examined by measuring conversion of xylose and glucose in the stream of monosaccharides and pretreated liquor, according to methodology presented in the above section, over five consecutive reaction cycles. After each conversion cycle, the immobilized GDH and XDH was separated from the reaction mixture by centrifugation and washed with Tris-HCl buffer solution before the next cycle. Free enzyme was separated from the reaction mixture by nanofiltration at 4 bar in an Amicon 8050 (Millipore, USA) using an NF90 membrane. The conversion of glucose and xylose by GDH and XDH, respectively, in the first catalytic cycle was defined as 100%. The biocatalytic productivity of free and immobilized enzyme was expressed as mass of product formed (mg) by mass of the enzyme used.

Statistical Analysis

Statistically significant differences were determined by one-way ANOVA performed in SigmaPlot 12 (Systat Software Inc., USA) using Tukey's test. Statistical significance was established at a $p < 0.05$ level.

Acknowledgements

This work was supported by research grant funds from the National Science Center Poland in accordance with decision no. DEC-2016/20/T/ST8/00391.

Conflict of Interest

The authors declare no conflict of interest.

Keywords: glucose dehydrogenase · xylose dehydrogenase · enzyme immobilization · silica · biomass conversion

[1] B. V. Twala, B. T. Sewell, J. Jordaan, *Enzyme Microb. Technol.* **2012**, *50*, 331–336.
[2] T. Pongtharangkul, P. Chuekitkumchorn, N. Suwanampa, P. Payongsri, K. Honda, W. Panbangred, *AMB Express* **2015**, *5*, 68–79.
[3] S. Ferri, K. Kojima, K. Sode, *J. Diabetes Sci. Technol.* **2011**, *5*, 1068–1076.
[4] S. T. Morthensen, A. S. Meyer, H. Jørgensen, M. Pinelo, *Biochem. Eng. J.* **2017**, *117*, 41–47.
[5] T. Werpy, G. Petersen, *U.S. Department of Energy*, National Renewable Energy Laboratory, **2004**.
[6] S. Ramachandran, P. Fontanille, A. Pandey, C. Larroche, *Food Technol. Biotechnol.* **2006**, *44*, 185–195.
[7] W. Niu, M. N. Molefe, J. W. Frost, *J. Am. Chem. Soc.* **2003**, *125*, 12998–12999.
[8] H. Liu, K. N. G. Valdehuesa, G. M. Nisola, K. R. M. Ramos, W. J. Chung, *Bioresour. Technol.* **2012**, *115*, 244–248.
[9] J. Atalah, Y. Zhou, G. Espina, J. M. Blamey, R. P. Ramasamy, *Catal. Sci. Technol.* **2018**, *8*, 1272.
[10] K. Murai, T. Nonoyama, T. Saito, K. Kato, *Catal. Sci. Technol.* **2012**, *2*, 310.
[11] J. Zdarta, A. S. Meyer, T. Jesionowski, M. Pinelo, *Adv. Colloid Interface Sci.* **2018**, *258*, 1–20.
[12] J. Zdarta, K. Antecka, R. Frankowski, A. Zgoła-Grześkowiak, H. Ehrlich, T. Jesionowski, *Sci. Total Environ.* **2018**, *615*, 784–795.
[13] M. Markiton, S. Boncel, D. Janas, A. Chrobok, *ACS Sustainable Chem. Eng.* **2017**, *5*, 1685–1691.
[14] P. F. Fulvio, S. Pikus, M. Jaroniec, *J. Colloid Interface Sci.* **2005**, *287*, 717–720.
[15] J. Zdarta, A. S. Meyer, T. Jesionowski, M. Pinelo, *Catalysts* **2018**, *8*, 92.
[16] P. Zucca, E. Sanjust, *Molecules* **2014**, *19*, 14139–14194.
[17] K. Yamanaka, M. Gino, R. Kaneda, *Agric. Biol. Chem.* **1977**, *41*, 1493–1499.
[18] P. K. Srivastava, S. Singh, *Prep. Biochem. Biotechnol.* **2013**, *43*, 376–384.
[19] L. Li, B. Liang, F. Li, J. Shi, M. Mascini, Q. Lang, A. Liu, *Biosens. Bioelectron.* **2013**, *42*, 156–162.
[20] M. Baron, J. D. Fontana, M. F. Guimaraes, J. Woodward, *Appl. Biochem. Biotechnol.* **1997**, *63*, 257–268.
[21] N. Aissaoui, J. Landoulsi, L. Bergaoui, S. Boujdaya, J. Lambert, *Enzyme Microb. Technol.* **2013**, *52*, 336–343.
[22] C. M. Moore, N.L Akers, A. D. Hill, Z. C. Johnson, S. D. Minteer, *Biomacromolecules* **2004**, *5*, 1241–1247.
[23] F. Secundo, *Chem. Soc. Rev.* **2013**, *42*, 6250–6261.
[24] H. Li, W. Xiao, P. Xie, L. Zheng, *Enzyme Microb. Technol.* **2018**, *10*, 66–73.
[25] S. Singh, P. K. Srivastava, *Advances in Enzyme Research* **2014**, *2*, 134–149.
[26] N. N. Mubarak, J. R. Wong, K. W. Tan, J. N. Sahu, E. C. Abdullah, N. N. Jayakumar, P. Ganesan, *J. Mol. Catal. B* **2014**, *107*, 124–131.
[27] Q. Z. K. Zhou, X. D. Chen, *Biochem. Eng. J.* **2001**, *9*, 33-40.
[28] Q. Z. K. Zhou, X. D. Chen, *J. Food Eng.* **2001**, *48*, 69–74.
[29] F. Marpani, Z. Sarossy, M. Pinelo, A. S. Meyer, *Biotechnol. Bioeng.* **2017**, *117*, 2762–2770.
[30] S. A. Yamanaka, B. Dunn, J. S. Valentine, J. I. Zink, *Journal of American Chemical Society* **1995**, *117*, 9095–9096.
[31] M. Zheng, Z. Su, X. Ji, G. Ma, P. Wang, S. Zhang, *J. Biotechnol.*, **2013**, *168*, 212–217.
[32] S. Sahin, I. Ozmen, *J. Mol. Catal. B* **2016**, *133*, S25–S33.
[33] P. L. James, C. Anthony, *Biophysica Acta* **2003**, *1674*, 200–205.
[34] J. Jordan, C. S. S. R. Kumar, C. Theegala, *J. Mol. Catal. B* **2011**, *68*, 139–146.
[35] S. Cumana, I. Ardao, A. P. Zeng, I. Smirnova, *Eng. Life Sci.* **2014**, *14*, 170–179.
[36] M. M. Bradford, *Analytical Biochemistry* **1976**, *72*, 248–254.
[37] C. L. Lee, R. E. Kibblewhite, C. D. Paavola, W. J. Orts, K. Wagschal, *J. Microbiol. Biotechnol.* **2017**, *27*, 77–83.

Manuscript received: August 17, 2018
Accepted Article published: September 11, 2018
Version of record online: October 16, 2018

materials

MDPI

Article

Co-Immobilization of Glucose Dehydrogenase and Xylose Dehydrogenase as a New Approach for Simultaneous Production of Gluconic and Xylonic Acid

Jakub Zdarta [1,*], Karolina Bachosz [1], Oliwia Degórska [1], Agata Zdarta [1], Ewa Kaczorek [1], Manuel Pinelo [2], Anne S. Meyer [3] and Teofil Jesionowski [1,*]

1 Institute of Chemical Technology and Engineering, Faculty of Chemical Technology, Poznan University of Technology, Berdychowo 4, PL-60965 Poznan, Poland
2 Department of Chemical and Biochemical Engineering, DTU Chemical Engineering, Technical University of Denmark, Soltofts Plads 229, DK-2800 Kgs. Lyngby, Denmark
3 Department of Biotechnology and Biomedicine, DTU Bioengineering, Technical University of Denmark, Soltofts Plads 224, DK-2800 Kgs. Lyngby, Denmark
* Correspondence: jakub.zdarta@put.poznan.pl (J.Z.); teofil.jesionowski@put.poznan.pl (T.J.); Tel.: +48-616-653-747 (J.Z.)

Received: 24 August 2019; Accepted: 24 September 2019; Published: 27 September 2019

Abstract: The conversion of biomass components catalyzed via immobilized enzymes is a promising way of obtaining valuable compounds with high efficiency under mild conditions. However, simultaneous transformation of glucose and xylose into gluconic acid and xylonic acid, respectively, is an overlooked research area. Therefore, in this work we have undertaken a study focused on the co-immobilization of glucose dehydrogenase (GDH, EC 1.1.1.118) and xylose dehydrogenase (XDH, EC 1.1.1.175) using mesoporous Santa Barbara Amorphous silica (SBA 15) for the simultaneous production of gluconic acid and xylonic acid. The effective co-immobilization of enzymes onto the surface and into the pores of the silica support was confirmed. A GDH:XDH ratio equal to 1:5 was the most suitable for the conversion of xylose and glucose, as the reaction yield reached over 90% for both monosaccharides after 45 min of the process. Upon co-immobilization, reaction yields exceeding 80% were noticed over wide pH (7–9) and temperature (40–60 °C) ranges. Additionally, the co-immobilized GDH and XDH exhibited a significant enhancement of their thermal, chemical and storage stability. Furthermore, the co-immobilized enzymes are characterized by good reusability, as they facilitated the reaction yields by over 80%, even after 5 consecutive reaction steps.

Keywords: glucose dehydrogenase; xylose dehydrogenase; enzymes immobilization; co-immobilization; silica SBA 15; biomass conversion

1. Introduction

Over the last decades, the number of porous materials has significantly increased. Due to their various properties, such as a high porosity, defined pore structure and size, as well as numerous functional groups, they find application in many fields of science and industry [1]. Mesoporous silicas, due to their properties, are widely employed in different fields, such as catalysis, adsorption, enzyme immobilization or drug delivery [1,2]. Among others, Santa Barbara Amorphous 15 silica (SBA 15) is a great example of these materials, owing its name to the place where it was discovered. The structure of the SBA 15 mesoporous silica is composed of hexagonal, two-dimensional internal pores with diameters between 5 nm and 30 nm [3]. Due to such a system, SBA 15 silica is characterized by a considerably

expanded surface area, which is why it is a good material for the adsorption of various compounds and/or enzyme immobilization [4]. In contrast to other types of silicas, during the adsorption or immobilization of biologically active substances (for example enzymes) using mesoporous SBA 15, the substances are adsorbed inside the pores, resulting in changes in their volume and size, as well as a better protection of the attached molecules against harsh reaction conditions [5].

As has already been mentioned, numerous molecules, including enzymes, can be attached using the mesoporous silica SBA 15. Immobilization is the process leading to the total or partial limitation of the movement of substances or biological materials by binding them to a carrier. There are three main types of immobilization: (i) without a carrier, (ii) inside the carrier or (iii) onto a carrier [6]. By applying the enzyme to the carrier, the scope of its action is usually broadened, the separation of products from the reaction mixture is enhanced, and the reuse as well as biocatalytic productivity of the biomolecules are improved [7]. However, the selection of a support material plays a key role in the immobilization process. A carrier that is ideal for any type of enzyme has not yet been created; however, among other materials, silica-based materials seem to be a suitable enzyme support due to their susceptibility to surface modification, their non-toxicity, as well as their chemical and physical stability. Moreover, silica possesses numerous hydroxyl groups that promote immobilization, by both covalent binding and adsorption [6]. Mesoporous silica materials, embracing SBA 15, have been previously used as supports for the immobilization of enzymes for various applications, including processes of biomass pretreatment and its further conversion. For instance, Xie et al. confirmed that by immobilizing the biomolecules on a carrier such as silica, their catalytic efficiency can be increased. The carrier was completely inert during the transesterification of soybean oil, but enabled the easy removal of the biocatalysts from the system. Furthermore, after five cycles of oil conversion, the SBA 15-based catalytic system showed great stability and activity, as it retained over 90% of its initial activity [8].

Plant-based biomass is of particular interest, mainly due to the fact that it can be an alternative for the fossil fuels platform, for the production of energy or biofuels, such as ethanol [7]. Biomass consists mainly of cellulose, hemicellulose and lignin, compounds which might act as a platform for obtaining valuable chemical substances [9]. Biomass is acquired from products, waste and residues from agricultural and forestry production, as well as from part of the waste originating from industrial processing. However, in order to obtain valuable compounds from biomass, it has to be properly pretreated to release valuable sugars, such as pentoses (mainly xylose) and hexoses (mainly glucose). Various pretreatment and conversion methods have been developed, including mechanical, physical and biological techniques [10]. Nevertheless, due to mild process conditions, the limited requirement for sophisticated apparatuses and high selectivity, biological methods based on enzymes are of particular interest [11]. It should be emphasized that the effectiveness of hydrolysis or the conversion of lignocellulose substrates depends on their effective preparation and the precise selection of the enzyme combination.

In our previous study, we demonstrated and explored the protocol for the separate immobilization of glucose dehydrogenase and xylose dehydrogenase using nano-SiO_2 and mesoporous SBA 15 silica supports. It has been established that, among others, immobilized enzymes exhibited a significantly higher activity over a wide temperature and pH range as compared to the free form of the biocatalysts. Furthermore, we have proved that immobilized biocatalysts are capable of an independent and efficient conversion of xylose into xylonic acid and glucose into gluconic acid [12]. Nevertheless, further study concerning the improvement of the process efficiency as well as facilitating its simplicity are still highly required. In addition, we would like to emphasize that the literature data related to the co-immobilization of enzymes for the simultaneous conversion of biomass compounds are limited.

Therefore, we have here undertaken a study related to the co-immobilization of two industrially relevant enzymes—glucose dehydrogenase (GDH) and xylose dehydrogenase (XDH)—using mesoporous SBA 15 silica for the efficient and concurrent conversion of glucose and xylose into gluconic acid (GA) and xylonic acid (XA), respectively. As part of the research, we also determined the optimal GDH:XDH activity ratio, as well as the effect of process duration and various pH and

temperature conditions on the simultaneous production yield of GA and XA. Moreover, the parameters that are important from a practical application point of view, such as the stability and reusability of the co-immobilized biocatalysts, have also been investigated in detail.

2. Materials and Methods

2.1. Chemicals and Reagents

Commercial mesoporous SBA 15 silica (<150 mm particle size) with a hexagonal pore morphology and pore size of up to 20 nm (SBA 15), glucose dehydrogenase from *Pseudomonas* sp. (EC 1.1.1.118) (GDH), D-glucose (Glu), D-xylose (Xyl), gluconic acid sodium salt (GA), xylonic acid lithium salt (XA), acetate buffer, phosphate buffer and tris-HCl buffer were provided by Sigma-Aldrich (Steinheim, Germany). β-Nicotinamide adenine dinucleotide hydrate (NAD^+), β-nicotinamide adenine dinucleotide, reduced disodium salt hydrate (NADH), Coomassie Brilliant Blue CBB G-250, pyridine, MSTFA, hexane, 96% ethanol, hydrochloric acid and 85% H_3PO_4 were purchased from Sigma-Aldrich (Steinheim, Germany). Xylose dehydrogenase (EC 1.1.1.175) (XDH) was provided by Megazyme (Bray, Wicklow, Ireland). All chemicals were of analytical grade and were used as received, without further purification.

2.2. Co-Immobilization of GDH and XDH

For the co-immobilization of GDH and XDH, 100 mg of SBA 15 silica was immersed in 1 mL of phosphate buffer at pH 8 containing 0.15 mg (30 U) of glucose dehydrogenase or 150 U of xylose dehydrogenase. To evaluate the most suitable activity ratio of GDH:XDH, the immobilization was carried out using various initial GDH:XDH ratios (1:1, 1:2, 1:5, 1:10). The immobilization was performed via the incubation of the samples for 2 h at 4 °C using an IKA KS 4000i control incubator (IKA Werke GmbH, Staufen im Breisgau, Germany) with mixing at 150 rpm. Afterwards, the obtained biocatalytic systems were centrifuged for 15 min (4000 rpm at a temperature of 4 °C) and used for the glucose and xylose conversion experiments. The amount of co-immobilized enzymes (U/g) was determined spectrophotometrically (Jasco V-750 spectrophotometer, Jasco, Tokyo, Japan) based on the Bradford method [13] and was considered as the difference between the initial enzyme amount and the concentration of the proteins in the supernatant after immobilization, also taking into account the mass of the used support material. Based on these measurements, the immobilization yield was also determined by considering the initial and final concentrations of the enzyme and the volume of the solution before and after immobilization.

2.3. Activity and Kinetic Parameters of the Free and Immobilized Enzymes

The activity of the free and co-immobilized glucose dehydrogenase and xylose dehydrogenase was examined based on the spectrophotometric measurements at $\lambda = 340$ nm (Jasco V-750 spectrophotometer, Jasco, Tokyo, Japan), carried out based on the model reaction of the reduction of the enzymatic cofactor NAD^+ to NADH. Briefly, the reaction was performed in 3 mL of phosphate buffer at pH 8 containing 20 mM of NAD^+, and 100 mM of D-glucose or D-xylose, to which 10 U of GDH and 50 U of XDH (the ADH:XDH ratio was 1:5) of the free or co-immobilized enzymes was added. The reaction mixture was than vigorously shaken on a KS260 Basic incubator (IKA Werke GmbH, Staufen im Breisgau, Germany) at 40 °C for 5 min. One unit of free or co-immobilized enzymes activity was defined as the amount of the biocatalyst required to produce 1 mM of product per minute under the optimal assay conditions. The specific activities of the free and co-immobilized GDH and XDH were expressed in U/mg or U/mL (for XDH) and represent the initial enzyme activity retained per unit mass of enzyme, or per unit mass of enzyme and solid support, respectively.

The kinetic parameters, Michaelis-Menten constant (K_M) and maximum reaction rate (V_{max}) of the free and co-immobilized XDH and GDH were examined based on the above-presented reaction, using various concentrations of NAD^+, ranging from 0.01 to 50 mM, by measuring the initial reaction

rates. The progress of the reaction was followed spectrophotometrically at λ = 340 nm (Jasco V-750 spectrophotometer, Jasco, Tokyo, Japan). The kinetic parameters were examined using a Hanes-Woolf plot under optimum assay conditions.

2.4. Conversion of Glucose to Gluconic Acid and Xylose to Xylonic Acid Catalyzed by Free and Co-Immobilized Enzymes

The simultaneous enzymatic conversion of glucose to gluconic acid and xylose to xylonic acid was performed using an activity ratio of 1:5 of free or co-immobilized GDH:XDH. For this reason, 30 U of GDH and 150 U of XDH of the free or co-immobilized biocatalysts were added to the 1 mL of reaction mixture containing: 55 mM of D-glucose, 345 mM of D-xylose and 100 mM of NAD^+ in phosphate buffer at pH 8. The reaction was carried out for 60 min at 40 °C with mixing at 100 rpm using an IKA KS 4000i control incubator (IKA Werke GmbH, Staufen im Breisgau, Germany). After 60 min, the process was terminated by adding 1 M HCl, and the obtained samples were analyzed by gas chromatography (GC-MS) to determine the concentration of the gluconic acid, xylonic acid and reaction yield. One unit of enzyme activity (U) of the free and co-immobilized enzymes was defined as the amount of GDH or XDH that produced 1 μmol of gluconic and xylonic acid, respectively, per minute. The yields (%) of the gluconic and xylonic acid were calculated as the ratio of the molar concentration of gluconic and xylonic acid obtained in relation to the initial molar concentration of glucose and xylose, respectively. All of the experiments were performed in triplicate, and error bars were presented as mean values ± standard deviation.

2.4.1. Time Course of the Conversion of Glucose to Gluconic Acid and Xylose to Xylonic Acid

The effect of the process duration on the changes of the concentration of gluconic acid and xylonic acid was determined based on the above-mentioned reaction performed under optimal process conditions (pH 8, temperature 40 °C) over 60 min. The reaction was followed by collecting samples at every specified period of time, and the production of GA and XA was evaluated using GC-MS measurements.

2.4.2. Effect of pH and Temperature on Enzymatic Conversion of Glucose to Gluconic Acid and Xylose to Xylonic Acid

The effect of the pH and temperature (pH and temperature profiles of co-immobilized GDH and XDH) on the conversion of glucose and xylose was examined based on the above-mentioned reaction over a pH ranging from 5 to 10 (at a temperature of 40 °C) using buffer solutions at the desired pH to adjust the pH and at temperature values ranging from 20 to 70 °C with a step size of 10 °C (at pH 8). After 60 min of the process, the reaction was terminated and the samples were analyzed using GC-MS.

2.4.3. Stability of the Free and Co-Immobilized GDH and XDH

The stability the free and co-immobilized GDH and XDH over time was determined based on the simultaneous catalytic conversion of glucose and xylose, after incubating the samples for 120 min in a phosphate buffer solution at pH 8 at 40 °C. After the specified period of time, the samples were used to catalyze the conversion of glucose into gluconic acid and xylose into xylonic acid, as described in Section 2.3. Furthermore, the samples were subjected to a GC-MS analysis, and, based on the obtained results, the relative activity in terms of the GA and XA production was determined. The initial activity of the free and co-immobilized GDH and XDH was defined as a 100% activity. The inactivation constant (k_D) and enzymes' half-life values ($t_{1/2}$) were determined based on the linear regression slope for ln(RA) vs. time.

2.4.4. Storage Stability and Reusability of the Free and Co-Immobilized GDH and XDH

The storage stability of the free and co-immobilized GDH and XDH, stored in phosphate buffer at pH 8 and 4 °C, was examined based on the above-mentioned reaction of glucose and xylose conversion

over 20 days of storage. After the process, the samples were analyzed using GC-MS, and the results were used to calculate the relative activity. For the purposes of the study of the storage stability, the initial value of the activity of the free and co-immobilized GDH and XDH was defined as a 100% activity.

The reusability of the co-immobilized GDH and XDH was determined during the production of GA and XA over ten repeated simultaneous conversion cycles of glucose and xylose carried out under optimal process conditions for 60 min. After each conversion step, the biocatalytic system was centrifuged from the reaction mixture, washed several times using a phosphate buffer at pH 8 and placed into a fresh reaction solution. After the process, the samples were analyzed using GC-MS, and the results were used to calculate the GA and XA yields.

2.5. Analytical Techniques

The morphology of the silica SBA 15 before and after the GDH and XDH co-immobilization was investigated using a transmission electron microscopy (TEM) JEOL JEM-1200EX II (JEOL, Tokyo, Japan) instrument at an accelerating voltage of 80 kV.

In order to identify the functional groups that were present on the surface of the analyzed materials and to confirm the effective enzyme immobilization, Fourier transform infrared spectroscopy (FTIR) was used. The samples were analyzed in the form of KBr pellets formed by mixing 1 mg of the sample with 200 mg of anhydrous potassium bromide, over a wavenumber range of 4000–400 cm^{-1}, with a resolution of 1 cm^{-1} using a Bruker Vertex 70 apparatus (Bruker, Billerica, MA, Germany).

The porous structure parameters of the SBA 15 silica before and after immobilization were determined using an ASAP 2020 instrument (Micromeritics Instrument Co., Norcross, GA, USA). The surface area was determined based on the multipoint BET (Brunauer–Emmett–Teller) method, while the mean size and total volume of the pores were examined based on the BJH (Barrett–Joyner–Halenda) algorithm, using data for adsorption under relative pressure (p/p_0) at 77 K. The obtained values are presented as the mean of three measurements, and the equipment accuracy (measured error) does not exceed 0.1% of the obtained values.

For the chromatography analysis, the samples were dried using a SpeedVac concentrator (37 °C, ok. 4.5–5 h). The derivatization was preceded by the modification of the carbonyl groups with an oxime formation (reaction with methoxamine). For that purpose, 50 µL of methoxyamine solution (pyridine 20 mg/mL) was added to the samples and mixed well using a thermomixer (Eppendorf, Hamburg, Germany) for 90 min, at 37 °C and 950 rpm. The oxime formation was followed by the sylilation of the hydroxyl groups using 100 µL MSTFA and incubation for 30 min at 37 °C. The samples were dissolved in 500 µL of hexane, mixed using a vortex, and then 500 µL of the samples were transferred to chromatography vials. The samples were analyzed using a GC-MS/MS chromatograph (Pegasus 4D, GCxGC-TOMFMS, LECO, St Joseph, MI, USA) with a BPX-5 column (28 m, 250 µm, 0.25 µm; SGE Analytical Science, Ringwood, Australia). The analyses were performed with helium as a carrier gas (1 mL/min) for 36 min under the following conditions: 70 °C for 2 min, after which the temperature was increased at 10 °C/min to 300 °C, and the final temperature was maintained for 10 min. The sample volume was 1 µL, and the dosage temperature was set to 250 °C. The temperature of the ion source was equal to 250 °C with an electron energy of 70 eV, and the mass spectra between 33–800 m/z were recorded. The data were analyzed using Chroma TOF-GC software (v4.51.6.0), and quantitative analyses for the ion signals at 217 m/z (xylonic acid) and at 333 and 292 m/z (gluconic acid) were performed for all analyzed compounds. Calibration curves based on the measurement of the analogous samples with the known xylonic acid and gluconic acid concentrations (in the range of 0.1 to 2 µg) were used to determine the contents of the compounds that were analyzed in the samples.

2.6. Statistical Analysis

All reactions and measurements were carried out in triplicate, and the presented error bars as well as error values represent the mean values ± standard deviation. Tukey's test by a one-way ANOVA

was performed using SigmaPlot 12 (Systat Software Inc., San Jose, CA, USA). Statistically significant differences were established at the level $p < 0.05$.

3. Results

3.1. Enzyme Co-Immobilization and Characterization

The characteristic of the SBA 15 silica material before and after co-immobilization and the efficiency of the immobilization were examined based on images obtained using a transmission electron microscope (TEM), changes in the porous structure parameters and Fourier transform infrared spectra (FTIR). The SBA 15 silica exhibited a well-ordered hexagonal array of pores, similar to a honeycomb, with the mesopores characterized by diameters of approx. 20 nm (Figure 1a). As can be observed in Figure 1b, after the co-immobilization of GDH and XDH, the surface of the support material is coated by the layer of the enzymes. Furthermore, it can be observed that after the deposition of enzymes, the pores' diameters decreased to approx. 13 nm. Based on the FTIR spectrum (Figure 1c) and the presence of the signal at 3400 cm^{-1}, which was attributed to stretching vibrations of –OH groups, it is clear that hydroxyl groups are present on the silica surface. In addition, signals at a wavenumber range between 1050 and 460 cm^{-1}, characteristic for stretching and bending vibrations of ≡Si–O bonds, can be observed. After the co-immobilization of GDH and XDH, additional signals with maxima at 3450 cm^{-1} (ν–OH groups), 2950 cm^{-1} (ν C–H bonds in CH_2 and CH_3), 1650 and 1545 cm^{-1} (ν amide I and amide II bonds), 1020 cm^{-1} (ν C–O–C bonds) and 650 cm^{-1} (δ C–C bonds) appeared. The results of the analysis of the porous structure parameters of the SBA 15 silica before and after the co-immobilization (Table 1) showed that upon GDH and XDH co-immobilization, the surface area of the support material dropped by around 35 m^2/g. Furthermore, significantly lower values of the pore size and pore diameters of around 40% were noticed.

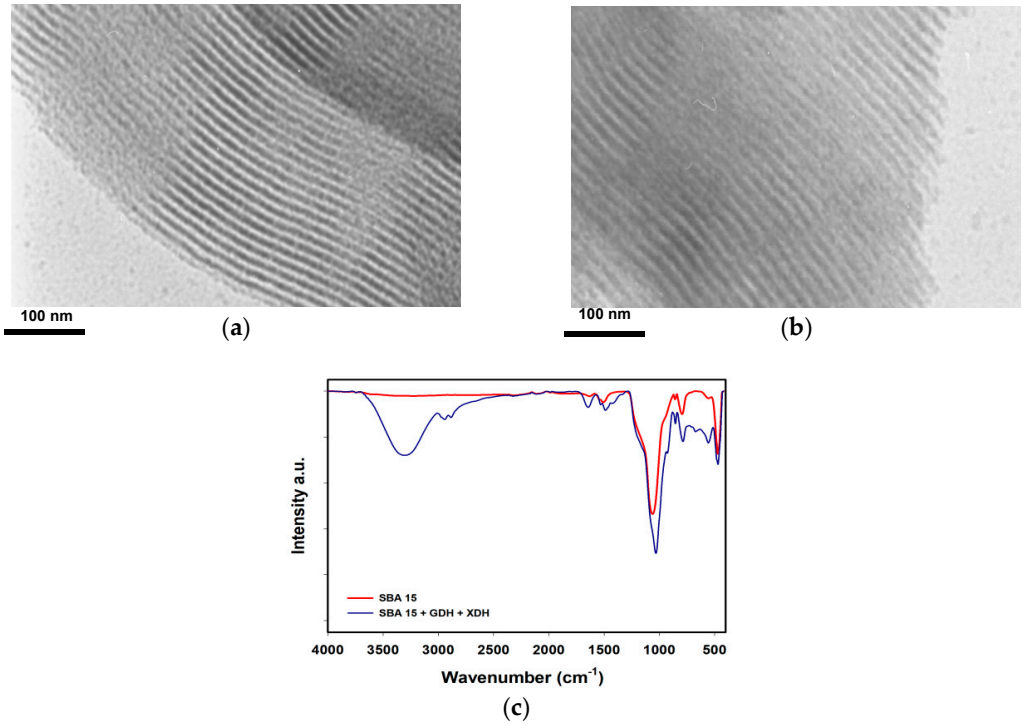

Figure 1. (**a**,**b**) TEM photos and (**c**) FTIR spectra of the SBA 15 silica before and after the GDH and XDH co-immobilization.

Table 1. The porous structure parameters of the SBA15 silica before and after the immobilization.

Sample Name	BET Surface Area (m^2/g)	Pore Volume (cm^3/g)	Pore Size (nm)
SBA 15	564.8	0.804	20.362
SBA 15 + GDH + XDH	529.7	0.473	13.573

To follow the co-immobilization of the GDH and XDH and to examine the changes in the substrate affinity of the biomolecules upon the c0-immobilization, the kinetic parameters of the free and co-immobilized enzymes as well as their specific activity were examined and compared (Table 2). It can be seen that the specific activity of the free GDH and XDH were comparable and reached, respectively, 39.8 U/mg and 43.3 U/mL. Meanwhile, after the immobilization, the specific activity of the co-immobilized GDH was lower and reached 25.9 U/mg. An even greater decrease was observed for the co-immobilized xylose dehydrogenase, whose specific activity values were about two times lower, as compared to the native enzyme, reaching 21.6 U/mg. It has also been found that the Michaelis-Menten constant (K_M) and the maximum reaction velocity rate (V_{max}) for the free GDH reached, respectively, 23.2 mM and 6.4 U/mg. By contrast, the K_M and V_{max} of the free XDH were significantly lower and were found to be 0.116 mM and 0.63 U/mL. Nevertheless, the obtained values are still in the range of the values of the kinetic parameters that are characteristic for both of the above-mentioned enzymes. After the co-immobilization, the substrate affinity of both enzymes decreased, as the K_M value increased by around 30–40%, reaching 30.1 mM for GDH and 0.149 mM for XDH. Furthermore, a lower substrate affinity finds its reflection in the lower values of V_{max} for both co-immobilized enzymes. The maximum velocity rate of the co-immobilized glucose dehydrogenase dropped by around 30%, as compared to the free enzyme, and was found to be 4.6 U/mg, (6.4 U/mg for the free GDH). Meanwhile, a less prominent decrease of the V_{max} of the co-immobilized xylose dehydrogenase of around 20% was noticed; as for the free XDH and co-immobilized XDH, these values reached, respectively, 0.63 U/mL and 0.48 U/mg. Finally, in the present study, to examine the sorption capacity of the SBA 15 toward enzymes' co-immobilization, the total amount of the co-immobilized GDH and XDH was also examined, resulting in 1458 U of the co-immobilized enzymes per 1 gram of the silica support. This value corresponds to a total immobilization yield of 81%.

Table 2. Data representing the kinetic parameters (Michaelis-Menten constant (K_M) and maximum velocity rate (V_{max})) and specific activity of the free and co-immobilized GDH and XDH, as well as the co-immobilization yield and amount of co-immobilized enzymes. * denotes (U/mL).

Sample Name	K_M (mM)	V_{max} (U/mg)	Specific Activity (U/mg)
free GDH	23.2 ± 1.5	6.4 ± 0.6	39.8 ± 2.3
co-immobilized GDH	30.1 ± 1.6	4.6 ± 0.4	25.9 ± 2.1
free XDH	0.116 ± 0.008	0.63 ± 0.09 *	43.3 ± 1.8 *
co-immobilized XDH	0.149 ± 0.011	0.48 ± 0.07	21.6 ± 2.3

3.2. Enzymes Co-Immobilization and Gluconic Acid and Xylonic Acid Production

3.2.1. Effect of GDH:XDH Ratio on the Production of Gluconic Acid and Xylonic Acid

It is commonly known that xylose dehydrogenase and glucose dehydrogenase are characterized by different catalytic activities and kinetics; hence, in order to achieve a high efficiency of gluconic acid and xylonic acid production, as well as to optimize the required quantity of enzymes, the effect of various GDH:XDH ratios on the conversion yield was examined (Figure 2). Although the highest productivity of gluconic acid (95%) was noticed for a GDH:XDH ratio equal to 1:1 and 1:2, the observed yields of xylonic acid were equal to approx. 50% and 60%, respectively. The maximal concentration of xylonic acid (89%) was obtained when the GDH:XDH ratio was equal to 1:5, and in this case the efficiency of the gluconic acid production was also very high and reached approx. 90%, which was

very similar to the case of the above-mentioned ratios. Furthermore, the differences in the productivity of both acids when comparing GDH:XDH ratios equal to 1:5 and 1:10 were insignificant. Therefore, a GDH:XDH ratio of 1:5 was selected as the most suitable due to the fact that a smaller amount of xylose dehydrogenase was used to achieve a high reaction yield.

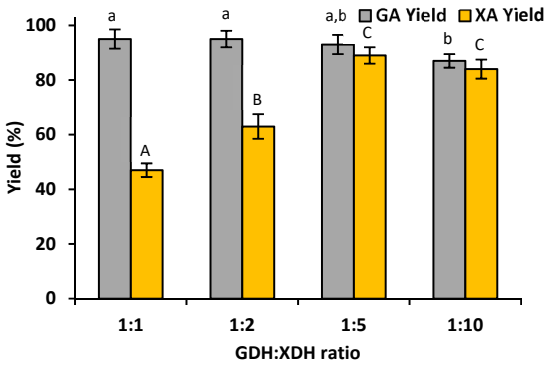

Figure 2. The effect of the ratio of the co-immobilized GDH:XDH on the production of gluconic acid and xylonic acid. The results were analyzed statistically with $p < 0.05$; the lowercase letters refer to statistical differences between the GA yields, while the uppercase letters refer to statistical differences in the XA yields between the different samples.

3.2.2. Time Course of The Production of Gluconic Acid and Xylonic Acid Catalysed by Co-Immobilized GDH and XDH.

The time course of the conversion of glucose and xylose catalyzed by co-immobilized GDH and XDH was investigated in order to examine the optimal reaction time that allows for a high process yield and in order to compare the productivity of the gluconic acid and xylonic acid. As can be seen in Figure 3, irrespective of the analyzed enzyme, the concentration of the product increased gradually during the first 30 min of the process and reached its maximum after 60 min, which for gluconic acid was equal to 51 mM and for xylonic acid was equal to 307 mM. Simultaneously, the concentration of the substrates also decreased gradually at the beginning of the process and reached a plateau after 60 min. After this time, over 90% of the glucose and 85% of the xylose were converted into corresponding acids, and the further prolongation of the reaction time did not result in higher concentrations of the products. Moreover, the rapid action of the co-immobilized enzymes was confirmed by the fact that the concentrations of the products exceeded 50% after 15 min and after 20 min of the process for GDH and XDH, respectively.

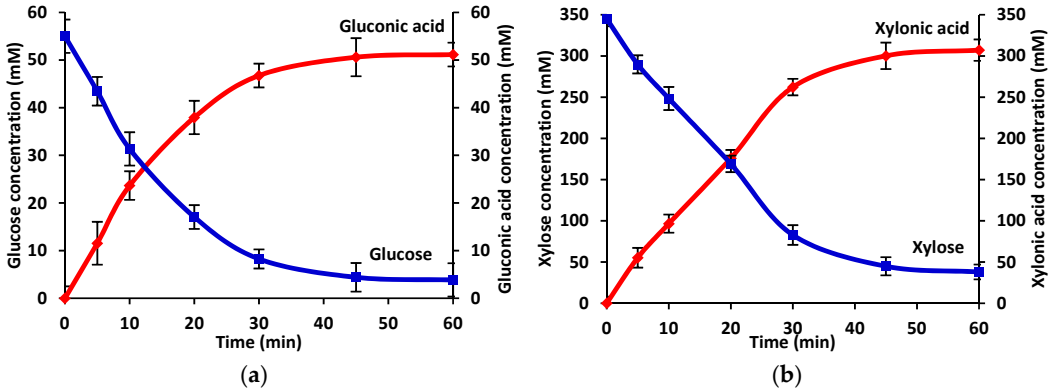

Figure 3. Time course for the reaction of: (**a**) the conversion of glucose into gluconic acid and (**b**) the conversion of xylose into xylonic acid catalyzed by co-immobilized GDH and XDH under optimal process conditions (the blue lines denote the glucose and xylose concentrations, while the red lines denote the concentrations of gluconic and xylonic acid).

3.2.3. Effect of pH and Temperature on The Production of Gluconic and Xylonic Acid Catalyzed by Co-Immobilized GDH and XDH

The effect of the pH and temperature on the production yield of xylonic acid and gluconic acid was studied over a wide range of pHs from 5 to 10 and temperature values ranging from 20 °C to 70 °C in order to evaluate the most suitable reaction conditions for the highest conversion of glucose and xylose. It can be seen that in a slightly acidic and neutral environment (pH 5–8), the productivity of gluconic acid was definitely higher than the productivity of xylonic acid (Figure 4a). Moreover, under acidic conditions, both biocatalysts possessed the lowest activity and the process yield decreased below 50%. The highest reaction yield was observed at pH 8 for both co-immobilized XDH and GDH. Under such pH conditions, the productivity of gluconic acid was equal to 93%, while the xylonic acid yield reached 89%. A high reaction efficiency was also noticed at pH 9, at which the productivity of both acids was equal to approx. 85%. A high gluconic acid yield (90%) was also observed at pH 7; however, at this pH, the productivity of xylonic acid reached 82%. Moreover, the co-immobilized enzymes retained their high catalytic properties even at pH 10, as the yield of both analyzed acids exceeded 80%. Based on Figure 4b, it can be noticed that at temperatures below 40 °C and above 60 °C, the production yield of gluconic acid and xylonic acid was lower than 80%. This was particularly observed at a temperature of 20 °C, at which the conversion of glucose and xylose was lower than 40%. On the other hand, the maximum productivity of gluconic acid and xylonic acid was noticed at temperatures of 40 °C and 50 °C. The yields of gluconic acid and xylonic acid at 40 °C reached 93% and 89%, respectively, while at 50 °C they were equal to 91% and 88%. Moreover, it should be underlined that the efficiency of the catalytic production of GA and XA was above 80%, even when the reaction was carried out at 60 °C.

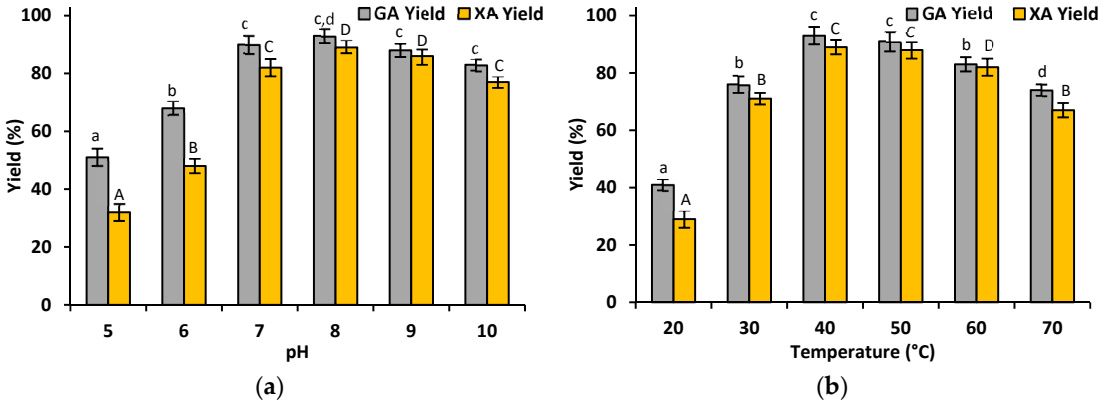

Figure 4. The effect of the (**a**) pH and (**b**) temperature on the conversion of xylose into xylonic acid catalyzed by co-immobilized GDH and XDH. The results were analyzed statistically with $p < 0.05$; the lowercase letters refer to statistical differences between the GA yields, while the uppercase letters refer to statistical differences in the XA yields between the different samples.

3.2.4. Stability of the Free and Co-Immobilized GDH and XDH

The determination of the stability of the co-immobilized enzymes over time under the process conditions is a crucial step that strongly influences the possible practical applications of the obtained biocatalytic systems. It can be seen that, irrespective of the type and form of the enzymes used, a progressive decrease of the catalytic activity over time was observed (Figure 5). However, the attachment of the glucose dehydrogenase to the silica support resulted in an enhancement of its stability. After 120 min of incubation at pH 8 and 40 °C, the co-immobilized GDH retained 80% of its initial activity; meanwhile, the free enzyme maintained less than 40% of its catalytic properties. On the other hand, xylose dehydrogenase was characterized by a higher stability over the analysed time range, as compared to GDH. Nevertheless, after co-immobilization using SBA 15 silica as a support, XDH exhibited approx. 85% of its initial activity, while the free enzyme exhibited less than

50% of its properties after the same period of time. A significant improvement of the stability of the co-immobilized GDH is also reflected by the values of the inactivation constant (k_D) and enzyme half-life ($t_{1/2}$). Free glucose dehydrogenase was characterized by k_D and $t_{1/2}$ equal to 0.0075 1/min and 95.4 min, respectively; meanwhile, for the free XDH, these values were equal to 0.0061 1/min and 115.7 min. As a result of the enzymes' co-immobilization, the inactivation constant and enzyme half-life were also significantly enhanced. For the co-immobilized GDH, these parameters were 3-fold lower and 2.5-fold higher than those of the free enzyme (0.0025 1/min and 275.5 min), respectively, whereas for the co-immobilized XDH the k_D and $t_{1/2}$ reached 0.0021 1/min and 323.7 min, which was improved by more than 3-fold when compared to the native biocatalyst.

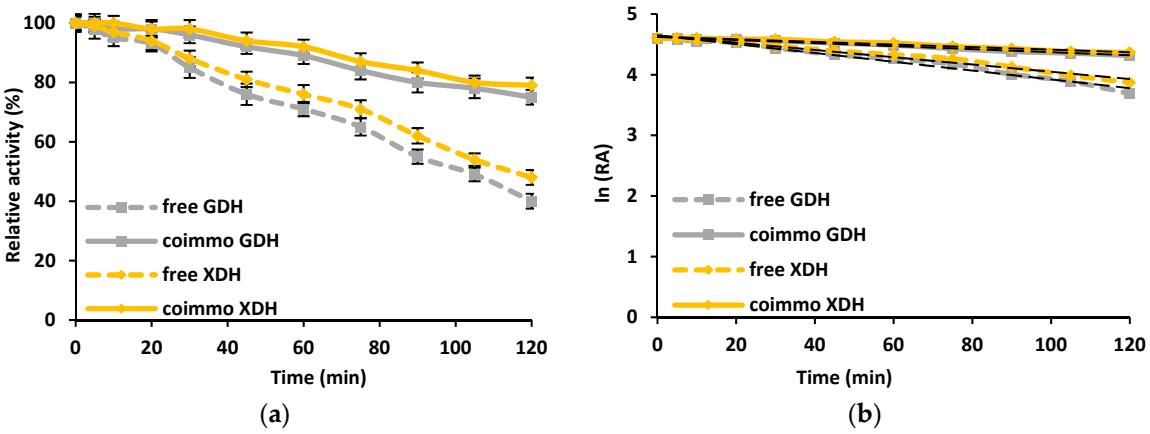

(**a**) (**b**)

Figure 5. The stability of free and co-immobilized GDH and XDH under optimal process conditions (**a**). The inactivation constants (k_D) were evaluated based on the linear regression slope for free and co-immobilized GDH and XDH under optimal process conditions (**b**).

3.2.5. Storage Stability and Reusability of the Co-Immobilized GDH and XDH

The storage stability as well as reusability of the co-immobilized GDH and XDH are of particular interest from a practical application point of view. The reusability of the co-immobilized biocatalysts was examined on the basis of the conversion efficiency of xylose and glucose into xylonic acid and gluconic acid over ten consecutive reaction cycles, while the storage stability was determined by analyzing the relative activity of the co-immobilized GDH and XDH over 20 days of storage at 4 °C (Figure 6a,b).

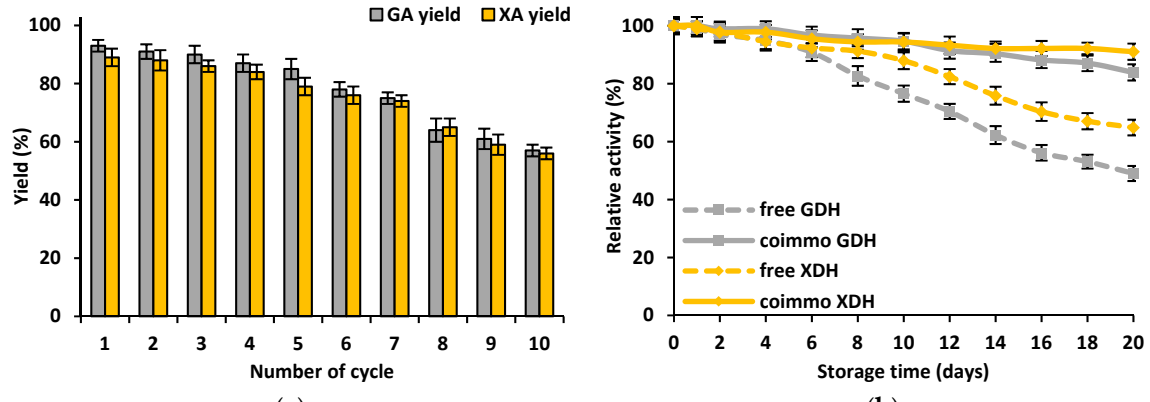

(**a**) (**b**)

Figure 6. The (**a**) storage stability and (**b**) reusability of the of free and co-immobilized GDH and XDH. The results were analyzed statistically with $p < 0.05$; the lowercase letters refer to statistical differences between the GA yields, while the uppercase letters refer to statistical differences in the XA yields between the different samples.

The results of the reusability test (Figure 6a) showed that the productivity of gluconic acid and xylonic acid was almost unaltered over the first five reaction steps and decreased only by approx. 10%. The further reaction yield decreased more significantly and after ten conversion cycles reached approx. 60% and 55%, respectively, for gluconic acid and xylonic acid. The results of the storage stability of the free and co-immobilized GDH and XDH (Figure 6b) indicate that both co-immobilized enzymes were characterized by a better storage stability, as compared to the free enzymes. For the first five days of storage, the catalytic activity of all the tested enzymes remained unaltered and after that started to decrease. Finally, after 20 days of storage, the relative activity of the free GDH was equal to only 49%, while for the immobilized GDH it reached 84%. Furthermore, the co-immobilized XDH was also characterized by a higher relative activity, which was equal to 91%, as the free biocatalyst retained only approx. 65% of its initial properties.

4. Discussion

4.1. Enzyme Co-Immobilization and Characterization

The morphology and the presence of chemical groups in the structure of the SBA 15 silica before and after immobilization as well as the immobilization effectivity were investigated using transmission electron microscopy and FTIR spectra. Based on the TEM image of the pure silica matrix, it can be observed that this material is characterized by ordered arrays of pores with diameters of approx. 20 nm, which facilitate enzyme binding not only onto the surface of the support but also inside pores. Indeed, after the co-immobilization of biomolecules, a uniform layer of the enzyme molecules can be seen in the TEM image. Furthermore, GDH and XDH molecules are deposited both onto the surface as well as into the pores of the silica material, which enhances the protection of the biomolecules against inactivation and improves their stability [14]. These observations are in agreement with the results of the porous structure analysis, which revealed a significant decrease of the pore size and pore volume, indicating enzyme deposition into the pores of the matrix. The effective co-immobilization of glucose dehydrogenase and xylose dehydrogenase was also indirectly confirmed by the presence of the signals attributed to the –OH, C–H, amide I and amide II, C–O and C–C bands in the FTIR spectrum of the SBA 15 after immobilization. Moreover, slight shifts (by approx. 5 to 10 cm^{-1}) of signals attributed to amide I and amide II toward lower wavenumber values were observed. This fact indicates that the biomolecules were bounded by the adsorption immobilization, by the formation of hydrogen bonds and electrostatic interactions between mainly amine groups present in the enzymes' structure and hydroxyl groups incorporated into the silica structure, as previously reported [15,16].

In the study we have also examined the specific activity of the free GDH and XDH and its changes upon co-immobilization. As was expected, after their co-immobilization both enzymes exhibited a lower specific activity. This fact might be related to changes in the microenvironment of the biocatalysts upon immobilization, as well as to the limited access of the substrate molecules to the enzymes' active sites due to biomolecule deposition into the pores of the silica support [17]. Moreover, as suggested earlier by Sánchez-Moreno, a more prominent decrease of the specific activity of the co-immobilized XDH is probably related to larger changes of the three-dimensional conformation of the amino acid residues in the active site of the XDH, as compared to the GDH [18]. Nevertheless, in the present study, the specific activity of the co-immobilized GDH reached over 25 U/mg, which was significantly higher than the specific activity of the glucose dehydrogenase co-immobilized with amine dehydrogenase by Liu et al. using magnetic nanoparticles, whose specific activity was 18.7 U/mg [19]. These results, together with the results representing the amount of immobilized enzyme (almost 1500 U of the co-immobilized enzymes per 1 gram of the silica SBA 15 support) and high co-immobilization yield, exceeding 80%, clearly show that mesoporous silica is a suitable carrier for enzyme co-immobilization and facilitates the retention of high catalytic properties. By contrast, Delgove et al. co-immobilized cyclohexanone monooxygenase and glucose dehydrogenase on an amino-functionalized agarose-based support. In their study, the total co-immobilization yield reached around 75%, and a significantly

lower enzyme loading was noticed, as less than 100 U of the enzymes were co-immobilized on the agarose support [20].

To examine the changes in the substrate affinity of the jointly co-immobilized glucose dehydrogenase and xylose dehydrogenase, the kinetic parameters of the free and immobilized enzymes were examined. It can be seen that the Michaelis-Menten constant of both immobilized dehydrogenases increased upon immobilization, indicating a lower substrate affinity. This fact is directly related to the creation of the diffusional limitations in the transport of the substrates due to the deposition of the biomolecules inside the pores of the support material. Another explanation might be related to the fact that almost 1500 U of the enzyme was co-immobilized, which might lead to the local enzyme overcrowding and blocking the enzymes active sites [21]. Furthermore, as suggested earlier by Baron et al., due to the requirement of the GDH and XDH for cofactor molecules, an additional interaction between the cofactor and support material as well as between the cofactor and substrate molecules cannot be excluded, leading to a lower substrate affinity [22]. Simultaneously, a lower value of the maximum velocity rate was also noticed for both co-immobilized enzymes. Thus, to overcome this limitations and facilitate the reaction rate, a higher substrate concentration should be used in reaction with the co-immobilized enzymes [23]. However, less significant changes in the values of the kinetic parameters were observed in the case of the co-immobilized XDH. These observations are in agreement with our previous study and might be explained by the lower molecular weight and size of the XDH, as compared to the GDH, which reduces the diffusional limitations and enhances the accessibility of the active sites for substrate molecules [24]. Nevertheless, we would like to emphasize that information related to the immobilization of dehydrogenases is very limited; thus, the novelty of the present study is certain.

4.2. Enzymes Co-Immobilization and Gluconic Acid and Xylonic Acid Production

It is known that, after the pretreatment, the concentrations of glucose and xylose in the biomass liquors vary depending on the source of the biomass and the pretreatment method; however, the total amount of xylose is usually approx. 5 to even 10 times higher than the glucose content [11,25]. Moreover, both co-immobilized enzymes are characterized by different activities as well as various pH and temperature optima. Thus, it was crucial to find the most suitable process conditions that would facilitate the achievement of a high reaction yield. In the first step of the investigation, the effect of various GDH:XDH ratios was examined. It was established that at a GDH:XDH ratio equal to 1:5, the highest conversion yield (over 90%) of glucose and xylose occurred. Although a higher conversion yield of glucose was noticed at a lower enzyme ratio (1:1; 1:2), a low yield of xylose conversion was also noticed due to the insufficient amount of xylose dehydrogenase in the system. On the other hand, when a GDH:XHD ratio of 1:10 was used, the conversion of monosaccharides decreased. This might be explained by the overcrowding of enzymes, which leads to steric hindrances, blocking the enzyme active sites and, in consequence, lowering the conversion yield, as presented earlier by Zhang et al [26]. A significant effect of the optimal co-immobilized enzymes ratio for effective catalytic action was also observed in our previous study. We found that a co-immobilized xylose dehydrogenase to alcohol dehydrogenase ratio equal to 2:1 was the most effective for the simultaneous conversion of xylose and cofactor regeneration [27]. However, in this study, a GDH:XDH ratio equal to 1:5 was selected as the most suitable and was used in the further steps of the investigation.

It is also known that immobilization may alter the three-dimensional structure of enzymes, leading to changes in their pH and temperature optima. According to our previous study and previously published articles, glucose dehydrogenase from *Pseudomonas* sp. (EC 1.1.1.118) exhibited its highest activity at a pH equal to approx. 8 and at 40 to 45 °C [12,28], while free xylose dehydrogenase possesses its optimum at a pH equal to approx. 8 and at a temperature of 35 °C [12,29]. After enzyme co-immobilization, the optimal conditions for the highest conversion of xylose and glucose were pH 8 and a temperature of 40 °C. Therefore, it could be concluded that the temperature optimum of XDH was slightly shifted toward higher values, probably due to slight changes in the microenvironment

of the enzyme active sites upon immobilization [30], while the optimal process conditions for GDH were unaltered after immobilization. It should also be clearly stated that the free enzymes only exhibited a high activity under the above-mentioned conditions, and changes in these parameters resulted in a significant decrease of the conversion yield (data not presented). In contrast, the co-immobilized enzymes were able to achieve an over 80% glucose and xylose conversion yield over a wide range of pHs ranging from 7 to 10 and temperatures ranging from 40 to 60 °C. The significant improvement of the enzyme activity and, in consequence, also of the conversion yield, as compared to the free enzymes, might be explained by several factors. First of all, GDH and XDH are known to be multimeric enzymes that tend to dissociate at temperatures over 50 °C [31]. Using silica-based support materials, multipoint enzyme binding is facilitated, enhancing the rigidity of the biomolecules, stabilizing their structure and preventing the dissociation of subunits. Furthermore, SBA 15 support material provides a protective effect for the biocatalysts against harsh reaction conditions that lead to a significant reduction of the conformational changes of the enzyme structure after immobilization [32]. Our observations stay in agreement with those noticed by Zhuang et al., who used silica SBA 15 for the adsorption immobilization of alkaline protease. The immobilized enzyme exhibited over 20% higher activity recovery over the whole analysed pH range (5–9) [33]. An even better protective effect of mesoporous material on the enzyme activity was presented by Li et al., who synthesized (3-aminopropyl) triethoxysilane (APTES) functionalized mesoporous SBA 15 silica for the covalent immobilization of lipase from *Candida rugosa*. Due to the rigidization of the enzyme structure and protective effect of the silica matrix, the covalently attached enzyme exhibited over 40% higher activity over a temperature range of 40 °C to 70 °C, as compared to the free biocatalyst [34]. Nevertheless, a decrease of the reaction yield at low temperatures and at an acidic pH is probably related to the insufficient thermal activation of the enzyme as well as to the protonation of the ionic groups and side chains of the enzyme, respectively. Due to these facts, electrostatic repulsion occurred, leading to the distortion and/or destruction of the active sites of the biomolecules [35].

Data related to the thermal and chemical stability of the free and co-immobilized GDH and XDH indicate that the stability of the biomolecules was significantly improved after immobilization using SBA 15 silica, as the relative activity of both co-immobilized enzymes was approx. 20% higher compared to free dehydrogenases. These results find a reflection in the values of the enzymes' half-lives and inactivation constants, which upon immobilization were improved over 3-fold. This is probably related to the fact that upon immobilization an external backbone for the biomolecules was provided, stabilizing the entire enzyme structure due to the creation of the enzyme-support interaction [36]. It has also been previously mentioned that GDH and XDH were immobilized into the pores of the support, providing an additional protection of the biomolecules. Finally, the vibrations of glucose dehydrogenase and xylose dehydrogenase caused by heating were limited, reducing the conformational changes of the enzymes and facilitating the preservation of the proper enzyme shape and properties [37]. The above-mentioned facts hampered the thermal and chemical denaturation of the enzymes, which are the main reasons for the lower relative activity observed for the free enzymes. These findings were also highlighted in another study by Karimi et al., who immobilized trypsin by adsorption using nanostructured mesoporous SBA-15 with compatible pore sizes. The presented results indicated that the adsorbed trypsin retained over 90% of its initial activity after 2 h incubation at 45 °C [38].

The reusability and storage stability are of key importance from the point of view of practical applications of the produced biocatalytic systems. The great advantage of the co-immobilized GDH and XDH is associated with the significant improvement of the above-mentioned features, as they retained over 80% of their initial catalytic properties after five consecutive reaction cycles and after 20 days of storage at 4 °C. The retention of a high activity might be explained by several factors, which also improve the thermal stability of the co-immobilized GDH and XDH. Nevertheless, the fact that dehydrogenases are also co-immobilized into the pores of hexagonal silica, providing protection against inactivation caused by thermal and pH denaturation and limiting the elution of the enzyme

from the support, should emphasized. However, a decrease in the conversion yield after several reaction steps is probably related to the inhibition of the biomolecules by the substrates and products, and/or to the enzymes' inactivation by the repeated use and effect of process conditions [39]. Similar observations have also been reported by Mureşeanu at al. and Wongvitvitchot et al., who immobilized, respectively, laccase from *Trametes versicolor* and cellulase from *Trichoderma reesei* by adsorption using SBA 15 silica as the support. In their studies, however, immobilized enzymes retained approx. 60% of their initial catalytic activity [40,41].

5. Conclusions

The main difficulties for the widespread application of enzymatic systems for the conversion of valuable biomass components are related to the high cost of the enzymes and their limited reusability. Therefore, in this study, we present the simultaneous co-immobilization of glucose dehydrogenase and xylose dehydrogenase using mesoporous SBA 15 silica for the concurrent conversion of glucose and xylose into gluconic acid and xylonic acid, respectively. Based on the FTIR and TEM results, it has been confirmed that the enzymes' molecules have been effectively attached onto the surface of the support as well as into its pores, ensuring the additional protection of the biomolecules against harsh reaction conditions. It has been also established that the optimal GDH:XDH ratio for the highest yield of GA and XA was equal to 1:5. The use of the above-mentioned system resulted in an approx. 90% conversion of both glucose and xylose after just 60 min of the process. Furthermore, the stability of the enzymes was significantly improved upon immobilization compared to the free GDH and XDH, as the co-immobilized biocatalysts exhibited over a 30% higher activity after 20 days of storage and after 2 h of incubation in harsh conditions. Finally, the co-immobilized enzymes showed a great reusability, as after 5 reaction cycles the conversion yield of glucose and xylose reached over 80%. The presented data clearly illustrate the exceptional potential of silica SBA 15 co-immobilized glucose dehydrogenase and xylose dehydrogenase for the efficient simultaneous conversion of glucose and xylose into valuable products. We believe that the present study may further stimulate the development of catalysts based on immobilized enzymes for the conversion of biomass components; however, further studies in this research area are still required.

Author Contributions: Conceptualization, J.Z., K.B., M.P. and T.J.; methodology, J.Z., A.Z. and O.D.; formal analysis, K.B., A.Z. and O.D.; investigation, K.B. and O.D.; resources, J.Z. and T.J.; writing—original draft preparation, J.Z., K.B., A.Z. and O.D.; writing—review and editing, J.Z., T.J. E.K. and M.P.; visualization, J.Z. and A.Z.; supervision, T.J. A.S.M. and M.P.; project administration, T.J.

Funding: This research was funded by Ministry of Science and Higher Education (Poland) as financial subsidy to PUT under the grant no. 03/32/SBAD/0906.

Conflicts of Interest: The authors declare no conflict of interest.

References

1. Feliczak-Guzik, A.; Nowak, I. Mesoporous niobosilicates serving as catalysts for synthesis of fragrances. *Cat. Today* **2009**, *142*, 288–292. [CrossRef]
2. Jesionowski, T.; Zdarta, J.; Krajewska, B. Enzyme immobilization by adsorption: A review. *Adsorption* **2014**, *20*, 801–821. [CrossRef]
3. Yu, C.; Tian, B.; Liu, X.; Fan, J.; Yang, H.; Zhao, D. Advances in mesoporous materials templated by nonionic block copolymers. In *Nanoporous Materials: Science and Engineering*; Lu, G.Q., Zhao, X.S., Eds.; Imperial College Press: London, Great Britain, 2004; pp. 115–136.
4. Hartmann, M.; Kostrov, X. Immobilization of enzymes on porous silicas – benefits and challenges. *Chem. Soc. Rev.* **2013**, *42*, 6277–6289. [CrossRef] [PubMed]
5. Zdarta, J.; Meyer, A.S.; Jesionowski, T.; Pinelo, M. Multifaceted strategy based on enzyme immobilization with reactant adsorption and membrane technology for biocatalytic removal of pollutants: A critical review. *Biotechnol. Adv.* in press.

6. Górecka, E.; Jastrzębska, M. Immobilization techniques and biopolymer carriers. *Biotechnol. Food Sci.* **2011**, *75*, 65–86.
7. Datta, S.; Christena, L.R.; Rajaram, Y.R.S. Enzyme immobilization: An overview on techniques and support materials. *3 Biotech* **2012**, *3*, 1–9. [CrossRef] [PubMed]
8. Xie, W.; Fan, M. Immobilization of tetramethylguanidine on mesoporous SBA-15 silica: A heterogeneous basic catalyst for transesterification of soybean oil. *Bioresour. Technol.* **2013**, *139*, 388–392. [CrossRef]
9. Roche, C.M.; Dibble, C.J.; Stickel, J.J. Laboratory-scale method for enzymatic saccharification of lignocellulosic biomass at high-solids loadings. *Biotechnol. Biofuels* **2009**, *2*, 28–37. [CrossRef]
10. Jørgensen, H.; Pinelo, M. Enzyme recycling in lignocellulosic biorefineries. *Biofuels Bioprod. Bioeng.* **2017**, *11*, 150–167. [CrossRef]
11. Sueb, M.S.M.; Zdarta, J.; Jesionowski, T.; Jonsson, G.; Meyer, A.S.; Jørgensen, H.; Pinelo, M. High-performance removal of acids and furans from wheat straw pretreatment liquid by dianafiltration. *Sep. Sci. Technol.* **2017**, *52*, 1901–1912. [CrossRef]
12. Zdarta, J.; Pinelo, M.; Jesionowski, T.; Meyer, A. Upgrading of biomass monosaccharides by immobilized glucose dehydrogenase and xylose dehydrogenase. *ChemCatChem* **2018**, *10*, 5164–5173. [CrossRef]
13. Bradford, M.M. A rapid and sensitive method for the quantitation of microgram quantities of protein utilizing the principle of protein-dye binding. *Anal. Biochem.* **1976**, *72*, 248–254. [CrossRef]
14. Srivastava, P.K.; Singh, S. Immobilization and applications of glucose-6-phosphate dehydrogenase: A review. *Prep. Biochem. Biotechnol.* **2013**, *43*, 376–384. [CrossRef]
15. Eslamipour, F.; Hejazi, P. Evaluating effective factors on activity and loading of immobilized a-amylase onto magnetic nanoparticles using response surface desirability approach. *RSC Adv.* **2016**, *6*, 20187–20197. [CrossRef]
16. Gholamzadeh, P.; Ziarani, G.M.; Badiei, A. Immobilization of lipases onto the SBA-15 mesoporous silica. *Biocatal. Biotransform.* **2017**, *35*, 131–150. [CrossRef]
17. Zdarta, J.; Feliczak-Guzik, A.; Siwińska-Ciesielczyk, K.; Nowak, I.; Jesionowski, T. Mesostructured cellular foam silica materials for laccase immobilization and tetracycline removal: A comprehensive study. *Micropor. Mesopor. Mater.* **2020**, *291*, 109688. [CrossRef]
18. Sánchez-Moreno, I.; García-Junceda, E.; Hermida, C.; Fernández-Mayoralas, A. Development of a new method for d -xylose detection and quantification in urine, based on the use of recombinant xylose dehydrogenase from *Caulobacter crescentus*. *J. Biotechnol.* **2016**, *234*, 50–57. [CrossRef]
19. Liu, J.; Pang, B.Q.W.; Adams, J.P.; Snajdrova, R.; Li, Z. Coupled immobilized amine dehydrogenase and glucose dehydrogenase for asymmetric synthesis of amines by reductive amination with cofactor recycling. *ChemCatChem* **2017**, *9*, 425–431. [CrossRef]
20. Delgove, M.; Valencia, D.; Solé, J.; Bernaerts, K.; de Wildeman, S.; Guillén, M.; Álvaro, G. High performing immobilized Baeyer-Villiger monooxygenase and glucose dehydrogenase for the synthesis of ε-caprolactone derivative. *Appl. Catal. A* **2019**, *572*, 134–141. [CrossRef]
21. Li, L.; Liang, B.; Li, F.; Shi, J.; Mascini, M.; Lang, Q.; Liu, A. Co-immobilization of glucose oxidase and xylose dehydrogenase displayed whole cell on multiwalled carbon nanotube nanocomposite films modified electrode for simultaneous voltammetric detection of D-glucose and D-xylose. *Biosens. Bioelectron.* **2013**, *42*, 156–162. [CrossRef]
22. Baron, M.; Fontana, J.D.; Guimaraes, M.F.; Woodward, J. Stabilization and reutilization of Bacillus megaterium glucose dehydrogenase by immobilization. *Appl. Biochem. Biotechnol.* **1997**, *63*, 257–268. [CrossRef]
23. Zhou, Q.Z.; Chen, X.D. Effects of temperature and pH on the catalytic activity of the immobilized β-galactosidase from *Kluyveromyces lactis*. *Biochem. Eng. J.* **2001**, *9*, 33–40. [CrossRef]
24. Zdarta, J.; Meyer, A.S.; Jesionowski, T.; Pinelo, M. Developments in support materials for immobilization of oxidoreductases: A comprehensive review. *Adv. Colloid. Interfac. Sci.* **2018**, *258*, 1–20. [CrossRef]
25. Hendriks, A.T.W.M.; Zeeman, G. Pretreatments to enhance the digestibility of lignocellulosic biomass. *Bioresour. Technol.* **2009**, *100*, 10–17. [CrossRef]
26. Zhang, D.H.; Zhang, Y.F.; Zhi, G.Y.; Xie, Y.L. Effect of hydrophobic/hydrophilic characteristics of magnetic microspheres on the immobilization of BSA. *Colloid. Surface. B* **2011**, *82*, 302–306. [CrossRef]
27. Bachosz, K.; Synoradzki, K.; Staszak, M.; Pinelo, M.; Meyer, A.S.; Zdarta, J.; Jesionowski, T. Bioconversion of xylose to xylonic acid via co-immobilized dehydrogenases for conjunct cofactor regeneration. *Bioorg. Chem.* in press. [CrossRef]

28. Gao, F.; Ding, H.; Xu, X.; Zhao, Y. A self-sufficient system for removal of synthetic dye by coupling of spore-displayed triphenylmethane reductase and glucose 1-dehydrogenase. *Environ. Sci. Pollut. Res. Int.* **2016**, *23*, 21319–21326. [CrossRef]
29. Yamanaka, K.; Gino, M. Purification and properties of D-xylose dehydrogenase in bacteria. *Hakko Kogaku Kaishi* **1979**, *57*, 322–331.
30. Secundo, F. Conformational changes of enzymes upon immobilisation. *Chem. Soc. Rev.* **2013**, *42*, 6250–6261. [CrossRef]
31. Aissaoui, N.; Landoulsi, J.; Bergaoui, L.; Boujdaya, S.; Lambert, J. Catalytic activity and thermostability of enzymes immobilized on silanized surface: Influence of the crosslinking agent. *Enzyme Microb. Technol.* **2013**, *52*, 336–343. [CrossRef]
32. Twala, B.V.; Sewell, B.T.; Jordaan, J. Immobilisation and characterisation of biocatalytic co-factor recycling enzymes, glucose dehydrogenase and NADH oxidase, on aldehyde functional ReSyn™ polymer microspheres. *Enzyme Microb. Technol.* **2012**, *50*, 331–336. [CrossRef]
33. Zhuang, H.; Dong, S.; Zhang, T.; Tang, M.; Xu, N.; Sun, B.; Liu, J.; Zhang, M.; Yuan, Y. Study on alkaline protease immobilized on mesoporous materials. *Asian J. Chem.* **2014**, *26*, 1139–1144. [CrossRef]
34. Li, X.; Xu, Y.; Zhou, G. Functionalization of mesoporous SBA-15 with APTES by co-condensation and its effect on immobilization of *Candida rugose* lipase. *Key Eng. Mater.* **2015**, *645–646*, 1261–1266. [CrossRef]
35. Zhou, Q.Z.K.; Chen, X.D. Immobilization of β-galactosidase on graphite surface by glutaraldehyde. *J. Food Eng.* **2001**, *48*, 69–74. [CrossRef]
36. Liu, X.H.; Du, X.; Feng, J.R.; Wu, M.B.; Lin, J.P.; Guan, J.; Wang, T.; Zhang, Z.H. Co-immobilization of Short-chain dehydrogenase/reductase and glucose dehydrogenase for the efficient production of (±)-ethyl mandelate. *Catal. Lett.* **2019**, *149*, 1710–1720. [CrossRef]
37. Solé, J.; Caminal, G.; Schürmann, M.; Álvaroa, G.; Guilléna, M. Co-immobilization of P450 BM3 and glucose dehydrogenase on different supports for application as a self-sufficient oxidative biocatalyst. *J. Chem. Technol. Biotechnol.* **2019**, *94*, 244–255. [CrossRef]
38. Karimi, B.; Emadi, S.; Safaria, A.A.; Kermaniana, M. Immobilization, stability and enzymatic activity of albumin and trypsin adsorbed onto nanostructured mesoporous SBA-15 with compatible pore sizes. *RSC Adv.* **2014**, *4*, 4387–4394. [CrossRef]
39. Sahin, S.; Ozmen, I. Determination of optimum conditions for glucose-6-phosphate dehydrogenase immobilization on chitosan-coated magnetic nanoparticles and its characterization. *J. Mol. Catal. B* **2016**, *133*, S25–S33. [CrossRef]
40. Mureşeanu, M.; Trandafir, I.; Băbeanu, C.; Pârvulescu, V.; Păun, G. Laccase immobilized on mesoporous silica supports as an efficient system for wastewater bioremediation. *Environ. Protect. Eng.* **2016**, *42*, 81–95.
41. Wongvitvitchot, W.; Siamnikorn, K.; Pithakratanayothin, S.; Chaisuwan, T.; Wongkasemjit, S. Effective and reusable *T. reesei* immobilized on SBA-15 for monomeric sugar production from cellulose hydrolysis. *Bioresour. Technol. Rep.* **2019**, *5*, 199–205. [CrossRef]

Colloids and Surfaces B: Biointerfaces 169 (2018) 118–125

Contents lists available at ScienceDirect

Colloids and Surfaces B: Biointerfaces

journal homepage: www.elsevier.com/locate/colsurfb

Biopolymers conjugated with magnetite as support materials for trypsin immobilization and protein digestion

Jakub Zdarta[a,*], Katarzyna Antecka[a], Artur Jędrzak[a], Karol Synoradzki[b,c], Magdalena Łuczak[a,d], Teofil Jesionowski[a,*]

[a] Institute of Chemical Technology and Engineering, Faculty of Chemical Technology, Poznan University of Technology, Berdychowo 4, 60965 Poznan, Poland
[b] Institute of Molecular Physics, Polish Academy of Sciences, Smoluchowskiego 17, 60179 Poznan, Poland
[c] Institute of Low Temperature and Structure Research, Polish Academy of Sciences, Okolna 2, 50422 Wroclaw, Poland
[d] European Centre for Bioinformatics and Genomics, Institute of Bioorganic Chemistry, Polish Academy of Sciences, Noskowskiego 12/14, 61704 Poznan, Poland

ARTICLE INFO

Article history:
Received 5 March 2018
Received in revised form 6 May 2018
Accepted 7 May 2018
Available online 8 May 2018

Keywords:
Magnetic materials
Hybrid supports
Enzyme immobilization
Trypsin
Peptide digestion

ABSTRACT

In the presented study synthesized magnetic nanoparticles were used as an inorganic precursor for the preparation of novel magnetite-lignin and magnetite-chitin hybrid supports for enzyme immobilization. Effective synthesis of the hybrids was confirmed by Fourier transform infrared spectroscopy and powder X-ray diffraction analysis. The materials exhibited good thermal stability and surface areas of 4.3 and 5.6 m^2/g respectively. The magnetite-lignin + trypsin and magnetite-chitin + trypsin systems were found to have good storage stability and reusability. After 20 days they retained over 75% and 90% respectively of their initial activity, and after 10 consecutive biocatalytic cycles retained over 60% and 80% respectively of their initial activity. The kinetic parameters of the free and immobilized enzyme were also comprehensively examined and compared. The results of peptide digestion tests confirmed the high proteolytic activity of the produced trypsin-based magnetic biocatalytic systems.

1. Introduction

There have been many reports in recent years concerning the various valuable features of magnetite, including chemical inertness, biocompatibility, non-toxicity, good thermal stability and high surface area, together with its ferromagnetic properties, which facilitate its simple separation from a mixture by the application of an external magnetic field [1–4]. In addition, many varied materials can be attached to the surface of magnetite to form magnetic hybrids [4,5]. Hybrids formed by the combination of inorganic and organic compounds are characterized by homogeneity, thermal resistance, and mechanical, chemical and electrokinetic stability [6,7]. In particular, magnetic nanoparticles of Fe_3O_4 have been investigated with biopolymers such as chitosan and cellulose [8–10] and with other components including carbon nanostructures (graphene, multi- and single-walled carbon nanotubes) [11–16], as well as biomolecules such as peptides [17] and saccharides such as alginic acid [18], to produce functional hybrid nanomaterials or nanocomposites. The incorporation of magnetic nanoparticles into hybrids gives these materials unique features that have greatly enhanced their practical applications in many fields of industry and science, for instance as adsorbents of dyes, pigments or harmful ions [8], as polymer fillers [5–7] and in the construction of biosensors [19]. However, in recent years, magnetite, used as a base for hybrid materials, has also been intensively studied as an enzyme carrier, mainly due to the fact that magnetic nanoparticles facilitate the fast and simple isolation of immobilized biomolecules using an external magnetic field. In consequence, the reusability of the biocatalytic system is greatly improved and products of higher purity can be obtained. For instance, Atacan et al. immobilized trypsin on tannin-modified magnetite nanoparticles [20]; Slováková et al. confined trypsin on magnetite coated with silica [21]; and Nicolás et al. presented interesting findings concerning the immobilization of CALB (*Candida antarctica* Lipase B) on lysine-modified magnetic nanoparticles [22]. Also Sun et al. used carboxymethyl chitosan-functionalized magnetic nanoparticles for cross-linking immobilization of trypsin [23]. These magnetite hybrids have been shown to significantly enhance the stability of the immobilized enzymes and make them into more effective and reusable biocatalytic systems, as they provide better adsorption parameters together with good biocompatibility or bioactivity.

* Corresponding authors.
E-mail addresses: jakub.zdarta@put.poznan.pl (J. Zdarta), teofil.jesionowski@put.poznan.pl (T. Jesionowski).

https://doi.org/10.1016/j.colsurfb.2018.05.018
0927-7765/

Trypsin (EC 3.4.21.4) is an enzyme belonging to the hydrolase group. This biomolecule is classified as a serine protease, a subclass of enzymes catalyzing the breakdown of peptide and ester bonds on the lysine and arginine amino acid residue side chain [24]. This serine protease is a globular protein of medium size, which is produced in the form of an inactive proenzyme: trypsinogen. The dominant forms of trypsin are α-trypsin, whose structure contains two peptide chains, and β-trypsin, which has one protein chain. The two forms differ in activity and thermal stability [25]. Trypsin is successfully used in the separation of dissected cells or proteolysis of caseins, which are the most important proteins found in milk. It is also used in the food industry, especially in the extraction of spices and aromas from vegetable proteins, the control of aroma formation in dairy products, the stabilization of beer and the production of hypoallergenic food [26].

Due to the wide practical application of industrially relevant enzyme, which is trypsin, we made an attempt to evaluate novel immobilization protocol using magnetic support materials. Thus, the aim of the present study was to synthesize and characterize magnetite-lignin and magnetite-chitin hybrids with properties suitable for trypsin immobilization. Effective enzyme immobilization was confirmed and the quantity of attached enzyme was determined. An investigation was also made of storage stability and reusability, features that are important for practical applications. The kinetic characteristics of the free and immobilized enzyme were investigated and compared. Finally, the trypsin-based magnetic biocatalytic systems were successfully used for the digestion of human serum albumin. Hydrolyzed fragments of albumin were detected and identified via MALDI-TOF MS.

2. Materials and methods

2.1. Chemicals and materials

Iron(III) chloride hexahydrate, iron(II) chloride tetrahydrate, tetramethylammonium hydroxide solution, kraft lignin (lignin, Mw ~10 000 u), α-chitin from shrimp shells (chitin), trypsin from bovine pancreas (EC 3.4.21.4), N-α-benzoyl-DL-arginine-4-nitroanilide hydrochloride (BAPNA), N,N-dimethylformamide, *p*-nitroanilide, benzamidine, Coomassie Brilliant Blue G-250 (CBBG-250) dye, bovine serum albumin (BSA), dithiothreitol (DTT), iodoacetamide and ammonium bicarbonate were obtained from Sigma-Aldrich (USA). Phosphate buffer at pH 7.2 (PBS) and 100 mM Tris-HCl buffer were supplied by Amresco (USA). Hydrochloric acid, 85% phosphoric acid, 96% ethyl alcohol, calcium chloride and acetic acid were purchased from Chempur (Poland). α-Cyano-4-hydroxycinnamic acid (CHCA) and Peptide Calibration Standard were obtained from Bruker Daltonics (Poland).

2.2. Synthesis of magnetite nanoparticles

Magnetite nanoparticles were synthesized by a co-precipitation method, as described in our previous work [27], with slight modifications. Briefly, iron(II) chloride and iron(III) chloride were dissolved in 2 M HCl in a molar ratio of 2:1 and mixed in an atmosphere of inert gas (nitrogen) at 80 °C. During mixing, a solution of tetramethylammonium hydroxide solution was dropped in for 1 h. Finally, the reaction mixture was centrifuged, washed several times with deionized water and dried at 50 °C for 12 h.

2.3. Synthesis of magnetite-lignin and magnetite-chitin hybrid materials

In the first stage, chitin and lignin were ground on a mechanical mortar. In the second stage, 500 mg of each of the biopolymer was placed in a reactor in 100 mL of deionized water, and 500 mg of the previously synthesized magnetite nanoparticles were added. The mixture was then stirred for 2 h using an MS-H-S10 magnetic stirrer (ChemLand, Poland). After synthesis, the hybrid materials were separated from the mixture with the use of a magnet, washed several times with deionized water, and dried at 40 °C for 12 h.

2.4. Trypsin immobilization

For the immobilization, 5 mL of trypsin solution at a concentration of 5 mg/mL in phosphate buffer at pH 7.2 (containing 1 mg of benzamidine) was added to 100 mg of the previously obtained hybrid support. The mixture was shaken in a KS260 Basic incubator (IKA Werke GmbH, Germany) at ambient temperature for 20 h. The biocatalytic systems obtained were then separated magnetically, and washed five times with the phosphate buffer. The resulting biocatalytic systems and filtrates were subjected to further analysis.

2.5. Storage stability and reusability of free and immobilized trypsin and desorption tests

Storage stability and reusability of the free and immobilized trypsin were evaluated by the method of Gaertner and Puigserver [28], based on the hydrolysis reaction of N-α-benzoyl-DL-arginine-4-nitroanilide hydrochloride (BAPNA) in N,N-dimethylformamide to *p*-nitroanilide (pNA). The reaction was performed at ambient temperature in a 100 mM Tris-HCl buffer solution at pH 7.8 containing 1 mM of BAPNA, 20 mM of $CaCl_2$ and 10 mg of free or immobilized enzyme. The reaction was carried out for 30 min and was stopped by addition of 2 mL of acetic acid. The quantity of pNA released was measured spectrophotometrically (Jasco V750, Japan) at λ = 405 nm and determined based on the calibration curve of *p*-nitroanilide. All measurements were made in duplicate. One unit of free or immobilized trypsin activity is defined as the quantity of enzyme catalyzing the production of 1 μmol of *p*-nitroanilide per 1 min under assay conditions. For the study of storage stability and reusability, the initial value of free or immobilized enzyme activity was defined as 100% activity. Reusability was evaluated over 10 consecutive catalytic cycles. After each reuse the immobilized trypsin was separated magnetically from the reaction mixture, washed with a phosphate buffer and reintroduced into a fresh reaction mixture. Storage stability was evaluated every two days for free and immobilized enzyme stored at 4 °C.

The desorption of immobilized trypsin by phosphate buffer at pH 7.2 and 0.1 M sodium chloride solutions was evaluated over a time of 12 h. For this purpose, both the magnetite-lignin and magnetite-chitin hybrids with immobilized trypsin were dispersed in PBS and 0.1 M sodium chloride solution. After the specified period of time, the amount of the trypsin eluted from the support was evaluated based on the Bradford method [29].

2.6. Kinetic measurements of free and immobilized trypsin

The Michaelis–Menten kinetic constant (K_m), maximum reaction rate (V_{max}), turnover number (k_{cat}) and specificity constant (k_{cat}/K_m) of free and immobilized trypsin were determined as described in Section 2.5, using various initial concentrations of BAPNA. Kinetic parameters were examined according to Lineweaver–Burk plots under optimum reaction assay conditions. All measurements were made in duplicate.

2.7. Digestion of human serum albumin by free and immobilized trypsin

A human blood sample from a healthy donor who had provided written informed consent (approval no. 926/166 15.09.2016

from the Bioethical Committee of Karol Marcinkowski University of Medical Sciences, Poznan, Poland) was harvested in collection tubes with EDTA. Two microliters of plasma sample was diluted with 50 mM NH_4HCO_3 to a final volume of 120 μL. Next 10 μL of the diluted sample was reduced with 5.6 mM DTT for 5 min at 95 °C. The sample was then alkylated with 5 mM iodoacetamide for 20 min in the dark. The proteins were digested with 2 μL of 0.5 μg/μL free trypsin or 10 mg of immobilized trypsin overnight at 37 °C. Each sample was prepared for digestion in duplicate.

Digested proteins were analyzed using MALDI-TOF/TOF. MALDI spectra were acquired on an UltrafleXtreme mass spectrometer (Bruker Daltonics, Germany) operating in reflector mode using delayed ion extraction. Positively charged ions in the *m/z* range 900–3500 were analyzed. For each sample, 0.5 μL was co-crystallized with CHCA matrix and spotted directly onto the MALDI AnchorChip target. The MS spectra were externally calibrated using the Peptide Calibration Standard mixture. Flex control v. 3.3 was used for the acquisition of spectra, and all further data processing was performed using Flex analysis v. 3.3 and Biotools 3.2. Proteins were identified using the Mascot (Matrix Science, London, UK) program against human albumin fasta. The protein search was performed using the following search parameters: precursor-ion mass tolerance +/−0.3 Da; cysteine treated with iodoacetamide to form carbamidomethyl-cysteine and oxidized methionine. Trypsin was set as the enzyme, with a maximum of two missed cleavages.

2.8. Characterization of hybrid materials and products after immobilization

The quality of the obtained hybrid materials was verified by X-ray diffraction on an X'pert Pro PANalytical (Netherlands) powder diffractometer with Cu Kα radiation. All measurements were made at room temperature. Structure refinement was performed using the FULLPROF program.

Porous structure parameters (surface area, total volume and mean size of pores) were analyzed using an ASAP 2020 apparatus (Micromeritics Instrument Co., USA). The BET (Brunauer–Emmett–Teller) method was used to determine the surface area using data for adsorption under relative pressure (p/p_0) at 77 K, and the BJH (Barrett–Joyner–Halenda) algorithm was used to evaluate pore volume and mean pore size.

The quantity of immobilized trypsin was determined using the Bradford method, by measuring the quantities of trypsin in the samples before and after immobilization. The quantity of immobilized enzyme (expressed in milligrams of immobilized enzyme per gram of support) was determined according to the calibration curve of BSA solutions at known concentration.

Magnetic characterization of the prepared hybrid materials was carried out in the temperature range 2–300 K and in magnetic fields up to 5T using a SQUID magnetometer (MPMS Quantum Design, USA). The temperature dependence of magnetization was measured in zero field cooled (ZFC) and field cooled (FC) conditions in a magnetic field of 1 kOe. Hysteresis curves were recorded at room temperature and at 5 K.

3. Results and discussion

3.1. Characterization of hybrid materials

3.1.1. XRD analysis

Figure 1 shows X-ray diffraction patterns for pure (magnetite – Fe_3O_4, lignin, and chitin) and hybrid materials (M-C, M-L). For pure Fe_3O_4, peaks related only to the cubic structure were observed. The lattice constant obtained from Rietveld refinement is close to the values obtained in our previous study [27]. The broadening

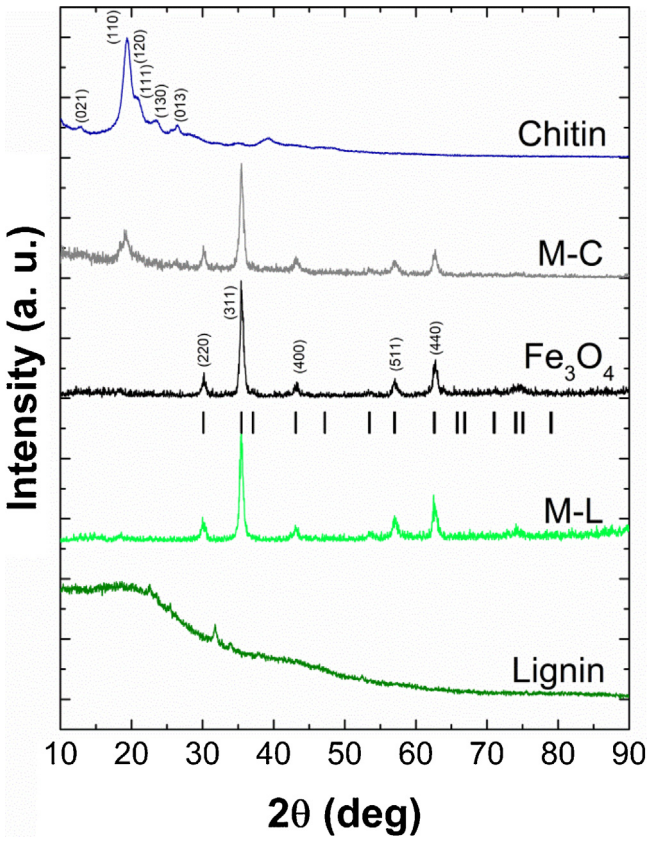

Fig. 1. XRD patterns of raw (magnetite, chitin, and lignin) and synthesized magnetite-lignin (M-L) and magnetite-chitin (M-C) hybrid materials. The ticks represent Bragg positions corresponding to the cubic phase of Fe_3O_4. The Miller indices are shown for the most pronounced peaks for pure chitin and Fe_3O_4.

of the Bragg peaks is mostly related to the size effect. The average crystalline size obtained from the Scherrer's equation is about 16 nm. Pure lignin, which is an amorphous polymer, does not shows Bragg peaks in XRD pattern [30]. In contrast, chitin revels several well-defined broad peaks corresponding to the crystallographic order [31,32]. The most pronounced diffraction peaks observed at 12.8°, 19.3°, 23.4°, and 26.4°, corresponds to the (021), (110), (130), and (013) planes, respectively. Obtained result are typical for α-chitin. The XRD patterns for the hybrids are composite of the starting materials patterns. This provides confirmation that the proposed methods of synthesis are effective, and additionally that the synthesis procedure does not affect the crystal structure of the starting materials. Additionally, detailed dispersive-morphological and physicochemical characterization of the synthesized hybrid materials was carried out (see Supplementary Materials).

3.2. Characterization of systems after immobilization

3.2.1. Porous structure parameters and amount of immobilized enzyme

As regards structural properties, magnetite has higher BET surface area, pore sizes and pore volume (16.6 m^2/g, 30.7 nm and 0.143 cm^3/g) than the other precursors (lignin and chitin), mainly due to its nanometric-scale particles (Table 1). The results are due to the formation of conjugates and agglomerates by the magnetite particles. The porous structure parameters of lignin and chitin are significantly lower than those of magnetite mainly due to the natural origin of these materials. The hybrids have BET surface areas of 4.3 and 5.6 m^2/g for magnetite-lignin and magnetite-chitin respectively; these values are higher than for

Table 1
Porous structure parameters of magnetite, lignin, chitin and synthesized hybrid materials before and after trypsin immobilization, and quantity of immobilized trypsin and immobilization yield.

Analyzed parameter	Analyzed sample						
	Magnetite	Lignin	Chitin	Magnetite-lignin	Magnetite-lignin+ trypsin	Magnetite-chitin	Magnetite-chitin+ trypsin
BET surface area (m^2/g)	16.6	1.1	2.5	4.3	4	5.6	5.1
Mean size of pores (nm)	30.7	12.5	23.4	21.2	19.6	27.6	24.2
Total pores volume (cm^3/g)	0.143	0.002	0.015	0.038	0.035	0.089	0.082
Amount of immobilized enzyme (mg/g)	–	–	–	–	155 ± 3.8	–	207.5 ± 5.6
Immobilization yield (%)	–	–	–	–	62 ± 4	–	83 ± 5

the pure biomaterials, but lower than for magnetite nanoparticles. The pore sizes and total pore volumes followed the same pattern. Trypsin immobilization led to a further decrease in all of the analyzed parameters. The BET surface area, pore size and total pore volume were 4 m^2/g, 19.6 nm and 0.035 cm^3/g respectively for magnetite-lignin + trypsin, and 5.1 m^2/g, 24.2 nm and 0.082 cm^3/g for magnetite-chitin + trypsin. The decrease in the porous structure parameters confirmed the effective immobilization of trypsin [33]. Furthermore, the drop in the values of pore size and pores volume suggested that trypsin was bound also in the pores of the material [34]. It should also be noted that the larger drop in the porous structure parameters of the magnetite-chitin support after immobilization is linked to the greater amount of immobilized trypsin (207.5 mg/g) compared with magnetite-lignin. Also a higher immobilization efficiency (83%) was recorded with the use of the magnetite-chitin material. The greater amount of immobilized enzyme and higher immobilization efficiency observed for magnetite-chitin support is probably related to the greater amount of the functional moieties, such as hydroxyl, carbonyl and amine groups, presented in the structure of the chitin, and their higher accessibility, as compared to lignin, which are responsible for the effective binding of the enzyme. It also should be added, that chitin, and in consequence also magnetite-chitin support, are characterized by higher porous structure parameters, compared to lignin, that results in greater amount of active sites allowing effective attachment of the enzyme molecules. These data are in agreement with the results obtained in our previous study, in which α-amylase was immobilized on a titania/lignin hybrid. A drop in the values of all analyzed parameters of samples after immobilization was also recorded in that case, confirming the effective attachment of the enzyme [35].

3.2.2. Magnetic properties of the obtained systems

All of the prepared materials exhibit similar magnetic properties (Fig. 2). The magnetization at 300 K and 5 T for pure nanosized Fe_3O_4 (71 emu/g) is lower than the theoretical value for bulk magnetite (92 emu/g) [36]. For the hybrid materials the magnetization values are significantly smaller, primarily due to the different quantities of Fe_3O_4. The change in magnetization may also be related to an increase in the shell layer thickness, as has been suggested by other researchers [37]. At 5 K (lower inset of Fig. 2) all materials show a clear hysteresis of ~450 Oe, while at room temperature there is no hysteresis. For the temperature dependence of magnetization (upper inset of Fig. 2) we observed a bifurcation for zero field cooled (ZFC) and field cooled (FC) curves at ~265 K. The ZFC curve has a broad maximum at around 110 K, which may indicate the superparamagnetic behavior of nanosized Fe_3O_4 particles. In the literature, a blocking temperature of 110 K was observed for Fe_3O_4 nanoparticles with an average diameter of ~10 nm [38,39]. On the other hand the FC curves increase monotonically with decreasing temperature. Our results suggest that the performed modification does not change the magnetic properties of pure nanosized Fe_3O_4, which exhibits superparamagnetic behavior. It should be emphasized that the prepared hybrid materials can be easily separated from water solution by applying an external magnet to the container (Fig. 2b).

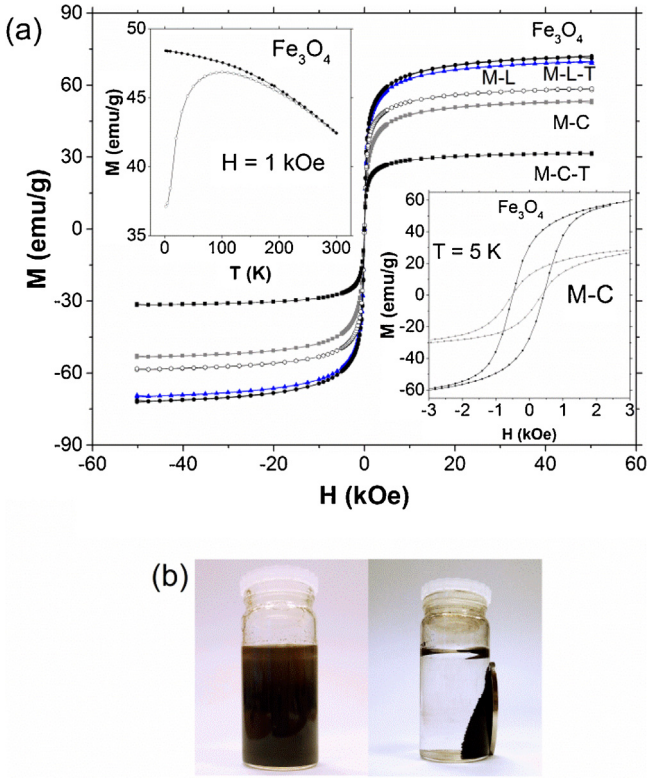

Fig. 2. Magnetization curves at room temperature for the studied hybrid materials. Upper inset: magnetization vs. temperature for pure magnetite. Lower inset: magnetization curves at 5 K for pure magnetite and M-C hybrid material (a) magnetic separation of magnetite-chitin + trypsin from reaction mixture solution by a permanent magnet (b).

3.3. Free and immobilized trypsin stability

Reusability is an important factor for the practical application of immobilized trypsin in protein digestion. In the case of magnetic supports this property is enhanced due to the easy recovery of biocatalytic systems using magnets. The trypsin immobilized on magnetite-lignin and magnetite-chitin hybrid supports retained 61% and 80% respectively of its initial activity after 10 consecutive cycles (Fig. 3a). The higher activity of trypsin attached to the magnetite-chitin support, in comparison with magnetite-lignin hybrid, is probably related to the formation of stronger enzyme–support interactions, due to the greater number of functional moieties present in this support material, which prevent the leaching of enzyme molecules from the matrix [40]. The storage stability of free and immobilized trypsin was evaluated over 20 days of storage. After this time the free enzyme had lost over 60% of its catalytic activity, while trypsin immobilized on Fe_3O_4-lignin and

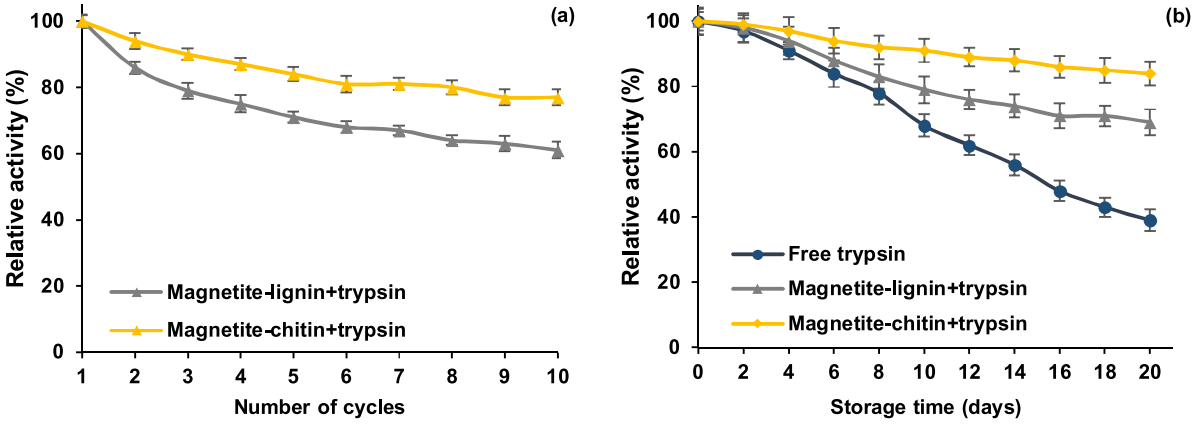

Fig. 3. Reusability (a) and storage stability (b) of free and immobilized trypsin.

Fe_3O_4-chitin retained 69% and 84% respectively of its initial activity (Fig. 3b). This may be attributed to an increase in the stability of the three-dimensional structure of the biocatalyst occurring as a result of immobilization. Nevertheless, the good reusability and storage stability of immobilized trypsin might also be explained by the formation of relatively strong and stable interactions between the enzyme and support. Formed interactions protect the trypsin from auto-dissociation and conformational changes during reuse and storage [41]. Obtained results are in agreement with the results of the desorption tests. When trypsin immobilized onto magnetite-lignin and magnetite-chitin hybrids was incubated for 12 h at PBS solution at pH 7.2 about 25 mg and 17 mg of the enzyme was leaked from the matrix. On the other hand, when immobilized enzyme was stored in 0.1 M NaOH solution for the same period of time, greater amount of enzyme was desorbed. Around 70 mg and less than 40 mg of trypsin, respectively, was eluted form magnetite-lignin and magnetite-chitin support. Shifting of the maxima of the signals in the FTIR spectra (detailed discussion is presented in Supplementary Materials, Fig. 3S), results of the desorption tests as well as presence of many functional moieties onto the surface of support materials suggest mixed adsorption (mainly hydrogen bonds) and covalent binding of the enzyme to the surface of hybrid supports as it was presented in the previous study [26,42].

3.4. Kinetic study of free and immobilized enzyme

To investigate the changes undergone by the trypsin on immobilization, kinetic parameters—the Michaelis–Menten constant (K_m), maximum reaction rate (V_{max}) and turnover number (k_{cat})—were calculated (Table 2). The K_m value of the free enzyme was 1.036 mM, while for trypsin immobilized on magnetite-lignin and magnetite-chitin supports it was 1.863 and 1.351 mM respectively. Lower values of V_{max} were recorded for magnetite-lignin + trypsin (0.893 U/mg) and for magnetite-chitin + trypsin (1.157 U/mg) than for the free enzyme (1.486 U/mg). The lower affinity of the substrate to the immobilized biocatalysts (indicated by higher values of K_m), and consequently the lower values of V_{max} recorded for both biocatalytic systems, may be explained by the creation of steric hindrances that limit transport of the substrates and block active sites of the enzyme [43]. However, lower substrate affinity and lower maximum reaction rate were noticed for trypsin immobilized onto lignin-based support indicating that amorphous character of this biopolymer enhances creation of diffusional limitations and decreases catalytic properties of the enzyme. These observations are in agreement with results reported by Sun et al., who showed that trypsin immobilized on carboxymethyl chitosan-functionalized magnetic nanoparticles also exhibited higher K_m and lower V_{max} values than free enzyme. However, due to the covalent immobilization of the enzyme in their study, an even greater decrease in substrate affinity and maximum reaction rate was recorded [44]. The value of the turnover number (85 1/s) computed for trypsin attached to the magnetite-chitin support was almost the same as for the free biocatalyst (87 1/s) and significantly higher than for the magnetite-lignin + trypsin system (53 1/s). The results suggest that both obtained biocatalytic systems retained their catalytic properties, but the magnetite-chitin hybrid support, due to its spatial structure and properties, appears to be more suitable for the immobilization of trypsin, as is also implied by the results of proteolysis of human serum albumin (see Section 3.5).

3.5. Digestion of human serum albumin by free and immobilized trypsin

The efficiency of digestion by immobilized trypsin was investigated using real biological samples. Human plasma samples subjected to proteolysis were analyzed by MALDI-TOF/TOF mass spectrometry. For comparison, plasma digestion by the free enzyme in solution was also investigated. Peptide mass spectra were obtained with an MS tolerance of ±0.3 Da. Because albumin accounts for about 60% of blood plasma proteins, in the next steps we focused only on this protein. The obtained spectra were compared and peptide fragments were identified using Mascot. Figure 4 shows the mass spectra of digested plasma protein fragments acquired using trypsin in solution and immobilized trypsin. Direct comparison of all spectra showed a high level of similarity between the spectra of soluble and magnetite-chitin immobilized trypsin: 59% of the signals present on the spectrum obtained from digestion by free trypsin were also observed

Table 2
Kinetic parameters of trypsin from bovine pancreas, free and immobilized on hybrid magnetic supports.

Kinetic parameters	Free trypsin	Magnetite-lignin + trypsin	Magnetite-chitin + trypsin
K_m (mM)	1.036 ± 0.035	1.863 ± 0.085	1.351 ± 0.094
V_{max} (U/mg)	1.486 ± 0.105	0.893 ± 0.092	1.157 ± 0.113
k_{cat} (1/s)	87 ± 9	53 ± 8	85 ± 11
k_{cat}/K_m (1/s*mM)	83.98	28.45	62.92

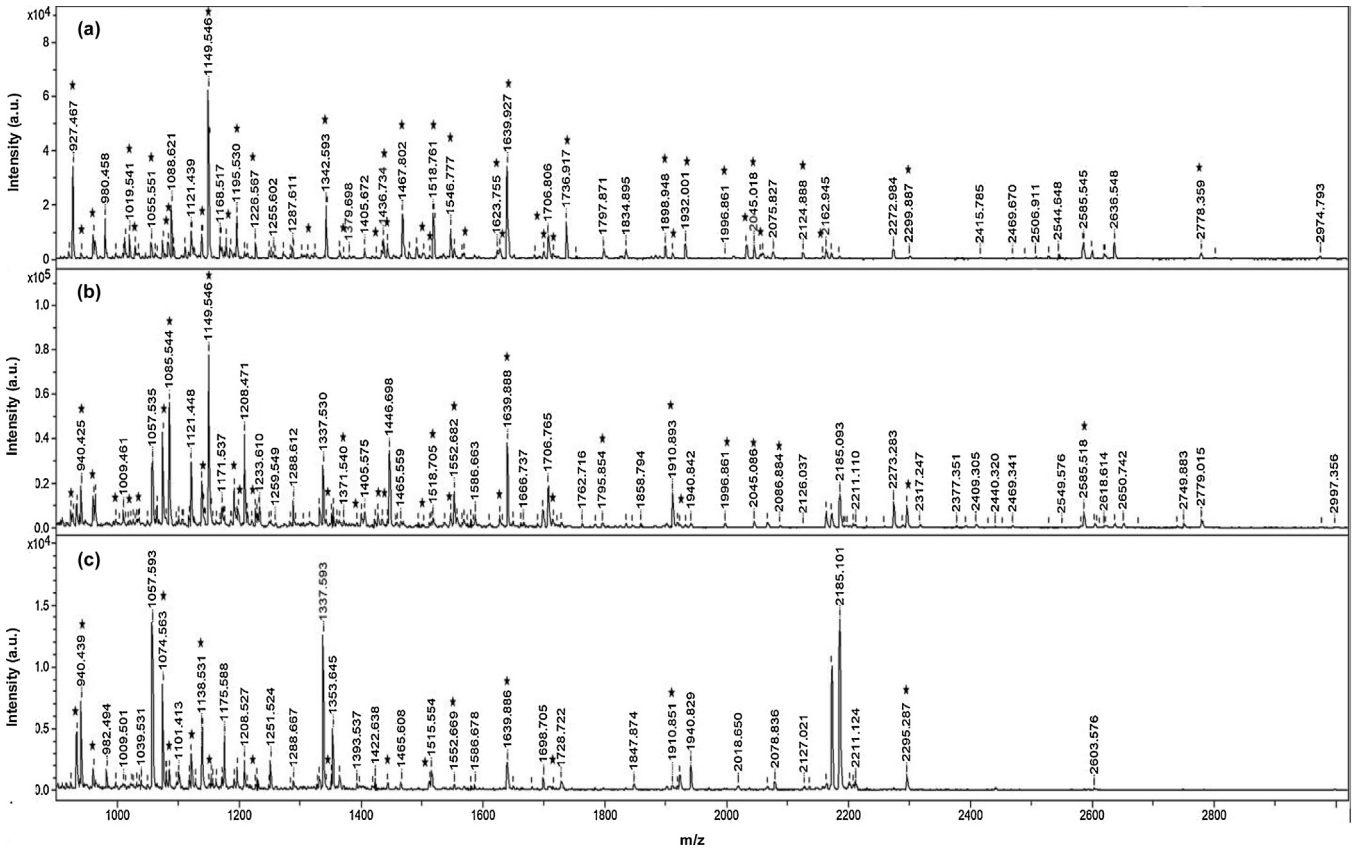

Fig. 4. Representative MALDI spectra of peptides obtained by digestion of plasma proteins with free (a), magnetite-chitin-immobilized (b) and magnetite-lignin-immobilized (c) trypsin. Asterisks show the specific fragments of human albumin identified by Mascot analysis.

on the spectrum obtained from digestion using trypsin immobilized on magnetite-chitin. Both spectra also contained the same most intensive albumin peptide peak at *m*/*z* 1149. This signal was also present on the spectrum for magnetite-lignin immobilized trypsin, but with a signal-to-noise threshold of 4.3, whereas the same parameter for magnetite-chitin immobilized trypsin was calculated as 110. The spectra obtained for magnetite-lignin immobilized trypsin contained a higher proportion of chemical noise compared with the soluble trypsin and trypsin immobilized on magnetite-chitin nanoparticles. As can be seen, the most intensive peaks on these spectra, at *m*/*z* 1057, 1337 and 2185, were not matched to plasma proteins. These peaks were also present on the spectra for magnetite-chitin immobilized trypsin, but were completely absent on the spectra for the free enzyme. This suggests that these unspecific signals may be linked to certain impurities introduced into the samples during preparation of the nanomaterial.

According to Mascot analysis, a large number of tryptic peptides from albumin were detected and identified [45]. The peaks labeled with asterisks were identified as peptides from the albumin sequence. Digestion by magnetite-chitin immobilized trypsin resulted in the identification of 36 peptides with albumin sequence coverage of 51% (Table 3). The same procedure for magnetite-lignin immobilized trypsin led to the identification of 17 fragments

Table 3
List of identified albumin peptides obtained after plasma digestion with free or immobilized trypsin. Measurement errors are given only for identified fragments for each variant. Unique fragments for immobilized digestion mode are in bold.

Calculated *m*/*z*	Sequence	Deviation (Da)		
		Free trypsin	Magnetite-chitin+ trypsin	Magnetite-lignin+ trypsin
927.493	YLYEIAR	−0.027	−0.034	
933.519	LCTVATLR		**−0.037**	**−0.016**
940.448	DDNPNLPR	−0.02	−0.023	−0.009
960.563	FQNALLVR	−0.033	−0.039	−0.027
1002.558	TPVSDRVTK		**−0.063**	
1017.536	SLHTLFGDK		**−0.036**	
1019.578	AFKAWAVAR	−0.037		
1029.46	CCKHPEAK	−0.007	0.001	
1055.588	KYLYEIAR	−0.037		
1074.543	LDELRDEGK	−0.033	−0.03	0.021
1083.595	YLYEIARR	−0.043		
1085.596	GVFRRDAHK		**−0.052**	**−0.016**
1128.699	KQTALVELVK			**−0.162**
1138.498	CCTESLVNR	−0.03	−0.028	0.033
1149.576	DAHKSEVAHR	−0.03	−0.03	0.005

Table 3 (*Continued*)

Calculated *m*/*z*	Sequence	Deviation (Da)		
		Free trypsin	Magnetite-chitin+ trypsin	Magnetite-lignin+ trypsin
1185.562	CCKHPEAKR	−0.034	0.013	
1195.589	CASLQKFGER	−0.059	−0.059	
1198.541	ETCFAEEGKK		**0.07**	
1226.605	FKDLGEENFK	−0.038	−0.044	−0.034
1231.694	QRLKCASLQK		**−0.205**	
1311.742	HPDYSVVLLLR	−0.062		
1342.635	AVMDDFAAFVEK	−0.041	−0.045	−0.019
1371.567	AAFTECCQAADK	−0.029	−0.027	
1400.677	VGSKCCKHPEAK		**−0.059**	
1424.739	DAHKSEVAHRFK	−0.038		
1434.533	ETYGEMADCCAK	−0.028	−0.017	
1436.768	LKCASLQKFGER	−0.033		
1443.642	YICENQDSISSK	−0.023	−0.037	−0.022
1467.843	RHPDYSVVLLLR	−0.041		
1490.905	QTALVELVKHKPK	−0.182		
1511.843	VPQVSTPTLVEVSR	−0.044	−0.08	−0.043
1518.776	LDELRDEGKASSAK	−0.014	−0.07	
1546.797	LKECCEKPLLEK	−0.02	−0.05	
1552.598	CCAAADPHECYAK	0.02	0.085	0.072
1623.788	DVFLGMFLYEYAR	−0.033		
1627.727	ADDKETCFAEEGKK	−0.009	−0.04	
1639.938	KVPQVSTPTLVEVSR	−0.011	−0.05	−0.052
1684.821	YICENQDSISSKLK	0.013		
1714.797	QEPERNECFLQHK	−0.013	−0.062	−0.076
1736.933	LSQRFPKAEFAEVSK	−0.016		
1795.884	DVFLGMFLYEYARR	−0.016	−0.029	
1898.995	HPYFYAPELLFFAKR	−0.048		
1910.932	RPCFSALEVDETYVPK	−0.031	−0.039	−0.081
1932.037	SLHTLFGDKLCTVATLR	−0.036	−0.074	
1996.929	NECFLQHKDDNPNLPR	−0.068	−0.068	
2032.144	YTKKVPQVSTPTLVEVSR	−0.05		
2045.095	VFDEFKPLVEEPQNLIK	−0.077	−0.009	
2055.096	RHPYFYAPELLFFAKR	−0.092		
2086.838	VHTECCHGDLLECADDR		**0.047**	
2124.987	AAFTECCQAADKAACLLPK	−0.099		
2157.09	ATKEQLKAVMDDFAAFVEK	−0.14		
2295.303	VPQVSTPTLVEVSRNLGKVGSK		**−0.03**	**−0.016**
2300.106	NYAEAKDVFLGMFLYEYAR	−0.218		
2585.118	VHTECCHGDLLECADDRADLAK		**0.401**	
2778.359	LVRPEVDVMCTAFHDNEETFLKK	0.001		

and 27% sequence coverage. For comparison, plasma digestion by the free enzyme yielded a sequence coverage of 61% with a peptide number of 43. However, 11 unique fragments were found after digestion by magnetite-chitin or magnetite-lignin immobilized trypsin. The absence of these peaks on the spectra after digestion by free trypsin may suggest some level of proteolysis specificity in the immobilized mode. The contribution of albumin peptides to the total ion current (TIC) was also determined. Ions for albumin fragments derived from digestion with magnetite-chitin and magnetite-lignin immobilized trypsin represented 43.37% and 24.25% of TIC respectively. For comparison, the corresponding value for free trypsin was 51.35%. Trypsin is an autodigestive enzyme, and the formation of autocatalysis products usually accompanies the analyzed peptides. Therefore, in the next step, the products of autocatalysis were compared. However, only a signal with *m*/*z* 2211 was present on both spectra obtained for immobilized trypsin. Moreover, the signal-to-noise thresholds for both signals were very low: 10 and 4.1 for magnetite-chitin and magnetite-lignin immobilized trypsin respectively. These results confirm the utility of the trypsin immobilized on nanomaterials in digestion, and suggest that the magnetite-chitin system is more efficient in the proteolysis of biological samples, mainly due to immobilization of the greater amount of trypsin and reduced diffusional limitations, as compared to magnetite-lignin hybrid support.

4. Conclusions

In this study, magnetite-lignin and magnetite-chitin hybrids, to the best of our knowledge were for the first time synthesized, characterized and used as support materials for trypsin immobilization. The results of XRD and FTIR analysis confirmed the effective synthesis of hybrid materials and enzyme immobilization. Over 150 mg and over 200 mg of trypsin per 1 g of matrix were bound to the surface of magnetite-lignin and magnetite-chitin hybrids respectively, with immobilization yields of 62% and 83%. The immobilized trypsin has been shown to have significantly improved storage stability: after 20 days of storage trypsin immobilized on magnetite-lignin and magnetite-chitin hybrids retained over 70% and over 80% of its initial activity. Moreover, due to the increased stability of immobilized trypsin and the use of magnetic supports, the reusability of the systems was also improved. After 10 consecutive biocatalytic cycles, trypsin immobilized on magnetite-lignin and magnetite-chitin hybrids retained respectively 69% and 84% relative activity. The obtained biocatalytic systems were applied in protein digestion, resulting in protein sequences similar to the peptide fragments obtained after digestion by free trypsin. Presented results suggest that obtained hybrid materials in the future might also be used for immobilization of different enzymes, however further study in this subject are required.

Acknowledgements

This work was supported by research grant funds from the National Science Center Poland in accordance with decision no. DEC-2015/19/N/ST8/02220.

Appendix A. Supplementary data

Supplementary data associated with this article can be found, in the online version, at https://doi.org/10.1016/j.colsurfb.2018.05.018.

References

[1] C. Su, J. Hazard. Mater. 322 (2017) 48.
[2] R. Sharma, S. Dutta, S. Sharma, R. Zboril, R. Varma, M.B. Gawande, Green Chem. 18 (2016) 3184.
[3] S. Laurent, D. Forge, M. Port, A. Roch, C. Robic, L. Vander Elst, R.N. Muller, Chem. Rev. 108 (2008) 2064.
[4] B. Andrzejewski, W. Bednarski, M. Kaźmierczak, A. Łapiński, K. Pogorzelec-Glaser, B. Hilczer, S. Jurga, G. Nowaczyk, K. Załęski, M. Matczak, B. Łeska, R. Pankiewicz, L. Kępiński, Compos. B: Eng. 64 (2014) 147.
[5] K. Tadyszak, A. Kertmen, E. Coy, R. Andruszkiewicz, S. Milewski, I. Kardava, B. Scheibe, S. Jurga, K. Chybczyńska, J. Magnet. Magn. Mater. 433 (2017) 254.
[6] T. Jesionowski, J. Zdarta, B. Krajewska, Adsorption 20 (2014) 801.
[7] A. Jędrzak, T. Rębiś, Ł. Klapiszewski, J. Zdarta, G. Milczarek, T. Jesionowski, Sens. Actuators B 256 (2018) 176.
[8] M.R. Lasheen, I.Y. El-Sherif, M.E. Tawfik, S.T. El-Wakeel, M.F. El-Shahat, Mater. Res. Bull. 80 (2016) 344.
[9] D. Honarmand, S.M. Ghoreishi, N. Habibi, E.T. Nicknejad, J. Appl. Polym. Sci. 133 (2016) 1.
[10] X. Luo, S. Liu, J. Zhou, L. Zhang, J. Mater. Chem. 19 (2009) 3538.
[11] J. Shen, Y. Li, Y. Zhu, Y. Hu, C. Li, J. Environ. Chem. Eng. 4 (2016) 2469.
[12] L. Ai, C. Zhang, Z. Chen, J. Hazard. Mater. 192 (2011) 1515.
[13] A. Tayyebi, M. Outokesh, S. Moradi, A. Doram, Appl. Surf. Sci. 353 (2015) 350.
[14] Y. Tang, H. Guo, L. Xiao, S. Yu, N. Gao, Y. Wang, Colloid Surf. A: Physicochem. Eng. Aspects 424 (2013) 74.
[15] Y. Zhan, R. Zhao, Y. Lei, F. Meng, J. Zhong, X. Liu, J. Magnet. Magn. Mater. 323 (2011) 1006.
[16] L. Jiang, L. Gao, Chem. Mater. 15 (2003) 2848.
[17] Z. Durmus, H. Kavas, A. Baykal, H. Sozeri, L. Alpsoy, S.Ü. Celik, M.S. Toprak, J. Alloys Compd. 509 (2011) 2555.
[18] Z. Durmus, H. Sözeri, B. Unal, A. Baykal, R. Topkay, S. Kazan, M.S. Toprak, Polyhedron 30 (2011) 322.
[19] R. DiCosimo, J. McAuliffe, A. Poulose, G. Bohlmann, Chem. Soc. Rev. 42 (2013) 6437.
[20] K. Atacan, B. Cakıroglu, M. Özacar, Colloids Surf. B: Biointerfaces 156 (2017) 9.
[21] M. Slováková, M. Sedlák, B. Krizková, R. Kupcik, R. Bulánek, L. Korecká, C. Drasar, Z. Bílková, Proc. Biochem. 50 (2015) 2088.
[22] P. Nicolás, V. Lassalle, M.L. Ferreira, Bioproc. Biosyst. Eng. 41 (2018) 171.
[23] J. Sun, L. Yang, M. Jiang, Y. Shi, B. Xu, H. Ma, J. Chromatogr. B 1054 (2017) 57.
[24] A. Bougatef, J. Clean. Prod. 57 (2013) 257.
[25] H. Yang, M.W. Wong, J. Am. Chem. Soc. 135 (2013) 5808.
[26] K. Atacan, B. Cakiroglu, M. Özacar, Food Chem. 212 (2016) 460.
[27] Ł. Klapiszewski, J. Zdarta, K. Antecka, K. Synoradzki, K. Siwińska-Stefańska, D. Moszyński, T. Jesionowski, Appl. Surf. Sci. 422 (2017) 94.
[28] H.F. Gaertner, A.J. Puigserver, Enzym. Microb. Technol. 14 (1992) 150.
[29] M.M. Bradford, Anal. Biochem. 72 (1976) 248.
[30] A. Goudarzi, L.T. Lin, F.K. Ko,J. Nanotechnol. Eng. Med. 5 (2014), 021006.
[31] Y. Zhang, C. Xue, Y. Xue, R. Gao, X. Zhang, Carbohydr. Res. 340 (2005) 1914.
[32] E.L. Mogilevskaya, T.A. Akopova, A.N. Zelenetskii, A.N. Ozerin, Polym. Sci. Ser. A 48 (2006) 116.
[33] N. Miletić, Z. Vuković, A. Nastasović, K. Loos, Macromol. Biosci. 11 (2011) 1537.
[34] A.B. Jastrzębski, K. Szymańska, J. Bryjak, J. Mrowiec-Białoń, Catal. Today 124 (2007) 2.
[35] Ł. Klapiszewski, J. Zdarta, T. Jesionowski, Colloids Surf. B: Biointerfaces 162 (2018) 90.
[36] D.H. Han, J.P. Wang, H.L. Luo, J. Magnet. Magn. Mater. 136 (1994) 176.
[37] Y.T. Zhu, X.Y. Ren, Y.M. Liu, Y. Wei, L.S. Qing, X. Liao, Mater. Sci. Eng. C 38 (2014) 278.
[38] G.F. Goya, T.S. Berquó, F.C. Fonseca, M.P. Morales, J. Appl. Phys. 94 (2003) 3520.
[39] A. Mitra, J. Mohapatra, S.S. Meena, C.V. Tomy, M. Aslam, J. Phys. Chem. C 118 (2014) 19356.
[40] J. Srbová, M. Slováková, Z. Křípalová, M. Žárská, M. Špačková, D. Stránská, Z. Bílková, React. Funct. Polym. 104 (2016) 38.
[41] M. Chellapandian, C.A. Sastry, Bioproc. Eng. 11 (1994) 17.
[42] S. Altun, B. Cakıroğlu, M. Özacar, M. Özacar, Colloids Surf. B: Biointerfaces 136 (2015) 963.
[43] M. Yakup Arica, S. Senel, N.G. Alaeddinoglu, S. Patir, A. Denizli, J. Appl. Polym. Sci. 75 (2000) 1685.
[44] J. Sun, L. Yang, M. Jiang, Y. Shi, B. Xu, H. Ma, J. Chromatogr. B 1054 (2017) 57.
[45] T. Koenig, B.H. Menze, M. Kirchner, F. Monigatti, K.C. Parker, T. Patterson, J.J. Steen, F.A. Hamprecht, H. Steen, J. Proteome Res. 7 (2008) 3708.

Advances in Colloid and Interface Science 258 (2018) 1–20

Contents lists available at ScienceDirect

Advances in Colloid and Interface Science

journal homepage: www.elsevier.com/locate/cis

Historical Perspective

Developments in support materials for immobilization of oxidoreductases: A comprehensive review

Jakub Zdarta [a,b,*], Anne S. Meyer [b], Teofil Jesionowski [a], Manuel Pinelo [b]

[a] Institute of Chemical Technology and Engineering, Faculty of Chemical Technology, Poznan University of Technology, Berdychowo 4, PL-60965 Poznan, Poland
[b] Department of Chemical and Biochemical Engineering, Center for BioProcess Engineering, Technical University of Denmark, Soltofts Plads 229, DK-2800 Kgs. Lyngby, Denmark

ARTICLE INFO

Available online 24 July 2018

Keywords:
Support materials
Materials properties
Enzyme immobilization
Oxidoreductases
Hazardous pollutants
Environmental protection

ABSTRACT

Bioremediation, a biologically mediated transformation or degradation of persistent chemicals into nonhazardous or less-hazardous substances, has been recognized as a key strategy to control levels of pollutants in water and soils. The use of enzymes, notably oxidoreductases such as laccases, tyrosinases, various oxygenases, aromatic dioxygenases, and different peroxidases (all of EC class 1) is receiving significant research attention in this regard. It should be stated that immobilization is emphasized as a powerful tool for enhancement of enzyme activity and stability as well as for protection of the enzyme proteins against negative effects of harsh reaction conditions. As proper selection of support materials for immobilization and their performance is overlooked when it comes to comparing performance of immobilized enzyme in academic studies, this review summarizes the current state of knowledge regarding the materials used for enzyme immobilization of these oxidoreductase enzymes for environmental applications. In the presented study, thorough physicochemical characteristics of the support materials was presented. Moreover, various types of reactions and notably operational modes of enzymatic processes for biodegradation of harmful pollutants are summarized, and future trends in use of immobilized oxidoreductases for environmental applications are discussed. Our goal is to provide an improved foundation on which new technological advancements can be made to achieve efficient enzyme-assisted bioremediation.

Contents

* Corresponding author at: Institute of Chemical Technology and Engineering, Faculty of Chemical Technology, Poznan University of Technology, Berdychowo 4, PL-60965 Poznan, Poland.
E-mail address: jakub.zdarta@put.poznan.pl (J. Zdarta).

https://doi.org/10.1016/j.cis.2018.07.004
0001-8686/

1. Introduction

Over recent years the production and wide application of synthetic chemical compounds has become essential in many branches of industry. There are, however, some serious drawbacks related to the use of these compounds because they are poorly biodegradable [1]. Interest therefore continues to grow in remediation of endocrine disrupting chemicals (EDCs), hormones, pesticides, synthetic dyes and pharmaceuticals because these substances may alter the functions of hormonal and nervous systems, cause diseases of the male and female reproductive system, disorders and alterations of neurological and metabolism and cause adverse effects in intact organisms [2–4]. These synthetic chemicals exhibit genotoxic activity, can cause diabetes, obesity, cardiovascular diseases, reproductive disorder or even cancer [5, 6]. Another cause for serious environmental concern is pollution of communal wastewater and effluents released by the textile or paper industries, agriculture or houses. Nowadays, there are a plenty of both physical and chemical methods for removal of persistent compounds. One of the most effective and eco-friendly of these methods is application of enzymes for biodegradation of hazardous pollutants.

Enzymes have for years been known as extremely efficient and highly effective biocatalysts that additionally are characterized by high chemo-, regio- and stereoselectivity. Furthermore, enzymes through decreasing the amount of toxic solvents and reducing the number of synthesis steps and activation energy, make the catalytic process more cost-effective and environmentally friendly [7]. In the current review, attention is given to laccases, tyrosinases, manganese and horseradish, lignin and phenol peroxidases, however also other oxidoreductases such as monooxygenases, oxygenases and even oxidases might be employed as highly efficient green biocatalysts for remediation of environmental pollutions [8], but literature references about efficient immobilization of monooxygenases and oxygenases for environmental protection are strongly limited. Above-mentioned types of enzymes are able to catalyze redox-transformations and degradation of a large number of organic compounds, in particular phenolic and non-phenolic aromatic compounds such as phenol and its derivatives, EDCs, synthetic and natural dyes, pesticides and pharmaceuticals [9, 10]. The catalytic action of these enzymes might range from simple transformation of contaminants to less toxic derivatives to manipulation of contaminated environments or even to bioaccumulation of pollutants [11].

Enzyme immobilization can be accomplished in various ways, but usually involves attachment of the enzyme molecules to a solid carrier, which is usually insoluble in the reaction environment [12]. The result is immobilized biocatalyst where the form of the enzyme has been changed from homogenous (free enzyme) to heterogeneous (immobilized enzyme). Enzyme immobilization allows maximal reuse or recycling of the enzyme in continuous processes where the substrate is fed continuously into the reaction to increase the biocatalytic productivity (amount of substrate molecules converted per amount of enzyme). Immobilized enzymes are usually characterized by enhanced stability against harsh conditions of pH, temperature and pressure [13]. Moreover, storage stability and reusability of the immobilized biocatalyst increases significantly compared with free enzyme [14]. So it could be summarized that immobilization represent simple and effective routes for improvement of enzyme properties as compared to application of the native biocatalysts [15]. The five main immobilization techniques are covalent binding, adsorption, encapsulation, entrapment and cross-linking. However, it should be emphasized that there is no universal method for any particular enzyme [16]. Selection and optimization of the most suitable support material and technique of immobilization is dependent on the type of the enzyme and biocatalytic process. It should also be mentioned that proper selection of support for enzymes such as laccases or tyrosinases for environmental applications not only ensured highly efficient biodegradation of toxic compounds but also protected enzyme molecules from denaturation and allowed their reusability [17]. Many different materials can potentially be used as support materials for enzyme immobilization. Nevertheless, the material has to fulfill some requirements in order to be used as a carrier. First, physicochemical features like the presence of chemical moieties, large surface area or good sorption properties are crucial for establishing of strong and stable interactions between the enzyme and a support material [18]. It is important that for environmental use, support materials should also be biocompatible, non-toxic, and environmentally friendly/acceptable and cannot negatively affect solution after biodegradation. Also, hydrophilicity of the carrier, its structure and mechanical or operational stability strongly affect the properties of the produced biocatalytic system and ultimately determine successful immobilization [19]. It should be stressed that for attachment of a biocatalyst for environmental applications, materials of organic, inorganic as well as hybrid or composite origin have been frequently studied [20]. Their selection is dictated by type of enzyme, type of biocatalytic conversion, character of the process and required form and shape of biocatalytic beads, all of which influence the efficiency of the whole bioremediation process [21].

The present review briefly describes various immobilization protocols used for binding of oxidoreductases. The main purpose of the literature study was to summarize and compare the current state of knowledge about support materials for enzyme immobilization with particular reference to immobilization of laccases, tyrosinases and phenyloxidases and use of the resulting biocatalytic systems in the removal of hazardous pollutants. The properties of inorganic, organic and hybrid support materials required for effective enzyme binding are specified and presented. Various types and configurations of degradation processes, and types of reactors are highlighted. Furthermore, the effect of operational parameters such as time, pH and temperature on the removal efficiencies of undesirable compounds are compared, as well as storage stability and reusability of the immobilized biocatalysts. We also discuss present and future perspectives for application of immobilized oxidoreductases for environmental protection with emphasis on pollutants removal.

2. Enzymes for environmental applications

As previously mentioned, enzymes belonging to the oxidoreductases (EC 1), such as laccases, tyrosinases, manganese, lignin and horseradish peroxidases, and phenoloxidases, are the most frequently employed for environmental applications [22]. These enzymes are

being investigated due to their applicability as "green catalysts" in the bioremediation of various dangerous chemicals such as phenols and derivatives, bisphenols, organic dyes or pharmaceuticals [23]. They have been found to be efficient biocatalysts for remediation of toxic compounds, but the structures, cofactors and mechanisms of action differ for each type of catalyst. Selected examples of the enzymes most frequently used for environmental protection are discussed in detail below.

2.1. Laccases

Laccases of various origin are the most commonly used for environmental protection. Laccases, which are extracellular enzymes also known as *p*-diphenol: dioxygen oxidoreductases (EC 1.10.3.2), are oxidoreductases omnipresent in plants and bacteria, however, laccases from fungi like *Trametes versicolor*, *Trametes vilosa* or *Cerrena unicolor* are of the greatest interest due to their high catalytic activity, availability and low price [24]. Laccases, due to their low substrate specificity, are enzymes that can catalyze wide range of reactions, mainly one-electron oxidation of monophenols, diphenols and polyphenols as well as diamines, aromatic amines and related substances such as N-heterocycles, phenothiazines and many others. These oxidation processes generate reactive phenoxy radicals with a simultaneous reduction of oxygen to water, without the need for hydrogen peroxide [25]. These laccases constitute a wide group of multi copper oxidase enzymes that contain four copper ions in their structure that exhibit different properties. A type-1 copper atom (T1) is responsible for the blue color of the laccase and together with the type-2 atom (T2) and two atoms of type 3 (T3) take part in oxidation-reductions reactions catalyzed by laccases [26]. In detailsd, the bioconversion acts are initiated at the type-1 copper atom where electrons from substrate molecules are extracted and transferred via His-Cys-His triade to the T2/T3 group. Further, accumulated electrons enable the oxidation reaction and simultaneously allow the reduction of molecular oxygen to water [27]. It also should be added that laccases are employed in various applications such as in the food, textile, fuel and medical industries [28]. Due to their wide substrate specificity and ubiquitous properties, they are able to act on a wide range of phenolic compounds and are increasingly used for bioremediation of environmental pollutants from soils and water [29, 30]. The example of the catalytic pathways of conversion of bisphenol A and tetracycline by laccase are presented in Fig. 1. Most laccases are extracellular proteins with isoelectric points ranging from 3 to 7 for fungal laccases and around 9 for plant laccases. Moreover, differences in optimal pH for both sources of laccases have been found: fungal laccases exhibit maximal catalytic properties at pH between 3.5 and 5 as laccases from plants have pH optima around pH 7. Differences in the temperature optima between various laccases have also been found [31].

2.2. Tyrosinases

Tyrosinases, *o*-diphenol: oxygen oxidoreductases (EC 1.14.18.1), also contain copper atoms in their active site. These copper atoms are known as CuA and CuB and are coordinated by histidine residues [34]. Tyrosinases are frequently abundant in nature and are found in plants, fungi, bacteria, insects and in mammalian issues [35]. They play a key role in the synthesis of melanin – the dye that is responsible for the color of human skin. Tyrosinases differ essentially from laccases in the mechanism of oxidation of phenol and its derivatives. Although tyrosinases also use oxygen as a cofactor, they generate quinones instead of free radicals and water molecules as a by-product [36]. The mechanism of catalytic action of tyrosinases has been defined as a two-step consecutive reaction of monophenol hydroxylation to corresponding ortho-diphenols and their further oxidation to ortho-quinones using O_2 molecules in both steps. Later release of water molecules terminates catalytic oxidation and leads to a polymerization reaction of *o*-quinones to macromolecular compounds [37] (See Fig. 2). Due to the fact that tyrosinases can occur in various molecular forms, different intermediates may be formed during catalysis of phenolic compounds [9]. It should be clearly stated that due to their wide specificity, tyrosinases similarly to laccases are able to catalyze transformation of various compounds such as phenol, monophenols and its multisubstituted derivatives, including chloro- and nitrophenols and bisphenols [38]. The effect of temperature and pH on the stability and activity of various tyrosinases has been thoroughly analyzed. A previous study reported pH ranging from 5.5 to 8 as the most suitable for the highest activity of free tyrosinases [39]. The effect of temperature on the activity of tyrosinases has also been studied. Published data showed that free tyrosinases exhibit the highest activity at temperatures ranging from 30 to 40 °C and that activity significantly decreases above 60 °C.·It should be added that most of tyrosinases under optimal conditions exhibit relatively good stability and retain high activity (80–100%) even for 8 h [40].

2.3. Lignin peroxidases

Besides laccases and tyrosinases, lignin peroxidases are also used for remediation of hazardous phenolic compounds from water and soil. Lignin peroxidase, 1,2-bis(3,4-dimethoxyphenyl)propane-1,3-diol:-hydrogen peroxide oxidoreductase (EC 1.11.1.14), also known as LiP, contains 1 mol of iron protoporphyrin (heme) as its cofactor for 1 mol of protein [41]. Lignin peroxidases catalyze the oxidative depolymerization of lignin in the presence of H_2O_2. Exemplary reaction, which characterizes catalytic action of LiP (oxidation of 1,2-bis (3,4-dimethoxyphenyl)propane-1,3-diol) could be presented as [42]:

$$1,2\text{–}bis(3,4\text{–}dimethoxyphenyl)propane\text{–}1,3\text{–}diol + H_2O_2 \leftrightarrow 3,4\text{–}dimethoxybenzaldehyde + 1\text{–}(3,4\text{–}dimethoxyphenyl)ethane\text{–}1,2\text{–}diol + H_2O.$$

It should be added that LiP is characterized by low substrate specificity with high, non-specific oxidation-reduction potential and is known for its ability to oxidize aromatic phenolic and non-phenolic compounds as well as a wide range of organic chemical compounds, such as xenobiotics with a redox potential of up to 1.4 V [43]. LiP was extracted for the first time from *Phanerochaete chrysosporium* but these enzymes are also known to be found in many microorganisms and white-rot fungi [44]. It should be mentioned further that lignin peroxidase is known from its low optimum pH value, as these enzymes reach their maximum catalytic activity at a pH near 3. The temperature optimum for LiP is similar to other peroxidases and is within a range of 40 to 50 °C [45].

2.4. Manganese peroxidases

Another enzyme with high biotechnology potential that belongs to the oxidoreductase group is manganese peroxidase (EC 1.11.1.13), also known as Mn(II):hydrogen-peroxide oxidoreductase or MnP. These glycosylated heme-containing enzymes can oxidize a wide variety of phenolic compounds, such as dyes and various monomeric and dimeric phenols as well as oxidize Mn(II) ions to Mn(III) using hydrogen peroxide [46]. The catalytic cycle of MnP is initiated by binding of H_2O_2 and formation of an iron-peroxide complex and subsequent transfer of 2 electrons from the heme resulting in formation of MnP Compound I. Later, one water molecule is formed by subsequent cleaving of the dioxygen bond and reduction proceeds through MnP Compound II. Afterwards, monochelated Mn^{2+} ion acts as electron donor for this porphyrin intermediate and is oxidized to Mn^{3+}. Another Mn^{3+} is formed by reduction of Compounds II leading to regeneration of native enzyme and releasing of the second water molecule [47]. Manganese peroxidase is a protein found in multiple forms with a typical molecular weight ranging from 40 to 50 kDa [47]. MnPs exhibit their maximal activity at Mn(II) concentrations above 100 μM and calcium cations enhance their catalytic properties [48]. Manganese

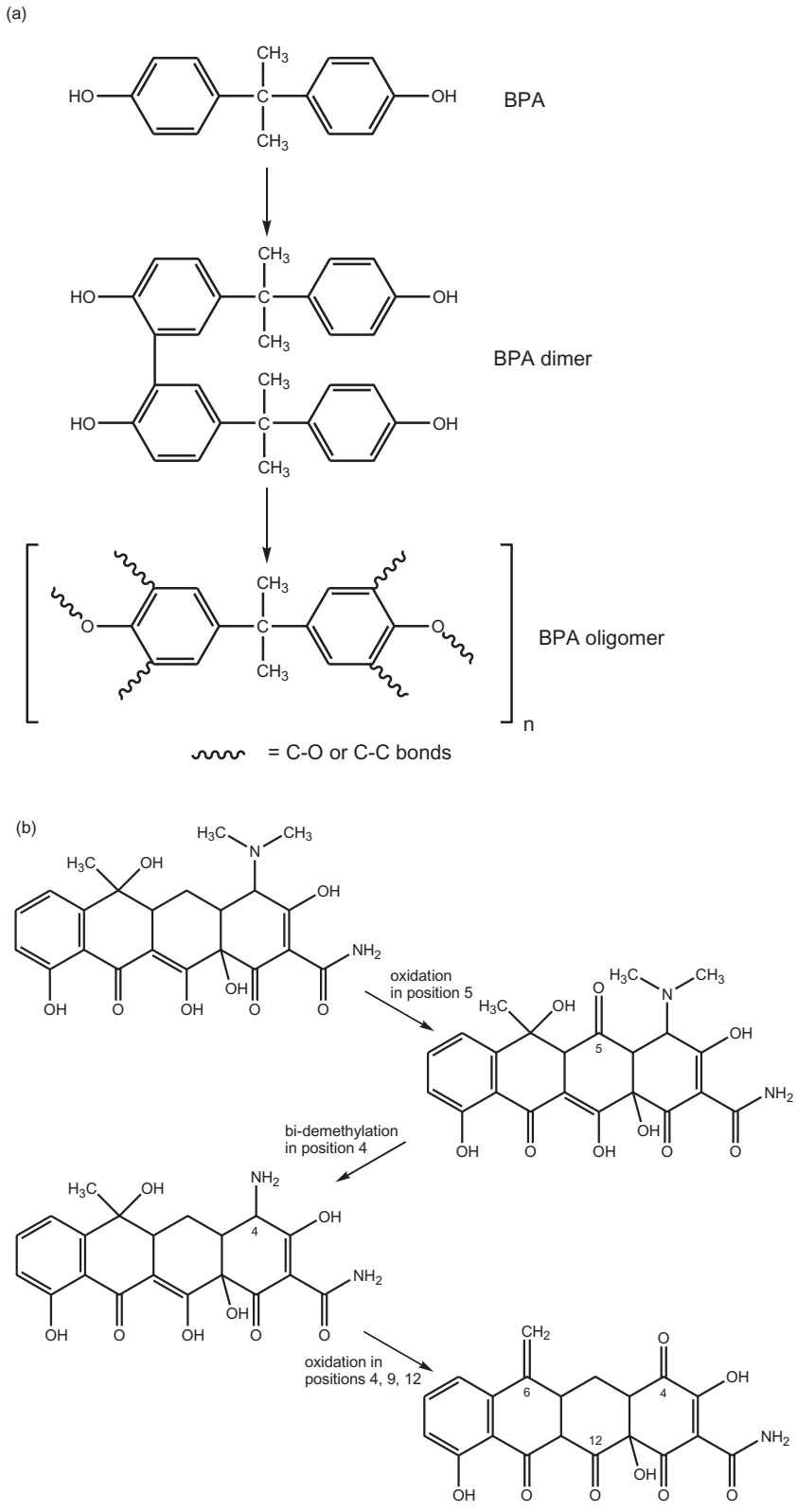

Fig. 1. Degradation pathways of: (a) bishenol A and (b) tetracycline by laccase (adapted from [32 and 33]).

peroxidase was discovered for the first time in *P. chrysosporium* but in later years the enzyme has also been found in bacteria and other white-rot fungi [49]. The optimum temperature for the highest catalytic activity of manganese peroxidases depends on its source, but in most cases lies the range of 30 to 40 °C. These enzymes exhibit their highest catalytic properties at slightly acidic pH levels of around 4 [50].

2.5. Horseradish peroxidases

Enzymes extracted from the roots of horseradish have also been assessed in environmental applications. A number of distinctive peroxidase isoenzymes have been found in nature, however, the most abundant is horseradish peroxidase C [51]. Horseradish peroxidase

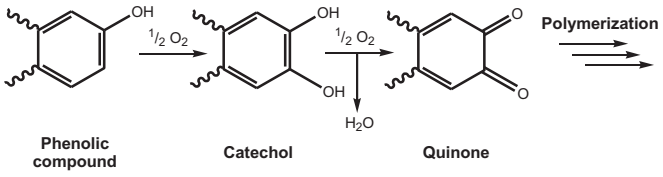

Fig. 2. Catalytic pathway of phenolic substrate by tyrosinase.

(EC 1.11.1.7) or HRP is also a heme-containing enzyme that includes in its structure iron(III) protoporphyrin and two atoms of calcium. The presence of calcium atoms is important, because loss of calcium results in significant decrease of enzyme activity and thermal stability [52]. Horseradish peroxidase catalyzes an oxidation reaction of phenolic acids, aromatic phenols such as pyrogallol and their derivatives (i.e. various bisphenols), non-aromatic amines such as 4-aminoantipyrine, indoles, etc. in the presence of hydrogen peroxide, producing two molecules of water. The second products of the catalytic reaction are radicals that can result in formation of polymeric compounds as the final products of oxidation [53, 54]. The main practical applications of HRPs includes treatment of the wastewaters contain phenolic compounds, environmental remediation, elimination of toxic compounds such as dyes from drinking water and industrial [55–57]. HRP, particularly its isoenzyme C, exhibits its greatest catalytic activity at temperatures of 25–40 °C and at neutral pH, close to 7 [58].

In recent years, lignolytic enzymes, such as laccase, tyrosinase, manganese, lignin and horseradish peroxidases have been used in numerous industrial processes, such as biomass conversion and chemical synthesis. However their great oxidizing potential caused that they have found an application in environmental protection to degrade xenobiotics, as dyes, pharmaceuticals and hazardous pollutants that are usually resistant to microbial biodegradation [59]. In our opinion, further study leading to the development of the techniques that improve practical features of the lignolytic enzymes is highly required as might facilitate use of these important biomolecules for various biotechnology applications and environmental protection.

3. Immobilization of enzymes

Many advanced research studies have been carried out in connection with the low stability and reusability of enzymes. Immobilization, a process through which the enzyme is bound to a solid support, changes the form of the catalyst from homogenous (free enzyme) to heterogenous (immobilized enzyme) [60]. Creation of interactions between the enzyme and a matrix (immobilization) stabilizes the peptide structure of the biocatalyst and results in improvement of enzyme stability towards strong pH, high temperature or the presence of organic solvents [61]. The possibility of separation of the biocatalytic system from the reaction mixture is strongly enhanced and thus contamination of products by the enzyme particles is minimalized. Additionally, after the immobilization, the biocatalysts can easily be removed by simple mechanical separation or centrifugation without using sophisticated analytical techniques. However, the greatest advantage of immobilization is the production of an enzymatic system that could be reused in many catalytic cycles without significant loss of its unique properties [62, 63].

According to the previously published reviews, methods of immobilization have been classified in many different ways [64–66]. The techniques differ between each other by the types of the created interactions and by type and form of the solid support. In each case, for selection of the immobilization technique, a compromise has been made between retention of high catalytic activity and operational benefits. For the purpose of the current discussion, five different immobilization techniques are distinguished, namely: (i) non-covalent (adsorption) immobilization; (ii) covalent immobilization on a carrier; (iii) encapsulation; (iv) entrapment and (v) cross-linking of the enzyme particles by creation of the cross-linked enzyme aggregates (CLEA) and cross-linked enzyme crystals (CLEC), as summarized in Table 1.

Non-covalent immobilization, also known as adsorption immobilization, is based on the creation of non-specific interactions mainly via hydrogen bonds and ionic and hydrophobic interactions. In effect, conformational changes in the enzyme particle are limited and retention of high catalytic activities by the immobilized enzymes is usually observed [67, 68]. Immobilization by covalent binding is based on the reaction of functional groups of the support material with functional groups of the enzyme (mainly $-NH_2$, –SH and –OH). Creation of strong chemical bonds between the biocatalyst and matrix significantly reduces leakage of the enzyme and enhances its reusability [69, 70]. When the biomolecule is immobilized by encapsulation or entrapment it is physically placed in the pores of the support material but its structure remains unaltered. Single enzymes as well as complex biocatalytic systems built from different types of enzymes may by immobilized by the use of these methods. The disadvantage of these techniques is that due to the location of the enzyme within the porous system of the matrix, transfer of the reaction mixture ingredients is more difficult [71]. Enzymes in the form of single crystals (CLEC) or as aggregates (CLEA) are cross-linked within bifunctional compounds such as glutaraldehyde (GA) or carbodiimides. Establishing covalent bonds through the use of cross-linking agents allows formation of a stable structure without the use of a solid support [72, 73].

Different techniques could be applied for immobilization of the same enzyme, however, changes in the enzyme structure and its properties are usually not equal with improvements of the biocatalysts properties. Thus, mild process conditions are highly required to retain good catalytic properties of the immobilized enzymes. Moreover, the more simple is the immobilization method, such as adsorption immobilization, the more cost effective is the process. As every enzyme differ from each other, it could be concluded that proper selection of the immobilization protocol is a key step to obtain biocatalytic systems which might be applied for practical applications.

Table 1
Main immobilization techniques, their characteristic and advantages.

Immobilization technique	Main functional groups of the support	Type of interactions	Strength of interactions	Advantages
Non-covalent (adsorption)	$-NH_2$, –SH, –OH, C=O, COOH, epoxy groups	hydrogen bonds, ionic interactions, hydrophobic interactions	weak	no enzyme modification, simple and inexpensive reusability of the support
Covalent binding	$-NH_2$, –SH, –OH, C=O	covalent bonds	strong	strong and stable interactions, multipoint attachment, reducing of enzyme leakage
Encapsulation	$-NH_2$, –OH,	ionic interactions, hydrophobic interactions	weak	no enzyme modification, protection of the enzyme
Entrapment	$-NH_2$, –OH, C=O	ionic interactions, hydrophobic interactions, covalent bonds	weak/strong	no enzyme modification
Cross-linking	C=O, $-NH_2$	covalent bonds	strong	no support needed, high strength of interactions

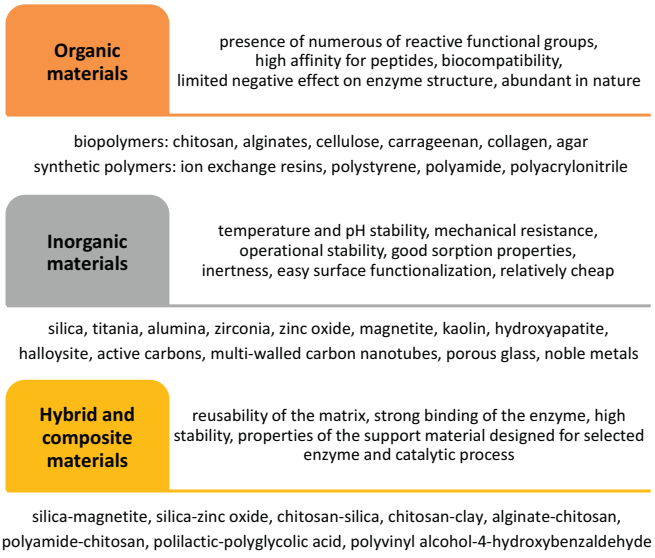

Fig. 3. Selected examples and the most important properties of support materials used for immobilization of enzymes for environmental application.

4. Materials for immobilization of enzymes used for environmental protection

As was mentioned earlier, the main purpose of the current review is to present and characterize various enzyme support materials that can be applied in processes related to environmental protection. Free oxidoreductases have been applied for removal of micropollutants from environments, however, large-scale use of these enzymes in biodegradation requires their immobilization to increase stability and prolong activity [74]. These biocatalysts can be immobilized through the use of various materials of different origin, from inorganic through organic to hybrids and composite supports. The most important properties of selected examples of these support materials are presented in Fig. 3. The great variety of the possible carriers with regard to shapes, sizes and forms means that enzymes can be immobilized via various protocols. In this section the effect of different features of support material on enzyme activity and biodegradation efficiency is presented and discussed.

4.1. Materials of organic origin

Many different materials of organic origin, both natural and synthetic, have been employed for immobilization of enzymes for environmental protection using different immobilization techniques (See Table 2).

4.1.1. Biopolymers

4.1.1.1. Chitosan. As was previously stated, chitosan is one of the most frequently used support materials for immobilization due to its easy availability, low cost, biocompatibility and hydrophilicity. The presence of many hydroxyl and amine groups in the structure of this biopolymer facilitates effective binding of laccases and other peroxidases without involving any modifying or cross-linking agents [111]. The ability of chitosan to create various forms, such as fibers, beads, microspheres or membranes, enhances its application as a support material for enzymes like laccase or lignin peroxidase and makes immobilized biomolecules more stable. For instance, Zhang et al. have covalently attached laccase from *Coriolus versicolor* via glutaraldehyde to the surface of chitosan. The obtained biocatalytic system was used for biodegradation of mono- and dichlorophenols and brought about the degradation of over 90% of 2,4-dichlorophenol in water solution. Moreover, immobilized enzyme was characterized by higher stability in comparison to free enzyme and exhibited good reusability [75]. In another study, chitosan, chitosan microspheres with high specific surface area and chitosan beads were used for immobilization of laccase, manganese peroxidase and lignin peroxidase by entrapment, covalent binding and adsorption, respectively. The produced biocatalysts, due to their wide specificity, were used for degradation of synthetic and natural azo-dyes in model and real water solutions. Enzymatic systems are characterized by various thermal and chemical stabilities, but under optimal conditions (temperature range 30–50 °C, pH range 5–8) they usually enable degradation of over 70% of the pollutants. Lack of electron mediator and low transfer of the electrons as well as complicated structure of the dyes are the main factors, which limit biodegradation efficiency [78]. However, the presence of the mediator agent is not necessary for total degradation of the contaminating dye. As Jaiswal et al. have shown, after 8 h at 37 °C laccase from papaya entrapped in chitosan beads was able to remove Indigo carmine completely from water solution due among other factors to low diffusional limitation [79].

4.1.1.2. Alginates. Other extensively used support materials for environmental applications of enzymes are various alginate salts derived from brown algae, *Phaeophyceae*, under alkaline conditions. After gelation under mild conditions and after addition of mono- or divalent cations like Na^{+}, Ca^{2+}, Cu^{2+}, Zn^{2+} and Mn^{2+} [112], alginates are characterized by viscosity and stiffness, which can easily be controlled by manipulation of the pH and molecular weight of the alginate solution. For enzyme immobilization, alginates are used in the form of beads, hydrogels and capsules. And as a consequence of the features and diversity of form of alginates, immobilization of laccases, tyrosinases and other peroxidases by alginates mainly occurs through entrapment and encapsulation. Usually, after biomolecules have been immobilized in alginates, there is a lack of covalent bonds between the enzyme and a support, and thus functional groups of the matrix and the enzyme interact based on relatively weak, ionic or adsorption forces [113]. Because interference in the structure of the enzyme is strongly limited, immobilized enzymes usually retain most of their catalytic properties. On the other hand, creation of relatively weak interactions might lead to leakage of the enzyme from the matrix and result in a decrease in biocatalytic activity of the produced system. Additionally, lower catalytic properties may be related to diffusional limitations in transport of the substrates and the products through the alginates layer. Sodium and calcium ions are the most commonly used ions for gelation of alginates. For instance, calcium alginate was used for immobilization of manganese peroxidase from *G. lucidum* and tyrosinase from *Agaricus bisporus* [80, 81], and tyrosinase from *Streptomyces espinosus* and laccase from *Bacillus subtilis* were entrapped in sodium alginate [82, 83]. Irrespective of metal cation used for gelation, immobilized tyrosinases were used for removal of phenol from water solutions. Immobilized enzyme exhibited high catalytic activity and under optimal conditions was able to totally degrade phenol from solution after 1 h of the process [81]. Silica ions have also been used to increase the mechanical stability of the alginate. Silica alginates were further used for encapsulation and entrapment of tyrosinase and the obtained biocatalytic system then applied for biodegradation of bisphenol A (BPA). This biocatalytic system not only allowed highly efficient removal of BPA in a relatively short time, but most of all was characterized by much higher pH and temperature resistance in comparison to free enzyme. However, fast drop of the catalytic properties over consecutive catalytic cycles related to the enzyme leakage should be presented as the weak point of this study [85]. Special attention should also be paid to copper alginates as supports for environmentally enzymes. Due to the fact that laccase contains three different copper ions in its structure, utilization of supports containing copper ions increases the bioactivity of the immobilized biomolecules. Laccases or polyphenol oxidases were entrapped and encapsulated in materials prepared in this way and used for degradation of natural and synthetic dyes and phenol derivatives with removal efficiencies that reached over 80%. However, the significant effect of copper ions on the immobilized enzyme should be emphasized. Phetsom et al. encapsulated laccase

Table 2
Materials of organic origin used for immobilization of laccases, tyrosinases and lignin, manganese and phenols oxidases for biodegradation of various environmental pollutants.

Support material	Enzyme	Immobilization technique	Contaminants	Process conditions	Removal efficiency	Reference
Chitosan	Laccase from *Coriolus versicolor*	Covalent immobilization	2,4-dichlorophenol, 4-chlorophenol, 2-chlorophenol	pH 5.5, 35°C, 24 h	94%, 75%, 69%	[75]
Chitosan	Laccase from *Trametes pubescens*	Entrapment	Reactive Brilliant Blue X-BR, Remazol Brilliant Blue R, Congo Red, Acid Black 172, Methylene Blue, Neutral Red, Indigo Blue, Naphthol Green B, Direct Fast Blue FBL, Crystal Violet	pH 5, 50 °C,	55%, 50%, 55%, 70%, 25%, 45%, 45%, 40%, 60%, 20%	[76]
Chitosan microspheres	Lignin peroxidase and manganese peroxidase from *Coriolus versicolor*	Covalent immobilization/cross-linking	Decolorizing of molasses waste water	pH 8.4, 30 °C, 6 h	80%	[77]
Chitosan beads	Lignin peroxidase from *Schizophyllum commune* IBL-06	Adsorption immobilization	Synthetic textile dyes	30 °C, 4 h	95.5%	[78]
Chitosan beads	Laccase from papaya	Entrapment	Indigo Carmine	pH 10, 37 °C, 8 h	100%	[79]
Calcium alginate	Manganese peroxidase from *G. lucidum* BL05	Entrapment	Sandal tree reactive dyes	pH 4.5, 35 °C, 12 h	up to 95%	[80]
Calcium alginate	Tyrosinase from *Agaricus bisporus*	Entrapment	Phenol	pH 7.2, 25 °C, 1 h	100%	[81]
Sodium alginate	Tyrosinase from *Streptomyces espinosus*	Entrapment	Phenol	4 h	up to 60%	[82]
Sodium alginate	Laccase from *Bacillus subtilis* MTCC 2414	Entrapment	Orange 3R, Yellow GR, T-Blue	40 °C, 120 h	74%, 79%, 71%	[83]
Silica alginate	Tyrosinase from *Agaricus bisporus*	Entrapment	Bisphenol A	20 °C, 24 h	100%	[84]
Silica alginate	Tyrosinase from *Agaricus bisporus*	Encapsulation	Bisphenol A	20 °C, 0.5 h	35%	[85]
Alginate beads	Polyphenol oxidase from *Taraxacum officinale*	Entrapment	synthetic dyes from industrial effluents	25 °C, 1 h	80%	[86]
Alginate beads	Horseradish peroxidase	Entrapment	Pyrogallol	pH 7, 25 °C	75%	[87]
Alginate beads	Laccase from *Coriolopsis gallica*	Entrapment	Remazol Brilliant Blue R, Reactive Black 5, Bismark Brown R, Lanaset Grey G	pH 5, 30 °C 24 h	90%, 81%, 53%, 87%	[88]
Alginate beads	Laccase	Entrapment	Direct Blue 2	pH 5, 30 °C	86%	[89]
Copper alginate beads	Polyphenol oxidase from *Cynarascolymus* L.	Entrapment	L-DOPA	pH 7, 25 °C	88%	[90]
Copper alginate beads	Laccase from *Lentinus polychrous*	Encapsulation	Remazol Brilliant Blue R, Methyl red, Indigo carmine, Bromophenol blue	30 °C, 2.5 h	89%, 91%, 100%, 86%	[91]
Cellulose	Polyphenol oxidase	Adsorption immobilization	Phenol, 4-chlorophenol, 4-bromophenol	pH 8, 5 h	20%, 30%, 45%	[92]
Cellulose paper	Tyrosinase from mushroom	Covalent immobilization	L-DOPA	pH 7, 22 °C, 2 h	70%	[93]
Cellulose nanofibers	Laccase	Covalent immobilization	Simulated dye effluent consist of Remazol Black 5, Remazol Brilliant Blue R, Remazol Brilliant Violet 5R, Reactive Orange 16 and Reactive Red 120	30 °C, 12 h	39%	[94]
Carboxymethylcellulose beads	Polyphenol oxidase	Covalent immobilization	L-tyrosine	pH 6.5, 25 °C	93%	[95]
Diethylaminoethyl cellulose	Tyrosinase from mushroom	Covalent immobilization	L-DOPA	pH 9, 4 h	60%	[96]
Thiolsulfinate-agarose	Laccase from *Trametes villosa*	Covalent immobilization	Remazol Brilliant Blue R	pH 4.8, 22 °C, 24 h	80%	[97]
Gum Arabic	Laccase	Covalent immobilization	Remazol Brilliant Blue R	pH 5, 40 °C, 2 h	81%	[98]
Green coconut fiber	Laccase from *Aspergillus*	Covalent immobilization	Reactive Black 5, Reactive Blue 114, Reactive Yellow 15, Reactive Yellow 176, Reactive Red 239, Reactive Red 180	pH 7, 35 °C	90%, 90%, 77%, 5%, 33%, 35%	[99]
Polyvinyl alcohol	Horseradish peroxidase	Covalent immobilization	pyrogallol	pH 6, 25 °C, 1 h	80%	[100]
Polyvinyl alcohol capsules	Laccase from *Trametes versicolor*	Encapsulation	Saturn Blue L4G dye	pH 5.5, 25 °C, 24 h	48%	[101]
Polyvinyl alcohol beads	Laccase from *Cyathus bulleri*	Entrapment	Acid Violet 17, Basic Green 4, Acid Red 27	pH 5.5, 30 °C,	90%, 95%, 90%	[102]

(continued on next page)

Table 2 (*continued*)

Support material	Enzyme	Immobilization technique	Contaminants	Process conditions	Removal efficiency	Reference
Polyacrylamide hydrogel	Lignin peroxidase from *P. chrysosporium*	Encapsulation	Bisphenol A	pH 5, 25 °C, 8 h	90%	[103]
Polyacrylonitrile beads	Tyrosinase	Covalent immobilization	Bisphenol A, Bisphenol B, Bisphenol F, Tetrachlorobisphenol A	25 °C, 1.5 h	92%, 93%, 94%, 91%	[104]
Poly-N-vinylpyrrolidone	Tyrosinase from *Agaricu sbisporus*	Covalent immobilization	Phenol	25 °C, 1 h	100%	[105]
Poly(2-hydroxyethyl methacrylate-*co*-glycidyl methacrylate)	Laccase from *Trametes versicolor*	Covalent immobilization	3,5-dinitro salicylic acid	pH 5, 55 °C, 2 h	75%	[106]
Epoxy activated polyethersulfone beads	Laccase from *Trametes versicolor*	Covalent immobilization	Acid Red 1	pH 5, 65 °C, 10 days	88%	[107]
Nylon membrane	Polyphenol oxidase from *Agaricus bisporus*	Covalent immobilization	Phenol, *p*-cresol, *m*-cresol, 4-chlorophenol, 4-methoxyphenol	25 °C, 8 h	Over 80% for *p*-cresol	[108]
Amberlite IRA 400 resin	Lignin peroxidase from *Phanerochaete chrysosporium*	Adsorption immobilization	Kraft E1 effluent	pH 3 and 7, 25 °C, 3 h	50%	[109]
Anion-exchange resin	Tyrosinase from mushroom	Covalent immobilization	*p*-cresol	25 °C, 72 h	83%	[110]

from *Lentinus polychrous* in Cu-alginate beads. The immobilized biomolecule exhibited more than two times the catalytic activity of free enzyme after 7 days of storage at pH 5.5 due to the presence of Cu^{2+} ions [91]. Alginates are also used in the form of beads for immobilization mainly by entrapment of laccases, tyrosinases and various peroxidases. Due to the mechanical stability of the capsules with biomolecules that form beads, these products are commonly employed in bioreactors of different configurations used for degradation of synthetic textile dyes as well as phenol and its derivatives in water solutions. As reported by Daassi et al., laccase from *Coriolopsis gallica* immobilized in alginate beads exhibited over 80% of its catalytic activity over a wide pH range from 5 to 9, but the free enzyme was most active only at pH 7. Furthermore, immobilized biocatalyst was characterized by high thermal stability. After incubation for 3 h at 55 °C, immobilized laccase still exhibited over 80% of initial activity, meanwhile free laccase under the same conditions completely lost its properties after 2 h of heating [88].

4.1.1.3. Cellulose. Another organic material used as support for environmental enzymes is cellulose and its modified forms. Cellulose is known from its great sorption capacity and the presence of many hydroxyl groups in its structure. This facts allows effective attachment of enzyme molecules and enhances opportunities for modification of cellulose surfaces by glutaraldehyde, diethylaminoethanol or introduction of epoxy groups [114]. Cellulose is also relatively easy to obtain, is nontoxic and biocompatible. The above-mentioned features taken together mean that cellulose and its derivatives are suitable support materials for adsorption or covalent immobilization of oxidoreductase enzymes. Application of cellulose-based materials is therefore growing quickly as a response to the importance of sustainable and cost-effective immobilization. As a result, many new cellulosic materials with desired properties and stability are under development for attachment of biomolecules. Sathishkumar et al. used cellulose nanofibers modified by glutaraldehyde for covalent immobilization of laccase. Thermal and pH stability as well as storage stability of the immobilized enzyme was considerably improved compared to the free enzyme. Laccase-cellulose nanofibers also exhibited great reusability and retained over 80% of the initial properties after five catalytic cycles. The biocatalyst thus obtained was applied for decolorization of simulated dye effluent (SDE) consisting of Remazol Black 5, Remazol Brilliant Blue R, Remazol Brilliant Violet 5R, Reactive Orange 16 and Reactive Red 120. The authors demonstrated that in the presence of the mediator, 1-hydroxybenzotriazole, decolorization of SDE reached around 40%. Although the stability of the immobilized enzyme was improved, changes in the structure of biomolecules due to covalent binding, caused that relatively low biodegradation efficiency was achieved. Also multiply of the dyes in the solution decreases process effectivity [94]. In another study, cellulose modified by diethylaminoethanol formed diethylaminoethyl-cellulose (DEAE-cellulose) was used by Cienska et al. for immobilization of tyrosinase. The authors report that tyrosinase immobilized on modified cellulose exhibited good storage stability and great reusability, and could be used in five subsequent catalytic cycles without loss of the initial activity. Moreover, after binding to the polysaccharide support, the negative effect of the toxic mixture component was strongly limited and the catalytic properties of the enzyme were retained at a high level [96]. Firooz and his team have also modified cellulose surfaces for covalent immobilization of tyrosinase. They used commercially available sheets of Whatman paper and immersed the sheets in a solution of ethylenediamine or propylenediamine to introduce amine groups. Laccase immobilized on amine-functionalized cellulose paper exhibited even higher catalytic activity – over 150% of that of free enzyme – under optimal pH (7.0) and temperature (35 °C) conditions. Although immobilized laccase is characterized by lower substrate affinity (higher value of Michaelis-Menten constant) than free enzyme, it still seems to be a very promising biocatalyst for degradation of dihydroxyphenylalanine (L-DOPA) [93]. It should be stated that other forms of cellulose such as cellulose beads or cellulose beads modified by carboxyl groups (carboxymethyl cellulose) may also be used for immobilization of polyphenol oxidases. The resulting systems could be further used for degradation of phenolic compounds and synthetic dyes, with efficiencies of over 90% [95].

4.1.1.4. Other biopolymers. Other biopolymers, mainly polysaccharides, may also be used for immobilization of laccases. A broad range of materials, including agarose, κ-carrageenan, gum Arabic and other natural products such as coconut fibers or wood sawdust, can be used as support for oxidoreductase immobilization [97, 98, 115]. These materials are known for their biocompatibility and high affinity for peptides, which makes them useful for many practical applications, including industrial processes with immobilized enzymes. Gioia and co-workers applied thiolsulfinate-agarose for reversible covalent immobilization of laccase from *Trametes villosa*. The great advantage of this support material is that after enzyme inactivation using a reducing agent like dithiothreitol (DTT), the biomolecules can be easily removed from the support surface and the matrix can be used for the next cycle of

immobilization. Presented results indicated that after 24 h of the process at 22 °C and pH 4.8, it would likely be possible to remove over 80% of Remazol Brilliant Blue R from textile industry effluents [97]. In another study, Cristovao et al. used green coconut fiber modified by 3-glycidoxypropyl-trimethoxysilane for immobilization of laccase at pH 7 for one-point and at pH 10 for multipoint covalent immobilization. Comparison of the systems so obtained showed that conducting the process under neutral pH resulted in production of biocatalyst with higher activity and affinity to the substrates. Both biocatalytic products were used for decolorization of reactive textile dyes such as Reactive Black 5 and Reactive Blue 114. Over 90% of the dyes could be degraded in the solution through use of the laccase-coconut fiber system [99].

4.1.2. Synthetic polymers

Besides many different organic materials of natural origin, synthetic polymers of different sizes and shapes are also used for immobilization of laccases, tyrosinases and peroxidases. Due to the presence of many functional moieties in the structure of synthetic polymers, the creation of relatively strong interactions has been observed between the enzymes and the support. Polymers can be formed into various shapes that are tailored to enzymes and products according to the particular immobilization application. Additionally, due to their structure and high stability, synthetic polymers usually protect biomolecules against degradation and enhance their stability. One of the most frequently used polymeric supports for environmental enzymes is polyvinyl alcohol (PVA). PVA is rich in hydroxyl groups, and is a strongly hydrophilic material which may be easily modified to achieve a suitable enzymatic matrix. For instance, PVA was used as fibers, beads or microspheres for covalent immobilization of horseradish peroxidase and for entrapment and encapsulation of laccase [100–102]. Chhabra and his team entrapped laccase from *Cyathus bulleri* in polyvinyl alcohol beads for degradation of azo-dyes in a continuous packed column. The biocatalytic system they thus obtained, in addition to retaining high activity (over 90%), was characterized by good storage stability (70% after 5 months of storage at 4 °C) and reusability (over 90% of initial activity after 5 days of the process). Continuous batch decolorization in a packed bed bioreactor under optimal conditions led to nearly 90% decolorization of Acid Violet 17, Basic Green 4 and Acid Red 27 [102]. Other common synthetic polymers might also be useful for enzyme immobilization. Laccases and tyrosinases of different origin as well as lignin or manganese peroxidases could be immobilized mainly by encapsulation or covalent immobilization through use of polyacrylamide hydrogel, polyacrylonitrile beads, poly-N-vinylpyrrolidone or epoxy activated polyethersulfone beads. The produced biocatalytic systems have been utilized for various environmental applications, but these systems are most commonly applied for degradation of phenol and its derivatives and to allow selected removal of environmental contaminants at relatively high efficiencies. For example, Nicolucci et al. applied tyrosinase immobilized on polyacrylonitrile beads to eliminate bisphenol A, B, F and tetracholorobisphenol A. In a degradation process carried out in bed reactor, a degradation of over 90% was obtained for each of the tested endocrine disruptor [104]. In study by Shesterenko and co-workers, tyrosinase from *Agaricus bisporus* was immobilized on poly-N-vinylpyrrolidone and used for removal of phenol. After 1 h of the process at 25 °C, total degradation of phenol was observed [105]. Polyamide in the form of a nylon membrane has also been applied for immobilization of polyphenol oxidases. This solution not only increases stability of the immobilized enzyme and permits continuous use of the immobilized oxidase, but also limits inhibition of the biocatalyst due to easy separation of the product from the reaction mixture. Nylon membrane with loaded enzyme was used for continuous biodegradation of phenol and its derivatives carried out in a bioreactor; the system has potential as a biocatalyst for biotransformation of phenols or bioremediation of phenol-polluted water [108]. Supports based on polymeric resins have been used to achieve multisubunit or multipoint immobilization of enzymes. Application of multipoint immobilization is required as its usually prevents biomolecule structure from denaturation, inactivation and structural damage and therefore helps to maintain catalytic activity at a high level. However, on the other hand might also leads to creation of diffusional limitations due to the blocking of enzymes active sites. Thus, Satoh et al. used a commercially available anion-exchange resin for covalent immobilization of mushroom tyrosinase. The immobilized enzyme exhibited high catalytic properties and stability under reaction conditions as well as reusability, as indicated by almost unaltered enzyme activity after five repeated catalytic cycles. Furthermore, a column-packed reactor with immobilized tyrosinase was used for effective degradation of *p*-cresol and allowed its removal at an efficiency of around 80%. To achieve higher effectivity of reactor, additional hydrogen peroxide supply must be ensured, that is the main limitation of the presented concept [110].

According to the references presented above it can be concluded that application of organic support materials for enzymes used for environmental decontamination is quite popular. The great advantage of these materials is that they can be used in different shapes (particles fibers), forms (membranes, beads) and sizes. For instance, nylon membrane, fibers obtained from green coconut and chitosan microspheres was applied for covalent immobilization of polyphenol oxidase, laccase from *Aspergillus* and lignin peroxidase from *Coriolus versicolor*, respectively and used for removal of various pollutants, like *p*-cresol, Reactive Black 5 or even waste waters after molasses conversion [77, 99, 108]. Biocatalytic systems obtained, irrespectively of the applied form of support material, allowed degradation of over 80% of hazardous compounds. As it was also presented above, alginate-based materials were employed for entrapment of i.e. tyrosinase from *Streptomyces espinosus*, manganese peroxidase from *G. lucidum* BL05 or horseradish peroxidase and used for degradation of natural reactive dyes, phenol or pyrogallol [80, 82, 87]. Obtained removal efficiencies that exceed 75% proved versatility of these materials as the support that could be used for immobilization of different enzymes and applied for removal of various contaminants. On the one hand the great variety of the enzymes could be immobilized, but on the other hand high diffusional limitations and leakage of the biomolecules from the support limit higher biodegradation efficiencies.

It could be concluded that using organic support for immobilization of oxidoreductases, there is some freedom in selection of attachment technique, because all above-mentioned immobilization protocols, that could be applied results in production of immobilized enzymes characterized by improved thermal, chemical and operational stability. Biocatalytic systems based on the organic matrices are employed for degradation of a very large number of environmental pollutants, ranging from synthetic and natural dyes, through phenol and its derivatives, to more complex compounds like pharmaceuticals. However, compared to the synthetic polymers, application of biopolymers have received wider consideration over the recent years. Several factors can justify this fact. Among others, the presence of many functional groups, ability to form various geometrical structures that increase protection of enzymes against the reaction conditions, biocompatibility, abundance in nature and fact that they are renewable should be enumerated. We believe that even though biopolymers, such as chitosan, alginates or cellulose are commonly used as a carriers for enzyme immobilization, these materials still have a great potential which can be used to develop a multidisciplinary approach covering the areas of biocatalysis, environmental protection and bioprocess engineering.

4.2. Inorganic materials

Besides the many organic materials presented above, inorganic supports are also widely used for immobilization of enzymes for environmental applications. Inorganic materials are suitable for enzyme immobilization due to their exceptional mechanical and chemical stability and electrical properties and are known for their large specific surface area, which may even be up to 1000 m^2/g for silica SBA 15 [116], porous structure, and controllable nanometer sizes similar to that of

enzyme molecules [117, 118]. The great advantage of inorganic supports in comparison to other materials is that they can be obtained relatively cheaply and simply due to their abundant presence and usually non-complicated synthesis procedure. Moreover, the presence of many hydroxyl, carbonyl and carboxyl groups on the surface of the inorganic carriers causes easier enzyme attachment and facilitates support functionalization through the use of surface modifying agents like glutaraldehyde or 3-aminpropyltriethoxysilane (APTES) [119]. Thus, inorganic materials are commonly used for immobilization of laccases, tyrosinases and phenoloxidases. Selected examples of the various inorganic materials of different origins and their application for immobilization of laccases, tyrosinases and lignin, manganese and phenol oxidases to biodegrade environmental pollutants are presented in Table 3, followed by discussion.

4.2.1. Silicas

Silica in various forms and sizes is the most commonly used inorganic support material for immobilization of oxidoreductases for environmental protection. It should be stressed that the hydrophilic character of the silica surface as well as presence of many hydroxyl groups on its surface leads to immobilization of biomolecules not only via adsorption [125] but also by creation of covalent bonds [123, 127] and even by encapsulation [131]. Special attention should be paid to multiplicity of forms of silica which could be exploited for immobilization. For example, mesoporous, ordered silica at pore sizes of 14.1 nm was used for immobilization of lignin peroxidase from *Phanerochaete chrysosporium*. The resulting product was used for degradation of Acid Orange II and removed over 75% of the dye from water solution [122]. In another study, Nair and co-workers used mesoporous silica spheres with a high surface area for covalent attachment of laccase from *Coriolopsis gallica* using glutaraldehyde as cross-linking agent. The biocatalytic system thus produced was characterized by high catalytic activity (over 380 U/g) and allowed for effective biodegradation of bisphenol A, diclofenac and 17-α-ethinylestradiol at efficiencies of over 70% for each compound [124]. Laccase from *Cerrena unicolor* has been covalently immobilized via glutaraldehyde on the surface of silica beads at control porosity with a pore size at around 375 Å. Immobilized enzyme was more active than its free form over a wide pH range from 4 to 9 and at temperatures of up to 70 °C. The resulting systems were used for elimination of 80% of bisphenol A, 40% of nonylphenol, and 60% of triclosan from water solution [129]. An interesting example of use of a silica matrix for immobilization of enzymes was presented by Sani et al. In their study, they used semi-transparent and fluffy powder of silica aerogel with a surface area of around 600 m^2/g for encapsulation of tyrosinase. The structure of the matrix strongly reduced diffusional limitation in transport of the substrates and as a result helped to retain high catalytic activity by the immobilized biomolecules. Furthermore, leakage of tyrosinase from the carrier was reduced by its encapsulation in the silica matrix which also protected tyrosinase from harsh reaction conditions. This effects resulted in reusability of the produced system, which after 10 repeated degradation cycles still retained over 70% of the initial catalytic properties. The biocatalytic system was used for degradation of phenol in water solution. After 3 h of biodegradation under optimal conditions (pH 7, 30 °C), over 90% of the pollutant was removed [131]. In summary, oxidoreductases have thus been immobilized on various types of silica supports and applied for biodegradation of a several organic compounds ranging from phenol and its derivatives, and endocrine disrupting chemicals, to synthetic and natural dyes, with high efficiencies, usually over 80%. However, it also should be noticed that the limitation of the silica-based materials is fact that whit out surface modification, usually adsorption immobilization occurred. This results in enzyme leakage and decrease in catalytic properties.

4.2.2. Inorganic oxides

Besides silica, other inorganic oxides such as titania, zinc oxide, alumina and magnetic iron (II,III) oxide are also used for immobilization of enzymes for environmental applications due to the presence of many functional groups, mainly hydroxyl and carbonyl groups. These materials are known from their high surface area and defined porosity that enhance attachment of a large amount of enzyme and increase catalytic activity of the produced systems. The above-mentioned materials are characterized by thermal, chemical and mechanical resistance, which in comparison with free enzyme significantly extends the tolerated pH and temperature ranges over which immobilized enzyme exhibits high catalytic activity. For instance, laccase covalently immobilized on alumina pellets exhibited over 80% of its catalytic activity at pH 4 to 6 and at temperature from 35 to 60 °C. By contrast, free laccase exhibited its maximum activity only at pH 4 and temperatures of 35–45 °C [126]. Another advantage of the inorganic oxides is that they can be used in various morphological forms. Hou and co-workers used titania nanoparticles for adsorption immobilization of laccase from *Trametes versicolor* and degradation of 2,4-dichlorophenol and 2,6-dimethoxyphenol. The produced biocatalytic systems, besides increases in thermal and chemical stability, seemed to be effective tools for biodegradation of disubstituted phenol derivatives. At pH 3.5 and 25 °C, over 85% of 2,4-dichlorophenol and over 60% of 2,6-dimethoxyphenol were removed from water solution [133]. In this study higher degradation rates were unachievable due to the sorption of the phenols on the nanoparticles. In consequence, actives sites are overloaded by the substrate molecules and catalytic efficiency decreases. In recent years magnetite has become a very promising support material for enzymes due to its magnetic properties and easy separation of the produced biocatalytic systems from the reaction mixture using external magnetic field. For instance, Balaji et al. used this material for covalent binding of laccase using glutaraldehyde and further for decolourization of water solution by removal of Reactive Green 19A dye. According to the presented results, over 75% of the dye was removed by using the described biocatalytic system. Moreover, use of magnetic particles for laccase immobilization significantly increased reusability of the biocatalytic system and facilitated control of the technological process [138].

4.2.3. Minerals

Inorganic materials such as minerals are also used for immobilization of oxidoreductases. The biggest advantage of these materials is that they are abundant in nature and inexpensive. They offer high surface areas, the presence of various functional moieties, high sorption capacity and stiffness as well as high thermal stability and resistance against mechanical destruction [151]. Various minerals, for example halloysite, kaolin, clays or bentonite could be used for immobilization of laccases and peroxidases. Due to good resistance of these supports, irrespectively of the material used, the produced biocatalytic systems are characterized by increase in their stability in comparison to free enzyme and are known for their great reusability. For instance, Chao and co-workers used halloysite nanotubes modified by dopamine for effective covalent immobilization of laccase from *Trametes versicolor*. The support material exhibited high loading ability to enzyme binding which facilitated the attachment of almost 170 mg of the peptide on 1 g of the support. This biocatalytic system was used for biodegradation of 2,4-dichlorophenol in waste water. Under optimal operational conditions, laccase bound to halloysite nanotubes was able to remove over 90% of the pollutants in 10 h [139]. In another study, horseradish peroxidase was immobilized by adsorption on the surface of aluminum-pillared interlayered clay for the treatment of wastewater polluted with phenolic compounds. After immobilization, the system exerted a perfect removal of phenol products over a broader pH range of 4.5 to 9.3 than the free biocatalyst was able to achieve. Furthermore, addition of polyethylene glycol to the wastewater was shown to significantly enhance phenol removal efficiency while reducing the amount of immobilized enzyme required to achieve a removal efficiency of over 90% [142].

4.2.4. Carbon-based materials

Special attention should be paid to carbon-based materials from among the very wide range of inorganic materials used for

Table 3
Materials of inorganic origin used for immobilization of laccases, tyrosinases and lignin, manganese and phenol oxidases for biodegradation of various environmental pollutants.

Support material	Enzyme	Immobilization technique	Contaminants	Process conditions	Removal efficiency	Reference
Silica SBA-15	Laccase from *Trametes versicolor*	Adsorption immobilization	Naphthalene	pH 4.5, 5 h	30%	[120]
Nanoporous silica beads	Laccase from *Trametes versicolor*	Adsorption immobilization	2,4-dinitrophenol	pH 5, 50 °C, 12 h	<90%	[121]
Mesoporous silica	Lignin peroxidase from *Phanerochaete chrysosporium*	Covalent immobilization	Acid Orange II	pH 4, 35 °C	77%	[122]
Mesoporous silica	Laccase from *Cerrena unicolor*	Covalent immobilization	Bisphenol A, 4-nonylphenol, Triclosan	pH 5, 1 h	80%, 40%, 60%	[123]
Mesoporous silica spheres	Laccase from *Coriolopsis gallica*	Covalent immobilization	Bisphenol A, Diclofenac, 17-α-ethinylestradiol	pH 5, 25 °C	90%, 85%, 70%	[124]
Mesoporous 2D silica	Lignin peroxidase	Adsorption immobilization	Phenol	pH 5, 25 °C	60%	[125]
Macroporous silica	Phenol oxidase from *Mycelia sterilia* IBR 35219/2	Covalent immobilization	Phenolic compounds of the green tea extract	pH 5.2, 30 °C	45%	[126]
Fumed silica	Laccase from *Coriolopsis polyzona*	Covalent immobilization	Bisphenol A	pH 7.5, 24 °C, 72 h	80%	[127]
Sol-gel silica	Rot fungi laccase	Adsorption immobilization	2,4-dichlorophenol, 2,4,6-trichlorophenol	25 °C, 4 h	95%, 100%	[128]
Silica beads	Laccase from *Cerrena unicolor*	Covalent immobilization	Bisphenol A, Nonylphenol, Triclosan	pH 5, 30 °C	80%, 40%, 60%	[129]
Silica gel	Tyrosinase from mushroom	Adsorption immobilization	Phenol	pH 6.8, 72 h	58%	[130]
Silica aerogel	Tyrosinase	Encapsulation	Phenol	pH 7, 30 °C, 3 h	90%	[131]
Diatom-biosilica particles	Tyrosinase from mushroom	Covalent immobilization	Phenol, *p*-cresol, Phenyl acetate	pH 7, 35 °C, 12 h	84%, 74%, 90%	[132]
Titania nanoparticles	Laccase from *Trametes versicolor*	Adsorption immobilization	2,4-dichlorophenol, 2,6-dimethoxyphenol	pH 3.5, 25 °C	85%, 63%	[133]
Titania nanoparticles	Laccase	Adsorption immobilization	Direct Red 31, Acid Blue 92, Direct Green 6	pH 3, 25 °C, 1 h	87%, 84%, 83%	[134]
Zinc oxide	Horseradish peroxidase	Covalent immobilization	4-aminoantipyrine	pH 4.5, 35 °C,	<95%	[135]
Alumina pellets	Laccase	Covalent immobilization	Melanoidins	pH 4.5, 28 °C, 6 h	47%	[136]
Alumina pellets	Laccase from *Trametes hirsuta*	Covalent immobilization	Basic Red 9, Reactive Blue 19, Acid Blue 225	pH 4.5, 30 °C	62%, 85%, 78%	[137]
Magnetic nanoparticles	Laccase	Covalent immobilization	Reactive Green 19A	pH 5, 25 °C	75%	[138]
Halloysite nanotubes	Laccase from *Trametes versicolor*	Covalent immobilization	2,4-dichlorophen	pH 5, 30 °C, 10 h	93%	[139]
Kaolin	Horseradish peroxidase	Adsorption immobilization	Pyrogallol, Acid Violet 109	pH 5, 24 °C, 1 h	70%, 87%	[140]
Vulcanic nanoclay	Manganese peroxidase from *Anthracophyllum discolor*	Adsorption immobilization	Pyrene, Anthracene, Fluoranthene, Phenanthrene	pH 4.5, 35 °C, 24 h	86%, 65%, 15%, 10%	[141]
Aluminum-pillared interlayered clay	Horseradish peroxidase	Adsorption immobilization	Phenol	pH 5, 25 °C, 4 h	<95%	[142]
Carbon nanotubes	Lignin peroxidase from *Ganoderma lucidum*	Covalent immobilization	Remazol Brilliant Blue R	pH 3.5, 25 °C, 24 h	78%	[143]
Multi-walled carbon nanotubes	Laccase from *Myceliophthora thermophile*	Covalent immobilization	Reactive Black 5	pH 5, 25 °C, 24 h	84%	[144]
Multi-walled carbon nanotubes	Tyrosinase from *Agaricus bisporus*	Covalent immobilization	Phenol	pH 7, 25 °C, 24 h	85%	[145]
Carbon nanospheres	Horseradish peroxidase	Covalent immobilization	2,4 dichlorophenol, 4-methoxyphenol, bisphenol A	pH 7, 25 °C, 1.5 h	95%, 99%, 52%	[146]
Mesoporous carbon from pecan shells	Laccase from *Trametes versicolor*	Adsorption immobilization	Acid Orange 7, Acid Blue 74, Reactive Red 2, Reactive Black 5	pH 6, 30 °C, 72 h	94%, 92%, 48%, 5%	[147]
Fullerene C_{60}	Laccase from *Trametes versicolor*	Covalent immobilization	Bisphenol A, Catechol	pH 5, 25 °C, 24 h	23%, 33%	[148]
Porous glass beads	Laccase from *Trametes versicolor*	Adsorption immobilization	Reactive Blue 19, Dispersed Blue 3, Acid Blue 74, Acid Red 27, Reactive Black 5	pH 5, 23 °C,	76%, 82% 82%, 27%, 10%	[149]
Nanoporous gold	Lignin peroxidase from *Phanerochaete chrysosporium*	Adsorption immobilization	Fuchsine, Rhodamine B, Pyrogallol Red	pH 7, 25 °C, 10 h	85%, 75%, 87%	[150]

immobilization of enzymes for environmental applications. Carbon-based materials are considered as a valuable support for enzyme immobilization because they have well-developed porous structures with pores of various size or volume and high specific surface areas (up to 1000 m^2/g), which means that these materials have a large number of contact sites on their surface for enzyme immobilization [152]. Carbon-based materials are also characterized by the presence of many functional groups on their surface [153]. Single-walled and multi-walled carbon nanotubes are those mostly used for covalent immobilization of laccases and tyrosinases. Carbon nanotubes could significantly enhance the electron transfer rate between substrates and laccase and as a consequence increase the catalytic activity of the

immobilized biomolecules. Additionally, through the creation of relatively strong chemical interactions between enzyme and support, carbon nanotubes increase the stability of the immobilized biomolecule towards harsh reaction conditions and enhance its reusability. In addition to carbon nanotubes, other materials such as carbon nanospheres or mesoporous carbon materials may also be used for immobilization of horseradish peroxidase or laccase [146, 147]. Subrizi and his team used multi-walled carbon nanotubes functionalized by poly (diallyldimethylammonium chloride) for covalent immobilization of tyrosinase from *Agaricus bisporus*. The obtained biocatalytic systems were used for degradation of phenol in aqueous media and removed of over 85% of phenol after 24 h of the process. It should be noted that immobilized tyrosinase was also able to catalyze removal of phenol derivatives of complicated chemical structure that react only to a small extent with the native enzyme [145]. Another example of carbon-based materials for laccase immobilization is fullerene C_{60}. It was used by Pang et al. for covalent immobilization of laccase from *Trametes versicolor* and applied for degradation of bisphenol A and catechol in water solution. Though immobilized laccase, due to creation of diffusional limitations, exhibited lower affinity to the substrate (higher value of Michaelis-Menten constant), it could still be used for efficient degradation of the pollutants under mild reaction conditions [148]. As the above-mentioned materials exhibited a great variety of advantages, it should be considered that their synthesis and production is usually complex and expensive.

4.2.5. Other inorganic materials

It should be added that other inorganic materials such as porous glass, calcium carbonate and noble metals can also be used for oxidoreductase immobilization. Due to inertness, large surface area and electronic properties which provide good electron transfer between the enzyme and a substrate, noble metals such as gold can be used for enzyme immobilization for environmental protection. Moreover, through the use of glass nanoparticles, biomolecules can be attached to the support homogeneously and retain their rigidity and catalytic activity [154]. Qiu et al. used nanoporous gold particles with pores of diameter around 40 nm for adsorption immobilization of lignin peroxidase from *Phanerochaete chrysosporium*. Gold-bounded enzyme retained over two times higher catalytic activity than free enzyme after incubation for 2 h at pH 5 and 45 °C. The resulting biocatalytic system was used for degradation of fuchsine, rhodamine B and pyrogallol red and removed over 75% of each compound [150]. Highly viscous liquids such as porous glass was used as beads for adsorption immobilization of laccase from *Trametes versicolor*. The obtained biocatalytic system, which was characterized by high thermal stability, was used in a recirculating packed or fluidized bed reactor for decolorization of textile dyes like Reactive Blue 19, Dispersed Blue 3, Acid Blue 74, Acid Red 27 and Reactive Black 5. After 30 min treatment in a fluidized bed reactor at pH 5 and 23 °C, over 80% of the Dispersed Blue 3 and Acid Blue 74 were removed from textile industry wastewater [149]. The limitation in this this study was the adsorption binding of the enzyme, as in the recirculation mode of the reactor it caused leakage of the laccase from the support.

As has been clearly shown, various inorganic materials including inorganic oxides (mainly silica or titanium dioxide), minerals, noble metals and carbon based materials, such as single- and multi-walled carbon nanotubes, are the most commonly used for immobilization of oxidoreductases for environmental applications. For example, laccase was covalently immobilized onto the surface of alumina pellets and multi-walled carbon nanotubes without any additional cross-linker [137, 145]. Produced immobilized enzymes were applied for degradation of Reactive Black 5 and Reactive Blue 19 with removal efficiencies exceed 85% and showed great reusability. These materials are known for their thermal and pH stability, mechanical resistance and good operational stability. Some attention should also be paid to the possibility of reuse of selected inorganic compounds after enzyme deactivation as a result of their high stability. Following immobilization on the surface of inorganic compounds, the range of pH and temperature over which the immobilized enzymes could effectively be used is often extended. For instance, laccase from *Trametes versicolor* or *Coriolopsis polyzona* was immobilized onto the surface of titania nanoparticles, porous glass beads or fumed silica, respectively [127, 133, 149]. Obtained systems were used for degradation of phenol derivatives and reactive dyes over a broad range pH from 3.5 up to 7.5 that confirmed stabilization of enzyme structure in both, acidic and base conditions. It also should be added that inorganic support materials, due to their presence in nature or easy preparation methodology are relatively inexpensive, which increases their application possibilities. According to the studies reviewed above, biocatalytic systems for removal of toxic compounds produced on the basis of inorganic supports bring highly efficient biodegradation of endocrine disruptor chemicals or dyes. To support this statement it could be presented, that various fungal laccases, immobilized onto the surface of nanoporous, mesoporous and sol-gel silica were applied for degradation of 2,4-dinitrophenol, 2,4,6-trichlorophenol, bisphenol A, diclofenac or triclosan [121, 123, 128]. It should be emphasized that silica is very versatile support material as each of the produced biocatalytic system degraded over 85% of the contaminant.

Factors such as high stability, mechanical resistance, the presence of many functional groups, mainly hydroxyl, and abundance in nature caused that inorganic materials as supports for oxidoreductases are commonly used for environmental applications. Enzymes may be effectively attached to these materials principally mainly via adsorption immobilization due to the good sorption properties of these carriers. However, the formation of covalent bonds due to the presence of many functional groups, should not be excluded, which results in creation of stable and reusable biocatalytic systems. It has been shown that immobilized oxidoreductases could be applied in large scale processes for effective remediation of wastewater contaminated with toxic pollutants. However, in our opinion some operational parameters still needs an improvement. Even so, due to the enhanced sensitivity and selectivity of the enzymes after immobilization using for instance noble metals or materials that enhance transfer of the electrons, biocatalytic systems containing oxidoreductases could be soon applied not only for environmental protection, but also in biosensors to detect even trace amounts of various compounds in effluents from industry or in human body fluids.

4.3. Hybrid materials

As previously mentioned, composite and hybrid materials as supports for enzymes have attracted researchers' attention over the last two decades. A combination of the properties of their precursors maximizes the benefits of these materials and makes them suitable supports for enzymes for many practical environmental applications. Many components of both organic and inorganic origin have been combined to create new supports for immobilization of oxidoreductases. Increases in stability and reusability of the immobilized enzyme can be achieved by the use of these types of matrices. Hybrid/composite support materials also protect biomolecules against denaturation and loss of the bioactivity under reaction conditions. Moreover, the properties of these support materials are usually designed for selected enzymes and the technological process in which the product will be applied after immobilization. An additional advantage of these materials is that due to their properties they can be applied in all immobilization techniques [155]. Selected examples of the various hybrid and composite materials used for immobilization of enzymes for environmental pollutants degradation are presented in Table 4, followed by comments.

4.3.1. Inorganic-inorganic hybrid materials

With regards to inorganic materials, mainly inorganic oxides such as silica or zinc and titanium oxide are used to produce hybrid supports for

Table 4
Hybrid and composite support materials used for immobilization of laccases, tyrosinases and lignin, manganese and phenol oxidases for biodegradation of various environmental pollutants.

Support material	Enzyme	Immobilization technique	Contaminants	Process conditions	Removal efficiency	Reference
Macroporous SiO_2/ZnO nanowires	Horseradish peroxidase	Covalent immobilization	Acid Blue 113, Acid Black 10 BX	pH 7, 25 °C, 35 min	95%, 90%	[156]
Multi-walled carbon nanotube/cordierite	Horseradish peroxidase	Covalent immobilization	4-aminoantipyrine	pH 7, 25 °C, 1 h	96%	[157]
Silica/magnetic/methacrylyol particles	Laccase from *Trametes versicolor*	Adsorption immobilization	Methyl Red	pH 6, 35 °C, 12 h	90%	[158]
Cu^{2+}/silica magnetic particles	Laccase	Covalent immobilization	2,4-dichlorophenol	pH 5, 25 °C, 12 h	100%	[159]
Silica magnetic particles	Laccase	Covalent immobilization	2,4-dichlorophenol	pH 5, 35 °C, 6 h	85%	[160]
Magnetic mesoporous silica nanoparticles	Laccase from *Trametes versicolor*	Covalent immobilization	Phenol	25 °C, 40 h	90%	[161]
Magnetic tubular mesoporous silica	Laccase	Covalent immobilization	Methoxychlor	pH 4.5, 35 °C, 10 h	69%	[162]
Magnetic nanoparticles/graphene oxide nanocomposite	Horseradish peroxidase	Covalent immobilization	2-chlorophenol, 4-chlorophenol, 2,4-dichlorophenol	pH 6, 25 °C, 3 h	82%, 52%, 33%	[163]
Carbon mesoporous magnetic composites	Laccase from *Trametes versicolor*	Covalent immobilization	Phenol, *p*-chlorophenol	pH 6, 45 °C, 12 h	74%, 82%	[164]
Magnetic chitosan/clay beads	Laccase from *Trametes versicolor*	Covalent immobilization	Phenol	pH 5, 25 °C, 4 h	80%	[165]
Superparamagnetic/chitosan microspheres	Tyrosinase	Covalent immobilization	Phenol	pH 7, 25 °C, 48 h	65%	[166]
Cyanuric chloride/silica magnetic nanoparticles	Tyrosinase	Covalent immobilization	2,2′-azinobis-(3-ethylbenzothiazoline-6-sulphonic acid)	pH 7, 35 °C, 1 h	95%	[167]
Chitosan/SiO_2 gel	Polyphenol oxidase from potato	Covalent immobilization	Phenol	pH 7, 25 °C, 24 h	86%	[168]
Chitosan/biomimetic silica nanoparticles	Manganese peroxidase from *Phanerochaete chrysosporium*	Covalent immobilization	2,6-dimethoxyphenol	pH 4.5, 30 °C, 1 h	95%	[169]
Chitosan/CeO_2 microspheres	Laccase from *Trametes versicolor*	Covalent immobilization	Methyl Red, Orange II	pH 6, 25 °C, 9 days	83%, 93%	[170]
Chitosan/clay composite	Tyrosinase from mushroom	Covalent immobilization	Phenol	pH 7, 25 °C, 6 h	100%	[171]
Chitosan nanoparticles/glass beads	Laccase *Paraconiothyrium variabile*	Covalent immobilization	Congo Red	pH 5, 40 °C, 15 min	98%	[172]
Chitosan/polyacrylamide hydrogel	Laccase from *Trametes versicolor*	Encapsulation	Acid Orange 7, Malachite Green	pH 5, 25 °C, 6 h	70%, 97%	[173]
Chitosan/alginate/magnetic capsules	Tyrosinase from mushroom	Encapsulation	Phenol, Bisphenol A	pH 6, 25 °C, 39 h	100%, 85%	[174]
Magnetic Cu alginate beads	Laccase from *Trametes versicolor*	Encapsulation	Triclosan, Remazol Brilliant Blue R	pH 5.2, 25 °C, 8 h	89%, 76%	[175]
Alginate/SiO_2 gel	Polyphenol oxidase from potato	Entrapment	Phenol	pH 7, 25 °C, 8 h	90%	[176]
Poly(acrylamide-crotonic acid)/Na alginate	Laccase from *Trametes versicolor*	Covalent immobilization	Acid Orange 52	pH 4.5, 30 °C, 6 h	73%	[177]
Poly(vinyl alcohol)/Ca alginate beads	Manganese peroxidase from *Ganoderma lucidum* IBL-05	Entrapment	Sandal reactive dyes, Textile wastewater	pH 5, 25 °C	92%, 80%	[178]
Polyamide 6/chitosan nanofibers	Laccase from *Trametes versicolor*	Covalent immobilization	Bisphenol A, 17-*α*-ethinylestradiol	pH 5, 37 °C, 6 h	92%, 100%	[179]
Poly(2-chloroethyl acrylate)/zeolite particles	Laccase from *Trametes versicolor*	Covalent immobilization	Reactive Red 120	pH 6.5, 35 °C, 3 h	100%	[180]
Poly(acrylic acid)/SiO_2 nanofibers	Laccase	Covalent immobilization	Triclosan	pH 4, 30 °C, 2 h	60%	[181]
Graphene oxide/latex hydrogel	Laccase	Covalent immobilization	Remazol Brilliant Blue R	pH 4.5, 25 °C, 17 h	100%	[182]
Cu tetra-aminophthalocyanine/magnetic nanoparticles	Laccase from *Pycnoporuss anguineus*	Covalent immobilization	2,2′-azinobis-(3-ethylbenzothiazoline-6-sulphonic acid)	pH 3, 45 °C	100%	[183]
Poly(4-vinyl pyridine)/Cu(II) magnetic beads	Laccase from *Trametes versicolor*	Adsorption immobilization	Reactive Green 19, Reactive Red 2, Reactive Brown 10	pH 5.5, 30 °C, 18 h	64%, 88%, 91%	[184]
Poly (*p*-phenylenediamine)/magnetic nanocomposite	Laccase	Covalent immobilization	Reactive Blue 19	pH 4, 25 °C, 2 h	90%	[185]
Poly(styrene-*co*-methacrylic acid) nanofibers	Horseradish peroxidase	Covalent immobilization	*o*-methoxyphenol	pH 5, 2 h	80%	[186]
Poly(lactic-*co*-glycolic acid) nanofibers	Laccase from *Pleurotus florida*	Covalent immobilization	Diclofenac	pH 4, 30 °C, 5 h	100%	[187]
Poly(acryl-amide) gel	Manganese peroxidase from *Ganoderma lucidum* IBL-05	Entrapment	Textile dyes	pH 5.5, 30 °C	<70%	[188]
Poly(methyl methacrylate-co-glycidyl	Laccase from *Trametes*	Covalent	Procion Red, Reactive Green 5,	pH 4, 45 °C, 10 h	81%, 60%,	[189]

(continued on next page)

Table 4 (*continued*)

Support material	Enzyme	Immobilization technique	Contaminants	Process conditions	Removal efficiency	Reference
methacrylate) cryogel	*versicolor*	immobilization	Reactive Brown 10, Reactive Green 19, Cibacron Blue F3GA, Alkali Blue 6B, Brilliant Blue 6		74%, 66%, 63%, 60%, 62%	
Poly(vinyl alcohol)/4-hydroxybenz-aldehyde cinnamate	Horseradish peroxidase	Covalent immobilization	2,2′-azinobis-(3-ethylbenzothiazoline-6-sulphonic acid)	pH 4.5, 25 °C	98%	[190]

oxidoreductase immobilization. Other oxides, minerals, carbon-based materials and noble metal ions are also frequently involved in the design of the new supports. Inorganic-inorganic hybrids are usually characterized by inertness, resistance against harsh reaction conditions and good mechanical stability. As a result, the immobilized enzyme also possesses improved thermal and chemical stability and its structure is protected by the composite matrix from denaturation [181]. A great advantage of inorganic-inorganic hybrids is that they may be used in a wide variety of shapes and sizes, such as nanoparticles, nanowires, fibers, tubes and even as membranes [159, 160, 192]. Sun et al. used macroporous SiO_2/ZnO nanowires modified by diethylene glycol diglycidyl ether for covalent immobilization of horseradish peroxidase. The immobilized enzyme exhibited high activity in decolorization of azo dyes, like Acid Blue 113 and Acid black 10 BX, and removed as much as 95 and 90% of these dyes, respectively. The support-bonded enzyme was able to remove over 90% of the selected dye from a solution containing dye at over 50 mg/L after <1 h. Furthermore, storage stability and reusability of the immobilized biomolecule was significantly improved in comparison with the free enzyme [156]. Special attention, though, among others inorganic materials should also be paid to magnetic particles representing by i.e. magnetite. Biocatalytic systems based on hybrids incorporating magnetic particles may be easily separated from reaction mixtures by an external magnetic field. Magnetite particles for immobilization of laccases and removal of phenol derivatives have been combined with silica particles or mesoporous carbon material [161, 164]. Superparamagnetic nanoparticles were successfully deposited on graphene oxide sheets by ultrasound-assisted co-precipitation by Chang and his team. Synthesized material was then used for immobilization of horseradish peroxidase and applied for batch biodegradation of 2-chlorophenol, 4-chlorophenol and 2,4-dichlorophenol. On the one hand, removal efficiency was strongly affected by the number and position of electron-withdrawing substituents in the phenol ring, but on the other hand also lack of proper hydrogen peroxide supplying limit high removal rates. Nevertheless, the highest removal efficiency, over 80%, was observed for 2-chlorophenol. The results presented by these authors suggest that storage stability and tolerance to changes in temperature and pH of the immobilized biomolecules were better than for the free biomolecules [163].

4.3.2. Inorganic-organic hybrid materials

Though magnetite is often combined with inorganic moieties, it can be also mixed with organic materials such as biopolymers, for example chitosan or alginates [166, 175] as well as synthetic polymers like poly(*p*-phenylenediamine) or poly(4-vinyl pyridine) [184, 185]. In a bench study magnetite nanoparticles were combined with chitosan to increase the bioaffinity of the hybrid and with clay to increase stability and mechanical resistance of the hybrid. The produced material was applied for covalent immobilization of laccase from *Trametes versicolor*. In comparison to the free enzyme, the immobilized biomolecules exhibited improved storage stability and better tolerance to changes in pH and temperature, and retained over 70% of initial activity after 10 repeated cycles. This biocatalytic system was then used for phenol degradation. After 4 h of treatment under optimal conditions, about 80% of phenol was removed from solution [165]. In another study, highly biocompatible chitosan core alginate capsules were enriched by magnetite nanoparticles and used for encapsulation of mushroom tyrosinase. The biomagnetic capsules thus obtained showed great storage stability, faster removal rate and greater reproducibility. This biocatalytic system could be applied for remediation of phenol and bisphenol A from real environmental water samples, because after 39 h of treatment of this process, 100% and over 85%, respectively, of the two pollutants were degraded [174]. In work by Bayramoglu and co-workers, synthetic polymer - poly(4-vinyl pyridine) was grafted on magnetic nanoparticle beads. Next, the polymer was chelated by Cu(II) ions for adsorption immobilization of laccase from *Trametes versicolor* and enhancement of the catalytic activity of the enzyme. The biocatalyst thus produced was used in an enzyme reactor for degradation of three textile dyes - Reactive Green 19, Reactive Red 2 and Reactive Brown 10 - in a batch system. The described results show that immobilized laccase could successfully remove the three test dyes from water solution at efficiencies of 64%, 88% and 91%, respectively. However, as the main factor that limit the decolorization rate was the chemical structure and type of substitute group of the dye molecules [184]. Biopolymers can also be combined with other inorganic materials to create suitable supports for immobilization of enzymes for environmental applications. For instance, chitosan was mixed with silica or cesium oxide, minerals or glass beads [169, 170, 172], while alginate was combined with silica gel [176]. An interesting example of the creation of inorganic-organic hybrids was presented by Dincer and co-workers. They mixed clay with chitosan and cross-linked hybrid material by glutaraldehyde to form beads that were used for covalent immobilization of tyrosinase. The authors reported high enzyme activity and loading efficiency due to the presence of many functional groups in the structure of the support. The immobilized tyrosinase was used for degradation of phenol in water solution. After treatment for 6 h at 25 °C and pH 7, all of the phenol was removed. The biocatalytic system was able to retain over 50% of its initial activity after seven repeated tests [171]. In this study achievement of the better reusability was limited by the inhibition and inactivation of the enzymes over consecutive catalytic cycles. Besides biopolymers, synthetic polymers may also be combined with inorganic components to form suitable matrices for immobilization of enzymes for environmental protection. For instance, poly(2-chloroethyl acrylate) was combined with zeolite particles, as latex hydrogel was mixed with graphene oxide to formed nanobeads. Both hybrids were then used for immobilization of laccase and applied for degradation of textile dyes with high efficiencies [180, 182]. Xu et al. used mesoporous SiO_2 nanofibers and connected them with poly(acrylic acid). Finally, the hybrid system was modified by vinyl groups to increase its affinity for laccase. The synthesized matrix was characterized by a mesoporous structure (pore size 1.73–3.54 nm) and a high specific surface area (542.91 m^2/g) which allowed covalent bonding of about 420 mg of the enzyme per 1 g of the support. The immobilized biomolecule exhibited better storage stability and higher tolerance to harsh pH and temperature conditions in comparison with free laccase. The biocatalytic system, after 2 h of triclosan treatment, under optimal process conditions (pH 4, 30 °C) removed around 65% of the pollutant from water solution [181]. The factor that limit degradation efficiency might be an enzyme overloading, which blocked active sites of the biocatalysts and decrease their activity.

4.3.3. Organic-organic hybrid materials

When there is a need for materials with more sophisticated features such as special reactive functional groups or unusual shape, polymers can be fixed with biopolymers or other synthetic polymer. Synthesized organic-organic hybrids due to the presence of biopolymers, such as calcium or sodium alginate, are biocompatible and non-toxic, because the presence of the polymers such as poly(acrylamide-crotonic acid) or polyvinyl alcohol ensures stability, mechanical resistance and stiffness of the hybrid support [177, 178]. Polyamide 6/chitosan nanofibers modified by using two different spacers (bovine serum albumin and hexamethylenediamine) have been used for immobilization of laccase from *Trametes versicolor* and applied for biodegradation of endocrine disrupting chemicals like bisphenol A and 17-α-ethinylestradiol. The resulting biocatalytic systems proved to be efficient not only in removal of a mixture of the pollutants (92% of bisphenol A removal, total degradation of 17-α-ethinylestradiol) but also showed great reusability. After three treatment cycles, the initial activity of this system was unaltered [179]. It should also be mentioned that hybrid supports built from two synthetic polymers may be used for immobilization of various oxidoreductases. Synthetic polymer hybrids are formed by polymerization using various monomers with desired properties. These materials exhibit chemical and mechanical stability and possess many desirable functional groups and are characterized by a large specific surface area that allows a great number of biomolecules to be attached in a stable way mainly via covalent bonds. For example, horseradish peroxidase was immobilized on composite poly(vinyl alcohol)/4-hydroxybenzaldehyde cinnamate or poly(styrene-*co*-methacrylic acid) nanofibers [186, 190]. The produced biocatalytic systems were applied for degradation of phenol derivatives and were able to remove over 80% of the pollutants from water solution. But the limitation of the presented biocatalytic system was covalent binding of the molecules and disruption in the structure of the enzyme active sites. In another study, Uygun and co-workers used poly(methyl methacrylate-*co*-glycidyl methacrylate) cryogel for immobilization of laccase from *Trametes versicolor* and degradation of textile dyes effluent. The immobilized enzyme degraded up to 80% of the selected dye with degree of degradation dependent on the chemical structure and molecular mass of the pollutants [189]. Sathishkumar et al. applied poly(lactic-*co*-glycolic acid) nanofibers for covalent immobilization of laccase from *Pleurotus florida*. The obtained biocatalytic system was used for biodegradation of diclofenac from aqueous sources. The results the authors present demonstrated that the environmental pollutant could be completely transformed into non-hazardous compounds. Moreover, their biocatalytic system exhibited great reusability. After three reuse cycles diclofenac was completely removed. Additionally, after addition of syringaldehyde, reusability of the system was extended to six catalytic cycles. The immobilized laccase had better storage, pH and thermal stability than the free biocatalyst [187]. It should be also noted that when synthetic polymer hybrids are used, entrapment also takes place. For this reason poly(acryl-amide) gel was used for entrapment of manganese peroxidase from *Ganoder malucidum* IBL-05. The immobilized enzyme exhibited good storage stability and could retain over 50% of initial activity after storage for two months at 4 °C. The thermal stability of the immobilized peroxidase was also significantly improved. After incubation for 72 h at 50 °C, the enzyme retained over 40% of its initial properties while the free biomolecule was completely inactive. The immobilized catalyst was further used for removal of textile dyes from real water solutions [188].

As has been clearly demonstrated various types of hybrids and composite materials can be applied for immobilization of enzymes for remediation of parlous pollutants. It is becoming more and more common to use these materials due to the possibility of designing their properties to fulfill the requirements of the technological process and of the enzyme. Precursor materials may be chosen to protect of the enzyme structure, increase thermal and chemical resistance of the immobilized biomolecules as well as to improve their catalytic properties. For example, carbon nanotubes could enhance transfer of the electron during catalytic reaction as the addition of Cu^{2+} ions in general increases the catalytic activity of the oxidoreductases. For example, copper ions were incorporated into the structure of tetra-aminophthalocyanine/magnetic nanoparticles and poly(4-vinyl pyridine)/magnetic beads. Hybrid supports were further used for covalent and adsorption immobilization of laccase from *Pycnoporuss anguineus* and *Trametes versicolor*, respectively. Produced immobilized enzymes were applied for degradation of 2,2′-azinobis-(3-ethylbenzothiazoline-6-sulphonic acid) and reactive dyes and allowed total removal of pollutants from water solution [184, 186]. Presented examples proved that addition of inorganic ions into the structure of polymeric matrix could significantly improve removal efficiency. Other precursor materials are chosen in order to improve operational control of the remediation process. For instance, magnetic nanoparticles make separation of the immobilized enzyme from reaction mixture fast and simple as inorganic oxides ensure high mechanical stability of the biocatalytic system and its reusability. Application of the hybrid supports for enzymes and their use in bioremediation of environmental pollutants, such as phenol and its derivatives, dyes and even estrogens from wastewater, results in high efficiency of the removal process. Pollutants like 2,4-dichlorophenol was efficiently removed by laccase covalently immobilized on silica magnetic particles and Cu^{2+}/silica magnetic particles [159, 160] as organic dye Reactive Green 19 was degraded with efficiency exceed 65% by laccase from *Trametes versicolor* immobilized on poly(4-vinyl pyridine)/Cu(II) magnetic beads or poly(methyl methacrylate-*co*-glycidyl methacrylate) cryogel [184, 189]. Undesirable compounds are effectively transformed into non-hazardous products, under mild conditions, whilst immobilized enzymes retain their high catalytic activity over repeated reaction cycles. Hybrids and composite materials can be formed into the shape that will be most suitable for the process. Therefore all techniques of immobilization may be used for immobilization of laccases of various origins, and for tyrosinases or peroxidases. However, note should be stated that proper selection of the immobilization technique is required to avoid diffusional limitations and enzyme inactivation. Hybrid support of inorganic-inorganic, organic-organic and mixed inorganic-organic origin, like magnetic nanoparticles/graphene oxide nanocomposite, chitosan/polyacrylamide hydrogel and alginate/SiO_2 gel were applied for covalent immobilization of horseradish peroxidase, encapsulation of laccase from *Trametes versicolor* and entrapment of polyphenol oxidase, respectively [163, 173, 176]. Immobilized enzymes were then used for degradation of phenol and its derivatives and organic dyes with removal efficiencies around 80% that proved versatility of the hybrid materials. However, higher degradation rate is limited by the diffusional limitations of reaction mixture.

Irrespectively of the origin of precursors, properties of the hybrid and composites materials could be tailored to meet the requirements of the enzymes and the process, making these materials particularly interesting as support for immobilization. Therefore, we strongly suggest more advanced research related to the application of the abovementioned materials as a carriers for oxidoreductases which should result in formation of active biocatalytic systems for removal of hazardous compounds with high efficiencies despite the fact that they are expensive and methodology for their synthesis is usually complicated. We also believe that hybrid and composite materials has continued to grow during recent years, as these materials are also particularly interesting in terms of potential for further exploitation. In the near future, hybrid and composite supports materials could be used for immobilization of enzymes for production of highly sensitive biosensors, as well as for efficient, more specific and “cleaner” catalysts in chemicals synthesis, or might even find application in clinical medicine. It should be mentioned that hybrids materials could be also used as an efficient and stable support for co-immobilization of enzymes and application of the resulting biocatalytic systems in multienzymatic bioconversion processes.

5. Effect of support materials and immobilization technique on substrates accessibility

As it was previously stated, laccases and tyrosinases required molecular oxygen as a substrate that is reduced to water during catalytic pathways of these enzymes [191, 192]. Similarly, peroxidases (LiP, MnP, HRP) need hydrogen peroxide, that during reaction is also reduced to water. The catalytic mechanism of laccases, tyrosinases and peroxidases differ from each other, but accessibility of the molecular oxygen and hydrogen peroxide, beside availability of phenolic substrates, is a key factor that limits catalytic efficiency of the immobilized oxidoreductases [193, 194].

To ensure high exposition of the enzyme active site for contact with substrates, proper selection of immobilization protocol has to be done. For instance, in case of adsorption immobilization by limited number of formed interactions, interference in the structure of the enzyme and amino acids rearrangements is reduced, as it facilitates easy binding of O_2 or H_2O_2. In contrast, covalent binding of the biocatalysts usually disrupts the structure of enzyme and its catalytic site, what makes interactions with reducing substrates more difficult. Enzymes immobilized by encapsulation or entrapment are usually physically locked into the matrix that limits structural changes of the biomolecules. But on the other hand, significant diffusional limitations occurs that reduce efficient transfer of substrates and decrease catalytic activity [195]. To support this statement some examples are presented below. For instance, fungal laccases were immobilized by adsorption, covalent binding and entrapment, using supports of organic origin, and applied for degradation of reactive dyes. Acid Orange 7 was almost totally removed from water solution by adsorbed enzyme, as 80% of Reactive Yellow 15 and about 50% of Remazol Brilliant Blue R were degraded by laccase immobilized by covalent binding and entrapment, respectively [76, 99, 147]. Different values of removal efficiencies might be explained mainly by various immobilization strategies and related to this different diffusional limitations, which are the lowest in adsorption immobilization and the highest in encapsulation due to enzyme surrounding by the support layer. Formed diffusional limitations strongly influence accessibility of the molecular oxygen and hydrogen peroxide to the active site of the enzymes and in consequence affect effectivity of biodegradation [196, 197].

When the supply of the oxygen or hydrogen peroxide is hindered, mesoporous materials at highly ordered structure of pores should be use, while they enable ease penetration of the oxygen or hydrogen peroxide molecules. In consequence higher removal efficiencies might be achieved using these materials. That proves, that application of various matrix for immobilization of the same enzyme could results in different degradation values and indicates that structural composition and properties of support material affect accessibility of O_2 or H_2O_2. Although most of the bioremediation processes using immobilized oxidoreductases are carried out without additional supply of reducing substrates there is a room for improvements leading to the higher robustness of the enzymes and cost reduction. For instance, some additional process like bubbling, oxygenation, aeration and even simple shaking could be applied to increase accessibility of the reducing substrates for immobilized enzymes.

6. Summary and comparison of the support materials of various origin

In the presented study it has been clearly shown that many various materials of organic, inorganic and hybrid/composite origin could be efficiently applied for immobilization of oxidoreductases for environmental application. The most important advantages and disadvantages of each type of the support materials were briefly summarized and are presented in Fig. 4.

The multiplicity of the possible supports caused that their proper selection is strongly governed by the type of the enzyme, immobilization technique and undesirable compound that has to be removed. For instance for immobilization of laccase from *Trametes versicolor*, the most commonly applied oxidoreductase for environmental application, materials of different hydrophilicity and functional moieties (–OH, $–NH_2$, C=O) of organic, inorganic and hybrid origin, such as chitosan and poly(vinyl alcohol) capsules [76, 101], mesoporous silica and Fullere C_{60} [121, 148] as well as magnetic chitosan/clay beads or poly

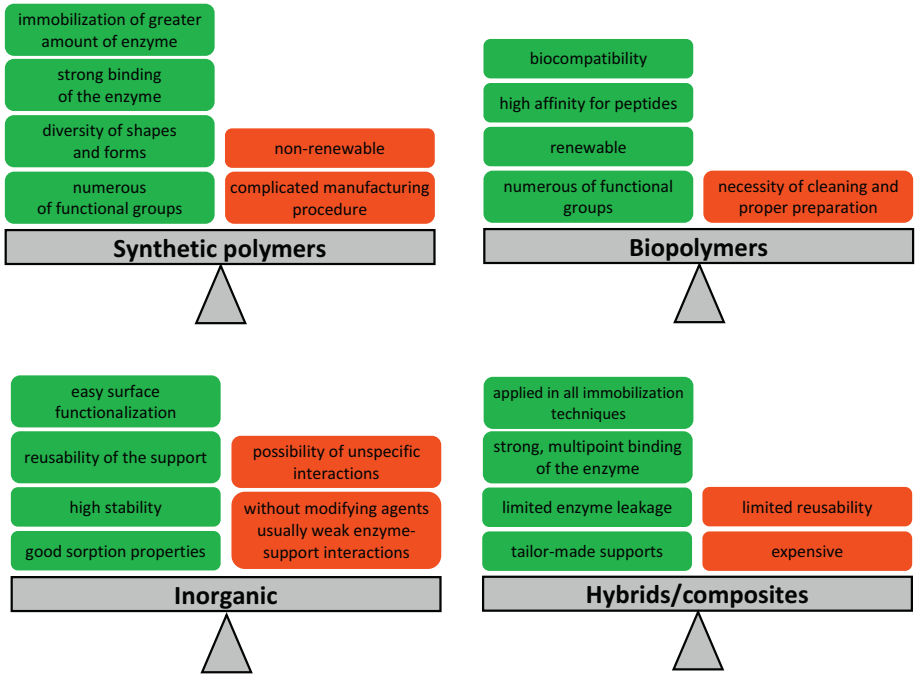

Fig. 4. Summary of advantages and disadvantages of support materials for immobilization of oxidoreductases.

(4-vinyl pyridine)/Cu(II) magnetic beads [165, 184] were applied. Also mushroom tyrosinase was immobilized using wide range of support materials, such as cellulose paper [83], silica gel [130] and chitosan/clay and chitosan/alginate magnetic capsules [171, 174]. Obtained biocatalytic systems were applied for degradation of synthetic and natural dyes and phenol and its derivatives with removal efficiencies usually higher than 80%, which proves that immobilized oxidoreductases are stable, irrespectively of the origin of support material. More attention should be paid on immobilization of laccase and tyrosinase on hybrid supports, such as poly(4-vinyl pyridine)/Cu(II) magnetic beads and chitosan/alginate magnetic capsules by adsorption and encapsulation, respectively. Immobilized laccase was used for degradation of Reactive Brown 91 and removed over 90% of the dye [184] as encapsulated tyrosinase degraded about 85% of bisphenol A from water solution [174]. Presented results prove that immobilized enzymes not only retain their robustness but also might be easily separated from reaction mixture by addition of magnetic particles. That suggest that hybrid and composite materials might be interesting for immobilization of laccases and tyrosinases and their practical application on larger scale for bioremediation of pollutants. Although various supports could be used for immobilization of laccases, tyrosinases and peroxidases, during selection of the specific material for practical applications mainly its accessibility and costs of its obtaining, purification and synthesis should be taken into account. Also high stability in harsh process conditions and mechanical resistance are a crucial factors determining selection of the carrier for immobilization of oxidoreductases. As inorganic carriers and biopolymers seems to be particularly interesting from the point of view of economy and stability, hybrid and composites materials are outstandingly attractive because they might be tailored and produced to enhance catalytic activity of the immobilized enzymes and in consequence to improve efficiencies of the processes carried out.

As it was previously mentioned, immobilization methodology also strongly influence the selection of enzyme support. Highly porous materials, at high specific surface area facilitate adsorption immobilization and enhance attachment of greater amounts of enzyme. As an example, chitosan beads, titania nanoparticles, mesoporous carbon and silica/magnetic/methacrylyol particles should be enumerated [78, 133, 147, 158]. These materials were used for immobilization of laccase, tyrosinase and even lignin peroxidase and applied for removal of mainly dyes and phenol from water solutions with removal efficiencies not exceeding 90%. This might be related to the binding of great amount of enzyme, which might leads to biomolecules overcrowding and in consequence decrease in catalytic activity [196]. On the other hand, immobilization of oxidoreductases on materials with numerous of functional groups facilitate covalent immobilization and multipoint attachment of the enzyme molecules. That is preferred in terms of improving stability of immobilized enzyme, however might also lead to creation of diffusional limitations in transport of substrates. From that point of view, particularly interesting are hybrid materials, such as magnetic chitosan/clay beads and poly(lactic-*co*-glycolic acid) nanofibers that were used for covalent binding of laccase from *Trametes versicolor* and applied for degradation of phenol and diclofenac, respectively [165, 187]. Even taking into account diffusional limitations, stability of the enzyme was significantly improved and allow total removal of phenol and diclofenac from the tested solution. Inorganic materials such as mesoporous silica spheres and halloysite nanotubes [124, 139] and organic carriers of natural origin like chitosan or coconut fibers could be applied for covalent immobilization [75, 99]. The above-mentioned supports were used for immobilization of all reviewed oxidoreductases and applied for biodegradation of synthetic and natural dyes, pharmaceuticals and phenols usually with efficiencies exceeding 80%. However, it should be emphasized that inorganic and organic materials for covalent attachment of the enzyme usually require intermediate agents, such as glutaraldehyde, that facilitate creation of covalent bonds. For immobilization of oxidoreductases also encapsulation and entrapment are applied. As supports for these techniques of immobilization mainly alginates-based materials are adapted due to their remarkable abilities for gelation under mild conditions and high operational stability [78–91]. Also poly(vinyl alcohol) beads, silica aerogel and hybrid chitosan/polyacrylamide hydrogel were used for encapsulation of laccases and tyrosinases [102, 131, 173]. For instance laccase was immobilized by encapsulation into chitosan beads and by entrapment into copper alginate beads and they were applied for degradation of Indigo carmine [79, 91]. Both biocatalytic systems allowed total degradation of the dye, but addition of copper ions into alginate beads increased activity of the laccase and caused that degradation process was four times shorter and was carried out in milder temperature conditions (30 °C) as compared to chitosan beads (37 °C). It is our belief that among the existing immobilization protocols, two approaches are of particular interest. Firstly, immobilization of oxidoreductases in the way where interference in the enzyme structure is highly limited as it results in no conformational changes in the biocatalysts structure and retention of high catalytic properties. The second approach is a multipoint immobilization of the enzyme. As a result biomolecule is permanently attached to the support material that results in the improvement of the reusability of the immobilized biocatalysts. However, we would like to emphasize that selection of the most suitable immobilization protocol is governed mainly by the type of the support and practical requirements for the biocatalytic system.

Irrespectively of the origin, support materials could be applied for biodegradation of the same type of the persistent pollutants. For instance, fungal laccases covalently immobilized using mesoporous silica and polyamide/chitosan composite [123, 179] as well as mushroom tyrosinase immobilized by entrapment using silica alginate and by covalent binding on polyacrylonitrile beads [85, 104] were applied for remediation of bisphenol A. Removal efficiencies ranging from 80% (mesoporous silica) up to 92% (composite support) were noticed for immobilized laccase as for tyrosinase it was 35% (silica alginate) and 90% (hybrid support). On the other hand, synthetic dyes could be efficiently removed by oxidoreductases immobilized using wide range of support materials. For example, for remediation of synthetic dye Remazol Brilliant Blue R, laccase immobilized by covalent binding on gum Arabic and graphene oxide/latex hydrogel and encapsulated into magnetic Cu alginate beads were applied [97, 175, 182]. The remediation efficiencies varied from 80% (gum Arabic) to 100% (hybrid material) for covalently immobilized enzyme. In case of encapsulated laccase, mainly due to the occurrence of diffusional limitations, biodegradation efficiency reached 76% and even the presence of copper ions in the support material did not improve performance of the process. These data clearly shows that porosity of the support material, type of surface functional groups and immobilization technique strongly affect degradation process of bisphenol A and Remazol Brilliant Blue R.

Many studies from research laboratories show promising early stage proof-of-concept results for application of oxidoreductases for environmental application, however, they suffer because there is a significant lack of work targeting the whole chain including production costs of the immobilized enzymes, any scale-up advantages of manufacturing of matrices and biocatalytic systems, as well as presenting their storage stability and practical implementation. Also broader comparison of several different types of immobilized enzyme systems, for example laccase systems that have broad substrate selectivity, are warranted. Presented studies and their limitations show that the time is now ripe for moving to the next level of multidisciplinary assessment and there is a need to involve the companies and environmental agencies in the research as they should help to overcome various practical limitations. As the results of these studies we should obtain immobilization protocols allowing production of universal biocatalytic systems for degradation and remediation of hazardous pollutants.

7. General summary and remarks

In recent years, environmental pollutants such as synthetic and natural dyes, pharmaceuticals and phenol and its derivatives have become

a very serious problem that needs to be solved to minimize the direct threats posed by these compounds to the health and life of living organisms. One possible way to remove hazardous contamination from wastewater and soils is their biodegradation using enzymes. It has been shown that phenyloxidase enzymes, such as laccase, tyrosinase or lignin, manganese and horseradish peroxidases, as a members of oxidoreductase catalytic class, may catalyze oxidation and transformation of numerous persistent compounds into non-toxic derivatives. These processes were usually carried out without addition of cofactors or mediators except molecular oxygen or hydrogen peroxide, which are widely available. The studies reviewed here can lead to a better understanding of enzymatic biodegradation and illustrate the following benefits of oxidoreductase enzymes:

(i) biodegradation processes may be carried out in highly efficient way under mild conditions,
(ii) removal of environmental contaminants is possible without use of toxic solvents or high energy consumption, in accordance with the rules of green chemistry,
(iii) remediation of pollutants may usually be carried out in more cost-effective way, without the need for advanced equipment,
(iv) conversion of hazardous compounds into their non-toxic derivatives may be achieved.

Despite the many promising results, it is evident that more research is needed to clarify the levels of different pollutants and residual pharmaceuticals locally, particular near industrial area and near hospitals. Next, a much better understanding of the competitive kinetics of different substrates on enzymatic removal by oxidoreductases, such as laccases or tyrosinases is clearly missing. Lastly, durability and robustness of different types of enzymes in genuine application environments should be assessed. This review also shows the need for larger comparative application trial among different types of enzymatic options for removal of pharmaceutical residues in particular.

It should further be pointed out that the immobilization process is frequently applied to increase stability of the enzymes and enhance their reusability as well as to create insoluble biocatalyst that may be reused. Here we have summarized and reviewed materials and their properties that could be used as supports in immobilization of enzymes for environmental applications. As we have described, materials of both organic and inorganic origin as well as hybrids and composites supports have been be applied for immobilization of oxidoreductases. We have also reported the key factors that determine selection of the support for immobilization of enzymes for contaminants removal as being the following:

(i) the presence of numerous functional groups for effective enzyme binding,
(ii) good sorption properties,
(iii) good thermal and chemical resistance and mechanical and operational stability.

However, materials with desired properties that increase activity and stability of the immobilized biocatalysts have also been examined. Furthermore, we have summarized the possible ways to perform the biodegradation processes and possibilities for increasing their efficiency.

Thus, our aim has been to review support materials that may be applied for immobilization of enzymes for environmental applications and show how these materials affect catalytic activity and stability of the biocatalysts. We wanted to present criteria for selection of support materials to produce biocatalytic systems which have excellent catalytic properties and good stability for use in modern remediation of undesirable pollutants from domestic and industrial wastewaters. Information presented in this review could form a basis for evaluation of a novel, highly efficient detoxification process conducted under mild conditions, without utilization of a hazardous reagents, in accordance with the rules of green chemistry.

While applications of immobilized laccases have been well studied, only few previous studies have dealt with the efficient use of other oxidoreductases for environmental protection. The information displayed on this review confirms that tyrosinases, and peroxidases such as horseradish, manganese and lignin peroxidase show promise as efficient treatments for removal of hazardous pollutants after immobilization, even at industrial scale. The main challenge to this respect is to build systems able to operate in continuous mode, so the operational costs of such bioremediation processes can be reduced. Additionally, further studies on the role of these enzymes on the removal of other compounds such as hormones or antibiotics will have to be also addressed in future studies.

Acknowledgements

This work was supported by research grant funds from the National Science Center Poland in accordance with decision no. DEC-2016/20/T/ST8/00391.

References

[1] Ning B, Graham N, Zhang Y, Nakonechny M, El-Din MG. Ozone Sci Eng 2007;29:153.
[2] Rezg R, El-Faza S, Gharbi N, Mornagui B. Environ Int 2014;64:83.
[3] Barrios-Estrada C, de Jesús Rostro-Alanis M, Muñoz-Gutiérrez BD, Iqbal HMN, Kannan S, Parra-Saldívar R. Sci Total Environ 2018;612:1516.
[4] Bilal M, Asgher M, Iqbal HMN, Hu H, Zhang X. Environ Sci Pollut Res 2017;24:7035.
[5] Tiwari D, Kamble J, Chilgunde S, Patil P, Maru G, Kawle D, et al. Mutat Res 2012;743:83.
[6] Rochester JR. Reprod Toxicol 2013;42:132.
[7] Cowan DA, Fernandez-Lafuente R. Enzyme Microb Technol 2011;49:326.
[8] Arora PK, Kumar M, Chauhan A, Raghava GP, Jain RK. BMC Res Notes. 2009;67 2.
[9] Sanchez-Ferrer A, Rodriguez-Lopez JN, Garcia-Canovas G, Garcia-Camona V. Biochimica et Biophysica Acta – Protein Struct Mol Enzymol 1995;1247:1.
[10] Kalyani DC, Munk L, Mikkelsen JD, Meyer AS. RSC Adv 2016;6:3910.
[11] Demarche P, Junghanns C, Nair RR, Agathos SN. Biotechnol Adv 2012;30:933.
[12] Zhao H. J Chem Technol Biotechnol 2010;85:891.
[13] Zhang Y, Ge J, Liu Z. ACS Catal 2015;5:4503.
[14] Iyer PV, Ananthanarayan L. Process Biochem 2008;43:1019.
[15] Bilal M, Iqbal HMN, Guo S, Hu H, Wang W, Zhang X. Int J Biol Macromol 2018;108:893.
[16] Krajewska B, Zaborska W, Leszko M. J Mol Catal B: Enzym 1997;3:231.
[17] Ba S, Arsenault A, Hassani T, Jones JP, Cabana H. Crit Rev Biotechnol 2013;33:404.
[18] Mateo C, Abian O, Bernedo M, Cuenca E, Fuentes M, Fernandez-Lorente G, et al. Enzyme Microb Technol 2005;37:456.
[19] Barbosa O, Torres R, Ortiz C, Berenguer-Murcia A, Rodrigues RC, Fernandez-Lafuente R. Biomacromolecules 2013;14:2433.
[20] Mateo C, Grazu V, Palomo JM, Lopez-Gallego F, Fernandez-Lafuente R, Guisan JM. Nat Protoc 2007;2:1022.
[21] Rao M, Scelza R, Acevedo F, Diez MC, Gianfreda L. Chemosphere 2014;107:145.
[22] Bilal M, Asgher M, Parra-Saldivar R, Hu H, Wang W, Zhang X, et al. Sci Total Environ 2017;576:646.
[23] Ba S, Haroune L, Cruz-Morato C, Jacquet C, Touahar IE, Bellenger JP, et al. Sci Total Environ 2014;487:748.
[24] Cha J, Kim T, Choi J, Jang K, Khaleda L, Kim W, et al. J Agric Food Chem 2017;65:1167.
[25] Bronikowski A, Hagedoorn PL, Koschorreck K, Urlacher VB. AMB Express 2017;73:1.
[26] Abdel-Hamind AM, Solbiati JO, Cann IKO. Adv Appl Microbiol 2013;82:1.
[27] Giardina P, Faraco V, Pezzella C, Piscitelli A, Vanhulle S, Sannia G. Cell Mol Life Sci 2010;67:369.
[28] Mogharabi M, Faramarzi MA. Adv Synthesis Catal 2014;356:897.
[29] Le TT, Murugesan K, Lee CS, Vu CH, Chang YS, Jeon JK. Bioresour Technol 2016;216:203.
[30] Barrios-Estrada C, Rostro-Alanis MJ, Parra AL, Belleville MP, Sanchez-Marcano J, Iqbal HMN, et al. Int J Biol Macromol 2018;108:837.
[31] Tagger S, Perissol C, Gil G, Vogt G, Le Petit J. Enzyme Microb Technol 1998;23:372.
[32] Fukuda T, Uchida H, Suzuki M, Miyamoto H, Morinaga H, Nawata H, et al. J Chem Technol Biotechnol 2004;79:1212.
[33] Yang J, Lin Y, Yang X, Ng TB, Ye X, Lin J. J Hazard Mater 2016;322:525.
[34] Olivares C, Solano F. Pigment Cell Melanoma Res 2009;22:750.
[35] Selinheimo E, NiEidhin D, Steffensen C, Nielsen J, Lomascolo A, Halaouli S, et al. J Australas Biotechnol 2007;130:471.
[36] Land CA, Ramsden PA, Riley PA. Acc Chem Res 2003;36:300.
[37] Shuster V, Fishman A. J Mol Microbiol Biotechnol 2009;17:188.
[38] Faccio G, Kruus K, Saloheimo M, Thöny-Meyer L. Process Biochem 2012;47:1749.
[39] Ihekata K, Nicell JA. Bioresour Technol 2000;74:191.

[40] Munjal N, Sawhney SK. Enzyme Microb Technol 2002;30:613.
[41] Blodig W, Smith AT, Doyle WA, Piontek K. J Mol Biol 2001;305:851.
[42] Wong DWS. Appl Biochem Biotechnol 2009;157:174.
[43] Valli K, Wariishi H, Gold MH. Biochemistry 1990;29:8535.
[44] Tien M, Kirt TK. Science 1983;221:661.
[45] Shaheen R, Asgher M, Hussain F, Bhatti HN. Int J Biol Macromol 2017;103:57.
[46] Glenn JK, Akileswaran L, Gold MH. Arch Biochem Biophys 1986;251:688.
[47] Hofrichter M. Enzyme Microb Technol 2002;30:454.
[48] Glenn JK, Gold MH. Arch Biochem Biophys 1985;242:329.
[49] Bonnarme P, Jeffries TW. Appl Environ Microbiol 1990;56:210–7.
[50] Yehia RS, Rodriguez-Couto S. Appl Biochem Microbiol 2017;53:222.
[51] Veitch NC. Phytochemistry 2004;65:249.
[52] Haschke RH, Friedhoff JM. Biochem Biophys Res Commun 1978;80:1039.
[53] Shigeoka S, Ishikawa T, Tamoi M, Miyagawa Y, Takeda T, Yabuta Y, et al. J Exp Biol 2002;53:1305.
[54] Bilal M, Rasheed T, Iqbal HMN, Hu H, Wang W, Zhang X. Int J Biol Macromol 2018; 113:983.
[55] Bilal M, Iqbal HMN, Shah SZH, Hu H, Wang W, Zhang X. J Environ Manage 2016; 183:836.
[56] Bilal M, Asgher M, Iqbal HMN, Hu H, Wang W, Zhang X. Int J Biol Macromol 2017; 102:582.
[57] Bilal M, Rasheed T, Iqbal HMN, Hu H, Wang W, Zhang X. Int J Biol Macromol 2017; 105:328.
[58] Chattopadhyay K, Mazumdar S. Biochemistry 2000;39:263.
[59] Jesionowski T, Zdarta J, Krajewska B. Adsorption 2014;20:801.
[60] Garcia-Galan C, Berenguer-Murcia A, Fernandez-Lafuente R, Rodrigues RC. Adv Synthesis Catal 2011;353:2885.
[61] Dicosimo R, McAuliffe J, Poulose AJ, Bohlmann G. Chem Soc Rev 2013;42:6437.
[62] Reetz MT. J Am Chem Soc 2013;135:12480.
[63] Adlercreutz P. Chem Soc Rev 2013;42:6406.
[64] Guzik U, Hupert-Kocurek K, Wojcieszynska D. Molecules 2014;19:8995.
[65] Krasnan V, Stloukal R, Rosenberg M, Rebroš M. Appl Microbiol Biotechnol 2016; 100:2535.
[66] Spahn C, Minteer SD. Recent Patents Eng 2008;2:195.
[67] Hernandez K, Fernandez-Lafuente R. Enzyme Microb Technol 2011;48:107.
[68] Mateo C, Palomo JM, Fernandez-Lorente G, Guisan JM, Fernandez-Lafuente R. Enzyme Microb Technol 2007;40:1451.
[69] Cao L. Curr Opin Chem Biol 2005;9:217.
[70] Brady D, Jordaan J. Biotechnol Lett 2009;31:1639.
[71] Sheldon RA. Adv Synthesis Catal 2007;349:1289.
[72] Sheldon RA. Org Process Res Dev 2011;15:213.
[73] Mukherjee S, Basak B, Bhunia B, Dey A, Mondal B. Rev Environ Sci Bio/Technol 2013;12:61.
[74] Ba S, Kumar VV. Crit Rev Biotechnol 2017;37:819.
[75] Zhang J, Liu X, Xu Z, Chen H, Yang Y. Int Biodeter Biodegr 2008;61:351.
[76] Zheng F, Cui BK, Wu XJ, Meng G, Liu HX, Si J. Int Biodeter Biodegr 2016;110:69.
[77] Ran Y, Zhifeiche X, Chen W. Appl Mech Mater 2012;138–139:1067.
[78] Sofia P, Asgher M, Shahid M, Randhawa MA. J Anim Plant Sci 2016;26:1451.
[79] Jaiswal N, Pandey VP, Dwived UN. Int J Biol Macromol 2016;86:288.
[80] Bilal M, Asgher M. BMC Biotechnol 2015;15:111.
[81] Romanovskaya II, Shesterenko YA, Sevastyanov OA, Brusilovskii IE. J Water Chem Technol 2010;32:61.
[82] Roy S, Das I, Munjal M, Karthik L, Kumar G, Kumar S, et al. Front Biol 2014;9:306.
[83] Narayanan PM, Murugan S, Eva AS, Devina SU, Kalidass S. Res J Microbiol 2015;10: 421.
[84] Kampmann M, Boll S, Kossuch J, Bielecki J, Uhl S, Kleiner B, et al. Water Res 2014; 57:295.
[85] Kampmann M, Hoffrichter AC, Stalinski D, Wichmann R. J Mol Catal B: Enzym 2015;116:124.
[86] Usluoglu A, Arabaci G. Res J Chem Environ 2013;17:16.
[87] Spasojević D, Prokopijevic M, Prodanović O, Pirtea MG, Radotić K, Prodanović R. Hemijska Industrija 2014;68:117.
[88] Daassi D, Rodríguez-Couto S, Nasri M, Mechichi T. Int Biodeter Biodegr 2014;90:71.
[89] Sanlier SH, Gider S, Köprülü A. Artificial Cells Nanomed Australas Biotechnol 2013; 41:259.
[90] Kocaturk S, Yagar H. Artificial Cells Blood Substitut Biotechnol 2010;38:157.
[91] Phetsom J, Khammuang S, Suwannawong P, Sarnthima R. J Biol Sci 2009;9:573.
[92] Loncar N, Božić N, Anđelković I, Milovanović A, Dojnov B, Vujčić M, et al. J Serb Chem Soc 2011;76:513.
[93] Firooz NS, Panahi R, Mokhtarani B, Yazdani F. Cellul 2017;24:1407.
[94] Sathishkumar P, Kamala-Kannan S, Cho M, Kim JS, Hadibarata T, Salim MR, et al. J Mol Catal B: Enzym 2014;100:111.
[95] Arica MY. Polymer Int 2000;49:775.
[96] Cienska M, Labus K, Lewańczuk M, Koźlecki T, Liesiene J, Bryjak J. PLoS One 2016;11:1.
[97] Gioia L, Rodriguez-Couto S, del Pilar MM, Manta C, Ovsejevi K. Biotechnol Appl Biochem 2014;87:502.
[98] Jadhav SW, Singhal RS. Int Biodeter Biodegr 2013;85:271.
[99] Cristovao RO, Silverio SC, Tavares APM, Brigida AIS, Loureiro JM, Boaventura RAR, et al. World J Microbiol Biotechnol 2012;28:2827.
[100] Rodrıguez-deLuna SE, Moreno-Cortez IE, Garza-Navarro MA, Lucio-Porto R, Pavon LL, Gonzalez-Gonzalez VA. J Appl Polym Sci 2017;134:1.
[101] Stloukal R, Watzková J, Gregušová B. Chem Papers 2014;68:1514.
[102] Chhabra M, Mishra S, Sreekrishnan TR. J Environ Health Sci Eng 2015;13:38.
[103] Gassara F, Brar SK, Verma M, Tyagi RD. Chemosphere 2013;92:1356.
[104] Nicolucci C, Rossi S, Menale C, Godjevargova T, Ivanov Y, Bianco M, et al. Biodegradation 2011;22:673.
[105] Shesterenko YA, Sevastyanov OV, Romanovskaya II. J Water Chem Technol 2012; 34:107.
[106] Dogan T, Bayram E, Uzun L, Senel S, Denizli A. J Appl Polym Sci 2015;132:1.
[107] Misra N, Kumar V, Goel NK, Varshney L. Polymer 2014;55:6017.
[108] Burton SG, Boshoff A, Edwards W, Rose PD. J Mol Catal B: Enzym 1998;5:411.
[109] Peralta-Zamora P, Gomes de Moraes S, Esposito E, Antunes R, Reyes J, Durán N. Environ Technol 1998;19:521.
[110] Satoh E, Tamura A, Kawagoe J, Ichimura Y, Nishi K, Yamada K. Kobunshi Ronbunsyu 2008;65:104.
[111] Li Z, Shang W, Liu W, Li H. Desalination Water Treatment 2014;52:2594.
[112] Gombotz WR, Wee SF. Adv Drug Deliv Rev 1998;31:267.
[113] Lee KY, Mooney DJ. Prog Polym Sci 2012;37:106.
[114] Feng Q, Hou D, Zhao Y, Xu T, Menkhaus TJ, Fong H. ACS Appl Mater Interfaces 2014; 6:20958.
[115] Makas YG, Kalkan NA, Aksoy S, Altinok H, Nesrin NH. J Biotechnol 2010;148:216.
[116] Thielemann JP, Girgsdies F, Schlögl R, Hess C. Beilstein J Nanotechnol 2011;2:110.
[117] Bapat G, Labade C, Chaudhari A, Zinjarde S. Adv Colloid Interface Sci 2016;237:1.
[118] Carlsson N, Gustafsson H, Thörn C, Olsson L, Holmberg K, Åkerman B. Adv Colloid Interface Sci 2014;205:339.
[119] Zucca P, Sanjust E. Molecules 2014;19:14139.
[120] Bautista LF, Morales G, Sanz R. Bioresour Technol 2010;101:8541.
[121] Dehghanifard E, Jafari AJ, Kalantary RR, Mahvi AH, Faramarzi MA, Esrafili A. Iran J Environ Health Sci Eng 2013;10:25.
[122] Hu Z, Xu L, Wen X. J Environ Sci 2012;25:181.
[123] Debaste F, Songulashvili G, Penninckx MJ. Desalination Water Treatment 2014;52: 2344.
[124] Nair RP, Demarche P, Agathos SN. N Biotechnol 2013;30:814.
[125] Xu LQ, Wen XH, Ding HJ. Environ Sci 2010;31:2493.
[126] McHedlishvili NI, Pruidze GN, Omiadze NT, Zukhbaya RV. Prikladnaya Biokhimiyai Mikrobiologiya 2000;36:141.
[127] Hommes G, Gasser CA, Howald CB, Goers R, Schlosser D, Shahgaldian P, et al. Bioresour Technol 2012;115:8.
[128] Qiu L, Huang Z. World J Microbiol Biotechnol 2010;26:775.
[129] Songulashvili G, Jimenez-Tobon GA, Jaspers C, Penninckx MJ. Fungal Biol 2012;116: 883.
[130] Seetharam GB, Saville BA. Water Res 2003;37:436.
[131] Sani S, Muhid MNM, Hamdan H. J Sol-Gel Sci Technol 2011;59:7.
[132] Bayramoglu G, Akbulut A, Arica MY. J Hazard Mater 2013;244-245:528.
[133] Hou J, Dong G, Ye Y, Chenn V. J Membr Sci 2014;452:229.
[134] Mohajershojaei K, Mahmoodi NM, Khosravi A. Biotechnol Bioprocess Eng 2015;20: 109.
[135] Zhang Y, Wu H, Huang X, Zhang J, Guo S. Nanoscale Res Lett 2011;6:450.
[136] Singh N, Basu S, Vankelecom IFJ, Balakrishna M. Appl Biochem Biotechnol 2015; 177:76.
[137] Abadulla E, Tzanov T, Costa S, Robra KH, Cavaco-Paulo A, Gubitz GM. Appl Environ Microbiol 2000;66:3357.
[138] Balaji N, Kumar KS, Seenuvasan M, Vinodhini G, Kumar MA. J Environ Biol 2016;37: 1489.
[139] Chao C, Liu J, Wang J, Zhang Y, Zhang B, Zhang Y, et al. ACS Appl Mater Interfaces 2013;5:10559.
[140] Sekuljica N, Prlainovic ZZ, Jovanovic JR, Stefanovic AB, Djokic VR, Mijin DZ, et al. Bioprocess Biosyst Eng 2016;39:461.
[141] Acevedo F, Pizzul L, MdP Castillo, González ME, Cea M, Gianfreda L, et al. Chemosphere 2010;80:271.
[142] Cheng J, Yu SM, Zuo P. Water Res 2006;40:283.
[143] S.F. Oliveira, J.M. Rodrigues da Luz, M.C.M. Kasuya, L.O. Ladeira and A.C. Junior, *Saudi J Biol Sci*, https://doi.org/10.1016/j.sjbs.2016.02.018.
[144] Othman AM, Gonzalez-Dominguez E, Sanroman A, Correa-Duartec M, Moldes D. RSC Adv 2016;6:114690.
[145] Subrizi F, Crucianelli M, Grossi V, Passacantando M, Pesci L, Saladino R. ACS Catal 2014;4:810.
[146] Lu YM, Yang QY, Wang LM, Zhang MZ, Guo WQ, Ca ZN, et al. Clean – Soil Air Water 2017;45:1600077.
[147] Ramírez-Montoya LA, Hernández-Montoya V, Montes-Morán MA, Jáuregui-Rincón J, Cervantes FJ. J Mol Liquids 2015;212:30.
[148] Pang R, Li M, Zhang C. Talanta 2015;131:38.
[149] Champagne PP, Ramsay JA. Bioresour Technol 2010;101:2230.
[150] Qiu H, Li Y, Ji G, Zhou G, Huang X, Qu Y, et al. Bioresour Technol 2009;100:3837.
[151] Lvov Y, Aerov A, Fakhrullin R. Adv Colloid Interface Sci 2014;207:189.
[152] Daoud FBO, Kaddour S, Sadoun T. Colloid Surfaces B: Biointerfaces 2010;75:93.
[153] Zhang C, Luo S, Chen W. Talanta 2013;113:142.
[154] Delvaux M, Demoustier-Champagne S. Biosens Bioelectron 2003;18:943.
[155] Ge J, Lei J, Zare RN. Nat Nanotechnol 2012;7:428.
[156] Sun H, Jin X, Long N, Zhang R. Int J Biol Macromol 2017;95:1049.
[157] Li ZL, Cheng L, Zhang LW, Liu W, Ma WQ, Liu L. Process Safety Environ Protect 2017;107:463.
[158] Lin J, Lai Q, Liu Y, Chen S, Le X, Zhou X. Int J Biol Macromol 2017;102:144.
[159] Wang Y, Chen X, Liu J, He F, Wang R. Environ Sci Pollut Res 2013;20:6222.
[160] Huan W, Yang Y, Wu B, Yuan H, Zhang Y. Chin J Chem 2012;30:2849.
[161] Wang F, Hu Y, Guo C, Huang W, Liu CZ. Bioresour Technol 2012;110:120.
[162] Yang Y, Wei Q, Zhang J, Xi Y, Yuan H, Chen C, et al. Biochem Eng J 2015;97:111.
[163] Chang Q, Jiang G, Tang H, Li N, Huang J, Wu L. Chin J Catal 2015;36:961.
[164] Liu Y, Zeng Z, Zeng G, Tang L, Pang Y, Li Z, et al. Bioresour Technol 2012;115:21.
[165] Aydemir T, Guler S. Artificial Cells Nanomed Biotechnol 2015;43:425.
[166] Peniche H, Osorio A, Acosta N, de la Campa A, Peniche C. J Appl Polym Sci 2005;98: 651.

[167] Abdollahi K, Yazdani F, Panahi R. Int J Biol Macromol 2017;94:396.
[168] Shao J, Ge H, Yang Y. Biotechnol Lett 2007;29:901.
[169] Luan PP, Jiang YJ, Zhang SP, Gao J, Su ZG, Ma GH, et al. J Biosci Bioeng 2014;118:575.
[170] Lin J, Fan L, Miao R, Le X, Chen S, Zhou X. Int J Biol Macromol 2015;78:1.
[171] Dincer A, Becerik S, Aydemir T. Int J Biol Macromol 2012;50:815.
[172] Sadighi A, Faramarzi MA. J Taiwan Inst Chem Eng 2013;44:156.
[173] Sun H, Yang H, Huang W, Zhang S. J Colloid Interface Sci 2015;450:353.
[174] Ispas CR, Ravalli MT, Steere A, Andreescu S. Water Res 2010;11:1961.
[175] Le TT, Murugesan K, Lee CS, Vu CH, Chang YS, Jeon JR. Bioresour Technol 2016;216:203.
[176] Shao J, Huang LL, Yang YM. J Chem Technol Biotechnol 2009;84:633.
[177] Koklukaya SZ, Sezer S, Aksoy S, Hasirci N. Biotechnol Appl Biochem 2016;32:699.
[178] Bilal M, Asgher I. Chem Central J 2015;9 (Article number 47).
[179] Maryskova M, Ardao I, García-Gonzalez CA, Martinova L, Rotkova J, Sevcu A. Enzyme Microb Technol 2016;89:31.
[180] Celikbicak O, Bayramoglu G, Yilmaz M, Ersoy G, Bicak N, Salih B, et al. Microporous Mesoporous Mater 2014;199:57.
[181] Xu R, Si Y, Wu X, Li F, Zhang B. Chem Eng J 2015;255:63.
[182] Ormategui N, Veloso A, Leal GP, Rodriguez-Couto S, Tomovska R. ACS Appl Mater Interfaces 2015;7:14104.
[183] Huang J, Xiao H, Li B, Wang J, Jiang D. Biotechnol Appl Biochem 2006;44:93.
[184] Bayramoglu G, Yilmaz M, Arica MY. Bioresour Technol 2010;101:6615.
[185] Liu Y, Yan M, Geng Y, Huang J. Appl Sci 2016;6:232.
[186] Pan C, Ding R, Dong L, Wang J, Hu Y. J Nanomater 2015;2015 (Article number 47).
[187] Sathishkumar P, Chae JC, Unnithan AR, Palvannan T, Kim HY, Lee KJ, et al. Enzyme Microb Technol 2012;51:113.
[188] Bilal M, Asgher M, Iqbal HM. Protein Pept Lett 2016;23:812.
[189] Uygun M. J Chem 2013;2013:387181.
[190] Rojas-Melgarejo F, Rodriguez-Lopez JN, Garcia-Canovas F, Garcia-Ruiz PA. Carbohydr Polym 2004;58:79–88.
[191] Nashar RME. Talanta 2012;96:161.
[192] Shang CY, Li WX, Zhang RF. Mater Res Bull 2015;68:336.
[193] Gouveia S, Fernández-Costas C, Sanromán MA, Moldes D. Bioresour Technol 2012;121:131.
[194] Baldrian P. Fungal laccases – occurrence and properties. FEMS Microbiol Rev 2006;30:215.
[195] Willner I, Yan YM, Willner B, Tel-Vered R. Fuel Cells 2009;9:7.
[196] Kumar S, Jana AK, Dhamija I, Singla Y, Maiti M. Eur J Pharm Biopharm 2013;85:413.
[197] Ortner A, Huber D, Haske-Cornelius O, Weber HK, Hofer K, Bauer W, et al. Process Biochem 2015;50:1277.

Biotechnology Advances 37 (2019) 107401

Contents lists available at ScienceDirect

Biotechnology Advances

journal homepage: www.elsevier.com/locate/biotechadv

Research review paper

Multi-faceted strategy based on enzyme immobilization with reactant adsorption and membrane technology for biocatalytic removal of pollutants: A critical review

Jakub Zdarta[a,c,*], Anne S. Meyer[b], Teofil Jesionowski[a], Manuel Pinelo[c]

[a] Institute of Chemical Technology and Engineering, Faculty of Chemical Technology, Poznan University of Technology, Berdychowo 4, PL-60965 Poznan, Poland
[b] Department of Biotechnology and Biomedicine, Technical University of Denmark, Soltofts Plads 224, DK-2800 Kgs. Lyngby, Denmark
[c] Department of Chemical and Biochemical Engineering, Center for BioProcess Engineering, Technical University of Denmark, Soltofts Plads 229, DK-2800 Kgs. Lyngby, Denmark

ARTICLE INFO

Keywords:
Oxidoreductases
Enzyme immobilization
Support materials
Hazardous pollutants removal
Pharmaceuticals
Enzymatic biodegradation
Enzymatic adsorption
Enzymatic bioreactors
Enzymatic membrane reactors

ABSTRACT

In the modern era, the use of sustainable, environmentally friendly alternatives for removal of recalcitrant pollutants in streams resulting from industrial processes is of key importance. In this context, biodegradation of phenolic compounds, pharmaceuticals and dyes in wastewater by using oxidoreductases offers numerous benefits. Tremendous research efforts have been made to develop novel, hybrid strategies for simultaneous immobilization of oxidoreductase and removal of toxic compounds. The use of support materials with the options for combining enzyme immobilization with adsorption technology focused on phenolic pollutants and products of biocatalytic conversion seems to be of particular interest. Application of enzymatic reactors based on immobilized oxidoreductases for coupling enzyme-aided degradation and membrane separation also attract still growing attention. However, prior selection of the most suitable support/sorbent material and/or membrane as well as operational mode and immobilization technique is required in order to achieve high removal efficiency. Thus, in the framework of this review, we present an overview of the impact of support/sorbent material on the catalytic properties of immobilized enzymes and sorption of pollutants as well as parameters of membranes for effective bioconversion and separation. Finally, future perspectives of the use of processes combining enzyme immobilization and sorption technology as well as application of enzymatic reactors for removal of environmental pollutants are discussed.

1. Introduction

The total amount of active pharmaceutical ingredients used in the medicine has exceeded 100,000 tons per year (Weber et al., 2016). This number includes antibiotics, anti-inflammatory drugs, pain killers and contraceptive hormones, and it is known that many of these substances are introduced into the environment (Kümmerer, 2009). Another group of pollutants includes dyes, colorants and pigments which are used in various industrial sectors, such as textiles, food and other consumer goods, in the amount of approx. 10^5 tons per year (Vikrant et al., 2018) and are also commonly released into the environment. Consequently, the risk of water pollution with such compounds is high and there are no signs that this problem is decreasing. The reported values of specific phenolic compounds, pharmaceuticals and dyes in aqueous environmental systems such as hospital wastewaters, industrial effluents, surface water, ground water and even seawater are scarce, but usually are within the range from ng/L to μg/L for pharmaceuticals (Heberer, 2002; Cruz-Morato et al., 2014) and to mg/L and even g/L for dyes (Li et al., 2017; Vikrant et al., 2018), with large variations depending on the type of substance, type of effluent and sampling places as well as the type of the water reservoir (ground water, surface waters or wastewaters) which contributes to a global scale of the problem (Table 1). These pollutants may negatively affect living organisms as well as the ecosystem, thus there is a need to remove them from the environment in order to ensure a healthier and more sustainable development (Lonappan et al., 2016; Rasheed et al., 2019). Data regarding the type, structure and level of the selected examples of pharmaceutical environmental pollutants collected from various reports was presented in Table 1.

Despite their highly diverse uses, the chemical structures of phenols, dyes and pigments as well as some key antibiotics, pain kilers and contraceptive hormones are similar in the sense that the majority of compounds, but not all, contain a phenolic group in their chemical

* Corresponding author.
E-mail address: jakub.zdarta@put.poznan.pl (J. Zdarta).

https://doi.org/10.1016/j.biotechadv.2019.05.007
Received 29 November 2018; Received in revised form 29 April 2019; Accepted 20 May 2019
Available online 22 May 2019

Table 1
Selected examples of the various types of pharmaceutical environmental pollutants[a].

Type Compound	Base chemical structure[a]	Levels reported in environment	References
Antibiotics	Example: Tetracyclin 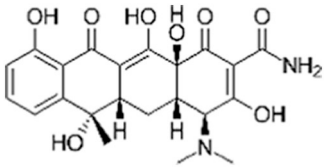	Wastewaters: 280–540 ng/L Ground waters: 4.4–9.3 ng/L Surface waters: 5.7–8.7 ng/L	(Javid et al., 2016)
Pain killers	Example: Paracetamol 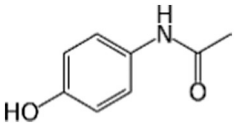	Wastewaters: 120–900 μg/L Ground waters: 4.4/–30 ng/L Surface waters: 0.3–4.5 μg/L	(Cruz-Morato et al., 2014; Sousa et al., 2016; Rivera-Jaimes et al., 2017)
Antidepressants	Example: Carbamazepine 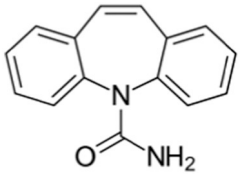	Wastewaters: 0.5 μg/L Ground waters: N/A Surface waters: up to 1.8 μg/L	(Cruz-Morato et al., 2014, Sousa et al., 2016)
Anti-inflammatories	Example: Naproxen 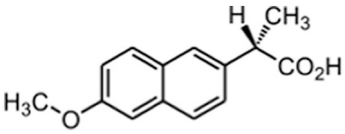	Wastewaters: 13 μg/L Ground waters: N/A Surface waters: up to 1.6 μg/L	(Cruz-Morato et al., 2014, Sousa et al., 2016)
Contraceptive hormones/ estrogenes	Example: Estradiol 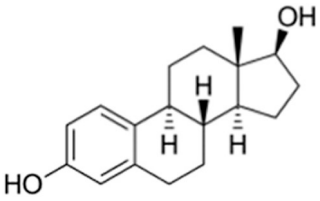	Wastewaters: 6.2–42.2 ng/L Ground waters: 2.5 ng/L Surface waters: 1–22 ng/L	(Adeel et al., 2017)

N/A – not available

[a] Several other pharmaceuticals *do not* contain a phenolic group, but some of their impurities do e.g. *p*-salicylic acid and 4-hydroxy iso-phthalic acid, which are impurities of acetylsalicylic acid (aspirin). No immediate data are available on their occurrence in the environment.

structure (Anku et al., 2017). As discussed below, phenolic compounds and non-phenolic pharmaceuticals are target substrates for several natural enzymes, which is why enzymatic conversion can be crucial for the removal of these diverse compounds from the environment (Ba and Kumar, 2017). Biodegradation with the use of enzymes seems to be a promising strategy to control the level of dyes as well as pharmaceutical pollutants and their derivatives in waters and soils, mainly because enzymes are characterized by distinct selectivity and can catalyze targeted conversion reactions. Inspection of the discussed data infers that the reduction of the quantities of pharmaceutical residue compounds present in the environment, particularly in wastewaters, is an important environmental challenge (Ba et al., 2013; Barrios-Estrada et al., 2018a; Zdarta et al., 2018a). However, it should be clearly stated that enzymes cannot be used for detoxification of raw wastewater due to the high content of organic and inorganic substances, which should be treated before the recalcitrant phenols or pharmaceuticals. Thus, only properly pretreated wastewater, without interferents and lower concentration of pollutants, can be treated by oxidoreductases in order to remove toxic compounds.

Enzymes which belong to the oxidoreductase class (EC 1.x.x.x, where 1 denotes type of the catalytic group and type of catalyzed reaction [redox - oxidation/reduction reactions for oxidoreductases], the second and the third x denote the enzyme's sub-class and sub-sub-class, respectively, and describe the reaction with respect to the compound, group, bond or product involved in the process, and the final x indicates the position in the sub-sub class and denotes specific metabolites and cofactors involved), such as tyrosinases, laccases and peroxidases (Table 2) are increasingly investigated as green biocatalysts for the removal of hazardous compounds, including phenol and its derivatives, synthetic and natural dyes, pharmaceuticals and even hormones (Cabana et al., 2009a, 2009b; Bilal et al., 2017a; Skoronski et al., 2017; Bilal et al., 2019a; Costa et al., 2019). The oxidoreductases are generally known for their high specificity constants, however, they vary depending on the type of enzyme, its origin and type of the substrate (Baldrian, 2005). This means that these enzymes can not only efficiently convert the above-mentioned compounds, but also exhibit high affinity to the pollutants. This is particularly important due to the low concentrations of phenols and their derivatives in wastewater. Notably,

Table 2
Oxidoreductase enzymes most frequently used for environmental applications and their selected properties.

Enzyme name	EC number	Sources	Main substrates	pH and temperature optimum	References
Laccase (Lac)	1.10.3.2	Fungi, bacteria, plants	Monophenols, diphenols, polyphenols, diamines, aromatic amines, N-heterocycles, phenothiazines	pH 3.5–5 temp. 20–25 °C	(Faccio et al., 2012, Senthivelan et al., 2016)
Tyrosinase (Tyr)	1.14.18.1	Fungi, bacteria, plants, insects and mammalian issues	Phenol, monophenols, bisphenols, multi-substituted phenol derivatives, including chloro- and nitrophenols	pH 5.5–8 temp. 30–40 °C	(Ihekata and Nicell, 2000, Tonin et al., 2016)
Horseradish peroxidase (HRP)	1.11.1.7	Roots of horseradish	Phenolic acids, aromatic phenols and their derivatives, non-aromatic amines, indoles	pH 7 temp. 25–40 °C	(Bilal et al., 2017b, Bilal et al., 2018b)
Lignin peroxidase (LiP)	1.11.1.14	White-rot fungi and microorganisms	Aromatic phenolic and non-phenolic compounds, xenobiotics with redox potential up to 1.4 V	pH around 3 temp. 35–45 °C	(Valli et al., 1990, Shaheen et al., 2017)
Manganese peroxidase (MnP)	1.11.1.13	White-rot fungi and bacteria	Dyes, monomeric and dimeric phenols	pH around 4 temp. 30–40 °C	(Bilal et al., 2017c, 2017d, Yehia and Rodriguez-Couto, 2017)

laccases (EC 1.10.3.2, where 10 denotes acting on diphenols and related substances as donors, 3 denotes reaction with oxygen as acceptor and 2 indicates second place in this sub-sub group), which are produced by both fungi and bacteria, can catalyse the conversion and hence "destruction" of many of the above-mentioned compounds *via* their ability to catalyse the oxidation of phenolic OH-groups during the reduction of oxygen to water (Lloret et al., 2013a, 2013b, 2013c; Tavares et al., 2017). The main substrates of the laccases include monophenols, polyphenols, methoxy-substituted phenols as well as aromatic amines and diamines. On the other hand, tyrosinases (EC 1.14.18.1, where 14 denotes acting on paired donors, with incorporation or reduction of molecular oxygen, 17 indicates acting with another compound as one donor, and incorporation of one atom of oxygen and 1 indicates first place in this sub-sub group) possess the narrowest substrate specificity. They are mainly active in case of phenols and catechols, if they do not bear electron-withdrawing substituents and O_2 molecules required for catalytic action. However, their mechanism is different compared to that observed for laccases. The oxidation process catalysed by tyrosinases generates ortho-quinones (Land et al., 2003), whereas the conversion with the use of laccases generates mainly reactive phenoxy radicals as intermediate products (Bronikowski et al., 2017). Regardless, oligomers and polymers are formed as the products of the oxidation of phenolic compounds in case of both enzymes. On the other hand, horseradish peroxidase (EC 1.11.1.7), manganese peroxidase (EC 1.11.1.13), and lignin peroxidase (EC 1.11.1.14) where 11 denotes acting on a peroxide as a separate acceptor, 1 denotes use of peroxides as substrates and 7, 13 and 14 indicate the place of these enzymes in the sub-sub group, are characterized by different substrate specificity. These enzymes exhibit activity towards phenolics, aromatic amines and also non-phenolic compounds with various efficiency and require hydrogen peroxide which is reduced to water during the catalytic conversion of phenolic compounds. For instance, horseradish peroxidase is a heme-containing enzyme which catalyses the oxidation of phenolic acids, aromatic phenols and non-aromatic amines. Manganese peroxidase can catalyse the oxidation of a wide spectrum of phenolic compounds, different mono- and dimeric phenols, and even dyes. Meanwhile, lignin peroxidase oxidizes a wide range of aromatic phenolic and non-phenolic compounds as well as other organic substances, such as xenobiotics (Bilal et al., 2019b). Nevertheless all of the above-mentioned biocatalysts possess a high biotechnological potential and several reports confirm their ability to catalyse the oxidation of a wide range of hazardous environmental pollutants (Nicolucci et al., 2011; Mukherjee et al., 2013; Le et al., 2016; Bilal et al., 2018a).

However, in order to efficiently exploit enzymes for such purposes – involving low but significant concentrations of the problematic pollutants in aqueous ecosystems – high efficiency and robustness of the enzymatic reaction systems are of key importance. As it was previously mentioned, the concentration of the pharmaceuticals in wastewaters usually does not exceed several μg/L (Table 1) which affects the enzymatic kinetics and conversion rates. In order to enhance the removal efficiencies of phenolic compounds by oxidoreductases, various mediators can be used (Husain and Husain, 2008). There are two possible mechanisms of action of mediators. They may act as electron transfer agents between the oxidoreductase and the substrate, in case of which the oxidized form of the mediator diffuses from the enzyme catalytic pocket and is able to oxidize the substrates molecules which are inaccessible or too bulky for the enzymes. On the other hand, the mediator may expand the oxidizing capability of the oxidoreductases towards oxidation of non-phenolic compounds at higher redox potential by providing alternative reaction pathways of oxidation (Munk et al., 2018). It should be mentioned that the addition of mediator agents also alters the enzymatic kinetics. However, the Michaelis–Menten kinetic model could be used to estimate the affinity of the oxidoreductases towards different mediators and reaction substrates after the addition of the mediators, and to evaluate the changes in the enzyme kinetics (Lyons, 2003). The most frequently used mediator agents include e.g.

2,2′-azino-bis(3-ethylbenzothiazoline-6-sulphonic acid) (ABTS), 1-hydroxybenzotriazole (HBT), N-hydroxyphthalimide (HPI) or 2,2,6,6-tetramethylpiperidin-1-yloxy (TEMPO). However, the selection of a suitable mediator is directly associated with the enzyme (redox potential, substrate specificity) and the type of substrate (Baiocco et al., 2006; D'Acunzo et al., 2006). Although the use of mediators affects the costs of the remediation process, their application is constantly growing over recent years due to the significant improvement of the removal efficiencies. Moreover, the use of such compounds may also significantly reduce the duration of the process which at least partially justifies the costs of the mediators.

It should also be mentioned that use of oxidoreductases has not been scaling up yet due to several obstacles. The most important issue is related e.g. to the market price of the enzymes. According to Sigma-Aldrich web page, the price of the commercially available laccase from *Trametes versicolor* is approximately equal to $1000 per 10 g, however the costs of the mushroom tyrosinase and horseradish peroxidase are higher and amount to approx. $2000 per 1 g and even $15000 per 1 g, respectively (Sigma-Aldrich, 2019a, 2019b, 2019c). Moreover, these enzymes suffer due to insufficient catalytic activity. Thus, it would not be feasible to use the commercially available biocatalysts at an industrial scale. One of the possible solutions to overcome this problem is the on-site production of enzymes and their purification to obtain highly active biocatalysts which results in a reduction of total process costs. Nevertheless, it is difficult to establish the total costs of the enzymes required for wastewater purification as they depend on several factors, such as enzyme dosage, its activity, the type of removed compounds and the required process efficiency (Liu et al., 2016). In addition, other strategies have been employed in order to improve the efficiency of enzymatic removal of hazardous pollutants. The most important one is enzyme immobilization, which significantly improves enzyme stability and reusability. Moreover, optimization of the process conditions, particularly in terms of pH and temperature, as well as the use of enzymatic reactors and recycling of enzymes should be highlighted and considered as promising to obtain high process efficiency (Østergaard et al., 2015; Aguilar et al., 2018). Enzyme immobilization facilitates the recycling and reusability of enzymes which allows to reduce the cost of the process even by up to 50% (Jørgensen and Pinelo, 2017).

A notable number of scientific and technical (engineering) reports testing novel enzyme immobilization strategies and reaction designs are available, thus indicating that bioremediation *via* enzymatic technology can be a new step forward which provides alternative strategies and materials involving e.g. adsorption technology (Hai et al., 2007; Su et al., 2016; Bilal et al., 2018c). Enzyme immobilization technology is crucial for environmental technology to maximize the reuse of enzymes in order to provide maximal biocatalytic productivity and hence lowest possible enzyme costs (Jesionowski et al., 2014; Zucca and Sanjust, 2014; Bilal and Iqbal, 2019). Immobilization of the enzymes provides long-term usability and high biological activity and effectivity of the immobilized oxidoreductases for the removal of pharmaceutical products (Zdarta et al., 2018c) and other environmentally undesirable phenolic compounds such as colorants (Ahmad et al., 2015). However, the immobilization process also possess drawbacks, e.g. its costs, required equipment as well as conformational restrictions of the immobilized enzyme which lead to a decrease of catalytic properties (Bilal et al., 2018d). In addition, there is a need to find suitable support material, characterized by operational resistance and the presence of functional moieties which facilitate stable attachment of the biomolecules. Moreover, it should be emphasized that only a proper immobilization allows for enzyme stabilization and retention of high catalytic properties by the biomolecules (Adeel et al., 2018). From this point of view, the particular interest is oriented to multipoint enzyme immobilization which may improve the enzyme activity, specificity or selectivity or even purify the enzyme (Bilal et al., 2019c, 2019d). This technique facilitates stable binding of the enzyme which reduces enzyme leakage and enhances the catalytic activity (Mateo et al., 2007). Finally, oriented immobilization contributes to the fact that immobilized biomolecules are deposited onto the surface in such way that their active sites are accessible for the substrate molecules. This is critical for the oxidoreductases, as their active site require a proper enzyme-support connection to facilitate the efficient transfer or uptake of the electrons to or from the support (Hernandez and Fernandez-Lafuente, 2011). Nevertheless, enzyme immobilization combined with substrate adsorption technology as well as the use of enzymatic bioreactors appear to be a particularly promising strategy.

Simultaneous enzymatic biodegradation with adsorption or separation enhance the removal efficiency of pollutants using oxidoreductase-based systems at an industrial and environmentally-relevant scale during bioremediation, and maximize the effectiveness of the process combinations (Martínez-Hernández et al., 2016). The combination of conversion and removal results in numerous advantages, including increased effectiveness of remediation, reduced time of the process by avoiding product accumulation and potential inhibition and, in turn, cleaner effluents; sorption is notably relevant as a new technology in such reactions due to the sorption of products of enzymatic conversion. Additionally, by means of simultaneous sorption and biodegradation, easier operational control of the process and cost reduction can be achieved, which is important for high biocatalytic productivity and thus competitive applications of immobilized enzymes (Homem and Santos, 2011).

Furthermore, precise catalysis of low substrate levels and handling of large volumes of effluents are required in order to efficiently convert and remove environmental pollutants as these compounds are usually present in dilute levels of μg/L. From this point of view, membranes-based technologies are very suitable and of particular interest. However, the use of enzymatic bioreactor systems involving immobilized enzymes has been found to work effectively rather than removal of pollutants by simple filtration, such as micro- or nanofiltration (Rondon et al., 2015). The greatest advantage of bioreactors with immobilized enzymes is the fact that biodegradation and removal processes can occur separately, simultaneously or consecutively, depending on the pollutant and the process requirements (Li et al., 2007). Moreover, through careful process control, parameters such as pH and temperature can be properly adjusted and maintained to ensure constant operational conditions (Al-Khalid and El-Naas, 2012). These facts contribute to a more effective and less expensive enzyme-catalysed biodegradation of hazardous pollutants.

In this article, we review the current state of knowledge concerning the application of simultaneous adsorption/enzymatic biodegradation processes *via* employment of enzymatic bioreactors for the removal of hazardous compounds. Various types of degradation processes, types of reactors and their operating modes which allow to achieve the highest removal efficiency, and properties of support material for enzyme immobilization for such processes are highlighted and discussed. It is also emphasized how the immobilization technique and operational parameters of the process affect the degradation of toxic compounds. Possible directions and future trends for development of advanced methods for removal of persistent pollutants by immobilized enzymes are also presented and discussed.

2. Simultaneous enzymatic biodegradation and adsorption of environmental pollutants

As it is well known, immobilized oxidoreductases are commonly used to degrade numerous hazardous pollutants present in the environment. Nevertheless, it should be emphasized, that attempts are currently made to combine biodegradation and adsorption methods in order to develop even more efficient and economically justified strategies for the degradation of hazardous compounds (Fig. 1). This solution concerns the use of the same material as support for enzyme adsorption and/or covalent immobilization, which improves the

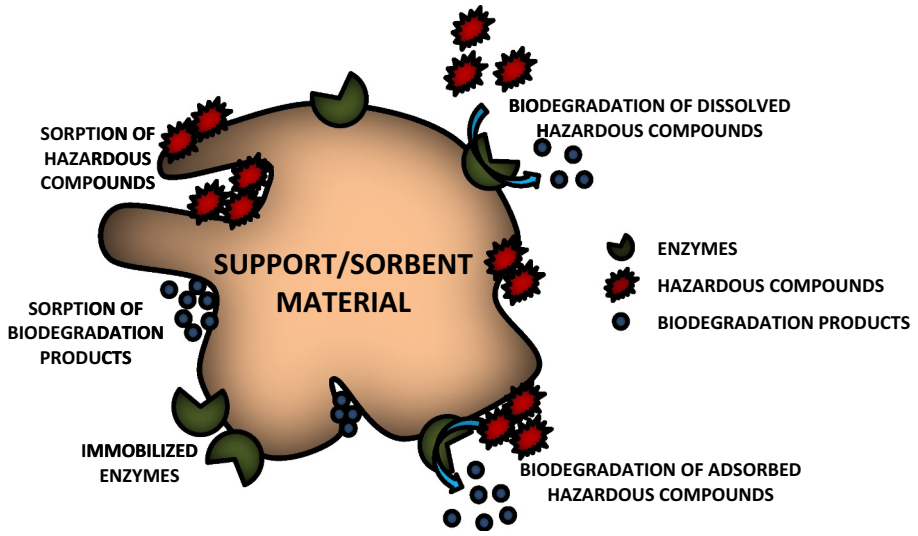

Fig. 1. Schematic diagram of simultaneous enzyme immobilization and sorption/biodegradation processes of environmental pollutants.

stability and reusability of the biocatalyst, in order to achieve higher bioconversion rates and simultaneous physical sorption of selected undesired compounds, which enhances the total removal effectivity (Antecka et al., 2018).

Although the biodegradation of hazardous compounds with the use of immobilized enzymes is generally highly efficient, it also possesses some limitations and disadvantages. First of all, due to the fact that enzymes exhibit high catalytic properties only within relatively narrow ranges of temperature and pH, incomplete removal or degradation of pollutants is observed. Moreover, the formation of oligomeric and polymeric products with high molecular weight may block the active sites of the biomolecules and thus reduce the remediation ability of the enzyme, as it has been reported in case of biodegradation of various bisphenols (Gasser et al., 2014).

In contrast, adsorption is much less sensitive to changes of the process conditions and can occurs over much wider pH and temperature ranges, even when the enzyme has lost its catalytic properties. The adsorption process is also very useful when biodegradation of a solution with a high concentration of toxic compounds is carried out. Since enzymes are highly efficient, mainly in lower concentration ranges, on the one hand high concentrations may increase conversion rates, but on the other the high quantity of pollutants extends the biodegradation time, which in turn increases the costs of the process. Adsorption strongly enhances the elimination of hazardous compounds and allows to attain high removal efficiencies at a shorter time (Chung et al., 2003). It should also be noted that adsorption of the pollutants may occur in two ways:

(i) by adsorption of the hazardous pollutants (enzyme substrate),
(ii) by adsorption of the products of enzymatic conversion (biodegradation products) (Imran et al., 2012).

In the first case, adsorption not only increases the final efficiency of the removal of toxic compounds, but also ensures the continuous supply of substrates for high enzyme activity. However, adsorption is also used for elimination of the biodegradation products. The compounds formed after enzymatic treatment are usually less toxic, but are still undesired in the reaction mixture. They can be removed by using appropriate sorbents, making the solution even more environmentally friendly (Castellana and Loffredo, 2014). It should be added that sorption processes are generally less selective than enzymatic biodegradation, which corresponds to the fact that a wider range of pollutants can be removed. However, the reusability of the support material for the immobilization of a new batch of enzyme is greatly limited by the fact that various toxic compounds are adsorbed on its surface, which causes fouling due to the affinity towards both the immobilized enzyme and pollutants to be adsorbed. Fouling of the support may lead to a significant loss of enzyme activity as well as changes in the physicochemical properties of the support. Furthermore, when pollutants are adsorbed onto the surface of the matrix, active sites of the enzyme molecules might be inhibited, which results in a decrease of enzymatic activity. In addition, fouling of the support may also negatively affect the structure of the enzyme, leading to its inactivation. In fact, fouling of the support is one of the most important reasons which limits the practical application of the simultaneous sorption/enzymatic degradation at a wider scale. Moreover, after adsorption of the pollutants, the availability of the functional groups and porosity of the support decrease and, in consequence, a decrease of sorption capacity is also observed. In this case, the regeneration of the sorbent is expensive and unfavourable in terms of practical applications. This means that the degradation parameters must be carefully controlled, which makes the process more complex and less cost-effective (Zhou and Hartmann, 2013). Nevertheless, in order to retain high catalytic properties of the immobilized enzyme and good sorption properties of the sorbent, there is a need to regenerate the support. One of the possible solution is selective desorption of the pollutant from the support material (Al-Jabari et al., 2017). In this case, the enzyme remains immobilized onto the support surface. However, this technique possess some limitations, e.g. stable enzyme-support interactions or formation of the multipoint biomolecules attachment are required to avoid enzyme leaching. Moreover, a proper eluent should be selected to remove the pollutants from the support. On the other hand, after inactivation of the immobilized enzyme, mainly due to repeated use and complete loading of the support with toxic compounds, there is a possibility to elute both the inactive enzyme and adsorbed pollutant. This solution is much easier, as compared to the previous one, however there is a risk that the use of a toxic eluent may partially damage the structure of the support/sorbent material.

The degradation of environmental pollutants by immobilized enzymes combined with adsorption process has become a subject area of interest to many research groups, particularly during the last decade. Nevertheless, we strongly believe that this approach should still be of high interest and further studies should be undertaken to develop this technique. This solution is highly effective due to the sorption of both environmental pollutants as well as products of their enzymatic conversion by the sorbent. These facts facilitate the process feasibility and result in less toxic and less polluted effluents (Shen et al., 2011). Moreover, catalytic properties of the biocatalyst are usually improved

Table 3
Materials of various origin used for simultaneous immobilization of oxidoreductases and adsorption/biodegradation of environmental pollutants.

Adsorption/ immobilization material	Enzyme	Immobilization technique	Pollutants (enzyme substrates)	Process conditions	Sorption	Degradation	Reference
					Total removal efficiency		
Alumina spherical pellets	Laccase from *Trametes villosa*	Adsorption immobilization	Reactive Black 5	pH 5, 45 °C, 24 h	79%	5% 82%	(Zille et al., 2003)
Alumina pellets	Laccase from *Trametes versicolor*	Covalent immobilization	Reactive Black 5	pH 5, 50 °C, 36 h	<10%	>90% 100%	(Osma et al., 2010)
Multi-walled carbon nanotubes	Laccase from *Trametes versicolor*	Adsorption immobilization	Bisphenol A,	pH 7, 25 °C, 24 h	9%	71% 80%	(Pang et al., 2015)
			Catechol		5%	85% 90%	
Epoxy-functionalized silica	Laccase from *Myceliophthora thermophila*	Covalent immobilization	Phenol,	pH 4.5, 25 °C, 24 h	10%	70% 80%	(Mohammadi et al., 2018)
			p-Chlorophenol		<5%	60% 60%	
Hollow mesoporous carbon spheres	Laccase from *Trametes versicolor*	Covalent immobilization	Tetracycline	pH 5, 25 °C, 3 h	77%	55% 100%	(Shao et al., 2019)
Potato dextrose agar	Laccase from *Pleurotus ostreatus*	Adsorption immobilization	Municipal landfill leachate	30 °C, 20 days	65%	15% >75%	(Loffredo et al., 2014)
Chitosan film	Tyrosinase from mushroom	Covalent immobilization	*p*-Cresol,	pH 7, 45 °C, 1 h	92%	100% 92%	(Yamada et al., 2005)
			m-Cresol,		94%	100% 94%	
			Catechol,		100%	98% 98%	
			p-Chlorophenol,		99%	100% 99%	
			m-Chlorophenol		68%	72% 70%	
Cross-linked chitosan beads	Laccase from *Trametes versicolor*	Covalent immobilization	Sulfur Blue 15,	pH 6.5, 30 °C,	20%	65% 82%	(Nguyen et al., 2016a)
			Sulfur Brown GD		20%	50% 71%	
Chitosan beads	Manganese peroxidase	Entrapment	Textile effluent	pH 4.5, 5 h	20%	90% 97%	(Bilal et al., 2016)
Polyacrylonitrile	Horseradish peroxidase	Covalent immobilization	Phenol	pH 6, 25 °C	<10%	>90% 95%	(Wang et al., 2016)
Chitosan/Fe membrane	Laccase from *Myrothecium verrucaria* I-5	Adsorption immobilization	Acid Red 73,	pH 7, 28 °C, 12 h	30%	70% 100%	(Wen et al., 2015)
			Acid Blue 113		25%	70% 95%	
Chitosan/Diaion WK-20 (cation exchange resin)	Tyrosinase	Covalent immobilization	Phenol,	pH 7, 25 °C, 2 h	100%	100% 100%	(Wada et al., 1993)
			p-Chlorophenol,		100%	100% 100%	
			p-Methoxypheno l,		100%	100% 100%	
			p-Cresol,		100%	100% 100%	
			Catechol		85%	90% 90%	
Chitosan/Diaion WK-10 beads	Tyrosinase from mushroom	Covalent immobilization	*p*-Cresol,	25 °C, 4 h	65%	98% 100%	(Tamura et al., 2010)
			4-*n*-Nonylphenol,		50%	99% 96%	
			4-*sec*-Butylphenol		60%	96% 100%	
Chitosan/alginate beads	Tyrosinase from *Agaricus bisporus*	Entrapment	Phenol	25 °C, 4 h	30%	85% 92%	(Ensuncho et al., 2005)
Cellulose/cellulose fibril/maleic anhydride	Laccase	Covalent immobilization	Chlorinated biphenyl	pH 4, 25 °C, 3 h	45%	40% 85%	(Li et al., 2017)
Polyacrylonitrile/montmorillonite/ graphene oxide nanofibers	Laccase from *Trametes versicolor*	Covalent immobilization	Catechol	pH 4, 25 °C	60%	35% 39%	(Wang et al., 2014)
Poly(vinyl alcohol)/poly(acrylic acid)/SiO_2	Horseradish peroxidase	Covalent immobilization	Paracetamol	pH 3, 25 °C, 1.5 h	15%	83% 98%	(Xu et al., 2015)
Polyvinyl alcohol/ halloysite beads	Laccase from Aspergillus sp.	Covalent immobilization	Reactive blue	pH 5, 25 °C, 8 h	16%	74% 90%	(Chao et al., 2018)
Poly(D,L-lactide-co-glycolide)/multi-walled carbon nanotubes	Laccase from *Trametes versicolor*	Encapsulation	Bisphenol A	pH 5, 25 °C, 5 h	10%	85% 95%	(Dai et al., 2016)
Poly(acrylic acid)/SiO_2 nanofibrous membranes	Laccase from white-rot fun	Covalent immobilization	Triclosan	pH 4, 30 °C, 2 h	45%	20% 65%	Xu et al., 2014
Poly(D,L-lactide-co-glycolide) /polyethylene glycol/poly(*p*-phenylene oxide) fibers	Horseradish peroxidase	Encapsulation	Pentachlorophenol	pH 3, 25 °C, 2 h	55%	30% 85%	(Niu et al., 2013)

as a result of its immobilization. Although the type of the used enzyme is associated with the environmental pollutant which should be removed, the proper selection of the support/sorbent material is the crucial step in this methodology as this material affects both enzyme immobilization and sorption processes. Thus, examples of the materials which are used for both enzyme immobilization and simultaneous adsorption of toxic compounds were presented in Table 3 (to enable clearer understanding, the sorption and biodegradation efficiencies were presented separately).

2.1. Materials used for simultaneous adsorption of pollutants and enzyme immobilization

Several different compounds of inorganic, organic and hybrid/composite origin, characterized by various morphology, porous structure and different features have been applied for simultaneous enzyme immobilization and sorption of pollutants. Selected examples of the above-mentioned materials and removed pollutants were summarized in Table 3. Nevertheless, materials used for concurrent biosorption and biodegradation processes possess some limitations and must fulfil certain criteria in order to become effective support materials for biomolecules and, at the same time, highly efficient sorbents. First of all, such materials must offer high stability and mechanical resistance under harsh reaction conditions (Zdarta et al., 2018b). Furthermore, their porous structure, including pore diameter and surface area, should grant them appreciable affinity not only for effective enzyme immobilization, but also for adsorption of hazardous compounds (Bhatnagar and Sillanpaa, 2010). Moreover, according to Loffredo and Senesi (2006), high contents of carbon and oxygen and a stable chemical structure of the sorbent also increase adsorption efficiency. However, the presence of many various functional groups on the surface of the material is the most important feature for an effective immobilization of enzymes and sorption of pollutants. This strongly enhances enzyme binding, but also determines the surface properties of the material as a sorbent (Gao et al., 2011). For instance, a significant amount of hydrophilic groups is essential for immobilized oxidoreductases, which exhibit better catalytic activity when supported using hydrophilic supports (Strong and Claus, 2011). Moreover, it should be clearly stated that improvement of enzyme stability and reusability is usually observed after providing covalent bonds between the enzyme and the support. In this case, heterofunctional supports are of particular interest which are defined as materials that possesses several different functional moieties capable to bind the protein (Barbosa et al., 2013; Rodrigues de Melo et al., 2017). Groups which facilitate the formation of the enzyme-support covalent bonds include e.g. glyoxyl, epoxy and divinyl sulfone groups. Although such functional groups might be very useful in enzyme immobilization, they possess several limitations. A two steps immobilization protocol is required for most of these strategies, in which the enzyme is immobilized by adsorption at first followed by formation of covalent interactions at alkaline pH (Santos et al., 2015). This might have negative effect on the protein structure and enzyme activity (Barbosa et al., 2014). The use of glutaraldehyde (GA) is an interesting alternative, as one the most universal and, in fact, commonly used surface modifying agents. Techniques in which GA is used are simple, efficient, relatively cheap and are among the most frequently used in enzyme immobilization. Although glutaraldehyde reacts mainly with primary amino groups in the enzyme structure, biomolecules might also be bound by reaction of GA with thiols, phenols and imidazoles moieties creating stable, single or multipoint enzyme-support interactions (Fernández-Lorente et al., 2006).

The simultaneous use of a material for enzyme immobilization and for adsorption also means that the functional groups must not only be compatible with chemical groups of the biomolecule, but should also exhibit affinity to the pollutant or to the products of its bioremediation. Due to the variation in the structure and chemistry of the immobilized and/or adsorbed molecules, there is a great diversity of interactions formed between the attached enzyme and support as well as the hazardous pollutants and sorbent. In general, hazardous compounds may be attached to the surface of sorbents by means of several complex mechanisms, such as surface adsorption, ion exchange, complexation (coordination) or chelation (Crini, 2006). On the other hand, enzymes are linked with the matrix mainly by adsorption and covalent bonds, however, immobilization by entrapment and encapsulation has also been reported (Koyani and Vazquez-Duhalt, 2016; Bilal et al., 2017c). Nevertheless, the immobilization of the enzyme onto the surface of the support (adsorption and covalent immobilization) is particularly desirable for removal of toxic compounds due to reduced diffusional limitations and improved exposure of the biocatalysts active sites for the substrates dissolved in the solution as well as adsorbed on the support material (Bilal et al., 2018e). Thus, the selection of a material with appropriate features plays a key role for effective immobilization and sorption of pollutants. Additionally, the surface properties of the sorbent should be selected in order to minimize the negative impact of the adsorbed compound on the catalytic activity of the biomolecules.

2.1.1. Inorganic materials

A wide variety of different inorganic materials has been used for simultaneous removal of hazardous pollutants by both immobilized enzymes and by adsorption. Organic oxides including e.g. silica, titanium, alumina and iron oxides have been used for the immobilization of oxidoreductases and selective sorption of pollutants such as synthetic and natural dyes, phenolic compounds and antibiotics due to the presence of many functional moieties, mainly hydroxyl groups, as well as well defined porous structure, good sorption properties and high stability (Champagne and Ramsay, 2007; Kim et al., 2011; Yu et al., 2015). There are also other inorganic materials, such as minerals and carbon-based materials, which offer high stability and good sorption properties that can be successfully applied for pollutant removal by enzymatic oxidation and subsequent adsorption (Choi et al., 2008; Ding et al., 2016). An interesting example of the utilization of inorganic oxides (alumina) was reported by Zille et al. and Osma et al. Laccase was immobilized by adsorption onto spherical alumina pellets or by covalent binding onto Al_2O_3 pellets, respectively, and used for the decolorization of industrial effluents containing Reactive Black 5. It was found that in both cases the decolorization occurred due to two processes: adsorption of the dye on the support material and its degradation by the laccase. However, an interesting phenomenon was observed: when the biomolecule was attached to the matrix *via* weak adsorption interactions, approx. 80% of the dye was removed due to the adsorption process and only 4% was degraded by the immobilized laccase (Zille et al., 2003). On the other hand, covalent binding of the biomolecules completely reversed these proportions: in this case over 90% of the Reactive Black 5 was biodegraded and less than 10% was adsorbed onto the alumina pellets. These observations may be explained by the type of the interactions formed between the enzyme and support. Covalent immobilization of the enzyme and the usually accompanying multipoint attachment of the biocatalysts resulted in the saturation of the majority of active sites on the surface of the support. This limited the number of free active sites available for the dye molecules and, as a consequence, the sorption capacity of the material with immobilized enzyme towards the dye was decreased (Osma et al., 2010). Furthermore covalent binding of the laccase increased its stability and enzyme leakage was strongly reduced, which also enhanced the enzymatic removal of the RB5 dye. Nevertheless, under optimal conditions, the biodegradation process was highly efficient in both batch and continuous modes, indicating that such biocatalytic systems may be suitable for potential implementation at an industrial scale.

It can be briefly summarize that use of the inorganic materials as support for simultaneous immobilization and removal of pollutants allows to achieve high removal efficiencies which exceed 90%. A wide range of toxic compounds may be removed, including dyes, phenols and antibiotics. However, enzymatic conversion is the main mechanism of

degradation of phenols, as the adsorption process enhances the total removal efficiency. For this technique, mainly laccases are immobilized using adsorption or covalent binding which facilitate the activity of the used biocatalytic systems. Moreover, enzymes immobilized onto inorganic materials are characterized by improved stability and exceptional operational and mechanical resistance.

Simultaneous enzyme immobilization and adsorption of toxic pollutants using inorganic materials is facilitated due to the presence of numerous functional groups, mainly hydroxyl, extraordinary stability and their mechanical resistance. Using these materials, enzymes are immobilized mainly by adsorption which protects their catalytic properties due to the fact that the three-dimensional structure of the biocatalysts is unaltered. However, due to the multipoint attachment, elution of the enzyme molecules from the support is restricted. Moreover, due to the presence of many functional moieties, the formation of the covalent bonds also cannot be excluded, which additionally reduces enzyme leakage. Also effective sorption of both environmental pollutants and products of their bioconversion is enhanced by the presence of several functional groups. It should be emphasized that among inorganic materials, inorganic oxides should be of particular interest for researchers and industrial applications. This is mainly due to their well-developed surface area and porous structure (numerous micropores and macropores) as well as particle sizes, defined morphology and exceptional stability. These features are directly associated with the properties of the naturally occurring inorganic oxides and the methodology of their synthesis which allows for the production of materials with desired physico-chemical characteristics. Moreover, it should be added that such materials are frequently and are easy to obtain, which makes them relatively cheap. Furthermore, the use of inorganic oxides for simultaneous enzyme immobilization and pollutants adsorption results in high removal efficiencies. It should also be added that inorganic oxides exhibit supplementary properties, such as magnetic properties in case of magnetite or photocatalytic properties in case of titanium, which, respectively, facilitate rapid separation of the material after the process by using external magnetic field or may enhance the removal efficiency by photocatalysis.

2.1.2. Organic materials

Aside from many inorganic materials, biopolymers and synthetic polymers are also used for simultaneous enzyme immobilization and sorption of hazardous compounds. The presence of numerous of chemical moieties, such as: –OH, $–NH_2$, C = O and COOH, in their structure enhances efficient immobilization of biocatalysts and sorption of environmental pollutants from water solutions. Biopolymers of different origin, abundant in nature, such as agar, starch and carrageenan, are used for the simultaneous biodegradation and adsorption of toxic compounds mainly due to their good sorption properties and relatively low cost (Costa and Reis, 2004; Srinivasan and Viraraghavan, 2010; Loffredo et al., 2014). Generally, due to the presence of functional moieties and their natural origin, most of these materials exhibit rather high affinity to peptides (Bilal and Iqbal, 2019). Moreover, due to their negligible negative effect on the biocatalysts, biopolymeric supports improve the operational and storage stability of the immobilized enzymes and prolong their catalytic activity which in consequence enhances the practical applications of the produced biocatalytic systems. The most commonly used biopolymer is chitosan, in a variety of forms and sizes. For instance, Nguyen et al. used chitosan beads crosslinked by glutaraldehyde for the removal of sulfur dyes (Sulfur Blue 15 and Sulfur Brown GD) from a water solution through biosorption and subsequent degradation by immobilized laccase. Enzymatic biodegradation was the leading mechanism of pollutant removal. Even at low laccase concentration, over 70 and 80% of Sulfur Brown GD and Sulfur Blue 15, respectively was removed at pH 6.5 from the dye solution at a concentration of 200 mg/L. However, when a mixture of dyes was treated under the same conditions, the efficiency of removal of each dye significantly decreased (Nguyen et al., 2016a). This is associated with the fact that dye molecules compete with each other for access to the active sites of enzymes and not every dye molecule could be converted due to their overcrowding. That is the main limitation of the presented solution and more enzymes should be immobilized to increase the amount of catalytic active sites in order to overcome this problem. In another study, chitosan film was used as a support for covalent immobilization of mushroom tyrosinase. The produced biocatalytic system was applied for the biodegradation of phenol derivatives from artificial wastewater and subsequent sorption of quinone derivatives formed after tyrosinase-catalyzed oxidation of toxic compounds. It was found that pH 7 and a temperature of 45 °C were the optimal conditions for both enzymatic biodegradation and quinone adsorption, which additionally improved the efficiency of the process. After biodegradation and subsequent sorption of products of phenol bioconversion, over 90% of *p*-cresol, *m*-cresol, catechol and *p*-chlorophenol were removed by this procedure (Yamada et al., 2005). Apart from polymers of natural origin, synthetic polymers are also used for simultaneous biodegradation and adsorption of hazardous compounds. Monomers commonly applied in enzyme immobilization, including polystyrene and polyvinyl alcohol, have also been used for the production of materials for both attachment of laccases or tyrosinases and the sorption of dyes or other phenolic derivatives in one process (Leidig et al., 1999; Zhang et al., 2014). Wang et al. investigated the use of polyacrylonitrile membranes for the immobilization of horseradish peroxidase and further degradation of phenol. The immobilized peroxidase was additionally crosslinked with glutaraldehyde, which on the one hand reduced the elution of the biomolecules from the matrix, but on the other hand significantly decreased the number of chemical moieties able to adsorb phenol. The removal process could be divided into two steps: (i) adsorption of phenol on the surface and in pores of the membrane to increase its availability to the immobilized enzyme and (ii) enzymatic conversion. Nevertheless, the main mechanism of removal was enzymatic biodegradation, and ultimately less than 10% of the phenol was removed by sorption. With the use of the described system, almost total removal of phenol from water solutions at concentrations up to 10 mg/L was achieved, which suggests that a polyacrylonitrile membrane with immobilized horseradish peroxidase has promising applications for the removal of phenol from water solutions (Wang et al., 2016).

It can be briefly summarized that the use of organic materials of both synthetic and natural origin, such as polyacrylonitrile or chitosan, for simultaneous enzyme immobilization and adsorption of hazardous compounds, mainly phenol and its derivatives and dyes, allows for their removal from wastewaters with high efficiencies, which usually exceed 90%. Moreover, oxidoreductases retained their high catalytic properties after immobilization as an effect of their attachment to the support, mainly by stable covalent bonds. Due to this fact, enzymatic conversion is the main mechanism which determines the removal processes of the pollutants. Furthermore, a wide range of enzymes, including laccases, tyrosinases and peroxidases, can be immobilized by adsorption, covalent binding and even encapsulation using polymeric supports. Nevertheless, in our opinion, biopolymers such as chitosan, are more suitable for application in simultaneous immobilization and sorption due to the presence of many chemical groups, formation of various geometrical shapes (which is of particular interest for application in bioreactors and in continuous processes) as well as biocompatibility and frequent abundance in nature, that makes them renewable and relatively cheap.

2.1.3. Hybrid and composite materials

During recent years, hybrid and composite materials are of particular interest among wide range of supports/sorbents used for enzyme immobilization and simultaneous removal of pollutants. Hybrid materials may be a combination of inorganic-organic, inorganic-inorganic and organic-organic species. The role of their formation results from the possibility to obtain novel materials which combine the properties of both components. Depending on the requirements, the hybrid materials

may be synthesized using different methods, and the selection of an appropriate method determines their physicochemical properties, such as morphology and dispersive character, electrokinetic and thermal stability as well as parameters of the porous structure and hydrophilic-hydrophobic nature. A broad spectrum of synthesis methods allows to design hybrid materials characterized by diverse physicochemical and structural parameters suitable for enzyme immobilization and removal of hazardous compounds. Another advantage is associated with the fact that their properties may be freely designed by selection of the components which are included in the hybrid materials as well as by means of further treatment using different surface modifications with multifunctional organic or bioorganic substances. On the other hand, composite materials include at least two components – one of them is dispersed in the second one. The most commonly known composite materials are polymers, metallic and ceramic composites. Compared to hybrid materials, properties of the composite materials are not a sum of the properties of its components. Nevertheless, both types of the above-mentioned materials exhibit unique properties which enable their application as effective supports/sorbents used for enzyme immobilization and simultaneous removal of pollutants.

2.1.3.1. Organic-inorganic hybrid materials. There are numerous reports concerning the use of combinations of precursors of different origin to produce functional hybrid materials with different properties. For example, polyacrylonitrile was combined with a naturally occurring montmorillonite to create nanofibers, which were enriched with graphene oxide to increase electron transfer. This material was used for the immobilization of laccase from *Trametes versicolor*, and then for the removal of catechol (Wang et al., 2014). Although addition of graphene oxide enhanced the catalytic properties of the enzyme, most of the functional groups of the precursors are involved in the formation of a hybrid. In consequence, the amount of immobilized enzyme as well as sorption capacity of the above-mentioned material are limited, which is the main disadvantage of the proposed support/sorbent resulting in relatively low total removal efficiency. In a similar study by Dai et al. (2016), poly(D,L-lactide-co-glycolide)/multi-walled carbon nanotubes hybrid fibers, produced *via* an electrospinning technique, were used for the encapsulation of laccase. The resulting biocatalytic system with a high electron transfer rate was further used for the biodegradation of bisphenol A from a water solution. The immobilized enzyme exhibited good storage stability and reusability, and was more stable than native laccase even at a temperature of 60 °C. It has been reported that the removal of BPA was mainly due to the enzymatic biodegradation, as adsorption of the pollutant did not exceed 10%. Other synthetic polymers, including poly(vinyl alcohol), poly(acrylic acid) and polyamine, as well as biopolymers such as chitosan or alginate, have also been combined with inorganic precursors such as silica, clays and iron ions to produce stable and efficient materials for enzyme immobilization and for further application of such systems in the biodegradation and simultaneous adsorption of dyes, phenols and pharmaceuticals (Perullini et al., 2010; Xu et al., 2015). The combination of a biopolymer (chitosan) with iron ions and creation of a hybrid membrane was suggested by Wen et al. (2015) for the economical and effective degradation of dyes. The membrane demonstrated excellent sorption capacity with respect to the laccase as well as the dye. The results proved that the dyes can be removed by the enzyme and the membrane synergistically; however, the dyes were first adsorbed on the membrane and then degraded by the enzyme. This solution improved substrate accessibility for the immobilized enzyme which resulted in the total removal of Acid Red 73 and Acid Blue 113 at mild conditions.

2.1.3.2. Organic-organic hybrid materials. Aside from combinations of inorganic and organic precursors, hybrids produced by linking of organic materials are also used. These materials are characterized by biocompatibility and high affinity towards peptides which is highly desirable for effective enzyme immobilization. Moreover, the presence of functional moieties additionally increases the efficiency of sorption properties of both hazardous pollutants and products of their conversion. An interesting example was reported by Ensuncho et al. (2005) regarding the combination of two biopolymers, chitosan and alginate, to form a chitosan matrix crosslinked with glutaraldehyde with an alginate-filled pore space, for entrapment immobilization of tyrosinase from *Agaricus bisporus*. The produced beads presented good mechanical properties and preserved the unique adsorption characteristics of chitosan. The biocatalytic system was used for the removal of phenol from water solution and further sorption of *o*-quinone as the product of enzymatic conversion. This solution allowed to retain good catalytic properties of tyrosinase over repeated biodegradation cycles, while protecting the immobilized enzyme against inactivation caused by the by-products of bioconversion. With the use of this system, over 90% of the phenol was removed under optimal conditions after four hours of the process. However, adsorption efficiency reached approx. 30% as enzymatic conversion reached over 60%. Materials which combine synthetic polymers and biopolymers are also used for effective simultaneous enzymatic biodegradation and adsorption of pollutants. For instance, chitosan was linked with the weakly acidic cation exchange resins Diaion WK10 and WK20. Tyrosinase was then covalently immobilized on the hybrid material and used for the removal of alkylphenols from aqueous solutions. In both cases the enzyme exhibited its highest catalytic activity in the temperature range of 30–45 °C and the pH range of 7–10. Under such conditions, alkylphenols were effectively removed through quinone oxidation by the immobilized biomolecules with efficiencies equal to 100% (Wada et al., 1993; Tamura et al., 2010). After enzymatic oxidation, subsequent quinone adsorption by the chitosan beads was observed. Moreover, the authors suggested that the removal efficiency would increase with increased quantity of chitosan in the beads due to the fact that quinone adsorption may exceed enzymatic conversion of quinones at a certain point (Tamura et al., 2010). Furthermore, they reported that the total amount of phenol was removed after two hours from the solution by the immobilized tyrosinase and chitosan beads. The presented solution is highly effective and ensures great enzyme reusability due to the combination of cationic resin, responsible for covalent binding of the tyrosinase, and chitosan, which plays a crucial role in adsorption process (Wada et al., 1993). For efficient encapsulation of horseradish peroxidase, the poly(D,L-lactide-co-glycolide)/polyethylene glycol/poly(*p*-phenylene oxide) fibers were produced *via* emulsion electrospinning. Furthermore, adsorption and degradation of pentachlorophenol (PCP) by the immobilized peroxidase was investigated. It was found that the sorption of PCP follows the pseudo-second-order model and its efficiency reached 55%. Additionally, sorption of the pollutant strongly enhanced the efficiency of its removal, due to interactions between the adsorbed pentachlorophenol and immobilized enzyme. A total removal efficiency of over 85% of PCP at the temperature of 25 °C and pH ranging from 2 to 4 was observed. Moreover, after encapsulation by emulsion electrospinning, the operational and storage stability of the immobilized biomolecules were significantly improved. This indicates that the produced biocatalytic system may find practical applications in the biodegradation of PCP from actual wastewaters. However, it should also be underlined that pH of the solution is the factor which limits the application of the above-mentioned system in alkaline conditions, as no adsorption and degradation were observed at pH above 4.7, due to the deprotonation of PCP, enzyme inactivation and its leakage from the support (Niu et al., 2013).

In order to briefly summarize the presented literature review, we would like to highlight that there is a fairly wide group of support materials of various origin that can be applied for the simultaneous biodegradation and adsorption process; however, inorganic materials characterized by good mechanical and operational properties together with synthetic or natural organic substances known from their

biocompatibility, are used most frequently. Aside from operational stability, such materials must also exhibit good sorption properties, a favorable and defined porous structure, and the presence of numerous functional groups for effective enzyme binding and sorption of hazardous pollutants. Over recent years hybrid and/or composite materials are also more and more commonly used for simultaneous immobilization and adsorption, mainly due to their tailor-made properties suitable for both the immobilized enzyme and pollutant or product of its conversion to be adsorbed. Therefore we encourage to carry out even more advanced studies in the topic of application of hybrid/composite materials for oxidoreductase immobilization and toxic compounds sorption, as the development of solutions resulting in high removal rates of dyes or phenolic compounds could be important in terms of environmental protection. However, we would like to emphasize that each of the above-mentioned groups of materials also possesses disadvantages. For instance, most of the organic materials are characterized by low sorption properties due to low porosity and low surface area. On the other hand, the presence of mainly hydroxyl groups on surface of the inorganic materials results in the fact that their functionalization is required to form stable enzyme-matrix interactions. Moreover, hybrid materials, aside from exhibiting tailor-made properties, are relatively expensive to obtain.

This technique dates back to the beginning of the last decade, but a rapidly growing interest in applications of the method has been observed during the last few years. The greatest advantage of this method is the fact that compounds which are resistant to enzymatic degradation are effectively removed from polluted solutions by adsorption. Additionally, due to the complex mechanism of remediation, a very wide group of toxic compounds could be efficiently eliminated from solution, usually with extraordinary efficiencies. However, reusability of the matrix after inactivation of the enzyme is limited, since desorption of the pollutants and regeneration of the sorbent are expensive and unfavorable. Consequently, extensive research is still required to improve the process control and efficiency, and to identify new groups of compounds which may be used for effective simultaneous enzyme immobilization and pollutant removal, thus increasing the applicability of the method in the bioremediation of toxic compounds from wastewaters and industrial effluents.

3. Enzymatic reactors for removal of environmental pollutants

Due to the increasing amount of pollutants prevalent in the environment, there is still a need to evaluate and develop efficient, ecofriendly and cost-effective solutions for their removal. Aside from simultaneous enzyme immobilization and sorption of toxic compounds, another interesting solution based on the use of enzymes is application of bioreactors for biodegradation and removal of persistent substances from wastewaters and industrial effluents. Enzymatic bioreactors usually offer a very good flow regime, reducing the mass transfer limitations which are commonly observed when heterogeneous catalysts are used (Luckarift, 2008). These features mean that removal and biodegradation processes performed in bioreactors are usually characterized by high selectivity and efficiency. Furthermore, due to the reduced time and energy consumption, processes carried out in bioreactors are more environmentally friendly and cost-effective (Balcao et al., 1996). Additionally, it should be emphasized that the effectivity of an enzymatic bioreactor is improved when immobilized enzymes are used as catalysts, due to their improved stability and reusability compared to free enzymes (Husain, 2017).

Many different configurations of enzymatic reactors for environmental applications have been developed in recent years. In general, these bioreactors may be divided into two groups: (i) enzymatic bioreactors (EBRs) and (ii) enzymatic membrane reactors (EMRs) (Nanba et al., 2007; Rios et al., 2014). In both EBRs and EMRs immobilized laccases, tyrosinases and other oxidoreductases (mainly horseradish peroxidase) are employed for the removal of hazardous compounds. However, there are great differences between these two types. EBRs are frequently used in various operational modes, such as batch reaction or continuous reaction, to increase the efficiency of the biocatalytic process. However, after biocatalytic conversion, an additional step is required, namely the separation of the immobilized enzyme from the reaction mixture. In the EMR, however, the catalytic action is simultaneous with membrane separation of the products from the reaction mixture, which results in high purity of the products and reaction effluents (Sanchez-Marcano and Tsotsis, 2002). Selected examples of the use of EBRs with immobilized oxidoreductases for environmental applications were reviewed in Section 3.1 whereas instances of the use of EMRs for biodegradation and removal of hazardous pollutants were discussed in detail in Section 3.2.

3.1. Enzymatic bioreactors (EBRs)

An enzymatic bioreactor, in broad terms, is a device in which enzyme-catalyzed transformation of substrates into products occur under mild reaction conditions (Miyazaki and Maeda, 2006). Selection of the reactor type and operational mode is conducted according to the process conditions, enzyme activity and required product purity. Immobilized oxidoreductases are, in general, used in two types of bioreactors: (i) batch reactors and (ii) continuous reactors (Webb et al., 2004; Xue and Woodley, 2012; Barrios-Estrada et al., 2018b) as presented in Fig. 2.

Batch reactors used for the removal of environmental pollutants by immobilized oxidoreductases include the stirred-tank reactor, the most frequently used type of enzyme reactor, as well as the fluidized bed reactor. Batch reactors are characterized by simplicity and flexibility of use at an industrial scale, offer easy control of the process and are very useful for slow reactions in a viscous mixture (Darnoko and Cheryan, 2000; Shimada et al., 2002). Furthermore, due to their simple construction and relatively high efficiencies, batch reactors require less capital investment than continuous processes. It should be added that immobilized laccases and tyrosinases applied in batch bioreactors offer very good reusability as they can often be used in more than ten consecutive biodegradation cycles (Srikanlayanukul et al., 2016). On the other hand, the advantage of continuous-mode reactors is that immobilized enzymes are constantly in contact with the stream of substrates, which enhances the activity of the biomolecules. Moreover, the flux of the reaction mixture through the biocatalytic beads can be controlled to meet process requirements (Bolivar et al., 2011). The use of a bioreactor in continuous mode also allows to avoid the usually costly separation of the biocatalyst from the reaction mixture (Almeida et al., 2003). In consequence, after detoxification by immobilized laccases, effluent streams with a purity of over 95% can be obtained (Palli et al., 2017). Since both batch and continuous processes have advantages in practical use, it is impossible to clearly indicate the best operational mode.

It should be highlighted that the design of an enzymatic bioreactor

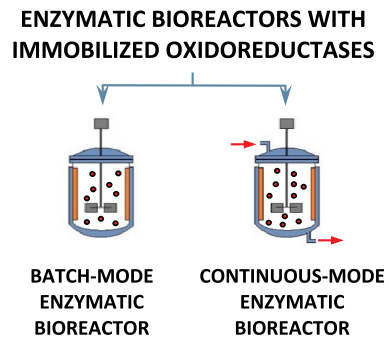

Fig. 2. Schematic representation of the batch-mode and continuous-mode enzymatic bioreactors for environmental applications.

is a complex engineering task. Nevertheless, the key idea is to design reactors capable of achieving the highest conversion rate and the highest quality of products at the lowest costs. First of all, to ensure high efficiencies of the enzymatic reaction, the bioreactor should provide optimal process conditions for the biomolecules, such as substrate supply, product and by-product removal, controlled pH, temperature and agitation speed (Benz, 2011; Le-Clech et al., 2006). Thus, prior to bioreactor design, a detailed study concerning type of the enzyme and substrate as well as conditions for the highest bioconversion efficiency should be carried out. Furthermore, enzymatic bioreactors should ensure the efficient use of the biomolecules and their substrates, reduce diffusional limitations and exhibit low energy requirements (Pino et al., 2018). Finally, the bioreactors should be characterized by simplicity and optimized volume of the vessel to ensure high rate of substrate conversion per volume of the reactor.

Nevertheless, we would like to point out that selection of the most suitable operational method is usually influenced by several variables, such as enzyme stability, type of support materials, process time and required purity of the solution after the process. However, to increase the efficiency of the processes carried out in enzymatic bioreactors and to enhance the biocatalytic properties of the enzymes, biomolecules in immobilized form are commonly used. Support materials of inorganic, organic and hybrid or composite origin may be used for the immobilization of tyrosinases, laccases and horseradish peroxidase for subsequent use in the biodegradation of hazardous pollutants. Selected examples of biocatalytic systems used in enzymatic bioreactors (EBRs) for environmental applications were summarized in Table 4.

As is shown in Table 4, materials of both inorganic and organic origin as well as hybrids and composites are used as supports for the immobilization of enzymes for application in bioreactors. These materials must be insoluble in the reaction environment and offer good mechanical and operational stability, with regard to the long duration of the process and its repeatability. Moreover, these supports are notable for their good sorption properties and the presence of many functional groups in their structure, for effective binding of the enzyme molecules to prevent elution of the catalyst from the support during the process (Illaes and Wilson, 2003).

3.1.1. Inorganic materials as support materials in EBRs

Among various inorganic materials, minerals, silicas, inorganic oxides such as γ-aluminum oxide, and carbon-based materials are the most frequently used to produce enzyme-matrix systems for application in EBRs (Kandelbauer et al., 2004). For example, in a study described by Nguyen et al., laccase was immobilized by adsorption on granular activated carbon, known for its good sorption properties, and applied for the degradation of sulfamethoxazole, carbamazepine, diclofenac and bisphenol A in a packed bed column bioreactor. The pollutants were removed with efficiencies of over 90% by enzymatic degradation following their adsorption onto activated carbon. The significantly higher efficiency of bioremoval achieved in the EBR with immobilized biomolecules compared to the EBR with free enzyme is associated with the fact that after enzyme immobilization on carbon material, transfer of electrons between the laccase and adsorbed substrate molecules was enhanced and bioreactor effectivity was improved. Moreover, the system demonstrated exceptional reusability: the immobilized biocatalyst retained its activity even after two months of continuous operation (Nguyen et al., 2016b).

3.1.2. Organic materials as support materials in EBRs

Synthetic polymers and biopolymers such as chitosan are also used, due to their mechanical stability under operational conditions and strong binding of the enzyme to the support. In view of their very good gelation properties and the mechanical resistance of the formed beads, alginates are a commonly used biopolymer (Ganaie et al., 2014). In another study, polyurethane foam cubes were used for covalent immobilization of laccase from *Trametes versicolor* by Yang et al. (2012). This biocatalytic system was used in a packed bed reactor for decolorization of Remazol Brilliant Blue R, Anthraquinone dye B4 and Acid Black 24 from model and industrial wastewaters. The immobilized laccase was used in five sequential degradation cycles and was able to decolorize all tested dyes efficiently, even at a concentration of 2000 ppm. Furthermore, the duckweed test showed a significant reduction of the toxicity of the effluents after enzymatic treatment. In another study, alginate was additionally cross-linked by $CuSO_4$ to form blue spherical beads with entrapped laccase from *Pleurotus ostreatus*. Copper ions were used not only for the gelation of the biopolymer, but also to enhance the catalytic properties of the immobilized enzyme. A fixed bed reactor with enzymatic beads working in continuous mode was used for decolorization of the anthraquinonic dye. Degradation efficiency of 70% was achieved after four hours of the process at pH 4.5 and temperature of 20 °C. The immobilized laccase exhibited remarkable reusability, achieving a high efficiency of decolorization (over 60%) even after 20 catalytic cycles (Palmieri et al., 2005). Although copper ions improve the activity of the immobilized laccase, the limitation of this solution, resulting in approx. 70% degradation, is associated with fact that formed coordinative bonds distort the enzyme structure and decrease its properties. Moreover, cross-linking of the alginate beads resulted in the occurrence of some diffusional limitations, which could additionally decrease the total removal efficiency.

3.1.3. EBRs operational modes

Aside from type of the support material, the operational mode of the bioreactor also affects its operational effectivity. As has been shown, there are different types of enzymatic bioreactors with immobilized enzymes for environmental applications working in batch and continuous modes. These may be classified as: (i) packed bed reactors, (ii) fixed bed reactors, (iii) fluidized bed reactors and (iv) continuous flow reactors (Williams, 2002). The type of used reactor as well as the support material are selected appropriately to the enzyme and the type of catalytic process. Moreover, the choice of reactor and operational mode is usually intended to increase the operational effectiveness of the equipment and the reaction yield. For example, Krastanov (2000) used a continuous fixed bed tubular bioreactor with laccase from *Pyricularia oryzae* and mushroom tyrosinase co-immobilized onto KC-Microperl MP100, for a rapid degradation of phenols from aqueous solutions. The bioreactor achieved high operational efficiency. With the use of the described method, phenolic derivatives such as α-naphthol or catechin could be totally removed from the mixture after a single pass through the reactor. Moreover, after immobilization, the operational stability of the immobilized enzymes with respect to particular substrate types, such as 2,4-dichloropenol and guaiacol, was significantly improved. In another study by Du et al. (2013), a fluidized bed reactor in which the biocatalytic beads consisted of laccase immobilized by entrapment into sodium alginate capsules was applied in order to increase the intensity of contact between the enzyme and substrates and to reduce reaction time. It was found that the optimal capacity of the bioreactor was 1.5 L and the following conditions were optimal for the degradation of pharmaceuticals: pH 5, temperature 20 °C and reaction time 100 min. Under these conditions, more than 75% of the pharmaceuticals were removed from wastewater. However, low mediator concentration and insufficient quantity of used laccase should be indicated as the main limitation factors which did not allow to achieve total removal efficiency. As it was mentioned above, it is hard to clearly indicate and suggest a universal and, at the same time, the most suitable operational mode for the removal of all of the environmental pollutants by immobilized oxidoreductases in EBRs. Thus we suggest careful consideration of the type of the enzymatic bioreactor, taking the type and form of the support material with immobilized enzyme into account, to ensure enzymatic activity as high as possible and its contact with stream of the substrates.

Table 4
Materials of various origin used for immobilization of laccases and tyrosinases for application in enzymatic bioreactors (EBRs) towards biodegradation of various environmental pollutants.

Reactor type	Process conditions	Support material	Enzyme	Immobilization technique	Pollutants (enzyme substrate)	Removal efficiency	Reference
Packed bed reactor	pH 7, 28 °C, 60 days	Granular activated carbon	Laccase from *Aspergillus oryzae*	Adsorption immobilization	Sulfamethoxazole, Carbamazepine, Diclofenac, Bisphenol A	94% 92%, 95%, 97%	(Nguyen et al., 2016b)
Packed bed reactor	pH 4, 40 °C, 30 h	γ-Aluminum oxide pellets	Laccase from *Trametes modesta*	Covalent immobilization	Lanaset Blue 2R, Terasil Pink 2GLA, Indigo Carmine, Crystal Violet	100%, 70%, 99%, 97%	(Kandelbauer et al., 2004)
Bioreactor	pH 6.5, 20 °C, 7 h	Aminopropyl-controlled pore glass	Tyrosinase from mushroom	Covalent immobilization	Phenol, *p*-Cresol, Catechol, 4-Methylcatechol, 4-Chlorophenol	60%, 100%, 100%, 100%, 100%	(Girelli et al., 2006)
Core-shell microreactor	pH 6.5, 25 °C, 15 min	Superparamagnetic hydrophobic particles/glass plates	Laccase	Covalent immobilization	Syringaldazine	75%	(Al-Kaidy and Tippkotter, 2016)
Column-packed reactor	pH 5, 28 °C, 5 days	Na-alginate beads	Laccase from *Polyporus rubidus*	Entrapment	Reactive Blue, Remazol Black 5, Reactive Orange, Congo Red	85%, 100%, 90%, 100%	(Dayaram and Dasgupta, 2008)
Fluidized bed bioreactor	pH 5, 20 °C, 100 min	Na-alginate beads	Laccase	Entrapment	Pharmaceuticals	75%	(Du et al., 2013)
Packed bed reactor	30 °C, 6 h	Ca-alginate beads	Laccase from *Streptomyces psammoticus*	Entrapment	Phenol	70%	(Niladevi and Prema, 2008)
Fixed bed reactor	pH 4.5, 20 °C, 4 h	Cu-alginate beads	Laccase from *Pleurotus ostreatus*	Entrapment	Remazol Brilliant Blue R	70%	(Palmieri et al., 2005)
Bioreactor	pH 7, 25 °C, 12 h	Cu-alginate beads	Laccase from *Ganoderma* sp. KU-Alk4,	Entrapment	Indigo Carmine, Remazol Brilliant Blue R, Bromophenol Blue, Direct Blue 15	100%, 100%, 65%, 54%	(Teerapatsakul et al., 2017)
Continuous-flow microreactor	pH 5, 30 °C, 1 h	Glutaraldehyde and paraformaldehyde	Laccase from *Trametes versicolor*	Cross-linking	Estrone, 17-*β*-Estradiol, 17-*α*-Ethinylestradiol	100%, 100%, 100%	(Lloret et al., 2013a, 2013b, 2013c)
Perfusion basket reactor	pH 4.5, 35 °C	Poly(ethylene glycol) and glutaraldehyde	Laccase from *Cirripectes polyzona*	Cross-linking	Nonylphenol, Bisphenol A, Triclosan	95%, 100%, 100%	(Cabana et al., 2009a, 2009b)
Packed bed reactor	25 °C, 5 days	Polyurethane foam cubes	Laccase from *Trametes versicolor*	Covalent immobilization	Remazol Brilliant Blue R, Anthraquinone dye B4, Acid Black 24	100%, 98%, 65%	(Yang et al., 2012)
Packed bed reactor	pH 7, 24 °C, 30 min	Eupergit C 250L	Laccase from *Myceliophthora thermophila*	Covalent immobilization	Estrone, 17-*β*-Estradiol, 17-*α*-Ethinylestradiol	65%, 80%, 80%	(Lloret et al., 2012)
Fixed bed tubular bioreactor	pH 6.5, 25 °C, 60 h	KC-Microperl MP100	Co-immobilized laccase *Pyricularia oryzae* and tyrosinase	Covalent immobilization	*α*-Naphthol, 4-Chlorophenol, 2-Chlorophenol, *p*-Cresol	100%, 66%, 50%, 28%	(Krastanov, 2000)

3.1.4. Enzyme immobilization techniques in EBRs

Depending on the type and form of support material and the reactor construction, enzymes can be immobilized *via* different techniques to increase the efficiency of the degradation process. However, the main concern is that the immobilized enzyme has to be strongly connected with the support to prevent its elution during repeated reaction cycles and to maintain good catalytic properties. Thus, mainly covalent immobilization as well as entrapment are frequently applied, however, adsorption, encapsulation and even cross-linking, are also used to produce biocatalytic beads for bioreactors (McMorn and Hutchings, 2004). An interesting example was reported by Dayaram and Dasgupta (2008) regarding the use of laccase from *Polyporus rubidus* for the degradation of four reactive dyes commonly occurring in effluents. The enzyme was immobilized *via* an entrapment method into calcium alginate beads and used in an enzymatic column-packed reactor. The biocatalytic system demonstrated excellent operational stability, and over 85% of the dyes were removed from wastewater. Additionally, due to the limited interference in the enzyme structure, the systems produced by entrapment exhibited good storage stability as their properties were unaltered after ten days of storage. Thus, immobilization by entrapment may be indicated as a promising way to develop easy and cost-effective methods for production of biocatalytic systems for remediation of hazardous dyes. Moreover, it should be emphasized that with the use of immobilized oxidoreductases as a beads in bioreactors, usually over 80% of toxic compounds can be removed. For instance, phenol and its derivatives, such as *p*-cresol, catechol and 4-methylcatechol, were biodegraded using a bioreactor with mushroom tyrosinase covalently immobilized onto aminopropyl-controlled pore glass. Under pH 6.5 and at ambient temperature, total removal of phenolic compounds was observed. Additionally, in order to obtain effluent which was as pure as possible after the enzymatic treatment, adsorption of colored quinone-type biodegradation products on a chitosan trap was applied (Girelli et al., 2006). This solution should be indicated as particularly interesting since the pollutants were removed *via* simultaneous enzymatic biodegradation by immobilized enzymes and adsorption by support/sorbent material, which additionally

increased the removal efficiency, improved the purity of the effluents and decreased their toxicity. In another study, laccase entrapped into copper alginate beads was used in a bioreactor for remediation of selected commercial aromatic dyes. The immobilized laccase exhibited better stability than the free enzyme and higher efficiency in the removal of various synthetic dyes under non-buffered conditions. The airflow rate was the key parameter affecting degradation time and number of batch runs. An airflow rate of 4 L/min was the most suitable for degradation of Indigo Carmine and Remazol Brilliant Blue R. Under this airflow, the total quantity of the dyes was removed from aqueous solution at pH 7 and temperature of 25 °C (Teerapatsakul et al., 2017).

To summarize the application of EBRs equipment based on the immobilized oxidoreductases for removal of environmental pollutants, it can be concluded that conversion of hazardous compounds can be achieved in a shorter time and under mild conditions. A great advantage of the EBRs is associated with the fact that materials of various origin could be used as a supports for immobilized enzyme. However, substances characterized by high stability and resistance as well as numerous functional groups on their surface, which enable the creation of stable enzyme-support interactions, such as inorganic oxides and synthetic polymers should be of particular interest. As noted above, enzymatic bioreactors can be classified as packed bed, fixed bed and fluidized bed reactors, which can operate in both continuous and batch modes. The selection of the bioreactor's operational mode is usually dictated by the process conditions, the type of pollutant and the form of the immobilized enzyme. Various immobilization techniques can be applied to improve process efficiency and different sizes and forms of the produced biocatalytic beads may be obtained. The form of beads is selected to increase the contact time of the enzyme with substrate molecules and the efficiency of the reaction. It is governed mainly by the operational mode of the process and concentration of the toxic compound. Nevertheless, in our opinion, the spherical beads, usually at nano- or microscale, based on materials characterized by high stability and mechanical resistance should be of particular interest due to their operational stability and low diffusional limitations between the immobilized enzyme and ingredients of the reaction mixture. It should also be added that the type and form of the support material also affects the type of the immobilization. Although various techniques were applied, we encourage the use of covalent immobilization, as this method enhanced the formation of stable, covalent enzyme-support interactions which prevents enzyme elution and ensures high operational stability and reusability of the formed biocatalytic beads. Furthermore, the foregoing examples have shown that a wide range of toxic organic compounds can be effectively removed with the use of EBRs; however, the type of pollutant and the used biocatalyst strongly affect the bioremediation conditions. In our opinion, future research will focus increasingly on the appropriate selection of the operational mode and the form of the biocatalytic beads in order to maximize the efficiency of the processes carried out in EBRs. As a result, enzymatic bioreactors should be used as effective and efficient tools not only for the remediation of hazardous compounds but also in biocatalytic conversion of biomass or production of biofuels.

3.2. Enzymatic membrane reactors (EMRs)

Among enzymatic bioreactors, in recent years there has been an increasing interest in the use of enzymatic membrane reactors (EMRs) with the immobilized oxidoreductases for the biodegradation of environmental pollutants from wastewaters. The greatest advantage of EMRs is that they combine selective mass transport with simultaneous biocatalytic conversion. Thus, selective removal of products from the reaction mixture is achieved. This increases the efficiency of the process by enhancement of the conversion of product-inhibited molecules and by forcing of thermodynamically unfavourable reactions (Rasera et al., 2009). Enzymatic membrane reactors are applied at an industrial scale mainly for production and bioconversion processes (Agustian et al., 2011); however, in this review, particular attention is paid to the use of EMRs in wastewater treatment as a sustainable, eco-friendly and efficient alternative for the currently used techniques. Moreover, the recent trends towards environmentally friendly technologies make EMRs an attractive solution, because they operate under mild conditions in terms of pH, temperature and pressure, reduce diffusional limitations, and allow for easy separation of by-products. Moreover, they do not require complex equipment or chemical additives (Brindle and Stephenson, 1996). The use of immobilized oxidoreductases in EMRs provides the possibility of application of biocatalytic transformations carried out in bioreactors at a large scale (Busca et al., 2008). Additionally, the high reusability of the immobilized enzymes ensures that EMRs offer excellent operational stability, reusability and high productivity in repeated biodegradation cycles. Depending on the immobilization technique, the form of the immobilized biocatalysts and the required purity of the products, microfiltration or ultrafiltration membranes can be used in EMRs for applications in wastewater treatments (Prazeres and Cabral, 2001). However, the most frequently used membrane configurations are: (i) flat sheet (frame and plate), (ii) hollow fibers and (iii) tubular (Gallucci et al., 2011). In addition, enzymatic membrane reactors can operate in both batch and continuous modes. It should be also strongly emphasized that EMRs use membranes as both a porous separator, to selectively divide components of the reaction mixture, as well as a matrix for enzyme immobilization. This solution allows to reduce operation cost associated with the use of additional support materials and provides an opportunity to design the optimal parameters and duration of the process to achieve high efficiency and productivity (Marshall et al., 1993). Enzymatic membrane reactors with immobilized laccases, tyrosinases and other oxidoreductases "over" and "in" the membranes are nowadays more and more frequently used for the degradation of toxic compounds, mainly with regard to the increased operability of the process and purity of the effluents (Fig. 3). Different types of membranes of various origin as well as various immobilization techniques are used to produce biocatalytic systems for use in EMRs. Selected examples of the application of enzymatic membrane reactors with immobilized oxidoreductases for the bioremoval of environmental pollutants from aqueous solution were summarized in Table 5.

3.2.1. Membranes properties and materials used in EMRs

As it was shown in Table 5, various materials of different origin have been used to prepare membranes with immobilized enzymes for use in enzymatic membrane reactors. The selection of membrane material and its properties, including pore size, the presence of functional groups, hydrophilicity and surface charge, have a crucial effect on the catalytic activity and stability. For instance, membranes with small pores may limit the access of the substrates to the enzymatic active sites or block changes of the laccase conformation after attachment,

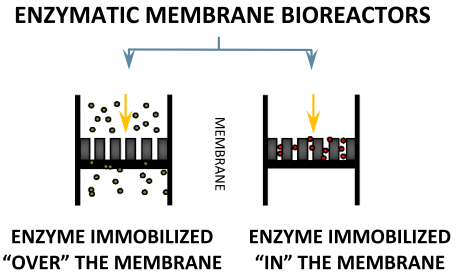

Fig. 3. Schematic representation of enzymatic membrane bioreactors for environmental application. Immobilized enzyme "over" the membrane means that enzyme is immobilized on support material and placed in the reactor together with the support (membrane is not a support and acts as a separation unit), whereas in case of enzyme immobilized "in" the membrane, there is no support material, the membrane acts as a support for biomolecules and a separation unit.

Table 5
Reactor operational mode and materials of various origin used for immobilization of laccases, tyrosinases and peroxidases for application in enzymatic membrane reactors for the biodegradation of various environmental pollutants.

Reactor operational mode	Process conditions	Support material	Enzyme	Immobilization technique	Pollutants (enzyme substrate)	Removal efficiency	Reference
Continuous reactor	pH 6, 25 °C	Ceramic membrane	Laccase from *Trametes versicolor*	Covalent immobilization	Tetracycline	>75%	(Abejon et al., 2015)
Continuous reactor	pH 6, 25 °C, 24 h	Ceramic membrane	Laccase from *Trametes versicolor*	Adsorption immobilization	Bisphenol A	97%	(Arca-Ramos et al., 2015)
Continuous reactor	pH 7, 24 h	Ceramic membrane	Laccase	Covalent immobilization	Sulfadiazine, Penicillin G, Doxycycline	99% 94%, 60%,	(Becker et al., 2016)
Fully-recycling continuous reactor	pH 5.5, 22 °C, 48 h	Carbon nanotubes/ poly (vinylidene fluoride) membrane	Laccase from *Trametes versicolor*	Covalent immobilization	Bisphenol A, Carbamazepine, Diclofenac, Clofibric acid, Ibuprofen	90%, 45%, 75%, 40%, 60%	(Ji et al., 2016)
Batch reactor	pH 6, 30 °C, 2 h	Chitosan membrane	Laccase from *Pleurotus ostreatus* 1804	Covalent immobilization	Acid black 10 BX	95%	(Katuri et al., 2009)
Batch reactor	25 °C, 24 h	Gelatin-ceramic membrane	Laccase from *Trametes versicolor*	Covalent immobilization	Tetracycline	87%	(de Cazes et al., 2015)
Batch reactor	pH 7, 25 °C, 48 h	Microporous polypropylene hollow fiber membranes	Co-immobilized laccase from *Rhus vernificera* and horseradish peroxidase	Entrapment	3,4-Dimethylphenols, 4-Ethylphenol, 2-Hydroxy-1,2,3,4-tetrahydronaphthalene, 2-Hydroxy-decahydronaphthalene, 4-Hydroxy-biphenyl	80%, 56%, 87%, 34%, 85%	(Moeder et al., 2004)
Isothermal and non-isothermal continuous reactor	pH 7.5, 25 °C	Nylon membrane	Laccase from *Rhus vernicifera*	Covalent immobilization	Hydroquinone	>80%	(Durante et al., 2004)
Non-isothermal batch reactor	pH 5.5, 25 °C, 1 h	Nylon membrane	Laccase from *Trametes versicolor*	Covalent immobilization	Bisphenol A	85%	(Diano et al., 2007)
Isothermal and non-isothermal batch reactor	30 °C, 1 h	Nylon membrane	Laccase from *Trametes versicolor*	Covalent immobilization	Bisphenol A	>95%	(Mita et al., 2009)
Continuous reactor	pH 5.3, 30 °C, 2 h	Polyethersulfone membrane	Laccase from *Cerrena unicolor*	Adsorption immobilization	Acid Blue 62	100%	(Lewanczuk and Bryjak, 2015)
Stirred tank continuous reactor	pH 5, 26 °C, 100 h	Polyethersulfone membrane	Laccase from *Myceliophthora thermophila*	Covalent immobilization	Estrone, 17-β-Estradiol, 17-α-Ethinylestradiol	80%, 100%, 100%	(Lloret et al., 2013a, 2013b, 2013c)
Non-isothermal batch reactor	pH 5.5, 30 °C, 30 min	Polypropylene membranes	Laccase from *Trametes versicolor*	Covalent immobilization	Phenol, 3-Methoxyphenol, 4-Acetamidophenol,	100%, 78%, 44%	(Georgieva et al., 2010)
Batch reactor	pH 4, 22 °C, 48 h	Poly(vinylidene fluoride) membrane	Laccase from *Trametes versicolor*	Adsorption immobilization	Bisphenol A	95%	(Jahangiri et al., 2014)
Batch reactor	pH 5, 25 °C, 24 h	Poly(vinylidene fluoride) microfiltration membrane	Laccase from *Trametes versicolor*	Covalent immobilization	*N',N'*-(dimethyl)-*N*-(2-hydroxyphenyl) urea	100%	(Jolivalt et al., 2000)
Fully-recycling batch reactor	pH 7, 30 °C, 3 h	NF270 polyamide membrane	Co-immobilized laccase from *Trametes versicolor* and horseradish peroxidase	Adsorption immobilization	Bisphenol A	95%	(Escalona et al., 2014)

reducing the efficiency of the entire biocatalytic process (Butterfield et al., 2001). On the other hand, it is known that the use of a permeable membrane enables the integration of the separation process with the chemical reaction. However, from a structural point of view, each pore in the membrane may be considered as a separate microsystem. Thus, the correct deposition of enzyme molecules in a membrane plays a significant role in ensuring the capture of substrate molecules by the immobilized enzymes and increasing the contact time between the substrate and the biocatalyst (Hou et al., 2014), as high permeate flux and, in consequence, shorter contact time may be the limiting factors which significantly reduce the efficiency of the process. The selection of a membrane with properties suitable for the immobilized biomolecules and for the separation of the stream of substrates and products, and stable under operational conditions, provides the possibility of precise control of the process and can minimize losses of substrate and products. Furthermore, an appropriate selection of the membrane can lead to a faster reaction rate and higher yields. It is also possible to achieve lower operational costs and a cleaner products stream (Taboada-Puig et al., 2016).

Nevertheless, membrane fouling is one of the most critical factor influencing efficiency of the EMRs. This is due to the fact that fouling may result in a decrease of the permeate flux and water permeability as well as lead to the changes in membrane selectivity and retention due to deposition of solid molecules onto membrane surface (Guo et al., 2012). There are few main mechanisms of membrane fouling, such as pore blocking, surface adsorption, gel or cake formation as well as inorganic precipitation and biological fouling (Luo et al., 2014a). It should be clearly stated that the fouling phenomenon depends on various factors, however the most important include the type, material and properties of the membrane, process conditions, nature of the solution and interactions between membrane and a solutes (Pino et al., 2018). Enzymes are usually immobilized into pores of the membrane, thus tend to form internal fouling. However, biomolecules might also be deposited onto the surface of the membrane. In this case, fouling is usually observed due to cake layer formation. In order to counter the above-mentioned facts, various strategies have been applied to completely avoid or at

least to minimize the fouling effect. According to the previously published reports, the most promising approach consist of operating in a cross-flow filtration mode and using a properly pretreated solution, without solids (Jørgensen and Pinelo, 2017, Pino et al., 2018).

The materials used as supports (membranes) in EMRs can be classified in three main groups: (i) inorganic (mainly ceramic), (ii) metallic, and (iii) polymeric, however, biopolymeric and hybrid membranes are also used. The applied materials should offer excellent stability and good mechanical resistance to provide operational stability and repeatability for enzymatic bioreactors (Jochems et al., 2011). Also, the presence of many functional groups in the structure of the material is required for effective enzyme binding. For example, the presence of numerous hydroxyl groups on the surface of a ceramic membrane with a mean pore diameter of 1.4 μm was exploited for the covalent immobilization of laccase. The membrane was then used in a continuous enzymatic bioreactor for the degradation of tetracycline, a commonly known antibiotic, in the treatment of effluents from hospital, municipal and industrial wastewater. The results showed that the efficiency of biodegradation strongly depended on the quantity of immobilized laccase. When this quantity was appropriately selected, 75% of the tetracycline was removed under optimal conditions of pH 5 and temperature of 25 °C. This demonstrates that in order to ensure the economic and technical competitiveness of the proposed technique, all parameters must meet the process requirements (Abejon et al., 2015). However, high pore diameter, far exceeding the size of the tetracycline and enzyme molecules, is the factor which limits higher removal efficiency as some of the pollutant molecules pass through the membrane unconverted. Aside from inorganic membranes, some polymeric materials also possess features which make them a suitable barrier for both enzyme immobilization and mixture separation. The use of polyethersulfone, a hydrophilic, water-insoluble polymer with a high quantity of free sulfone groups, enables the formation of effective interactions with an immobilized enzyme. Moreover, this polymer is known for its high resistance to mineral acids, alkalis and electrolytes, at pH ranging from 2 to 13, and is commonly used as a skin layer material for various membranes. A polyethersulfone membrane was used for adsorption immobilization of laccase from *Cerrena unicolor*, and the obtained system was applied for the degradation of Acid Blue 62 dye at he temperature of 30 °C and pH equal to 5.3. After two hours of the process, total decolorization of the solution was observed. With the EMR operating in continuous mode, the immobilized laccase was used for dye removal for four days, achieving over 98% conversion of Acid Blue 62. It should also be noted that the immobilized enzyme was stable over six successive reaction cycles without additional aeration (Lewanczuk and Bryjak, 2015). Nevertheless, at the membrane selection stage, particular care must be taken to prevent the destruction and decomposition of the immobilized enzyme, so as to maintain the high catalytic activity of the biomolecules during repeated catalytic cycles. For this reason, a microporous polypropylene hollow-fiber membrane was used for entrapment co-immobilization of laccase from *Rhus vernicifera* and horseradish peroxidase. This membrane offers low interference in the structure of the enzyme, and thus the catalytic activity is maintained at a high level. Moreover, the membrane protects the biocatalysts against the negative effects of the reaction conditions by the formation of the shell by the membrane fibers around enzyme molecules, and additionally increases the stability of the entrapped biomolecules. The system was used in a batch reactor for the remediation of selected hydroxylated aromatic compounds. It was demonstrated that after 48 h of the process, the prepared membrane can remove hazardous compounds from aqueous solution with efficiencies of over 80% (Moeder et al., 2004). The drawback of this solution is the fact, that deposition of the enzyme into the membrane fibers is associated with diffusional limitations which decrease the total removal efficiency. Moreover, the use of membranes in bioreactors has a great impact on the permeate flux. This is affected by the quantity of immobilized enzyme, the transmembrane pressure, the axial velocity and the operational mode (He et al., 2017). Usually, substrate particles accumulate on the top of the membrane, which on one hand ensures a supply of new substrate molecules to the immobilized biocatalysts, but on the other hand may create diffusional limitations and, in consequence, decrease the remediation effectivity. This was observed in case of a nylon membrane grafted with glycidyl methacrylate and phenylenediamine, with covalently immobilized laccase from *Trametes versicolor*, in a study by Diano et al. (2007). This biocatalytic system was used for the bioremediation of water polluted with bisphenol A (BPA). Under optimal conditions (pH 5.5 and temperature 25 °C), and after only one hour over 85% of the BPA was remediated. It was also established that the affinity of the immobilized laccase to the BPA molecules increased with an increase of temperature, under non-isothermal conditions. Nevertheless, the formation of a substrate layer on the membrane induced a diffusional resistance, which reduced the catalytic efficiency of the immobilized enzyme.

Simultaneous catalytic action and separation, which is a significant advantage of enzymatic membrane reactors, provides the ability to retain undesired by-products and unreacted substrates above the membrane and to obtain a stream of products characterized by high purity. This is particularly important in the case of laccase enzymes, due to the formation of products with high molecular mass (oligomers and polymers) during the catalytic transformation of phenolic pollutants (Nazari et al., 2007). The pore size of the membrane must be selected appropriately for the used enzyme and the molecular weight of the undesired compounds. The pore size must be such as to retain the enzyme on the membrane's surface and to prevent it from passing through the membrane, so as to allow the bioreaction. Furthermore, the pores should be large enough to allow the products to pass through and to retain other ingredients of the reaction mixture. For example, commercially available nylon membrane with a pore diameter of 0.2 μm was used for covalent immobilization of laccase from *Trametes versicolor*. The bioremediation of bisphenol A was investigated under isothermal and non-isothermal conditions. After one hour of the process in non-isothermal conditions, over 95% of the BPA was degraded. It was also found that increasing the concentration of bisphenol caused a decrease in the efficiency of the membrane, due to overcrowding of the substrate molecules. Nevertheless, it was shown that the membrane was able to fully retain high-molecular-weight products of the reaction, as these compounds were not detected in the effluent (Mita et al., 2009).

Various materials of different origin have been used for fabrication of membranes which act as a support material for enzyme immobilization and a separation barrier in enzymatic membranes reactors. The production of a membrane based on the selected materials should be simple and such material should be characterized by mechanical resistance to ensure the long-term operational stability of the membrane. From this point of view, in our opinion, synthetic polymers should particularly attract growing attention as to fulfill the abovementioned requirements and moreover offer the presence of numerous functional groups which enhance enzyme immobilization and may affect selective membrane separation. However, the main drawback of the polymeric materials as membranes is their tendency to undergo fouling, which is highly undesirable as it could affect both the catalytic conversion and flux properties. Aside from membrane materials, another important factor which has to be taken under consideration during membrane selection is its pore size, which on the one hand ensures enzyme retention but on the other hand must ensure high flux-regime to reduce operational time of the process and avoid enzyme inhibition. Membranes with different pore sizes are used as supports in EMRs, however, we strongly believe that the polymeric micro- and ultrafiltration membranes are most suitable for both enzyme immobilization and removal/separation of environmental pollutants, due to their pore size as well as mechanical and operational stability. Moreover, we would like to add that in the recently published studies there is generally little information related to the costs of the membranes for use in EMRs as they depend on membrane material,

bioreactor operational mode and energy demand. Nevertheless, based on the available data, it has been assumed that the total costs of the membrane for use in bioreactor should not exceed 30% of the total costs of bioreactor construction (Young et al., 2013; Lo et al., 2015).

3.2.2. EMRs operational modes

Apart from the type of the support material and the type of membrane used, the configuration of an enzymatic reactor also has a significant impact on its operational effectivity. There are two main types of configuration for EMRs: (i) a reactor integrated with a membrane operation unit and (ii) a reactor with a membrane used as an active catalytic and separation unit (Lopez et al., 2002). Both configurations can operate in batch and continuous mode. In the case of the reactor with a membrane operation unit, immobilized enzymes usually circulate freely in the operational volume of the bioreactor. After the biocatalytic process, immobilized biomolecules are fully retained on the retentate side following membrane filtration and are easy to reuse in the next catalytic cycle. In the case of EMRs, in which the membrane is used as a simultaneous catalytic and separation unit, enzymes are immobilized on the surface of the membrane or are loaded inside its pores. An enzymatic membrane reactor with laccase immobilized onto a ceramic membrane, operating in continuous mode, was designed by Arca-Ramos et al. (2015). The continuous removal of toxic compounds was carried out from synthetic and actual biologically treated wastewaters at pH 6 and temperature of 25 °C, for 48 h. After that time 97% and over 70% of BPA was removed from the model and actual solution, respectively. In contrast, a study by Katuri et al. (2009) present the use of a batch mode reactor with laccase from *Pleurotus ostreatus* 1804 immobilized in a chitosan membrane for decolorization of Acid Black 10 BX. The optimal process parameters for each batch of the degradation cycle were established as follows: pH 6, temperature 30 °C and 2 h process duration. Under these conditions, over 95% of the dye was removed. Moreover, it was found that the EMR with immobilized laccase operating in batch mode was characterized by a short contact time and ensured reusability of the immobilized biocatalyst for a number of cycles. It also exhibited excellent operational stability in repeated applications of the immobilized laccase and achieved high efficiency of dye removal. Although both solutions with enzyme immobilized “over” and “onto/in” membrane are interesting, in order to avoid additional expenses and to simplify the process and the equipment, we encourage to develop solutions which utilize membranes as simultaneous catalytic and separation unit. Moreover, the use of such systems allows to obtain a stream of products characterized by higher purity.

3.2.3. Immobilization techniques for EMRs

In comparison with enzymatic membrane reactors with free biomolecules, EMRs with biocatalysts immobilized in the membrane or onto its surface can significantly improve the reusability of enzymes and limit their inhibition by product molecules. The technique of immobilization, and consequently the form of the immobilized enzyme, used to produce biocatalytic systems for EMRs is determined mainly by the reactor configuration, but increasing the quantity of protein usually increases the catalytic activity until it reaches the maximum, after which the binding of additional amounts of the enzyme does not improve the catalytic properties (Rekuc et al., 2010). Enzyme molecules can be immobilized in or on the membrane *via* covalent bonds as well as by various non-covalent interactions, such as electrostatic or hydrophobic adsorption and hydrogen bonds, or by entrapment (Zhao et al., 2014). Nevertheless, enzymes for use in EMRs are immobilized mainly by covalent binding or adsorption to ensure stable binding and reusability of the biocatalytic system. For example, an efficient technology was developed based on an EMR with laccase from *Myceliophthora thermophila* covalently immobilized with the use of polyethersulfone membrane for continuous removal of estrogenic compounds from wastewaters. The immobilized enzyme enabled the effective conversion of estrone, 17-β-estradiol and 17-α-ethinylestradiol with efficiencies over 80%. Moreover, the immobilized biocatalysts exhibited improved thermal stability and excellent operational stability, allowing the enzymatic membrane reactor to operate effectively for 100 h, which confirms its high productivity and potential as an enzymatic reactor system (Lloret et al., 2013a, 2013b, 2013c). As immobilization is carried out using covalent binding, a study associated with the optimization of the amount of immobilized biocatalysts and some surface modification of the membrane to increase enzyme-membrane distance should be performed to achieve higher removal efficiency.

However, enzyme immobilization using membranes as support materials is also a promising method for co-immobilization of biocatalysts, because it can be carried out under mild conditions in a single step and the formed interactions maintain the enzymatic activity at a high level (Luo et al., 2014b). The co-immobilization involves the integration of at least two types of enzymes immobilized on the same matrix to increase the catalytic ability of the system for the conversion of compounds (Morthensen et al., 2017). A very good example of this technique was reported by Escalona et al. (2014). Laccase from *Trametes versicolor* and horseradish peroxidase were co-immobilized by adsorption onto the surface of a polyamide NF270 commercial membrane to facilitate the removal of bisphenol A. It was found that over 95% of the BPA was removed after 3 h of the process at the temperature of 30 °C and pH 7. The EMR coupled with an enzyme recycling system was tested and found to achieve a similar removal efficiency to that of a classic membrane reactor with co-immobilized laccase and horseradish peroxidase. The nanofiltration membrane retained the products of BPA remediation and produced an effluent of high purity. Additionally, only approx. 30% flux decay was observed. The results show that the system is very interesting from the point of view of potential large-scale applications.

Attention should also be paid to the immobilization of enzymes in membranes using a simple and effective method based on membrane fouling. The immobilization technique presented in Fig. 4 is based on adsorption and/or entrapment of the biomolecules in the pores of the membrane and/or on its surface, and is called fouling-induced enzyme immobilization (Luo et al., 2013, 2015).

Based on the above-mentioned examples, it can be briefly concluded, that enzymatic membranes reactors (EMRs) based on the immobilized oxidoreductases still attract increasing attention for application in conversion and removal of environmental pollutants over recent years. Pure and less toxic effluents can be obtained mainly due to the fact that high bioremoval efficiencies can be achieved under mild conditions and due to simultaneous bioconversion and separation of reaction mixture. This results from the selection of the most suitable operational mode, membrane and technique of the immobilization. As it was presented above, two operational modes are applied, however, in our opinion, a bioreactor with a membrane acting as an biocatalytic and separation unit should be of particular attention. In this solution, there is no need to use additional support material because the membrane is the matrix for the biomolecules. To ensure high operational efficiency of the EMRs, stable and mechanically resistant membranes are required. Attention should be paid to the polymeric, commercially available membranes due to their availability and possibility of selection of membranes with desired pores size. These membranes also offer the presence of functional groups on their surface and in the pores, which enhance the formation of covalent bonds. Formation of covalent linkage prevents enzyme leakage and usually increases the reusability of the system. Nevertheless, it should be emphasized that after proper selection of operational conditions, various environmental pollutants, such as dyes, phenols, bisphenols and even estrogenes can be removed with efficiencies usually exceeding 90%. It should be added that enzymatic membranes reactors are also used in different branches of life sciences and industry, such as pharmacy, chemical synthesis or biomass conversion. This fact confirms the flexibility and significance of the EMRs-based approaches in their application at the broad industrial scale.

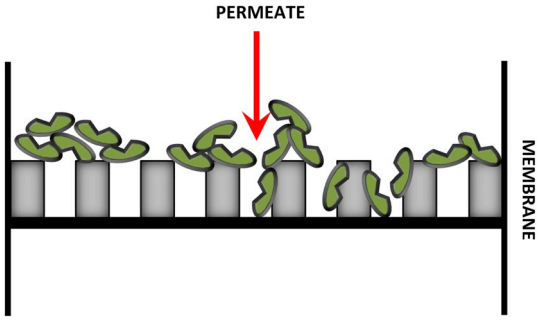

Fig. 4. Graphical representation of fouling-induced enzyme immobilization.

4. General remarks and future perspectives

Environmental pollutants, including a wide range of phenolic compounds as well as natural and synthetic dyes, are produced as waste substances by many branches of industry and consequently these compounds occur in waters and soils. Their removal at an industrial scale, in green and sustainable ways, has become an important problem over recent years, which might be solved by the use of free or immobilized biocatalysts such as laccases or tyrosinases. These enzymes are able to convert numerous pollutants of environmental concern into less toxic derivatives. To achieve high bioconversion efficiency, more advanced solutions, based on immobilized oxidoreductases, have been developed. Thus, in this review, we have presented brief information regarding simultaneous sorption and biodegradation processes as well as the use of bioreactors with immobilized enzymes for bioremediation processes. We have highlighted the advantages of these processes and established that with their use:

(i) bioconversion of environmental pollutants is carried out under mild conditions, without organic solvents, in line with the principles of green chemistry;
(ii) total conversion of hazardous pollutants into less toxic compounds can be achieved;
(iii) biodegradation can be carried out in more efficient and cost-effective ways;
(iv) one-step removal and separation of toxic compounds and their conversion products can be achieved, to obtain an effluent stream of high purity.

Information concerning support materials, immobilization techniques, and the equipment and operational modes of bioreactors used for the biodegradation of toxic compounds has also been presented which allowed to indicate the most suitable solutions for achievement of high process efficiency. We have also summarized the criteria for the selection of factors which enable the production of highly stable and highly resistant biocatalytic systems for the removal processes.

Although many methods which apply free or immobilized enzymes for the biodegradation of hazardous compounds have been reported, there is still a need to develop more advanced solutions that increase the efficiency and cost-effectiveness of the removal process. Application of enzymatic bioreactors and simultaneous separation and catalytic conversion to be a promising option for large-scale bioremediation processes under mild conditions in the future appears (meaning that the reactions can be accomplished at the natural water temperature and pH), in accordance with the rules of green chemistry. In contrast to "industrial manufacture" processes, the discussed processes are focused on the removal of undesirable compounds but not necessarily on the production of a commercial product, hence particular attention has to be paid to the operational efficiency and maximal conversion. Thus, further studies to identify the most suitable and most long-term robust carriers for oxidoreductases are required. Future development of support/sorbent materials will be focused on use of microporous nanomaterials and their modification for: (i) targeting enzyme immobilization, to retain high catalytic properties and (ii) selective sorption of pollutants, by ensuring higher affinity of the sorbent to the molecules of toxic compounds. Also hybrid/composite materials will be intensively studied in future due to the possibility of fabrication of tailored support, with desired properties for both enzyme immobilization and adsorption. This will improve the biodegradation efficiency even more and reduce the time and costs of the process. We strongly believe that further study leading to new enzymes development will be carried out, as there is still a need to look for oxidoreductases characterized by high long-term and operational stability. Moreover, the mechanism of catalytic conversion and oxygen/hydrogen peroxide supply for oxidoreductases will be investigated in order to obtain high biocatalysts efficiency. Future development of enzymatic reactors will be focused on new, stable and reusable membranes with numerous functional groups for stable binding of the biocatalysts. In our opinion, the application of the solution using membrane as a support for immobilization of oxidoreductase and, simultaneously, as separation unit will also be more common. This solution enhances the bioconversion efficiency and allows to obtain pure streams of effluents. Moreover, future investigations will focus on the implementations of the developed solutions at large-scale applications for the bioremediation of wastewaters. We hope that this review may provide certain suggestions and ideas for the design and implementation of novel, more efficient solutions for detoxification processes of actual wastewaters with the use of immobilized oxidoreductases.

Acknowledgements

This work was supported by research grant funds from the National Science Center Poland in accordance with decision no. DEC-2015/19/N/ST8/02220.

References

Abejon, R., De Cazes, M., Belleville, M.P., Sanchez-Marcano, J., 2015. Large-scale enzymatic membrane reactors for tetracycline degradation in WWTP effluents. Water Res. 73, 118–131.
Adeel, M., Song, X., Wang, Y., Francis, D., Yang, Y., 2017. Environmental impact of estrogens on human, animal and plant life: a critical review. Environ. Int. 99, 107–119.
Adeel, M., Bilal, M., Rasheed, T., Sharma, A., Iqbal, H.M.N., 2018. Graphene and graphene oxide: functionalization and nano-bio-catalytic system for enzyme immobilization and biotechnological perspective. Int. J. Biol. Macromol. 120, 1430–1440.
Aguilar, D.L., Rodríguez-Jasso, R.M., Zanuso, E., Lara-Flores, A.A., Aguilar, C.N., Sanchez, A., Ruiz, H.A., 2018. Operational strategies for enzymatic hydrolysis in a biorefinery. Biorefin. Biomass Biofuel. 14, 223–248.
Agustian, J., Kamaruddin, A.H., Bhatia, S., 2011. Enzymatic membrane reactors: the determining factors in two separate phase operations. J. Chem. Technol. Biotechnol. 86, 1032–1048.
Ahmad, A., Mohd-Setapar, S.H., Chuong, C.S., Khatoon, A., Wani, W.A., Kumar, R., Rafatullah, M., 2015. Recent advances in new generation dye removal technologies: novel search for approaches to reprocess wastewater. RSC Adv. 5, 30801–30818.
Al-Jabari, M., Iqefan, N., Zahdeh, N., Dweik, H., 2017. Adsorption of organic pollutants from dairy wastewater on soil: pollution problem and control. Int. J. Global Environ. Issues 16, 149–161.
Al-Kaidy, H., Tippkotter, N., 2016. Superparamagnetic hydrophobic particles as shell material for digital microfluidic droplets and proof-of-principle reaction assessments with immobilized laccase. Eng. Life Sci. 16, 222–230.
Al-Khalid, T., El-Naas, M., 2012. Aerobic biodegradation of phenols: a comprehensive review. Crit. Rev. Environ. Sci. Technol. 42, 1631–1690.
Almeida, C., Branyik, T., Moradas-Ferreira, P., Teixeira, J., 2003. Continuous production of pectinase by immobilized yeast cells on spent grains. J. Biosci. Bioeng. 96, 513–518.
Anku, W.W., Mamo, M.A., Govender, P.P., 2017. Phenolic compounds in water: sources, reactivity, toxicity and treatment methods. In: Soto-Hernández, M., Tenango, M.P., García-Mateos, R. (Eds.), Phenolic Compounds Natural Sources, Importance and Applications. InTech, London, pp. 419–443.
Antecka, K., Zdarta, J., Siwińska-Stefańska, K., Sztuk, G., Jankowska, E., Oleskowicz-Popiel, P., Jesionowski, T., 2018. Synergistic degradation of dye wastewaters using binary or ternary oxide systems with immobilized laccase. Catalysts 8, 402–420.
Arca-Ramos, A., Eibes, G., Feijoo, G., Lema, J.M., Moreira, M.T., 2015. Potentiality of a ceramic membrane reactor for the laccase-catalyzed removal of bisphenol a from secondary effluents. Appl. Microbiol. Biotechnol. 99, 9299–9308.

Ba, S., Kumar, V.V., 2017. Recent developments in the use of tyrosinase and laccase in environmental applications. Crit. Rev. Biotechnol. 37, 819–832.
Ba, S., Arsenault, A., Hassani, T., Jones, P., Cabana, H., 2013. Laccase immobilization and insolubilization: from fundamentals to applications for the elimination of emerging contaminants in wastewater treatment. Crit. Rev. Biotechnol. 33, 404–418.
Baiocco, P., Barreca, A.M., Fabbrini, M., Galli, C., Gentili, P., 2006. Promoting laccase activity towards non-phenolic substrates: a mechanistic investigation with some laccase-mediator systems. Org. Biomol. Chem. 1, 191–197.
Balcao, V.M., Paiva, A.L., Malcata, F.X., 1996. Bioreactors with immobilized lipases: state of the art. Enzym. Microb. Technol. 18, 392–416.
Baldrian, P., 2005. Fungal laccases: occurrence and properties. FEMS Microbiol. Rev. 30, 215–242.
Barbosa, O., Torres, R., Ortiz, C., Berenguer-Murcia, A., Rodrigues, R.C., Fernandez-Lafuente, R., 2013. Heterofunctional supports in enzyme immobilization: from traditional immobilization protocols to opportunities in tuning enzyme properties. Biomacromology 14, 2433–2462.
Barbosa, O., Ortiz, C., Berenguer-Murcia, Á., Torres, R., Rodrigues, R.C., Fernandez-Lafuente, R., 2014. Glutaraldehyde in bio-catalysts design: a useful crosslinker and a versatile tool in enzyme immobilization. RSC Adv. 4, 1583–1600.
Barrios-Estrada, C., de Jesús Rostro-Alanis, M., Muñoz-Gutiérrez, B.D., Iqbal, H.M.N., Kannan, S., Parra-Saldívar, R., 2018a. Emergent contaminants: endocrine disruptors and their laccase-assisted degradation-a review. Sci. Total Environ. 612, 1516–1531.
Barrios-Estrada, C., Rostro-Alanis, M.J., Parra, A.L., Belleville, M.P., Sanchez-Marcano, J., Iqbal, H.M.N., Parra-Saldívar, R., 2018b. Potentialities of active membranes with immobilized laccase for Bisphenol A degradation. Int. J. Biol. Macromol. 108, 837–844.
Becker, D., Giustina, S.V.D., Rodriguez-Mozaz, S., Schoevaart, R., Barcelo, D., de Cazes, M., Belleville, M.P., Sanchez-Marcano, J., de Gunzburg, J., Couillerotf, O., Völker, J., Oehlmann, J., Wagner, M., 2016. Removal of antibiotics in wastewater by enzymatic treatment with fungal laccase – degradation of compounds does not always eliminate toxicity. Bioresour. Technol. 219, 500–509.
Benz, G.T., 2011. Bioreactor design for chemical engineers. Am. Inst. Chem. Eng. 1, 21–26.
Bhatnagar, A., Sillanpaa, M., 2010. Utilization of agroindustrial and municipal waste materials as potential adsorbents for water treatment – a review. Chem. Eng. J. 157, 277–296.
Bilal, M., Iqbal, H.F.Z., 2019. Naturally-derived biopolymers: potential platforms for enzyme immobilization. Int. J. Biol. Macromol. https://doi.org/10.1016/j.ijbiomac.2019.02.152. (article in press).
Bilal, M., Asgher, M., Iqbal, H.M.N., Hua, H., Zhang, X., 2016. Chitosan beads immobilized manganese peroxidase catalytic potential for detoxification and decolorization of textile effluent. Int. J. Biol. Macromol. 89, 181–189.
Bilal, M., Asgher, M., Parra-Saldivar, R., Hu, H., Wang, W., Zhang, X., Iqbal, H.M.N., 2017a. Immobilized ligninolytic enzymes: an innovative and environmental responsive technology to tackle dye-based industrial pollutants – a review. Sci. Total Environ. 576, 646–659.
Bilal, M., Iqbal, H.M.N., Hu, H., Wang, W., Zhang, X., 2017b. Development of horseradish peroxidase-based cross-linked enzyme aggregates and their environmental exploitation for bioremediation purposes. J. Environ. Manag. 188, 137–143.
Bilal, M., Rasheed, T., Iqbal, H.M.N., Hu, H., Wang, W., Zhang, X., 2017c. Novel characteristics of horseradish peroxidase immobilized onto the polyvinyl alcohol-alginate beads and its methyl orange degradation potential. Int. J. Biol. Macromol. 105, 328–335.
Bilal, M., Asgher, M., Iqbal, H.M.N., Hu, H., Wang, W., Zhang, X., 2017d. Bio-catalytic performance and dye-based industrial pollutants degradation potential of agarose-immobilized MnP using a packed bed reactor system. Int. J. Biol. Macromol. 102, 582–590.
Bilal, M., Rasheed, T., Iqbal, H.M.N., Yan, Y., 2018a. Peroxidases-assisted removal of environmentally-related hazardous pollutants with reference to the reaction mechanisms of industrial dyes. Sci. Total Environ. 644, 1–13.
Bilal, M., Rasheed, T., Iqbal, H.M.N., Hu, H., Wang, W., Zhang, X., 2018b. Horseradish peroxidase immobilization by copolymerization into cross-linked polyacrylamide gel and its dye degradation and detoxification potential. Int. J. Biol. Macromol. 113, 983–990.
Bilal, M., Iqbal, H.M.N., Guo, S., Hu, H., Wang, W., Zhang, X., 2018c. State-of-the-art protein engineering approaches using biological macromolecules: a review from immobilization to implementation view point. Int. J. Biol. Macromol. 108, 893–901.
Bilal, M., Zhao, Y., Rasheed, T., Iqbal, H.M.N., 2018d. Magnetic nanoparticles as versatile carriers for enzymes immobilization: a review. Int. J. Biol. Macromol. 120, 2530–2544.
Bilal, M., Rasheed, T., Zhao, Y., Iqbal, H.M.N., Cui, J., 2018e. “Smart” chemistry and its application in peroxidase immobilization using different support materials. Int. J. Biol. Macromol. 119, 278–290.
Bilal, M., Rasheed, T., Zhao, Y., Iqbal, H.M.N., 2019a. Agarose-chitosan hydrogel-immobilized horseradish peroxidase with sustainable bio-catalytic and dye degradation properties. Int. J. Biol. Macromol. 124, 742–749.
Bilal, M., Adeel, M., Rasheed, T., Zhao, Y., Iqbal, H.M.N., 2019b. Emerging contaminants of high concern and their enzyme-assisted biodegradation – a review. Environ. Int. 124, 336–353.
Bilal, M., Asgher, M., Cheng, H., Yan, Y., Iqbal, H.M.N., 2019c. Multi-point enzyme immobilization, surface chemistry, and novel platforms: a paradigm shift in biocatalyst design. Crit. Rev. Biotechnol. 39, 202–219.
Bilal, M., Rasheed, T., Nabeel, F., Iqbal, H.M.N., Zhao, Y., 2019d. Hazardous contaminants in the environment and their laccase-assisted degradation - a review. J. Environ. Manag. 15, 253–264.
Bolivar, J.M., Wiesbauer, J., Nidetzky, B., 2011. Biotransformations in microstructured reactors: more than flowing with the stream? Trends Biotechnol. 29, 333–342.
Brindle, K., Stephenson, T., 1996. The application of membrane biological reactors for the treatment of waste-waters. Biotechnol. Bioeng. 49, 601–610.
Bronikowski, A., Hagedoorn, P.L., Koschorreck, K., Urlacher, V.B., 2017. Expression of a new laccase from *Moniliophthora roreri* at high levels in *Pichia pastoris* and its potential application in micropollutant degradation. AMB Express 73, 1–13.
Busca, G., Berardinelli, S., Resini, C., Arrighi, L., 2008. Technologies for the removal of phenol from fluid streams: a short review of recent developments. J. Hazard. Mater. 160, 265–288.
Butterfield, D.A., Bhattacharyya, D., Daunert, S., Bachas, L.G., 2001. Catalytic biofunctional membranes containing site-specifically immobilized enzyme arrays. J. Membr. Sci. 181, 29–37.
Cabana, H., Alexandre, C., Agathos, S.N., Jones, J.P., 2009a. Immobilization of laccase from the white rot fungus *Coriolopsis polyzona* and use of the immobilized biocatalyst for the continuous elimination of endocrine disrupting chemicals. Bioresour. Technol. 100, 3447–3458.
Cabana, H., Jones, J.P., Agathos, S.N., 2009b. Utilization of cross-linked laccase aggregates in a perfusion basket reactor for the continuous elimination of endocrine-disrupting chemicals. Biotechnol. Bioeng. 102, 1582–1592.
Castellana, G., Loffredo, E., 2014. Simultaneous removal of endocrine disruptors from a wastewater using white rot fungi and various adsorbents. Water Air Soil Pollut. 225, 1872–1884.
Champagne, P.P., Ramsay, J.A., 2007. Reactive blue 19 decolouration by laccase immobilized on silica beads. Appl. Microbiol. Biotechnol. 77, 819–823.
Chao, C., Guan, H., Zhang, J., Liu, Y., Zhao, Y., Zhang, B., 2018. Immobilization of laccase onto porous polyvinyl alcohol/halloysite hybrid beads for dye removal. Water Sci. Technol. 77, 809–818.
Choi, K.J., Kim, S.G., Kim, S.H., 2008. Removal of antibiotics by coagulation and granular activated carbon filtration. J. Hazard. Mater. 151, 38–43.
Chung, T.P., Tseng, H.Y., Juang, R.S., 2003. Mass transfer effect and intermediate detection for phenol degradation in immobilized *Pseudomonas putida* systems. Process Biochem. 38, 1497–1507.
Costa, S.A., Reis, R.L., 2004. Immobilisation of catalase on the surface of biodegradable starch-based polymers as a way to change its surface characteristics. J. Mater. Sci. Mater. Med. 15, 335–342.
Costa, J.B., Lima, M.J., Sampaio, M.J., Neves, M.C., Faria, J.L., Morales-Torres, S., Tavares, A.P.M., Silva, C.G., 2019. Enhanced biocatalytic sustainability of laccase by immobilization on functionalized carbon nanotubes/polysulfone membranes. Chem. Eng. J. 355, 974–985.
Crini, G., 2006. Non-conventional low-cost adsorbents for dye removal: a review. Bioresour. Technol. 97, 1061–1085.
Cruz-Morato, C., Lucas, D., Llorca, M., Rodriguez-Mozaz, S., Gorga, M., Petrovic, M., Barceló, D., Vicent, T., Sarrà, M., Marco-Urrea, M., 2014. Hospital wastewater treatment by fungal bioreactor: removal efficiency for pharmaceuticals and endocrine disruptor compounds. Sci. Total Environ. 493, 365–376.
D’Acunzo, F., Galli, C., Gentili, P., Sergi, F., 2006. Mechanistic and steric issues in the oxidation of phenolic and non-phenolic compounds by laccase or laccase-mediator systems. The case of bifunctional substrates. New J. Chem. 30, 583–591.
Dai, Y., Yao, J., Song, Y., Liu, X., Wang, S., Yuan, Y., 2016. Enhanced performance of immobilized laccase in electrospun fibrous membranes by carbon nanotubes modification and its application for bisphenol a removal from water. J. Hazard. Mater. 317, 485–493.
Darnoko, D., Cheryan, M., 2000. Kinetics of palm oil transesterification in a batch reactor. J. Amer. Oil Chem. Soc. 77, 1263–1267.
Dayaram, P., Dasgupta, D., 2008. Decolorisation of synthetic dyes and textile wastewater using *Polyporus rubidus*. J. Environ. Biol. 29, 831–836.
de Cazes, M., Belleville, M.P., Mougel, M., Kellner, H., Sanchez-Marcano, J., 2015. Characterization of laccase-grafted ceramic membranes for pharmaceuticals degradation. J. Membr. Sci. 476, 384–393.
Diano, N., Grano, V., Fraconte, L., Caputo, P., Ricupito, A., Attanasio, A., Bianco, M., Bencivenga, U., Rossi, S., Manco, I., Mita, L., Del Pozzo, G., Mita, D.G., 2007. Non-isothermal bioreactors in enzymatic remediation of waters polluted by endocrine disruptors: BPA as a model of pollutant. Appl. Catal. B Environ. 69, 252–261.
Ding, H., Wu, Y., Zou, B., Lou, Q., Zhang, Q., Zhong, J., Lu, L., Dai, G., 2016. Simultaneous removal and degradation characteristics of sulfonamide, tetracycline, and quinolone antibiotics by laccase-mediated oxidation coupled with soil adsorption. J. Hazard. Mater. 307, 350–358.
Du, F., Li, Z., Zhang, A., 2013. Study on advanced treatment of pharmaceutical wastewater by fluidized bed laccase bioreactor. J. Chem. Pharm. Res. 5, 223–227.
Durante, D., Casadio, R., Martelli, L., Tasco, G., Portaccio, M., de Luca, P., Bencivenga, U., Rossi, S., Di Martino, S., Grano, V., Diano, N., Mita, D.G., 2004. Isothermal and non-isothermal bioreactors in the detoxification of wastewaters polluted by aromatic compounds by means of immobilized laccase from *Rhus vernicifera*. J. Mol. Catal. B Enzym. 27, 191–206.
Ensuncho, L., Alvarez-Cuenca, M., Legge, L.R., 2005. Removal of aqueous phenol using immobilized enzymes in a bench scale and pilot scale three-phase fluidized bed reactor. Bioprocess Biosyst. Eng. 27, 185–191.
Escalona, I., de Grooth, J., Font, J., Nijmeijer, K., 2014. Removal of BPA by enzyme polymerization using NF membranes. J. Membr. Sci. 468, 192–201.
Faccio, G., Kruus, K., Saloheimo, M., Thöny-Meyer, L., 2012. Bacterial tyrosinases and their applications. Process Biochem. 47, 1749–1760.
Fernández-Lorente, G., Palomo, J.M., Mateo, C., Munilla, R., Ortiz, C., Cabrera, Z., Guisán, J.M., Fernández-Lafuente, R., 2006. Glutaraldehyde cross-linking of lipases adsorbed on aminated supports in the presence of detergents leads to improved performance. Biomacromology 7, 2610–2615.
Gallucci, F., Basile, A., Hai, F.I., 2011. Membranes for Membrane Reactors: Preparation,

Optimization and Selection. Wiley InterScience, New Jersey.
Ganaie, M.A., Rawat, H.K., Wani, O.A., Gupta, U.S., Kango, J., 2014. Immobilization of fructosyl transferase by chitosan and alginate for efficient production of fructooligosaccharides. Process Biochem. 49, 840–844.
Gao, Z., Du, B., Zhang, G., Gao, Y., Li, Z., Zhang, H., Duan, X., 2011. Adsorption of pentachlorophenol from aqueous solution on dodecylbenzenesulfonate modified nickel–titanium layered double hydroxide nanocomposites. Ind. Eng. Chem. Res. 50, 5334–5345.
Gasser, C., Yu, L., Svojitka, J., Wintgens, T., Ammann, E., Shahgaldian, P., Corvini, P.X., Hommes, G., 2014. Advanced enzymatic elimination of phenolic contaminants in wastewater: a nano approach at field scale. Appl. Microbiol. Biotechnol. 98, 3305–3316.
Georgieva, S., Godjevargova, T., Mita, T.G., Diano, N., Menale, C., Nicolucci, C., Carratelli, C.R., Mita, L., Golovinsky, E., 2010. Non-isothermal bioremediation of waters polluted by phenol and some of its derivatives by laccase covalently immobilized on polypropylene membranes. J. Mol. Catal. B Enzym. 66, 210–218.
Girelli, A.M., Mattei, E., Messina, A., 2006. Phenols removal by immobilized tyrosinase reactor in on-line high performance liquid chromatography. Anal. Chim. Acta 580, 271–277.
Guo, W., Ngo, H.-H., Li, J., 2012. A mini-review on membrane fouling. Bioresour. Technol. 122, 27–34.
Hai, F.I., Yamamoto, K., Fukushi, K., 2007. Hybrid treatment systems for dye wastewater. Crit. Rev. Environ. Sci. Technol. 37, 315–377.
He, Z., Miller, D.J., Kasemset, S., Paul, D.R., Freeman, B.D., 2017. The effect of permeate flux on membrane fouling during microfiltration of oily water. J. Membr. Sci. 525, 25–34.
Heberer, T., 2002. Occurrence, fate, and removal of pharmaceutical residues in the aquatic environment: a review of recent research data. Toxicol. Lett. 131, 5–17.
Hernandez, K., Fernandez-Lafuente, R., 2011. Control of protein immobilization: coupling immobilization and site-directed mutagenesis to improve biocatalyst or biosensor performance. Enzym. Microb. Technol. 48, 107–122.
Homem, V., Santos, L., 2011. Degradation and removal methods of antibiotics from aqueous matrices – a review. J. Environ. Manag. 92, 2304–2347.
Hou, J., Dong, G., Ye, Y., 2014. Enzymatic degradation of bisphenol-A with immobilized laccase on TiO_2 sol-gel coated PVDF membrane. J. Membr. Sci. 469, 19–30.
Husain, Q., 2017. Nanomaterials as novel supports for the immobilization of amylolytic enzymes and their applications: a review. Biocatal 3, 37–53.
Husain, M., Husain, Q., 2008. Applications of redox mediators in the treatment of organic pollutants by using oxidoreductive enzymes: a review. Crit. Rev. Environ. Sci. Technol. 38, 1–42.
Ihekata, K., Nicell, J.A., 2000. Characterization of tyrosinase for the treatment of aqueous phenols. Bioresour. Technol. 74, 191–199.
Illaes, A., Wilson, L., 2003. Enzyme reactor design under thermal inactivation. Crit. Rev. Biotechnol. 23, 61–93.
Imran, A., Asim, M., Tabrez, A.K., 2012. Low cost adsorbents for the removal of organic pollutants from wastewater. J. Environ. Manag. 113, 170–183.
Jahangiri, E., Reichelt, S., Thomas, I., Hausmann, K., Schlosser, D., Schulze, A., 2014. Electron beam-induced immobilization of laccase on porous supports for wastewater treatment applications. Molecules 19, 11860–11882.
Javid, A., Mesdaghinia, A., Nasseri, S., Mahvi, A.H., Alimohammadi, M., Gharibi, H., 2016. Assessment of tetracycline contamination in surface and groundwater resources proximal to animal farming houses in Tehran, Iran. J. Environ. Health Sci. Eng. 14, 4–9.
Jesionowski, T., Zdarta, J., Krajewska, B., 2014. Enzymes immobilization by adsorption: a review. Adsorption 20, 801–821.
Ji, C., Hou, J., Chen, V., 2016. Cross-linked carbon nanotubes-based biocatalytic membranes for micro-pollutants degradation: performance, stability, and regeneration. J. Membr. Sci. 520, 869–880.
Jochems, P., Satyawali, Y., Diels, L., Dejonghe, W., 2011. Enzyme immobilization on/in polymeric membranes: status, challenges and perspectives in biocatalytic membrane reactors (BMRs). Green Chem. 13, 1609–1623.
Jolivalt, C., Brenon, S., Caminade, E., Mougin, C., Pontie, M., 2000. Immobilization of laccase from *Trametes versicolor* on a modified PVDF microfiltration membrane: characterization of the grafted support and application in removing a phenylurea pesticide in wastewater. J. Membr. Sci. 180, 103–113.
Jørgensen, H., Pinelo, M., 2017. Enzyme recycling in lignocellulosic biorefineries. Biofuels Bioprod. Biorefin. 11, 150–167.
Kandelbauer, A., Maute, O., Kessler, R.W., Erlacher, A., Gubitz, G.M., 2004. Study of dye decolorization in an immobilized laccase enzyme-reactor using online spectroscopy. Biotechnol. Bioeng. 87, 552–563.
Katuri, K.P., Mohan, S.V., Sridhar, S., Pati, B.R., Sarma, P.N., 2009. Laccase-membrane reactors for decolorization of an acid azo dye in aqueous phase: process optimization. Water Res. 43, 3647–3658.
Kim, B.C., Lee, J., Um, W., Kim, J., Joo, J., Lee, J.H., Kwak, J.H., Kim, J.H., Lee, C., Lee, H., Addleman, R.S., Hyeon, T., Gu, M.B., Kim, J., 2011. Magnetic mesoporous materials for removal of environmental wastes. J. Hazard. Mater. 192, 1140–1147.
Koyani, R.D., Vazquez-Duhalt, R., 2016. Laccase encapsulation in chitosan nanoparticles enhances the protein stability against microbial degradation. Environ. Sci. Pollut. Res. Int. 23, 18850–18857.
Krastanov, A., 2000. Removal of phenols from mixture by co-immobilized laccase/tyrosinase and Polycar adsorption. J. Ind. Microbiol. Biotechnol. 24, 383–388.
Kümmerer, K., 2009. Antibiotics in the aquatic environment – a review – Part I. Chemosphere 75, 417–434.
Land, E.J., Ramsden, C.A., Riley, P.A., 2003. Tyrosinase autoactivation and the chemistry of ortho-quinone amines. Acc. Chem. Res. 36, 300–308.
Le, T.T., Murugesan, K., Lee, C.S., Vu, C.H., Chang, Y.S., Jeon, J.R., 2016. Degradation of synthetic pollutants in real wastewater using laccase encapsulated in core–shell magnetic copper alginate beads. Bioresour. Technol. 216, 203–210.
Le-Clech, P., Chen, V., Fane, T.A.G., 2006. Fouling in membrane bioreactors used in wastewater treatment. J. Membr. Sci. 284, 17–53.
Leidig, E., Prusse, U., Vorlop, K.D., Winter, J., 1999. Biotransformation of poly R-478 by continuous cultures of PVAL- encapsulated *Trametes versicolor* under non-sterile conditions. Bioprocess Eng. 21, 5–12.
Lewanczuk, M., Bryjak, J., 2015. Continuous decolorization of Acid Blue 62 solution in an enzyme membrane reactor. Appl. Biochem. Biotechnol. 177, 237–252.
Li, X., Xu, H., Wu, Q., 2007. Large-scale biodiesel production from microalga *Chlorella protothecoides* through heterotrophic cultivation in bioreactors. Biotechnol. Bioeng. 98, 764–771.
Li, R., Gao, B., Guo, K., Yue, Q., Zheng, H., Wang, Y., 2017. Effects of papermaking sludge-based polymer on coagulation behavior in the disperse and reactive dyes wastewater treatment. Bioresour. Technol. 240, 59–67.
Liu, G., Zhang, J., Bao, J., 2016. Cost evaluation of cellulase enzyme for industrial-scale cellulosic ethanol production based on rigorous Aspen Plus modelling. Bioprocess Biosyst. Eng. 39, 133–140.
Lloret, L., Hollmann, F., Eibes, G., Feijoo, G., Moreira, M.T., Lema, J.M., 2012. Immobilisation of laccase on Eupergit supports and its application for the removal of endocrine disrupting chemicals in a packed-bed reactor. Biodegradat 23, 373–386.
Lloret, L., Eibes, G., Moreira, M.T., Feijoo, G., Lema, J.M., 2013a. On the use of a high-redox potential laccase as an alternative for thetransformation of non-steroidal anti-inflammatory drugs (NSAIDs). J. Mol. Catal. B Enzym. 97, 233–242.
Lloret, L., Eibes, G., Moreira, M.T., Feijoo, G., Lema, J.M., 2013b. Removal of estrogenic compounds from filtered secondary wastewater effluent in a continuous enzymatic membrane reactor. Identification of biotransformation products. Environ. Sci. Technol. 2013, 4536–4543.
Lloret, L., Eibes, G., Moreira, M.T., Feijoo, G., Lema, J.M., Miyazaki, M., 2013c. Improving the catalytic performance of laccase using a novel continuous-flow microreactor. Chem. Eng. J. 223, 497–506.
Lo, C.H., McAdam, E., Judd, S., 2015. The cost of a small membrane bioreactor. Water Sci. Technol. 2015, 1739–1746.
Loffredo, E., Senesi, N., 2006. In Viable Methods of Soil and Water Pollution Monitoring, Protection and Remediation. Springer, Dordrecht.
Loffredo, E., Castellana, G., Senesi, N., 2014. Decontamination of a municipal landfill leachate from endocrine disruptors using a combined sorption/bioremoval approach. Environ. Sci. Pollut. Res. 21, 2654–2662.
Lonappan, L., Pulicharla, R., Rouissi, T., Brar, S.K., Verma, M., Surampalli, R.Y., Valero, J.R., 2016. Diclofenac in municipal wastewater treatment plant: quantification using laser diode thermal desorption – atmospheric pressure chemical ionization – tandem mass spectrometry approach in comparison with an established liquid chromatography electrospray ionization – tandem mass spectrometry method. J. Chromatogr. A 1433, 106–113.
Lopez, C., Mielgo, I., Moreira, M.T., Feijoo, G., Lemo, J.M., 2002. Enzymatic membrane reactors for biodegradation of recalcitrant compounds. Application to dye decolourization. J. Biotechnol. 99, 249–257.
Luckarift, H.R., 2008. Silica-immobilized enzyme reactors. J. Liquid Chromat. Related Technol. 31, 1568–1592.
Luo, J., Meyer, A.S., Jonsson, G., Pinelo, M., 2013. Fouling-induced enzyme immobilization for membrane reactors. Bioresour. Technol. 147, 260–268.
Luo, J., Meyer, A.S., Jonsson, G., Pinelo, M., 2014a. Enzyme immobilization by fouling in ultrafiltration membranes: impact of membrane configuration and type on flux behavior and biocatalytic conversion efficacy. Biochem. Eng. J. 83, 79–89.
Luo, J., Marpani, F., Brites, R., Frederiksen, L., Meyer, A.S., Jonsson, G., Pinelo, M., 2014b. Directing filtration to optimize enzyme immobilization in reactive membranes. J. Membr. Sci. 459, 1–11.
Luo, J., Meyer, A.S., Mateiu, R.V., Pinelo, M., 2015. Cascade catalysis in membranes with enzyme immobilization for multienzymatic conversion of CO_2 to methanol. New Biotechnol. 32, 319–327.
Lyons, M.E.G., 2003. Mediated electron transfer at redox active monolayers. Part 4: kinetics of redox enzymes coupled with electron mediators. Sensors 3, 19–42.
Marshall, A.D., Munro, P.A., Tragardh, G., 1993. The effect of protein fouling in microfiltration and ultrafiltration on permeate flux, protein retention, and selectivity: a literature review. Desal 1993 (91), 65–108.
Martínez-Hernández, V., Meffe, R., López, S.H., de Bustamante, I., 2016. The role of sorption and biodegradation in the removal of acetaminophen, carbamazepine, caffeine, naproxen and sulfamethoxazole during soil contact: a kinetics study. Sci. Total Environ. 556, 232–241.
Mateo, C., Grazu, V., Palomo, J.M., Lopez-Gallego, F., Fernandez-Lafuente, R., Guisan, J.M., 2007. Immobilization of enzymes on heterofunctional epoxy supports. Nat. Protoc. 2, 1022–1033.
McMorn, P., Hutchings, G.J., 2004. Heterogeneous enantioselective catalysts: strategies for the immobilisation of homogeneous catalysts. Chem. Soc. Rev. 33, 108–122.
Mita, D.G., Diano, N., Grano, V., Portaccio, M., Rossi, S., Bencivenga, U., Manco, I., Nicolucci, C., Bianco, M., Grimaldi, T., Mita, L., Georgieva, S., Godjevargova, T., 2009. The process of thermodialysis in bioremediation of waters polluted by endocrine disruptors. J. Mol. Catal. B Enzym. 58, 199–207.
Miyazaki, M., Maeda, M., 2006. Microchannel enzyme reactors and their applications for processing. Trends Biotechnol. 24, 463–470.
Moeder, M., Martin, C., Koeller, G., 2004. Degradation of hydroxylated compounds using laccase and horseradish peroxidase immobilized on microporous polypropylene hollow fiber membranes. J. Membr. Sci. 245, 183–190.
Mohammadi, M., As'habi, M.A., Salehi, P., Yousefi, M., Nazari, M., Brask, J., 2018. Immobilization of laccase on epoxy-functionalized silica and its application in biodegradation of phenolic compounds. Int. J. Biol. Macromol. 109, 443–447.

Morthensen, S.T., Meyer, A.S., Jørgensen, H., Pinelo, M., 2017. Significance of membrane bioreactor design on the biocatalytic performance of glucose oxidase and catalase: free vs. immobilized enzyme systems. Biochem. Eng. J. 15, 41–47.
Mukherjee, S., Basak, B., Bhunia, B., Dey, A., Mondalet, B., 2013. Potential use of polyphenol oxidases (PPO) in the bioremediation of phenolic contaminants containing industrial wastewater. Rev. Environ. Sci. Biotechnol. 12, 61–73.
Munk, L., Andersen, M.L., Meyer, A.S., 2018. Influence of mediators on laccase catalyzed radical formation in lignin. Enzym. Microb. Technol. 116, 48–56.
Nanba, H., Yasohara, Y., Hasegawa, J., Takahashi, S., 2007. Bioreactor systems for the production of optically active amino acids and alcohols. Org. Proc. Res. Dev. 11, 503–508.
Nazari, K., Esmaeili, N., Mahmoudi, A., Rahimi, H., Moosavi-Movahedi, A.A., 2007. Peroxidative phenol removal from aqueous solutions using activated peroxidase biocatalyst. Enzym. Microb. Technol. 41, 226–233.
Nguyen, T.A., Fu, C.C., Juang, R.S., 2016a. Effective removal of sulfur dyes from water by biosorption and subsequent immobilized laccase degradation on crosslinked chitosan beads. Chem. Eng. J. 304, 313–324.
Nguyen, L.N., Hai, F.I., Desseto, A., Richardson, C., Price, W.E., Nghiem, L.D., 2016b. Continuous adsorption and biotransformation of micropollutants by granular activated carbon-bound laccase in a packed-bed enzyme reactor. Bioresour. Technol. 210, 108–116.
Nicolucci, C., Rossi, S., Menale, C., Godjevargova, T., Ivanov, Y., Bianco, M., Mita, L., Bencivenga, U., Mita, D.G., Diano, N., 2011. Biodegradation of bisphenols with immobilized laccase or tyrosinase on polyacrylonitrile beads. Biodegrad 22, 673–683.
Niladevi, K.N., Prema, P., 2008. Immobilization of laccase from *Streptomyces psammoticus* and its application in phenol removal using packed bed reactor. World J. Microbiol. Biotechnol. 24, 1215–1222.
Niu, J., Xu, J., Dai, Y., Xu, J., Guo, H., Sun, K., Liu, R., 2013. Immobilization of horseradish peroxidase by electrospun fibrous membranes for adsorption and degradation of pentachlorophenol in water. J. Hazard. Mater. 246–247, 119–125.
Osma, J.F., Toca-Herrera, J.L., Rodriguez-Couto, S., 2010. Biodegradation of a simulated textile effluent by immobilised-coated laccase in laboratory-scale reactors. Appl. Catal. A 373, 147–153.
Østergaard, M., Lindedam, J., Dan, M., Elleskov, M., Cristina, A., Gama, M., Jørgensen, J., Felby, C., 2015. Continuous recycling of enzymes during production of lignocellulosic bioethanol in demonstration scale. Appl. Energy 159, 188–195.
Palli, L., Castellet-Rovira, F., Pérez-Trujillo, M., Caniani, D., Sarrà-Adroguer, M., Gori, R., 2017. Preliminary evaluation of *Pleurotus ostreatus* for the removal of selected pharmaceuticals from hospital wastewater. Biotechnol. Prog. 33, 1529–1537.
Palmieri, G., Giardina, P., Sannia, G., 2005. Laccase-mediated Remazol Brilliant Blue R decolorization in a fixed-bed bioreactor. Biotechnol. Prog. 21, 1436–1441.
Pang, R., Li, M., Zhang, C., 2015. Degradation of phenolic compounds by laccase immobilized on carbon nanomaterials: diffusional limitation investigation. Talanta 131, 38–45.
Perullini, M., Jobbagy, M., Mouso, N., Forchiassin, F., Bilmes, S.A., 2010. Silica-alginate-fungi biocomposites for remediation of polluted water. J. Mater. Chem. 20, 6479–6483.
Pino, M.S., Rodríguez-Jasso, R.M., Michelin, M.-, Flores-Gallegos, A.C., Morales-Rodriguez, R., Teixeira, J.A., Ruiz, H.A., 2018. Bioreactor design for enzymatic hydrolysis of biomass under the iorefinery concept. Chem. Eng. J. 347, 119–136.
Prazeres, D.M.F., Cabral, J.M.S., 2001. Multiphase Bioreactor Design. Taylor & Francis, London.
Rasera, K., Ferla, J., Dillon, A.J.P., Riveiros, R., Zeni, M., 2009. Immobilization of laccase from *Pleurotus sajorcaju* in polyamide membranes. Desal 245, 657–661.
Rasheed, T., Bilal, M., Nabeel, F., Adeel, M., Iqbal, H.M.N., 2019. Environmentally-related contaminants of high concern: potential sources and analytical modalities for detection, quantification, and treatment. Environ. Int. 122, 52–66.
Rekuc, A., Bryjak, J., Szymanska, K., Jarzebski, A.B., 2010. Very stable silica-gel-bound laccase biocatalysts for the selective oxidation in continuous systems. Bioresour. Technol. 101, 2076–2083.
Rios, G.M., Belleville, M.P., Paolucci, D., Sanchez, J., 2014. Progress in enzymatic membrane reactors – a review. J. Membr. Sci. 242, 189–196.
Rivera-Jaimes, J.A., Postigo, C., Melgoza-Alemán, R.M., Aceña, J., Barceló, D., López de Alda, M., 2017. Study of pharmaceuticals in surface and wastewater from Cuernavaca, Morelos, Mexico: occurrence and environmental risk assessment. Sci. Total Environ. 613 (614), 1263–1274.
Rodrigues de Melo, R., Alnoch, R.C., Vilela, A.F.L., Maltempi de Souza, E., Krieger, N., Ruller, R., Sato, H.H., Mateo, C., 2017. New heterofunctional supports based on glutaraldehyde-activation: a tool for enzyme immobilization at neutral pH. Molecules 22 article number 1088.
Rondon, H., El-Cheikh, W., Boluarte, I.A.R., Chang, C.-Y., Bagshaw, S., Farago, L., Jegatheesan, V., Shu, L., 2015. Application of enhanced membrane bioreactor (eMBR) to treat dye wastewater. Bioresour. Technol. 183, 78–85.
Sanchez-Marcano, J., Tsotsis, T.T., 2002. Catalytic Membranes and Membrane Reactors. Wiley VCH, Weinheim.
Santos, J.C.S.D., Barbosa, O., Ortiz, C., Berenguer-Murcia, A., Rodrigues, R.C., Fernandez-Lafuente, R., 2015. Importance of the support properties for immobilization or purification of enzymes. ChemCatChem 7, 2413–2432.
Senthivelan, T., Kanagaraj, J., Panda, R.C., 2016. Recent trends in fungal laccase for various industrial applications: an eco-friendly approach – a review. Biotechnol. Bioprocess Eng. 21, 19–38.
Shaheen, R., Asgher, M., Hussain, F., Bhatti, H.N., 2017. Immobilized lignin peroxidase from *Ganoderma lucidum* IBL-05 with improved dye decolorization and cytotoxicity reduction properties. Int. J. Biol. Macromol. 103, 57–64.
Shao, B., Liu, Z., Zeng, G., Liu, Y., Yang, X., Zhou, C., Chen, M., Liu, Y., Jiang, Y., Yan, M., 2019. Immobilization of laccase on hollow mesoporous carbon nanospheres: noteworthy immobilization, excellent stability and efficacious for antibiotic contaminants removal. J. Hazard. Mater. 312, 318–326.
Shen, S., Shen, Y., Wen, Y., Wang, H., Liu, W., 2011. Fast and highly efficient removal of dyes under alkaline conditions using magnetic chitosan-Fe(III) hydrogel. Water Res. 45, 5200–5210.
Shimada, Y., Watanabe, Y., Sugihara, A., Tominaga, Y., 2002. Enzymatic alcoholysis for biodiesel fuel production and application of the reaction to oil processing. J. Mol. Catal. B Enzym. 17, 133–142.
Sigma-Aldrich, 2019a. laccase from *Trametes versicolor*. Enzyme pricing. https://www.sigmaaldrich.com/catalog/search?term=Laccase&interface=All&N=0&mode=partialmax&lang=pl&region=PL&focus=product/ accessed 16 March 2019.
Sigma-Aldrich, 2019b. Mushroom Tyrosianse. Enzyme pricing. https://www.sigmaaldrich.com/catalog/product/sigma/t3824?lang=pl&region=PL/ accessed 16 March 2019.
Sigma-Aldrich, 2019c. horseradish Peroxidase. Enzyme pricing. https://www.sigmaaldrich.com/catalog/search?term=hrp&interface=All&N=0&mode=match%20partialmax&lang=pl&region=PL&focus=product/ (accessed 16 March 2019).
Skoronski, E., Souza, D.H., Ely, C., Broilo, F., Fernandes, M., Furigo Junior, A., Ghislandi, M.G., 2017. Immobilization of laccase from *Aspergillus oryzae* on graphene nanosheets. Int. J. Biol. Macromol. 99, 121–127.
Sousa, J.C.G., Ribeiro, A.R., Barbosa, M.O., Pereira, M.F.R., Silva, A.M.T., 2016. A review on environmental monitoring of water organic pollutants identified by EU guidelines. J. Hazard. Mater. 344, 146–162.
Srikanlayanukul, M., Khanongnuch, C., Lumyong, S., 2016. Decolorization of textile wastewater by immobilized *Coriolus versicolor* RC3 in repeated-batch system with the effect of sugar addition. Chiang Mai University J. Nat. Sci. 5, 301–306.
Srinivasan, A., Viraraghavan, T., 2010. Decolorization of dye wastewaters by biosorbents: a review. J. Environ. Manag. 91, 1915–1929.
Strong, P.J., Claus, H., 2011. Laccase: a review of its past and its future in bioremediation. Crit. Rev. Environ. Sci. Technol. 41, 373–434.
Su, C.X.H., Low, L.W., Teng, T.T., Wong, Y.S., 2016. Combination and hybridization of treatments in dye wastewater treatment: a review. J. Environ. Chem. Eng. 4, 3618–3631.
Taboada-Puig, R., Eibes, G., Lloret, L., Lu-Chau, T.A., Feijoo, G., Moreira, M.T., Lema, J.M., 2016. Fostering the action of versa-tile peroxidase as a highly efficient biocatalyst for the removal of endocrine disrupting compounds. New Biotechnol. 3, 187–195.
Tamura, A., Satoh, E., Kashiwada, A., Matsuda, K., Yamada, K., 2010. Removal of alkylphenols by the combined use of tyrosinase immobilized on ion-exchange resins and chitosan beads. J. Appl. Polym. Sci. 115, 137–145.
Tavares, A.P.M., Silva, C.G., Xavier, A.M.R.B., 2017. Laccase Properties, Reaction Mechanisms and Applications: An overview in Laccase: Applications, Investigations and Insights. Nova Science Publishers.
Teerapatsakul, C., Parra, R., Keshavarz, T., Chitradon, L., 2017. Repeated batch for dye degradation in an airlift bioreactor by laccase entrapped in copper alginate. Int. Biodeterior. Biodegrad. 120, 52–57.
Tonin, F., Melis, R., Cordes, A., Sanchez-Amat, A., Pollegioni, L., Rosini, E., 2016. Comparison of different microbial laccases as tools for industrial uses. New Biotechnol. 33, 387–398.
Valli, K., Wariishi, H., Gold, M.H., 1990. Oxidation of monomethoxylated aromatic compounds by lignin peroxidase: role of veratryl alcohol in lignin biodegradation. Biochemical 29, 8535–8539.
Vikrant, K., Giri, B.S., Raza, N., Roy, K., Kim, K.-H., Rai, B.N., Singh, R.S., 2018. Recent advancements in bioremediation of dye: current status and challenges. Bioresour. Technol. 253, 355–367.
Wada, S., Ichikawa, H., Tatsun, K., 1993. Removal of phenols from wastewater by soluble and immobilized tyrosinase. Biotechnol. Bioeng. 42, 854–858.
Wang, Q., Cui, J., Li, G., Zhang, J., Li, D., Huang, F., Wei, Q., 2014. Laccase immobilized on a PAN/adsorbents composite nanofibrous membrane for catechol treatment by a biocatalysis/adsorption process. Molecules 19, 3376–3388.
Wang, S., Liu, W., Zheng, J., Xu, X., 2016. Immobilization of horseradish peroxidase on modified PAN-based membranes for the removal of phenol from buffer solutions. Can. J. Chem. Eng. 94, 865–871.
Webb, C., Koutinas, W.R., Wang, R., 2004. Developing a sustainable bioprocessing strategy based on a generic feedstock. Adv. Biochem. Eng. Biotechnol. 87, 195–268.
Weber, F.A., aus der Beek, T., Bergmann, A., Carius, A., Grüttner, G., Hickmann, S., Ebert, I., Hein, A., Küster, A., Rose, J., Koch-Jugl, J., Stolzenberg, H.-Ch, 2016. Pharmaceuticals in the environment – the global perspective. In: Occurrence, Effects, and Potential Cooperative Action Under SAICM. Federal Ministry of the Environment, Berlin.
Wen, Y., Liang, Y., Shen, C., Wang, H., Fue, D., Wang, H., 2015. Synergistic removal of dyes by *Myrothecium verrucaria* immobilization on a chitosan–Fe membrane. RSC Adv. 5, 68200–68208.
Williams, J.A., 2002. Keys to bioreactor selections. Chem. Eng. Prog. 98, 34–41.
Xu, R., Si, Y., Wu, X., Li, F., Zhang, B., 2014. Triclosan removal by laccase immobilized on mesoporous nanofibers: strong adsorption and efficient degradation. Chem. Eng. J. 255, 63–70.
Xu, R., Si, Y., Li, F., Zhang, B., 2015. Enzymatic removal of paracetamol from aqueous phase: horseradish peroxidase immobilized on nanofibrous membranes. Environ. Sci. Pollut. Res. 22, 3838–3846.
Xue, R., Woodley, J.M., 2012. Process technology for multi-enzymatic reaction systems. Bioresour. Technol. 115, 183–195.
Yamada, K., Akiba, Y., Shibuya, T., Kashiwada, A., Matsuda, K., Hirata, M., 2005. Water purification through bioconversion of phenol compounds by tyrosinase and chemical adsorption by chitosan beads. Biotechnol. Prog. 21, 823–829.
Yang, G., Lu, K., Su, X., 2012. Decolorization and detoxication of reactive industrial dyes

by immobilized laccases. Adv. Mater. Res. 550, 2279–2283.
Yehia, R.S., Rodriguez-Couto, S., 2017. Discoloration of the azo dye Congo Red by manganese-dependent peroxidase from *Pleurotus sajor-caju*. Appl. Biochem. Microbiol. 53, 222–229.
Young, T., Smoot, S., Peeters, J., Côté, P., 2013. When does building an MBR make sense? how variations of local construction and operating cost parameters impact overall project economics. Proc. Water Environ. Fed. (8), 6354–6365.
Yu, L., Zhang, X.Y., Tang, Q.W., Li, J., Xie, T., Liu, C., Cao, M.Y., Zhang, R.C., Wang, S., Hu, J.M., Qiao, W.C., Li, W.W., Ruan, H.H., 2015. Decolorization characteristics of a newly isolated salt-tolerant Bacillus sp. strain and its application for azo dye-containing wastewater in immobilized form. Appl. Microbiol. Biotechnol. (21), 9277–9287.
Zdarta, J., Antecka, K., Frankowski, R., Zgoła-Grześkowiak, A., Ehrlich, H., Jesionowski, T., 2018a. The effect of operational parameters on the biodegradation of bisphenols by *Trametes versicolor* laccase immobilized on *Hippospongia communis* spongin scaffolds. Sci. Total Environ. 615, 784–795.
Zdarta, J., Meyer, A.S., Jesionowski, T., Pinelo, M., 2018b. A general overview of support materials for enzyme immobilization: characteristics, properties, practical utility. Catalysts 8, 9.
Zdarta, J., Meyer, A.S., Jesionowski, T., Pinelo, M., 2018c. Developments in support materials for immobilization of oxidoreductases: a comprehensive review. Adv. Colloid Interf. Sci. 258, 1–20.
Zhang, X., Pan, B., Wu, B., Zhang, W., Lv, L., 2014. A new polymer-based laccase for decolorization of AO7: long-term storage and mediator reuse. Bioresour. Technol. 164, 248–253.
Zhao, F., Li, H., Jiang, Y., Wang, X., Mu, X., 2014. Co-immobilization of multi-enzyme on control-reduced graphene oxide by non-covalent bonds: an artificial biocatalytic system for the one-pot production of gluconic acid from starch. Green Chem. 16, 2558–2565.
Zhou, Z., Hartmann, M., 2013. Progress in enzyme immobilization in ordered mesoporous materials and related applications. Chem. Soc. Rev. 42, 3894–3912.
Zille, A., Tzanov, T., Gubitz, G.M., Cavaco-Paulo, A., 2003. Immobilized laccase for decolourization of Reactive Black 5 dyeing effluent. Biotechnol. Lett. 25, 1473–1477.
Zucca, P., Sanjust, E., 2014. Inorganic materials as supports for covalent enzyme immobilization: methods and mechanisms. Molecules 19, 14139–14194.

Microporous and Mesoporous Materials 291 (2020) 109688

Contents lists available at ScienceDirect

Microporous and Mesoporous Materials

journal homepage: www.elsevier.com/locate/micromeso

Mesostructured cellular foam silica materials for laccase immobilization and tetracycline removal: A comprehensive study

Jakub Zdarta[a,**], Agnieszka Feliczak-Guzik[b], Katarzyna Siwińska-Ciesielczyk[a], Izabela Nowak[b], Teofil Jesionowski[a,*]

[a] Institute of Chemical Technology and Engineering, Faculty of Chemical Technology, Poznan University of Technology, Berdychowo 4, PL-60965, Poznan, Poland
[b] Faculty of Chemistry, Adam Mickiewicz University, Uniwersytetu Poznańskiego 8, PL-02507, Poznan, Poland

ARTICLE INFO

Keywords:
MCF materials
MCF characterization
Enzyme immobilization
Catalytic activity
Teracycline removal

ABSTRACT

Due to its exceptional textural, morphological and mechanical properties, mesostructured cellular foam (MCF) silica is a suitable support material for enzyme immobilization. However, the simple and efficient protocol of enzyme immobilization using MCF is often overlooked. Thus, in the presented study, we describe the synthesis, modification and characterization of mesostructured cellular foam silica for use in laccase immobilization. It has been established that the synthesized materials are characterized by high surface area equal to approx. 550 $m^2 g^{-1}$ and pores with diameters of approx. 20 nm, which makes them suitable for effective enzyme binding. Furthermore, immobilization of the laccase onto both, unmodified and Cu-modified MCF has been carried out, resulting in process yield of over 95% and 85%, respectively. Upon immobilization, irrespectively of the support used, laccase retained higher activity (over 80%) at a wider temperature (20–40 °C) and pH (4–7) range, as compared to the free enzyme, which exhibited such high activity only at pH 5 and 30 °C. In addition, the reusability of the laccase immobilized onto MCF + Cu material has also been improved as it still retained approx. 90% of its initial activity after 10 reaction cycles. Finally, the obtained biocatalytic systems have been applied for degradation of tetracycline from aqueous solutions resulting in 100% removal of the antibiotic by the MCF + Cu + lac system due to simultaneous adsorption and biocatalytic conversion.

1. Introduction

According to the IUPAC definition, mesoporous materials are characterized by pores with diameters ranging from 2 to 50 nm and usually possess pores at a volume up to 2 $cm^3 g^{-1}$ and high surface area, which may reach even 1500 $m^2 g^{-1}$ [1]. Furthermore, the multiplicity of the synthesis methods, such as sol-gel, microwave, hydro- and solvothermal, precipitation in polar and nonpolar media as well as sonochemical approaches, allow to obtain the tailor-made materials with desired properties [2–10]. Mesoporous materials are also well-known for their high chemical and biological stability, mechanical resistance, biocompatibility as well as biodegradability and susceptibility to surface functionalization. Due to the above-mentioned features, mesoporous materials still attract growing attention for application in various fields of science and engineering, including biomedicine, energy storage, separation, adsorption, catalysis and biocatalysis [11,12].

Currently, a great variety of the mesoporous materials is known and frequently applied, among which carbon mesoporous materials as well as inorganic oxides, such as titania, zirconia, alumina or even cerium and tin oxide should be enumerated. However, since methods of their synthesis have been developed at the turn of 1960s and 1970s, mesoporous silica materials mainly are of particular interest due to their remarkable textural properties, such as high surface area and pore volume [13]. Moreover, at the begging of 1990s, the first reports regarding the synthesis of mesoporous silica nanoparticles have been published, opening new fields for potential application for the above-mentioned materials. Various types of mesoporous silica have been developed, among which the most commonly known and frequently applied include Mobil Composition of Matter (Mobil Crystalline Materials, MCM), Santa Barbara Amorphous (SBA) and Mesostructured Cellular Foam (MCF), which differ in terms of morphological structure as well as the pore array, size and volume [14,15]. MCF is a wide class of three-dimensional materials characterized by high stability and resistance with surface area up to 1500 $m^2 g^{-1}$ and pores with diameters usually ranging from 20 to 50 nm, however with a narrow pore size distribution [16]. Moreover, these materials are composed of uniform

* Corresponding author.
** Corresponding author.
E-mail addresses: jakub.zdarta@put.poznan.pl (J. Zdarta), teofil.jesionowski@put.poznan.pl (T. Jesionowski).

https://doi.org/10.1016/j.micromeso.2019.109688
Received 16 July 2019; Received in revised form 26 August 2019; Accepted 28 August 2019
Available online 29 August 2019

spherical cells interconnected by window pores, which is an advantage in terms of better diffusion of reactants and products, and are known due to their water insolubility, hydrophilic character and numerous of hydroxyl functional groups [17]. These remarkable properties make mesoporous silica materials suitable for use as a supports for enzyme immobilization.

Enzyme immobilization is based on the attachment of the enzyme molecules to the solid support that provides high activity and effectivity of the biomolecules and improves their stability and reusability [18]. Furthermore, immobilization is a promising technology for maximization of the enzyme biocatalytic productivity and their reuse to reduce the operational costs of the catalytic processes [19,20]. Materials of various origin may be used as supports for enzyme immobilization, among which mesoporous silica materials are one of the most frequently applied. For example, α-chymotrypsin and lipase were immobilized in SBA-15 mesoporous silica and additionally cross-linked by glutaraldehyde in the study by Kim et al. [21]. The presented approach was very effective in enzyme leaching limitations and, as a consequence, enhancement of the enzyme stability. In another study, chloroperoxidase from *Caldariomyces fumago* was covalently immobilized using SBA-15 silica and applied for the enzymatic oxidation of azo dyes allowing for total removal of Acid Blue 120 and Direct Blue 85 [22]. Mesostructured cellular foams have also been previously used as enzyme supports. For instance, Fried et al. [23] reported immobilization of glucose-6-phosphate dehydrogenase onto MCF grafted with aminosilanes with different chain length to select the most suitable support for the highest enzyme activity. In another work, aminopropyl-modified MCF was used for covalent immobilization of penicillin G acylase through the Schiff base reaction. It has been shown that enzyme attached by the covalent bonds exhibited improved stability compared to biocatalyst adsorbed onto unmodified MCF [24]. Finally, enzymes from oxidoreductase group, such as tyrosinase from *Agaricus bisporus* have also been covalently immobilized using amine-grafted MCF by Zynek et al. [25]. The presented data clearly indicated that stability of the tyrosinase against thermal inactivation has been significantly improved upon immobilization. Nevertheless, data regarding the immobilization of laccase using mesoporous supports for removal of pharmaceuticals are limited and simple as well as efficient protocols for immobilization of laccase are still required. Up to date, laccase have been immobilized by adsorption and covalent binding using mesostructured siliceous cellular foams [26–29]. Properties of the free and silica immobilized enzymes have been examined and compared and it has been found that immobilized laccase exhibited improved stability and higher activity over wider pH and temperature ranges, as compared to free laccase.

Therefore, in the presented study, we have undertaken a research concerning the synthesis of mesoporous cellular foam (MCF), its modification using copper ions and characterization including high-resolution transmission electron microscopy, energy dispersive X-ray spectroscopy as well as evaluation of porous structure parameters and thermal stability. Furthermore, the obtained materials have been used as a support for immobilization of laccase from *Trametes versicolor* and the produced biocatalytic systems were applied for removal of tetracycline from aqueous solutions. As part of the study, we have also evaluated and compared the kinetic parameters of the immobilized enzymes and examined the effect of various pH and temperature conditions on the stability of free and immobilized laccase. Finally, the biocatalytic systems have been applied for removal of tetracycline allowing total removal of the antibiotic by simultaneous sorption of the pollutant and its catalytic conversion.

2. Experimental

2.1. Materials

Laccase from *Trametes versicolor* (EC 1.10.3.2 ≥ 0.5 U mg^{-1}), tetracycline (≥98.0%), 2,2-azinobis-3-ethylbenzothiazoline-6-sulfonate (ABTS, ≥99%), Coomassie Brilliant Blue G-250, phosphate, acetate and Tris-HCl buffers at specific pH value, copper(II) sulfate, tetraethyl orthosilicate (TEOS, > 99%), copper(II) chloride (97%), 1,3,5-timethylbenzene (> 99%) and ammonium fluoride (> 99%) as well as methanol, 96% ethanol and 85% H_3PO_4 (all laboratory grade) were supplied by Sigma-Aldrich. Pluronic P123 was manufactured by BASF. In turn, HCl (35% v./v.) was bought from Chempur.

2.2. MCF synthesis and modification

MCF materials were obtained using the hydrothermal sol-gel process according to Trejda and co-workers [30]. Pluronic P123 (32 g) was dissolved in a HCl solution (70.08 g hydrochloric acid and 1142 g H_2O). Afterwards, after 1 h, tetraethyl orthosilicate (68.22 g) was added to the mixture and then stirred at 40 °C for 20 h. Next, the mixture was heated in the oven, at 100 °C for 24 h under static conditions. The solids were then recovered by filtration, washed with distilled water, and air dried at 60 °C for 12 h. The template was removed by calcination in air at 550 °C for 8 h.

Next, the unmodified MCF support was modified by incipient wetness impregnation. The vessel with a weighted portion of the MCF was charged dropwise with a water solution of copper(II) chloride. The mass fraction of copper was kept as 10 wt% in respect to the support. The vessel with the impregnated support was tightly closed with polyolefin-paraffin foil and left to rest for 24 h. Next, the modified material was dried for 1 h at 30 °C, then for 1 h at 40 °C and finally for 18 h at 60 °C.

2.3. Enzyme immobilization

For the immobilization of laccase from *Trametes versicolor,* 1 g of the MCF and MCF + Cu support material was used, to which 10 mL of the laccase solution at concentration of 5 mg mL^{-1} in acetate buffer at pH 5 was added. The mixture was shaken for 3 h in a KS 4000i Control incubator (IKA Werke GmbH, Germany) with mixing at 150 rpm at a temperature of 4 °C. Finally, the immobilized enzymes were centrifuged (Eppendorf Centrifuge 5810 R, Germany) and washed several times with the acetate buffer to remove the unbounded enzyme.

The amount of immobilized enzyme (mg g^{-1}) was determined based on the spectrophotometric measurements according to the Bradford method [31] as the difference between the initial enzyme dosage and the concentration of protein present in the supernatant after immobilization and considering the mass of the support material. The immobilization yield (%) was calculated considering the difference between the amount of the enzyme in the supernatant before and after immobilization and volume of the reaction mixture.

In order to calculate the enzyme leakage (%) from the support, both immobilized laccases were incubated for 12 h at 30 °C in 20 mL of acetate buffer at pH 5 and were mixed at 200 rpm using an IKA KS 4000i Control incubator. The percentage of eluted enzyme was calculated based on measurement of the protein content in the biocatalytic systems obtained after immobilization and the concentration of the enzyme after the leakage test, based on the Bradford method.

2.4. Enzyme activity, stability and kinetic study

The activity, temperature and pH profiles as well as storage stability and reusability of the free and immobilized laccases were evaluated based on spectrophotometric measurements with a Jasco V-750 (Japan) spectrophotometer at λ = 420 nm, using ABTS as the substrate, according to the methodology presented by Dai et al. [32], with a slight modification. For each reaction, 10 mg of the free or immobilized enzyme were used. The relative activity (A_R) (eq. (1)) was defined as the percentage ratio of the activity of laccase at a specific value (A_i) to the enzyme's maximum activity (A_{max}). A_{max} is the highest activity among all values of enzymatic activity recorded in this study.

$$A_R(\%) = \frac{A_i}{A_{max}} \cdot 100\% \quad (1)$$

The pH profiles were examined over a pH range from 3 to 9, using a buffer solution at an appropriate pH, at temperature of 30 °C. The temperature profiles of the free and immobilized laccase were evaluated over a temperature range from 10 °C to 60 °C at a pH 5. The reusability of the immobilized laccases was calculated based on spectrophotometric measurements over ten repeated reaction cycles. After each reaction step, the tested biocatalytic system was separated from the reaction mixture by centrifugation, washed several times with buffer solution at pH 5 and added to a mixture containing fresh substrate. Storage stability of the free and immobilized laccase was evaluated over 30 days of storage at 4 °C in acetate buffer at pH 5. For the reusability and storage stability the initial activity of the biocatalysts was defined as 100%.

The Michaelis–Menten constant (K_M), the maximum rate of reaction (V_{max}) and turnover number (k_{cat}) of free and immobilized laccases were examined based on the oxidation reaction of ABTS as a substrate, at concentrations from 0.01 mM to 0.5 mM under optimal process conditions using various concentrations of the substrate solution. To calculate the apparent kinetic parameters, the Hanes–Woolf plot was applied.

2.5. Tetracycline removal

The obtained biocatalytic systems were tested in the removal experiments of tetracycline. However, as MCF materials are known for their good sorption capacity, the efficiency of adsorption of the pharmaceutical using the unmodified and Cu modified MCF supports before and after immobilization was examined prior to evaluating the efficiency of the catalytic degradation of tetracycline.

2.5.1. Adsorption study

In order to evaluate the sorption properties of the MCF materials before and after immobilization, the tests were performed using pure support materials and biocatalytic systems with a thermally inactivated laccase. Prior to the adsorption tests, the immobilized enzymes were placed in a Memmert SF75 (Memmert, Germany) drier at 80 °C for 3 h for enzyme inactivation. For each of the adsorption experiments, 100 mg of the MCF material before immobilization and with the inactivated enzyme were placed in vials with 10 mL of tetracycline solution at pH 5 and concentration 1 mg L^{-1}. The duration of the test was 90 min. After a specified period of time, the concentration of tetracycline was examined spectrophotometrically using a Jasco V-750 spectrophotometer at wavelength 355 nm, based on the calibration curve of tetracycline. The adsorption efficiency (%) after a specified period of time was calculated considering the initial concentration of tetracycline and remaining concentration of the antibiotic after a certain time.

2.5.2. Biodegradation study

The biodegradation of the tetracycline by free and both MCF-immobilized laccases was investigated in darkness using an IKA KS 4000i incubator shaker (100 rpm). Briefly, 10 mg of free or immobilized laccases were added to 10 mL of tetracycline solution at pH 5 and concentration 1 mg L^{-1}. The experiment duration was 90 min and progress of the reaction was monitored spectrophotometrically at λ = 355 nm by collecting the samples (0.1 mL) every specified period of time. The concentration of the antibiotic after biodegradation was calculated based on a standard calibration curve of this compound. The removal efficiency of tetracycline (%) was calculated according to the following equation (eq. (2)):

$$Tetracycline\ removal\ (\%) = \frac{C_0 - C_t}{C_0} \cdot 100\% \quad (2)$$

where C_0 denotes initial tetracycline concentration and C_t denotes the remaining concentration of tetracycline after a certain time.

2.6. Analytical techniques

High-resolution transmission electron microscopic (HRTEM) measurements were performed with a Hitachi HT7700 microscope (Hitachi, Japan) operating at 100 kV. A small quantity of the sample was dispersed in 2 mL of deionized water with the use of ultrasound. Then, 1 μL of the solution was applied to a nickel mesh covered with a carbon film.

The surface composition of the samples before and after immobilization was analyzed by energy dispersive X-ray spectroscopy (EDS) using a Hitachi HT7700 microscope equipped with a UltraDry detector and microanalysis system from Thermo Scientific.

XRD measurements were performed on a Bruker AXS D8 Advance diffractometer with CuKα radiation generated radiation of the wavelength α = 0.154 nm in 2Θ range of 6–60° with the accuracy to 0.05° (wide-angle range).

Fourier transform infrared (FTIR) spectra of the support materials and samples after immobilization were recorded using a Vertex 70 apparatus (Bruker, Germany). The samples were analyzed in the form of KBr pellets, by mixing 1.5 mg of the sample and 250 mg of anhydrous potassium bromide, over a wavenumber range of 4000–420 cm^{-1} (at a resolution of 0.5 cm^{-1}).

The porous structure parameters of the materials before and after immobilization were determined using an ASAP 2020 instrument (Micromeritics Instrument Co., USA). The surface area was evaluated based on the multipoint BET (Brunauer–Emmett–Teller) method using data for adsorption under relative pressure (p/p_0) at 77 K. The mean size and total volume of pores were calculated based on the BJH (Barrett–Joyner–Halenda) algorithm.

Thermogravimetric analysis (TG) of the support materials was performed using a Jupiter STA 449F3 apparatus (Netzsch, Germany). Measurements were carried out over the temperature range from 25 °C to 1000 °C under nitrogen flow of 10 mL min^{-1} at a heating rate of 10 °C min^{-1}, with an initial sample weight of about 10 mg.

2.7. Statistical analysis

All of the above-presented experiments were performed in triplicate. The results were presented as mean value ± standard deviation. Statistically significant differences were determined by using one-way ANOVA performed using SigmaPlot 12 (Systat Software Inc., USA), based on Tukey's test. Statistical significance was established at $p < 0.05$.

3. Results and discussion

3.1. Physicochemical characterization

3.1.1. Morphological and surface composition study

It can be observed that the obtained MCF material is characterized by a rather spherical pores with an average size of approx. 25 nm, however, with a narrow pore size distribution (Fig. 1a). After MCF functionalization by the copper ions, an additional layer can be seen on the surface of the silica material, also resulting in a slight decrease of the pores diameters (Fig. 1c). Upon laccase immobilization onto both unmodified and modified MCF materials (Fig. 1b,d), irregular shapes representing enzyme aggregates, with the size of approx. 10 nm, can be observed, which confirms effective laccase deposition. Furthermore, it can be observed that enzymes molecules have been deposited onto the surface of the MCF as well as in its pores, which could provide a suitable micro-environment for immobilizing laccase. Effective MCF functionalization and laccase immobilization have also been confirmed by the EDS result. After Cu^{2+} coating, the presence of peaks characteristic for these ions can be seen, as signals assigned to carbon, nitrogen and sulfur

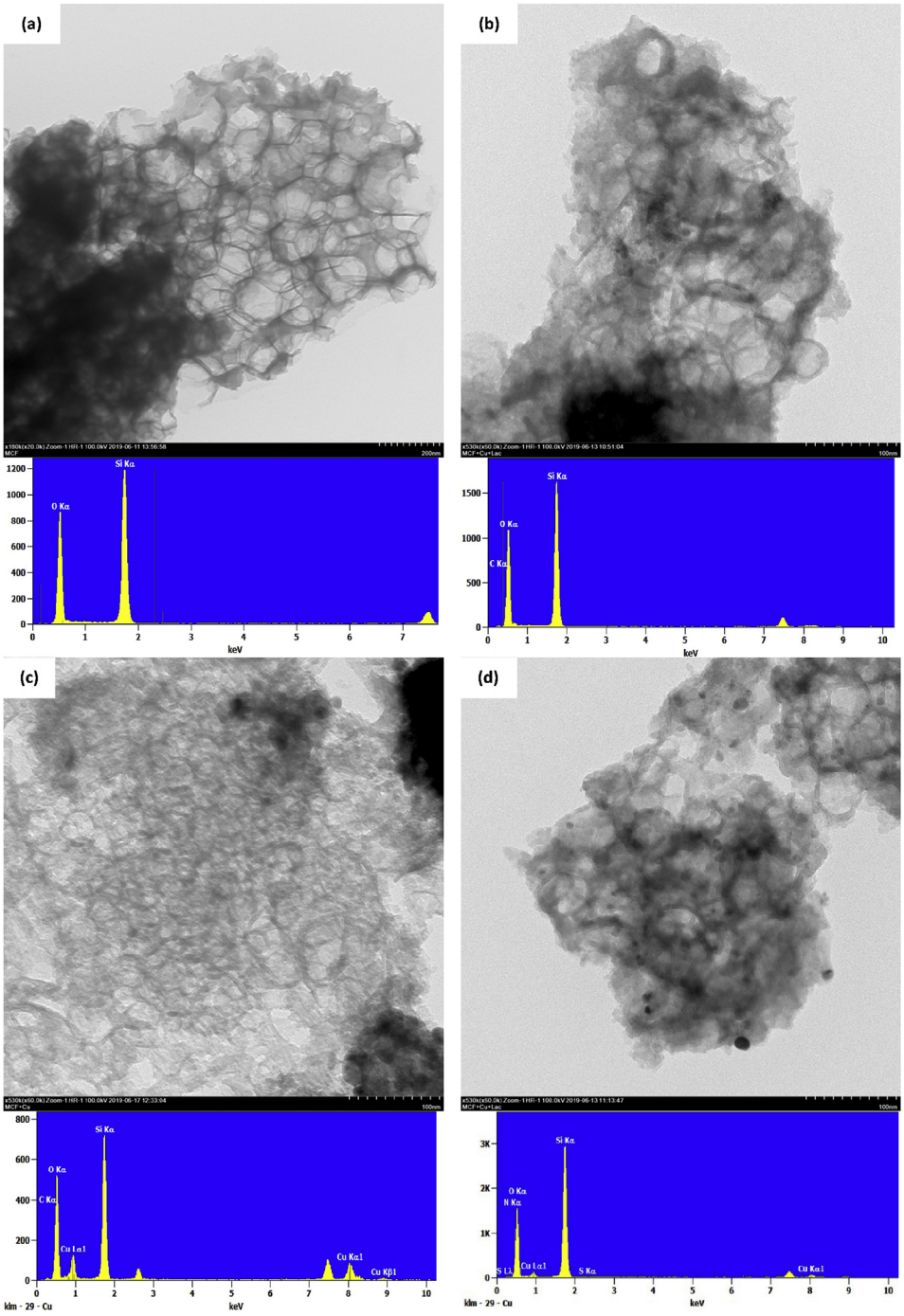

Fig. 1. HRTEM images and EDS spectra of: pure MCF (a), MCF + lac (b), MCF + Cu (c) and MCF + Cu + lac (d).

(elements which are present in the enzyme structure) can be observed on the EDS spectra after enzyme immobilization.

3.1.2. XRD and FTIR analysis

The XRD patterns of pure MCF and copper modified MCF before and after laccase immobilization in a wide range of angles were presented in Fig. 2. The presence of signals for MCF + Cu confirms the existence of a substance in the crystalline form. A number of peaks at 2θ = 16.2°, 21.9°, 28.9°, and 33.9° was assigned to $CuCl_2$, thereby confirming successful preparation of the copper-modified sample [33]. The powder XRD patterns of the pure MCF and modified MCF before and after laccase immobilization confirmed its amorphous form. These materials do not possess a long range order.

FTIR spectra of the MCF support material before and after laccase immobilization have been obtained in order to characterize the chemical groups present on the surface of the materials (Fig. 3). A band with maximum at 3320 cm^{-1}, assigned to the stretching vibration of –OH groups can be seen on the FTIR spectra of the MCF material before enzyme immobilization. Furthermore, signals at 1055, 795 and 475 cm^{-1}, characteristic for stretching vibrations of Si–O–Si bonds as well as bending and out of plane vibrations of Si–O bonds, respectively, can also be observed. After enzyme deposition on the MCF surface, irrespectively of the type of the support used, additional signals assigned to the enzyme structure can be observed. Among others, the most important is the increase of the intensity of the peak assigned to the –OH groups due to the presence of hydroxyl moieties in the enzyme

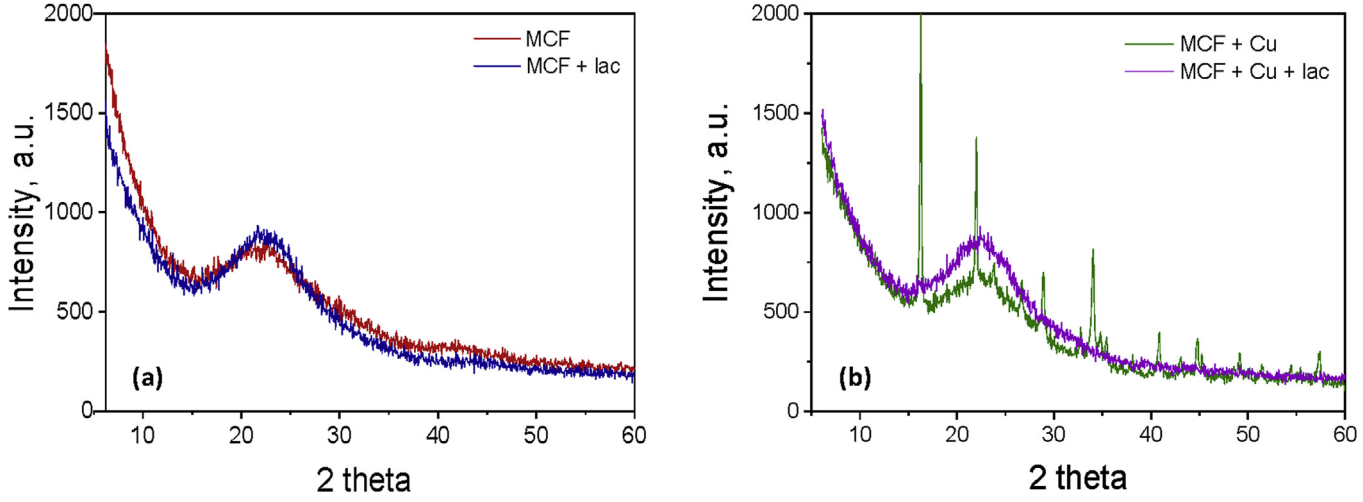

Fig. 2. Wide-angle XRD patterns of: pure MCF (a) and Cu modified MCF (b) before and after laccase immobilization.

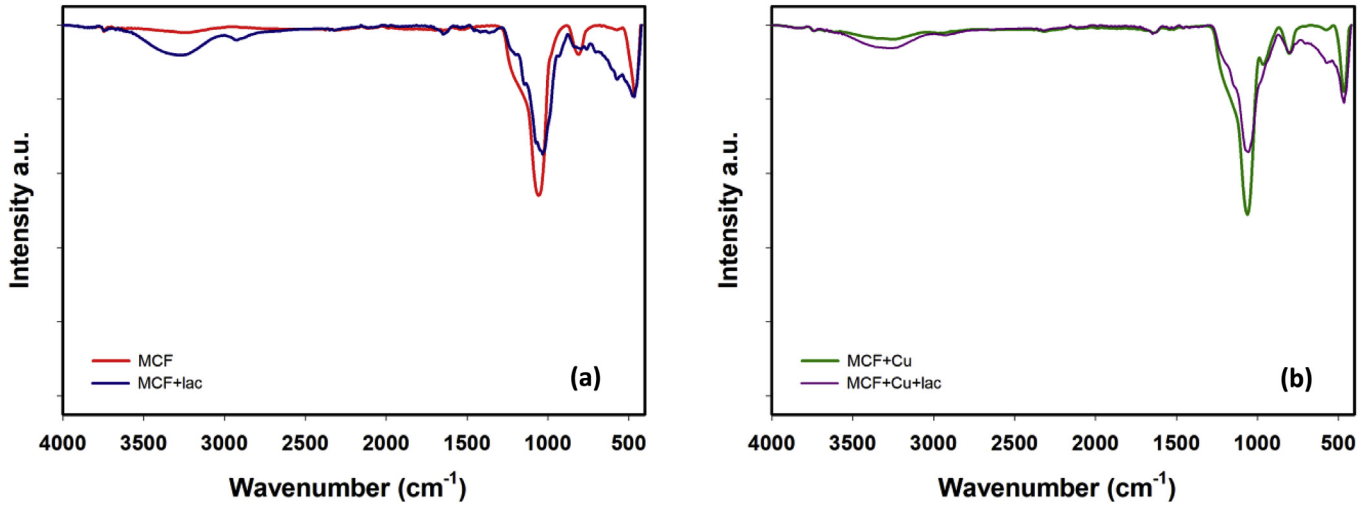

Fig. 3. FTIR spectra of: pure MCF (a) and Cu modified MCF (b) before and after laccase immobilization.

structure. Moreover, small peaks with maxima at 1655, 1545 and approx. 1250 cm^{-1}, characteristic for the amide I, amide II and amide III bands, respectively, have also been observed. Finally, signals related to the carbon skeleton of the enzyme at 2950 cm^{-1} (stretching vibrations of C–H bonds) and approx. 600 cm^{-1} (bending vibrations of C–C bonds) has appeared after immobilization. According to Wong et al. [34], the presence of the above-mentioned signals as well as slight shifts of their maxima towards higher wavenumbers indicate not only efficient enzyme immobilization but also retention of its catalytic properties.

3.1.3. Textural properties

In order to evaluate the textural properties, N_2 adsorption/desorption isotherms and pore size distribution for all prepared products were carried out. The isotherms of all analyzed materials were typical for type-IV with type H2 hysteresis loop, according to the IUPAC classification, which are characteristic for mesoporous structures (Fig. 4). The results of analysis of the parameters of the porous structure of MCF product indicate that the mentioned sample is characterized by a BET surface area equal to 586.5 $m^2 g^{-1}$. The mean pore diameter (S_p) and the total pore volume (V_p) of MCF material was equal to 22.1 nm and 2.218 $cm^3 g^{-1}$, respectively. After laccase immobilization on the MCF sample (MCF + lac sample), the resultant BET surface area, mean pore diameter and total pore volume were equal to 379.6 $m^2 g^{-1}$, 21.1 nm and 1.657 $cm^3 g^{-1}$, respectively. Moreover, interpretation of parameters of porous structure of the mentioned products confirmed that the hysteresis loops of MCF and MCF + lac samples cover the relative pressure range of p/p_o = 0.5–0.99. The amount of adsorbed nitrogen reached a maximum value of 1538.3 $cm^3 g^{-1}$ and 1124.3 $cm^3 g^{-1}$ at p/p_o = 0.99 for MCF and MCF + lac samples, respectively. The BET surface areas of the MCF + Cu and MCF + Cu + lac samples were significantly lower than that of pure MCF sample. The reduction of the BET surface area from 586.5 m^2/g (characteristic for MCF sample) to 431.9 m^2/g for MCF + Cu sample is probably associated with the blocking of active sites by Cu ions, which was used for functionalization of the support. The mean pore diameter and the total pore volume of MCF + Cu material were equal to 18.0 nm and 1.691 $cm^3 g^{-1}$, respectively. The interpretation of results of low-temperature sorption of nitrogen for MCF + Cu + lac sample confirmed that the mentioned product is characterized with the lowest BET surface area (406.2 $m^2 g^{-1}$). The total pore volume and mean pore diameter of the analyzed sample were equal to 1.556 $cm^3 g^{-1}$ and 17.8 nm, respectively. The hysteresis loop of MCF + Cu and MCF + Cu + lac samples covered the relative pressure range of p/p_o = 0.6–0.99. The amount of nitrogen adsorbed reached a maximum value of 1151.7 $cm^3 g^{-1}$ and 1062.7 $cm^3 g^{-1}$ at p/p_o = 0.99 for MCF + Cu and MCF + Cu + lac samples, respectively. The mean pore diameter and pore volume of MCF + lac, MCF + Cu and MCF + Cu + lac samples were lower that respective values of the MCF

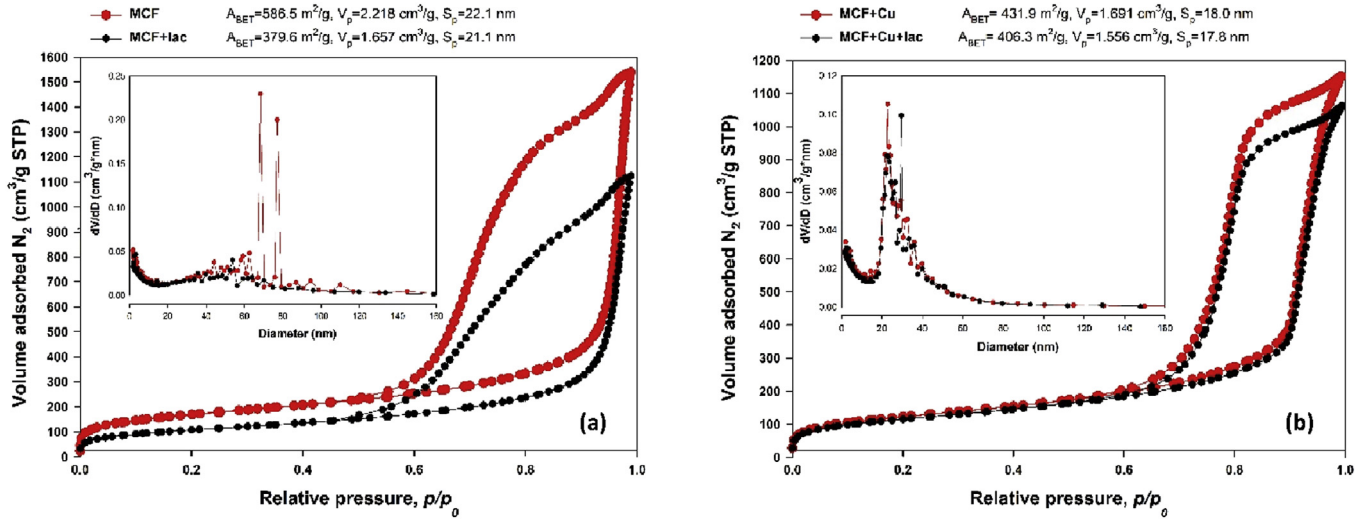

Fig. 4. N_2 adsorption/desorption isotherms and inset pore size diameters of: MCF and MCF + lac (a), and MCF + Cu and MCF + Cu + lac (b) materials.

material. The decrease of BET surface area for the MCF + lac, MCF + Cu and MCF + Cu + lac materials resulted from blocking the surface functional groups of MCF product by the laccase biomolecules or Cu ions. The obtained results which describe the parameters of the porous structure of the MCF-based materials confirmed the changes in the surface character of the analyzed products as well as the effectiveness of the immobilization process of laccase or Cu ions deposition. Our results are in agreement with previously published reports [35,36] which also indicated that immobilization of strictly defined molecules on MCF product had significant influence on the structure of mesoporous support material.

3.1.4. Thermal stability

The thermal stability of MCF and MCF + Cu samples was determined using TGA analysis (Fig. 5). The thermogram of the MCF sample indicated a minor weight loss by approx. 4.5% in the temperature range of 30–200 °C. The weight loss is mainly associated with the local elimination of water molecules which interact with the surface silanol groups. The next weight loss, by about 2%, was observed for MCF material in the temperature range of 200–1000 °C. The TGA curve of the MCF + Cu product showed a major weight loss by approx. 11% in the temperature range of 30–100 °C. The next weight loss by about 4% was observed on the TG curve in the temperature range of 100–400 °C. Those losses are associate with the desorption of physisorbed and chemisorbed water or probably with oxidation of Cu to Cu_2O, as reported in the literature [37–39]. The small endothermic and exothermic effects recorded in the DTA curve are a confirmation of the occurring changes. The third stage of the degradation, by approx. 10%, in the temperature range of 400–620 °C, may be attributed to the slow decomposition of copper in the MCF material leading to the formation of copper oxide. The mentioned stage of the degradation is also associated with a distinct endothermic effect observed on the DTA curve.

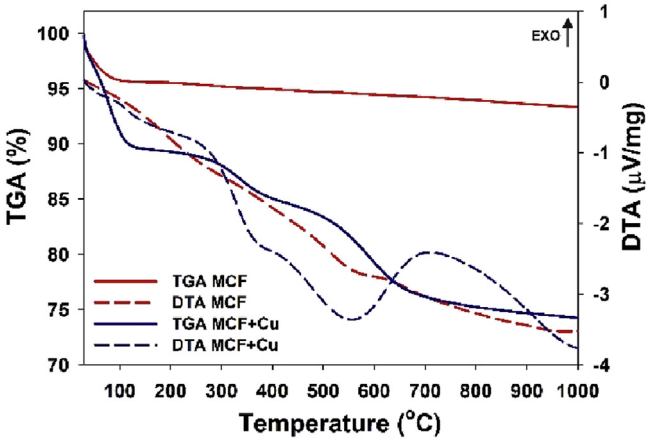

Fig. 5. TGA curves of MCF and MCF + Cu samples.

3.2. Enzyme immobilization and characterization

Based on the results presented in the above section, it is clear that MCF materials are characterized by defined and well-developed surface area, high thermal stability and possess numerous hydroxyl groups on their surface. These properties make MCF materials suitable for application as a supports for enzyme immobilization. Thus, in the further steps of the research, we have undertaken the study to evaluate efficient immobilization protocol of laccase from *Trametes versicolor* using MCF and Cu doped MCF materials, to examine the effect of copper ions on the activity of immobilized laccase. The immobilization process has been characterized and kinetic parameters of the free and immobilized enzymes have been calculated. Moreover, since it is known that the catalytic activity is strongly affected by the process conditions, it was important to examine optimal pH and temperature parameters as well as storage stability and reusability of the immobilized enzymes. All of the above-mentioned features of the immobilized laccases have been evaluated to examine the practical application potential of the obtained systems.

3.2.1. Immobilization yield and kinetic parameters

In order to examine the changes of the biocatalysts upon immobilization, their kinetic parameters, such as the Michaelis–Menten constant (K_M), maximum reaction rate (V_{max}) and turnover number (k_{cat}) were calculated (Table 1). It can be observed that the K_M value of free laccase was equal to 0.062 mM and was lower by approx. 25% and 45% compared to the K_M of MCF + lac and MCF + Cu + lac, respectively. Consequently, approx. 20% lower values of V_{max} for the immobilized laccases (0.039 mM min^{-1} and 0.035 mM min^{-1} for MCF + Lac and MCF + Cu + lac, respectively) were noticed, in comparison to the free enzyme, which reached 0.047 mM min^{-1}. Higher values of Michaelis-Menten constant indicate lower substrate affinity of the immobilized biocatalysts which leads to the decrease of the maximal reaction rate (V_{max}). This may be related to the formation of steric hindrances upon immobilization, which limit the transfer of substrates and products and block the enzyme active sites, as reported previously [40]. All of these factors affect the catalytic action and might

Table 1
Kinetic parameters of free and immobilized laccase and data describing performed immobilization process.

Analyzed parameter	Free laccase	MCF + lac	MCF + Cu + lac
K_M (mM)	0.062 ± 0.003	0.079 ± 0.004	0.088 ± 0.003
V_{max} (mM min^{-1})	0.047 ± 0.002	0.039 ± 0.003	0.035 ± 0.003
k_{cat} (s^{-1})	61 ± 3	56 ± 4	68 ± 4
k_{cat}/K_M (mM^{-1} s^{-1})	983 ± 10	620 ± 8	772 ± 11
Immobilization yield (%)	–	94 ± 3.5	85 ± 4.1
Amount of immobilized enzyme (mg g^{-1})	–	188 ± 4.3	170 ± 4.6
Enzyme leaching (%)	–	9 ± 2.1	13 ± 3.2

lead to its decrease. However, the value of the turnover number (k_{cat}) for the MCF + lac biocatalytic system (56 s^{-1}) was almost unaltered as compared to the k_{cat} of free laccase (61 s^{-1}). Surprisingly, even higher k_{cat} for the MCF + Cu + lac system (68 s^{-1}) was noticed, indicating that an activation effect of the copper ions on laccase activity occurred [41]. The obtained results clearly show that the produced biocatalytic systems retained their high catalytic properties but MCF + Cu support material appears to be more suitable for laccase immobilization and its further application for the removal of pharmaceuticals, as was also implied by the results of tetracycline removal (Section 3.3). Furthermore, in the study, the immobilization process was also investigated to examine the amount of immobilized enzymes and immobilization yield. According to the data presented in Table 1, the amount of laccase adsorbed onto MCF and Cu doped MCF reached 188 mg g^{-1} and 170 mg g^{-1}, respectively, which corresponds to an immobilization yield of 94% and 85%. The higher amount of the laccase immobilized onto unmodified support and, in consequence, also higher immobilization yield might be explained by the fact that after surface modification with copper ions some of the active sites of the support capable of enzyme binding were saturated by the metal ions, leading to the decrease in enzyme sorption capacity. However, although the amount of immobilized enzyme was lower when modified support was used, this biocatalytic system retained higher activity in the further tests, due to the activation effect of Cu ions, as mentioned previously. The obtained results confirmed the exceptional capacity of the mesoporous silicas towards enzyme immobilization and are in agreement with the previously published studies. For instance, Zhao et al. [42] used MCF silica and immobilized over 260 U of laccase per 1 g of the support, whereas Rekuć et al. [27] reported immobilization of over 390 U of enzyme on 1 g of mesoporous silica carrier.

3.2.2. Effect of pH and temperature

Effect of pH (from 3 to 9) and temperature (from 10 °C to 60 °C) on the activity of the free and immobilized enzymes was studied to plot pH and temperature profiles of the biocatalysts and to examine optimal process conditions. Based on Fig. 6a, it can be observed that the activity of free and immobilized enzymes increased with the increase of pH, reached its maximum at pH 5 and started to decrease with further pH increase. Nevertheless, it should be emphasized that the relative activity of the immobilized laccases reached over 70% at pH range from 4 to 7 (over 90% at pH 4 and 5) and was significantly higher compared to that of free laccase, which exhibited activity of over 80% only at pH 5. The decrease of the enzyme activity observed at basic pH might be explained by the formation of hydroxide ions, which affect the internal structure of the T2/T3 copper complex in the laccase molecule and, in consequence, lead to the reduction potential of oxygen and decrease the reaction efficiency [43]. The effect of the temperature on the relative activity of the free and immobilized laccases was presented in Fig. 6b. This indicates that catalytic properties of the tested biocatalysts increased up to 30 °C, reached a maximum and then sharply decreased. Nevertheless, MCF + Cu + lac and MCF + lac exhibited over 80% of relative activity at temperature ranging from 20 °C to 40 °C and even approx. 60% at 50 °C, which was much higher compared to free enzyme at the same temperature conditions. The decrease of the relative activity at higher temperatures (over 50 °C) is related to the partial enzyme inactivation due to thermal denaturation of the enzyme structure [44].

Nevertheless, based on the presented results, it could be stated that thermal and chemical stability of both the obtained biocatalytic systems was improved as compared with the free laccase. This can be explained by the protective effect of the MCF support material towards laccase molecules. At the tested pH range, the surface of the support is negatively charged and the enzyme is positively charged (IEP of MCF is equal to approx. 2.5, IEP of laccase is equal to approx. 8.5), which facilitate the formation of strong enzyme-support interactions and, in consequence, stabilize and rigidize the structure of the biocatalysts [45]. Furthermore, enzyme molecules are deposited into the pores of the support which protect them against denaturation and inactivation due to harsh reaction conditions. Moreover, as it was expected, due to activation effect of the copper ions, the MCF + Cu + lac exhibited higher relative activity over the analyzed pH and temperature ranges, which retained over 30% of its activity even at pH 8 and temperature 60 °C. Significant improvement of the thermal and chemical stability of laccase immobilized onto MCF material was also observed by Zhao et al. In their study, the immobilized enzyme exhibited the highest activity at temperature equal to 50 °C and at pH equal to 3. However, due to limitation of the conformational changes of the enzyme structure upon immobilization, it retained over 50% of relative activity over wider pH (form 4 to 6) and temperature range (35–55 °C) as compared to free enzyme [42].

3.2.3. Storage stability and reusability

Reusability and storage stability are of key importance in terms of practical application as they enhance the biocatalytic productivity and contribute to a more cost-effective process. The storage stability of the

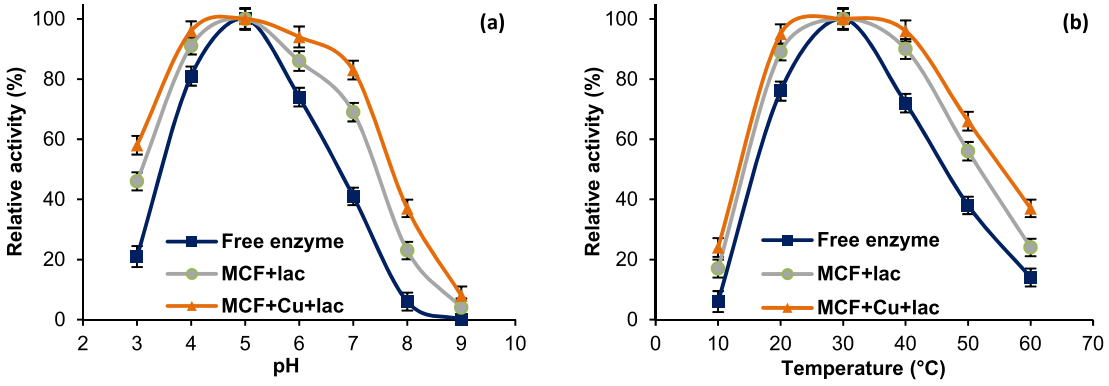

Fig. 6. Effect of: pH (a) and temperature (b) on the relative activity of free and immobilized laccase.

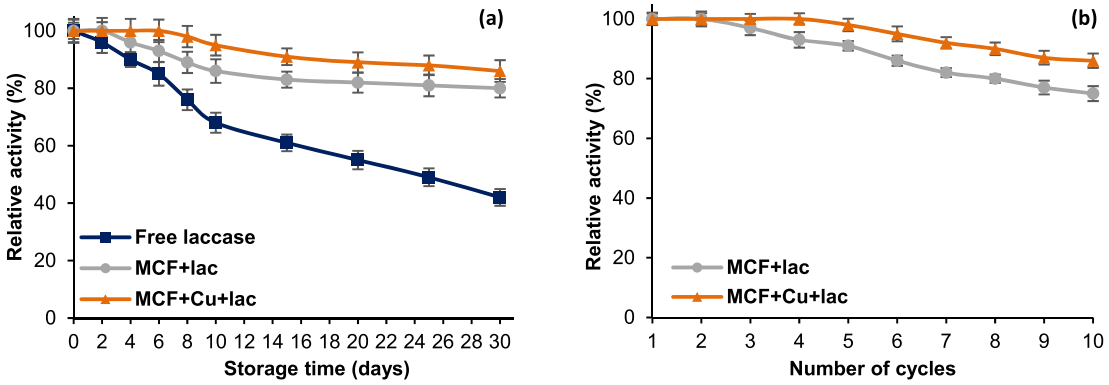

Fig. 7. Storage stability (a) and reusability (b) of the immobilized laccase.

MCF + lac and MCF + Cu + lac biocatalytic systems was examined over 30 days (Fig. 7a). Immobilized enzymes retained over 95% of their initial activity over 5 days. After that time, the relative activity slightly decreased and after 30 days reached 88% and 82%, respectively for MCF + Cu + lac and MCF + lac. These results indicate that storage stability of the laccase was significantly improved after immobilization, as the free enzymes retained less than 40% of their initial activity. To examine the capability to reuse the obtained biocatalytic systems, they were used in the 10 consecutive reaction cycles (Fig. 7b). The presented results indicate that the produced immobilized enzymes were characterized by exceptional reusability. After 5 reaction steps, the activity of the MCF + Cu + lac system was almost unaltered, whereas the activity of the MCF + lac decreased to 95%. Moreover, after 10 cycles, laccase immobilized onto the unmodified and modified MCF retained over 85% and 80% of its initial activity.

Significant improvement of the storage stability and reusability of the immobilized laccase may result from several factors. Firstly, enzymes are immobilized not only onto the surface of the MCF but also into its pores. As a result, the biomolecules are better protected against inactivation due to reaction conditions. Moreover, the immobilization into the pores of the support limited enzyme leakage as confirmed by the desorption test, which indicated that after 10 reaction cycles less than 25% of the laccase was eluted from the carrier. Moreover, as suggested in our previous study, silica supports provide protective effect for enzyme molecules and stabilize their structure upon immobilization [46]. Due to the above-mentioned facts, the obtained systems retain their catalytic properties over storage time and may be reused in consecutive reaction steps. Nevertheless, the observed decrease of the catalytic activity may be related to the partial elution of the enzyme, its denaturation by the products of the catalytic reaction as well as inactivation over time and reuse [47]. Similar results were also noticed by Moghrabi-Manzari et al., who coimmobilized laccase and 2,2,6,6-tetramethylpiperidin-1-oxyl (TEMPO) mediator using mesoporous SBA15 silica. Due to simultaneous coimmobilization of the enzyme and the mediator, the produced hybrid catalysts retained approx. 80% of its initial activity after 10 reaction cycles [36].

3.3. Tetracycline removal

The potential practical application of the produced biocatalytic systems in environmental protection was tested by using the obtained catalysts in the removal process of tetracycline, a commonly used antibiotic. However, since MCF and other silica-based materials are known from their high sorption properties, the adsorption efficiency of tetracycline by pure MCF materials and materials with thermally inactivated enzyme has also been examined in order to confirm the simultaneous adsorption/biodegradation mechanism of tetracycline removal (Fig. 8). Surprisingly, although the MCF materials exhibit good sorption properties towards pharmaceuticals [48,49], MCF and MCF

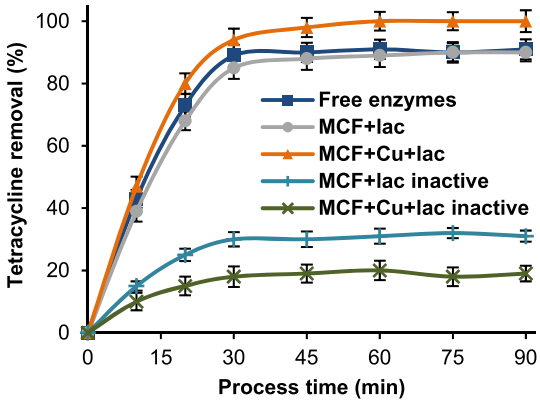

Fig. 8. Time course of the adsorption and biodegradation of tetracycline by free, inactive and active immobilized laccase.

modified by Cu ions before enzyme immobilization removed less than 80% of tetracycline after 90 min of the process (data not presented). This most likely resulted from the high molecular weight of tetracycline, the sorption of which saturated the active sites on the surface of the sorbent material. After immobilization of the enzyme, the sorption capacity of the MCF materials with inactive biocatalysts towards tetracycline significantly decreased, due to the attachment of enzymes on the surface of the support/sorbent material, and reached approx. 30% and 20% for MCF + lac and MCF + Cu + lac, respectively. On the other hand, free laccase exhibited high efficiency of tetracycline biodegradation as the removal rate reached 92% after just 30 min of the process. However, even higher total removal efficiencies of the antibiotic were obtained when immobilized biocatalysts were used. MCF doped with Cu ions completely removed tetracycline after 60 min of the process whereas the MCF + lac system allowed to reach 91% biodegradation efficiency. Higher removal rate obtained for the process carried out using the system based on modified MCF is associated with the presence of copper ions, which enhanced the enzyme activity and improved the transfer of electrons between the substrate and enzyme active site, as mentioned above. It should be emphasized that the obtained results clearly show that removal of tetracycline occurs as a result of simultaneous adsorption and catalytic biodegradation since the total removal efficiency was achieved only when the immobilized biocatalyst (MCF + Cu + lac system) was used, which makes them a promising approach for application in wastewater treatment. Application of separate adsorption and biocatalytic degradation was insufficient to completely remove the antibiotic.

4. Conclusions

The presented study provides a proof-of-concept for the

immobilization of laccase using mesostructured cellular foam silica, and application of the immobilized enzymes for efficient removal of tetracycline from model aqueous solutions. The obtained materials were characterized by spherical pores with diameters of approx. 25 nm, which makes MCF a suitable support for laccase binding. In addition, the synthesized MCF has been modified by copper ions to improve the catalytic activity of the enzyme. It has been shown that higher enzyme loading and immobilization yield, respectively equal to 188 mg g^{-1} and 94%, were obtained for unmodified MCF, as compared to the Cu-modified silica. However, laccase immobilized onto modified support is characterized by higher activity over wider pH and temperature range, conforming a positive effect of these ions onto the enzymatic activity. In addition, the produced biocatalytic systems were characterized by improved storage stability and reusability, since after 30 days of storage and ten consecutive catalytic cycles the MCF + lac and MCF + Cu + lac respectively exhibited approx. 80% and over 90% of their initial activity. Furthermore, the presented data clearly shows that laccase immobilized onto the modified MCF support allows for complete removal of tetracycline from the aqueous solution at the concentration of 1 mg L^{-1} due to simultaneous adsorption and biocatalytic conversion, which makes the presented approach attractive for practical applications. We strongly believe that the presented data may stimulate further development of the use of MCF materials for enzyme immobilization as well as application of the biocatalytic systems for removal of hazardous compounds from aqueous solutions.

Acknowledgements

We wish to express our sincere gratitude to Professor Mietek Jaroniec. His support was the foundation of our inspiration and his valuable suggestions were much appreciated.

This study was funded by Ministry of Science and Higher Education (Poland) as financial subsidy to PUT under the grant no. 03/32/SBAD/0906.

References

[1] F. Schüth, Angew. Chem. Int. Ed. 42 (2003) 3604–3622 https://doi.org/10.1002/anie.200300593.
[2] M. Kruk, M. Jaroniec, Chem. Mater. 13 (2001) 3169–3183 https://doi.org/10.1021/cm010106913.
[3] P.N.E. Diagboya, E.D. Dikio, Microporous Mesoporous Mater. 266 (2018) 252–267 https://doi.org/10.1016/j.micromeso.2018.03.008.
[4] X. Li, J. Yu, M. Jaroniec, Chem. Soc. Rev. 45 (2016) 2603–2636 https://doi.org/10.1039/c5cs00838g.
[5] R. Ryoo, C.H. Ko, M. Kruk, V. Antochshuk, M. Jaroniec, J. Phys. Chem. B 104 (2000) 11465–11471 https://doi.org/10.1021/jp002597a.
[6] X. Li, J. Yu, M. Jaroniec, C. Chen, Chem. Rev. 119 (2019) 3962–4179 https://doi.org/10.1021/acs.chemrev.8b00400.
[7] I. Sobczak, M. Ziolek, M. Renn, P. Decyk, I. Nowak, M. Daturi, J.C. Lavalley, Microporous Mesoporous Mater. 74 (2004) 23–36 https://doi.org/10.1016/j.micromeso.2004.05.015.
[8] A. Feliczak-Guzik, B. Jadach, H. Piotrowska, M. Murias, J. Lulek, I. Nowak, Microporous Mesoporous Mater. 220 (2016) 231–238 https://doi.org/10.1016/j.micromeso.2015.09.006.
[9] J. Choma, M. Jaroniec, W. Burakiewicz-Mortka, M. Kloske, Appl. Surf. Sci. 196 (2002) 216–223 https://doi.org/10.1016/S0169-4332(02)00060-0.
[10] B.J. Jankiewicz, D. Jamiola, J. Choma, M. Jaroniec, Adv. Colloid Interface Sci. 170 (2012) 28–47.
[11] A. Taguchi, F. Schüth, Microporous Mesoporous Mater. 77 (2005) 1–45 https://doi.org/10.1016/j.micromeso.2004.06.030.
[12] M. Hartmann, Chem. Mater. 17 (2005) 4577–4593 https://doi.org/10.1021/cm0485658.
[13] G.Z. Papageorgiou, A. Palani, D. Gilliopoulos, K.S. Triantafyllidis, D.N. Bikiaris, J. Therm. Anal. Calorim. 113 (2013) 1651–1665 https://doi.org/10.1007/s10973-013-3223-z.
[14] M.L. Cerrada, E. Perez, J.P. Lourenco, J.M. Campos, M.R. Ribeiro, Microporous Mesoporous Mater. 130 (2010) 215–223 https://doi.org/10.1016/j.micromeso.2009.11.009.
[15] V. Antochshuk, M. Jaroniec, Chem. Mater. 128 (2000) 496–501 https://doi.org/10.1021/cm000268p.
[16] P. Schmidt-Winkel, W.W. Lukens, D. Zhao, P. Yang, B.F. Chmelka, G.D. Stucky, J. Am. Chem. Soc. 12 (1999) 1254–1255.
[17] Z. Li, J.C. Barnes, A. Bosoy, J.F. Stoddart, J.I. Zink, Chem. Soc. Rev. 41 (2012) 2590–2605 https://doi.org/10.1039/C1CS15246G.
[18] T. Jesionowski, J. Zdarta, B. Krajewska, Adsorption 20 (2014) 801–821 https://doi.org/10.1007/s10450-014-9623-y.
[19] J. Zdarta, A.S. Meyer, T. Jesionowski, M. Pinelo, Adv. Colloid Interface Sci. 258 (2018) 1–20 https://doi.org/10.1016/j.cis.2018.07.004.
[20] J. Zdarta, A.S. Meyer, T. Jesionowski, M. Pinelo, Biotechnol. Adv. (2019) Article in press https://doi.org/10.1016/j.biotechadv.2019.05.007.
[21] M.I. Kim, J. Kim, J. Lee, S. Shin, H.B. Na, T. Hyeon, H.G. Park, H.N. Chang, Microporous Mesoporous Mater. 111 (2008) 18–23 https://doi.org/10.1016/j.micromeso.2007.07.009.
[22] E. Guerrero, P. Aburto, E. Terrés, O. Villegas, E. González, T. Zayas, F. Hernández, E. Torres, J. Porous Mater. 20 (2013) 387–396 https://doi.org/10.1007/s10934-012-9608-8.
[23] D.I. Fried, D. Bednarski, M. Dreifke, F.J. Brieler, M. Thommesband, M. Froba, J. Mater. Chem. B 3 (2015) 2341–2349 https://doi.org/10.1039/c4tb01700e.
[24] J. Zhao, Y. Wang, G. Luo, S. Zhu, Bioresour. Technol. 101 (2010) 7211–7217 https://doi.org/10.1016/j.biortech.2010.04.067.
[25] K. Zynek, J. Bryjak, K. Szymańska, A.B. Jarzębski, Biotechnol. Bioproc. Eng. 16 (2011) 180–189 https://doi.org/10.1007/s12257-010-0011-5.
[26] M. Zhao, Y. Wang, Z. Liu, D. Cui, X. Bian, J. Macromol. Sci., Part A Pure Appl. Chem. 48 (2011) 447–453 https://doi.org/10.1080/10601325.2011.573330.
[27] A. Rekuć, J. Bryjak, K. Szymańska, A.B. Jarzębski, Process Biochem. 44 (2009) 191–198 https://doi.org/10.1016/j.procbio.2008.10.007.
[28] E. Santalla, E. Serra, A. Mayoral, J. Losada, R.M. Blanco, I. Díaz, Solid State Sci. 13 (2011), https://doi.org/10.1016/j.solidstatesciences.2010.09.015.
[29] J. Bryjak, K. Szymańska, A.B. Jarzębski, Chem. Process Eng. 33 (2012) 611–620 https://doi.org/10.2478/v10176-012-0051-9.
[30] M. Trejda, B. Pokora, M. Ziółek, Catal. Today 254 (2015) 104–110 https://doi.org/10.1016/j.cattod.2014.11.034.
[31] M.M. Bradford, Anal. Biochem. 72 (1976) 248–254 https://doi.org/10.1006/abio.1976.9999.
[32] Y. Dai, J. Niu, J. Liu, L. Yin, J. Xu, Bioresour. Technol. 101 (2010) 8942–8947 https://doi.org/10.1016/j.biortech.2010.07.027.
[33] E. Santalla, E. Serra, A. Mayoral, J. Losada, R.M. Blanco, I. Diaz, Solid State Sci. 13 (2011) 691–697 https://doi.org/10.1016/j.solidstatesciences.2010.09.2015.
[34] P.T.T. Wong, R.K. Nong, T.A. Caputo, T.A. Godwin, B. Rigas, Proc. Natl. Acad. Sci. 88 (1991) 10988–10992 https://doi.org/10.1073/pnas.88.24.10988.
[35] S. Zhu, D. Zhang, N. Yang, J. Nanoparticle Res. 11 (2009) 561–568 https://doi.org/10.1007/s11051-007-9325-4.
[36] M. Mogharabi-Manzari, M. Amini, M. Abdollahi, M. Khoobi, G. Bagherzadeh, M. Ali Faramarzi, ChemCatChem 10 (2018) 1542–1546 https://doi.org/10.1002/cctc.201701527.
[37] L. Hermida, A.Z. Abdullah, A.R. Mohamed, J. Mater. Environ. Sci. 9 (2018) 2328–2333.
[38] S. Nanaki, M. Tseklima, Z. Terzopoulou, M. Nerantzaki, D.J. Giliopoulos, K. Triantafyllidis, M. Kostoglou, D.N. Bikiaris, Eur. J. Pharm. Biopharm. 117 (2017) 77–90, https://doi.org/10.1016/j.ejpb.2017.03.016.
[39] L.D. Jadhav, S.P. Patil, A.U. Chavan, A.P. Jamale, V.R. Puri, Micro & Nano Lett. 6 (2011) 812–815, https://doi.org/10.1049/mnl.2011.0372.
[40] M.Y. Arica, S. Senel, N.G. Alaeddinoglu, S. Patir, A. Denizli, J. Appl. Polym. Sci. 75 (2000) 1685–1692 https://doi.org/10.1002/1097-4628.7514.1685.26.
[41] O.M. Gomma, O.A. Momtaz, Braz. J. Microbiol. 46 (2015) 285–292 https://doi.org/10.1590/S1517-838246120120118.
[42] M. Zhao, Y. Wang, Z. liu, D. Cui, X. Bian, J. Macromol. Sci., Pure Appl. Chem. 48 (2011) 447–453 https://doi.org/10.1080/10601325.2011.573330.
[43] P.J. Strong, H. Claus, Crit. Rev. Environ. Sci. Technol. 41 (2011) 373–434 https://doi.org/10.1080/10643380902945706.
[44] S. Singh, P.K. Srivastava, Adv. Enzym. Res. 2 (2014) 134–149 https://doi.org/10.4236/aer.2014.24014.
[45] Q.Y. Li, P.Y. Wang, Y.L. Zhou, Z.R. Nie, Q. Wei, J. Sol. Gel Sci. Technol. 78 (2016) 523–530 https://doi.org/10.1007/s10971-016-3967-6.
[46] J. Zdarta, M. Pinelo, T. Jesionowski, A.S. Meyer, ChemCatChem 10 (2018) 5164–5173 https://doi.org/10.1002/cctc.201801335.
[47] J. Jordan, C.S.S.R. Kumar, C. Theegala, J. Mol. Catal. B Enzym. 68 (2011) 139–146 https://doi.org/10.1016/j.molcatb.2010.09.010.
[48] M. Barczak, Microporous Mesoporous Mater. 278 (2019) 354–365 https://doi.org/10.1016/j.micromeso.2019.01.012.
[49] C. Jung, A. Son, N. Her, K.-D. Zoh, J. Cho, Y. Yoon, J. Ind. Eng. Chem. 27 (2015) 1–11 https://doi.org/10.1016/j.jiec.2014.12.035.

biomolecules

MDPI

Article

3D Chitin Scaffolds from the Marine Demosponge *Aplysina archeri* as a Support for Laccase Immobilization and Its Use in the Removal of Pharmaceuticals

Jakub Zdarta [1,*], Tomasz Machałowski [1,2], Oliwia Degórska [1], Karolina Bachosz [1], Andriy Fursov [2], Hermann Ehrlich [2,3], Viatcheslav N. Ivanenko [4] and Teofil Jesionowski [1,*]

1 Faculty of Chemical Technology, Institute of Chemical Technology and Engineering, Poznan University of Technology, Berdychowo 4, 60965 Poznan, Poland; tomasz.g.machalowski@doctorate.put.poznan.pl (T.M.); oliwia.degorska@gmail.com (O.D.); karolinabachosz@gmail.com (K.B.)

2 Institute of Electronics and Sensor Materials, TU Bergakademie Freiberg, Gustav-Zeuner str. 3, 09599 Freiberg, Germany; andriyfur@gmail.com (A.F.); hermann.ehrlich@esm.tu-freiberg.de (H.E.)

3 Wielkopolska Center for Advanced Technologies (WCAT), Poznan University str. 10, 61614 Poznan, Poland

4 Department of Invertebrate Zoology, Biological Faculty, Lomonosov Moscow State University, 119992 Moscow, Russia; ivanenko.slava@gmail.com

* Correspondence: jakub.zdarta@put.poznan.pl (J.Z.); teofil.jesionowski@put.poznan.pl (T.J.)

Received: 19 March 2020; Accepted: 20 April 2020; Published: 22 April 2020

Abstract: For the first time, 3D chitin scaffolds from the marine demosponge *Aplysina archeri* were used for adsorption and immobilization of laccase from *Trametes versicolor*. The resulting chitin–enzyme biocatalytic systems were applied in the removal of tetracycline. Effective enzyme immobilization was confirmed by scanning electron microscopy. Immobilization yield and kinetic parameters were investigated in detail, in addition to the activity of the enzyme after immobilization. The designed systems were further used for the removal of tetracycline under various process conditions. Optimum process conditions, enabling total removal of tetracycline from solutions at concentrations up to 1 mg/L, were found to be pH 5, temperature between 25 and 35 °C, and 1 h process duration. Due to the protective effect of the chitinous scaffolds and stabilization of the enzyme by multipoint attachment, the storage stability and thermal stability of the immobilized biomolecules were significantly improved as compared to the free enzyme. The produced biocatalytic systems also exhibited good reusability, as after 10 repeated uses they removed over 90% of tetracycline from solution. Finally, the immobilized laccase was used in a packed bed reactor for continuous removal of tetracycline, and enabled the removal of over 80% of the antibiotic after 24 h of continuous use.

Keywords: chitin scaffolds; marine scaffolds; enzyme immobilization; laccase; tetracycline; pollutant removal

1. Introduction

Traditionally, diverse polymer-, carbon-, inorganic-, and hybrid-based ultralight porous three-dimensional (3D) materials have been used for enzyme immobilization [1–4]. Recently, modern porous 3D printing scaffolds with complex internal structures and channels have been the focus of much attention [5]. Our scaffolding strategy [6] is based, however, on naturally prefabricated 3D scaffolds of poriferan (sponge) origin. These unique biopolymer-containing constructs offer alternative immobilization matrices that can be isolated from demosponges cultivated worldwide, to provide appropriate supports for a broad range of enzymes. Thus, demosponges of the order Dictioceratida (also known as commercial bath

sponges) [7,8] represent a renewable source of proteinaceous spongin scaffolds which have recently been reported as effective in applications in extreme biomimetics [9–12], waste treatment [13–17], electrochemistry [18], and enzyme immobilization [19]. Meanwhile, marine demosponges of the order Verongiida have been recognized as a renewable source of uniquely pre-structured 3D chitinous scaffolds [20–28] which have found applications in tissue engineering [6,21,29–34], drug release [35], the development of hybrid materials [36–40], and environmental science [41,42]. Chitin of invertebrate origin has previously been studied by researchers in protein immobilization as a matrix for the immobilization of enzymes [43–48], including lipases [49,50] and papain [51]. However, in this study we investigated the ability of a unique, ready-to-use 3D chitinous scaffold isolated from the marine demosponge *Aplysina archeri* (Figure 1) to immobilize laccase as a selected enzyme, and an innovative application of this unique system in the removal of tetracycline by simultaneous adsorption and catalytic conversion.

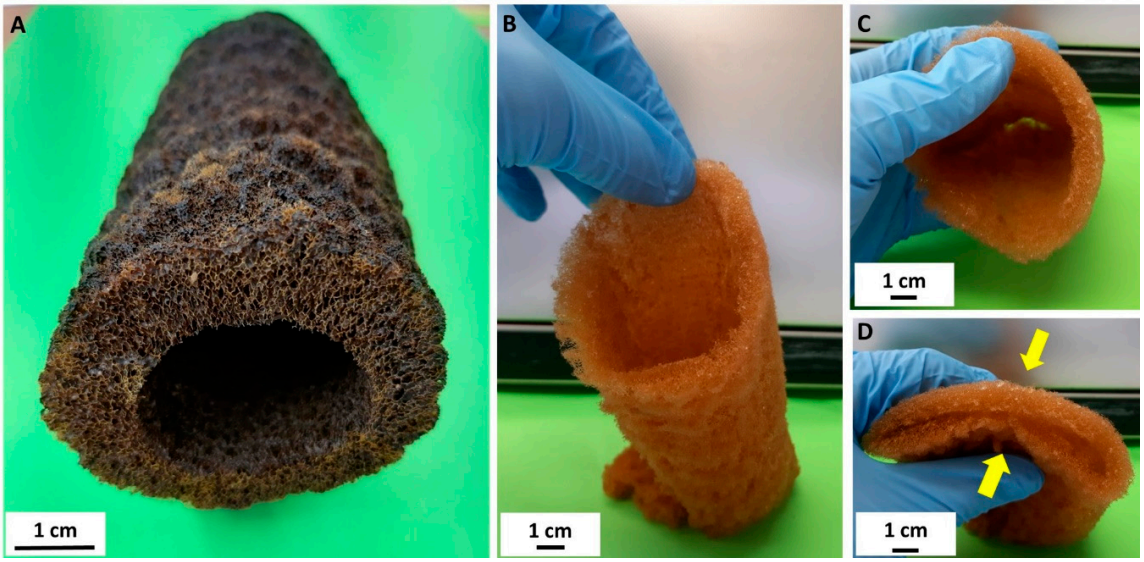

Figure 1. A selected air-dried fragment of *Aplysina archeri* sponge skeleton is rigid and represents the typical tube-like morphology of verongiids (**A**). Decellularization with subsequent demineralization of this construct [6,26] leads to isolation of the flexible chitinous scaffold (**B**–**D**), which reproduces the shape, form, and structural features of the original tubular sponge skeleton, with a length of up to 1.5 m.

The laccase (EC 1.10.3.2) is an enzyme classified as multicopper oxidoreductase, that occurs in numerous higher plants, several bacteria, and is secreted by many fungi [52]. Laccase catalyzes the oxygen reduction reaction directly to water with the simultaneous oxidation of polyphenols, aminophenols, polyamines, and lignins. The active center of the laccase contains four adjacent copper atoms, which represent three types distinguished by their specific properties. Type I copper gives the enzyme molecule blue color and is the site of oxidation of the substrate. Copper type II and two atoms of copper type III form a three-atomic assembly in which binding and reduction of molecular oxygen to water occurs. During each catalytic cycle of laccase, there is a reduction of one oxygen molecule to two water molecules, accompanying oxidation of four substrate molecules to four substrate radicals [53]. Laccases find a variety of applications in many industries due to a number of reactions involving them. This enzyme is used to remove impurities in wastewater thanks to the phenol oxidation reaction and to degrade industrial waste [54]. It is also used on a large scale in the process of lignin degradation and detoxification of aromas generated in this process [55]. In order to increase its activity and easier separation of the enzyme from the post-reaction mixture laccase can be immobilized on a variety of carriers, such as chitinous sponges.

2. Materials and Methods

2.1. Chemicals and Materials

Samples of the verongiid demosponge *Aplysina archeri* (Higgin, 1875) (Figure 1) were collected at depths of 10–25 m by scuba divers around the Caribbean islands of Saint Vincent and Curaçao in May–June 2017, during the Pacotilles expedition. All permits required for the study were obtained during that expedition, which complied with all relevant regulations [26]. The reagents used for isolation of chitin sponge skeleton—sodium hydroxide, acetic acid, and hydrogen peroxide—were supplied by Merck (Darmstadt, Germany). Reagents for enzyme immobilization—laccase from *Trametes versicolor* (EC 1.10.3.2, activity ≥0.5 U/mg), 50 mM phosphate buffer (at pH 7–9), and 100 mM acetate buffer (at pH 3–6)—were supplied by Sigma Aldrich (St. Louis, MO, USA). Tetracycline (>99%), 2,2′-azino-bis(3-ethylbenzothiazoline-6-sulfonic acid) (ABTS) and Bradford reagent used for examination of the quantity of immobilized enzyme were supplied by Sigma Aldrich (St. Louis, MO, USA).

2.2. Isolation of Chitin Sponge Skeletons

Modified Standard Method

The isolation of chitinous scaffold from *A. archeri* was performed by a modified version of the standard method proposed by Ehrlich et al. in 2007 [20]. First, a selected fragment of the sponge (see Figure 1) was placed in deionized water for 1 h at 24 °C to remove water-soluble compounds. A deproteinization process was then carried out using 2.5 M NaOH (Th. Geyer GmbH & Co. KG, Renningen, Germany) at 37 °C for 24 h. The skeletal scaffold was next washed with distilled water to neutral pH, and treated with 20% acetic acid (Th. Geyer GmbH & Co. KG, Renningen, Germany) at 24 °C for 6 h to remove residual calcium carbonates. It was then neutralized by rinsing with deionized water [26]. Deproteinization and demineralization of the sponge skeleton were repeated for 144 h to obtain a completely soft and pigment-free chitinous scaffold (Figure 2) for further use as a support in enzyme immobilization.

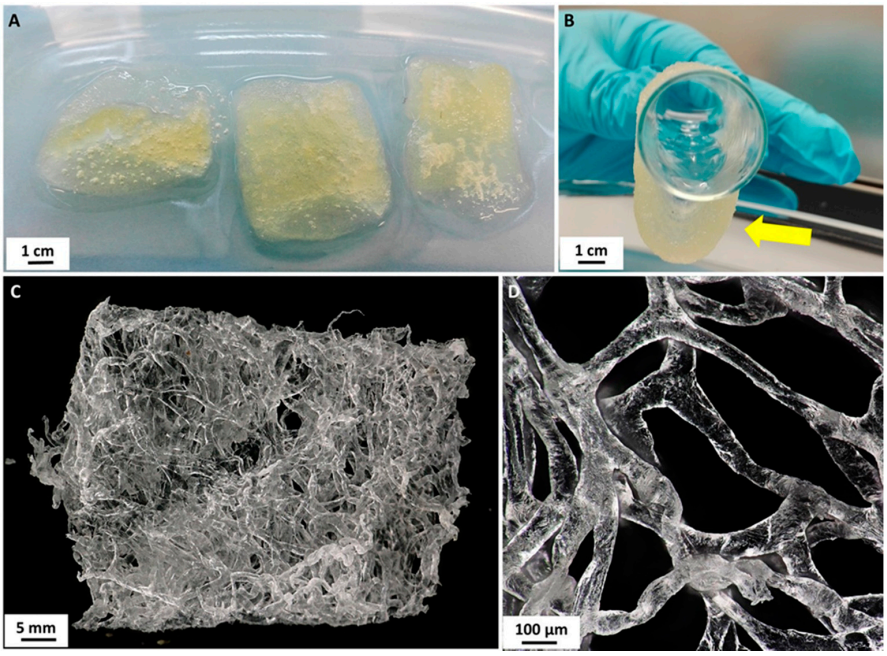

Figure 2. Isolated chitinous scaffolds (**A**) possess excellent ability to insert water (**B**, arrow). On drying in air at ambient temperature these constructs remained three-dimensional (**C**) and retained their characteristic interconnected microtubular architecture (**D**).

2.3. Laccase Immobilization

Prior to laccase immobilization, the chitinous scaffolds (Figure 2C) were cut into pieces weighing 5 mg. Then, 5 mg of the isolated scaffold was placed in a vial, to which 2 mL of laccase solution in acetate buffer at pH 5 and concentration 5 mg/mL was added. The mixture was placed in an incubator (IKA Werke GmbH, Staufen im Breisgau, Germany) and was shaken at 150 rpm for 1 h at 25 °C. After enzyme immobilization the samples were removed from the mixture, washed with acetate buffer at pH 5 to remove unbound enzyme, and used in tests involving the removal of tetracycline. The supernatant after immobilization was subjected to spectrophotometric measurements to evaluate the quantity of immobilized enzyme and the immobilization yield.

2.4. Characterization of Immobilized Enzymes

The amount of the immobilized enzyme was calculated based on the spectrophotometric measurements using the Bradford protein assay method [56]. The amount of immobilized enzyme, expressed in mg/g, was determined as the difference between the initial amount of enzyme and the final laccase concentration in the mixture after immobilization, relative to the mass of the chitin scaffold. Immobilization yield (%) was calculated by considering the difference in the amounts of the enzyme before and after immobilization in both, supernatant after immobilization and acetate buffer used to remove unbound enzyme, and the volume of the solution used in this process.

Activity assays for free and immobilized laccase were performed spectrophotometrically, based on a model reaction using 2,2′-azino-bis(3-ethylbenzothiazoline-6-sulfonic acid) (ABTS) as a substrate. Briefly, 10 mg of free or immobilized enzyme was added to 5 mL of a mixture containing 10 mM of ABTS in phosphate buffer at pH 5. The reaction was carried out for 60 min at 25 °C. After the process, spectrophotometric measurements were made at wavelength 420 nm. One unit of free or immobilized laccase activity was defined as the amount of enzyme needed to convert 1 mM of ABTS per minute under the assay conditions. Based on the results, using a standard calibration curve for ABTS, the specific activity of the free and immobilized enzyme (U/mg) was calculated as the initial enzyme activity retained, respectively, per unit mass of enzyme and per unit mass of enzyme and support. The activity retention (%) of immobilized laccase is presented as the percentage activity of the immobilized laccase, relative to the catalytic activity of the free enzyme.

The kinetic parameters of the free and immobilized laccase—the Michaelis–Menten constant (K_M) and the maximum reaction rate (V_{max})—were examined based on the above-mentioned ABTS oxidation reaction using solutions of substrate at concentrations ranging from 0.01 to 10 mM, performed under optimal assay conditions. The apparent kinetic parameters (K_M and V_{max}) of free and immobilized laccase were calculated using Hanes–Woolf plot.

The storage stability of free and immobilized laccase was tested spectrophotometrically over 30 days of storage at 4 °C in acetate buffer at pH 5. Storage stability was determined using ABTS as a substrate, according to the methodology described above, by evaluation of the activity retention of free and immobilized enzyme at specified time intervals.

The thermochemical stability of both free and immobilized laccase over time was examined after incubating the samples for 120 min under optimum pH and temperature conditions (pH 5, temperature 25 °C). Spectrophotometric measurements were performed based on the reaction using ABTS as a substrate. The relative activity of free and immobilized enzyme was determined at specified time intervals. For clearer presentation of the data, in these experiments the initial activity of free laccase was defined as 100% activity. The inactivation curves of free and immobilized enzyme, the inactivation constant (k_D) and the half-life ($t_{1/2}$) were calculated based on the linear regression slope.

2.5. Removal of Tetracycline

The main objective of the study was to use the obtained biocatalytic systems for efficient removal of tetracycline in various pH and temperature conditions and using antibiotic solutions

at various concentrations. To determine the contributions of adsorption and catalytic conversion to total tetracycline removal, experiments were performed to evaluate the efficiency of adsorption of tetracycline by pure chitin sponge skeleton and by the sponge skeleton with immobilized enzyme following thermal inactivation, as well as the efficiency of removal of the antibiotic by simultaneous adsorption and catalytic conversion by the produced biocatalytic systems.

2.5.1. Adsorption of Tetracycline by Pure Chitin Scaffolds

Before the overall efficiency of tetracycline removal was evaluated, a determination was made of the efficiency of adsorption of the antibiotic by the pure chitin scaffolds. For this purpose, 10 mg of the chitinous scaffold was placed in vials, to which 10 mL of the tetracycline solution at appropriate concentration was added. The process was carried out for 1 h. To examine the effect of pH, buffer solution was used to adjust the pH to values ranging from 3 to 9 (acetate buffer at pH 3–6 and phosphate buffer at pH 7–9). The experiments were performed at 25 °C, using tetracycline solution at concentration 1 mg/L. Tests to establish the effect of temperature on the adsorption efficiency were performed at temperatures ranging from 5 to 65 °C (10 °C step) using tetracycline solution at pH 5 and concentration 1 mg/L. The effect of antibiotic concentration on the efficiency of its adsorption was determined at 25 °C using solutions at pH 5 and concentrations 0.1, 0.5, 1.0, and 3.0 mg/L. After the adsorption process the chitinous sponges were separated and the reaction mixture underwent further spectrophotometric measurements.

2.5.2. Adsorption of Tetracycline by Chitin Scaffolds with Thermally Inactivated Enzyme

In the next step, a determination was made of the efficiency of adsorption of tetracycline by chitin scaffold with immobilized enzyme following thermal inactivation. For this purpose, the products obtained after the immobilization stage were placed in a dryer for 2 h at 80 °C for enzyme inactivation, and then used in the adsorption experiment. The adsorption tests were carried out for 1 h using 10 mL of the tetracycline solution, to which 10 mg of the chitinous scaffold with inactive enzyme was added. The effect of pH was examined over pH ranging from 3 to 9, at 25 °C using tetracycline solution at concentration 1 mg/L. The effect of temperature on the efficiency of adsorption of tetracycline was examined at temperatures from 5 to 65 °C (10 °C step) using antibiotic solution at concentration 1 mg/L and acetate buffer at pH 5. The effect of concentration of tetracycline solution on the efficiency of its adsorption was examined at 25 °C using solutions at pH 5 and concentrations 0.1, 0.5, 1.0, and 3.0 mg/L. After adsorption the chitinous skeletons were separated and the reaction mixture underwent spectrophotometric measurements.

2.5.3. Removal of Tetracycline by Simultaneous Adsorption and Catalytic Conversion

The next step involved determination of the efficiency of removal of tetracycline by simultaneous adsorption and catalytic conversion, catalyzed by the systems with immobilized enzyme. For this purpose, to 10 mg of the freshly obtained biocatalytic systems, 10 mL of tetracycline solution at the appropriate concentration was added. The process was carried out for 1 h. To evaluate the effect of tetracycline concentration on the rate of its removal, solutions at concentrations 0.1, 0.5, 1.0, and 3.0 mg/L, in acetate buffer at pH 5, were used. The process was performed at 25 °C. To study the effect of pH, solutions at concentration 1 mg/L at pH ranging from 3 to 9 were tested at 25 °C. The effect of temperature on the efficiency of removal of tetracycline was examined over the temperature range 5–65 °C (10 °C step) using antibiotic solution at concentration 1 mg/L at pH 5. After the removal experiments the biocatalytic systems were separated and the reaction mixture underwent spectrophotometric measurements.

2.5.4. Reusability of Immobilized Laccase

The reusability of the immobilized laccase was examined according to the methodology described above, by measuring the efficiency of removal of tetracycline over 10 repeated biocatalytic cycles using 10 mL of tetracycline solution at pH 5 and concentration 1 mg/L at 25 °C. After each removal cycle the chitinous scaffolds with immobilized laccase were separated from the reaction mixture, washed with pH 5 acetate buffer to remove unreacted substrates and products from the chitin scaffold, and transferred to fresh tetracycline solution.

2.6. Removal of Tetracycline in Packed Bed Reactor

Continuous removal of tetracycline by the chitinous scaffolds with immobilized laccase was performed in a packed bed bioreactor containing 500 mg of chitinous scaffold with immobilized laccase (the amount of immobilized enzyme was approx. 1 g). A schematic illustration of the packed bed reactor used in the study is presented in Figure 3. The process was performed for 24 h at temperature 25 °C using tetracycline solution at concentration 1 mg/L at pH 5. The tetracycline solution was placed in a substrate vessel and was passed through the column at a flow rate of 2 mL/min using a peristaltic pump. The effluents from the column were collected in separate vessels at specified intervals and underwent spectrophotometric measurements. The efficiency of removal of tetracycline was calculated using the following equation (Equation (1)):

$$\frac{Adsorption}{Removal}\ Efficiency\ (\%) = \frac{C_i - C_t}{C_i} \quad (1)$$

where C_i. denotes the initial tetracycline concentration and C_t. denotes the final tetracycline concentration after treatment.

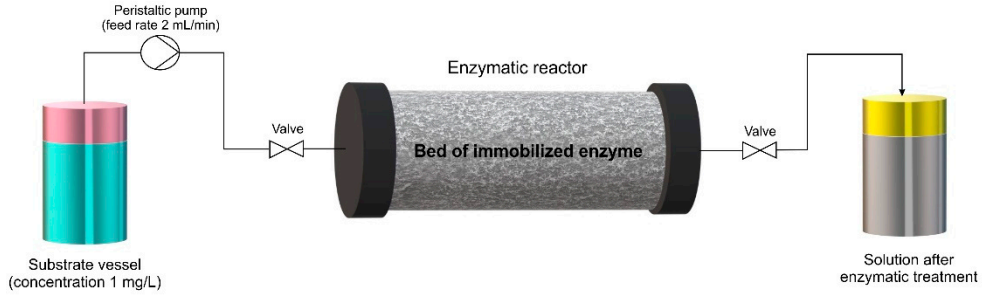

Figure 3. The packed bed reactor system used in the study for continuous removal of tetracycline.

2.7. Analytic Techniques

The morphology of the obtained chitinous materials before and after immobilization was examined by transmission electron microscopy (TEM) performed on a Hitachi HT7700 instrument (Hitachi, Japan) working in high contrast (HC) mode and operating at 100 kV. Prior to measurements, an appropriate quantity of the sample was dispersed in 2 mL of deionized water with the use of ultrasounds (Ultrasonic bath, Cavotator, Anaheim, CA, USA) and then 5 µL of the solution was applied on the nickel mesh grid covered with a carbon film. SEM photographs were obtained using an EVO40 scanning electron microscope (SEM, Zeiss, Oberkochen, Germany).

The structural features of the obtained chitinous scaffolds were observed using an advanced imaging and measurement system consisting of a Keyence VHX-6000 (Keyence, Tokyo, Japan) digital optical microscope and the swing-head zoom lenses VH-Z20R (magnification up to 200×) and VH-Z100UR (magnification up to 1000×).

The quantity of immobilized enzyme, immobilization yield, activity of free and immobilized enzyme, and efficiency of removal of tetracycline were examined based on spectrophotometric measurements using a Jasco V750 UV-Vis spectrophotometer (Jasco, Tokyo, Japan). The measurements

were performed at 595, 420, and 355 nm, respectively, for the Bradford method, ABTS, and tetracycline removal experiments. The final concentrations of laccase after the immobilization process, ABTS after oxidation, and tetracycline after treatment were obtained using calibration curves for bovine serum albumin, ABTS, and tetracycline, respectively. The rate of adsorption/removal of tetracycline (%) in all of the aforementioned experiments was calculated based on the Equation (1).

2.8. Statistical Analysis

All experiments and measurements in this study were performed in triplicate, and error values are defined as means ± standard deviation. Statistically significant differences were determined by one-way ANOVA using Tukey's test, performed in SigmaPlot 12 (Systat Software Inc., Los Angeles, CA, USA). Statistical significance was established at a level of $p < 0.05$.

3. Results

3.1. Characterization of Products after Immobilization

3.1.1. Morphological Analysis

In the first step of characterization, the surface morphology of the chitinous scaffolds before and after immobilization of laccase was determined based on analysis of SEM and TEM images (Figure 4).

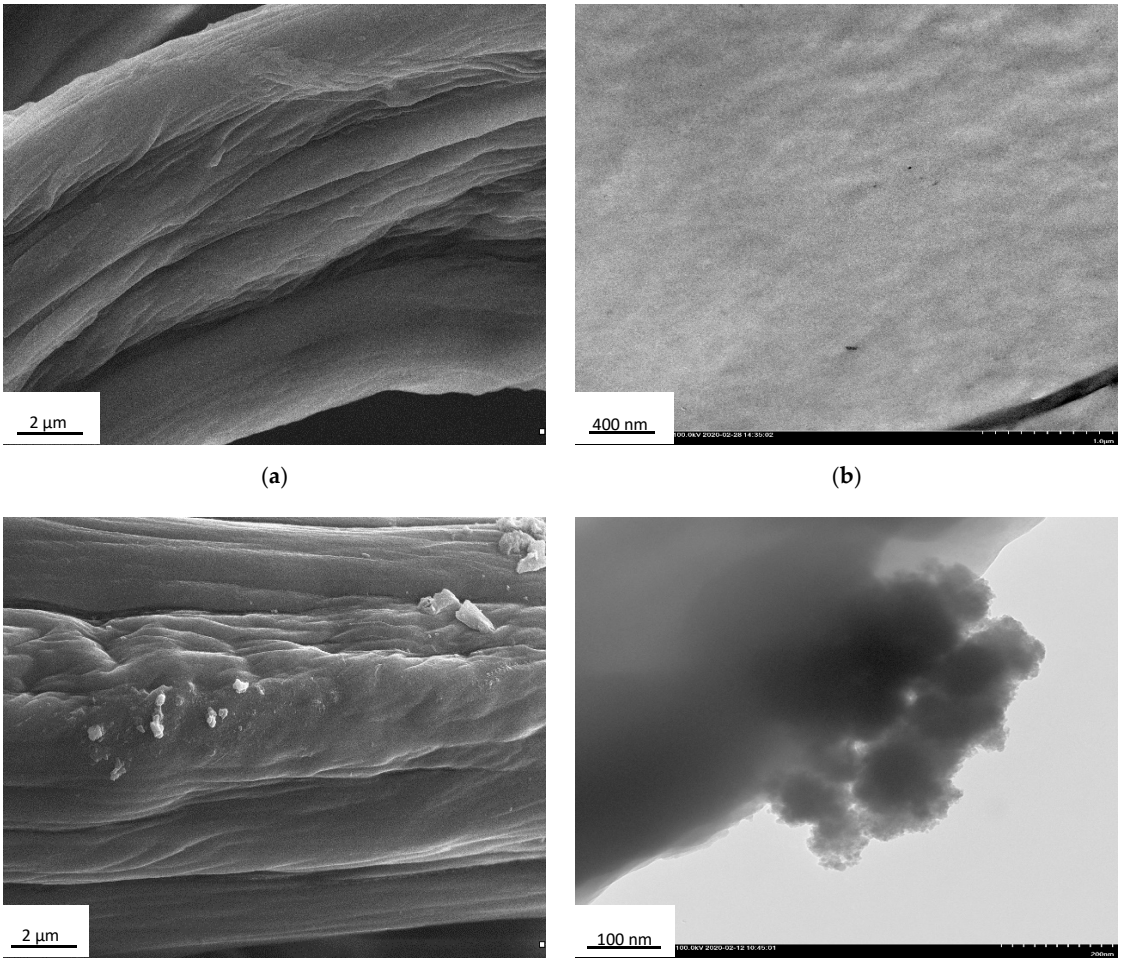

Figure 4. SEM and TEM images of the *A. archeri* sponge skeleton before (**a**,**b**) and after (**c**,**d**) laccase immobilization.

From Figures 2 and 4a it can be seen that the surface of chitinous scaffold from *A. archeri* before enzyme deposition is relatively uniform and smooth, being typically slightly folded after drying. Furthermore, no kind of microdamage was observed in the SEM and TEM images. By contrast, upon laccase immobilization, numerous aggregates with irregular shape and a size of around 500 nm are present on the surface of the chitinous scaffold. These aggregates may be interpreted as agglomerates of the enzyme molecules, and their presence confirms effective enzyme immobilization.

3.1.2. Characterization of the Immobilization Process and Kinetic Parameters of the Free and Immobilized Laccase

After confirmation of efficient immobilization, the process as well as the resulting chitin-based biocatalytic systems were characterized in terms of the process yield and the activity of the immobilized enzymes (Table 1). Furthermore, apparent kinetic parameters (K_M and V_{max}) of free and immobilized laccase were determined to examine changes in the substrate affinity of the enzyme upon immobilization.

Table 1. Parameters characterizing the immobilization process (amount of the immobilized enzyme, immobilization yield, specific activity and relative activity of free and immobilized laccase, and kinetic parameters of the free and immobilized enzyme.

Analyzed Parameter	Free Laccase	Immobilized Laccase
Immobilization yield (%)	-	91 ± 0.6
Amount of immobilized enzyme (mg/g)	-	1820 ± 90
Specific activity (U/mg)	56 ± 1.9	52.5 ± 1.5
Activity retention (%)	-	89 ± 3.2
K_M (mM)	0.093 ± 0.018	0.113 ± 0.022
V_{max} (mM/s)	0.048 ± 0.008	0.045 ± 0.011
V_{max}/K_M (1/s)	0.516	0.398

From Table 1 it can be seen that after 1 h of laccase immobilization from solution at concentration 5 mg/L, the relatively high immobilization yield of 91% was achieved. This results in an extremely high quantity of laccase immobilized on the chitinous scaffolds (around 1800 mg of the enzyme was immobilized per 1 g of the support). It is also evident from the data that almost 90% activity was retained by the immobilized laccase, as its specific activity was 52.5 U/mg, compared with 56 U/mg for the free enzyme. The study also included evaluation of the kinetic parameters of the free and immobilized laccase. Upon immobilization a slight increase in the value of the Michaelis–Menten constant (K_M), from 0.093 to 0.113 mM, was recorded. These results indicate a slightly lower substrate affinity in the case of the immobilized biomolecules, reflected in the lower values of the maximum reaction rate (0.048 mM/s) obtained for the immobilized laccase as compared to the free enzyme. Consequently, a lower catalytic efficiency (0.516 1/s) was also recorded for the immobilized laccase. Although the data show a slightly lower substrate affinity in the case of laccase bonded with the chitinous scaffold, the changes do not exceed 20%, clearly indicating that the obtained systems can be considered as a robust biocatalyst for further applications.

3.1.3. Storage Stability and Thermochemical Stability of Free and Immobilized Enzymes

The next part of the study concerned evaluation of changes in the relative activity of the free and immobilized laccase over time under storage and under process conditions (pH 5, temperature 25 °C) in order to determine their storage stability and thermochemical stability. The results are presented in Figure 5.

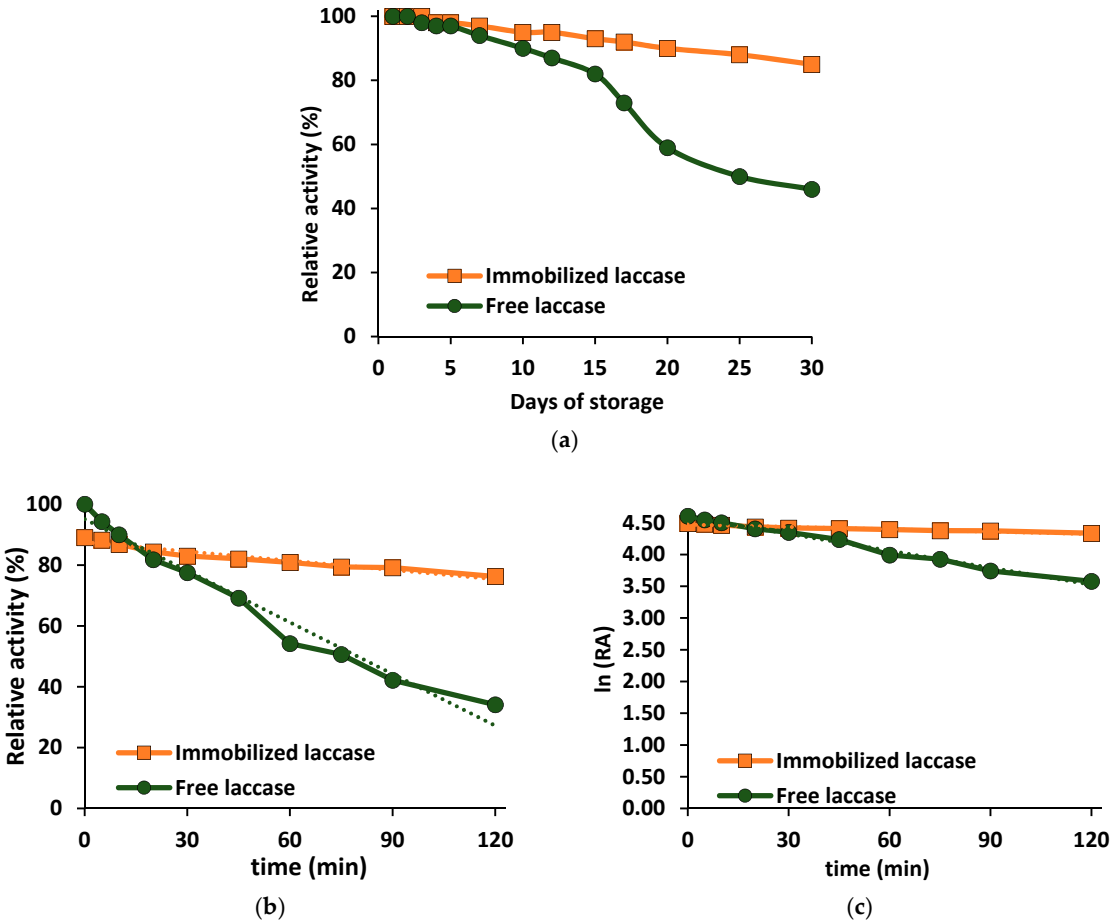

Figure 5. Storage stability of the free and immobilized enzyme (**a**) and stability under optimal process conditions (pH 5, temperature 25 °C) (**b**,**c**). The error value in each of the experiments (based on the mean and standard deviation from three experiments) does not exceed 3.5%.

From Figure 5a it can be seen that the activity of the free laccase decreased slightly from the first day of the storage stability test, and after 15 days reached around 80%. After that time a more gradual decrease in relative activity was recorded, and after 30 days of storage the relative activity of the free laccase did not exceed 50%. By contrast, the relative activity of the immobilized enzyme remained unaltered over the first 5 days of storage, and then began to decrease slightly. After 15 days it reached 93%, and after 30 days of storage at 4 °C almost 85% of the initial catalytic activity was retained, which is over 50% higher than the value for free laccase. The investigation also included determination of thermochemical stability profiles of the free and immobilized laccase under process conditions (pH 5, temperature 25 °C). The results (Figure 5b,c) clearly show that, although the initial activity of the immobilized laccase was slightly lower (see Table 1), the enzyme bound to the chitinous skeletons displayed a significant improvement in thermochemical stability as compared to the free biomolecules. After 30 and 120 min of incubation at process conditions, the immobilized laccase retained, respectively, 83% and 77% relative activity, indicating that the chitin-based biocatalytic systems were quite stable and prevented inactivation of the enzyme. Meanwhile, the activity of free laccase was gradually reduced: after incubation in the same conditions, after 15 and 120 min it retained, respectively, around 80% and less than 40% of its activity. Furthermore, the inactivation constant (k_D) and half-life ($t_{1/2}$) of free and immobilized laccase were examined and compared based on a linear regression slope. The results are in agreement with the data presented above; the values of k_D and $t_{1/2}$ for the immobilized enzyme were found to be 0.0038 1/min and 182.4 min, respectively, while for the free enzyme they were 0.0174 1/min and 39.8 min. Thus, the inactivation constant of the immobilized

laccase was more than four times lower than that of the free enzyme, while the enzyme half-life was increased by 4.5 times upon immobilization. The presented data clearly indicate that chitinous sponge skeletons are suitable matrices for laccase immobilization and protect the immobilized biomolecule against thermal and chemical inactivation.

3.2. Removal of Tetracycline

Following confirmation of the effective immobilization of laccase and evaluation of the stability of the produced biocatalytic systems, in the next step of the investigation the immobilized laccase was applied in the removal of tetracycline from water solutions under various process conditions, including different pH, temperature, and tetracycline solution concentration. This was the main objective of the study. Furthermore, as removal of tetracycline took place by simultaneous adsorption and biocatalytic conversion, we decided to follow these processes in detail to examine their contributions to the total removal of the antibiotic. It should be additionally noted that experiments on the use of pure chitinous scaffolds and free enzyme for adsorption and conversion of tetracycline under the most suitable process conditions (pH 5 and temperature 25 °C) result in removal rates of around 80% and 60%, respectively (full data not presented), indicating that total removal of the antibiotic by the separately applied techniques is not possible to achieve.

3.2.1. Effect of Concentration of Tetracycline Solution on Efficiency of Its Removal

In the first stage of the investigation, the effect of the concentration of tetracycline solution, in a range from 0.1 to 3.0 mg/L, on the efficiency of its adsorption, catalytic conversion, and total removal was determined at pH 5 and temperature 25 °C. The results are presented in Figure 6.

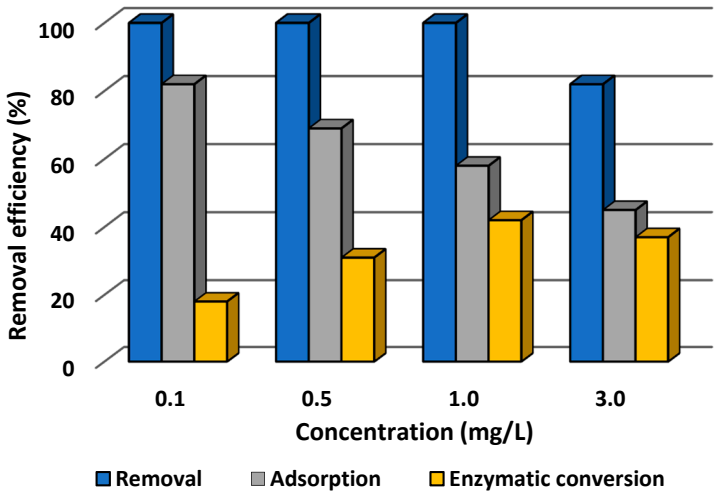

Figure 6. Effect of initial concentration of tetracycline solution on the efficiency of its adsorption, enzymatic conversion, and total removal by laccase immobilized on a chitin scaffold. The error value in each of the experiments (based on the mean and standard deviation from three experiments) does not exceed 3.5%. Adsorption efficiency denotes the efficiency of adsorption by the chitinous scaffold with immobilized laccase following thermal inactivation.

From Figure 6 it is evident that from solutions at concentration 0.1, 0.5, and 1.0 mg/L tetracycline was totally removed after 60 min of the process. A decrease of about 20% in the total efficiency of removal of the antibiotic was observed in the case of a solution at the highest concentration (3.0 mg/L). The data indicate that removal of tetracycline occurred as a result of simultaneous adsorption by the chitinous skeletons and catalytic conversion by the immobilized laccase. Furthermore, the higher is the tetracycline concentration, the lower the efficiency of its adsorption, which falls from 80% at concentration 0.1 mg/L to 42% for a 3.0 mg/L solution of tetracycline. By contrast, the efficiency of

enzymatic conversion increased with increasing concentrations of antibiotic in the solution, reaching around 40% for a concentration of 1.0 mg/L. The exception is the solution at the highest concentration, for which the efficiency of catalytic conversion was lower (around 35%) as compared to the 1.0 mg/L solution, and for which the lowest adsorption efficiency was recorded among all of the tested samples.

3.2.2. Effect of pH of Tetracycline Solution on Efficiency of Its Removal

It is recognized that pH may significantly affect both adsorption of the pollutant and the catalytic action of the immobilized laccase. Therefore, in the next step of the investigation, the effect of the pH of tetracycline solution on the efficiency of its removal was examined over a wide pH range from 3 to 9, at temperature 25 °C and using tetracycline solution at concentration 1.0 mg/L. The data obtained are presented in Figure 7.

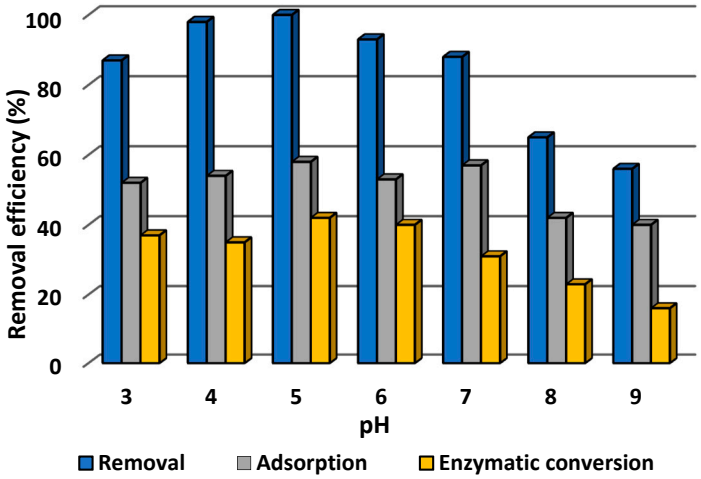

Figure 7. Effect of pH of tetracycline solution on the efficiency of its adsorption, enzymatic conversion, and total removal by laccase immobilized on a chitinous scaffold. The error value in each of the experiments (based on the mean and standard deviation from three experiments) does not exceed 3.5%. Adsorption efficiency denotes the efficiency of adsorption by the chitinous scaffolds with immobilized laccase following thermal inactivation.

It can be seen that the total efficiency of removal of tetracycline increased from 85% at pH 3 to reach 100% at pH 5, and then began to decrease, to around 55% at pH 9. Nevertheless, it should be noted that the total removal efficiency exceeded 90% in a pH range from 4 to 7, and remained above 80% at pH 3 and pH 7. These results are significantly higher than the efficiencies of adsorption by pure chitinous sponges and conversion by free enzyme, which were 80% and 60%, respectively, at pH 5, and decreased further on even slight changes in pH. It should be recalled that the removal of tetracycline took place by simultaneous adsorption and biocatalytic conversion. The adsorption process showed comparable efficiencies, at around 55%, at pH values ranging from 3 to 7; a decrease of around 15% in this parameter was recorded at highly basic pH (pH 8 and pH 9). By contrast, the contribution of catalytic conversion to the total removal of tetracycline is significantly higher in acidic conditions, reaching a maximum of around 40% at pH 5 and pH 6. Further increases in pH caused the efficiency of enzymatic action to fall to 30% at pH 7 and less than 15% at pH 9.

3.2.3. Effect of Temperature on Efficiency of Removal of Tetracycline

Process temperature is another important parameter which may affect the efficiency of both adsorption and catalytic conversion, and as a consequence the total rate of removal of tetracycline. Therefore, the effect of temperature was examined over a wide range, from 5 to 65 °C, using tetracycline solution at pH 5 and concentration 1.0 mg/L. The results are presented in Figure 8.

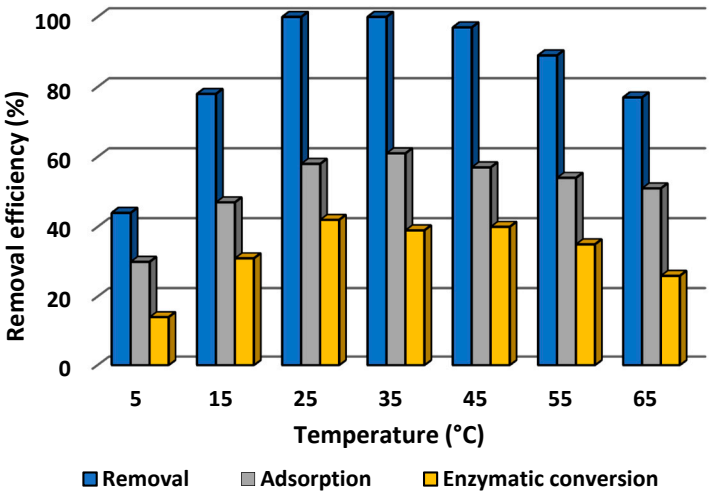

Figure 8. Effect of temperature on the efficiency of adsorption, enzymatic conversion and total removal of tetracycline by laccase immobilized on chitin scaffolds. The error value in each of the experiments (based on the mean and standard deviation from three experiments) does not exceed 3.5%. Adsorption efficiency denotes the efficiency of adsorption by the chitinous scaffolds with immobilized laccase following thermal inactivation.

From Figure 8 it can be seen that the efficiency of removal of tetracycline rose with increasing temperature, reached its maximum (100%) at 25 and 35 °C, and then decreased with further increase of the process temperature. However, although 100% removal was recorded only at 25 and 35 °C, the rate remained above 90% at temperatures of 45 and 55 °C, and over 80% of the antibiotic was removed at 15 °C and even at 65 °C. These results indicate that the obtained biocatalytic systems are capable of effectively eliminating tetracycline by simultaneous sorption and catalytic action over a much wider temperature range than in the case of adsorption by pure sponges and conversion by free laccase. Nevertheless, it should be highlighted that, although the efficiencies of adsorption and catalytic conversion exhibited similar profiles over the whole analyzed temperature range, the adsorption efficiency was about 20% higher than the efficiency of catalytic conversion of the antibiotic, reaching a maximum of around 60% at 35 °C. Notwithstanding, even at 65 °C, over 50% of the tetracycline was removed by adsorption. From Figure 8 it is also evident that the highest contribution of catalytic conversion to antibiotic removal occurred at temperatures ranging from 25 to 45 °C, and reached around 40%. At higher and lower temperatures, lower rates of catalytic conversion were recorded; however, even at 65 °C, over 25% of the pollutant was removed by the catalytic action.

3.2.4. Reusability of Immobilized Laccase

Immobilization appears to be the most promising technique for improving enzyme stability, resulting in the possibility of multiple use of immobilized biomolecules in repeated reaction cycles. This property is of particular interest from an industrial point of view, since it facilitates cost reduction and enhances process control. Therefore, in the present study, the recyclability of the immobilized laccase was examined over 10 repeated batch tests of tetracycline degradation under optimal process conditions (Figure 9).

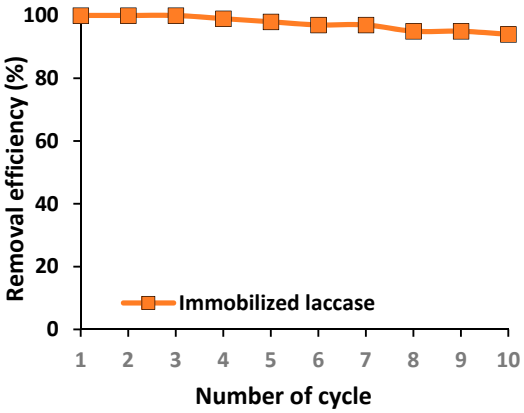

Figure 9. Reusability of the immobilized laccase over repeated catalytic cycles. The error value in each of the experiments (based on the mean and standard deviation from three experiments) does not exceed 3.5%.

From Figure 9 it is evident that the immobilized biocatalyst offers exceptional reusability, as the efficiency of removal of tetracycline decreased only slightly over 10 reaction cycles. Furthermore, over the first three catalytic cycles the biocatalytic system is capable of removing 100% of tetracycline from the solution, and even after 10 repeated steps the immobilized laccase enables removal of over 90% of the tetracycline. Although the contributions of each technique to the total removal of the antibiotic over repeated biocatalytic cycles were not determined in this part of the study, the observed decline in removal efficiency may be related to both a decrease in the sorption efficiency and decline in the catalytic properties of the immobilized laccase.

3.2.5. Removal of Tetracycline Using a Packed Bed Bioreactor

To evaluate the possible practical application of the produced chitin-based biocatalytic systems in the removal of antibiotics, such as tetracycline, from wastewaters, a packed bed bioreactor containing chitinous scaffolds with immobilized laccase was constructed for the first time for continuous removal of tetracycline. The process was performed over 24 h under the most suitable conditions for the highest removal of the antibiotic. Results are presented in Figure 10.

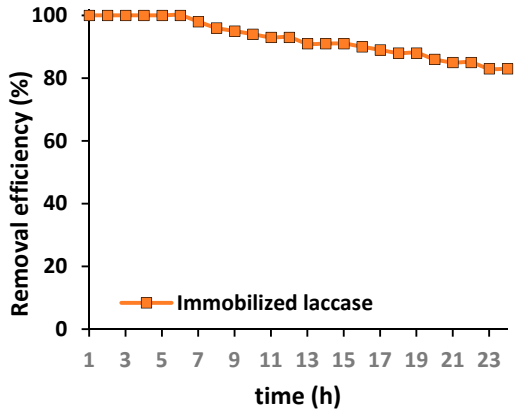

Figure 10. Efficiency of tetracycline removal over 24 h in a packed bed bioreactor containing chitinous scaffolds with immobilized laccase. The error value in each of the experiments (based on the mean and standard deviation from three experiments) does not exceed 3.5%.

The experiment was performed over 24 h; however, it should be highlighted that the process time was measured from the collection of the first drop of effluent after treatment. From Figure 9 it is evident that over the first 6 h of the process total removal of the tetracycline was achieved. Further,

a slight drop in the removal efficiency was recorded; however, even after 16 h of the continuous process, over 90% of the antibiotic was removed. Finally, 83% of the tetracycline was removed by the biocatalytic system after 24 h of continuous operation, by way of simultaneous adsorption and catalytic action. This provides clear indication of the enormous potential of the produced materials in practical applications.

4. Discussion

As was stated above, the main objective of the study was to use *A. archeri* sponge skeletons as a unique source of 3D chitinous scaffolds to serve as a support for enzyme immobilization, and to apply the obtained biocatalytic systems in the removal of tetracycline, as a model pollutant present in wastewaters. Effective immobilization of the enzyme was confirmed, and the effect of various process conditions on the efficiency of removal of the antibiotic was examined. Finally, a new packed bed bioreactor was constructed to evaluate the removal rate in a continuous process.

4.1. Characterization of Products Following Immobilization

In the first stage of the investigation, the morphology of the chitinous scaffolds before and after laccase immobilization was examined based on SEM and TEM images to check the suitability of the scaffolds as supports for enzyme deposition and to confirm effective binding of the enzyme. As shown in Figure 4, the chitinous scaffolds have an open, three-dimensional structure that facilitates transfer of the substrate and products to the immobilized molecules and reduces transfer limitations. The clearly visible, irregular shapes with sizes of a few micrometers, present on the chitin fibers after immobilization, should be interpreted as an enzyme aggregates. This clearly confirms effective deposition of the enzyme onto the surface of the chitinous scaffolds. Similar observations confirming laccase attachment were made in our previous study, in which scaffolds based on *Hippospongia communis* spongin were used for immobilization of laccase [19].

As shown, a very high immobilization yield of 91% was achieved, corresponding to the extraordinary amount of immobilized enzyme (1820 mg of laccase deposited per 1 g of chitinous scaffold). The high immobilization yield and large quantity of deposited enzyme may be explained by the exceptional sorption properties of *A. archeri* chitin [26] as well the presence of numerous functional groups typical for this aminopolysaccharide, mainly carbonyl and hydroxyl, that are capable of providing effective and stable enzyme binding [46]. However, it should be highlighted that although the interactions formed are stable, they are based mainly on hydrogen bonds and adsorption interactions. For this reason, interference in the structure of the enzyme and its distortion upon immobilization are limited [57]. This is a possible explanation of the high specific activity of the immobilized laccase (52.5 U/mg) as compared to the free enzyme (56 U/mg), corresponding to an activity retention of 89% [58]. By contrast, Das et al. immobilized laccase on magnetic iron nanoparticles and obtained specific activity of the immobilized protein was about 15 U/mg, that was almost two times lower as compared to free laccase (30 U/mg) [59]. Similar results were reported by Lin et al. who noticed specific activity of 20.1 and 30.1 U/mg for immobilized and free enzyme, respectively. However, in their tests chitosan/CeO_2 microspheres were used as a support in the immobilization of laccase from *Trametes versicolor* [60]. In another study by Ramirez-Montoya et al. the specific activities of free laccase and laccase immobilized on a mesoporous carbon obtained from pecan shells were found to be 10.85 and 0.038 U/mg, respectively [61]. Therefore, it might be assumed that presented in our study significantly higher specific activity of the immobilized laccase indicates production of an effective biocatalyst.

Furthermore, kinetic parameters of the free and immobilized enzymes were determined, to investigate changes in enzyme–substrate affinity before and after immobilization. A slight increase in the K_M value, of about 20%, and a similar drop in the maximum rate were obtained for immobilized laccase as compared to the free biomolecule, indicating a lower substrate affinity and lower reaction rate. These results are probably related to the fact that upon immobilization some of the active sites of the

immobilized laccase can be blocked, reducing their accessibility and impairing the catalytic properties of the immobilized enzyme [62]. However, it should be noted that due to the open structure of the chitinous matrix and limited deformation of the enzyme structure, only a slight worsening of catalytic properties was observed. Similar observations were made in our previous study concerning adsorption immobilization of laccase on poly(l-lactic acid)-co-poly(ε-caprolactone) electrospun nanofibers [63]. By contrast, in a study by Olajuyigbe et al. [64], laccase was immobilized by entrapment using calcium and copper alginate beads. Due to the creation of strong diffusional limitations, almost three times higher Michaelis–Menten constants were obtained. In summary, therefore, the present results clearly indicate that the obtained immobilized enzymes may be considered as effective biocatalytic systems for practical application, for instance in the removal of hazardous compounds.

Nevertheless, the retention of high catalytic properties by enzymes after immobilization is not in itself sufficient, as these systems should also provide significant improvements in thermal and chemical stability as compared to the free enzyme. In this study, both the thermochemical stability and storage stability of the free and immobilized laccase were examined and compared under optimal process conditions. The significant improvement of the enzyme's stability over time and under harsh reaction conditions can be explained mainly by the creation of stable enzyme–support interactions, which stabilize and stiffen the entire enzyme structure and protect it against thermal and chemical inactivation [65,66]. Moreover, the support material additionally protects laccase against inactivation [67]. These observations are confirmed by the values of the inactivation constant, which for immobilized laccase was found to be 0.0038 1/min, more than four times lower than the value for free laccase. Nevertheless, a drop in the catalytic properties over time and after incubation might be explained by both partial inactivation of the enzyme and its partial elution from the support. Similar observations were made by Yang et al. who immobilized laccase from *Cerrena* sp. by adsorption using chitosan beads as a support. In their study, due to stabilization of the enzyme upon immobilization, the half-life of the immobilized laccase was found to be almost twice that of the free biocatalyst [68]. By contrast, in a study by Tavares et al. in 2015 [69], commercial laccase was immobilized by adsorption using multi-walled carbon nanotubes. Although the immobilized enzyme retained high catalytic properties, surprisingly, its stability decreased upon immobilization.

4.2. Removal of Tetracycline

After the effective immobilization of laccase had been confirmed and the chitin-based biocatalytic systems thoroughly characterized in terms of their catalytic properties, the immobilized enzymes were applied in the removal of tetracycline from water solutions under various process conditions, including different pH, temperature, and initial concentration of tetracycline solution. Due to the excellent sorption properties of the chitinous scaffolds, removal by both adsorption and catalytic conversion was investigated in order to evaluate the contribution of each of these pathways to the total removal of the antibiotic. However, it should be noted that upon laccase immobilization, some of the active centers capable of adsorbing tetracycline might be saturated by the biomolecules. Therefore, data on the efficiency of adsorption of tetracycline refer to adsorption of the antibiotic by chitinous scaffolds with thermally inactivated enzyme, and total removal efficiency is based on simultaneous catalytic conversion and adsorption of tetracycline.

The concentration of tetracycline, one of the most frequently used antibiotics, in wastewater varies depending on the source, but it usually ranges from 100 to as much as 1000 μg/L [70]. Thus, in the first stage of the study, the effect of various initial concentrations of tetracycline solution on its removal rate was investigated. The data indicate the clear trend that the higher the concentration of the tetracycline solution is, the lower the percentage of adsorption and the higher the percentage of catalytic conversion in the removal of the antibiotic. This may be explained by the fact that with an increasing amount of tetracycline molecules in the solution, the maximal sorption capacity of the scaffold was attained and further adsorption was extremely limited [17]. The lowest efficiency of removal of tetracycline, around 80%, was recorded for antibiotic solution with a concentration of 3 mg/L. This may be because

the amount of pollutant in the solution is too high to allow its removal by adsorption or catalytic action, as previously reported by Yu et al. [71] and Kumar and Cabana [72]. In another study, by Ji et al. (2016), laccase was covalently immobilized on TiO_2 nanoparticles and used for the removal of pharmaceuticals. Although over 90% of the pollutants were removed from a solution at concentration 5 mg/L, addition of a mediator agent such as syringaldehyde was required to achieve high removal efficiency [73]. Nevertheless, it should be emphasized that the biocatalytic systems produced in this study enable the total removal of tetracycline by simultaneous adsorption and catalytic conversion from solutions at concentrations ranging from 0.1 to 1.0 mg/L.

It is also known that pH might significantly affect both adsorption and catalytic action; therefore, the effect of this parameter on the efficiency of removal of tetracycline was studied over a wide pH range from 3 to 9. Over 80% of tetracycline was removed by simultaneous adsorption and catalytic conversion in the pH range from 3 to 7. However, the data indicate that due to the high sorption capacity of the chitinous scaffolds, the adsorption efficiency was around 50% over the pH range 3–7. Meanwhile, the efficiency of catalytic conversion increased up to pH 5, reached a maximum (40%) at pH 5 and 6, and then decreased. This is related to the fact that in strongly acidic conditions, below pH 4, tetracycline molecules and chitinous scaffolds are negatively charged, leading to ionic repulsions and lowering adsorption efficiency [74]. The lower catalytic conversion rate at basic pH is related to the negative effect of OH^- ions, which influence the enzyme's microenvironment and reduce its activity [75]. Nevertheless, in the pH range 3–6 over 40% of the tetracycline was removed by catalytic conversion, which indicates that the stability of the enzyme was improved upon immobilization, due to the formation of stable enzyme–support interactions and the protective effect of the support [76,77]. Similar observations were made by Shao et al. (2019), who observed the high activity of laccase immobilized by covalent binding onto hollow mesoporous carbon spheres, at pH ranging from 2.5 to 6.5 [78]. By contrast, a significant effect of pH on the removal of hazardous pollutants was observed by Dai et al. (2016) who immobilized laccase using electrospun fibrous membrane modified by multi-walled carbon nanotubes. They reported that over 60% of bisphenol A was removed only in the pH range 3–6 [79].

The effect of temperature on the efficiency of removal of tetracycline was also examined, as temperature can significantly affect both of the processes involved in the removal of the antibiotic. Over the whole analyzed range, the percentage profiles of adsorption and catalytic conversion showed similar trends, although the percentage for adsorption was about 20% higher than for catalytic conversion, this being directly related to the sorption properties of the scaffolds [26] and temperature conditions [80]. The temperature profile of the catalytic conversion of tetracycline by immobilized laccase is directly related to the properties of the laccase from *Trametes versicolor*, which exhibits the best catalytic properties at 25–35 °C [81]. Similar observations were reported by Zhang et al. (2020) [82]. However, as compared to free laccase, the immobilized enzyme exhibited high activity over a wider temperature range, which indicates stabilization of the enzyme structure and its protection against thermal inactivation due to high temperature [83]. Furthermore, it should be highlighted that due to simultaneous adsorption and catalytic conversion, around 80% of the tetracycline was removed over a wide temperature range from 15 to 65 °C. By contrast, in our previous study concerning the immobilization of laccase using electrospun fabricated membranes, the highest removal rate of tetracycline (around 90%) was achieved in a slightly narrower temperature range, from 25 to 45 °C [84].

To sum up briefly, the efficiency of removal of the antibiotic by simultaneous adsorption and catalytic conversion was above 90% over the pH range from 4 to 6 and the temperature range from 25 to 45 °C, from solutions at concentrations up to 1 mg/L. Since the preliminary tests of the use of pure chitinous scaffolds and free enzyme for adsorption and catalytic conversion of tetracycline produced inadequate results (efficiencies of around 80% and 60%, respectively), the data presented suggest that the produced biocatalytic systems might be considered as a sustainable alternative for the removal of pollutants from wastewaters.

Nevertheless, from the practical point of view, one of the most crucial properties is the recyclability of the chitinous scaffolds with immobilized enzyme over repeated removal cycles. The results show that although the efficiency of removal of tetracycline declined slightly with repeated use, even in the 10th batch removal cycle over 90% of the antibiotic was removed. The exceptional reusability of these biocatalytic systems is related to the stability and durability of the chitinous scaffolds [26] as well as the ability of this material to protect the immobilized enzyme against inactivation as a result of process conditions [85]. Furthermore, the enzyme–support interactions protect the enzyme against elution from the matrix, as tetracycline is washed out from the scaffolds between repeated uses [86]. Although the data show that the immobilized laccase is stable during repeated use, the decrease in tetracycline removal is related mainly to inactivation of the enzyme due to its inhibition by the macromolecular products of the reaction [87], although partial elution of the laccase from the support should not be excluded. In another study, laccase was immobilized using bentonite-derived mesoporous materials and used for the removal of tetracycline in 10 removal cycles [88]. The efficiency of removal of the antibiotic gradually declined over repeated reaction steps, and after five cycles the degradation rate did not exceed 50%, significantly lower than the value obtained in our study.

The final stage of the investigation concerned application of the produced biocatalytic systems for the continuous removal of tetracycline in a packed bed reactor over 24 h. The exceptional removal efficiency over the initial process time is related mainly to the above-mentioned excellent sorption properties of the chitinous scaffolds. However, due to saturation of the scaffolds' active sites capable of adsorbing tetracycline, the longer the duration of the removal process, the higher the percentage contribution of catalytic conversion to the removal efficiency. This is related to the improved operational stability of the laccase upon immobilization, as well as the higher resistance of the immobilized enzyme to thermal and chemical inactivation [83]. Nevertheless, the observed slight decrease in the removal rate might be explained by partial elution of the enzyme from the support and its inactivation due to continuous use. In another study, laccase was immobilized using ceramic membranes for the continuous degradation of tetracycline from real wastewaters, and a relatively high removal rate of over 75% was achieved [89].

5. Conclusions

In this study, for the first time, 3D chitin scaffolds from the marine demosponge *A. archeri* were used as a support for effective immobilization of laccase. The immobilized enzyme exhibited high activity retention and high substrate affinity. Moreover, the thermal and storage stability of the immobilized enzyme were significantly improved as compared to the free enzyme, indicating the protective effect of the support on the biomolecules. The produced biocatalytic systems were used for removal of tetracycline, and after 1 h of the process at pH 5 and temperatures of 25 and 35 °C, total removal of the antibiotic was achieved from solutions at relatively high concentration, up to 1 mg/L. Moreover, the system consisting of chitinous scaffolds and immobilized laccase displayed good reusability: even after 10 repeated degradation cycles over 90% of the antibiotic was removed. This indicates the potential of the system for practical application in biotechnological processes. Finally, the possible continuous use of immobilized laccase was tested in a packed bed reactor. It was found that after 24 h of the continuous process over 80% of the pharmaceutical was removed. These features indicate the possibility of efficient removal of tetracycline over wide pH and temperature ranges by simultaneous adsorption and catalytic conversion, both over numerous process steps and in continuous use. Furthermore, they may provide economic advantages for the large-scale practical use of the produced biocatalytic systems in wastewater treatment. Nevertheless, further study concerning optimization of the removal process and evaluation of the effect of various inhibitors on the tetracycline removal rate is still required. In addition, in our opinion, future study related to the use of immobilized enzymes for removal of hazardous pollutants should be focused on practical application of the biocatalytic systems in continuous treatment in bioreactors, and on process optimization to achieve the highest possible removal rate.

Author Contributions: Conceptualization, J.Z., H.E. and T.J.; methodology, J.Z., H.E. and T.J.; formal analysis, J.Z. and K.B.; investigation, J.Z., T.M., O.D. and K.B.; resources, V.N.I., H.E. and T.J.; writing—original draft preparation, J.Z., T.M., O.D. and K.B.; writing—review and editing, J.Z., H.E. and T.J.; visualization, A.F., T.M., O.D. and K.B.; supervision, J.Z., H.E. and T.J.; project administration, H.E. and T.J.; funding acquisition, H.E. and T.J. All authors have read and agreed to the published version of the manuscript.

Funding: This research was partially funded by Ministry of Science and Higher Education (Poland) as financial subsidy to PUT no. 0912/SBAD/2006. This research was partially supported by DFG Project HE 394/3, SMWK Project no. 02010311 (Germany). Tomasz Machałowski was supported by DAAD (Personal ref. no. 91734605).

Conflicts of Interest: The authors declare no conflict of interest.

References

1. Nejadnik, M.R.; Deepak, F.L.; Garcia, C.D. Adsorption of glucose oxidase to 3-D scaffolds of carbon nanotubes: Analytical applications. *Electroanalysis* **2011**, *23*, 1462–1469. [CrossRef]
2. Dey, P. Polyglycerol based hydrogels for the immobilization of catalytically active enzymes and as scaffolds for cells. Ph.D. Thesis, Freie Universität Berlin, Berlin, Germany, 9 October 2015.
3. Duan, G. 3D porous sponges from electrospun polymer fibers and their applications. Ph.D. Thesis, Universität Bayreuth, Bayreuth, Germany, 26 July 2017.
4. Kowalski, A.E.; Johnson, L.B.; Dierl, H.K.; Park, S.; Huber, T.R.; Snow, C.D. Porous protein crystals as scaffolds for enzyme immobilization. *Biomater. Sci.* **2019**, *7*, 1898–1904. [CrossRef]
5. Ye, J.; Chu, T.; Chu, J.; Gao, B.; He, B. A versatile approach for enzyme immobilization using chemically modified 3D-printed scaffolds. *ACS Sustain. Chem. Eng.* **2019**, *7*, 18048–18054. [CrossRef]
6. Wysokowski, M.; Machałowski, T.; Petrenko, I.; Schimpf, C.; Rafaja, D.; Galli, R.; Ziętek, J.; Pantović, S.; Voronkina, A.; Kovalchuk, V.; et al. 3D chitin scaffolds of marine demosponge origin for biomimetic mollusk hemolymph-associated biomineralization *ex-vivo*. *Mar. Drugs* **2020**, *18*, 123. [CrossRef]
7. Jesionowski, T.; Norman, M.; Zółtowska-Aksamitowska, S.; Petrenko, I.; Joseph, Y.; Ehrlich, H. Marine spongin: Naturally prefabricated 3D scaffold-based biomaterial. *Mar. Drugs* **2018**, *16*, 1–23. [CrossRef]
8. Ehrlich, H.; Wysokowski, M.; Zółtowska-Aksamitowska, S.; Petrenko, I.; Jesionowski, T. Collagens of poriferan origin. *Mar. Drugs* **2018**, *16*, 79. [CrossRef]
9. Szatkowski, T.; Wysokowski, M.; Lota, G.; Pęziak, D.; Bazhenov, V.V.; Nowaczyk, G.; Walter, J.; Molodtsov, S.L.; Stöcker, H.; Himcinschi, C.; et al. Novel nanostructured hematite-spongin composite developed using an extreme biomimetic approach. *RSC Adv.* **2015**, *5*, 79031–79040. [CrossRef]
10. Szatkowski, T.; Siwińska-Stefańska, K.; Wysokowski, M.; Stelling, A.; Joseph, Y.; Ehrlich, H.; Jesionowski, T. Immobilization of titanium(IV) oxide onto 3D spongin scaffolds of marine sponge origin according to extreme biomimetics principles for removal of C.I. Basic Blue 9. *Biomimetics* **2017**, *2*, 4. [CrossRef]
11. Szatkowski, T.; Kopczyński, K.; Motylenko, M.; Borrmann, H.; Mania, B.; Graś, M.; Lota, G.; Bazhenov, V.V.; Rafaja, D.; Roth, F.; et al. Extreme biomimetics: A carbonized 3D spongin scaffold as a novel support for nanostructured manganese oxide(IV) and its electrochemical applications. *Nano Res.* **2018**, *11*, 4199–4214. [CrossRef]
12. Petrenko, I.; Summers, A.P.; Simon, P.; Żółtowska-Aksamitowska, S.; Motylenko, M.; Schimpf, C.; Rafaja, D.; Roth, F.; Kummer, K.; Brendler, E.; et al. Extreme biomimetics: Preservation of molecular detail in centimeter-scale samples of biological meshes laid down by sponges. *Sci. Adv.* **2019**, *5*, eaax2805. [CrossRef]
13. Norman, M.; Bartczak, P.; Zdarta, J.; Tylus, W.; Szatkowski, T.; Stelling, A.L.; Ehrlich, H.; Jesionowski, T. Adsorption of C.I. natural red 4 onto spongin skeleton of marine demosponge. *Materials (Basel)* **2015**, *8*, 96–116. [CrossRef]
14. Norman, M.; Bartczak, P.; Zdarta, J.; Ehrlich, H.; Jesionowski, T. Anthocyanin dye conjugated with *Hippospongia communis* marine demosponge skeleton and its antiradical activity. *Dyes Pigm.* **2016**, *134*, 541–552. [CrossRef]
15. Norman, M.; Bartczak, P.; Zdarta, J.; Tomala, W.; Żurańska, B.; Dobrowolska, A.; Piasecki, A.; Czaczyk, K.; Ehrlich, H.; Jesionowski, T. Sodium copper chlorophyllin immobilization onto *Hippospongia communis* marine demosponge skeleton and its antibacterial activity. *Int. J. Mol. Sci.* **2016**, *17*, 1564. [CrossRef]
16. Norman, M.; Zdarta, J.; Bartczak, P.; Piasecki, A.; Petrenko, I.; Ehrlich, H.; Jesionowski, T. Marine sponge skeleton photosensitized by copper phthalocyanine: A catalyst for Rhodamine B degradation. *Open Chem.* **2016**, *14*, 243–254. [CrossRef]

17. Norman, M.; Żółtowska-Aksamitowska, S.; Zgoła-Grześkowiak, A.; Ehrlich, H.; Jesionowski, T. Iron(III) phthalocyanine supported on a spongin scaffold as an advanced photocatalyst in a highly efficient removal process of halophenols and bisphenol A. *J. Hazard. Mater.* **2018**, *347*, 78–88. [CrossRef]
18. Stępniak, I.; Galiński, M.; Nowacki, K.; Wysokowski, M.; Jakubowska, P.; Bazhenov, V.V.; Leisegang, T.; Ehrlich, H.; Jesionowski, T. A novel chitosan/sponge chitin origin material as a membrane for supercapacitors-preparation and characterization. *RSC Adv.* **2016**, *6*, 4007–4013. [CrossRef]
19. Zdarta, J.; Antecka, K.; Frankowski, R.; Zgoła-Grześkowiak, A.; Ehrlich, H.; Jesionowski, T. The effect of operational parameters on the biodegradation of bisphenols by *Trametes versicolor* laccase immobilized on *Hippospongia communis* spongin scaffolds. *Sci. Total Environ.* **2018**, *615*, 784–795. [CrossRef]
20. Ehrlich, H.; Maldonado, M.; Spindler, K.D.; Eckert, C.; Hanke, T.; Born, R.; Goebel, C.; Simon, P.; Heinemann, S.; Worch, H. First evidence of chitin as a component of the skeletal fibers of marine sponges. Part I. Verongidae (demospongia: Porifera). *J. Exp. Zool. B Mol. Dev. Evol.* **2007**, *308B*, 347–356. [CrossRef]
21. Ehrlich, H.; Ilan, M.; Maldonado, M.; Muricy, G.; Bavestrello, G.; Kljajic, Z.; Carballo, J.L.; Schiaparelli, S.; Ereskovsky, A.; Schupp, P.; et al. Three-dimensional chitin-based scaffolds from Verongida sponges (Demospongiae: Porifera). Part I. Isolation and identification of chitin. *Int. J. Biol. Macromol.* **2010**, *47*, 132–140. [CrossRef]
22. Ehrlich, H.; Bazhenov, V.V.; Debitus, C.; de Voogd, N.; Galli, R.; Tsurkan, M.V.; Wysokowski, M.; Meissner, H.; Bulut, E.; Kaya, M.; et al. Isolation and identification of chitin from heavy mineralized skeleton of *Suberea clavata* (Verongida: Demospongiae: Porifera) marine demosponge. *Int. J. Biol. Macromol.* **2017**, *104*, 1706–1712. [CrossRef]
23. Brunner, E.; Ehrlich, H.; Schupp, P.; Hedrich, R.; Hunoldt, S.; Kammer, M.; Machill, S.; Paasch, S.; Bazhenov, V.V.; Kurek, D.V.; et al. Chitin-based scaffolds are an integral part of the skeleton of the marine demosponge *Ianthella basta*. *J. Struct. Biol.* **2009**, *168*, 539–547. [CrossRef] [PubMed]
24. Shaala, L.A.; Asfour, H.Z.; Youssef, D.T.A.; Zółtowska-Aksamitowska, S.; Wysokowski, M.; Tsurkan, M.; Galli, R.; Meissner, H.; Petrenko, I.; Tabachnick, K.; et al. New source of 3D chitin scaffolds: the Red Sea Demosponge *Pseudoceratina arabica* (Pseudoceratinidae, Verongiida). *Mar. Drugs* **2019**, *17*, 92. [CrossRef]
25. Zółtowska-Aksamitowska, S.; Shaala, L.A.; Youssef, D.T.A.; Elhady, S.S.; Tsurkan, M.V.; Petrenko, I.; Wysokowski, M.; Tabachnick, K.; Meissner, H.; Ivanenko, V.N.; et al. First report on chitin in a non-verongiid marine demosponge: The *Mycale euplectellioides* case. *Mar. Drugs* **2018**, *16*, 1–17. [CrossRef] [PubMed]
26. Klinger, C.; Żółtowska-Aksamitowska, S.; Wysokowski, M.; Tsurkan, M.V.; Galli, R.; Petrenko, I.; Machałowski, T.; Ereskovsky, A.; Martinović, R.; Muzychka, L.; et al. Express method for isolation of ready-to-use 3D chitin scaffolds from *Aplysina archeri* (Aplysineidae: Verongiida) demosponge. *Mar. Drugs* **2019**, *17*, 131. [CrossRef] [PubMed]
27. Fromont, J.; Żółtowska-Aksamitowska, S.; Galli, R.; Meissner, H.; Erpenbeck, D.; Vacelet, J.; Diaz, C.; Tsurkan, M.V.; Petrenko, I.; Youssef, D.T.A.; et al. New family and genus of a Dendrilla-like sponge with characters of Verongiida. Part II. Discovery of chitin in the skeleton of *Ernstilla lacunosa*. *Zool. Anz.* **2019**, *280*, 21–29. [CrossRef]
28. Vacelet, J.; Erpenbeck, D.; Diaz, C.; Ehrlich, H.; Fromont, J. New family and genus for Dendrilla-like sponges with characters of Verongiida. Part I redescription of *Dendrilla lacunosa* Hentschel 1912, diagnosis of the new family Ernstillidae and *Ernstilla* n. g. *Zool. Anz.* **2019**, *280*, 14–20. [CrossRef]
29. Steck, E.; Burkhardt, M.; Ehrlich, H.; Richter, W. Discrimination between cells of murine and human origin in xenotransplants by species specific genomic in situ hybridization. *Xenotransplantation* **2010**, *17*, 153–159. [CrossRef]
30. Mutsenko, V.V.; Bazhenov, V.V.; Rogulska, O.; Tarusin, D.N.; Schütz, K.; Brüggemeier, S.; Gossla, E.; Akkineni, A.R.; Meißner, H.; Lode, A.; et al. 3D chitinous scaffolds derived from cultivated marine demosponge *Aplysina aerophoba* for tissue engineering approaches based on human mesenchymal stromal cells. *Int. J. Biol. Macromol.* **2017**, *104*, 1966–1974. [CrossRef]
31. Mutsenko, V.V.; Gryshkov, O.; Lauterboeck, L.; Rogulska, O.; Tarusin, D.N.; Bazhenov, V.V.; Schütz, K.; Brüggemeier, S.; Gossla, E.; Akkineni, A.R.; et al. Novel chitin scaffolds derived from marine sponge *Ianthella basta* for tissue engineering approaches based on human mesenchymal stromal cells: Biocompatibility and cryopreservation. *Int. J. Biol. Macromol.* **2017**, *104*, 1955–1965. [CrossRef]

32. Mutsenko, V.; Gryshkov, O.; Rogulska, O.; Lode, A.; Petrenko, A.Y.G.M.; Glasmache, B.; Ehrlich, H. Chitinous scaffolds from marine sponges for tissue engineering. In *Marine-Derived Biomaterials for Tissue Engineering Applications*; Choi, A.H., Ben-Nissan, B., Eds.; Springer Nature: Singapore, 2019; pp. 285–307.
33. Schubert, M.; Binnewerg, B.; Voronkina, A.; Muzychka, L.; Wysokowski, M.; Petrenko, I.; Kovalchuk, V.; Tsurkan, M.; Martinovic, R.; Bechmann, N.; et al. Naturally prefabricated marine biomaterials: isolation and applications of flat chitinous 3D scaffolds from *Ianthella labyrinthus* (Demospongiae: Verongiida). *Int. J. Mol. Sci.* **2019**, *20*, 5105. [CrossRef]
34. Binnewerg, B.; Schubert, M.; Voronkina, A.; Muzychka, L.; Wysokowski, M.; Petrenko, I.; Djurović, M.; Kovalchuk, V.; Tsurkan, M.; Martinovic, R.; et al. Marine biomaterials: Biomimetic and pharmacological potential of cultivated *Aplysina aerophoba* marine demosponge. *Mater. Sci. Eng. C* **2020**, *109*, 110566. [CrossRef] [PubMed]
35. Kovalchuk, V.; Voronkina, A.; Binnewerg, B.; Schubert, M.; Muzychka, L.; Wysokowski, M.; Tsurkan, M.V.; Bechmann, N.; Petrenko, I.; Fursov, A.; et al. Naturally drug-loaded chitin: isolation and applications. *Mar. Drugs* **2019**, *17*, 574. [CrossRef] [PubMed]
36. Ehrlich, H. Biomimetic potential of chitin-based composite biomaterials of poriferan origin. In *Biomimetic Biomaterials: Structure and Applications*; Ruys, A.J., Ed.; Woodhead Publishing Limited: Cambridge, UK, 2013; pp. 46–66.
37. Wysokowski, M.; Behm, T.; Born, R.; Bazhenov, V.V.; Meißner, H.; Richter, G.; Szwarc-Rzepka, K.; Makarova, A.; Vyalikh, D.; Schupp, P.; et al. Preparation of chitin-silica composites by in vitro silicification of two-dimensional *Ianthella basta* demosponge chitinous scaffolds under modified Stöber conditions. *Mater. Sci. Eng. C* **2013**, *33*, 3935–3941.
38. Wysokowski, M.; Motylenko, M.; Walter, J.; Lota, G.; Wojciechowski, J.; Stöcker, H.; Galli, R.; Stelling, A.L.; Himcinschi, C.; Niederschlag, E.; et al. Synthesis of nanostructured chitin-hematite composites under extreme biomimetic conditions. *RSC Adv.* **2014**, *4*, 61743–61752. [CrossRef]
39. Wysokowski, M.; Petrenko, I.; Stelling, A.L.; Stawski, D.; Jesionowski, T.; Ehrlich, H. Poriferan chitin as a versatile template for extreme biomimetics. *Polymers (Basel)* **2015**, *7*, 235–265. [CrossRef]
40. Wysokowski, M.; Motylenko, M.; Rafaja, D.; Koltsov, I.; Stöcker, H.; Szalaty, T.J.; Bazhenov, V.V.; Stelling, A.L.; Beyer, J.; Heitmann, J.; et al. Extreme biomimetic approach for synthesis of nanocrystalline chitin-(Ti,Zr)O_2 multiphase composites. *Mater. Chem. Phys.* **2017**, *188*, 115–124. [CrossRef]
41. Schleuter, D.; Günther, A.; Paasch, S.; Ehrlich, H.; Kljajić, Z.; Hanke, T.; Bernhard, G.; Brunner, E. Chitin-based renewable materials from marine sponges for uranium adsorption. *Carbohydr. Polym.* **2013**, *92*, 712–718. [CrossRef]
42. Petrenko, I.; Bazhenov, V.V.; Galli, R.; Wysokowski, M.; Fromont, J.; Schupp, P.J.; Stelling, A.L.; Niederschlag, E.; Stöker, H.; Kutsova, V.Z.; et al. Chitin of poriferan origin and the bioelectrometallurgy of copper/copper oxide. *Int. J. Biol. Macromol.* **2017**, *104*, 1626–1632. [CrossRef]
43. Magalhães, J.M.C.S.; Machado, A.A.S.C. Enzyme immobilization on chitin and chitosan for construction of enzymatic sensors. *Uses Immobil. Biol. Compd.* **1993**, *252*, 191–200.
44. Illanes, A. Chitin as a matrix for enzyme immobilization. In *Advances in Bioprocess Engineering*; Galindo, E., Ramírez, O.T., Eds.; Springer: Dordrecht, Germany, 1994; pp. 461–466.
45. Krajewska, B. Chitin and its derivative as supports for immobilization of enzymes. *Acta Biotechnol.* **1991**, *11*, 269–277. [CrossRef]
46. Krajewska, B. Application of chitin- and chitosan-based materials for enzyme immobilizations: A review. *Enzyme Microb. Technol.* **2004**, *35*, 126–139. [CrossRef]
47. Huang, W.C.; Wang, W.; Xue, C.; Mao, X. Effective enzyme immobilization onto a magnetic chitin nanofiber composite. *ACS Sustain. Chem. Eng.* **2018**, *6*, 8118–8124. [CrossRef]
48. Verma, M.L.; Kumar, S.; Das, A.; Randhawa, J.S.; Chamundeeswari, M. Chitin and chitosan-based support materials for enzyme immobilization and biotechnological applications. *Environ. Chem. Lett.* **2020**, *18*, 315–323. [CrossRef]
49. Gomes, F.M.; Pereira, E.B.; de Castro, H.F. Immobilization of lipase on chitin and its use in nonconventional biocatalysis. *Biomacromolecules* **2004**, *5*, 17–23. [CrossRef]
50. Kilinç, A.; Teke, M.; Önal, S.; Telefoncu, A. Immobilization of pancreatic lipase on chitin and chitosan. *Prep. Biochem. Biotechnol.* **2006**, *36*, 153–163. [CrossRef] [PubMed]

51. Silva, D.F.; Rosa, H.; Carvalho, A.F.A.; Oliva-Neto, P. Immobilization of papain on chitin and chitosan and recycling of soluble enzyme for deflocculation of *Saccharomyces cerevisiae* from bioethanol distilleries. *Enzyme Res.* **2015**, *2015*, 1–10. [CrossRef] [PubMed]
52. Johannes, C.; Majcherczyk, A. Laccase activity tests and laccase inhibitors. *J. Biotechnol.* **2000**, *78*, 193–199. [CrossRef]
53. Solomon, E.I.; Sundaram, U.M.; Machonkin, T.E. Multicopper oxidases and oxygenases. *Chem. Rev.* **1996**, *96*, 2563–2606. [CrossRef] [PubMed]
54. Yaropolov, A.I.; Skorobogat'ko, O.V.; Vartanov, S.S.; Varfolomeyev, S.D. Laccase: Properties, catalytic mechanism, and applicability. *Appl. Biochem. Biotechnol.* **1994**, *49*, 257–280. [CrossRef]
55. Bajpai, P. Application of enzymes in the pulp and paper industry. *Biotechnol. Prog.* **1999**, *15*, 147–157. [CrossRef]
56. Bradford, M.M. A rapid and sensitive method for the quantitation of microgram quantities of protein utilizing the principle of protein-dye binding. *Anal. Biochem.* **1976**, *72*, 248–254. [CrossRef]
57. Rahmani, H.; Lakzian, A.; Karimi, A.; Halajnia, A. Efficient removal of 2,4-dinitrophenol from synthetic wastewater and contaminated soil samples using free and immobilized laccases. *J. Environ. Manage.* **2020**, *256*, 109740. [CrossRef] [PubMed]
58. Zdarta, J.; Jesionowski, T. *Luffa cylindrica* sponges as a thermally and chemically stable support for *Aspergillus niger* lipase. *Biotechnol. Prog.* **2016**, *32*, 657–665. [CrossRef]
59. Das, A.; Singh, J.; Yogalakshmi, K.N. Laccase immobilized magnetic iron nanoparticles: Fabrication and its performance evaluation in chlorpyrifos degradation. *Int. Biodeterior. Biodegradation* **2017**, *117*, 183–189. [CrossRef]
60. Lin, J.; Fan, L.; Miao, R.; Le, X.; Chen, S.; Zhou, X. Enhancing catalytic performance of laccase via immobilization on chitosan/CeO_2 microspheres. *Int. J. Biol. Macromol.* **2015**, *78*, 1–8. [CrossRef]
61. Ramirez-Montoya, L.A.; Hernandez-Montoya, V.; Montes-Moran, M.A.; Jauregui-Rincon, J.; Cervantes, F.J. Decolorization of dyes with different molecular properties using free and immobilized laccases from *Trametes versicolor*. *J. Mol. Liq.* **2015**, *212*, 30–37. [CrossRef]
62. Yamanaka, S.A.; Dunn, S.B.; Valentine, J.S.; Zink, J.I. Nicotinamide adenine dinucleotide phosphate fluorescence and adsorption monitoring of enzyme activity in silicate sol-gels for chemical sensing applications. *J. Am. Chem. Soc.* **1995**, *117*, 9095–9096. [CrossRef]
63. Zdarta, J.; Jankowska, K.; Wyszowska, M.; Kijeńska-Gawrońska, E.; Zgoła-Grześkowiak, A.; Pinelo, M.; Meyer, A.S.; Moszyński, D.; Jesionowski, T. Robust biodegradation of naproxen and diclofenac by laccase immobilized using electrospun nanofibers with enhanced stability and reusability. *Mater. Sci. Eng. C* **2019**, *103*, 109789.
64. Olajuyigbe, F.M.; Adetuyi, O.Y.; Fatokun, C.O. Characterization of free and immobilized laccase from *Cyberlindnera fabianii* and application in degradation of bisphenol A. *Int. J. Biol. Macromol.* **2019**, *125*, 856–864. [CrossRef]
65. Datta, S.; Christena, L.R.; Rajaram, Y.R.S. Enzyme immobilization: An overview on techniques and support materials. *3 Biotech* **2013**, *3*, 1–9. [CrossRef]
66. Lee, S.H.; Yeo, S.Y.; Cools, P.; Morent, R. Plasma polymerization onto nonwoven polyethylene/polypropylene fibers for laccase immobilization as dye decolorization filter media. *Text. Res. J.* **2019**, *89*, 3578–3590. [CrossRef]
67. Zdarta, J.; Pinelo, M.; Jesionowski, T.; Meyer, A.S. Upgrading of biomass monosaccharides by immobilized glucose dehydrogenase and xylose dehydrogenase. *ChemCatChem* **2018**, *10*, 5164–5173. [CrossRef]
68. Yang, J.; Wang, Z.; Lin, Y.; Ng, T.B.; Ye, X.; Lin, J. Immobilized *Cerrena* sp. laccase: Preparation, thermal inactivation, and operational stability in malachite green decolorization. *Sci. Rep.* **2017**, *7*, 16429. [CrossRef] [PubMed]
69. Tavares, A.P.; Silva, C.G.; Drazić, G.; Silva, A.M.; Loureiro, J.M.; Faria, J.L. Laccase immobilization over multi-walled carbon nanotubes: Kinetic, thermodynamic and stability studies. *J. Colloid Interface Sci.* **2015**, *454*, 52–60. [CrossRef] [PubMed]
70. Liu, H.; Ma, C.; Chen, G.; White, J.C.; Wang, Z.; Xing, B.; Dhankher, O.P. Titanium dioxide nanoparticles alleviate tetracycline toxicity to *Arabidopsis thaliana* (L.). *ACS Sustain. Chem. Eng.* **2017**, *5*, 3204–3213. [CrossRef]

71. Yu, B.W.; Bai, Y.T.; Ming, Z.; Yang, H.; Chen, L.Y.; Hu, X.J.; Feng, S.C.; Yang, S.T. Adsorption behaviors of tetracycline on magnetic graphene oxide sponge. *Mater. Chem. Phys.* **2017**, *198*, 283–290. [CrossRef]
72. Kumar, V.V.; Cabana, H. Towards high potential magnetic biocatalysts for on-demand elimination of pharmaceuticals. *Bioresour. Technol.* **2016**, *200*, 81–89. [CrossRef]
73. Ji, C.; Hou, J.; Wang, K.; Zhang, Y.; Chen, V. Biocatalytic degradation of carbamazepine with immobilized laccase-mediator membrane hybrid reactor. *J. Membr. Sci.* **2016**, *502*, 11–20. [CrossRef]
74. Nodeh, H.R.; Sereshti, H. Synthesis of magnetic graphene oxide doped with strontium titanium trioxide nanoparticles as a nanocomposite for the removal of antibiotics from aqueous media. *RSC Adv.* **2016**, *6*, 89953–89965. [CrossRef]
75. Georgiou, R.P.; Tsiakiri, E.P.; Lazaridis, N.K.; Pantazaki, A.A. Decolorization of melanoidins from simulated and industrial molasses effluents by immobilized laccase. *J. Environ. Chem. Eng.* **2016**, *4*, 1322–1331. [CrossRef]
76. Jiang, D.S.; Long, S.Y.; Huang, J.; Xiao, H.Y.; Zhou, J.Y. Immobilization of *Pycnoporus sanguineus* laccase on magnetic chitosan microspheres. *Biochem. Eng. J.* **2005**, *25*, 15–23. [CrossRef]
77. Lin, J.; Wen, Q.; Chen, S.; Le, X.; Zhou, X.; Huang, L. Synthesis of amine-functionalized Fe_3O_4@C nanoparticles for laccase immobilization. *Int. J. Biol. Macromol.* **2016**, *96*, 377–383. [CrossRef]
78. Shao, B.; Liu, Z.; Zeng, G.; Liu, Y.; Yang, X.; Zhou, C.; Chen, M.; Liu, Y.; Jiang, Y.; Yan, M. Immobilization of laccase on hollow mesoporous carbon nanospheres: Noteworthy immobilization, excellent stability and efficacious for antibiotic contaminants removal. *J. Hazard. Mater.* **2019**, *362*, 318–326. [CrossRef] [PubMed]
79. Dai, Y.; Yao, J.; Song, Y.; Liu, X.; Wang, S.; Yuan, Y. Enhanced performance of immobilized laccase in electrospun fibrous membranes by carbon nanotubes modification and its application for bisphenol A removal from water. *J. Hazard. Mater.* **2016**, *317*, 485–493. [CrossRef] [PubMed]
80. Chen, A.; Shang, C.; Shao, J.; Lin, Y.; Luo, S.; Zhang, J.; Huang, H.; Lei, M.; Zeng, Q. Carbon disulfide-modified magnetic ion-imprinted chitosan-Fe(III): A novel adsorbent for simultaneous removal of tetracycline and cadmium. *Carbohydr. Polym.* **2017**, *155*, 19–27. [CrossRef]
81. de Carvalho, M.E.; Monteiro, M.C.; Sant'Anna Jr, G.L. Laccase from *Trametes versicolor*: Stability at temperature and alkaline conditions and its effect on biobleaching of hardwood kraft pulp. *Appl. Biochem. Biotechnol.* **1999**, *77–79*, 723–733. [CrossRef]
82. Zhang, W.; Yang, Q.; Luo, Q.; Shi, L.; Meng, S. Laccase-carbon nanotube nanocomposites for enhancing dyes removal. *J. Clean. Prod.* **2020**, *242*, 118425. [CrossRef]
83. Bilal, M.; Asgher, M.; Shahid, M.; Bhatti, H.N. Characteristic features and dye degrading capability of agar-agar gel immobilized manganese peroxidase. *Int. J. Biol. Macromol.* **2016**, *86*, 728–740. [CrossRef]
84. Zdarta, J.; Jankowska, K.; Bachosz, K.; Kijeńska-Gawrońska, E.; Zgoła-Grześkowiak, A.; Kaczorek, E.; Jesionowski, T. A promising laccase immobilization using electrospun materials for biocatalytic degradation of tetracycline: Effect of process conditions and catalytic pathways. *Catal. Today* **2019**, in press. [CrossRef]
85. Andjelković, U.; Milutinović-Nikolić, A.; Jović-Jovićić, N.; Banković, P.; Bajt, T.; Mojović, Z.; Vujćić, Z.; Jovanović, D. Efficient stabilization of *Saccharomyces cerevisiae* external invertase by immobilisation on modified beidellite nanoclays. *Food Chem.* **2015**, *168*, 262–269. [CrossRef]
86. Skoronski, E.; Souza, D.H.; Ely, C.; Broilo, F.; Fernandes, M.; Fúrigo Jr, A.; Ghislandi, M.G. Immobilization of laccase from *Aspergillus oryzae* on graphene nanosheets. *Int. J. Biol. Macromol.* **2017**, *99*, 121–127. [CrossRef] [PubMed]
87. Zille, A.; Tzanov, T.; Gübitz, G.M.; Cavaco-Paulo, A. Immobilized laccase for decolourization of Reactive Black 5 dyeing effluent. *Biotechnol. Lett.* **2003**, *25*, 1473–1477. [CrossRef] [PubMed]
88. Wen, X.; Zeng, Z.; Du, C.; Huang, D.; Zeng, G.; Xiao, R.; Lai, C.; Xu, P.; Zhang, C.; Wan, J.; et al. Immobilized laccase on bentonite-derived mesoporous materials for removal of tetracycline. *Chemosphere* **2019**, *222*, 865–871. [CrossRef] [PubMed]
89. Abejón, R.; De Cazes, M.; Belleville, M.P.; Sanchez-Marcano, J. Large-scale enzymatic membrane reactors for tetracycline degradation in WWTP effluents. *Water Res.* **2015**, *73*, 118–131. [CrossRef]

Catalysis Today 348 (2020) 127–136

Contents lists available at ScienceDirect

Catalysis Today

journal homepage: www.elsevier.com/locate/cattod

A promising laccase immobilization using electrospun materials for biocatalytic degradation of tetracycline: Effect of process conditions and catalytic pathways

Jakub Zdarta[a,*], Katarzyna Jankowska[a], Karolina Bachosz[a], Ewa Kijeńska-Gawrońska[b], Agnieszka Zgoła-Grześkowiak[c], Ewa Kaczorek[a], Teofil Jesionowski[a,*]

[a] Institute of Chemical Technology and Engineering, Faculty of Chemical Technology, Poznan University of Technology, Berdychowo 4, PL-60965 Poznan, Poland
[b] Faculty of Materials Science and Engineering, Warsaw University of Technology, Wołoska 141, PL-02507 Warsaw, Poland
[c] Institute of Chemistry and Technical Electrochemistry, Faculty of Chemical Technology, Poznan University of Technology, Berdychowo 4, PL-60965 Poznan, Poland

ARTICLE INFO

Keywords:
Electrospun materials
Enzyme immobilization
Laccase
Tetracycline
Environmental protection
Biodegradation

ABSTRACT

In the presented study poly(methyl methacrylate) (PMMA) and magnetite nanoparticles were used to prepare novel PMMA/Fe_3O_4 electrospun nanofibers. The obtained materials were characterized, and then modified and used as supports for covalent binding and encapsulation of laccase from *Trametes versicolor*. High enzyme loading (63.2 mg of laccase per 1 cm^2 of support) was recorded for the system after covalent binding, and the formation of stable interactions was confirmed, as leaching of the enzyme from the support did not exceed 12%. Furthermore, the obtained biocatalytic systems exhibited excellent pH, thermal and storage stability as well as reusability: after 40 days of storage and 5 successive biocatalytic cycles they retained 80% of their initial properties. Experiments on the removal of antibiotic showed that both immobilized laccases possess high ability to convert tetracycline. Under optimal process conditions (pH 5, temperature 25 °C, tetracycline solution concentration 1.0 mg L^{-1}) the removal efficiency reached 100% and 94% for covalently bonded and encapsulated laccase. Finally, the degradation products were examined to investigate the degradation mechanism. The data showed that oxidation, dehydrogenation and demethylation are major reactions in the degradation of tetracycline using immobilized laccase. The findings demonstrate clearly that laccase immobilized by covalent binding and encapsulation using electrospun materials has the potential for application in environmental protection processes for the removal of antibiotics.

1. Introduction

Antibiotics are used as active agents in the prevention and treatment of all types of bacterial infections in humans and animals. Their annual global consumption is estimated at over 200,000 tons [1,2]. According to European Union regulations, the concentration of antibiotics in the environment should not exceed 10 μg L^{-1}; however, the estimated concentration of tetracycline, one of the most commonly used antibiotics, is significantly higher, reaching levels of 450–900 μg L^{-1} [2]. In addition, according to the United States Food and Drug Administration, high levels of tetracycline have been detected in soil, drinking water and groundwater, as well as hospital and municipal wastewaters [3]. The ubiquity of tetracycline and antibiotics in general could lead to the creation of bacteria strains resistant to these drugs, posing a potential threat to the ecosystem and human health.

There are many techniques for effective removal of tetracycline from the environment, including adsorption [4,5], ozonation [6], photocatalysis [7], electrolysis [8], advanced oxidation processes [9], and membrane techniques [10]. However, enzymatic bioremediation seems to be the most effective, this being directly related to the high specificity and selectivity of biocatalytic reactions. The use of enzymes in the degradation of antibiotics is environmentally friendly. What is more, in comparison with the above-mentioned chemical processes, enzymatic reactions take place under mild conditions (temperature and pH), which reduces energy costs [11]. In the bioremediation of pollutants from water and wastewater, enzymes from the class of oxidoreductases are used, among which the most important are laccases, tyrosinases, and peroxidases. For reasons of availability, low price, and absence of need for additional chemical reagents (only the presence of molecular oxygen is required for the oxidation reaction), the most

* Corresponding authors.
E-mail addresses: jakub.zdarta@put.poznan.pl (J. Zdarta), teofil.jesionowski@put.poznan.pl (T. Jesionowski).

https://doi.org/10.1016/j.cattod.2019.08.042
Received 17 May 2019; Received in revised form 21 August 2019; Accepted 27 August 2019
Available online 28 August 2019
0920-5861/

commonly used are laccases [12]. Although these enzymes are widespread in nature, mainly in fungi, as well as in the cells of some prokaryotes, insects and plants the most frequently used are laccases obtained from various species of white or red rot fungi, such as *Trametes versicolor* and *Trametes vilosa* [13].

However, the efficiency of reactions involving enzymes is closely related to their activity. Free proteins are sensitive to changes in temperature and pH conditions, as well as the presence of inhibitors in the reaction environment, which significantly affects their applicability. To increase the stability and reusability of biocatalytic systems, enzyme immobilization processes are applied. There are many methods for immobilizing proteins, including adsorption, covalent binding, encapsulation or cross-linking, depending on the type of interaction between the enzyme and the support [14,15]. The properties determining the choice of a suitable matrix include the physicochemical parameters of the support, such as porosity, surface area, the presence and type of functional groups, mechanical strength, and chemical and thermal stability. Supports used in the immobilization process constitute a diverse group of materials, which includes inorganic carriers, natural and synthetic polymers, as well as hybrid materials [16].

On the other hand, innovative materials created by the electrospinning method are gaining increasing interest. This technique allows to obtain tailor-made highly porous materials from nano- to micrometer size, composed of different precursors. Enzymes may be efficiently immobilized both by encapsulation inside the electrospun fibers and by adsorption or covalent binding on the surface of the fibers. Water-insoluble fibers are produced mainly from polymers, such as polystyrene (PS), polyacrylonitrile (PAN), poly(methyl methacrylate) (PMMA), polysulfone (PSF) and polyurethane (PU) [17]. For instance, in a previous study, Dai et al. [18] successfully immobilized laccase by encapsulation into the poly(D,L-lactide)/poly(ethylene oxide)-poly(propylene oxide)-poly(ethylene oxide) triblock copolymer. In another study, Koloti et al. [19] bounded laccase covalently with hyperbranched polyethyleneimine/polyethersulfone electrospun nanofibrous membrane. Furthermore, laccase was previously immobilized using electrospun materials made of polycaprolactone, polyacrylonitrile or polylactide for encapsulation and covalent binding of the enzyme molecules [20–23]. All of the biocatalytic systems were then used in environmental processes for the removal of organic pollutants, such as chlorophenols, bisphenols and dyes from water solutions.

Taking into account the above-mentioned information, in this study, for the first time, we present a proof-of-concept for the production of a novel electrospun poly(methyl methacrylate) (PMMA) material with embedded magnetic particles (Fe_3O_4), and its use for laccase immobilization by encapsulation and covalent binding. This material was chosen as a support due to its porosity and stability, the presence of numerous functional groups that facilitate its modification, as well as magnetic properties which facilitate the separation of the biocatalytic system from the reaction mixture by using external magnetic field. Further, immobilized laccase was used in experiments involving the biodegradation of tetracycline under various process conditions. Optimal reaction parameters leading to effective degradation of the antibiotic were investigated, as well as the stability and reusability of the obtained systems. The results indicate that an effective environmental tool for the removal of tetracycline has been developed, which might find practical applications in the biodegradation processes of hazardous pollutants from wastewaters.

2. Materials and methods

2.1. Chemicals and materials

Iron(III) chloride hexahydrate, iron(II) chloride tetrahydrate and 25% tetramethylammonium hydroxide solution, used for the synthesis of magnetite nanoparticles (MNPs), as well as poly(methyl methacrylate) (PMMA) at molecular weight 10,000 g mol^{-1} and 1,1,1,3,3,3-hexafluoro-2-propanol (HFP), used for the production of electrospun materials, were obtained from Sigma-Aldrich (USA). *N*-(3-dimethylaminopropyl)-*N'*-ethylcarbodiimide (EDC) and *N*-hydroxysuccinimide (NHS), used for modification of the nanofibers, laccase from *Trametes versicolor* (EC 1.10.3.2, ≥0.5 U/mg), tetracycline (≥98.0%), 2,2-azinobis-3-ethylbenzothiazoline-6-sulfonate (ABTS, ≥99%), Coomassie Brilliant Blue G-250, acetate, phosphate and Tris−HCl buffers at specific pH were supplied by Sigma-Aldrich. Methanol, ethanol and 85% H_3PO_4 (all laboratory grade) were obtained from Chempur (Poland). LC/MS-grade acetonitrile and ammonium acetate were obtained from Sigma-Aldrich (USA). HPLC-grade water was prepared by reverse osmosis in a Demiwa system from Watek (Czech Republic) followed by double distillation from a quartz apparatus.

2.2. Synthesis of magnetite nanoparticles

The magnetite nanoparticles were synthesized using a co-precipitation method based on our previous study [24] with slight modification. Briefly, $FeCl_3{\cdot}6H_2O$ and $FeCl_2{\cdot}4H_2O$ in a molar ratio of 2:1 were used as precursors and dissolved in degassed water and mixed for 1 h at a constant temperature of 80 °C under a neutral gas (nitrogen) atmosphere. During mixing, 30 mL of 25% tetramethylammonium hydroxide solution was added dropwise. After addition of the tetramethylammonium hydroxide the reaction mixture was stirred for 30 min. Finally, magnetic nanoparticles were separated from the reaction mixture using an external magnetic field, washed several times using deionized water, and dried for 12 h at 45 °C.

2.3. Production of electrospun materials

To prepare PMMA/magnetite nanofibers for covalent immobilization of laccase, 0.75 g of PMMA was dissolved in 6 mL of HFP to form a 12% (w/v) solution. Next, 200 mg of the previously prepared magnetite nanoparticles were added and the solution was stirred for 3 h at ambient temperature to obtain a final mixture ready for the electrospinning process. Electrospinning of the solution was carried out under optimized conditions using a NANON-01A apparatus (MECC Co., Japan). The apparatus was equipped with an 18 G flattened needle connected to a syringe by a PTFE tube fixed to a moving head. The speed of the moving head was 75 mm/sec, the working width was 150 mm, and the voltage applied through the needle was 20 kV. The feed rate was set at 1.0 mL h^{-1}, and the distance between the needle tip and the collector was 100 mm. The PMMA/Fe_3O_4 nanofibers were collected on a grounded steel plate collector covered with aluminum foil. At the final stage of production of the nanofibers they were dried for 48 h at a temperature of 27 °C in a vacuum dryer.

2.4. Support modification

Prior to immobilization, the previously obtained PMMA/Fe_3O_4 nanofibers underwent functionalization using EDC/NHS according to the methodology presented by Zhu et al. [25]. Briefly, 10 mg of EDC and 14 mg of NHS were dissolved in 5 mL of phosphate buffer at pH 6.5. Next, a few pieces of cut nanofibers with a surface area of 0.5 cm^2 (0.5 cm × 1.0 cm) were weighed, washed with deionized water and added to the solution of modifier. The mixture was then immersed for 5 h at ambient temperature. After the process, nanofibers were separated from the reaction mixture using an external magnetic field, washed with deionized water to remove unbound reactants, and used as a support for laccase immobilization. The idea of the functionalization of the PMMA/Fe_3O_4 nanofibers and covalent immobilization of laccase was presented in Fig. 1.

2.5. Laccase immobilization by covalent binding and encapsulation

Covalent immobilization was carried out by placing 2 pieces of the

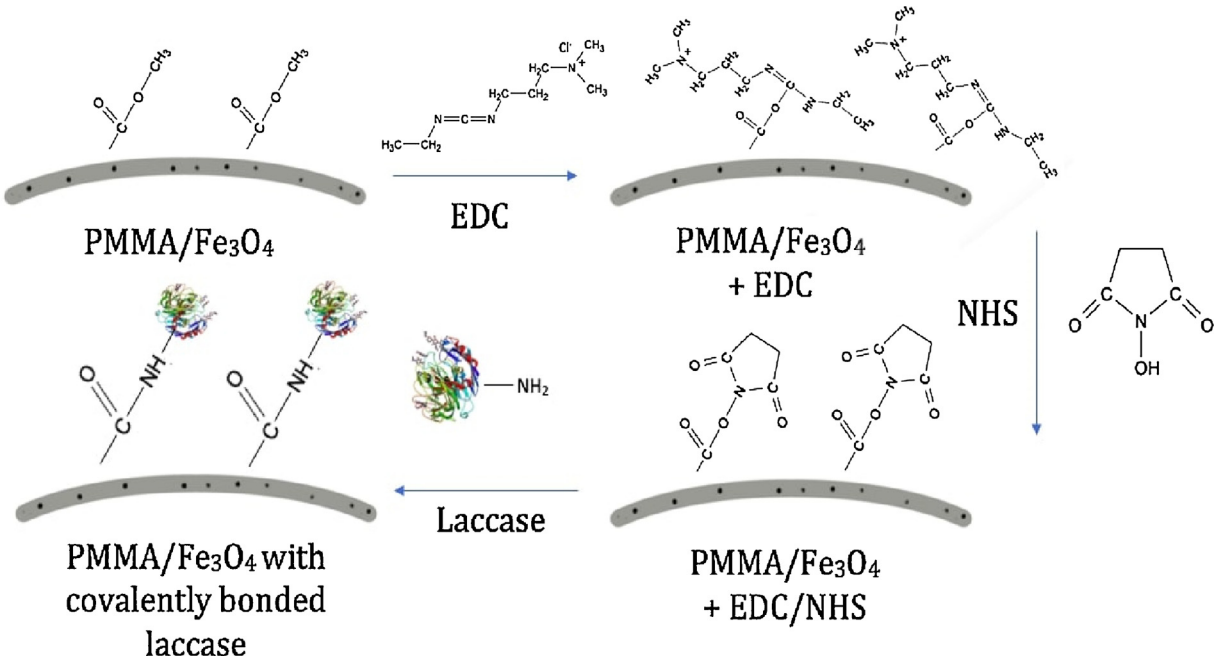

Fig. 1. The schematic diagram representing the idea of the functionalization of the PMMA/Fe3O4 nanofibers by EDC/NHS approach and covalent immobilization of laccase.

cut and modified nanofibers in 10 mL of laccase solution at a concentration of 8 mg mL^{-1} in acetate buffer at pH 5. The process was carried out for 2 h at 4 °C using an IKA KS 4000i incubator (Germany). After the process, the PMMA/Fe_3O_4 nanofibers with immobilized enzyme were separated from the mixture using an external magnetic field, and washed with acetate buffer to remove unbound enzyme.

For the fabrication of fibers with encapsulated enzyme, 0.75 g of PMMA was dissolved in 6 mL of HFP to form a 12% (w/v) solution. Next, 200 mg of the previously prepared magnetite nanoparticles were added and the solution was stirred for 3 h at ambient temperature to obtain a final mixture. In the separate flask laccase was dissolved in acetate buffer at pH 5 at a concentration of 40 mg mL^{-1}. Next, the solutions of PMMA and laccase were mixed in a volumetric ratio of 1:10 and stirred for 1 h using a magnetic stirrer. Electrospinning of the solution was carried out under optimized conditions using a NANON-01A apparatus (MECC Co., Japan). The apparatus was equipped with an 18 G flattened needle connected to a syringe by a PTFE tube fixed to a moving head. The speed of the moving head was 75 mm/sec, the working width was 150 mm, and the voltage applied through the needle was 20 kV. The feed rate was set at 1.0 mL h^{-1}, and the distance between the needle tip and the collector was 100 mm. The obtained nanofibers were collected on a grounded steel plate collector covered with aluminum foil and they were dried for 48 h at a temperature of 27 °C in a vacuum dryer.

2.6. Amount of immobilized enzyme and enzyme leakage

The amount of immobilized enzyme (mg cm^{-2}) was evaluated based on the Bradford method [26] as the difference between the initial dosage of the enzyme and the concentration of the protein in the supernatant after immobilization, considering the area of the support material. From the results the immobilization yield (%) was also calculated, based on the concentration of the laccase solutions before and after immobilization, and their volume.

In order to evaluate enzyme leakage (%) from the support, both covalently immobilized and encapsulated laccase were incubated for 24 h at 25 °C in 50 mL of acetate buffer at pH 5 and were mixed at 350 rpm using a shaker. The percentage of eluted laccase was calculated based on measurement of the protein content in the biocatalytic systems obtained after immobilization and the concentration of the enzyme after the leakage test, using the Bradford method.

2.7. Stability, reusability as well as kinetic parameters of free and immobilized enzymes

To evaluate storage stability, the free and immobilized enzymes were stored at 4 °C for 40 days, and their relative activity was examined after specified periods of time, based on the reaction with ABTS as a substrate, to which 10 mg of free or immobilized enzyme was added [27]. The reaction was carried out for 60 min at pH 5 and temperature 25 °C. Changes in the substrate concentration were followed spectrophotometrically at wavelength 420 nm using a Jasco V-750 spectrophotometer (Japan). The initial value of the activity of the free or immobilized enzyme was defined as 100%.

The reusability of the covalently immobilized and encapsulated laccase was examined based on the aforementioned reaction over eight consecutive catalytic cycles lasting 60 min at pH 5 and temperature 25 °C. After each reaction cycle, the material contains immobilized enzymes were separated from the reaction mixture using an external magnetic field, washed with acetate buffer at pH 5 and placed into a fresh ABTS solution. The activity of laccase in the first biodegradation cycle was defined as 100% activity.

Chemical and thermal stability of the free and immobilized enzymes over time were evaluated based on the reaction with ABTS as a substrate, after incubating the samples at pH 5 and temperature 25 °C (optimum conditions) for 180 min. The relative activity of free and immobilized enzymes was examined after a specified period of time. The initial activity of the tested systems was defined as 100% activity. The inactivation constant (k_D) and half-life ($t_{1/2}$) were evaluated based on the linear regression slope.

Evaluation of the kinetic parameters – the Michaelis-Menten constant (K_m) and the maximum rate of reaction ($Vmax$) – of free and immobilized laccase was performed based on the model reactions described above, using as a substrate solutions of ABTS at concentrations ranging from 0.001 to 0.5 mM. The kinetic parameters were calculated based on Hanes–Woolf plots under optimum assay conditions.

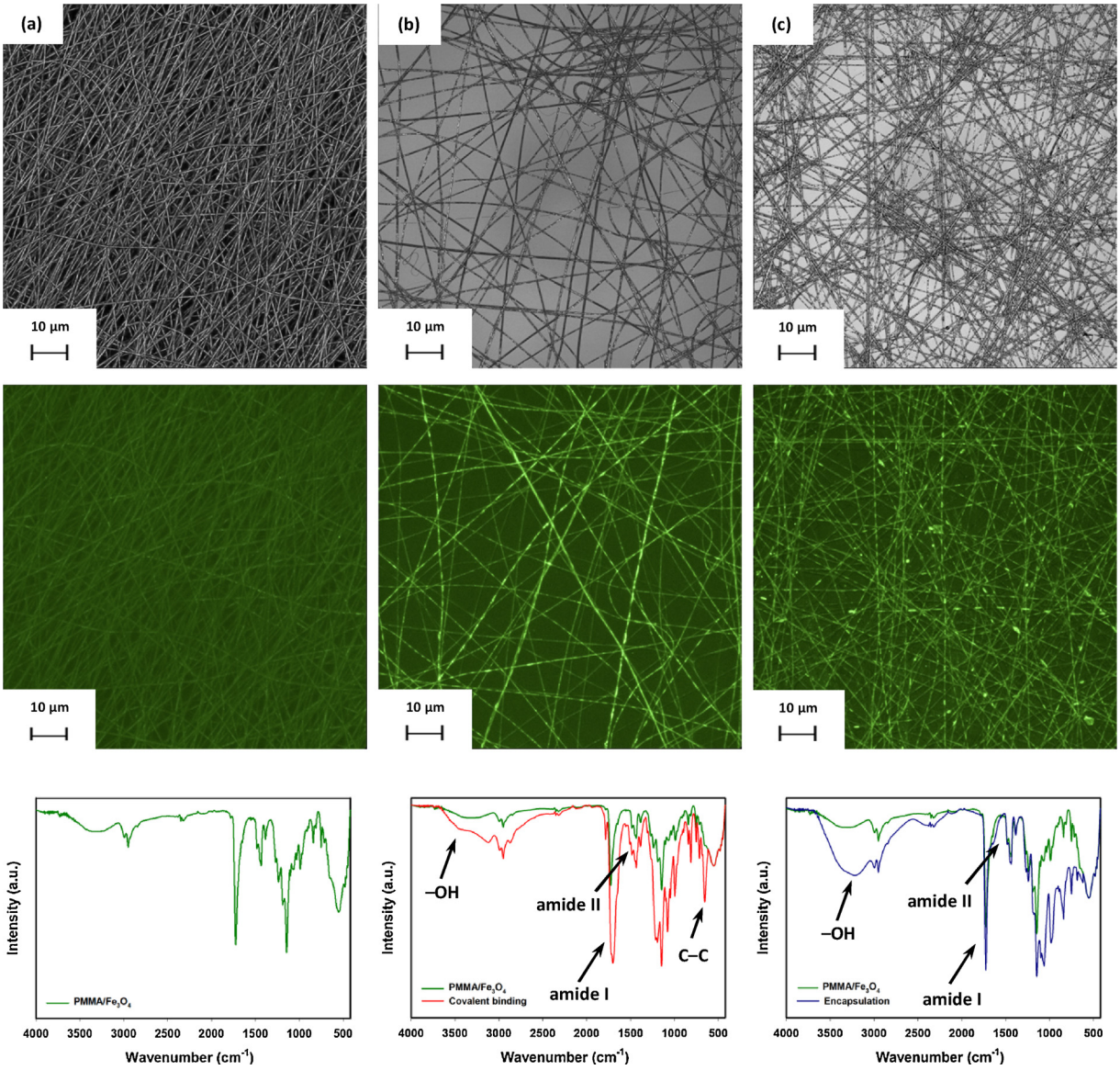

Fig. 2. Confocal laser scanning micrographs in the material (upper row) and fluorescent (lower row) mode, and FTIR spectra of: (a) PMMA/Fe_3O_4, (b) PMMA/Fe_3O_4 and PMMA/Fe_3O_4 with covalently bonded laccase, and (c) PMMA/Fe_3O_4 and PMMA/Fe_3O_4 with encapsulated laccase.

2.8. Removal of tetracycline

The tetracycline degradation ability of the free and immobilized enzymes was examined using an IKA KS 4000i incubator shaker (200 rpm) in complete darkness. To 20 mL of the tetracycline at various concentration in buffer solutions at desired pH, 10 mg of the free or immobilized enzyme was added. The reaction was carried out for 60 min, and samples (0.1 mL) were taken every 10 min. The progress of the reaction was observed spectrophotometrically using a Jasco V-750 spectrophotometer at wavelength 355 nm. The concentration of the tetracycline after degradation was evaluated based on a standard calibration curve for that compound. The efficiency of removal of tetracycline was calculated from the following equation (1):

$$\textit{Tetracycline removal}\ (\%) = \frac{C_0 - C_t}{C_0} \cdot 100\% \quad (1)$$

where C_0 denotes initial tetracycline concentration and C_t denotes the remaining concentration of tetracycline after a certain time.

The effect of pH on the tetracycline removal efficiency was evaluated using 1 mg L^{-1} solution at 25 °C over the pH range 3–9 (buffer solutions at desired pH). The effect of temperature on the removal efficiency was evaluated at temperatures of 5, 15, 25, 35 and 45 °C using tetracycline solution at concentration 1 mg L^{-1} in acetate buffer at pH 5. To examine the effect of the concentration of the antibiotic on the efficiency of its degradation, solutions at concentrations of 0.1, 1.0, 5.0 and 10.0 mg L^{-1} were used, and experiments were carried out at temperature 25 °C and pH 5.

In order to determine the possible adsorption of tetracycline by the PMMA/Fe_3O_4 with covalently immobilized or encapsulated laccase, a control experiment with thermally inactivated enzymes was carried out. For this purpose, immobilized laccase was subjected to thermal inactivation for 5 h at 80 °C and placed in 20 mL of tetracycline solution at concentration 1 mg L^{-1} at pH 5 for 60 min. The amount of adsorbed antibiotic was evaluated spectrophotometrically.

2.9. Analysis of the electrospun nanofibers before and after laccase immobilization

Differences in the structure of the electrospun materials before and after immobilization, and the distribution of the immobilized laccase,

Table 1
Kinetic parameters of free and immobilized enzymes and data illustrating immobilization efficiency and enzyme leakage.

	K_m (mM)	V_{max} (mM s^{-1})	Amount of immobilized enzyme (mg cm^{-2})	Immobilization yield (%)	Enzyme leakage (%)
Free laccase	0.059 ± 0.006	0.043 ± 0.003	–	–	–
Covalent binding	0.134 ± 0.007	0.032 ± 0.004	63.2 ± 2.8	79 ± 3.1	12.3 ± 1.2
Encapsulation	0.192 ± 0.01	0.027 ± 0.003	40.0	100	3.4 ± 0.9

were investigated using an LSM710 confocal laser scanning microscope (CLSM) from Zeiss (Germany). The microscope operated in the material (reflected light) and fluorescent modes using an argon ion laser at wavelengths of 458 nm and 488 nm respectively. Fourier transform infrared (FTIR) spectra of the electrospun materials before and after immobilization were obtained using a Bruker Vertex 70 spectrometer (Germany) operating in attenuated total reflectance (ATR) mode over the wavenumber range 4000–400 cm^{-1} at a resolution of 0.5 cm^{-1}.

2.10. Chromatographic measurements

Identification of degradation products was performed using an UltiMate 3000 HPLC instrument from Dionex (USA) coupled with a 4000 QTRAP mass spectrometer from ABSciex (USA). A Gemini-NX C18 analytical column (100 mm x 2.0 mm I.D.; 3 µm) from Phenomenex (USA) maintained at 35 °C was used in the study. The sample injection volume was 5 µL. The mobile phase consisted of 5 mM ammonium acetate in water and acetonitrile (ACN) at a flow rate of 0.3 mL min^{-1}, according to the following gradient: 0 min 10% ACN, 1 min 10% ACN, 3 min 40% ACN, 6 min 85% ACN. The electrospray ion source (ESI) operated in positive mode. Nitrogen was used in both the source and the mass spectrometer. The following parameters of the source and mass spectrometer were used: curtain gas pressure 10 psi, nebulization gas pressure 45 psi, auxiliary gas pressure 45 psi, source temperature 450 °C, ESI voltage 4500 V, declustering potential 45 V. Chromatograms were collected in enhanced mass spectra mode in the range 50–600 *m/z*. Selected ions were fragmented in enhanced product ion mode.

2.11. Statistical analysis

All of the above experiments were performed in triplicate, and the results are presented as mean ± standard deviation. Statistically significant differences were determined using one-way ANOVA performed using Systat Software Inc. SigmaPlot 12 (USA), based on Tukey's test. Statistical significance was established at $p < 0.05$.

3. Results and discussion

3.1. Characterization of support and enzyme immobilization

To confirm the effectiveness of the synthesis of PMMA/Fe_3O_4 electrospun material and the immobilization of laccase by covalent binding and encapsulation, CLSM photographs (material and fluorescence modes) and FTIR spectra were obtained (Fig. 2). Each of the electrospun materials, before and after the immobilization process, consists of fibers with diameters not exceeding 500 nm. However, after covalent binding of the laccase, a slight increase in the diameters of the nanofibers was observed due to the enzyme immobilization onto their surface. CLSM photographs in fluorescence mode clearly show the differences before and after laccase immobilization. The PMMA/Fe_3O_4 material (Fig. 2a) does not exhibit fluorescence. However, after the immobilization process the fibers emit green fluorescence under excitation, indicating effective enzyme immobilization [28]. The fibers with covalently immobilized enzyme emit brighter green fluorescence than the material with encapsulated laccase that is related to the laccase immobilization, respectively, onto and into PMMA/Fe_3O_4 nanofibers.

The FTIR spectra indicate differences between the electrospun materials before and after laccase immobilization. The spectrum of PMMA/Fe_3O_4 contains signals characteristic for PMMA and Fe_3O_4 at 2940 cm^{-1} (−CH bonds), 1720 cm^{-1} (C═O bonds), 1390 cm^{-1} (C−H bonds), 1150 cm^{-1} (C−O bonds), and 574 cm^{-1} (Fe−O bonds), indicating the effective synthesis of the PMMA/Fe_3O_4 material [24,29]. In the FTIR spectra of PMMA/Fe_3O_4 with immobilized laccase, beside the above-listed signals, peaks are also observed at 3420 cm^{-1} (O−H groups), 1655 cm^{-1} and 1540 cm^{-1} (amide I and II bands respectively) and 700 cm^{-1} (C−C bonds); these confirm effective immobilization of the enzyme [27]. Moreover, it should be noted that the maxima of some signals in the FTIR spectrum after enzyme encapsulation, such as peaks assigned to stretching vibrations of O−H, amide I and amide II bonds, were slightly shifted, at around 10 cm^{-1} towards higher wavenumber values. This suggests changes in the microenvironment of these groups as a result of the encapsulation.

In the next part of the study the characteristics of immobilization and enzyme leakage were investigated, and the kinetic parameters of the free and immobilized enzymes were calculated and compared (Table 1). As can be seen, the values of the K_m constant obtained for the immobilized enzymes, both covalently bonded and encapsulated, are significantly higher than for the free laccase, indicating the lower affinity of the immobilized enzymes to the substrate. The increase in the value of K_m observed for immobilized enzymes is associated with structural changes of the biomolecules resulting from the immobilization process, as well as spherical hindrances around enzyme active sites or loss of enzyme elasticity [30]. This fact is particularly visible for encapsulated laccase, due to the surrounding of the enzyme molecules by the PMMA/Fe_3O_4 material. Consequently, the values of the maximum reaction rate calculated for covalently immobilized and encapsulated laccase are lower by 25% and 35% respectively than the *Vmax* of free laccase, this being related mainly to the lower substrate affinity [31]. However, although the K_m of the immobilized enzymes increased significantly, the obtained biocatalytic systems can be considered effective biocatalysts due to the relatively small decrease in *Vmax*. This unexpected finding may be explained by the highly porous structure of the electrospun materials, which partially reduces diffusional limitations [32].

The immobilization yield of 100% recorded for encapsulated laccase is a natural result due to the presence of the enzyme in the solution prior to electrospinning. However, the high immobilization yield (around 80%) and the amount of over 60 mg of enzyme loaded per cm^2 of nanofibers in the case of covalent binding of the enzyme indicate the high enzyme affinity by the EDC/NHS modified fibers as well as the high immobilization capacity of the PMMA/Fe_3O_4 material, mainly due to its porosity and the presence of many chemical moieties. Furthermore, the results of the leakage test confirm the formation of stable enzyme–matrix covalent bonds and the protective effect of the polymeric support against laccase elution. Only 12% of the enzyme was eluted from the support after 24 h of the test. In the case of the encapsulated enzyme the value was even lower and reached 3.4%.

3.2. Stability and reusability of free and immobilized enzymes

Following the effective immobilization of laccase, the stability of the obtained biocatalytic systems and of the free enzyme over time under process conditions was investigated and compared. Storage stability and reusability are also important features and prerequisites for

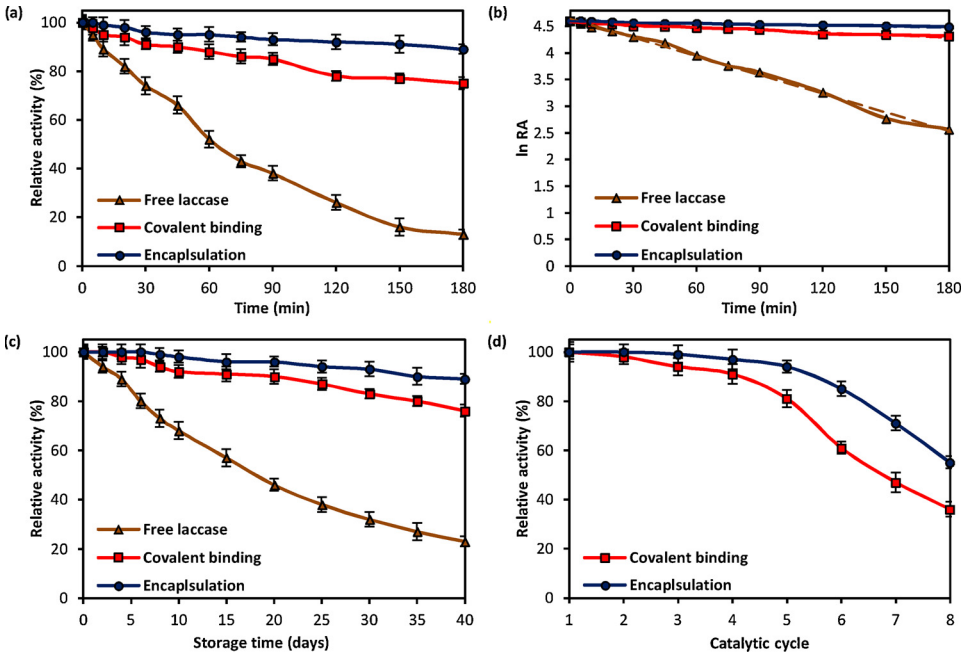

Fig. 3. Thermal and chemical stability (a, b), storage stability (c) and reusability (d) of the free and immobilized laccase.

practical applications. Fig. 3a shows that after 180 min of incubation, both immobilized enzymes exhibit excellent thermal stability as compared with free laccase. After this time the free enzyme retained less than 20% of its initial catalytic activity, compared with around 80% and over 90% for covalently bonded and encapsulated laccase respectively. The improvement in the stability of the immobilized laccases is reflected in the values of the inactivation constant (k_D) and enzyme half-life ($t_{1/2}$), which were calculated based on the data presented in Fig. 3b. The values of k_D and $t_{1/2}$ for free laccase were 0.0122 1/min and 57.1 min, while for laccase immobilized by covalent binding the values were 0.0016 1/min and 440.5 min. An even more significant improvement in these parameters was recorded for encapsulated laccase, for which the half-life was 20 times longer than that of the free enzyme (1122.6 min), and the inactivation constant was the lowest among all of those tested (0.0006 1/min). As shown in Fig. 3c, the relative activity of the immobilized enzymes decreased steadily but very slowly compared with free laccase; after 40 days of storage the enzymes immobilized by covalent binding and by encapsulation respectively preserved around 75% and 90% of their activity. Meanwhile free laccase lost half of its activity after 20 days, and after 40 days less than 20% of its initial activity was retained. The reusability test performed over eight successive catalytic cycles showed that both immobilized enzymes exhibit exceptional reusability: after five consecutive batches the fall in the relative activity did not exceed 10% and 20% for encapsulated and covalently bonded laccase respectively (Fig. 3d). Although a more significant drop occurs in further biocatalytic steps, after eight reaction cycles the biocatalytic systems retained around 50% of their initial activity, indicating the excellent reusability of the obtained biocatalysts.

The significant improvement in the thermostability, chemical stability, storage stability and reusability of the laccase after immobilization might be attributed to the protective effect of the PMMA/Fe_3O_4 material and the provision of a protective microenvironment for the immobilized enzymes by the support [33]. Moreover, after immobilization of the laccase its three-dimensional structure is more rigid, and is protected against conformational changes caused by reaction conditions which lead to enzyme deactivation. Furthermore, the stable covalent binding limits leaching of the enzyme from the support, and ensures the retention of high catalytic activity [34]. Nevertheless, the higher stability exhibited by the encapsulated laccase compared with the covalently bonded enzyme is related to the fact that the biomolecules are trapped in the PMMA/Fe_3O_4 nanofibers, which form a unique core-shell structure providing additional protection of laccase against deactivation [28]. On the other hand, the drop in the relative activity of the immobilized enzymes is related to enzyme inhibition by the products of the reaction as well as deactivation of the enzyme due to its repeated use. Nonetheless, the results clearly show that both of the obtained biocatalytic systems offer good operational stability and may be used with high efficiency for the removal of hazardous compounds from wastewater.

3.3. Removal of tetracycline

Many previous studies have shown that various process parameters might significantly affect the enzymatic removal of hazardous pollutants [35,36]. Thus, following evaluation of the stability and reusability of the immobilized laccase, it was crucial to determine the effect of various process conditions (pH, temperature, and concentration of tetracycline solution) on its efficiency and to determine optimal conditions enabling the effective removal of antibiotic. Moreover, to determine whether the removal of tetracycline results from catalytic action only or from both adsorption and catalytic treatment, adsorption experiments were performed using both biocatalytic systems with inactivated enzyme. It should be emphasized that although electrospun materials usually have good sorption capacity, the adsorption of tetracycline using nanofibers with thermally inactivated laccase did not exceed 5%, indicating that the removal of the antibiotic is mainly due to enzymatic conversion.

3.3.1. Effect of pH

The removal of antibiotic was investigated over a broad pH range from 3 to 9, at 25 °C (Fig. 4). It can be seen that irrespective of the form of biocatalyst used, the efficiency of removal of tetracycline increased with pH to reach a maximum at pH 5, and then decreased with increasing pH values. Similar observations were made in our previous studies [27,37] and may be explained by the nature of the laccase from *Trametes versicolor* (used in this study), which exhibits maximum catalytic activity in slightly acidic conditions (around pH 5). Free and covalently immobilized laccase removed 100% of the antibiotic from the solution, and the efficiency of the removal process using

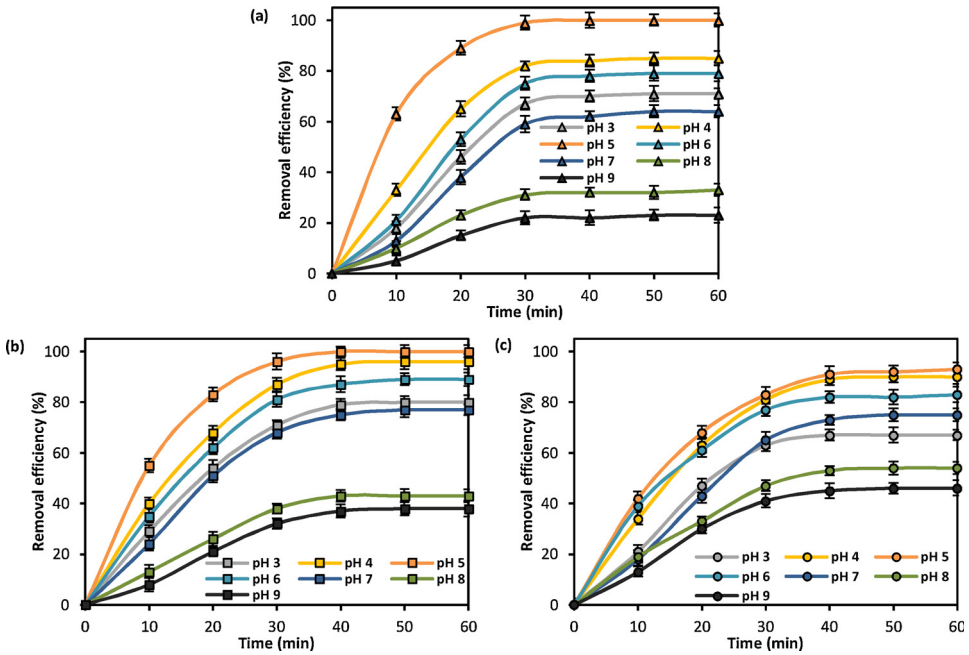

Fig. 4. Effect of pH on the efficiency of removal of tetracycline by: free enzyme (a), covalently bonded enzyme (b) and encapsulated enzyme (c).

encapsulated laccase was around 95%. This is related to the fact that the accessibility of the active sites of the encapsulated laccase is more restricted than in the free and covalently bonded enzyme, due to the polymer layer around the laccase biomolecules [37]. It should be added that the degradation curves obtained in the processes with both immobilized enzymes reached a plateau after 40 min of the reaction, compared with 30 min when free laccase was used. These results are in agreement with the kinetic data, and might be explained by the higher substrate affinity of free laccase as well as the lack of diffusional limitations.

However, it should be underlined that use of both immobilized enzymes leads to higher efficiencies of removal of tetracycline as compared with free laccase over broader analyzed pH range. This is due to the fact that laccase immobilized on or within the PMMA/Fe_3O_4 material is better protected against harsh reaction conditions and has higher pH resistance than the native enzyme [38]. This phenomenon is particularly visible in the efficiency of tetracycline degradation by encapsulated laccase, which even at pH 8 and pH 9 remained above 40% due to stabilization and protection of the enzyme structure [39]. These results are in agreement with those of Shao et al., [34], who immobilized laccase by covalent binding on hollow mesoporous carbon nanospheres and used it for the removal of tetracycline from aqueous solution. The removal efficiency over the whole analyzed pH range (3–9) was significantly higher than for the native enzyme.

3.3.2. Effect of temperature

The catalytic properties of the free and immobilized enzymes might also be affected by temperature. The efficiencies of removal of tetracycline were examined over a wide range of temperatures from 5 to 45 °C, at pH 5. Irrespective of the type of biocatalyst used, the highest removal efficiencies were observed at 25 °C; this is related to the properties of the laccase, which exhibits maximum activity in the temperature range 20–25 °C [40]. As Fig. 5a shows, free laccase degraded over 80% of tetracycline only at the temperatures 25 and 35 °C; decreasing or increasing the temperature caused a significant drop in the efficiency of removal of the pharmaceutical due to the instability of the free enzyme under the process conditions. Meanwhile, when immobilized biocatalysts were used for degradation of tetracycline, the removal efficiency exceeded 80% over a wide temperature range from 15 even up to 45 °C (Fig. 5b,c). Moreover, over the broader analyzed temperature range, encapsulated and covalently immobilized laccase degraded tetracycline with higher efficiencies than the native laccase. The significant improvement in the thermal tolerance of immobilized laccase is related to several factors; among others, the formation of stable covalent laccase–support interactions which stabilize the enzyme structure and protect it against conformational changes. Furthermore, the PMMA/Fe_3O_4 material reduces the negative effect of higher temperatures on enzyme activity and protects the biomolecules against thermal inactivation [41]. Similar results were previously reported by Taheran et al., who immobilized laccase on polyacrylonitrile – biochar composite nanofibrous membrane made by the electrospinning technique. The immobilized enzyme was used to degrade pharmaceuticals from water solutions, and attained around 20% higher catalytic activity than the native laccase over the whole temperature range from 10 to 70 °C [42].

3.3.3. Effect of solution concentration

Although concentrations of tetracycline in wastewater usually do not exceed 0.9 mg L^{-1} [43], we decided to use a higher concentration of antibiotic to test the effectivity of the obtained biocatalytic systems. The efficiency of removal of tetracycline was evaluated using solutions at concentrations ranging from 0.1 to 10 mg L^{-1}, under optimal process conditions (Fig. 6). After 60 min of the process the highest removal efficiencies reached 100% for free and covalently bonded laccase and 94% for the encapsulated enzyme when the tetracycline solution concentration was 0.1 or 1.0 mg L^{-1}. Above this value, the higher the concentration of the tetracycline solution, the lower the efficiency of removal. Nevertheless, the encapsulated laccase removed 60% of the pollutant even from the solution with concentration 10 mg L^{-1}. The highest removal rates recorded for the free enzyme are related to the accessibility of the enzyme's active sites; however, the high biodegradation efficiencies obtained using immobilized laccase from solution at high concentration are related to the porosity of the electrospun PMMA/Fe_3O_4 nanofibers and the high enzyme loading on the surface of the support. By contrast, as reported by Yang et al. [44], laccase immobilized on magnetic nanoparticles degraded tetracycline at a concentration of 0.1 mg L^{-1}. The efficiency of removal of the pharmaceutical was 80% in the first 12 h of the process. In another study, Dai et al. [28] removed bisphenol A from aqueous solution at concentration 50 mg L^{-1} using laccase encapsulated in electrospun fibrous

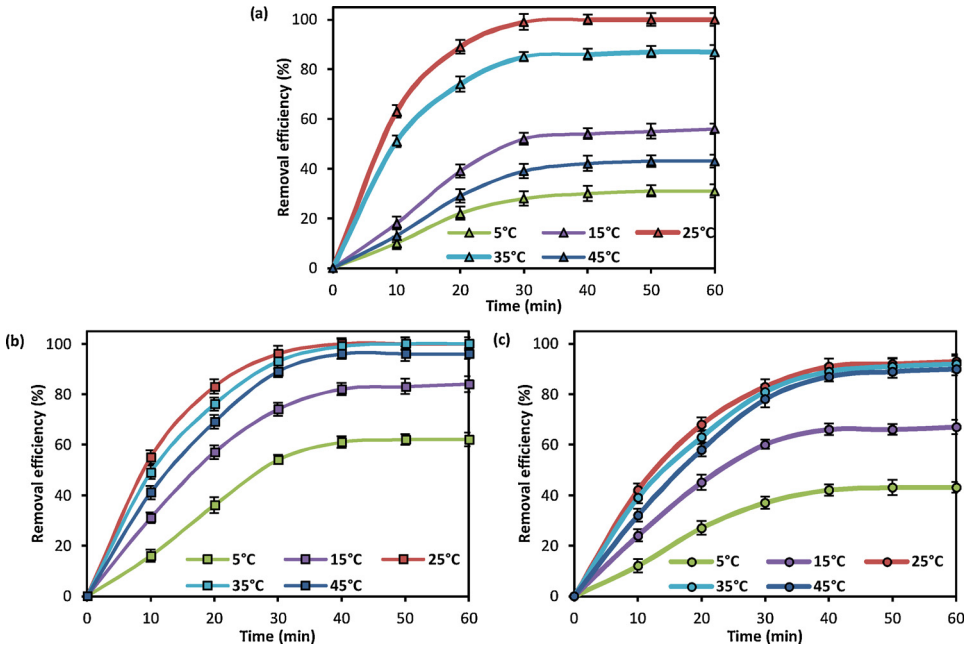

Fig. 5. Effect of temperature on the efficiency of removal of tetracycline by: free enzyme (a), covalently bonded enzyme (b), encapsulated enzyme (c).

membrane, with an efficiency of 80%. However, this high efficiency was due to a dual removal mechanism, with simultaneous sorption onto the electrospun fibers and enzymatic conversion by laccase. Nevertheless, it could be briefly summarized, that laccase immobilized using PMMA/Fe_3O_4 by covalent binding and encapsulation removed, respectively 100 and 95% of tetracycline form solution at pH 5 and concentration 1 mg L^{-1} at temperatures of 25 and 35 °C. The promising results obtained in this study indicate the possibility of using the biocatalytic system in the removal of pharmaceuticals from aqueous solutions even at higher concentrations.

3.4. Products of conversion and the transformation pathways

Following evaluation of the effect of various process parameters on tetracycline removal, the products of enzymatic conversion and possible transformation pathways were studied. During the conversion of tetracycline by laccase several processes were observed, including oxidation, dehydrogenation and demethylation (Fig. 7). The chromatogram obtained at the start of the degradation showed two peaks of protonated molecules characteristic of tetracycline, both at m/z = 445. These two peaks are typical of tetracyclines, which occur in two tautomeric forms (keto and enol) eluting at different retention times (2.42 and 3.38 min) [45]. Two degradation products were observed after only 30 min and remained in the degradation liquor up to 3 h: the first was formed after oxidation of the carbon atom at position 5 in the tetracycline structure (protonated molecule at m/z = 461) and the second after dehydrogenation of tetracycline, also at the C5 position (protonated molecule at m/z = 443). Further degradation of the oxidized

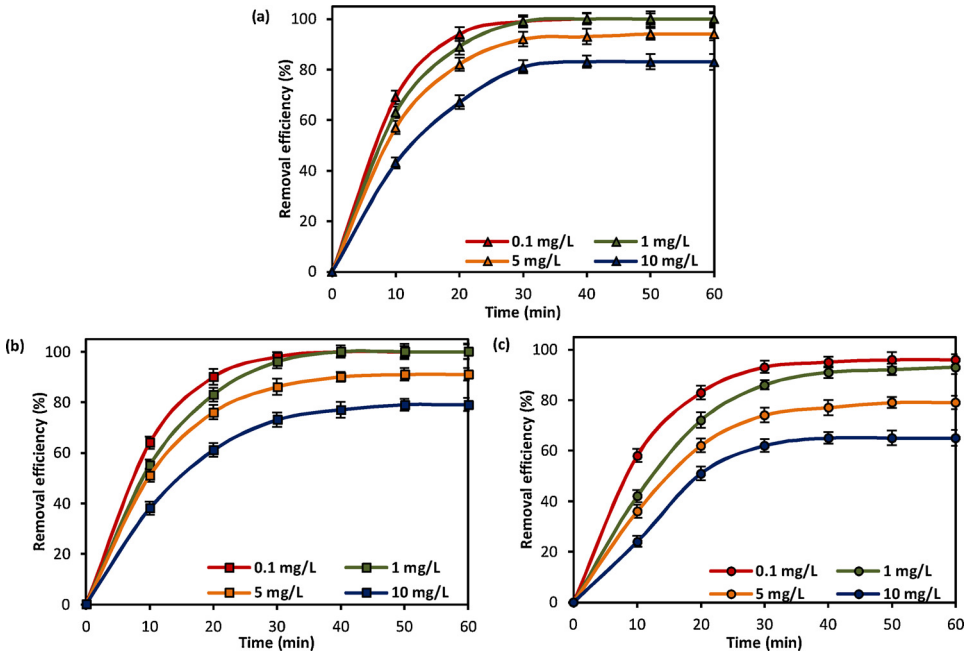

Fig. 6. Effect of solution concentration on the efficiency of removal of tetracycline by: free enzyme (a), covalently bonded enzyme(b) and encapsulated enzyme (c).

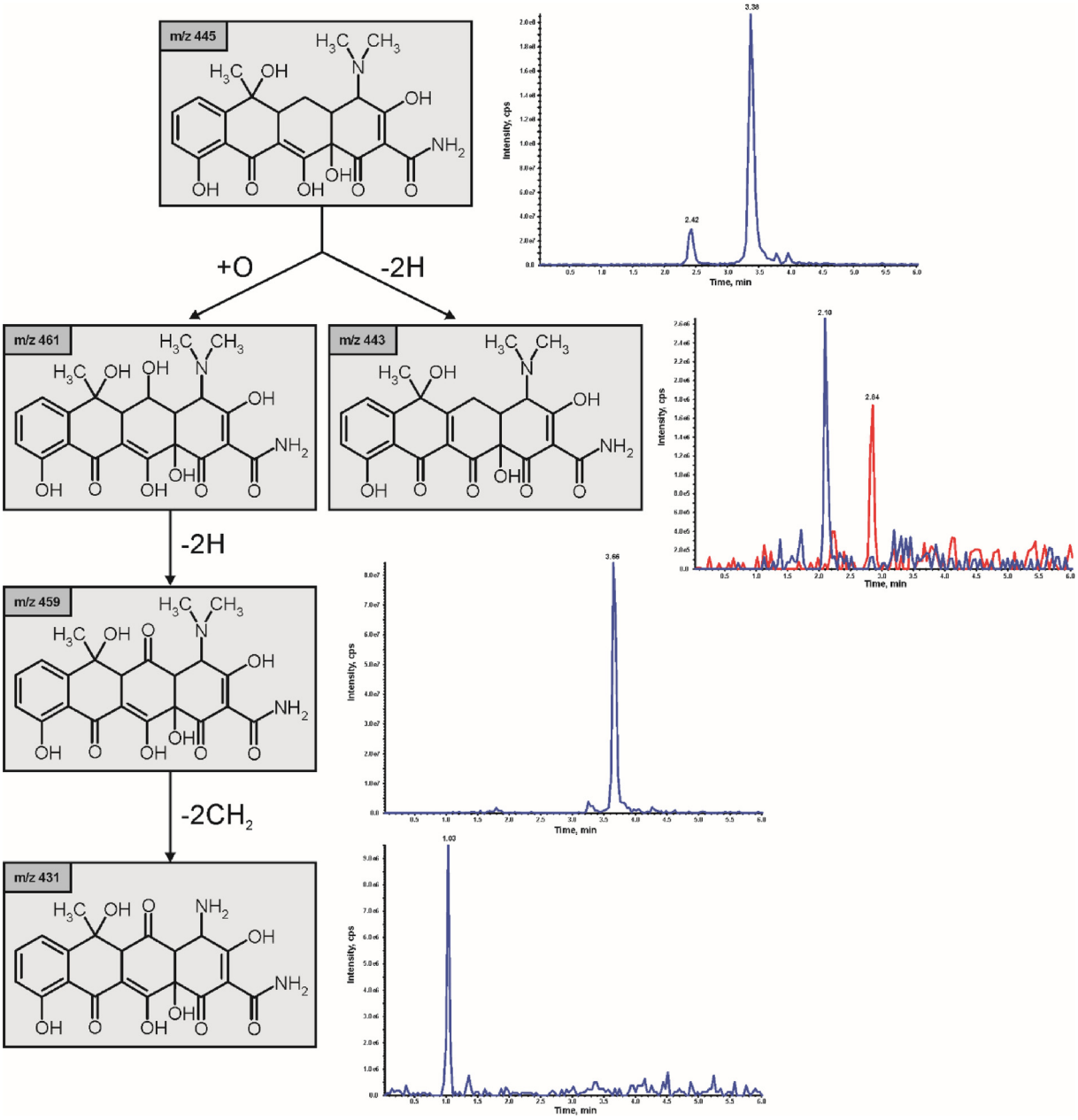

Fig. 7. Conversion products of tetracycline with extracted ion chromatograms of protonated molecules at *m/z*given by the structures of the compound.

product led to its dehydrogenation and formation of a corresponding ketone (protonated molecule at $m/z = 459$). This, based on its ion abundance, was the main degradation product of tetracycline. It was detected after one hour of degradation, and its concentration increased in the subsequent hours of the test. Finally, an ion at $m/z = 431$ was also found, indicating bi-demethylation of the amine groups at the carbon atom at position 4 in the main degradation product. The degradation products found in the test were in agreement with those described by Yang et al. [44] and Sun et al. [46], although the low-intensive ion at $m/z = 396$ (abundance only 1×10^4 according to Yang et al.) was not visible in the present study. Similarly, two compounds of molecular weight 426 g mol^{-1}, proposed by Sun et al., to be direct degradation products of tetracycline, were not found in this study. Instead, it was shown that the ions at $m/z = 427$ were formed by fragmentation of tetracycline, which was also confirmed by the identity of the retention times for the chromatographic peaks of ions at $m/z = 427$ and $m/z = 445$.

4. Conclusions

It may be stated in summary that in the present study, for the first time, novel PMMA/Fe_3O_4 electrospun nanofibers were fabricated, characterized, modified and used as a support for laccase immobilization. Due to the high enzyme loading (over 60 mg of enzyme per cm^2 of electrospun material), the formation of stable enzyme–support interactions (negligible leaching of laccase) and the protective effect of the support material, the immobilized biomolecules exhibit exceptional thermal, pH and storage stability as compared with the free enzyme. The immobilized laccases also offer excellent reusability: after five repeated biodegradation cycles both biocatalytic systems retained over 80% of their initial activity. Furthermore, covalently bonded and encapsulated laccase respectively removed 100% and 95% of tetracycline from a solution at concentration 1.0 mg L^{-1}. It has also been shown that due to improvement of the enzyme's stability against reaction conditions, effective removal of tetracycline (> 80%) by the immobilized laccases takes place over broader pH and temperature ranges as

compared with the free enzyme. Moreover, as the sorption of the antibiotic by the electrospun material does not exceed 5%, it is mainly catalytic action that is responsible for effective antibiotic conversion. Finally, analysis of the degradation products of the enzymatic conversion of tetracycline indicates that oxidation, dehydrogenation and demethylation are the main processes responsible for the conversion of antibiotic molecules. Hence, it can be concluded that the proposed immobilization approach results in the formation of highly stable biocatalytic systems with excellent potential for application in the removal of hazardous pollutants from wastewater on a large scale.

Declaration of Competing Interest

None.

Acknowledgement

This work was financed and prepared as part of research project supported by the National Science Centre Poland, No. 2017/27/B/ST8/01506.

References

[1] D. Becker, S. Varela Della Giustina, S. Rodriguez-Mozaz, R. Schoevaart, D. Barcelo, M. de Cazes, M.P. Belleville, J. Sanchez-Marcano, J. de Gunzburg, O. Couillerot, J. Volker, J. Oehlmann, M. Wagner, Bioresour. Technol. Rep. 219 (2016) 500–509.
[2] H. Liu, C. Ma, G. Chen, J.C. White, Z. Wang, B. Xing, O.P. Dhankher, ACS Sustain. Chem. Eng. 5 (2017) 3204–3213.
[3] V.T. Nguyen, C.M. Hung, T.B. Nguyen, J.H. Chang, T.H. Wang, C.H. Wu, Y.L. Lin, C.W. Chen, C.D. Dong, Catalysts 9 (2019) 1–14.
[4] J. Lyu, Z. Hu, Z. Li, M. Ge, J. Phys. Chem. Solids 129 (2019) 61–70.
[5] J. Rivera-Utrilla, C.V. Gomez-Pacheco, M. Sanchez-Polo, J.J. Lopez-Penalver, R. Ocampo-Perez, J. Environ. Manage. 131 (2013) 16–24.
[6] C.V. Gomez-Pacheco, M. Sanchez-Polo, J. Rivera-Utrilla, J. Lopez-Penalver, Chem. Eng. J. 178 (2011) 115–121.
[7] L. Jiang, D. Chen, L. Qin, J. Liang, X. Sun, Y. Huang, J. Alloys. Compd. 783 (2019) 10–18.
[8] I. Yahiaoui, L.Y. Cherif, K. Madi, F. Aissani-Benissad, F. Fourcade, A. Amrane, Sep. Sci. Technol. 53 (2018) 337–348.
[9] L.W. Matzek, K.E. Carter, Chemosphere 151 (2016) 178–188.
[10] T.T. Nguyen, X.T. Bui, V.P. Luu, P.D. Nguyen, W. Guo, H.H. Ngo, Bioresour. Technol. Rep. 240 (2017) 42–49.
[11] M. de Cazes, M.P. Belleville, M. Mougel, H. Kellner, J. Sanchez-Marcano, J. Membrane Sci. 476 (2015) 384–393.
[12] A.H. Alneyadi, M.A. Rauf, S.S. Ashraf, Crit. Rev. Biotechnol. 38 (2018) 971–988.
[13] Shraddha, S. Shekher, M. Sehgal, A.K. Kamthania, Enzyme Res. (2011) (2011) 1–11.
[14] R.C. Rodrigues, C. Ortiz, A. Berenguer-Murcia, R. Torres, R. Fernandez-Lafuente, Chem. Soc. Rev. 42 (2013) 6290–6307.
[15] M. Maryskova, I. Ardao, C.A. Garcia-Gonzalez, L. Martinova, J. Rotkova, A. Sevcu, Enzyme Microb. Tech. 89 (2016) 31–38.
[16] E. Fatarella, D. Spinelli, M. Ruzzante, R. Pogni, J. Mol. Cat. B: Enzym. 102 (2014) 41–47.
[17] D.N. Tran, K.J. Balkus Jr, Top. Catal. 55 (2012) 1057–1069.
[18] Y. Dai, J. Niu, J. Liu, L. Yin, J. Xu, Bioresour. Technol. Rep. 101 (2010) 8942–8947.
[19] L.E. Koloti, N.P. Gule, O.A. Arotiba, S.P. Malinga, Environ. Technol. 39 (2018) 392–404.
[20] R. Xu, C. Chi, F. Li, B. Zhang, ACS Appl. Mater. Interface 5 (2013) 12554–12560.
[21] M.F. Canbolat, H.B. Savas, F. Gultekin, Biochem. Anal. Biochem. 528 (2017) 13–18.
[22] Q. Feng, D. Wu, S. Huan, M. Li, X. Li, J. Eng. Fiber Fabric 11 (2016) 45–54.
[23] M.J.F. Jasni, P. Sathishkumar, S. Sornambikai, A.R.M. Yusoff, F. Ameen, N.A. Buang, M.R.A. Kadir, Z. Yusop, Bioproc. Biosys. Eng. 40 (2017) 191–200.
[24] Ł. Klapiszewski, J. Zdarta, K. Antecka, K. Synoradzki, K. Siwińska-Stefańska, D. Moszyński, T. Jesionowski, Appl. Surf. Sci. 422 (2017) 94–103.
[25] Y.T. Zhu, X.Y. Ren, Y.M. Liu, Y. Wei, L.S. Qing, X. Liao, Mater. Sci. Eng. C 38 (2014) 278–285.
[26] M.M. Bradford, Anal. Biochem. 72 (1976) 248–254.
[27] J. Zdarta, K. Antecka, R. Frankowski, A. Zgoła-Grześkowiak, H. Ehrlich, T. Jesionowski, Sci. Total Environ. 615 (2018) 784–795.
[28] Y. Dai, J. Yao, Y. Song, X. Liu, S. Wang, Y. Yuan, J. Hazard. Mater. 317 (2016) 485–493.
[29] A. Dazzi, A. Deniset-Besseau, P. Lasch, Analyst 138 (2013) 4191–4201.
[30] R.O. Cristovao, S.C. Silverio, A.P.M. Tavares, A.I.S. Brigida, J.M. Laureiro, R.A.R. Boaventura, E.A. Macedo, M.A.Z. Coelho, World J. Microbiol. Biotechnol. 28 (2012) 2827–2838.
[31] F. Salami, Z. Habibi, M. Yousefi, M. Mohammadi, Int. J. Biol. Macromol. 120 (2018) 144–151.
[32] S. Kumar, I. Haq, J. Prakash, A. Raj, Int. J. Biol. Macromol. 98 (2017) 24–33.
[33] S.A. Chaudhari, R.J. Kar, S.R. Singhal, Curr. Org. Chem. 19 (2015) 1732–1754.
[34] B. Shao, Z. Liu, G. Zeng, Y. Liu, X. Yang, C. Zhou, M. Chen, Y. Liu, Y. Jiang, M. Yan, J. Hazard. Mater. 362 (2019) 318–326.
[35] M. de Cazes, M.P. Belleville, E. Petit, M. Llorca, S. Rodríguez-Mozaz, J. de Gunzburg, D. Barceló, J. Sanchez-Marcano, Catal. Today 236 (2014) 146–152.
[36] F. Lassouane, H. Ait-Amar, S. Amrani, S. Rodriguez-Couto, Bioresour. Technol. Rep. 271 (2019) 360–367.
[37] K. Antecka, J. Zdarta, K. Siwińska-Stefańska, G. Sztuk, E. Jankowska, P. Oleskowicz-Popiel, T. Jesionowski, Catalysts 8 (2018) 1–18.
[38] X. Wen, Z. Zeng, C. Du, D. Huang, G. Zeng, R. Xiao, C. Lai, P. Xu, C. Zhang, J. Wan, L. Hu, L. Yin, C. Zhou, R. Deng, Chemosphere 222 (2019) 865–871.
[39] J. Liu, J. Niu, L. Yin, F. Jiang, Analyst 136 (2011) 4802–4808.
[40] S. Rangelov, J.A. Nicell, Biochem. Eng. J. 99 (2015) 1–15.
[41] S. Datta, L.R. Christena, Y.R.S. Rajaram, Biotech 3 (2013) 1–9.
[42] M. Taheran, M. Naghdi, S.K. Brar, E.J. Knystautas, M. Verma, R.Y. Surampalli, ACS Sustain. Chem. Eng. 5 (2017) 10430–10438.
[43] A. Pena, M. Paulo, L.J.G. Silva, M. Seifrtová, C.M. Lino, P. Solich, Anal. Bioanal. Chem. 396 (2010) 2929–2936.
[44] D.J. Yang, Y. Lin, X. Yang, T.B. Ng, X. Ye, D.J. Lin, J. Hazard. Mater. 322 (2017) 525–531.
[45] B. Ferraz Spisso, M.A. Gonçalves de Araújo Jr, M. Alves Monteiro, A.M. Belém Lima, M. Ulberg Pereira, R. Alves Luiz, A. Wanderley da Nóbrega, Anal. Chim. Acta 656 (2009) 72–84.
[46] K. Sun, Q. Huang, S. Li, J. Hazard. Mater. 331 (2017) 182–188.

Materials Science & Engineering C 103 (2019) 109789

Contents lists available at ScienceDirect

Materials Science & Engineering C

journal homepage: www.elsevier.com/locate/msec

Robust biodegradation of naproxen and diclofenac by laccase immobilized using electrospun nanofibers with enhanced stability and reusability

Jakub Zdarta[a,*], Katarzyna Jankowska[a], Marta Wyszowska[a], Ewa Kijeńska-Gawrońska[b], Agnieszka Zgoła-Grześkowiak[c], Manuel Pinelo[d], Anne S. Meyer[e], Dariusz Moszyński[f], Teofil Jesionowski[a,*]

[a] Institute of Chemical Technology and Engineering, Faculty of Chemical Technology, Poznan University of Technology, Berdychowo 4, PL-60965 Poznan, Poland
[b] Faculty of Materials Science and Engineering, Warsaw University of Technology, Wołoska 141, PL-02507 Warsaw, Poland
[c] Institute of Chemistry and Electrochemistry, Faculty of Chemical Technology, Poznan University of Technology, Berdychowo 4, PL-60965 Poznan, Poland
[d] Department of Chemical and Biochemical Engineering, DTU Chemical Engineering, Technical University of Denmark, Soltofts Plads 227, DK-2800 Kgs. Lyngby, Denmark
[e] Department of Biotechnology and Biomedicine, DTU Bioengineering, Technical University of Denmark, Soltofts Plads 229, DK-2800 Kgs. Lyngby, Denmark
[f] West Pomeranian University of Technology, Szczecin, Faculty of Chemical Technology and Engineering, Institute of Inorganic Chemical Technology and Environment Engineering, Pułaskiego 10, PL-70322 Szczecin, Poland

ARTICLE INFO

Keywords:
Laccase
Immobilization
Electrospun materials
Environmental pollutants
Pharmaceuticals
Biodegradation

ABSTRACT

Enzymatic biodegradation of pharmaceuticals, using enzymes such as laccase, is a green solution for the removal of toxic pollutants that has attracted growing interest over recent years. Moreover, the application of immobilized biocatalysts is relevant for industrial applications, due to the improved stability and reusability of the immobilized enzymes. Thus, in the present study, laccase was immobilized by adsorption and encapsulation using poly(l-lactic acid)-*co*-poly(ε-caprolactone) (PLCL) electrospun nanofibers as a tailor-made support. The produced biocatalytic systems were applied in the biodegradation of two commonly used anti-inflammatories, naproxen and diclofenac, which are present in wastewaters at environmentally relevant concentrations. The results showed that under optimal process conditions (temperature 25 °C, pH 5 and 3 for naproxen and diclofenac respectively), even from a solution at a concentration of 1 mg L^{-1}, over 90% of both pharmaceuticals was removed by encapsulated laccase in batch mode. Both immobilized enzymes also exhibited high reusability: after five reaction cycles approximately 60% and 40% of naproxen and diclofenac were removed by encapsulated and adsorbed laccase respectively. In addition, a thorough analysis was made of the products of biodegradation of the two studied pollutants. Furthermore, toxicity study of the mixture after biodegradation of the pharmaceuticals showed that the solutions obtained after the process were approximately 65% less toxic than the initial naproxen and diclofenac solutions.

1. Introduction

Due to its high production and consumption, pharmaceutically active compounds frequently occurred in wastewater, drinking water and even ground water at concentrations usually do not exceeding nanograms or micrograms per liter [1]. Accumulation of these compounds as well as their metabolites in water compartments in unknown and uncontrolled amounts has attracted attention as they are persistent and might have negative effect on human beings and environment. For instance long-term contact with diclofenac is associated with a serious atherothrombotic and gastrointestinal issues as well as vascular risk [2]. Moreover, the adverse effect of diclofenac on environment, such as on microbial consortia and selected aquatic organisms has been previously reported [3]. On the other hand, naproxen and its metabolites also could negatively affected on human body and caused some serious gastrointestinal and cardiovascular adverse effects and lead to an irreparable changes in a rover ecosystems [4]. Due to the low bioavailability and complex structure of these compounds, their biodegradation is a serious environmental challenge. Conventional treatment plants are not able to efficiently remove and have some issues, such as generation of toxic by-products and waste stream. Thus, increasing interest was focused on a sustainable biological alternative as an eco-friendly and powerful solutions [5]. As of particular interest, enzymatic-based methods should be presented, as biocatalysts can degrade a wide range

* Corresponding authors.
E-mail addresses: jakub.zdarta@put.poznan.pl (J. Zdarta), teofil.jesionowski@put.poznan.pl (T. Jesionowski).

https://doi.org/10.1016/j.msec.2019.109789
Received 24 January 2019; Received in revised form 10 May 2019; Accepted 23 May 2019
Available online 24 May 2019

of xenobiotics under mild conditions, without toxic effluents [6].

The catalytic conversion of pharmaceutical pollutants takes place by the action of fungal oxidative enzymes, such as laccases, tyrosinases and various peroxidases [7]. Laccases, however, are the most frequently applied enzymes for biodegradation of persistent compounds due to their availability, low price, low substrate specificity and high catalytic activity. There are some literature study related to the use of free laccase for degradation on anti-inflammatories. For instance, Lonappan et al., reported that laccase produced by white rot fungi *Trametes versicolor*, degraded over 90% of diclofenac after 48 h of the process [8]. In another study Aracagök et al., showed that crude laccase from *Trametes trogii* almost completely removed diclofenac with 97% efficiency in 48 h [9]. However, practical application of free enzymes suffers from their low stability and poor reusability. Enzyme immobilization is a possible approach to overcome these limitations and at the same time increase the biodegradation efficiency and enzyme reuse [10]. In the previous study it has been reported that laccase was immobilized onto polyacrylonitrile nanofibers [11], marine sponges scaffolds [12] or biochar microparticles at various organic origin [13], and efficiently used for removal of hazardous compounds. As proper selection of the support material in enzyme immobilization is the crucial affecting properties of the biocatalysts, more and more attention is paid to evaluate immobilization protocols based on using novel and tailor-made supports.

The materials produced by the electrospinning method are characterized by thin structures reaching a diameter in the range from 100 nm to 1 μm, and length to even several thousand meters [14]. One of the most important features of electrospun materials is the designed geometry in a quick and relatively cheap way [15]. Although all nanofibers combine common features, the final properties of a material depend on the polymer used to obtain electrospun materials. It should be pointed that electrospun nanofibers can be also successfully used to enzyme immobilization. The important feature of materials produced by electrospinning method is porosity, biocompatibility and a large number of functional groups on the surface of nanofibers. This is evidenced by the fact that it is possible to immobilize the protein by means of adsorption, encapsulation or covalent bonding on the electrospun material. A wide range of polymers are used to enzyme immobilization, and poly(ε-caprolactone) [16] and poly(vinyl alcohol) are one of them [17]. It is worth to paying attention that during the production of electrospun nanofibers it is possible to obtain composite which, having many functional groups, increase the affinity of the enzyme to the support, for example polycaprolactone/cellulose monoacetate [18] and poly(vinyl alcohol)/polyacrylamide [19].

Hence, in this study we aimed to evaluate novel immobilization protocol for laccase from *Trametes versicolor* by adsorption and encapsulation approach, using PLCL electrospun nanofibers as support material. This support was used due to its exceptional mechanical stability, numerous of functional groups facilitating stable attachment of the enzyme as well as its porosity that limit diffusional limitations and enhance activity of the biomolecules. Further, the biodegradation and conversion of diclofenac and naproxen by the biocatalytic systems obtained were investigated and the optimal process conditions for removal of both pharmaceuticals have been found during the study. Moreover, comprehensive work on characterization of degradation products and their toxicity have also been examined in details. Although degradation of pharmaceuticals by laccase has been reported, to the best of our knowledge, this is the first time, where effective removal of naproxen and diclofenac by PLCL-laccase biocatalytic systems is shown. Moreover, presented results might provide a novel and efficient technique for practical application of electrospun-based immobilized enzymes for biodegradation of hazardous pollutants from wastewaters.

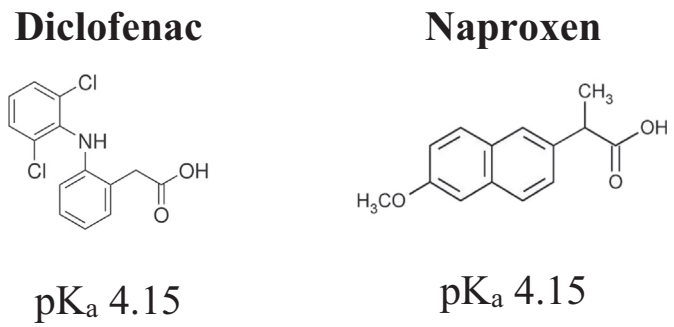

Fig. 1. Structures and pK_a values of diclofenac and naproxen.

2. Materials and methods

2.1. Chemicals and reagents

Poly(l-lactic acid)-*co*-poly(ε-caprolactone) (PLCL), laccase from *Trametes versicolor* (EC 1.10.3.2, ≥0.5 U/mg), diclofenac sodium salt (DCF, ≥98%), naproxen (NPR, ≥99%) (see Fig. 1), 2,2-azinobis-3-ethylbenzothiazoline-6-sulfonate (ABTS, ≥99%), Coomassie Brilliant Blue, acetate and phosphate buffers at specific pH, analytical grade chloroform and Span 80 were supplied by Sigma-Aldrich (USA). Ethanol, methanol and 85% H_3PO_4 (all laboratory grade) were supplied by Chempur (Poland). HPLC-grade methanol and LC-MS-grade acetonitrile were obtained from Merck (Germany). HPLC-grade water was produced in the laboratory using a Demiwa system (Watek, Czech Republic).

2.2. Fabrication of electrospun materials

Hydrophilic PLCL nanofibers were obtained by electrospinning of an emulsion. To prepare the oil phase, 0.5 g of PLCL was dissolved in 5 mL of analytical grade chloroform to form a 10% (w/v) solution. Next, 50 μL of the surfactant Span 80 was added dropwise. An acetate buffer at pH 5 was used as the water phase. The oil and aqueous solutions were mixed in a ratio of 1:20 (v/v), and the mixture was stirred at RT for 3 h to obtain a smooth water-in-oil emulsion. PLCL nanofibers with laccase encapsulated within the fibers were also prepared by emulsion electrospinning. The oil phase was prepared as in the case of the PLCL fibers. For the water phase, laccase was dissolved in acetate buffer at a concentration of 100 mg mL^{-1}. Next, the polymer and laccase solutions were mixed in a ratio of 1:20 (v/v) and stirred for 3 h at RT. The electrospinning of both emulsions was carried out under the same optimized conditions using a NANON-01A apparatus (MECC Co., Japan). An 18G flattened needle connected to a syringe by a PTFE tube was fixed to a moving head with a linear speed of 50 mm/s and a working width of 100 mm. A high voltage of 25 kV was applied through the needle. The distance from the needle tip to the collector was set at 150 mm. The feed rate was fixed at 1.5 mL h^{-1}. Nanofibrous meshes were collected on an aluminum foil-covered, grounded steel plate collector and dried for 24 h in a vacuum drier (25 °C).

2.3. Immobilization of laccase by adsorption on PLCL membrane

Prior to immobilization the membrane was washed with deionized water, cut into pieces of 0.25 cm^2 (0.5 × 0.5 cm) and weighed. The pieces were then immersed in 5 mL of 1 mg mL^{-1} laccase solution (acetate buffer at pH 5) for 2 h at 4 °C using a KS 4000i incubator (IKA Werke GmbH, Germany). After the process, the PLCL fibers with immobilized enzyme were separated from the mixture and washed with acetate buffer to remove unbound enzyme.

2.4. Storage stability and kinetic parameters of free and immobilized enzymes

The storage stability of free and immobilized enzyme stored at 4 °C was examined over 30 days. Briefly, ABTS was used as a substrate, to which 10 mg of free or immobilized laccase was added. Changes in the concentration of the substrate were measured spectrophotometrically (λ = 420 nm), using a Jasco V-750 (Japan) spectrophotometer. For the storage stability study, the initial value of the activity of the free or immobilized enzyme was defined as 100%. The inactivation constant (k_D), and half-life ($t_{1/2}$) were evaluated based on the linear regression slope.

The same reaction was used to evaluate the kinetic parameters: the Michaelis–Menten constant (K_m) and the maximum rate of reaction (V_{max}). For this purpose solutions of the substrate at concentrations ranging from 1 to 100 mM were used, and the experiments were carried out under optimum assay reaction conditions. The Hanes–Woolf plot was used to calculate the apparent kinetic parameters of the free and immobilized enzyme. All measurements were made in triplicate, and the results are presented as average ± standard deviation.

2.5. Biodegradation of pharmaceuticals

The biodegradation of naproxen and diclofenac by free, adsorbed and encapsulated laccase was studied using an IKA KS 4000i incubator shaker (100 rpm). To 10 mL of a mixture of diclofenac or naproxen in buffer solution, 5 mg of free or immobilized laccase was added. The mixtures were then kept for 24 h and sampled at specified time intervals. After sampling, 0.1 mL of methanol was added prior to quantitative analysis. As naproxen is known for its resistance to enzymatic biodegradation [20] 0.1 mM of ABTS was added as a mediator agent to the solutions of that pharmaceutical.

Prior to evaluation of the efficiency of pharmaceutical biodegradation, the efficiency of adsorption of naproxen and diclofenac by the electrospun materials was examined. For this purpose, 50 mg of fibers with adsorbed and encapsulated laccase were subjected to thermal deactivation (4 h, 80 °C) and placed in 10 mL of DCF and NPR solutions at concentration 1 mg L^{-1} at pH 5 and 3 respectively. Adsorption experiments were carried out for 24 h, and the quantity of the pharmaceuticals adsorbed onto the electrospun materials was evaluated using chromatographic techniques.

The effect of pH on the biodegradation efficiency was evaluated using solutions at concentration 1 mg L^{-1} at 25 °C over the pH range 3–7. To adjust the pH, a buffer solution with the desired pH was used. The effect of temperature on the removal efficiency was evaluated at temperatures of 5, 25 and 50 °C using diclofenac and naproxen solutions at concentration 1 mg L^{-1} in acetate buffer at pH 5 and 3 respectively. To assess the effect of the concentration of the pharmaceutical solution on degradation efficiency, solutions at concentrations of 0.1, 1.0 and 10.0 mg L^{-1} were used. Experiments were carried out at a temperature of 25 °C at pH 5 (diclofenac) and pH 3 (naproxen).

The reusability of the adsorbed and encapsulated laccase was tested using diclofenac and naproxen solutions at concentration 1 mg L^{-1} in acetate buffer at pH 5 and 3 respectively, at 25 °C. After each biodegradation cycle, the immobilized enzymes were separated from the reaction mixture, washed with acetate buffer at the desired pH and placed into a fresh pharmaceutical solution. The activity of laccase in the first biodegradation cycle was defined as 100% activity. All of the above experiments were performed in triplicate, and the results are presented as average ± standard deviation.

2.6. Analytical procedures

The morphology of the PLCL fibers before and after enzyme immobilization was evaluated based on SEM photographs (EVO40, Zeiss, Germany) after gold coating (Balzers PV205P, Switzerland). Individual fibers diameters were measured from the SEM micrographs of 100 randomly selected nanofibers using Image Analysis Software (ImageJ, National Institute of Health, USA). FTIR spectra were obtained using a Bruker Vertex 70 spectrometer (Germany) in the wavenumber range 4000–400 cm^{-1} (resolution 0.5 cm^{-1}) using anhydrous KBr for sample preparation. The amount of immobilized enzyme (mg g^{-1}) was determined using the Bradford method, by measuring the initial enzyme dosage and the concentration of the protein in the supernatant after immobilization, and considering the mass of the support material [21]. The surface composition of the PLCL fibers before and after enzyme immobilization was analyzed by means of X-ray photoelectron spectroscopy (XPS) applying a Prevac system (ESCA, Poland) with Scienta analyzer (SES2002, Sweden) and Mg $K\alpha$ ($h\nu$ = 1253.7 eV) excitation radiation.

2.7. Chromatographic measurements

A chromatographic system from Dionex (USA) consisting of a P580 A LPG gradient pump, an ASI-100 autosampler, an STH 585 oven and an RF 2000 fluorescence detector was used for naproxen determination. 5 μL samples were injected into a C18 Hypersil GOLD column (150 mm × 4.6 mm I.D.; 5 μm) with a 2.1 mm I.D. filter cartridge (0.2 μm) (Thermo Scientific, USA). The mobile phase consisted of 75% methanol at a flow rate of 1.5 mL min^{-1} at 35 °C. Signal responses were measured by fluorescence detection at wavelengths set to 230 nm for excitation and 355 nm for emission.

The chromatographic system UltiMate 3000 RSLC (Dionex, USA) coupled to an API 4000 QTRAP triple quadrupole mass spectrometer (AB Sciex, USA) was used for diclofenac determination. 5 μL samples were injected into a KinetexEvo C18 column (150 mm × 2.1 mm I.D.; 2.6 μm) (Phenomenex, USA) maintained at 35 °C. The mobile phase employed in the analysis consisted of 0.1% HCOOH in water and acetonitrile at a flow rate of 0.3 mL min^{-1}. The following gradient was used: 0 min 70%; 2.5 min 100%; 3.0 min 100% of acetonitrile. The LC column effluent was directed to the electrospray ionization source (Turbo Ion Spray) operating in negative ion mode. The following settings were applied for the ion source and mass spectrometer: curtain gas 10 psi, nebulizer gas 40 psi, auxiliary gas 40 psi, temperature 450 °C, ion spray voltage −4500 V, declustering potential −45 V, collision gas set to medium. The dwell time for each mass transition detected in the selected reaction monitoring mode was set to 200 ms. The quantitative transition was from 294 to 250 m/z at collision energy set to −16 V, and the confirmatory transition was from 294 to 214 m/z at collision energy set to −28 V.

Identification of degradation products was performed using the above-mentioned LC-MS system. 5 μL samples were injected into a Gemini-NX C18 column (100 mm × 2.0 mm I.D.; 3 μm) (Phenomenex, USA) maintained at 35 °C. The mobile phase consisted of 5 mM ammonium acetate in water and methanol at flow rate 0.3 mL min^{-1}, at a gradient from 50% to 100% methanol in 4 min and then for 2 min in isocratic conditions. The electrospray ion source operated in positive and negative mode. Nitrogen was used in both the source and the mass spectrometer. The following parameters of the ESI source and mass spectrometer were used: curtain gas pressure 10 psi, nebulization gas pressure 45 psi, auxiliary gas pressure 45 psi, source temperature 450 °C, ESI voltage ± 4500 V, declustering potential −40 V. Chromatograms were collected in enhanced mass spectra mode in the range 50–900 m/z.

The linearity of the methods was tested over a wide range for all analytes. The instrumental limit of detection (LOD) and the instrumental limit of quantitation (LOQ) were calculated on the basis of the signal-to-noise (S/N) ratio, using S/N = 3 for calculation of the LOD and S/N = 10 for calculation of the LOQ. Precision and accuracy were not tested, because sample preparation included only the dilution step. Therefore, only the injection precision of the instrument is applicable in this procedure, and this was always below 1%. The values obtained for

diclofenac were LOD = 0.09 (μg L^{-1}), LOQ = 0.3 (μg L^{-1}), linear range 0.5–1000 (μg L^{-1}); the values for naproxen were LOD = 0.3 (μg L^{-1}), LOQ = 1.0 (μg L^{-1}), linear range 1–5000 (μg L^{-1}).

2.8. Toxicity tests

The acute toxicity of the untreated solutions of naproxen and diclofenac and the solutions treated with adsorbed and encapsulated laccase was evaluated at ambient temperature using *Artemia salina* as the test microorganism, according to the methodology presented by Bilal et al. [22]. Briefly, the mobility rate of 48-hour-old shrimps was measured after 48 h of incubation in untreated and enzymatically treated solutions of the pharmaceuticals. The effective concentration (EC_{30}) was then calculated. EC_{30} is defined as the concentration of the pharmaceutical (%) at which 30% of the target population show a positive response after the exposure time. Solutions of artificial seawater and potassium permanganate were used as the negative and positive control respectively. The toxicity tests were performed in duplicate, and results are presented as average ± standard deviation.

2.9. Statistical analysis

Statistically significant differences were determined using one-way ANOVA performed in SigmaPlot 12 (Systat Software Inc., USA) using Tukey's test. Statistical significance was established at $p < 0.05$.

3. Results and discussion

3.1. Characterization of the fibers and enzyme immobilization

The PLCL electrospun materials before immobilization consisted of randomly arrayed linear and continuous fibers with diameters of around 0.3–0.5 μm, with a relatively uniform, folded and bead-free surface (Fig. 2a). After laccase encapsulation (Fig. 2b) the diameter of the fibers did not change significantly; however some tubercles could be observed in certain areas of the fibers and their surface was more uneven, implying effective insertion of the enzyme aggregates into the PLCL fibers. By contrast, as presented in Fig. 2c, after enzyme adsorption the total surface of the fibers became corrugated. In addition, the diameter of the fibers increased, reaching up to 0.8 μm, indicating that laccase was uniformly distributed on the surface of the fibers. In the study, also the average diameter of obtained fibers before and after laccase immobilization were calculated and reached 373 ± 127 nm; 469 ± 222 nm and 430 ± 143 for crude PLCL fibers, PLCL fibers with encapsulated laccase and PLCL fibers with adsorbed laccase, respectively (Fig. 2 inset).

Additionally, to investigate the functional groups present in the PLCL fibers and in the products after immobilization, FTIR spectroscopy was applied. The FTIR spectrum of the pristine fibers contains signals characteristic for the $–CH_3$ (2945 cm^{-1}), $–CH_2$ (1395 cm^{-1}) and C–O–C (1185 and 1020 cm^{-1}) groups present in the structure of PLCL. A significant peak with a maximum at 1756 cm^{-1} is attributed to stretching vibrations of carbonyl groups, which are responsible for enzyme binding. As expected, when laccase was encapsulated into the electrospun fibers, peaks related to the enzyme were not observed on the FTIR spectrum. However, slight shifts of the signal maxima were observed, suggesting changes in the chemical microenvironment of the PLCL moieties after enzyme encapsulation. Comparing the FTIR spectra of pristine PLCL fibers and those with adsorbed laccase, new signals appeared at 3430 cm^{-1} and 650 cm^{-1}, corresponding to stretching vibrations of –OH and $–NH_2$ groups and bending vibrations of C—C bonds, and thus characteristic of the enzyme structure, as shown in Fig. 2d. Moreover, compared with the spectra of PLCL and free laccase, after enzyme adsorption a shift of the signal maxima towards higher wavenumbers was observed. These indicate effective adsorption immobilization, by the formation of hydrogen bonds between carbonyl groups in the PLCL fibers and amine and hydroxyl groups in the laccase structure [23].

The structure of the PLCL crude nanofibers and immobilization of laccase were followed using the surface analysis by X-ray photoelectron spectroscopy. The surface composition of PLCL fibers before immobilization, after laccase encapsulation and after enzyme adsorption was analyzed. It has been found that on the surface of PLCL nanofibers before laccase immobilization mainly C—H, C–OH and carboxylic groups (COOH) occur. Furthermore, the elemental analysis of PLCL fibers and material after laccase encapsulation gives identical result. The surface of these materials is composed of about 77% of carbon atoms and about 22% of oxygen atoms. In case of the material after enzyme adsorption apart of the above mentioned elements a distinctive though low (about 0.5 at.%) signal of nitrogen was detected. Since immobilization of enzyme takes place on a surface of PLCL fibers only a presence of nitrogen atoms originating from peptide bonds is expected. Its low intensity is justified by a relatively high information depth for organic material and the fact that PLCL molecules dominates in the region of analysis. Therefore the presence of nitrogen is considered as a confirmation of successful immobilization of laccase. In the material after laccase encapsulation the outer material (PLCL fibers) screens the XPS signal from enzyme molecules inside capsules.

The high-resolution XPS N 1s spectrum from material after enzyme adsorption indicates that nitrogen atoms are in chemical environment characteristic for peptide bonds at 400.4 eV [24]. The XPS C 1s spectra of all investigated samples are shown in Fig. 3 The spectrum of PLCL fibers is presented as a grey fill and is virtually identical with a spectrum coming from encapsulated laccase (dotted line). A spectrum originating from adsorbed laccase differs in the region about 289 eV which is characteristic for carboxyl functional groups. The intensity of the peak in these region is lower than that from other samples. It indicates that part of the carboxylic groups from PLCL fibers is involved with the bonding of immobilized enzyme.

3.2. Characterization of products after laccase immobilization

According to the data in Table 1, the amount of encapsulated laccase (340 mg g^{-1}) was approximately 25% higher than the quantity of adsorbed laccase (292 mg g^{-1}). This is directly related to the fact that before encapsulation the laccase was dispersed in the solution used for electrospinning, and thus the total amount of the enzyme was incorporated into the fibers. Meanwhile, during adsorption immobilization, some enzyme losses were observed, resulting in lower laccase loading.

In line with expectations, the Michaelis–Menten constant (K_m) of adsorbed laccase was three times higher (0.143 mM) and K_m of encapsulated laccase was over four times higher (0.215 mM), than that of the free enzyme (0.051 mM), indicating lower substrate affinity to the enzyme after immobilization. Whereas, the maximum reaction rate (V_{max}) of both immobilized laccases was lower than that of the free enzyme. The differences in K_m and V_{max} between the free and immobilized enzymes might be explained by an increase in diffusional limitations and lower accessibility of the enzyme's active sites after immobilization, caused by the spatial barriers of the matrix [25]. The effect of the diffusion limitations on K_m is particularly pronounced for the encapsulated enzyme, as the PLCL surrounds the enzyme molecules and reduces their availability to the substrates. Nevertheless, in our study both immobilized laccases have a V_{max} value up to 75% of that of the free laccase, indicating that they can still be considered efficient catalytic systems for the removal of pharmaceuticals. The retention of such good catalytic properties, particularly in the case of encapsulated laccase, was an unexpected finding. It might be explained by the highly porous structure of the electrospun nanofibers used that partially reduces diffusional limitations, as has been reported previously [26].

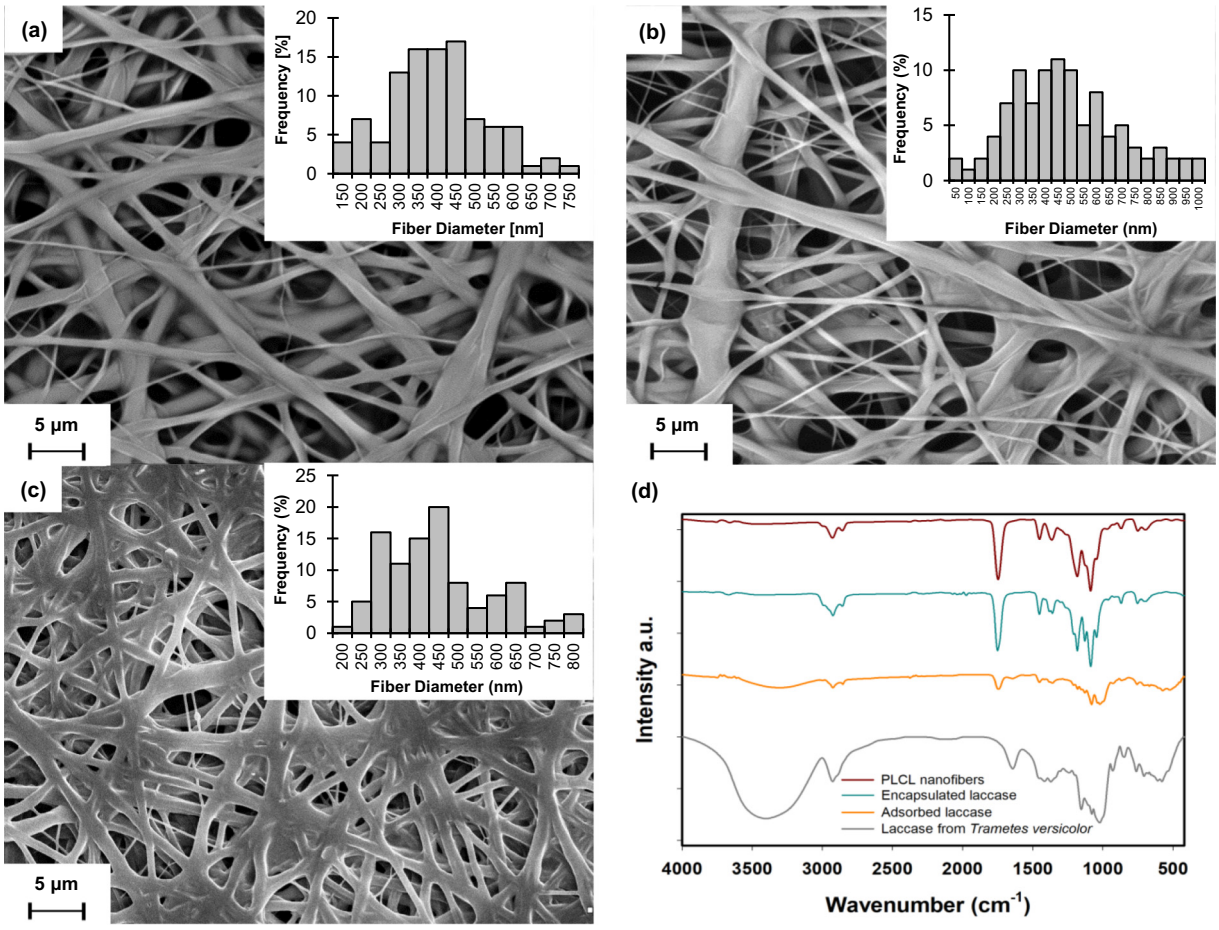

Fig. 2. SEM images of: (a) crude PLCL fibers, (b) PLCL fibers with encapsulated laccase, (c) PLCL with adsorbed laccase and (d) FTIR spectra of PLCL fibers before and after laccase immobilization. Inset, the diameter distribution for each types of fibers before and after laccase immobilization.

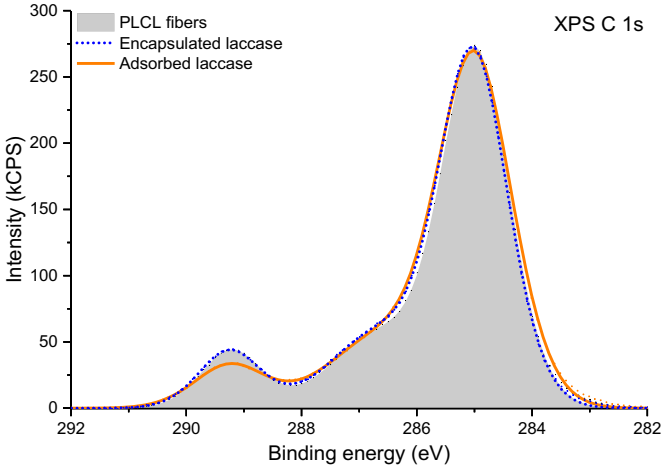

Fig. 3. XPS C 1s spectra of PLCL nanofibers, PLCL nanofibers with encapsulated laccase and PLCL nanofibers with adsorbed laccase.

3.3. Storage stability of free and PLCL-immobilized laccase

Irrespective of the immobilization protocol used, the storage stability of both PLCL-immobilized enzymes was significantly enhanced compared with the free laccase (Fig. 4). Accordingly, encapsulated and adsorbed laccase retained respectively over 90% and around 70% of their initial activity after 30 days of storage at 4 °C. These values correspond to the inactivation constant (k_D) of 0.004 and 0.014 1/day and

Table 1
Laccase loading and kinetic parameters of free and immobilized laccases. Standard deviation do not exceed 5%.

Laccase	Laccase loading (mg g^{-1} fibers)	K_m (mM)	V_{max} (mM/s)
free laccase	–	0.051	0.039
adsorbed laccase	292	0.143	0.033
encapsulated laccase	340	0.215	0.024

enzyme half-life ($t_{1/2}$) of 173.3 and 49.5 days for encapsulated and adsorbed laccase, respectively. By contrast, the free enzyme retained 60% of its initial activity after 10 days, and only around 30% after 30 days. Also noticed k_D and $t_{1/2}$ of free enzyme were significantly lower, as compared to immobilized biocatalysts and reached 0.0397 1/day and 17.5 days, indicating lower stability of the free enzyme. These results might be explained by the protection of the enzyme molecules against conformational changes by the PLCL electrospun supports. Thus, better stabilization of the three-dimensional structure of the enzyme is provided. The higher activity retention in the case of the encapsulated laccase is also related to the formation of a unique core-shell structure after laccase immobilization into PLCL fibers, which protects the enzyme molecules against deactivation caused by harsh reaction conditions [27].

3.4. Biodegradation of pharmaceuticals

It is known that the yield of enzymatic reactions is strongly affected by the process conditions. For practical applications it is important to

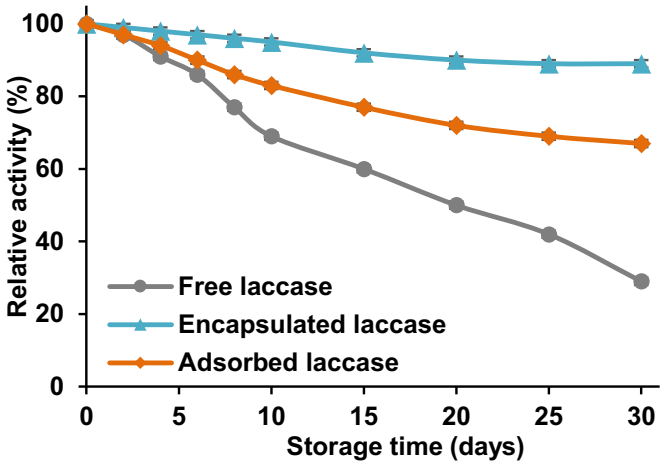

Fig. 4. Storage stability of laccase from *Trametes versicolor*, free, encapsulated into PLCL fibers and adsorbed onto PLCL fibers.

evaluate the effect of the reaction conditions and determine the most suitable parameters for diclofenac and naproxen degradation. For this reason, the degradation experiments were carried out under various pH and temperature conditions. Additionally, in view of the well-developed porous structure of the electrospun fibers, the sorption capacity of the produced materials with deactivated enzyme was evaluated. In the latter case, < 10% of both pharmaceuticals were removed from the solution by adsorption. It was thus concluded that the remediation of anti-inflammatories is related mainly to the catalytic action of the immobilized laccase. Moreover, to evaluate the effect of immobilization on the catalytic properties of the laccase, biodegradation processes were carried out using the free enzyme. Under optimal conditions (pH 5, temperature 25 °C) the removal of naproxen and diclofenac by water-soluble laccase reached about 95%. However, under conditions deviating from the optimum, degradation efficiencies were significantly lower than those noticed for the immobilized laccase, falling below 50% for both pharmaceuticals. Moreover, the reusability of the free biocatalyst is extremely limited.

3.4.1. Effect of pH

As Fig. 5 shows, the highest degradation of diclofenac, around 90%, was observed when encapsulated laccase was used in acidic conditions (pH 3 and 5). Degradation by adsorbed laccase in these conditions was lower, at around 60%. This may be explained by the fact that the adsorbed laccase is more exposed to deactivation by the process conditions, as well as some enzyme leakage occured, resulting in decreased biodegradation efficiency. The optimal pH range of 3 to 5 for diclofenac removal may also be related to its pK_a value (4.15). In this pH range the ratio of undissociated and dissociated molecules of diclofenac are equal; this creates the most suitable environment for the action of laccase [28]. Surprisingly, the highest rate of degradation of naproxen by the immobilized enzyme was observed at pH 3; it reached almost 100% and around 90% for encapsulated and adsorbed laccase respectively. However, even at pH 5, PLCL-laccase systems were able to degrade over 80% of the pollutant. The shift of the optimum pH and significantly higher rates of biodegradation by the adsorbed enzyme, compared with the case of diclofenac, are probably related to the presence of the mediator (ABTS in this study) in the reaction mixture, which slightly altered the microenvironment around the active sites of the enzyme and suppressed the laccase deactivation process [29]. The presence of the mediator is required to achieve satisfactory rates of reaction, as it is known that naproxen is insufficiently oxidized by the laccase and is resistant to enzymatic degradation [20]. The significant drop in the rates of degradation of both anti-inflammatory drugs at pH 7 is related to the formation of hydroxide ions, which can bind to the T2/T3 copper ions in the laccase structure. This causes the internal transfer of electrons from T1 to T2/T3 to be blocked, so that the reduction potential of oxygen is decreased and in consequence the reaction efficiency is reduced [30].

Nevertheless, it should be emphasized that both immobilized laccases exhibited higher removal rates at strongly acidic (pH 3) and even neutral pH, compared with the free enzyme (data not presented), indicating the lower sensitivity of the bound enzymes to changes in pH. This is probably due to the rigidification of the enzyme structure after immobilization and its better protection against conformational changes and chemical deactivation [31].

3.4.2. Effect of temperature

As it can be seen in Fig. 6, degradation of naproxen and diclofenac increased with an increase in temperature, reaching a maximum at 25 °C (92% and 99% respectively for encapsulated laccase, 62% and 87% for adsorbed laccase), and decreasing slightly at 50 °C. On the one hand, the lower degradation rates of both pharmaceuticals observed at 5 °C are related to inhibition of the enzyme and its insufficient activation. On the other hand, the high removal efficiencies observed even at 50 °C indicate that the negative effect of high temperature on the catalytic properties of the immobilized enzyme was strongly reduced. This might be related to the stabilization of the laccase structure after immobilization that prevent against conformational changes, as well as to the protective effect of the PLCL electrospun fibers. High degradation efficiencies at higher temperatures are also related to the better solubility and mobility of the pharmaceuticals at elevated temperatures, as well as reduced diffusional limitations of the substrate molecules [32]. However, it should be noted that the temperature of real effluents

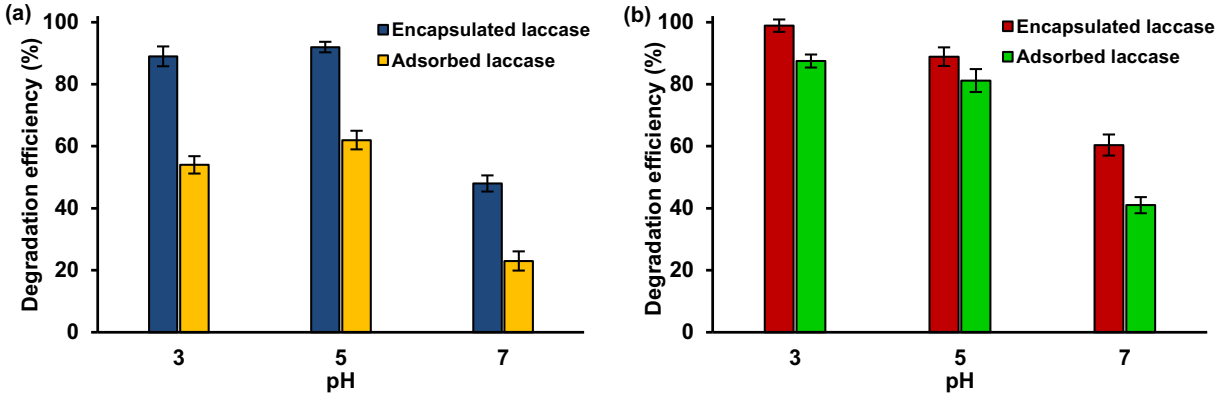

Fig. 5. Effect of solution pH on efficiencies of removal of: (a) diclofenac and (b) naproxen by encapsulated and adsorbed laccase. Degradation conditions: temperature 25 °C, pharmaceutical concentration 1.0 mg L^{-1}.

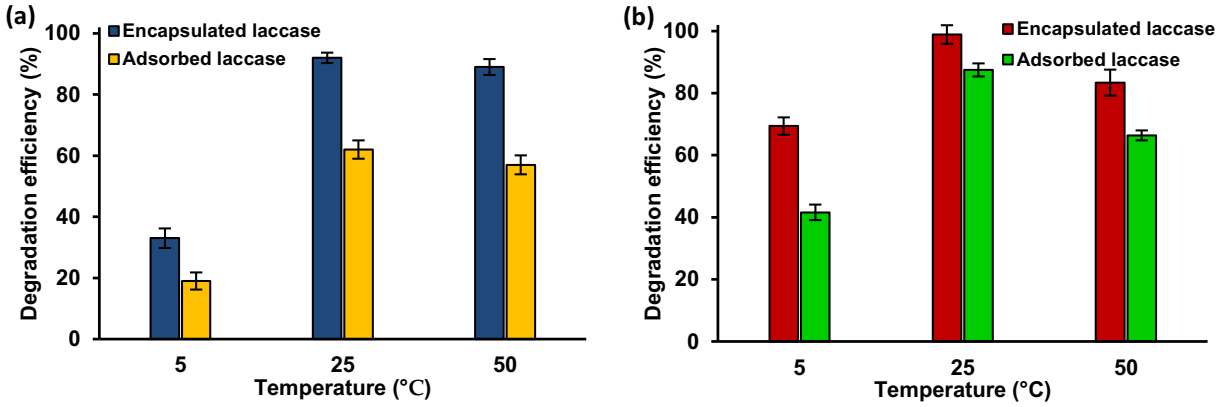

Fig. 6. Effect of process temperature on the efficiency of removal of: (a) diclofenac and (b) naproxen by encapsulated and adsorbed laccase. Degradation conditions: pharmaceutical concentration 1.0 mg L^{-1}, pH 5 and 3 respectively for diclofenac and naproxen.

containing pharmaceuticals is usually in the range 15–35 °C [33]; thus, the high degradation efficiencies observed at 25 and 50 °C indicate that the resistance of the enzyme to thermal deactivation was improved after immobilization and suggesting the possible practical application of the produced biocatalytic systems for wastewater treatment.

3.4.3. Effect of pharmaceutical solutions concentration

After determining the optimal pH and temperature conditions for the remediation processes (temperature 25 °C, pH 5 and 3 for diclofenac and naproxen respectively), we also examined how the concentration of the anti-inflammatory drugs affected the efficiency of their remediation (Fig. 7). Although the concentration of both compounds in municipal and pharmaceutical wastewaters is usually at levels of μg L^{-1} [34] we decided to test higher concentrations to determine whether the produced biocatalytic systems offer good potential for the bioconversion of hazardous pollutants from wastewaters. As expected, the higher is the concentration of the pharmaceutical, the lower is the degradation efficiency. This might be explained by two main factors: (i) insufficient amount of the immobilized enzyme and (ii) inhibition of the laccase active sites by substrates molecules, observed at higher concentrations of pharmaceutical. Similarly as in the previous experiments, in case of both analyzed compounds, encapsulated laccase is characterized by significantly higher biodegradation ability. However, less significant drop of the removal rates was observed during degradation of diclofenac (80% of diclofenac removal from 10 mg L^{-1} solution), compared to naproxen conversion, that is directly related to the presence of the mediator (ABTS) in the reaction mixture, which generates radical species. These radical species enhance biodegradation rate by the increasing of the laccase redox potential and reduce steric hindrances [35].

3.5. Operational stability of the immobilized enzymes

Reusability is the main advantage of immobilized enzymes, and is particularly important for practical applications. Hence, the operational stability of the encapsulated and adsorbed laccase was determined over five successive cycles of diclofenac and naproxen degradation (Fig. 8). The degradation of diclofenac and naproxen by adsorbed laccase followed the same trend, reaching approximately 20% and 40% respectively in the fifth reaction cycle. The sharp drop in the removal efficiency of the adsorbed enzyme is caused by laccase leakage (about 50% of the enzyme). As expected, encapsulated laccase demonstrated significantly higher reusability, enabling the removal of over 60% of diclofenac and 70% of naproxen in the fifth cycle. This is directly related to the effect of the core-shell structure of the PLCL nanofibers, which protects enzyme molecules against conformational changes caused by the external environment. Nevertheless, the activity of both immobilized laccases may also decline due to thermal and chemical denaturation and deactivation and due to partial inhibition of the biomolecules by the biodegradation products, as previously mentioned.

3.6. Products of biodegradation and reaction pathways

During the study, the degradation products of diclofenac and naproxen were identified by analyzing the mixture obtained after the process that resulted in the highest efficiency of degradation.

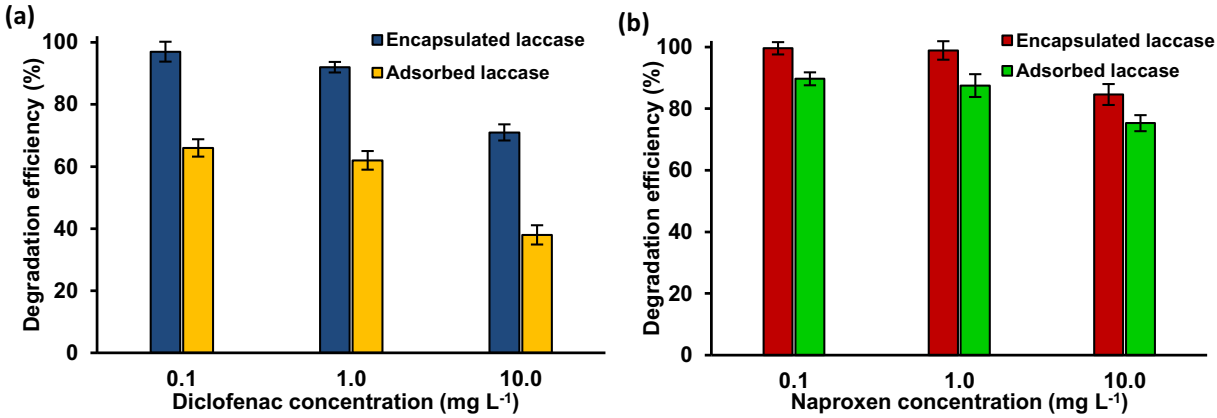

Fig. 7. Effect of initial concentration of: (a) diclofenac and (b) naproxen solution on the efficiency of their removal by encapsulated and adsorbed laccase. Degradation conditions: temperature 25 °C, pH 5 and 3 respectively for diclofenac and naproxen.

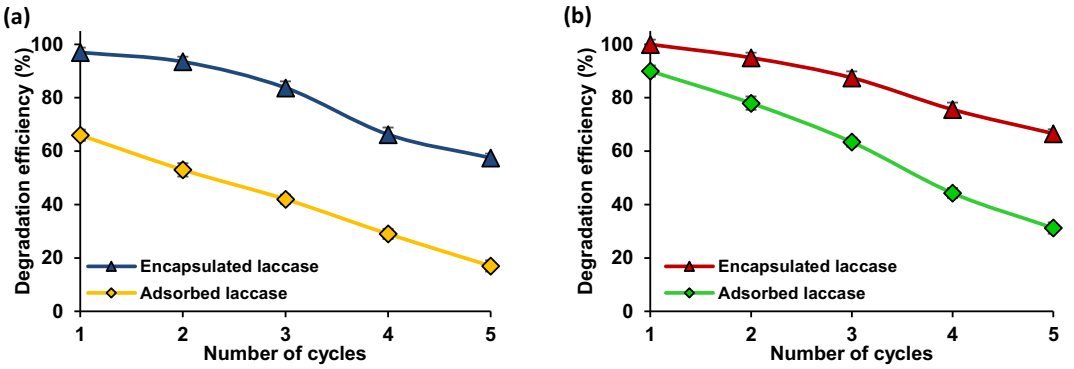

Fig. 8. Reusability of the encapsulated and adsorbed laccase for degradation of: (a) diclofenac and (b) naproxen over five removal cycles. Degradation conditions: temperature 25 °C, pharmaceutical concentration 1.0 mg L^{-1}, pH 5 and 3 respectively for diclofenac and naproxen.

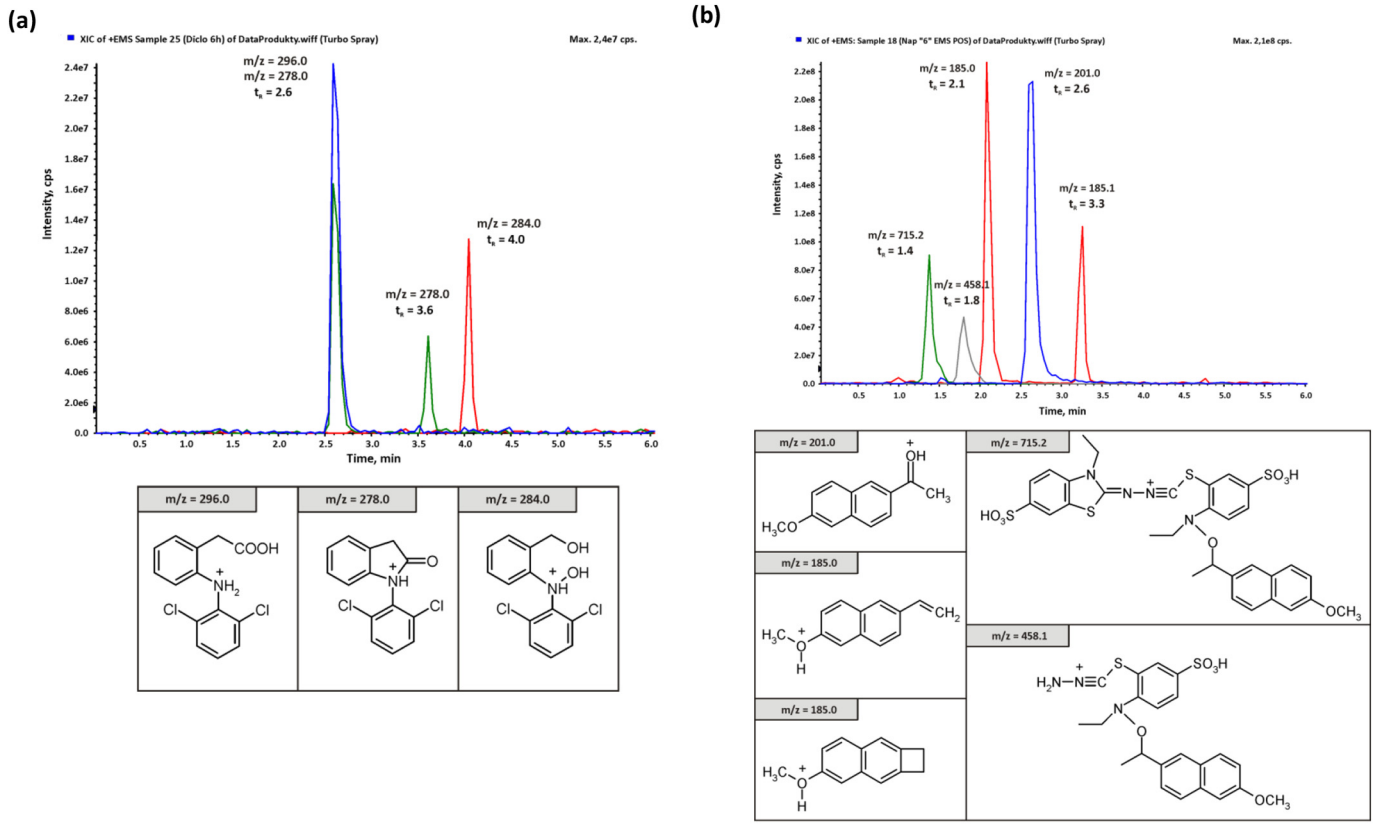

Fig. 9. Extracted ion chromatogram after 6 h of biodegradation by encapsulated laccase of: (a) diclofenac and (b) naproxen. The structures of ions found at retention times (a) 2.6, 3.6 and 4.0 min after diclofenac degradation and (b) 1.4, 1.8, 2.1, 2.6 and 3.3 min after naproxen degradation are given below the chromatogram.

Characteristic ions of diclofenac were found at a retention time of 2.6 min, namely the pseudomolecular ion (at $m/z = 296$) due to its incomplete conversion, and its daughter ions formed after elimination of the water molecule (at $m/z = 278$), the carbon monoxide molecule (at $m/z = 250$) and the chlorine radical (at $m/z = 215$). Two degradation products were identified at retention times of 3.6 and 4.0 min (Fig. 9a). The first was formed after elimination of the water molecule from diclofenac, and the pseudomolecular ion of this compound (found at $m/z = 278$) has the same structure as the first fragmentation ion of diclofenac. Further fragmentation ions were not found due to the low concentration of this degradation product and the rapid formation of the second bioconversion product, whose structure was confirmed by the presence of the pseudomolecular ion (at $m/z = 284$) and two abundant daughter ions formed after elimination of the hydrogen peroxide molecule (at $m/z = 250$) and the chlorine radical (at $m/z = 215$). Surprisingly, results show that hydroxy- and dihydroxydiclofenac (products of enzymatic conversion of diclofenac) were not detected, indicating the transformation of diclofenac into non-detected metabolites, as presented also earlier [8,36].

In the second test, apart from the naproxen peak at retention time 2.2 min, a number of other compounds were found and identified (Fig. 9b). The degradation process of naproxen led to the elimination of the formic acid molecule from the carboxylic group of naproxen. As a result three different degradation products were found: two formed immediately and one after oxidation of the carbon atom adjacent to the aromatic ring. For the first two compounds detected at retention times 2.1 and 3.3 min, only the pseudomolecular ion at $m/z = 185$ was found, due to their relatively stable nature under soft electrospray ionization. The first of these compounds had a similar retention time to naproxen and the same m/z value as the daughter ion of naproxen. It was

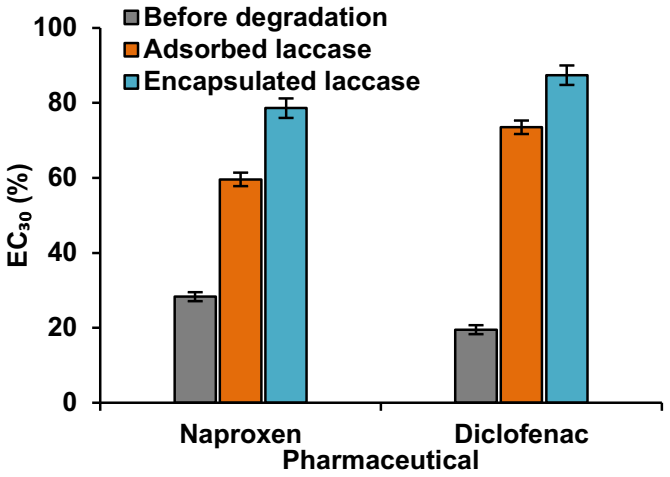

Fig. 10. Toxicity study of untreated solutions of naproxen and diclofenac and solutions treated with immobilized laccase, using the *A. salina* test. $EC_{30} \geq 100\%$ = nontoxic.

identified as a degradation product because during the test the pseudomolecular ion of naproxen (at $m/z = 231$) completely disappeared. The initially determined ratio of the ions at $m/z = 231$ to those at $m/z = 185$, equal to 3:4, is characteristic of naproxen in the given LC-MS system and the conditions of the analytical method. The disappearance of the first peak with simultaneous increase in the second is evidence of the formation of a new product found at a similar retention time. Unfortunately, due to lack of further fragmentation, the compounds eluted at retention times 2.1 and 3.3 min could not be distinguished from each other and assigned reliably to peaks. The third degradation product was found at retention time 2.6 min. The pseudomolecular ion of this compound found at $m/z = 201$ was decomposed by the loss of the ketene molecule, leading to an ion at $m/z = 159$. Thus, 1-(6-metoxynaphtalen-2-yl)ethanone was determined to be the main degradation product formed in the presence of laccase in our study. Moreover, as the test with naproxen was performed with the ABTS mediator, this compound was also present in the chromatogram. More interestingly, there were two ions found which may be attributed to conjugation products of the naproxen molecule with the ABTS molecule and a large part of that molecule. These two ions were found at retention times 1.4 min (at $m/z = 715$) and 1.8 min (at $m/z = 458$) respectively. These conjugation products of naproxen and ABTS mediator have not previously been reported in literature. In the course of the degradation, only the first can potentially be transformed back to ABTS. The formation of the second results in an inevitable loss of ABTS and a potentially lower rate of degradation of naproxen due to the lower concentration of the mediator.

3.7. Toxicity study

One of the most important objectives in research related to the removal of pollutants is to reduce the toxicity of the effluent after treatment. Thus, ecotoxicity studies against *A. salina* were carried out, to evaluate changes in the toxicity of the untreated and enzymatically treated solutions of both pharmaceuticals. For this purpose, mixtures produced after 24 h of biodegradation under optimal process conditions, were examined. The results are presented in terms of EC_{30} (%), the concentration of the pollutant at which 30% of the microorganisms showed a positive response after the exposure time (Fig. 10).

The untreated diclofenac and naproxen solutions have EC_{30} values of around 25% and 20%, indicating the high toxicity of both pharmaceutical solutions. After enzymatic treatment by obtained biocatalytic systems, the toxicity was substantially reduced, with EC_{30} ranging from 60% to around 85%. However, the use of encapsulated laccase led to higher EC_{30} values (79.6% and 84.7% for diclofenac and naproxen respectively) than in the case of the adsorbed enzyme. This suggests the lower toxicity of the effluent, and is consistent with the results obtained for biodegradation efficiency, which showed the removal rate to be higher when the encapsulated biocatalyst was used. The decrease in the toxicity of the tested solutions may be explained by the elimination of both anti-inflammatories from the mixture by way of enzymatic conversion [37]. It has been shown that both native laccase and laccase-containing fungal strains may be used for the removal of hazardous pharmaceuticals from wastewaters; however, monitoring of the toxicity of the effluents is key to determining the practical application of the evaluated methods, as intermediates and/or final products might be even more toxic than the initial compounds [38]. Nevertheless, the higher values of EC_{30} obtained suggest that the products of biodegradation are in fact less toxic than the initial solutions of the tested pharmaceuticals. Thus, our findings show that the use of laccase immobilized on electrospun PLCL nanofibers is a very promising choice for the effective biodegradation and detoxification of naproxen and diclofenac from water solutions, and may lead to practical applications.

4. Conclusions

The main obstacles to the widespread implementation of laccase-based systems for biodegradation of hazardous pollutants, including various pharmaceutical compounds, are the cost of the enzyme and its poor reusability. Thus, in the present study, we have demonstrated a proof-of-concept for the use of PLCL electrospun fibers as a support material for the adsorption and encapsulation of laccase, an enzyme of enormous environmental potential, and an application of the obtained biocatalytic systems in the removal of naproxen and diclofenac from water solutions. After 24 h of the process, encapsulated laccase biodegraded over 90% of naproxen and diclofenac under optimal process conditions, namely a temperature of 25 °C and pH of 5 and 3 respectively, from a solution at an environmentally relevant concentration (1 mg L^{-1}). The efficiency of removal of both compounds by the adsorbed enzyme was lower, mainly due to deactivation of the enzyme and its elution from the support. The obtained biocatalytic systems exhibited excellent operational stability: even after five consecutive degradation cycles the encapsulated laccase removed over 60% of the pollutants, which is of particular interest for practical applications. Furthermore, the storage stability of the immobilized laccase was significantly better than that of the free enzyme. Finally, we identified products of the enzymatic conversion of both anti-inflammatories, and showed them to be substantially less toxic than the parent compound. It should be added that the metabolites formed might be easily removed from water solutions using simple physical processes, such as precipitation. In summary, the presented results illustrate the excellent potential of PLCL-immobilized laccase for the removal of pharmaceuticals from aqueous solutions, and indicate the possibility of its practical application in real wastewater treatment on an industrial scale. However, further studies in this area are still needed.

Declaration of Competing Interest

None.

Acknowledgements

This research was funded by Ministry of Science and Higher Education (Poland) as financial subsidy to PUT under the grant no. 03/32/BSAD/0906.

References

[1] J.B. Costa, M.J. Lima, M.J. Sampaio, M.C. Neves, J.L. Faria, S. Morales-Torres, A.P.M. Tavares, C.G. Silva, Enhanced biocatalytic sustainability of laccase by

immobilization on functionalized carbon nanotubes/polysulfone membranes, Chem. Eng. J. 355 (2019) 974–985, https://doi.org/10.1016/j.cej.2018.08.178.
[2] L. Lloret, G. Eibes, T.A. Lú-Chau, M.T. Moreira, G. Feijoo, J.M. Lema, Laccase-catalyzed degradation of anti-inflammatories and estrogens, Biochem. Eng. J. 51 (2010) 124–131, https://doi.org/10.1016/j.bej.2010.06.005.
[3] N. Vieno, M. Sillanpää, Fate of diclofenac in municipal wastewater treatment plant - a review, Environ. Int. 69 (2014) 28–39, https://doi.org/10.1016/j.envint.2014.03.021.
[4] E. Marco-Urrea, M. Pérez-Tujillo, P. Blánqez, T. Vicent, G. Caminal, Biodegradation of the analgesic naproxen by *Tramates versicolor* and identification of intermediates using HPLC-DAD-MS and NMR, Bioresour. Technol. 101 (2010) 2159–2166, https://doi.org/10.1016/j.biortech.2009.11.019.
[5] L. Lonappan, Y. Liu, T. Rouissi, F. Pourcel, S.K. Brar, M. Verma, R.Y. Surampallic, Covalent immobilization of laccase on citric acid functionalized micro-biochars derived from different feedstock and removal of diclofenac, Chem. Eng. J. 351 (2018) 985–994, https://doi.org/10.1016/j.cej.2018.06.157.
[6] J. Zdarta, A.S. Meyer, T. Jesionowski, M. Pinelo, Developments in support materials for immobilization of oxidoreductases: a comprehensive review, Adv. Colloid Interf. Sci. 258 (2018) 1–20, https://doi.org/10.1016/j.cis.2018.07.004.
[7] G. Wu, X. Liu, P. Zhou, L. Wang, M. Hegazy, X. Huang, Y. Huang, A facile approach for the reduction of 4-nitrophenol and degradation of congo red using gold nanoparticles or laccase decorated hybrid inorganic nanoparticles/polymer-biomacromolecules vesicles, Mat. Sci. Eng. C. 94 (2019) 524–533, https://doi.org/10.1016/j.msec.2018.09.061.
[8] L. Lonappan, T. Rouissi, M.A. Laadila, S.K. Brar, L.H. Galan, M. Verma, R.Y. Surampalli, Agro-industrial-produced laccase for degradation of diclofenac and identification of transformation products, ACS Sustain. Chem. Eng. 5 (2017) 5772–5781, https://doi.org/10.1021/acssuschemeng.7b00390.
[9] Y.D. Aracagök, H. Göker, N. Cihangir, Biodegradation of diclofenac with fungal strains, Arch. Environ. Prot. 44 (2018) 55–62, https://doi.org/10.24425/118181.
[10] T. Jesionowski, J. Zdarta, B. Krajewska, Enzyme immobilization by adsorption: a review, Adsorption 20 (2014) 801–821, https://doi.org/10.1007/s10450-014-9623-y.
[11] R. Xu, C. Chi, F. Li, B. Zhang, Laccase-polyacrylonitrile nanofibrous membrane: highly immobilized, stable, reusable, and efficacious for 2,4,6-trichlorophenol removal, ACS Appl. Mater. Interface 5 (2013) 12554–12560, https://doi.org/10.1021/am403849q.
[12] J. Zdarta, K. Antecka, R. Frankowski, A. Zgoła-Grześkowiak, H. Ehrlich, T. Jesionowski, The effect of operational parameters on the biodegradation of bisphenols by *Trametes versicolor* laccase immobilized on *Hippospongia communis* spongin scaffolds, Sci. Total Environ. 615 (2018) 784–795, https://doi.org/10.1016/j.scitotenv.2017.09.213.
[13] L. Lonappan, Y. Liu, T. Rouissi, S.K. Brar, M. Verma, R.Y. Surampalli, Adsorptive immobilization of agro-industrially produced crude laccase on various micro-biochars and degradation of diclofenac, Sci. Total Environ. 640-641 (2018) 1251–1258, https://doi.org/10.1016/j.scitotenv.2018.06.005.
[14] E. Kijeńska, W. Święszkowski, General requirements of electrospun materials for tissue engineering: setups and strategy for successful electrospinning in laboratory and industry, in: T. Uvar, E. Kny (Eds.), Electrospun Materials for Tissue Engineering and Biomedical Applications: Research Design and Commercialization, Elsevier, Cambridge, 2017, pp. 43–56.
[15] E. Kijeńska, M.P. Prabhakaran, W. Święszkowski, K.J. Kurzydłowski, S. Ramakrishna, Electrospun bio-composite P(LLA-CL)/collagen I/collagen III scaffolds for nerve tissue engineering, J. Biomed. Mater. Res. Part B: Appl. Biomater. 100 (2012) 1093–1102, https://doi.org/10.1002/jbm.b.32676.
[16] M.F. Canbolat, H.B. Savas, F. Gultekin, Enzymatic behavior of laccase following interaction with γ-CD and immobilization into PCL nanofibers, Anal. Biochem. 528 (2017) 13–18, https://doi.org/10.1016/j.ab.2017.04.005.
[17] S.E. Rodríguez-de Luna, I.E. Moreno-Cortez, M.A. Garza-Navarro, R. Lucio-Porto, L. López Pavón, V.A. González-González, Thermal stability of the immobilization process of horseradish peroxidase in electrospun polymeric nanofibers, J. Appl. Polym. Sci.. 134 (2017) article number 44811. doi:10.1002/app.44811.
[18] Y. Aykut, T. Sevgi, E. Demirkan, Cellulose monoacetate/polycaprolactone and cellulose monoacetate/polycaprolactam blended nanofibers for protease immobilization, J. Appl. Polym. Sci. 134 (2017) 45479, , https://doi.org/10.1002/app.45479.
[19] Z. Temoçin, M. Inal, M. Gökgöz, M. Yiğitoğlu, Immobilization of horseradish peroxidase on electrospun poly(vinyl alcohol)–polyacrylamide blend nanofiber membrane and its use in the conversion of phenol, Polym. Bull. 75 (2018) 1843–1865, https://doi.org/10.1007/s00289-017-2129-5.
[20] L.N. Nguyen, F.I. Hai, J.A. McDonald, S.J. Khan, W.E. Price, L.D. Nghiem, Continuous transformation of chiral pharmaceuticals in enzymatic membrane bioreactors for advanced wastewater treatment, Water Sci. Technol. 76 (2017) 1816–1826, https://doi.org/10.2166/wst.2017.331.
[21] M.M. Bradford, A rapid and sensitive method for the quantitation of microgram quantities of protein utilizing the principle of protein-dye binding, Anal. Biochem. 72 (1976) 248–254, https://doi.org/10.1016/0003-2697(76)90527-3.
[22] M. Bilal, H.M.N. Iqbal, H. Hu, W. Wang, X. Zhang, Enhanced bio-catalytic performance and dye degradation potential of chitosan-encapsulated horseradish peroxidase in a packed bed reactor system, Sci. Total Environ. 575 (2017) 1352–1360, https://doi.org/10.1016/j.scitotenv.2016.09.215.
[23] E. Fatarella, D. Spinelli, M. Ruzzantea, R. Pogni, Nylon 6 film and nanofiber carriers: preparation and laccase immobilization performance, J. Mol. Catal. B Enzym. 102 (2014) 41–47, https://doi.org/10.1016/j.molcatb.2014.01.012.
[24] J. Zdarta, M. Wysokowski, M. Norman, A. Kołodziejczak-Radzimska, D. Moszyński, H. Maciejewski, H. Ehrlich, T. Jesionowski, *Candida antarctica* lipase B immobilized onto chitin conjugated with poss® compounds: useful tool for rapeseed oil conversion, Int. J. Mol. Sci. 17 (2016) 1581–1597, https://doi.org/10.3390/ijms17091581.
[25] Q. Feng, X. Xia, A. Wei, X. Wang, Q. Wei, D. Huo, A. Wei, Preparation of Cu(II)-chelated poly(vinyl alcohol) nanofibrous membranes for catalase immobilization, J. Appl. Polym. Sci. 120 (2011) 3291–3296, https://doi.org/10.1002/app.33493.
[26] A. Greiner, J.H. Wendorff, Electrospinning: a fascinating method for the preparation of ultrathin fibers, Angew. Chem. Int. Ed. 46 (2017) 5670–5703, https://doi.org/10.1002/anie.200604646.
[27] Y. Dai, L. Yin, J. Niu, Laccase-carrying electrospun fibrous membranes for adsorption and degradation of PAHs in shoal soils, Environ. Sci. Technol. 45 (2011) 10611–10618, https://doi.org/10.1021/es203286e.
[28] J. Margot, J. Maillard, L. Rossi, D.A. Barry, C. Holliger, Influence of treatment conditions on the oxidation of micropollutants by *Trametes versicolor* laccase, New Biotechnol. 30 (2013) 803–813, https://doi.org/10.1016/j.nbt.2013.06.004.
[29] B.S. Wolfenden, R.L. Willson, Radical-cations as reference chromogens in kinetic studies of Ono-electron transfer reactions: pulse radiolysis studies of 2,2′azinobis-(3-ethylbenzthiazoline-6-sulphonate), J. Chem. Soc. Perkin Trans. 2 (1982) 805–812, https://doi.org/10.1039/P29820000805.
[30] P.J. Strong, H. Claus, Laccase: a review of its past and its future in bioremediation, Crit. Rev. Environ. Sci. Technol. 41 (2011) 373–434, https://doi.org/10.1080/10643380902945706.
[31] L.N. Nguyen, F.I. Hai, A. Dosseto, C. Richardson, W.E. Price, L.D. Nghiem, Continuous adsorption and biotransformation of micropollutants by granular activated carbon-bound laccase in a packed-bed enzyme reactor, Bioresour. Technol. 210 (2016) 108–116, https://doi.org/10.1016/j.biortech.2016.01.014.
[32] S. Georgieva, T. Godjevargova, D.G. Mita, N. Diano, C. Menale, C. Nicolucci, C.R. Carratelli, L. Mita, E. Golovinsky, Non-isothermal bioremediation of water polluted by phenol and some of its derivatives by laccase covalently immobilized on polypropylene membranes, J. Mol. Catal. B Enzym. 66 (2010) 210–218, https://doi.org/10.1016/j.molcatb.2010.05.011.
[33] K. Hilden, T.K. Hakala, P. Maijala, T.K. Lundell, A. Hatakka, Novel thermotolerant laccases produced by the white-rot fungus *Physisporinus rivulosus*, Appl. Microbiol. Biotechnol. 77 (2007) 301–309, https://doi.org/10.1007/s00253-007-1155-x.
[34] L. Lonappan, S.K. Brar, R.K. Das, M. Verma, R.Y. Surampalli, Diclofenac and its transformation products: environmental occurrence and toxicity - a review, Environ. Int. 96 (2016) 127–138, https://doi.org/10.1016/j.envint.2016.09.014.
[35] L.N. Nguyen, F.I. Hai, W.E. Price, F.D. Leusch, F. Roddick, H.H. Ngo, W. Guo, S.F. Magram, L.D. Nghiem, The effects of mediator and granular activated carbon addition on degradation of trace organic contaminants by an enzymatic membrane reactor, Bioresour. Technol. 167 (2014) 169–177, https://doi.org/10.1016/j.biortech.2014.05.125.
[36] E. Marco-Urrea, M. Pérez-Tujillo, C. Cruz-Morató, G. Caminal, T. Vicent, Degradation of the drug sodium diclofenac by *Tramates versicolor* pellets and identification of some intermediates by NMR, J. Hazard. Mat. 176 (2010) 836–842, https://doi.org/10.1016/j.jhazmat.2009.11.112.
[37] M. Bilal, H.M.N. Iqbal, S.Z.H. Shah, H. Hu, W. Wang, X. Zhang, Horseradish peroxidase-assisted approach to decolorize and detoxify dye pollutants in a packed bed bioreactor, J. Environ. Manag. 183 (2016) 836–842, https://doi.org/10.1016/j.jenvman.2016.09.040.
[38] C. Cruz-Morató, D. Lucas, M. Llorca, S. Rodriguez-Mozaz, M. Gorga, M. Petrovic, D. Barceló, T. Vincet, M. Sarrà, E. Marco-Urrea, Hospital wastewater treatment by fungal bioreactor: removal efficiency for pharmaceuticals and endocrine disruptor compounds, Sci. Total Environ. 493 (2014) 365–376, https://doi.org/10.1016/j.scitotenv.2014.05.117.

International Journal of Biological Macromolecules 165 (2020) 2049–2059

Contents lists available at ScienceDirect

International Journal of Biological Macromolecules

journal homepage: http://www.elsevier.com/locate/ijbiomac

The response surface methodology for optimization of tyrosinase immobilization onto electrospun polycaprolactone–chitosan fibers for use in bisphenol A removal

Jakub Zdarta [a,*], Maciej Staszak [a], Katarzyna Jankowska [a], Karolina Kaźmierczak [a], Oliwia Degórska [a], Luong N. Nguyen [b], Ewa Kijeńska-Gawrońska [c,d], Manuel Pinelo [e], Teofil Jesionowski [a]

[a] Institute of Chemical Technology and Engineering, Faculty of Chemical Technology, Poznan University of Technology, Berdychowo 4, PL-60965 Poznan, Poland
[b] Centre for Technology in Water and Wastewater, University of Technology Sydney, Ultimo 2007, New South Wales, Australia
[c] Centre for Advanced Materials and Technologies CEZAMAT, Warsaw University of Technology, Poleczki 19, PL-02822 Warsaw, Poland
[d] Faculty of Materials Science and Engineering, Warsaw University of Technology, Woloska 141, PL-02507 Warsaw, Poland
[e] Department of Chemical and Biochemical Engineering, Technical University of Denmark, Soltofts Plads, Building 227, DK-2800 Kongens Lyngby, Denmark

ARTICLE INFO

Article history:
Received 5 May 2020
Received in revised form 3 September 2020
Accepted 12 October 2020
Available online 18 October 2020

Keywords:
Enzyme immobilization
Biocatalysts, Immobilization optimization
Bisphenol A removal

ABSTRACT

Composite polycaprolactone–chitosan material was produced by an electrospinning method and used as a support for immobilization of tyrosinase by mixed ionic interactions and hydrogen bonds formation. The morphology of the fibers and enzyme deposition were confirmed by SEM images. Further, multivariate polynomial regression was used to model the experimental data and to determine optimal conditions for immobilization process, which were found to be pH 7, temperature 25 °C and 16 h process duration. Under these conditions, novel type of biocatalytic system was produced with immobilization yield of 93% and expressed activity of 95%. Furthermore, as prepared system was applied in batch experiments related to biodegradation of bisphenol A under various remediation conditions. It was found that over 80% of the pollutant was removed after 120 min of the process, in the temperature range 15–45 °C and pH 6–9, using solutions at concentration up to 3 mg/L. Experimental data collected proved that the stability and reusability of the tyrosinase were significantly improved upon immobilization: the immobilized biomolecule retained around 90% of its initial activity after 30 days of storage, and was still capable to remove over 80% of bisphenol A even after 10 repeated uses. By contrast, free enzyme was able to remove over 80% of bisphenol A at pH 7–8 and temperature range 15–35 °C, and retained less than 60% of its initial activity after 30 days of storage.

1. Introduction

The widespread use of bisphenols in industry, and their adverse impact on living organisms, including mutagenic and cancerogenic effects, make it essential to monitor their circulation in the environment [1–4]. Many studies are focused on searching for efficient and environmentally friendly methods of degradation of phenolic compounds and their derivatives [5,6]. One of such approaches concerns biodegradation of toxic pollutants using enzymes: natural biocatalysts having the ability to oxidize phenols, dyes, pharmaceuticals and estrogens [7,8]. The most widely used enzymes in biodegradation are oxidoreductases, including peroxidases such as horseradish, lignin or chloroperoxidase, and polyphenol oxidases such as laccase and tyrosinase [9–11].

Recently published scientific reports suggest that tyrosinase is capable for efficient degradation of phenols and bisphenols by catalytic conversion into corresponding quinones, which tend to form oligomeric and polymeric compounds that can be easily separated from solution by precipitation [12,13]. Mechanism of such catalytic performance consists of hydroxylation and subsequent oxidation reaction of phenols into ortho-quinones with simultaneous reduction of oxygen, as a co-substrate, to water. The mushroom *Agaricus bisporus* tyrosinase, which was reported to be a glycosylated, tetrameric protein with a molecular mass of around 120 kDa, composed of two heavy subunits of~43 kDa (H subunit) and two lights subunits of ~14 kDa (L subunit), is mostly used [14,15]. This tyrosinase possesses isoelectric point at pH 4.7–5, whereas shows its maximum activity at pH around 7 and at mild temperature of around 25 °C [16]. In general, tyrosinase consists of three various domains, among which, the central domain, responsible for catalytic action contains two Cu binding sites, called CuA and CuB, which interact both with molecular oxygen and phenolic substrate. Moreover, the mushroom tyrosinase has 11 cysteine residues at N-terminal domain and 1 cysteine residue at C-terminal domain that stabilize protein structure by internal disulfide linkages [17].

* Corresponding author.
E-mail address: jakub.zdarta@put.poznan.pl (J. Zdarta).

https://doi.org/10.1016/j.ijbiomac.2020.10.081
0141-8130/

Application of free enzymes, due to their low activity, poor stability and lack of reusability is limited. In order to improve it, immobilization process might be used, after which the protein is bound to a solid support [18,19]. The immobilization of biomolecules provides some operational stability, higher resistance against adverse effects of the reaction conditions, as well as facilitates reuse of the enzymes [20]. In this context, a controlled immobilization, particularly using porous supports, has a positive effect on the enzyme maintenance and performance, reduces diffusional limitations and partitions as well as enzyme aggregation and its inhibition and prevents against internal conformational changes in its structure [21,22]. Furthermore, immobilization results in significant enzyme stabilization, especially when enzyme is multipointly immobilized [23], as well as when favorable environment for the enzyme is generated upon immobilization [24]. A properly performed immobilization also leads to enhancement of enzyme catalytic activity under harsh process conditions and its selectivity and/or specificity [22]. Finally, examples of enzyme purification by immobilization have been also reported [25,26].

Among others immobilization strategies, adsorption approach based on formation of ionic, hydrogen or mixed interactions, is the most commonly used. This is mainly due to the simplicity of the immobilization procedure, its low-cost and usually observed retention of high catalytic activity by the immobilized biomolecules [27,28]. Adsorption immobilization is characterized by low-force interaction, however, physical adsorption of biomacromolecules is a multipoint process having advantages and disadvantages [29,30]. On the one hand, the structure of the enzyme is insensibly altered and there is a possibility to reuse the support [22]. On the other hand, weak interactions lead to elution of the enzyme from the support, and thus fast decrease of catalytic properties and limited reusability might be observed [31]. It should be highlighted, that such enzymes as oxidoreductases have been immobilized via adsorption and other techniques in order to improve their properties in environmental applications. For instance, lignin peroxidase immobilized onto chitosan was able to degrade over 95% of textile dyes, and laccase immobilized onto nanoporous silica beads was capable for removal of over 90% of 2,4-dinitrophenol [32,33]. In another study, tyrosine immobilized onto silica alginate was reported as very efficient in removal of bisphenol A with an efficiency up to 100% [34].

It is important to note, however, that successful immobilization is highly dependent on a proper selection of a suitable support, as well as determination of optimal process conditions, which affect the final parameters of the immobilized enzymes [35,36]. The numerous research, concerning enzymes immobilization and supports selection, was presented in the literature in the past decade. In recent years, electrospun supports have raised particular interest, due to the possibility to prepare tailor-made, highly porous materials that exhibit affinity towards enzymes [37]. However, bearing in mind the specificity of enzymes and the nature of the process, it is extremely important to select the most favorable conditions for the immobilization of a given protein [38]. Parameters that require analysis include pH and temperature of the immobilization process, which may inactivate the biocatalyst, and the process time and initial enzyme concentration, which may affect the quantity of immobilized enzyme and its activity [39]. In this context, the one-factor-at-a-time (OFAT) method, response surface methodology (RSM) and Box–Behnken design (BBD) are techniques used for modeling of the immobilization process and selection of its optimal conditions [40,41]. However, methods of data matching have also been used to optimize enzyme immobilization [42]. The criteria listed above have a great impact on attainment of the maximum enzyme activity and on the possible applications of the immobilized biocatalysts.

Therefore, to address the issues related to the efficient immobilization of tyrosinase and optimization of this process, in presented study, to the best of our knowledge for the first time, an attempt was made to produce polycaprolactone–chitosan (PCL–chitosan) electrospun materials for tyrosinase immobilization in order to obtain novel type of biocatalytic systems capable for bisphenol A removal. These being the key and novel objectives of the study. The hypothesis that supports this research approach is that biocompatible PCL-chitosan materials facilitate tyrosinase immobilization by adsorption and improve enzyme stability as well its reusability. The produced PCL–chitosan material, beside relatively good mechanical stability, is characterized by the presence of hydroxyl, amine and carbonyl groups onto its surface. These groups are capable for creation of hydrogen bonds and ionic interactions during enzyme immobilization process with functional groups of biomolecule, including mainly amine, hydroxyl and carboxyl moieties (Fig. 1). Moreover, this support material was selected due to its open three-dimensional structure, high volume to mass ratio and relatively low-cost of its production. A thorough analysis of the produced electrospun support was performed and the response surface methodology was applied for modeling of the immobilization process and optimization of its

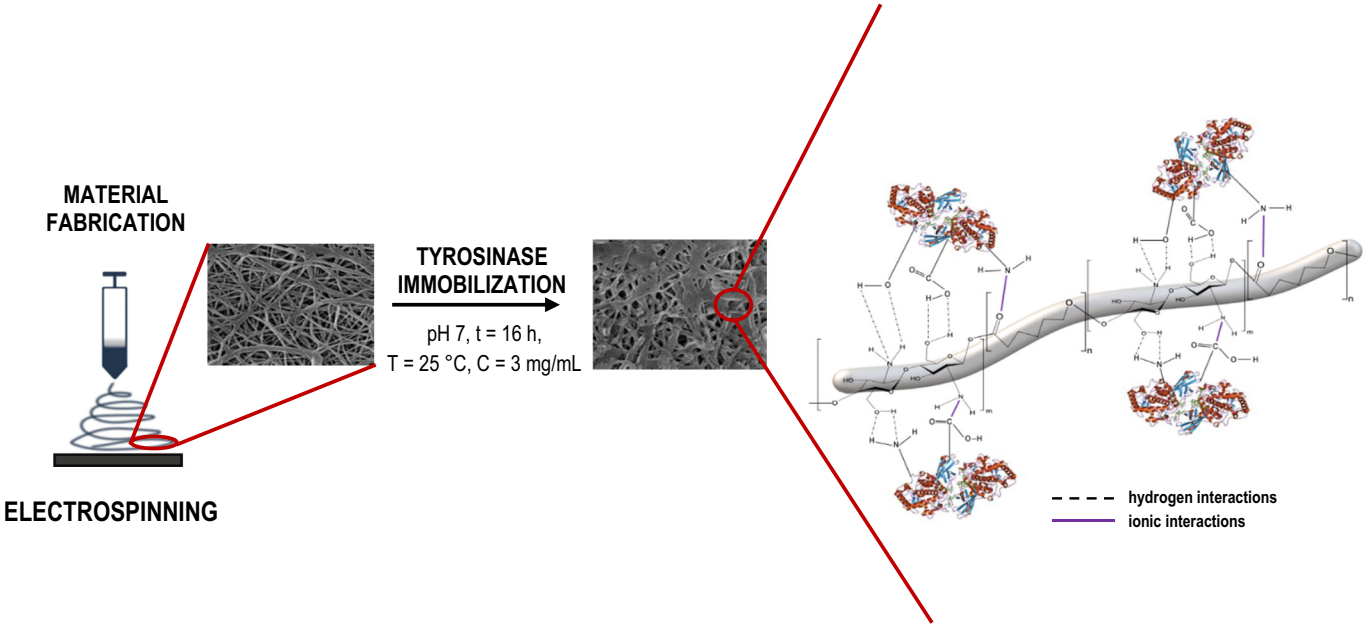

Fig. 1. Scheme presenting fabrication of polycaprolactone–chitosan (PCL–chitosan) electrospun material and immobilization process, with detailed insight into mechanism of performed process.

conditions to obtain a biocatalytic system offering high catalytic activity. The stability and reusability of the immobilized biomolecule were also examined. Finally, the possible practical application of the produced biocatalytic systems was validated in the biodegradation of bisphenol A under various reaction conditions. The research approach concerning immobilization of tyrosinase and its use for removal of bisphenol A is an overlooked research area in recently published articles.

2. Materials and methods

2.1. Materials

Polycaprolactone (PCL) with molecular weight of 80 kDa, chitosan with molecular weight of 1000 kDa, trifluoroacetic acid (TFA), mushroom tyrosinase (polyphenol oxidase, activity ~2000 U/mg solid, EC 1.14.18.1), 100 mM acetate buffer (pH 3–5), 100 mM phosphate buffer (pH 6–8), 100 mM bicarbonate buffer (pH 9, 10), bisphenol A (BPA) (purity ≥99%) and L-catechol, were supplied by Sigma-Aldrich (USA).

2.2. Fabrication of PCL–chitosan materials

PCL–chitosan electrospun fibers were prepared using a NANON-01A device (MECC Co. Ltd., Japan) by mixing two polymers solutions. To prepare chitosan solution, it was dissolved in TFA to obtain 5% (w/v) solution. The obtained mixture was then stirred for 4 h at 75 °C. To obtain second solution, polycaprolactone was dissolved in TFA to obtain 10% (w/v) solution - it was stirred for 4 h at room temperature. Next, both solutions were mixed together to obtain PCL:chitosan ratio of 15:85 (w/w) and further stirred for 1 h. The resulting PCL–chitosan solution was placed in a plastic syringe and electrospun. The applied voltage was set at 20 kV, the distance between nozzle and collector was 150 mm, and the ejection rate was 1 mL/h. The obtained PCL–chitosan fibers were dried in a vacuum drier at 25 °C.

2.3. Tyrosinase immobilization

Immobilization of mushroom tyrosinase was performed by adsorption under various process conditions in order to obtain immobilized enzymes with enhanced catalytic activity. For immobilization, 10 mg of PCL–chitosan material (two pieces 1 cm × 1 cm in size), washed with distilled water, was placed in 10 mL of tyrosinase solution at the desired concentration (from 0.5 to 5.0 mg/mL), prepared in 100 mM buffer solution at an appropriate pH (ranging from 4 to 9). The samples were then placed in a shaker (IKA Werke GmbH, Germany) and agitated at 150 rpm for a specified period of time ranging from 1 h to 24 h, at various temperatures (from 5 °C to 55 °C). After immobilization, samples were separated from the reaction mixture and were washed with 100 mM phosphate buffer (pH 7) to remove unbounded enzyme.

2.4. The effect of process conditions on the activity of immobilized enzyme – modeling study

The mathematical model proposed was formulated using Mathcad software. For the six distinct data sets, with different independent variables, the *polyfit* function was used to generate the response surface. Based on the least squares modelhood, the problem of fitting the surface consisted of searching of such parameters in order to obtain the smallest value of the sum of squared distances between data points and the surface. Calculating the partial derivatives of F is straightforward for the formulation chosen, although a numerical procedure might be required in the case of more complex surface functions. In presented example, symbolic solutions for the optimal parameters A_{opt} and B_{opt} were derived analytically.

2.5. Immobilization yield, enzyme activity and stability

The activity and stability of the free and immobilized enzyme were examined based on a model reaction using L-catechol as a substrate, by measuring the rate of formation of ortho-quinones, according to slightly modified methodology presented by Dincer et al. [43]. Briefly, 50 mg of free enzyme or an appropriate amount of the biocatalytic system produced containing 50 mg of immobilized tyrosinase was added to 10 mL of 20 mM L-catechol solution in 100 mM phosphate buffer (pH 7). The process was carried out for 60 min at 25 °C with a continuous oxygen supply at a flow rate of 1 mL/min. One unit of free and immobilized tyrosinase activity was defined as the amount of enzyme that liberates 1 mM of ortho-quinones per minute under assay conditions. Analyzing the storage and thermal stability, the initial value of enzyme relative activity was defined as 100% activity. Measurements of relative activity were performed at regular time intervals.

The storage stability of free and immobilized tyrosinase was examined by spectrophotometric measurements, over 20 days of storage at 4 °C in 100 mM phosphate buffer at pH 7, based on the above-mentioned model reaction.

The thermochemical stability of free and immobilized enzyme was determined over 120 min of incubation under optimal temperature and pH conditions (25 °C and pH 7), based on the same model reaction using 20 mM L-catechol as a substrate. Spectrophotometric measurements were performed after a specified heating time. Then the relative activity was calculated. In addition, inactivation parameters of the free and immobilized enzyme—the inactivation constant (k_D) and enzyme half-life ($t_{1/2}$)—were calculated based on the linear regression slope of inactivation curves.

The immobilization yield and expressed activity were calculated following Eqs. (1) and (2):

$$\textit{Immobilization yield}\ (\%) = \frac{A_i - A_f}{A_i} \cdot 100\% \tag{1}$$

$$\textit{Activity recovery}\ (\%) = \frac{A_t}{A_i} \cdot 100\% \tag{2}$$

where: A_i denotes the initial activity of tyrosinase added to the immobilization medium, A_f denotes the total activity of the enzyme in the supernatant and washing solution after the immobilization and A_t denotes the activity of the immobilized tyrosinase. The activities of the supernatant and reference samples were determined under standard conditions, based on the above-presented reaction.

The kinetic parameters of free and immobilized tyrosinase—the Michaelis–Menten constant (K_m) and maximum reaction rate (V_{max})—were determined against L-catechol, by measuring the initial reaction rates of L-catechol oxidation under optimal process conditions with a continuous oxygen supply with a flow rate 1 mL/min using various substrate solutions at concentrations ranging from 0.5 to 20 mM. The apparent kinetic parameters of free and immobilized tyrosinase (K_m and V_{max}) were calculated from Hanes–Woolf plot.

2.6. Removal of bisphenol A

Degradation of BPA by free and immobilized tyrosinase was performed using an IKA KS 4000i Control incubator (IKA Werke GmbH, Germany). For the BPA removal experiments, 10 mg of free or an appropriate amount of the biocatalyst produced containing 10 mg of immobilized enzyme was introduced to BPA solution at desired concentration. The samples were shaken under specified process conditions at 150 rpm for 120 min with a continuous oxygen supply at a flow rate of 1 mL/min, and furthermore analyzed at specified time intervals to determine the BPA removal efficiency.

The effect of initial BPA concentration on the removal efficiency was examined using solutions at concentrations of 0.1, 0.5, 1.0, 3.0 and

5 mg/L, pH 7 and 25 °C. The effect of pH on the percentage removal of bisphenol A was examined over a wide pH range of 3–10, using 100 mM buffer solutions to adjust an appropriate pH value. The process was performed at 25 °C using BPA solution in concentration of 3 mg/L. To assess the effect of temperature on the removal of BPA, biodegradation was performed at temperature ranging from 5 °C to 65 °C (with a 10 °C step), using BPA solution in concentration of 3 mg/L and at pH 7.

The reusability of the immobilized tyrosinase was examined over ten repeated cycles of bisphenol A removal. Briefly, each cycle was performed within 120 min at 25 °C, using BPA solution in an initial concentration of 3 mg/L and at pH 7. After each biodegradation step, the immobilized tyrosinase was separated from the reaction mixture, washed several times with 100 mM phosphate buffer (pH 7), and placed in a fresh BPA solution.

2.7. Analytical techniques

The morphology of the fabricated PCL–chitosan electrospun fibers, before and after tyrosinase immobilization, was presented in SEM images (EVO40, Zeiss, Germany). The average diameter of the obtained fibers, before and after enzyme attachment, was calculated using the Image J program (National Institute of Health, USA).

The porous structure parameters of the materials before immobilization were determined using an ASAP 2020 instrument (Micromeritics Instrument Co., USA). The surface area was evaluated according to the multipoint BET (Brunauer–Emmett–Teller) method using low temperature nitrogen (77 K) adsorption under relative pressure (p/p_0). The mean size and total volume of pores were calculated based on the BJH (Barrett–Joyner–Halenda) algorithm.

The Fourier transform infrared spectra (FTIR) of electrospun material, before and after tyrosinase immobilization, were recorded using Vertex 70 spectrometer (Bruker, Germany) working in attenuated total reflectance (ATR) mode. The measurements were conducted in the wavenumber range of 4000 to 400 cm^{-1}, at a resolution of 0.5 cm^{-1} and 64 scans.

The percentage mass contribution of selected elements present in the samples before and after immobilization was analyzed by means of energy dispersive X-ray spectroscopy (EDS) using a Princeton Gamma-Tech unit with a prism digital spectrometer (UK).

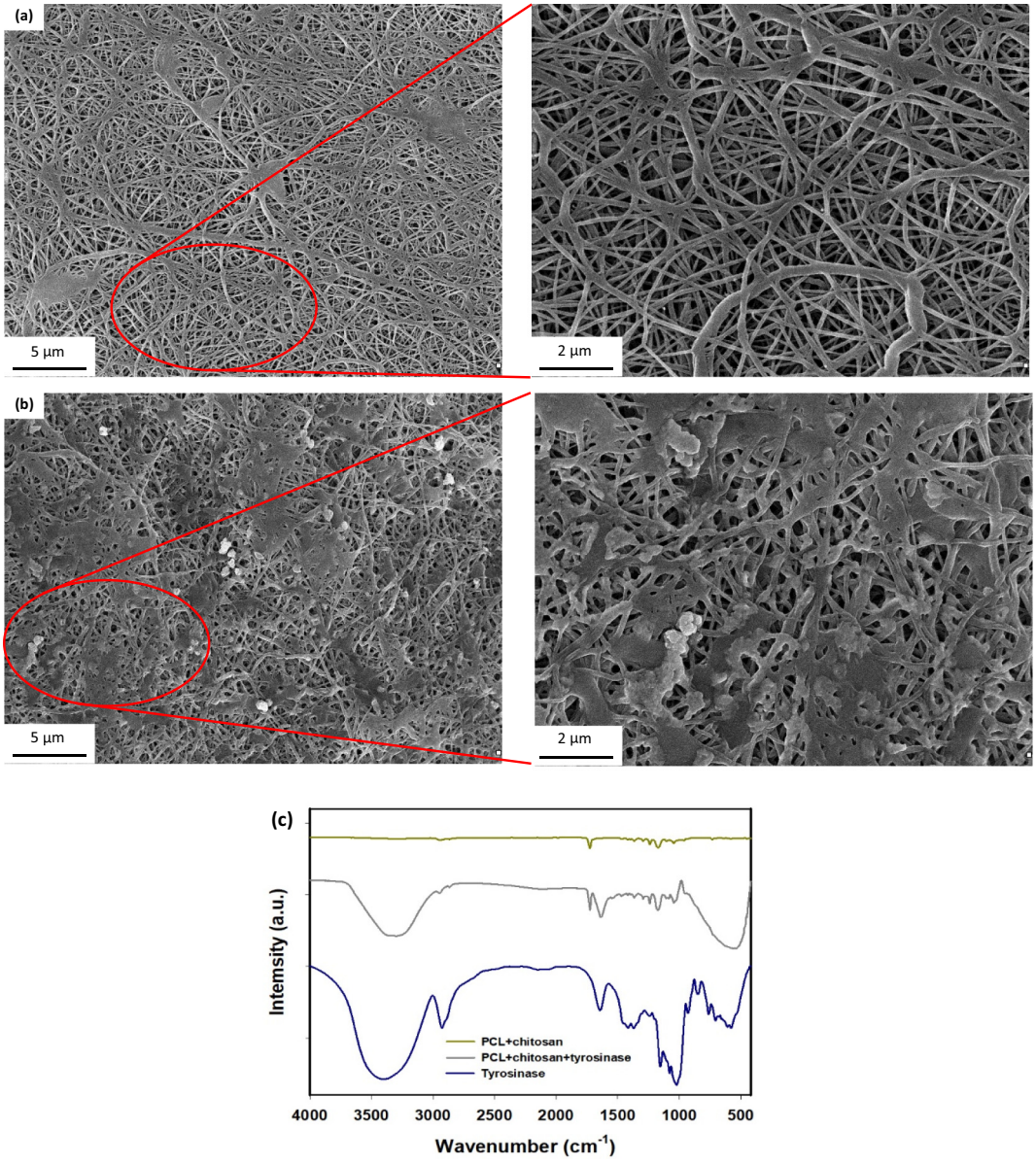

Fig. 2. SEM images of PCL-chitosan electrospun materials before (a) and after (b) enzyme immobilization and (c) FTIR spectra of tyrosinase, PCL-chitosan electrospun material and PCL-chitosan with immobilized enzyme.

The efficiency of bisphenol A removal, as well as the stability and reusability of free and immobilized enzyme, were determined based on spectrophotometric measurements using a Jasco V-750 spectrophotometer (Jasco, Japan), measuring the absorbance during ABTS oxidation at $\lambda = 420$ nm (stability study) and during BPA removal at $\lambda = 480$ nm. The final concentration of ortho-quinones after oxidation process, and the concentration of BPA after biodegradation, were obtained based on a proper calibration curves. The efficiency (%) of bisphenol A removal was calculated by considering the initial and the final concentration of the pollutant in the solution, before and after degradation performed under specified conditions.

2.8. Statistical analysis

All experiments and measurements were performed in triplicate, and error values are presented as means ± standard deviation. Statistically significant differences were determined by one-way ANOVA using Tukey's test, performed in SigmaPlot 12 software (Systat Software Inc., USA). Statistical significance was established at a level of $p < 0.05$.

3. Results and discussion

3.1. Morphological characterization of fibers before and after immobilization

In order to characterize the morphology of the obtained materials and confirm effective enzyme immobilization, in the first stage of the investigation, SEM images were taken for PCL–chitosan electrospun fibers before and after tyrosinase immobilization (Fig. 2). Electrospun fibers, before attachment of tyrosinase (Fig. 2a) are branched, with a smooth surface, and have an average diameter of 344 ± 121 nm. By contrast, after enzyme deposition a significant increase in fiber diameter (average diameter of 689 ± 365 nm) was observed, indicating attachment of the enzyme to the fibers surface. Mushroom tyrosinase is characterized by the molecular weight of around 120 kDa thus, irregular shapes almost uniformly covered surface of the fibers (Fig. 2b). This fact confirms effective enzyme immobilization and suggests formation of enzyme aggregates [44]. This might lead to the partition and diffusional problems upon immobilization that reduce enzyme activity. However, it should be noted that electrospun material has a multidimensional structure with relatively large pores irregular in shape and size, which reduce diffusional resistance and facilitate efficient transport of reaction substrates and products between active centers of the immobilized enzyme and the reaction mixture [45]; this makes such material a suitable support for the immobilization of biomolecules. BET surface area of the produced PCL–chitosan material was found to be 72.3 m^2/g. In addition, the average pore size of the single fiber was 19.64 nm, whereas its volume was 0.874 cm^3/g. Such values indicate porous nature of the produced support, making it suitable for enzyme immobilization. In the FTIR spectrum of PCL–chitosan material (Fig. 2c) the most important is the presence of signals noted at 3420 and 1720 cm^{-1}, assigned to hydroxyl and carbonyl functional groups, capable for enzyme binding. In the spectrum of produced biocatalytic system additional signals can be observed. Among them, those at 1645 and 1080 cm^{-1} are the most important ones and confirm effective enzyme deposition onto electrospun material. Additionally, results of elemental analysis confirm the effective enzyme adsorption, as higher percentage mass contribution of elements such as carbon, nitrogen, oxygen and sulfur, in the samples after immobilization was noticed.

3.2. Modeling the effect of process conditions on the activity of immobilized enzyme

As one the most important objectives of the study was to produce highly active biocatalytic system for removal of bisphenol A, a proper selection of immobilization conditions, including initial concentration of enzyme solution, pH and process duration, is of key importance. Therefore, in presented study, the effect of process conditions on the activity of immobilized tyrosinase was modeled in order to determine the optimal ones.

The response surface methodology was used for this purpose, leading to a model that serves to find the optimum immobilization conditions. Additionally, for specified pH and process time t, the influence of other parameters such as temperature T, initial concentration of enzyme solution C, and their dependencies vs. catalyst activity, were estimated and analyzed. The analysis consisted of selecting an appropriate multidimensional function $F(A, B)$ exhibiting a similar character to the data measured; see Eq. (3). The usual measure of the quality of model fit and data variance is standard deviation. It is important that mathematical model describing the data should not be too complex, to prevent overfitting and consequently to avoid identifying false trends. The model shouldn't also be too simple, so that it reflects all of the relevant relationships in the obtained data. The choice of the order of multivariate polynomial F in the form given by Eq. (3) is justified by the fact that for higher, even third-degree formulations the resultant models exhibit several extrema, which cannot be explained by the measured data variance. Besides, the existence of several maxima and saddle points in the model makes the problem more difficult to solve. Numerous extrema which might exist in a model fitted to the data will always lead to problems regarding the localness of the optimum; for example, the results obtained might not reflect a global optimum for the process parameters. Moreover, mathematical solution of the optimum search problem stated in terms of higher-order polynomials becomes impossible by analytical methods, and can only be done by a numerical approach, which should be avoided if possible due to the greater complexity involved. The higher quality of a fit obtainable using polynomials of higher degree than two does not compensate the risk of obtaining false positive optimization results.

For each model presented, the calculated value of standard deviation describes the amount of variation in the data that is not explained by the model; the lower this value, the better. The model's quality of a fit is also indicated by the determined value of R^2 coefficient. This indicates the fraction (or percentage) of the total variance of the data that is explained by the model; the closer this value is to 1 (or 100%), the better. The data fit procedure utilizes linear statistical estimation to obtain a nonlinear model of the dependence of activity on selected explanatory variables A and B. The explanatory variables A and B may denote pH, process time, temperature or concentration, according to the analysis selected.

$$F(A,B) = a_1 + a_2A + a_3B + a_4A{\cdot}B + a_5A^2 + a_6B^2 \tag{3}$$

The response surface methodology is implemented on the continuous domain over which the fitted model is defined, by applying partial derivative operators to a model mathematical function. The partial derivatives of model F are given by:

$$\frac{dF}{dA} = a_2 + a_4B + 2a_5A \tag{4}$$

$$\frac{dF}{dB} = a_3 + a_4A + 2a_6B \tag{5}$$

The resulting formulations for the analytical solution of equations obtained by setting the expressions in (4) and (5) equal to zero can be solved analytically, representing the optimization problem defined in terms of surface response methodology. The solutions to the problem are given by Eqs. (6) and (7).

$$A_{opt} = \frac{-a_3a_4 + 2a_6a_2}{a_4^2 - 4a_5a_6} \tag{6}$$

$$B_{opt} = -\frac{a_4a_2 - 2a_5a_3}{a_4^2 - 4a_5a_6} \tag{7}$$

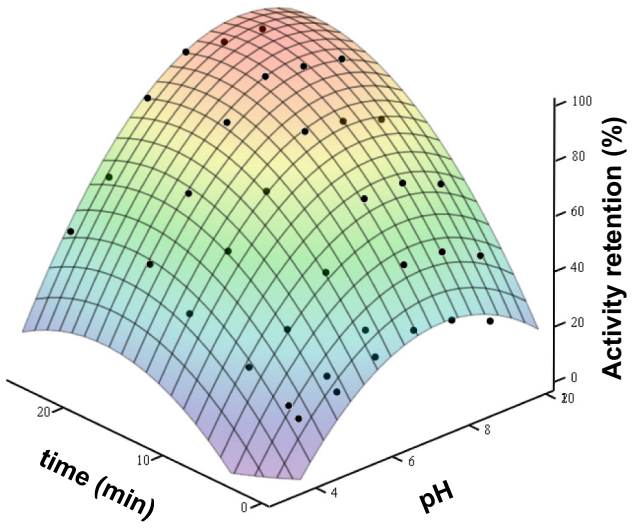

Fig. 3. Response surface for catalyst activity as a function of pH and process time. Dots indicate rescaled experimental values.

The advantage of the response surface methodology optimization presented in the analytical form of solutions (6) and (7) is that it is general in the sense of the model used, and does not require a numerical approach to find the optimal process conditions. It is important to note, however, that this solution is tailored only to the model F presented in (3).

A typical view of the response surface, based on the pH vs. process time model for catalyst activity, is shown in Fig. 3. The model F exhibits only one global maximum, which is justified by observing the measured experimental data. The response surface is a statistical fit, and therefore it extends far beyond the experimental values, in the range $(-\infty, \infty)$. The meaningful range of F is located inside the convex hull containing experimental data points. Although the formal convex hull is not calculated here, it can easily be estimated by examining the minimum and maximum values of the measured data, that is, the explanatory (A and B) variables. Only within this range and in its close neighborhood the response surface exhibits physically meaningful results.

The detailed results obtained by calculation are given in Table 1. Six distinct sets of experimental values were used, which relate selected independent variables A and B to the measured activity of the catalyst. The actual process variables denoted by A and B are given in the first two columns.

The values a_i represent the coefficients of a model F for a given relation between variables that affect the catalyst's activity. Their meaning is statistical only, and they have no physical significance. Nonetheless, they play a key role in the model formulation. The optimal values A_{opt} and B_{opt} for process parameters represent the results from the response surface analysis. These provide the values of process parameters—pH, time t, concentration C, and temperature T—that lead to the highest activity of the catalyst. The quality of the models is confirmed by high values of the determined coefficient R^2, close to one, and relatively low values of the standard deviation in comparison to the activity values.

3.3. Characterization of immobilized enzyme

Based on the result of modeling study and preliminary experiments, immobilization conditions allowing for obtaining the biocatalytic system with the highest catalytic activity were found to be: pH 7, temperature 25 °C, initial enzyme concentration 3 mg/mL and 16 h of immobilization duration. Under these conditions, immobilization yield reached 93% whereas activity recovery attained 95%. Slight decrease in enzyme activity, as compared to free counterpart, might be related to the formation of diffusional limitation in transport of L-catechol and oxygen [46] as well as some distortion of enzyme structure due to its binding to the support [21,47]. Immobilization of tyrosinase performed under process conditions differ than optimal one, results in a lower activity recovery due to the negative effect of the process conditions on enzyme structure and its activity. As produced immobilized tyrosinase is also characterized by the highest stability among all systems obtained and tested at various immobilization conditions. It should be noted that enzyme loading, beside its influence on enzyme activity [48], may also affect its stability due to possible changes in the distances of enzyme-support interactions in a highly-loaded enzymatic systems [49]. It has been reported that high immobilization yield, corresponding with high enzyme loading, leads to improvement in enzyme stability due to crowding formation and reduction of enzyme mobility [50,51]. On the other hand, internal enzyme hydrophobic interactions as well as enzyme-enzyme interactions in the highly loaded support may lead to the irreversible conformational changes resulting in the drop in enzyme activity [52]. Furthermore, the occurrence of diffusional limitations in highly loaded biocatalytic systems cause that apparent activity of these enzymes is higher as compared to the systems where diffusional restrictions did not occur [53].

In addition, to follow the immobilization progress a proper curve was plotted under optimal immobilization conditions (Fig. 4). After 3 h, less than 40% of the activity was immobilized that might be due to the homogenous distribution of support functional groups onto its surface [54]. After 16 h most of the enzyme's activity was immobilized and expressed activity of the immobilized tyrosinase reached 95%. Prolongation of the immobilization increased supernatant residual activity probably due to enzyme elution from the support.

3.4. Removal of bisphenol A

Free tyrosinase and biocatalytic system produced under optimal immobilization conditions and exhibiting the highest catalytic activity were further applied and compared in the removal of bisphenol A from model water solution under various remediation conditions. Tyrosinase was used in this study because this enzyme is capable for efficient degradation/conversion of mono- and bisphenols [55], and because biomolecules deposited on solid supports, unlike free enzymes, offer improved resistance against inactivation by harsh process conditions and can be easily separated from the reaction mixtures [56], which is of great importance for the treatment of large volume of wastewaters.

Fig. 5a shows the percentage removal of bisphenol A by free and immobilized enzyme over time. It can be seen that irrespective of the biocatalyst used, removal efficiency increased gradually over the initial stage of the process, reaching 100% after 60 min and 90 min of the

Table 1
Calculated parameters of models F for selected relations between explanatory (measured) variables A and B.

A	B	a_1	a_2	a_3	a_4	a_5	a_6	A_{opt}	B_{opt}	R^2	Std. dev.
pH	*t, min*	−111.80	39.404	4.226	0.234	−2.631	−0.146	8.433	21.187	0.944	6.598
pH	*C, g/L*	−128.46	40.853	37.696	0.363	−2.616	−5.874	8.048	3.458	0.906	8.814
pH	*T, °C*	−145.20	53.332	1.956	−0.043	−3.265	−0.024	7.946	33.669	0.979	3.163
T, °C	*C, g/L*	8.57	1.483	39.145	−0.0050	−0.02	−5.532	36.064	3.522	0.891	8.202
T, °C	*t, min*	4.592	1.774	7.001	−0.0037	−0.025	−0.188	33.725	18.294	0.96	5.19
C, g/L	*t, min*	4.303	27.46	4.631	0.326	−4.749	−0.146	3.57	19.78	0.893	8.842

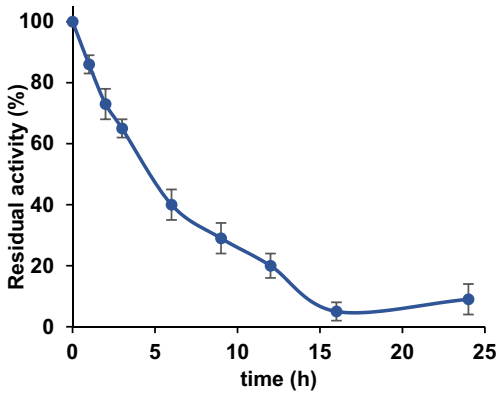

Fig. 4. Immobilization course of tyrosinase onto PCL-chitosan electrospun support material. Immobilization was performed at pH 7 and 25 °C using enzyme solution in concentration of 3 mg/mL.

process performed using free and immobilized tyrosinase, respectively. Nevertheless, over analyzed time intervals, the biocatalytic system produced exhibited slightly lower removal rate of BPA than the free enzyme, which may be due to the lower activity of PCL–chitosan-bonded tyrosinase (an activity recovery of 95%) and accumulation of the products of enzymatic conversion, that lead to the inhibition of the biocatalyst [57]. Furthermore, the results obtained are in agreement with the kinetic parameters obtained for model reaction concerning L-catechol oxidation. The values of the Michaelis–Menten constant (K_m) for free and immobilized enzyme were 1.46 mM and 2.53 mM, respectively. Moreover, the maximum velocity rate (V_{max}) of free enzyme (46.8 U/mg) was higher than the V_{max} of the immobilized enzyme (31.4 U/mg). These data indicate the lower substrate affinity towards tyrosinase after immobilization and may be explained by the formation of diffusional limitations upon immobilization due to partial blocking of enzyme active sites and aggregation of tyrosinase molecules [58]. The changes in the values of the kinetic parameters upon immobilization are also attributed to the fact that immobilized enzyme is located in an environment different from that of its free form, leading to alterations in its microenvironment and causing changes in the enzyme kinetic. Furthermore, changes in the substrate affinity may be related to the changes in enzyme structure and formation of enzyme-support interactions [59,60]. Similar observations were made by Dincer et al. (2012), who immobilized tyrosinase onto chitosan–clay composite beads and noticed high activity retention accompanied by pronounced changes in enzyme kinetic. Two times lower substrate affinity and 40% lower V_{max} of the immobilized tyrosinase were explained by diffusional limitations, steric effects and alteration of enzyme structure [43].

The effect of various process parameters on BPA removal process efficiency was further investigated. As bisphenol A is commonly used as an additive and intermediate product in polymer processing, it frequently occurs in wastewaters at different concentration [61]. Therefore, it was decided to examine the percentage removal of BPA over a wide range of its solution concentrations (from 0.1 mg/L to 5 mg/L), (Fig. 5b). It was evidenced that after 120 min of the process, both, free and immobilized tyrosinase demonstrated excellent catalytic activity, as BPA was totally removed from the solution in concentrations up to 3 mg/L. For solution in the highest concentration (5 mg/L), a drop in the total removal rate of bisphenol A was recorded. Although higher degradation efficiency of the immobilized tyrosinase was attained, as compared to its performance in lower concentrated BPA solutions, the 5 mg of BPA per 1 L of the solution was too high to be fully converted by the enzyme. Furthermore, some distortions of the enzyme structure caused by such high substrate concentration, may lead to the production of semiinextitated forms of BPA that also decrease the removal efficiency of bisphenol A. Nevertheless, even from the 5 mg/L solution, over 80% of the BPA was removed. For comparison, in our previous

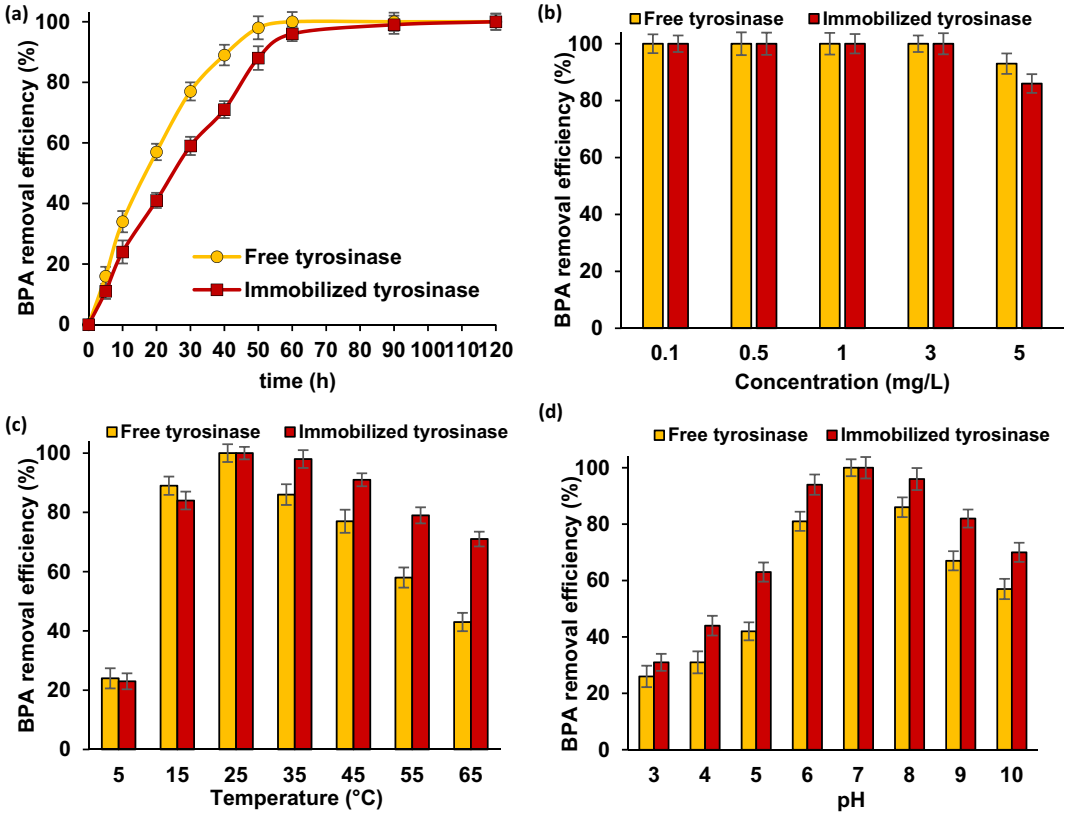

Fig. 5. Percentage removal of BPA using free and immobilized tyrosinase vs. process parameters: time (a), initial BPA concentration (b), process temperature (c) and pH of the solution (d).

study concerning immobilization of laccase onto spongin-based scaffolds, we demonstrated that the immobilized enzyme was capable to remove over 95% of bisphenol A from a solution in concentration of 2 mg/L after 24 h of the treatment process [62].

Another important parameter strongly influencing the stability and catalytic activity of the biocatalysts is the process temperature. The effect of this parameter on the efficiency of BPA removal was investigated over a temperature ranging from 5 °C to 65 °C (Fig. 5c). As shown, the optimum process temperature, for both, free and immobilized enzyme, was found to be 25 °C, as total removal of bisphenol A was noted. Changing the temperature to higher or lower values led to a significant drop in the removal rate of the pollutant by free enzyme. By contrast, immobilized tyrosinase exhibited higher activity over a wider temperature range; it removed over 80% of BPA at temperatures ranging from 15 °C to 55 °C. Even at 65 °C, around 70% of bisphenol A was converted by the immobilized biomolecule, that was over 30% more as compared to free enzyme. This clearly demonstrates that immobilized enzyme, protected against thermal inactivation, was more stable as its free counterpart, even at higher temperatures. The improvement in the enzyme's stability against harsh temperature conditions upon immobilization may be explained by the formation of enzyme–support interactions which stabilize the structure of the biomolecule, as well as rigidization of the enzyme, which facilitates its application at higher operational temperatures [63,64]. Similar observations have been reported by Tamura et al. [65] and Nicolucci et al. [66], who immobilized tyrosinase using ion-exchange resins and polyacrylonitrile beads, for use in the removal of alkylphenols and bisphenol A, respectively. Irrespective of the support material type, enzyme stabilization upon immobilization caused that pollutants were removed more efficiently over a wider temperature range than by free enzyme.

Another key parameter affecting the catalytic activity of biomolecule is pH. The effect of pH on the removal of BPA (pH range 3–10) was investigated (Fig. 5d). As the results demonstrate, pH 7 was found to be the optimum one for both free and immobilized tyrosinase; this is in agreement with previously published studies concerning immobilization and application of mushroom tyrosinase [67,68]. Beyond this value, BPA removal by the free enzyme gradually decreased: only at pH 7 and 8 it removed more than 80% of the pollutant. By contrast, immobilized tyrosinase displayed improved stability over the whole analyzed pH range. Furthermore, PCL–chitosan-bonded tyrosinase exhibited a less pronounced decline in the BPA removal under harsh pH conditions; it enabled the removal of over 80% of bisphenol A in the pH range 6–9. The improvement in the activity of tyrosinase upon immobilization, over a wide pH range, is attributed to the stabilization of the enzyme structure and protection of the biomolecule against the dissociation of amino acids caused by adverse effects of acidic and basic conditions (H^+ and OH^- ions) [69]. Similar observations have been reported by Wu et al. [70], who immobilized tyrosinase on polyacrylonitrile beads and used them in the biodegradation of phenol. Authors observed an improvement in enzyme stability over a pH range 6–9; however, total removal of the phenol was not achieved, indicating the higher capability of the biocatalytic system obtained in presented study for the removal of phenolic compounds under various pH conditions.

3.5. Stability and reusability of free and immobilized tyrosinase

It has been reported that immobilization improves the stability of enzymes and facilitates their reuse [7,36]. As thermochemical and storage stability, as well as reusability, are among the key criteria affecting the practical application of immobilized enzymes, these parameters for free and PCL–chitosan-immobilized tyrosinase were examined and compared (Fig. 6).

The free and immobilized biocatalysts were stored at 4 °C over 20 days, and the storage stability was examined at specified time intervals. As shown in Fig. 6a, the free tyrosinase gradually lost its activity during storage, and after 20 days of the test retained less than 50% of its initial activity. As expected, the decrease in the activity of the

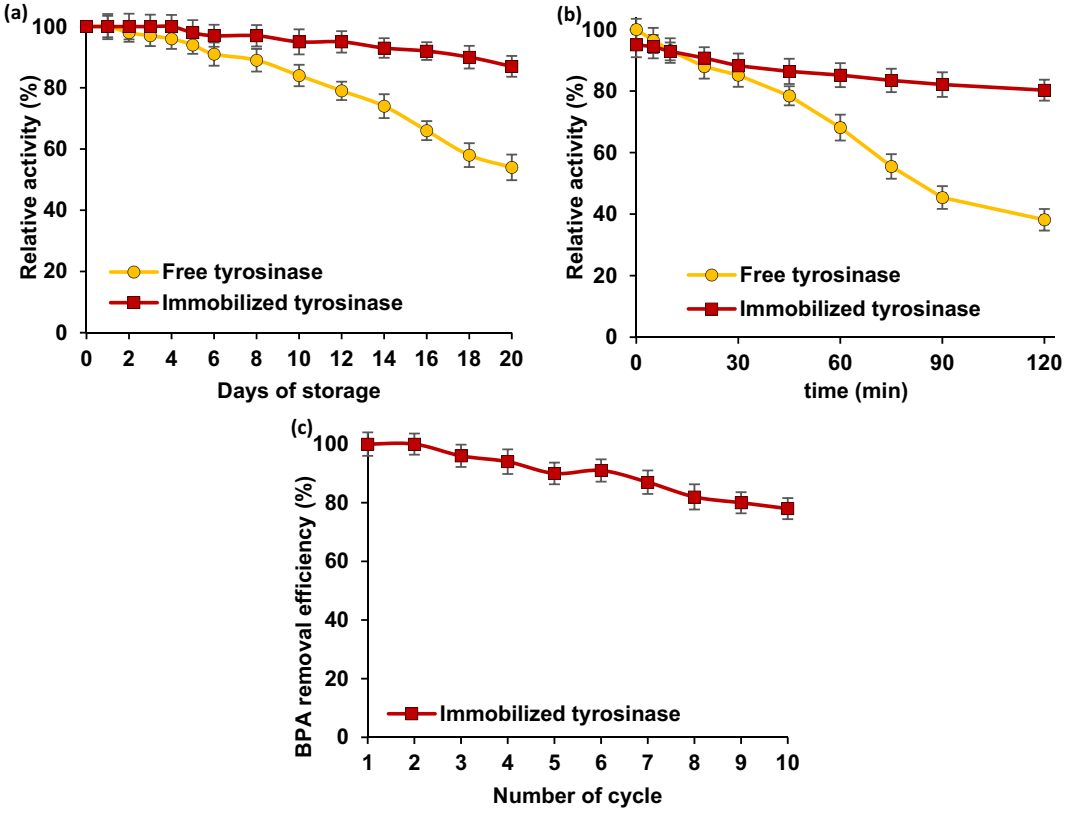

Fig. 6. Storage (a), thermochemical (b) stability of the and PCL-chitosan immobilized tyrosinase and reusability (c) of the immobilized enzyme over repeated reaction cycles.

immobilized enzyme was lower. Over 5 days of storage no activity loss was observed, and after 20 days of storage PCL–chitosan-immobilized tyrosinase retained over 85% of its initial activity. Although loss of enzymatic activity is a naturally occurring phenomenon, the presented data clearly indicate that upon immobilization of tyrosinase on PCL–chitosan electrospun fibers, followed by the stabilization of the enzyme structure and multiple enzyme attachment [71], this effect may be effectively reduced. Similar observations have been reported in other studies concerning immobilization of various polyphenol oxidases on chitosan-based materials, indicating the positive effect of this biomaterial on enzyme stability [34,72,73].

Evaluation of thermochemical stability of immobilized enzyme over time, under process conditions, is one of the most important criteria to be considered. The stability of free and immobilized tyrosinase over 120 min of a process carried out at pH 7 and 25 °C was examined and compared (Fig. 6b). The relative activities of both free and immobilized enzyme declined over time, and after 60 min of incubation reached 70% and 85%, respectively. Prolongation of the incubation time led to a further drop in the relative activity; however, a significantly smaller decrease was observed in case of immobilized tyrosinase. After 120 min of the test the relative activity of free enzyme was around 40%, while PCL–chitosan-bonded tyrosinase retained over 80% of its activity. Observed drop in the catalytic activity may be attributed to changes in the tertiary structure of the enzyme caused by the reaction environment [74]. Nevertheless, the enzyme's thermal stability improved significantly upon immobilization. These results correspond well with the values of the inactivation parameters. The inactivation constant (k_d) and half-life ($t_{1/2}$) of free tyrosinase were measured as 0.0083 1/min and 84.5 min, respectively. In the case of immobilized enzyme, the inactivation constant and half-life were improved more than fivefold as compared to free tyrosinase, taking values of 0.0015 1/min and 462 min, respectively. The higher thermal stability of immobilized tyrosinase may be explained by several factors, including stiffening of the enzyme structure upon immobilization [75], its protection against distortion and conformational changes of the amino acids in the enzyme structure [76], and the protective effect of the support material against process conditions [77]. All of these factors facilitate the retention of high catalytic activity by immobilized enzyme [78] and improve its stability.

The reusability of immobilized enzyme over repeated reaction cycles is the most important parameter affecting its practical application, as it can provide advantages—including cost reductions—for treatment processes. Thus, the reusability of the PCL–chitosan-immobilized tyrosinase over ten repeated cycles of bisphenol A removal, and under optimal process conditions was tested (Fig. 6c). The efficiency of BPA removal slightly decreased after repeated use, and reached approximately 90% after five reaction cycles and around 80% after ten repeated use. The decline in the removal efficiency is related mainly to the inhibition of the enzyme by the macromolecular products of catalytic conversion, but due to adsorption interaction, partial enzyme elution should not be excluded [79]. The maintenance of high removal of BPA by immobilized tyrosinase, over numerous treatment steps is attributed to the stabilization of the enzyme structure, and improvement of its durability under reaction conditions that facilitate the retention of catalytic activity, as previously reported [80,81]. Similar conclusions were reached by Veismoradi et al. [82] and Wu et al. [70], who immobilized tyrosinase using polyaniline membrane coated with chitosan, and polyacrylonitrile beads. The biocatalytic systems were used for the removal of azo dyes and phenols over repeated cycles, and because of the stabilization of the enzyme upon immobilization, the pollutants removal of 80% and 60%, after ten repeated uses, were noted, respectively.

4. Conclusions

Experimental data collected proved that PCL–chitosan electrospun composite material is well-suited for the efficient immobilization of mushroom tyrosinase. Data modeling has been applied to determine the optimal immobilization conditions. Multivariate regression analysis based on the least squares method provided values of polynomial coefficients which produced the statistical best fit to the experimental values, and gave a process parameters such as its duration - 16 h, pH 7 and temperature 25 °C as the optimal ones. The biocatalytic systems produced were further tested in biodegradation of bisphenol A. Obtained dependencies showed that PCL–chitosan-immobilized tyrosinase was capable to efficiently remove BPA over a significantly wider pH and temperature range than free enzyme, clearly indicating improvement of the enzyme stability upon immobilization. Furthermore, the reusability and stability of the immobilized biomolecule over time were also analyzed. The enhanced stability and reusability of immobilized tyrosinase provide economic advantages for large-scale practical applications of the produced systems, as the high biodegradation of bisphenol A suggests that the obtained biocatalytic systems may be considered as a promising tool for the removal of hazardous compounds from wastewaters. Moreover, the obtained electrospun PCL–chitosan material may be a promising alternative to synthetic and natural polymers commonly used as supports in enzyme immobilization; however, further study is still required.

Declaration of competing interest

The authors declare that they have no known competing financial interests or personal relationships that could have appeared to influence the work reported in this paper.

Acknowledgements

This work was supported by the National Science Centre, Poland under the research Grant number 2019/35/D/ST8/02087.

References

[1] M.Y. Chen, M. Ike, M. Fujita, Acute toxicity, mutagenicity, and estrogenicity of bisphenol A and other bisphenols, Environ. Toxicol. 17 (2002) 80–86, https://doi.org/10.1002/tox.10035.
[2] S. Kitamura, T. Suzuki, S. Sanoh, R. Kohta, N. Jinno, K. Sugihara, S. Yoshihara, N. Fujimoto, H. Watanabe, S. Ohta, Comparative study of the endocrine-disrupting activity of bisphenol A and 19 related compounds, Toxicol. Sci. 84 (2005) 249–259, https://doi.org/10.1093/toxsci/kfi074.
[3] S. Eladak, T. Grisin, D. Moison, M.J. Guerquin, T. N'Tumba–Byn, S. Pozzi–Gaudin, A. Benachi, G. Livera, V. Rouiller–Fabre, R. Habert, A new chapter in the bisphenol A story: bisphenol S and bisphenol F are not safe alternatives to this compound, Fertil. Steril. 103 (2015) 11–21, https://doi.org/10.1016/j.fertnstert.2014.11.005.
[4] J.M. Di Donato, G. Cernera, P. Giovannelli, G. Galasso, A. Bilancio, A. Migliaccio, G. Castoria, Recent advances on bisphenol-A and endocrine disruptor effect on human prostate cancer, Mol. Cell. Endocrinol. 457 (2017) 35–42, https://doi.org/10.1016/j.mce.2017.02.045.
[5] D.P. Mohapatra, S.K. Brar, R.D. Tyagi, R.Y. Surampalli, Physico – chemical pretreatment and biotransformation of wastewater and wastewater sludge – fate of bisphenol A, Chemosphere 78 (2010) 923–941, https://doi.org/10.1016/j.chemosphere.2009.12.053.
[6] V.A. Angelini, J. Orejas, M.I. Medina, E. Agostini, Scale up of 2,4– dichlorophenol removal from aqueous solutions using *Brassica napus* hairy roots, J. Hazard. Mater. 185 (2011) 269–274, https://doi.org/10.1016/j.jhazmat.2010.09.028.
[7] J. Zdarta, A.S. Meyer, T. Jesionowski, M. Pinelo, Developments in support materials for immobilization of oxidoreductases: a comprehensive review, Adv. Colloid Interf. Sci. 258 (2018) 1–20, https://doi.org/10.1016/j.cis.2018.07.004.
[8] K. Chang, T. Teng, Ch. Fu, Ch. Liu, Improving biodegradation of bisphenol a by immobilization and inducer, Process. Saf. Environ. Prot. 128 (2019) 128–134, https://doi.org/10.1016/j.psep.2019.05.038.
[9] A. Dwevedi, Enzyme immobilization: solution towards various environmental issues, Enzym. Immobil. (2016) 87–106, https://doi.org/10.1007/978-3-319-41418-8_5.
[10] V. Aranganathan, C. Kavya, M.S. Sheeja, C. Yuvraj, Construction of biosensor for detection of phenolic compound using thermostabilized *Agaricus bisporus* tyrosinase, Arab. J. Sci. Eng. 42 (2017) 11–18, https://doi.org/10.1007/s13369-016-2044-3.
[11] T. Senthivelan, J. Kanagaraj, R. Panda, Recent trends in fungal laccase for various industrial applications: an eco-friendly approach – a review, Biotechnol. Bioproc. 21 (2016) 19–38, https://doi.org/10.1007/s12257-015-0278-7.
[12] G. Faccio, K. Kruus, M. Saloheimo, L. Thöny-Meyer, Bacterial tyrosinases and their applications, Process Biochem. 47 (2012) 1749–1760, https://doi.org/10.1016/j.procbio.2012.08.018.

[13] M. Bilal, M.N. Hafiz, D.B. Iqbal, Mitigation of bisphenol A using an array of laccase-based robust bio-catalytic cues – a review, Sci. Total Environ. 689 (2019) 160–177, https://doi.org/10.1016/j.scitotenv.2019.06.403.
[14] T.-S. Chang, An updated review of tyrosinase inhibitors, Int. J. Mol. Sci. 10 (2009) 2440–2475, https://doi.org/10.3390/ijms10062440.
[15] S. Zolghadri, A. Bahrami, M.T.H. Khan, J. Munoz-Munoz, F. Garcia-Molina, F. Garcia-Canovas, A.A. Saboury, A comprehensive review on tyrosinase inhibitors, J. Enzym. Inhib. Med. Ch. 34 (2019) 297–309, https://doi.org/10.1080/14756366.2018.1545767.
[16] M.E. Marin-Zamora, F. Rojas-Melgarejo, F. Garcia-Canovas, P.A. Garcia-Ruiz, Cinnamic ester of D-sorbitol for immobilization of muschroom tyrosinase, J. Chem. Technol. Biotechnol. 80 (2005) 1356–1364, https://doi.org/10.1002/jctb.1334.
[17] S.-Y. Seo, V.K. Sharma, N. Sharma, Muschroom tyrosinase: recent prospects, J. Agric. Food Chem. 51 (2003) 2837–2853, https://doi.org/10.1021/jf020826f.
[18] A. Roger, S. van Pelt, Enzyme immobilisation in biocatalysis: why, what and how, Chem. Soc. Rev. 42 (2013) 6223–6235, https://doi.org/10.1039/C3CS60075K.
[19] U. Hanefeld, L. Cao, E. Magner, Enzyme immobilisation: fundamentals and application, Chem. Soc. Rev. 42 (2013) 6211–6212, https://doi.org/10.1039/C3CS90042H.
[20] Y. Zhang, J. Ge, Z. Liu, Enhanced activity of immobilized or chemically modified enzymes, ACS Catal. 5 (2015) 4503–4513, https://doi.org/10.1021/acscatal.5b00996.
[21] R.C. Rodrigues, C. Ortiz, A. Berenguer-Murcia, R. Torres, R. Fernandez-Lafuente, Modifying enzyme activity and selectivity by immobilization, Chem. Soc. Rev. 42 (2013) 6290–6307, https://doi.org/10.1039/C2CS35231A.
[22] C. Mateo, J.M. Palomo, G. Fernandez-Lorente, J.M. Guisan, R. Fernandez-Lafuente, Improvement of enzyme activity, stability and selectivity via immobilization techniques, Enzym. Microb. Technol. 40 (2007) 1451–1463, https://doi.org/10.1016/j.enzmictec.2007.01.018.
[23] C. Mateo, O. Abian, R. Fernandez-Lafuente, J.M. Guisan, Increase in conformational stability of enzymes immobilized on epoxy-activated supports by favoring additional multipoint covalent attachment, Enzym. Microb. Technol. 26 (2000) 509–515, https://doi.org/10.1016/S0141-0229(99)00188-X.
[24] C. Garcia-Galan, A. Berenguer-Murcia, R. Fernandez-Lafuente, R.C. Rodrigues, Potential of different enzyme immobilization strategies to improve enzyme performance, Adv. Synth. Catal. 353 (2011) 2885–2904, https://doi.org/10.1002/adsc.201100534.
[25] A.A. Khan, S. Akhtar, Q. Husain, Simultaneous purification and immobilization of mushroom tyrosinase on an immunoaffinity support, Process Biochem. 40 (2005) 2379–2386, https://doi.org/10.1016/j.procbio.2004.09.020.
[26] S. Akhtar, A.A. Khan, Q. Husain, Simultaneous purification and immobilization of bitter gourd (*Momordica charantia*) peroxidases on bioaffinity support, J. Chem. Technol. Biotechnol. 80 (2005) 198–205, https://doi.org/10.1002/jctb.1179.
[27] M.M. Ferreira, F.L.B. Santiago, N.A.G. DaSilva, J.H.H. Luiz, R. Fernandez-Lafuente, A.A. Mendes, D.B. Hirata, Different strategies to immobilize lipase from *Geotrichum candidum*: kinetic and thermodynamic studies, Process Biochem. 67 (2018) 55–63, https://doi.org/10.1016/j.procbio.2018.01.028.
[28] Y. Lokha, S. Arana-Pena, N.S. Rios, C. Mendez-Sanches, L.R.B. Goncalves, F. Lopez-Gallego, R. Fernandez-Lafuente, Modulating the properties of the lipase from *Thermomyces lanuginosus* immobilized on octyl agarose beads by altering the immobilization conditions, Enzym. Microb. Technol. 133 (2020) 109461, https://doi.org/10.1016/j.enzmictec.2019.109461.
[29] J.M. Bolivar, C. Mateo, J. Rocha-Martin, F. Cava, J. Bernguer, R. Fernandez-Lafuente, J.M. Guisan, The adsorption of multimeric enzymes on very lowly activated supports involves more enzyme subunits: stabilization of a glutamate dehydrogenase from *Thermus thermophilus* by immobilization on heterofunctional supports, Enzym. Microb. Technol. 44 (2009) 139–144, https://doi.org/10.1016/j.enzmictec.2008.10.004.
[30] Z. Cabrera, G. Fernandez-Lorente, R. Fernandez-Lafuente, J.M. Palomo, J.M. Guisan, Novozym 435 displays very different selectivity compared to lipase from *Candida antarctica* B adsorbed on other hydrophobic supports, J. Mol. Catal. B Enzym. 57 (2009) 171–176, https://doi.org/10.1016/j.molcatb.2008.08.012.
[31] M. Saleemuddin, Bioaffinity based immobilization of enzymes, in: P.K. Bhatia (Ed.), Thermal Biosensors, Bioactivity, Bioaffinity. Advances in Biochemical Engineering/Biotechnology, Springer, Berlin, Heidelberg 2001, pp. 203–226, https://doi.org/10.1007/3-540-49811-7_6.
[32] P. Sofia, M. Asgher, M. Shahid, M.A. Randhawa, Chitosan beads immobilized *Schizophyllum commune* IBL-06 lignin peroxidase with novel thermo stability, catalytic and dye removal properties, J. Anim. Plant Sci. 5 (2016) 1451–1463.
[33] E. Dehghanifard, A.J. Jafari, R.R. Kalantary, A.H. Mahvi, M.A. Faramarzi, A. Esrafili, Biodegradation of 2,4-dinitrophenol with laccase immobilized on nano-porous silica beads, J. Environ. Health. Sci. Eng. 10 (2013) e25, https://doi.org/10.1186/1735-2746-10-25.
[34] M. Kampmann, S. Boll, J. Kossuch, J. Bielecki, S. Uhl, B. Kleiner, R. Wichmann, Efficient immobilization of mushroom tyrosinase utilizing whole cells from *Agaricus bisporus* and its application for degradation of bisphenol A, Water Res. 57 (2014) 295–303, https://doi.org/10.1016/j.watres.2014.03.054.
[35] T. Jesionowski, J. Zdarta, B. Krajewska, Enzyme immobilization by adsorption: a review, Adsorption 20 (2014) 801–821, https://doi.org/10.1007/s10450-014-9623-y.
[36] J. Zdarta, A.S. Meyer, T. Jesionowski, M. Pinelo, Multi-faceted strategy based on enzyme immobilization with reactant adsorption and membrane technology for biocatalytic removal of pollutants: a critical review, Biotechnol. Adv. 37 (2019) e107401, https://doi.org/10.1016/j.biotechadv.2019.05.007.
[37] Y. Dai, J. Yao, Y. Song, X. Liu, S. Wang, Y. Yuan, Enhanced performance of immobilized laccase in electrospun fibrous membranes by carbon nanotubes modification and its application for bisphenol A removal from water, J. Hazard. Mater. 317 (2016) 485–493, https://doi.org/10.1016/j.jhazmat.2016.06.017.
[38] R.A. Sheldon, Enzyme immobilization: the quest for optimum performance, ChemInform 38 (2007) 1289–1307, https://doi.org/10.1002/chin.200736266.
[39] Y.F. Zhang, J. Ge, Z. Liu, Enhanced activity of immobilized or chemically modified enzymes, ACS Catal. 5 (2015) 4503–4513, https://doi.org/10.1021/acscatal.5b00996.
[40] J. Wu, H. Zhang, N. Oturan, Y. Wang, Lu Chen, M.A. Oturan, Application of response surface methodology to the removal of the antibiotic tetracycline by electrochemical process using carbon-felt cathode and DSA (Ti/RuO_2–IrO_2) anode, Chemosphere 87 (2012) 614–620, https://doi.org/10.1016/j.chemosphere.2012.01.036.
[41] A.F. Mansor, N.A. Mohidem, W.N. Izyani, W.M. Zawawi, N.S. Othman, S. Endud, H. Mat, The optimization of synthesis conditions for laccase entrapment in mesoporous silica microparticles by response surface methodology, Micropor. Mesopor. Mat. 220 (2016) 308–314, https://doi.org/10.1016/j.micromeso.2015.08.014.
[42] K. Bachosz, K. Synoradzki, M. Staszak, M. Pinelo, A.S. Meyer, J. Zdarta, T. Jesionowski, Bioconversion of xylose to xylonic acid via co-immobilized dehydrogenases for conjunct cofactor regeneration, Bioorg. Chem. 10 (2019) 1–10, https://doi.org/10.1016/j.bioorg.2019.01.043.
[43] A. Dincer, S. Becerik, T. Aydemir, Immobilization of tyrosinase on chitosan-clay composite beads, Int. J. Biol. Macromol. 50 (201) 815–820. https://doi.org/10.1016/j.ijbiomac.2011.11.020.
[44] J. Zdarta, T. Jesionowski, *Luffa cylindrica* sponges as a thermally and chemically stable support for *Aspergillus niger* lipase, Biotechnol. Prog. 32 (2016) 657–665, https://doi.org/10.1002/btpr.2253.
[45] M. Zhang, G. Zhou, Y. Feng, T. Xiong, H. Hou, Q. Guo, Flexible 3D-nitrogen-doped carbon nanotubes nanostructure: a good matrix for enzyme immobilization and biosensing, Sensor. Actuat. B Chem. 222 (2016) 829–838, https://doi.org/10.1016/j.snb.2015.09.030.
[46] P. Pialis, M.C.J. Hamann, B.A. Saville, L-DOPA production from tyrosinase immobilized on nylon 6,6, Biotechnol. Bioeng. 51 (1999) 141–147, https://doi.org/10.1002/(SICI)1097-0290(19960720)51:2<141::AID-BIT2>3.0.CO;2-J.
[47] J. Boundrant, J.M. Woodley, R. Fernandez-Lafuente, Parameters necessary to define an immobilized enzyme preparation, Process Biochem. 90 (2020) 66–80, https://doi.org/10.1016/j.procbio.2019.11.026.
[48] O. Barbosa, R. Torres, C. Ortiz, R. Fernandez-Lafuente, The slow-down of the CALB immobilization rate permits to control the inter and intra molecular modification produced by glutaraldehyde, Process Biochem. 47 (2012) 766–774, https://doi.org/10.1016/j.procbio.2012.02.009.
[49] L. Fernandez-Lopez, S.G. Pedrero, N. Lopez-Carrobles, B.C. Gorines, J.J. Virgen-Ortiz, R. Fernandez-Lafuente, Effect of protein load on stability of immobilized enzymes, Enzym. Microb. Technol. 98 (2017) 18–25, https://doi.org/10.1016/j.enzmictec.2016.12.002.
[50] A.P. Minton, Influence of macromolecular crowding upon the stability and state of association of proteins: predictions and observations, J. Pharm. Sci. 94 (2005) 1668–1675, https://doi.org/10.1002/jps.20417.
[51] S. Arana-Pena, N.S. Rios, D. Carballares, C. Mendez-Sanchez, Y. Lokha, L.R.B. Goncalves, R. Fernandez-Lafuente, Effects of enzyme loading and immobilization conditions on the catalytic features of lipase from *Pseudomonas fluorescens* immobilized on octyl-agarose beads, Front. Bioeng. Biotechnol. 8 (2020) 36, https://doi.org/10.3389/fbioe.2020.00036.
[52] M. Bilal, M. Asgher, H. Cheng, Y. Yan, H.M.N. Iqbal, Multi-point enzyme immobilization, surface chemistry and novel platforms: a paradigm shift in biocatalyst design, Crit. Rev. Biotechnol. 39 (2019) 202–219, https://doi.org/10.1080/07388551.2018.1531822.
[53] G.K. Leet, P.J. Reilly, The effect of slow intraparticle diffusion on observed immmobilized enzyme stability, Chem. Eng. Sci. 36 (1981) 1967–1975, https://doi.org/10.1016/0009-2509(81)80036-X.
[54] M. Bilal, T. Rasheed, Y. Zhao, H.M.N. Iqbal, J. Cui, "Smart" chemistry and its application in peroxidase immobilization using different support materials, Int. J. Biol. Macromol. 119 (2018) 278–290, https://doi.org/10.1016/j.ijbiomac.2018.07.134.
[55] Y.A.M. Gerritsen, C.G.J. Chapelon, H.J. Wichers, The low-isoelectric point tyrosinase of *Agaricus bisporous* may be a glycoprotein, Phytochemistry 35 (1994) 573–577, https://doi.org/10.1016/S0031-9422(00)90563-6.
[56] C.R. Ispas, M.T. Ravalli, A. Steere, A. Silvana, Multifunctional biomagnetic capsules for easy removal of phenol and bisphenol A, Water Res. 44 (2010) 1961–1969, https://doi.org/10.1016/j.watres.2009.11.049.
[57] M.Y. Arica, B. Altıntas, G. Bayramoglu, Immobilization of laccase onto spacer-arm attached non-porous poly(GMA/EGDMA) beads: application for textile dye degradation, Bioresour. Technol. 100 (2009) 665–669, https://doi.org/10.1016/j.biortech.2008.07.038.
[58] K.J. Laidler, P.S. Bunting, The kinetics of immobilized enzyme systems, in: D.L. Purich (Ed.), Methods in Enzymology: Enzyme Kinetics and Mechanism, DL Purich, Academic Press Inc, New York 1980, pp. 227–248.
[59] F. Sahin, G. Demirel, H. Tümtürk, A novel matrix for the immobilization of acetylcholinesterase, Int. J. Biol. Macromol. 37 (2005) 148–153, https://doi.org/10.1016/j.ijbiomac.2005.10.003.
[60] M.Y. Chang, R.S. Juang, Activities, stabilities, and reaction kinetics of three free and chitosan-clay composite immobilized enzymes, Enzym. Microb. Technol. 36 (2005) 75–82, https://doi.org/10.1016/j.enzmictec.2004.06.013.
[61] C.A. Staples, P.B. Dorn, G.M. Klecka, S.T. O'Block, L.R. Harris, A review of the environmental fate, effects, and exposures of bisphenol A, Chemosphere 36 (1998) 2149–2173, https://doi.org/10.1016/S0045-6535(97)10133-3.
[62] J. Zdarta, K. Antecka, R. Frankowski, A. Zgoła-Grześkowiak, H. Erlich, T. Jesionowski, The effect of operational parameters on the biodegradation of bisphenols by *Trametes versicolor* laccase immobilized on *Hippospongia communis* scaffolds, Sci. Total Environ. 615 (2018) 784–795, https://doi.org/10.1016/j.scitotenv.2017.09.213.
[63] A. Yashi, F. Sakin, G. Demirel, H. Tumturuk, Binary immobilization of tyrosinase by using alginate gel beads and poly(acrylamide-co-acrylic acid) hydrogels, Int. J. Biol. Macromol. 36 (2005) 253–258, https://doi.org/10.1016/j.ibiomac.2005.06.011.

[64] R.L.O.J.L. Dias, O. Soares de Silva, A. Porto, Immobilization of pectinase from *Aspergillus aculeatus* in alginate beads and clarification of apple and umbu juices in a packed bed reactor, Food Bioprod. Process. 109 (2018) 9–18, https://doi.org/10.1016/j.fbp.2018.02.005.
[65] A. Tamura, E. Satoh, A. Kashiwada, K. Matsuda, K. Yamada, Removal of alkylphenols by the combined use of tyrosinase immobilized on ion-exchange resins and chitosan beads, J. Appl. Polym. Sci. 115 (2010) 137–145, https://doi.org/10.1002/app.30947.
[66] C. Nicolucci, S. Rossi, C. Menale, T. Godjevargova, Y. Ivanov, M. Bianco, L. Mita, U. Bencivenga, D.G. Mita, N. Diano, Biodegradation of bisphenols with immobilized laccase or tyrosinase on polyacrylonitrile beads, Biodegradation 22 (2011) 673–683, https://doi.org/10.1007/s10532-010-9440-2.
[67] M.E. Marin-Zamora, F. Rojas-Melgarejo, F. Garcia-Canovas, P.A. Garcia-Ruiz, Effects of the immobilization supports on the catalytic properties of immobilized mushroom tyrosinase: a comparative study using several substrates, J. Biotechnol. 131 (2007) 388–396, https://doi.org/10.1016/j.jbiotec.2007.05.004.
[68] W.T. Ismaya, H.J. Rozeboom, A. Weijn, J.J. Mes, F. Fusetti, H.J. Wichers, B.W. Dijkstra, Crystal structure of *Agaricus bisporus* mushroom tyrosinase: identity of the tetramer subunits and interaction with tropolone, Biochemistry 50 (2011) 5477–5486, https://doi.org/10.1021/bi200395t.
[69] G. Bayramoglu, M.Y. Arica, Reversible immobilization of catalase on fibrous polymer grafted and metal chelated chitosan membrane, J. Mol. Catal. B Enzym. 62 (2010) 297–304, https://doi.org/10.1016/j.molcatb.2009.11.013.
[70] Q. Wu, Z. Xu, Y. Duan, Y. Zhu, M. Ou, X. Xu, Immobilization of tyrosinase on polyacrylonitrile beads: biodegradation of phenol from aqueous solution and the relevant cytotoxicity assessment, RSC Adv. 7 (2017) 28114–28123, https://doi.org/10.1039/C7RA03174B.
[71] K. Abollahi, F. Yazdani, R. Panahi, Fabrication of the robust and recyclable tyrosinase-harboring biocatalyst using ethylenediamine functionalized superparamagnetic nanoparticles: nanocarrier characterization and immobilized enzyme properties, J. Biol. Inorg. Chem. 24 (2019) 943–959, https://doi.org/10.1007/s00775-019-01690-1.
[72] J. Shao, H. Ge, Y. Yang, Immobilization of polyphenol oxidase on chitosan–SiO_2 gel for removal of aqueous phenol, Biotechnol. Lett. 29 (2007) 901–905, https://doi.org/10.1007/s10529-007-9329-2.
[73] G. Bayramoglu, M. Yilmaz, M.Y. Arica, Preparation and characterization of epoxy-functionalized magnetic chitosan beads: laccase immobilized for degradation of reactive dyes, Bioprocess Biosyst. Eng. 33 (2010) 439–448, https://doi.org/10.1007/s00449-009-0345-6.
[74] S.A. Cetinus, H.N. Oztop, Immobilization of catalase into chemically crosslinked chitosan beads, Enzym. Microb. Technol. 32 (2003) 889–894, https://doi.org/10.1016/S0141-0229(03)00065-6.
[75] J.L. Gomez, A. Bodalo, E. Gomez, J. Bastida, A.M. Hidalgo, M. Gomez, Immobilization of peroxidases on glass beads: an improved alternative for phenol removal, Enzym. Microb. Technol. 39 (2006) 1016–1022, https://doi.org/10.1016/j.enzmictec.2006.02.008.
[76] G. Bayramoglu, B. Altintas, M. Yilmaz, M.Y. Arica, Immobilization of chloroperoxidase onto highly hydrophilic polyethylene chains via bio-conjugation: catalytic properties and stabilities, Bioresour. Technol. 102 (2011) 475–482, https://doi.org/10.1016/j.biortech.2010.08.056.
[77] E. Arkan, C. Karami, R. Rafipur, Immobilization of tyrosinase on Fe_3O_4@Au core–shell nanoparticles as bio-probe for detection of dopamine, phenol and catechol, J. Biol. Inorg. Chem. 24 (2019) 961–969, https://doi.org/10.1007/s00775-019-01691-0.
[78] D. Dodor, H. Hwang, E. Sin, Oxidation of anthracene and benzo[a]pyrene by immobilized laccase from *Trametes versicolor*, Enzym. Microb. Technol. 35 (2004) 210–217, https://doi.org/10.1016/j.enzmictec.2004.04.007.
[79] C. Ji, L.N. Nguyen, J. Hou, F.I. Hai, V. Chen, Direct immobilization of laccase on titania nanoparticles from crude enzyme extracts of *P. ostreatus* culture for micropollutant degradation, Sep. Purif. Technol. 178 (2017) 215–223https://doi.org/10.1016/j.seppur.2017.01.043.
[80] F.A.D. Inroga, M.O. Rocha, V. Lavayen, J. Arguello, Development of a tyrosinase-based biosensor for bisphenol A detection using gold leaf–like microstructures, J. Solid State Electr. 23 (2019) 1659–1666, https://doi.org/10.1007/s10008-019-04252-2.
[81] M. Bilal, H.M.N. Iqbal, H. Hu, W. Wang, X. Zhang, Enhanced bio-catalytic performance and dye degradation potential of chitosan-encapsulated horseradish peroxidase in a packed bed reactor system, Sci. Total Environ. 575 (2017) 1352–1360, https://doi.org/10.1016/j.scitotenv.2016.09.215.
[82] A. Veismorandi, S.M. Mousavi, M. Taherian, Decolorization of dye solutions by tyrosinase in enzymatic membrane reactors, J. Chem. Technol. Biotechnol. 94 (2019) 3559–5568, https://doi.org/10.1002/jctb.6158.

Science of the Total Environment 615 (2018) 784–795

Contents lists available at ScienceDirect

Science of the Total Environment

journal homepage: www.elsevier.com/locate/scitotenv

The effect of operational parameters on the biodegradation of bisphenols by *Trametes versicolor* laccase immobilized on *Hippospongia communis* spongin scaffolds

Jakub Zdarta [a,*], Katarzyna Antecka [a], Robert Frankowski [b], Agnieszka Zgoła-Grześkowiak [b], Hermann Ehrlich [c], Teofil Jesionowski [a]

[a] Institute of Chemical Technology and Engineering, Faculty of Chemical Technology, Poznan University of Technology, Berdychowo 4, 60965 Poznan, Poland
[b] Institute of Chemistry and Electrochemistry, Faculty of Chemical Technology, Poznan University of Technology, Berdychowo 4, 60965 Poznan, Poland
[c] Institute of Experimental Physics, TU Bergakademie Freiberg, Leipziger Str. 23, 09599 Freiberg, Germany

HIGHLIGHTS

- Application of *H. communis* scaffolds as effective support for laccase immobilization.
- Enhancement of the pH, temperature and storage stability of immobilized laccase.
- Evaluation of optimal biodegradation conditions for the highest removal efficiency.
- Formation of dimers and trimers as main products of bisphenols enzymatic oxidation.
- Degradation over 95% of bisphenol A and bisphenol F at pH 5 and temperature of 30 °C.

GRAPHICAL ABSTRACT

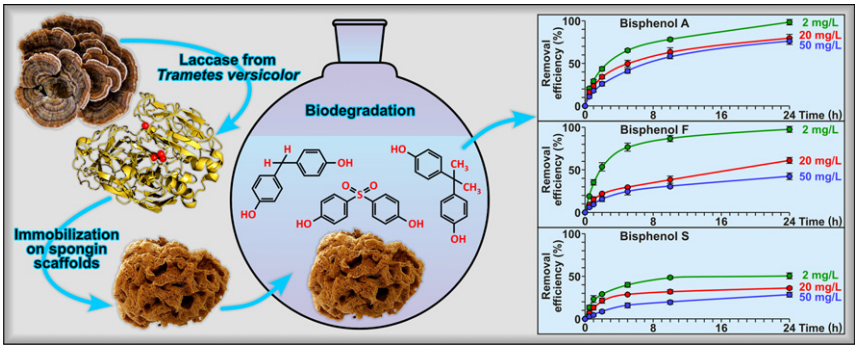

ARTICLE INFO

Article history:
Received 27 July 2017
Received in revised form 19 September 2017
Accepted 19 September 2017
Available online 7 October 2017

Editor: Jay Gan

Keywords:
Laccase
Immobilization
Environmental pollutants
Biodegradation
Bisphenol removal

ABSTRACT

Due to the rapid growth in quantities of phenolic compounds in wastewater, the development of efficient and environmentally friendly methods for their removal becomes a necessity. Thus, in a presented work, for the first time, a novel material, *Hippospongia communis* spongin-based scaffold, was used as a biopolymeric support for the immobilization of laccase from *Trametes versicolor*. The resulting biocatalytic systems were used for the biodegradation of three bisphenols: bisphenol A (BPA), bisphenol F (BPF) and bioremoval-resistant bisphenol S (BPS). Optimization of the immobilization and biodegradation methodologies was performed to increase bisphenols removal. The effect of temperature, pH and initial pollutant concentration was evaluated. It was shown that under optimal conditions, almost 100% of BPA (pH 5, 30 °C) and BPF (pH 5, 40 °C), and over 40% of BPS (pH 4, 30 °C) was removed from the solution at a concentration of 2 mg/mL. Furthermore, the immobilized laccase exhibited good reusability and storage stability, retaining over 80% of its initial activity after 50 days of storage. In addition, the main biodegradation products of BPA and BPF were identified. It was shown that mainly dimers and trimers were formed following the oxidation of bisphenols by the immobilized laccase.

* Corresponding author.
E-mail address: jakub.zdarta@put.poznan.pl (J. Zdarta).

https://doi.org/10.1016/j.scitotenv.2017.09.213
0048-9697/

1. Introduction

Bisphenols are a class of compounds that contain two phenol rings connected by a short spacer group. The most commonly known and widely used is bisphenol A (BPA), which is an intermediate product in the manufacture of polycarbonates, epoxy resins and flame retardants. There are many everyday products which may contain BPA, including compact discs, optical lenses, powder paints, thermal paper and food packaging (Staples et al., 1998). BPA can contaminate food or beverages by migrating from the container (Krishnan et al., 1993; EFSA, 2013). An even greater concern is the discovery that BPA is an endocrine disruptor. Endocrine disrupting compounds (EDCs) are substances or mixtures that can alter functions of the hormonal system and cause adverse effects in an intact organism, such as obesity, diabetes, cardiovascular diseases, breast cancer and reproductive disorder, and even exhibit genotoxic activity (Tiwari et al., 2012; Rochester, 2013; Rezg et al., 2014; Bilal et al., 2017a). Because of these properties, industry is beginning to look for substitutes for BPA in polymer production. Options include other bisphenols, such as bisphenol F (BPF) and bisphenol S (BPS), which are gradually replacing BPA (Eladak et al., 2015). Unfortunately, studies have shown that both BPF and BPS also have endocrine-disrupting and toxic properties (Chen et al., 2002; Eladak et al., 2015; Kitamura et al., 2005), although diverse results were presented by different authors. Chen et al. (2002) found BPF to have similar endocrine-disrupting activity to BPA, while BPS showed weak activity, and both BPF and BPS were less toxic than BPA. Eladak et al. (2015) reported that both BPF and BPS have anti-androgenic effects similar to those of BPA. On the other hand, Kitamura et al. (2005) showed BPA, BPF and BPS to have similar estrogenic activity, and BPF and BPS to have lower anti-androgenic activity than BPA.

Reported concentrations of BPA in river water vary between not detected and 68 ng/L in European countries (Kasprzyk-Hordern et al., 2008; Jonkers et al., 2009) and between 7 and 79 ng/L in Asia (Narasaki, 2002). Studies reported that BPA, alongside BPS and BPF, can be found not only in water and sediment (Song et al., 2012) but also in food and drinks (Grumetto et al., 2008; Liao and Kannan, 2013), in dust (Liao et al., 2012) and even in human urine samples (Yang et al., 2014).

The biodegradation of BPA in river water is rapid, with a half-life often under one day after a lag period of 2–7 days (Klecka et al., 2001), although in seawater its degradation generally takes slightly longer (Danzl et al., 2009). These studies showed that microorganisms capable of degrading BPA are present in the aquatic environment, thus BPA is not a persistent compound. BPA and BPF exhibit fairly good biodegradability in the environment, but BPS shows some problems. In aerobic and anaerobic conditions, BPF, which seems to be a better choice for the replacement of BPA, offers the best degradability properties (Ike et al., 2006).

Various enzymes, including laccase, tyrosinase, and manganese and horseradish peroxidase, are used for the biodegradation of hazardous compounds such as phenol and its derivatives, or synthetic and natural dyes (Bilal et al., 2016, 2017b, 2017c, 2017d). Among the enzymes, laccases (EC 1.10.3.2) are the most frequently applied. These oxygen oxidoreductases catalyze a wide range of chemical reactions, mainly by one-electron oxidation of mono-, di- and polyphenols (Bronikowski et al., 2017). As a multi copper oxidase, laccase contains four copper atoms in its structure, which exhibit different properties. A type-1 (T1) copper atom causes the blue color of the laccase, while a type-2 (T2) atom and two atoms of type 3 (T3) participate in oxidation reactions (Abdel-Hamind et al., 2013). These enzymes have found applications in the textile, food, fuel and medical industries (Mogharabi and Faramarzi, 2014; Zeeb et al., 2014; Kumar et al., 2017). However, it should be noted that laccase has ubiquitous properties enabling its use in many processes related to the biodegradation of environmental pollutants and their removal from soils and wastewaters (Yadav and Yadav, 2015; Le et al., 2016; Chatha et al., 2017). Laccase biocatalysts occur in bacteria, plants and insects (Singh et al., 2010; Geng et al., 2016), but fungal laccases deserve special attention due to their high adaptability (Cha et al., 2017).

In view of the potential increase in thermal stability and pH range, enabling the use of laccase in a wider range of conditions, in recent years increasing interest in laccase immobilization processes is observed [Jesionowski et al., 2014, Ba and Kumar, 2017]. There are many published studies that describe the immobilization of fungal laccase on different carriers (Cabana et al., 2007, 2009; Skoronski et al., 2017). For instance, Georgieva et al. (2010) described laccase immobilization on polypropylene membranes in non-isothermal conditions. This biocatalytic system was used in the degradation of phenol and its derivatives. Singh et al. (2010) studied γ-proteobacterium JB laccase and its immobilization on nitrocellulose membrane. Compounds such as syringaldazine, catechol, guaiacol and hydroquinone were degraded by the obtained biocatalytic system. In another study, Lin et al. (2016) proposed the immobilization of laccase on Cu(II) and Mn(II) chelated magnetic microspheres. The obtained system was used for the degradation of BPA, which resulted in the removal of over 85% of that compound. Furthermore, Aydemir and Guler (2015) described the synthesis of magnetic chitosan composite beads for the immobilization of laccase. The support with the immobilized enzyme removed phenol with an efficiency of 80%. Apart from the above examples, it should be noted that immobilization of laccases on biopolymeric supports is of increasing interest (Duran et al., 2002; Kues, 2015; Bilal et al., 2017e).

In this work, for the first time, spongin-based skeletons of *H. communis* marine sponges were used as a novel carrier for laccase immobilization. Spongin, as a collagen-like protein, is compatible with enzymes, but importantly it is more resistant to enzyme degradation than collagen. Moreover, marine sponge skeletons are renewable and do not require complicated preparation procedures or additional surface functionalization, due to their unique chemical and structural properties. Synthesized systems combine the beneficial properties of both substrates: the degradation activity of laccase and the three-dimensional architecture of the skeletons, which allows easy access of hazardous compounds to the active sites of the immobilized biocatalysts.

In the present study, the effect of various process parameters on the removal efficiency of BPA, BPF and the rarely studied BPS was determined. As an efficient biocatalytic system, laccase from *Trametes versicolor* immobilized on *H. communis* spongin scaffolds was used. Effective enzyme immobilization was confirmed by Fourier transform infrared spectroscopy (FTIR) and scanning electron microscopy (SEM). The effect of the initial immobilization conditions and the quantity of the biocatalytic system on the degradation of bisphenols was tested. Moreover, the storage stability of the free and immobilized enzyme was examined. Finally, the effect of pH, temperature, initial solution concentration and number of biodegradation cycles on the efficiency of removal of BPA, BPF and BPS was evaluated and compared.

2. Materials and methods

2.1. Materials

Hippospongia communis sponges, farmed on the Mediterranean coast in Tunisia, were purchased from INTIB GmbH (Germany). Laccase from *Trametes versicolor* (EC 1.10.3.2), bisphenol A (BPA, >99%), bisphenol F (BPF, >99%), bisphenol S (BPS, >98%),

2,2-azinobis-3-ethylbenzothiazoline-6-sulfonate (ABTS, 99%), Coomassie Brilliant Blue and sodium azide were received from Sigma-Aldrich (USA). Ethanol, methanol, hydrochloric acid and orthophosphoric acid (all laboratory grade) were purchased from Chempur (Poland). Acetate and phosphate buffers with specific pH were supplied by Sigma-Aldrich (USA). HPLC-grade methanol was purchased from Avantor (Poland). HPLC-grade water was prepared by reverse osmosis in a Demiwa system from Watek (Czech Republic), followed by double distillation from a quartz apparatus.

2.2. Preparation of spongin-based scaffolds from H. communis demosponge

The preparation of the *H. communis* spongin-based scaffolds was described in detail in our previous work (Norman et al., 2016). Briefly, skeletons were immersed in HCl for 72 h and rinsed with distilled water until neutral pH was attained. The scaffolds were then dried at 50 °C and stored at room temperature.

2.3. Laccase immobilization

Before immobilization, the spongin-based scaffolds were cut into pieces (0.5 × 0.5 × 0.5 cm). To evaluate the effect of the various initial immobilization parameters, an appropriate quantity, ranging from 10 to 100 mg, of the previously prepared scaffolds was placed in a reactor, to which enzyme solution (10 mL) at various concentrations (from 0.25 to 2.0 mg/mL) in pH 5 acetate buffer solution was added. Immobilization was carried out on a shaker (IKA Werke GmbH, Germany) for 1 h. After immobilization, the obtained systems were filtered under reduced pressure and washed with acetate buffer (pH 5) to remove unbound enzyme.

2.4. Storage stability and kinetic parameters of free and immobilized laccase

The storage stability of free and immobilized laccase stored at 4 °C in acetate buffer (pH 5) was tested spectrophotometrically over 50 days, using ABTS as the substrate, according to the procedure described by Dai et al. (2010) with slight modification. For the reaction, 5 mg of free enzyme and an appropriate amount of the product after immobilization containing 5 mg of laccase were used. Changes in the absorbance of the substrate after reaction were measured with a Jasco V-750 (Japan) spectrophotometer at $\lambda = 420$ nm.

The Michaelis–Menten constant (K_m) and the maximum rate of reaction (V_{max}) were evaluated based on the oxidation reaction of ABTS using various concentrations of the substrate solution. The Lineweaver–Burk plot was used to calculate the apparent kinetic parameters (K_m and V_{max}) of free and immobilized laccase.

2.5. Bisphenol removal experiments

Degradation of BPA, BPF and BPS was carried out in an IKA KS 4000i (IKA Werke GmbH, Germany) incubator shaker (150 rpm) using 30 mL of bisphenol solution. The mixtures were kept for 24 h and sampled at specified time intervals. After sampling, 100 μL of sodium azide (10 M) was added to the mixture to terminate the catalytic reaction, prior to further analysis.

Before the efficiency of bisphenols degradation was evaluated, the efficiency of adsorption of bisphenol on the sponge skeletons with immobilized laccase was examined. Sponge scaffolds with attached enzyme (immobilization time: 1 h, concentration of enzyme solution: 1 mg/mL) were subjected to thermal inactivation (2 h at 70 °C), after which the adsorption was carried out. For the adsorption experiments, 30 mL of a 2 mg/L solution of each bisphenol was mixed with 50 mg of the *H. communis* spongin scaffolds with inactivated enzyme. The system was than mixed for 24 h, and at specified time intervals the adsorption of the bisphenols was analyzed chromatographically.

To establish the effect of free laccase on degradation efficiency of BPA, BPF and BPS, experiments were carried out at 30 °C (BPA and BPS) and 40 °C (BPF) using bisphenols solutions at a concentration of 2 mg/mL at pH 5. For these experiments 5 mg of water-soluble laccase was used, and the process duration was 24 h.

To determine the effect of the initial process parameters on the efficiency of BPA degradation, initial enzyme solutions at concentrations ranging from 0.25 to 2.0 mg/mL in pH 5 acetate buffer were used for immobilization. To assess the influence of the quantity of the biocatalytic system on bisphenol degradation, it was tested in quantities ranging from 10 to 100 mg. These experiments were carried out using BPA solution at a concentration of 2 mg/L at pH 5 and at 30 °C.

Laccase solution in a concentration of 1 mg/mL and 50 mg of the produced biocatalytic system with approximately 5 mg of immobilized laccase were used as the initial process parameters for further bisphenol removal experiments to evaluate the effect of the initial degradation parameters on degradation efficiency. The effect of pH on the degradation efficiency of BPA, BPF and BPS was evaluated using the appropriate bisphenol solution at a concentration of 2 mg/L at 30 °C, with pH ranging from 4 to 8 for BPA and from 4 to 6 for BPF and BPS. A buffer solution at the desired pH was used to adjust the pH value. The influence of temperature on the removal of bisphenols was examined using bisphenol solutions at a concentration of 2 mg/L in pH 5 acetate buffer and at temperatures ranging from 10 to 50 °C for BPA and from 20 to 40 °C for BPF and BPS. To assess the effect of the bisphenol solution concentration on the removal efficiency, solutions at concentrations of 2, 20 and 50 mg/L were used. Experiments were carried out under optimal process conditions (pH 5, temperature 30 °C for BPA and BPS and 40 °C for BPF). The efficiency of bisphenol removal over 5 repeated degradation cycles was evaluated using BPA, BPF and BPS solutions (2 mg/L) at pH 5 and at 30 °C. After each reaction cycle the biocatalytic system was separated from the mixture by filtration under reduced pressure, washed with pH 5 acetate buffer and transferred to fresh bisphenol solution. All of the above experiments were performed in duplicate.

2.6. Analytical techniques

The morphology of the *H. communis* spongin-based scaffold before and after immobilization was described based on SEM images (EVO40, Zeiss, Germany) after gold coating (Balzers PV205P, Switzerland). FTIR spectra of the tested materials were obtained using a Vertex 70 spectrometer (Bruker, Germany). Samples were analyzed in the form of KBr pellets in the wavenumber range 4000–400 cm^{-1} at a resolution of 0.5 cm^{-1}. The quantity of immobilized laccase was evaluated according to the Bradford method using Coomassie Brilliant Blue (Bradford, 1976). Measurements were made on a Jasco V750 spectrophotometer (Japan) at wavelength 595 nm.

Determination of BPA and BPF was performed using a chromatographic system from Dionex (USA) consisting of a P580 A LPG gradient pump, an ASI-100 autosampler, an STH 585 oven and an RF 2000 fluorescence detector. Samples of exactly 5 μL were injected into a C18 Hypersil GOLD column (150 mm × 4.6 mm I.D.; 5 μm) with a 2.1 mm I.D. filter cartridge (0.2 μm) from Thermo Scientific (USA), maintained at 35 °C. The analysis was performed in isocratic mode with a 1.5 mL/min flow rate of 75% methanol as a mobile phase. Signal responses were measured by fluorescence detection at wavelengths set at 273 nm for excitation and 300 nm for emission.

For determination of BPS the UltiMate 3000 RSLC chromatographic system from Dionex (USA) was used, coupled with an API 4000 QTRAP triple quadrupole mass spectrometer from AB Sciex (USA). Samples of exactly 3 μL were injected into a C18 Hypersil GOLD column (100 mm × 2.1 mm I.D.; 1.9 μm) with a 2.1 mm I.D. filter cartridge (0.2 μm) from Thermo Scientific (USA), maintained at 35 °C. The mobile phase employed in the analysis consisted of $5 \cdot 10^{-3}$ mol/L ammonium acetate in water and methanol at a flow rate of 0.2 mL/min. Isocratic conditions were used for elution, with the mobile phase consisting of 70% methanol. The LC column effluent was directed to the electrospray ionization source operating in negative ion mode. The following settings for the ion source and mass spectrometer were used: curtain gas 20 psi, nebulizer gas 40 psi, auxiliary gas 45 psi, temperature 450 °C, ion spray voltage −4500 V, declustering potential −60 V, and collision gas set to medium. The dwell time for each mass transition detected in the selected reaction monitoring mode was equal to 100 ms. The quantitative transition was from 249 to 108 m/z with collision energy set to −39 V, and the confirmatory transition was from 249 to 92 m/z with collision energy set to −53 V.

LC-MS/MS identification of the degradation products of bisphenols was performed using the LC-MS/MS system described above. Samples of exactly 10 μL were injected into a Gemini-NX C18 column (100 mm × 2.0 mm I.D.; 3 μm) from Phenomenex (USA), maintained at 35 °C. The mobile phase consisted of 5 mM ammonium acetate in water and methanol at flow rate 0.3 mL/min, on a gradient from 50% to 100% methanol over 2 min and then for 4 min in isocratic conditions. The electrospray ion source operated in negative ion mode. Nitrogen was used in both the source and the mass spectrometer. The following parameters of the source and mass spectrometer were used: curtain gas pressure 10 psi, nebulization gas pressure 45 psi, auxiliary gas pressure 45 psi, source temperature 450 °C, ion spray voltage −4500 V, declustering potential −40 V. Spectra were collected in scan mode in the range 70–600 *m/z*.

3. Results and discussion

3.1. Characterization of H. communis spongin-based scaffolds and products obtained after immobilization

The morphology of the *H. communis* skeletons before (Fig. 1a, c) and its changes after (Fig. 1b, d) laccase immobilization was determined based on SEM images. As can be seen in Fig. 1, marine demosponges consist of an open, three-dimensional network built from triply branched fibers (Szatkowski et al., 2015; Zdarta et al., 2017). The fibers are corrugated and have diameters of around 20 μm. The morphological structure of the *H. communis* scaffolds allows easier access of the substrate molecules to the active sites of the enzyme, which reduces diffusional limitations. On the SEM images of the product after immobilization (Fig. 1b, d) irregularly shaped enzyme aggregates can be seen, which proved the effective immobilization of the laccase.

To identify the functional groups present in the structure of the sponge scaffolds and to confirm effective laccase immobilization, FTIR spectroscopy was used (Fig. 2). The FTIR spectrum of the spongin-based scaffolds contains signals attributed to various functional groups,

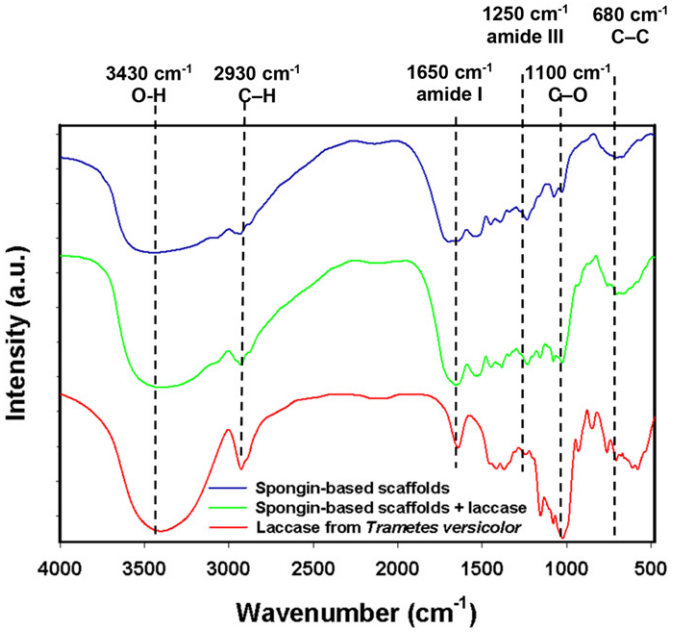

Fig. 2. FTIR spectra of *H. communis* spongin-based scaffolds, laccase from *Trametes versicolor* and the product obtained after immobilization.

for example at 3430 and 1380 cm^{-1} (υ —OH and δ C—OH), 1720 cm^{-1} (υ C═O) and 1100 cm^{-1} (υ C—O in COOH). Bands characteristic for the peptide structure of the spongin scaffolds are also present. In the FTIR spectrum of the produced biocatalytic system, changes in the intensity of the signals attributed to C—H stretching (2930 cm^{-1}) as well as amide I and III bands (1650 and 1250 cm^{-1} respectively) can be noted. According to Wong et al. (1991), this suggests that the immobilized laccase was successfully attached to the matrix and retains its catalytic properties. The presence of carboxyl, carbonyl and hydroxyl

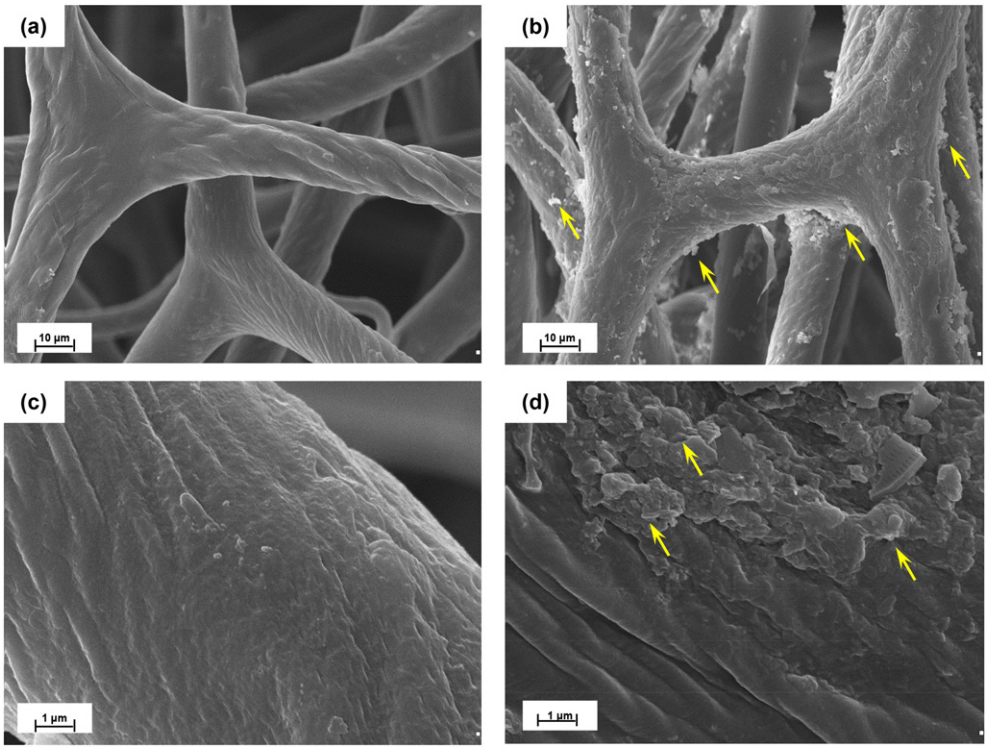

Fig. 1. SEM photographs of *H. communis* spongin-based scaffolds: (a), (c) before and (b), (d) after laccase immobilization (yellow arrows indicate immobilized laccase).

groups in the structure of the *H. communis* scaffolds not only enabled effective attachment of the laccase to the surface of the sponges and the creation of stable interaction, but also increased the transfer of electrons between substrates and the immobilized enzyme (Xu et al., 2013; Jones and Solomon, 2015). This made the degradation of pollutants more effective.

3.2. Storage stability and effect of initial degradation parameters

The storage stability of immobilized laccase is an important parameter that determines its practical application on an industrial scale, for example in wastewater treatment. The storage stability of the free and immobilized enzyme was tested for 50 days and compared (Fig. 3). The immobilized laccase retained around 90% of its initial activity after 20 days and over 80% after 50 days of storage. By comparison, free laccase retained only around 50% of its catalytic properties after 20 days and <20% after 50 days of storage, indicating that the storage stability of the immobilized enzyme is much higher than that of the free enzyme. This might be attributed to the stabilizing effect of the three-dimensional structure of the enzyme after immobilization, as well as the protective role of the matrix, which limits conformational changes of the biocatalyst (Xu et al., 2013). By contrast, Maryskova et al. (2016) showed that laccase immobilized on polyamide 6/chitosan nanofibers modified by bovine serum albumin or hexamethylenediamine as spacers retained <60% of its initial activity after 15 days of storage. It was concluded that laccase immobilized on *H. communis* spongin scaffolds has higher storage stability.

The effect of the enzyme solution concentration and the mass of the biocatalytic system used for BPA removal was evaluated to determine the most suitable initial process parameters in terms of the efficiency of bisphenol degradation (Fig. 4.) Solutions of laccase from *T. versicolor* with different enzyme concentrations (0.25–2.0 mg/mL) were used for immobilization. As Fig. 4a shows, BPA degradation efficiency increased with increasing initial quantity of enzyme, and reached its maximum for solutions at a concentration of 1.0 mg/mL. Further increase in the initial quantity of laccase did not improve BPA removal efficiency. These observations are in agreement with the results concerning the quantity of immobilized enzyme. From the solution at a concentration of 1 mg/mL, 89 mg of laccase per 1 g of matrix was immobilized, compared with 159 mg/g for the 2 mg/mL solution. These results suggest that an increase in the quantity of immobilized laccase leads to overcrowding of enzyme particles and loss of its activity, and consequently to a decrease in BPA removal efficiency (Rekuć et al., 2010).

To assess the effect of the quantity of the biocatalytic system on BPA degradation, immobilization was carried out for 1 h from a solution at a concentration of 1 mg/mL. The results (Fig. 4b) clearly show a rise in degradation efficiency with increasing dosage of the biocatalyst. When 50 mg of the biocatalytic system was used total removal of BPA was achieved, which indicates that there is no reason to use a larger amount of immobilized laccase. Thus, for further experiments related to the degradation of bisphenols, an initial enzyme solution concentration of 1 mg/mL and 50 mg of *H. communis* scaffolds with immobilized enzyme were used.

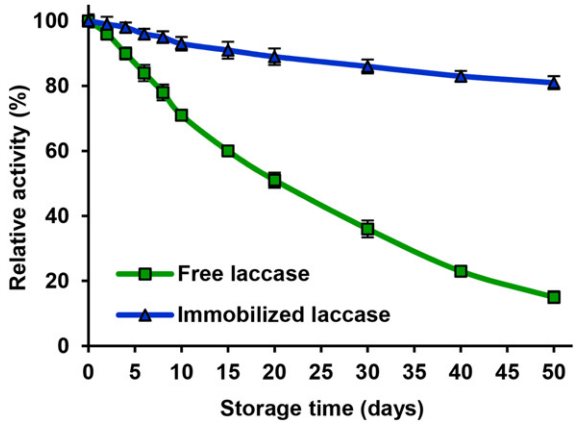

Fig. 3. Storage stability of laccase from *T. versicolor*, free and immobilized on *H. communis* spongin-based scaffolds.

3.3. Degradation of BPA, BPF and BPS

To establish how immobilization affects the ability of the laccase to degrade BPA, BPF and BPS, tests were performed using the free enzyme. Water-soluble laccase (5 mg) under optimal conditions (pH 5, temperature 30 °C for BPA and BPS and 40 °C for BPF) removed 98% of BPA and 96% of BPF after 24 h of the process. Degradation of BPS from water solution was significantly lower and reached 47% at the end of the process. This is related to the fact that compounds with higher molecular weight and more complex structure exhibit higher resistance to biodegradation than those with lower molecular weight (Uhnakova et al., 2009; Nicolucci et al., 2011). Moreover, according to Ike et al. (2006), the presence of the O═S═O group in the structure of BPS means that in water solutions this compound might be additionally stabilized by the transfer of electrons between aromatic rings and the SO_2 group, making it extremely resistant to biodegradation. By comparison, it was found that the degradation of bisphenols using the free enzyme reached its maximal efficiency after 10 h of the process. However, separation of the dissolved enzyme from the mixture after remediation is difficult and cost-effective. Moreover, the reusability of the free enzyme is very limited. Thus, in this study the biodegradation of bisphenols by immobilized laccase was emphasized and studied in detail.

It should be noted that *H. communis* spongin scaffolds are able to adsorb compounds from water solutions (Norman et al., 2016). The results showed that sponge skeletons adsorbed about 10% of each bisphenol, which proves that the removal is mainly caused by the immobilized enzyme.

3.3.1. Effect of temperature

The effect of temperature on the efficiency of removal of BPA was tested over a wide temperature range, from 10 to 50 °C, at pH 5. The highest degradation efficiencies of BPA, over 60%, were observed at temperatures of 20, 30 and 40 °C (Fig. 5a); thus the removal of BPF and BPS was carried out in the temperature range 20–40 °C (Fig. 5b, c), also at pH 5. As can be seen in Fig. 5, an increase in temperature from 10 to 30 °C enhanced the biocatalytic degradation of BPA. At this temperature degradation of 96% of BPA was observed. A further increase in process temperature up to 50 °C caused a decrease in the efficiency of removal of BPA. The observed removal efficiency for the immobilized laccase is similar to the value recorded for free biocatalyst. This is also in agreement with the calculated values of K_m (Michaelis–Menten constant) for free (0.92 mM) and immobilized enzyme (1.08 mM). This may suggest that the slight decrease in BPA removal efficiency might be related to steric hindrances which result from the attachment of the enzyme to the solid support (Landarani-Isfahani et al., 2015). Similar results were previously published by Bai et al. (2014), who showed that laccase immobilized on activated poly(vinyl alcohol) and crosslinked by glutaraldehyde also exhibited its highest catalytic activity at temperatures of 30 and 40 °C. High degradation efficiencies were also recorded for BPF: the highest efficiency, close to 95%, was observed at 40 °C; nevertheless, even at 30 °C, 85% of BPF can be removed from water solution. By contrast, Nicolucci et al. (2011) showed that laccase immobilized on polyacrylonitrile beads can remove over 90% of BPF at 50 °C. Thus, the biocatalytic system used in this work makes the biodegradation process less energy-consuming. The lowest degradation efficiencies were recorded for BPS. At 30 °C, 40% of BPS can be removed from water solution, but over 20% of BPS can be removed over the whole of the analyzed temperature range.

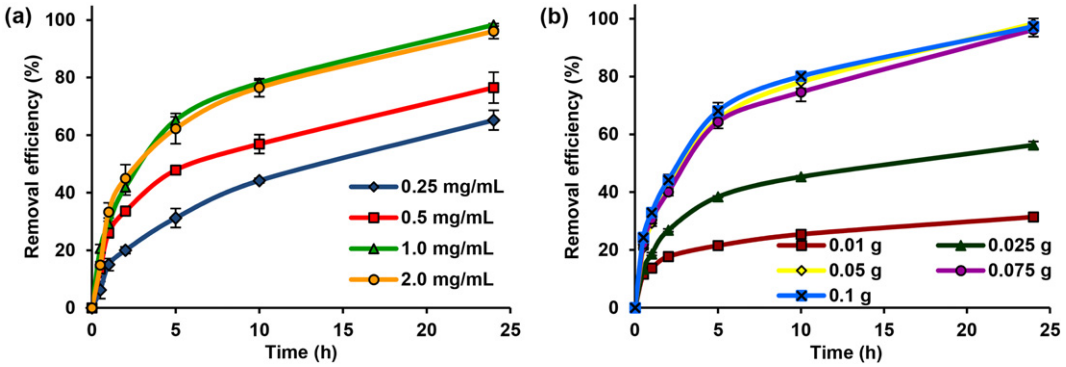

Fig. 4. Effect of (a) the initial concentration of the enzyme solution used in immobilization and (b) the mass of the biocatalytic system on the efficiency of degradation of bisphenol A.

At low temperatures, the catalytic activity of the immobilized laccase was strongly inhibited, results in low pollutant removal efficiencies. High temperature also negatively affected the oxidizing properties of the laccase. Heat causes conformational changes in the laccase structure, leading to its thermal denaturation and decreasing biodegradation efficiencies (Kim and Nicell, 2006). Free laccase from *T. versicolor* exhibited its temperature optimum at 30 °C, and even slight changes from this value caused significant changes in its catalytic properties (Marco-Urrea et al., 2010; Dwivedi et al., 2011). The presented results showed that laccase immobilized on *H. communis* skeletons removed over 80% of BPA and BPF over a broader temperature range, proves that immobilization increased the thermal stability of the laccase.

3.3.2. Effect of pH

In addition to temperature, the pH of the solution significantly affected the efficiency of removal of bisphenols. Removal of BPA was carried out over the broadest pH range, from 4 to 8, at 30 °C (Fig. 6a). The highest efficiencies were recorded at pH values from 4 to 6; therefore in that range the effect of pH on the degradation of BPF (at 40 °C) and BPS (at 30 °C) was examined (Fig. 6b, c). The experimental results indicated that the biodegradation efficiency for BPA increased to reach a maximum at pH 5, and then decreased as the pH became higher. The pH of the solution had a relatively significant influence on BPA removal; however, within the pH range from 4 to 6, over 80% of the BPA was biodegraded. This is directly related to the catalytic properties of the laccase, which was found to exhibit its highest catalytic activity and stability at pH 5 (Rangelov and Nicell, 2015; Donati et al., 2015). For comparison, in a study reported by Hou et al. (2014a), laccase was immobilized on TiO_2 nanoparticles. A degradation efficiency of over 80% was recorded in the pH range 3–5, although partial removal of the BPA was affected by the photo-degradation activity of the TiO_2. In the present work, the biodegradation of bisphenols is dependent mainly on the catalytic properties of the immobilized laccase (the adsorption of bisphenols by *H. communis* scaffolds is <10%). After 24 h of the process, over 80% of BPF was degraded from water solutions at pH 5 and 6 (Fig. 6b). At acidic pH the degradation efficiency felt markedly, to

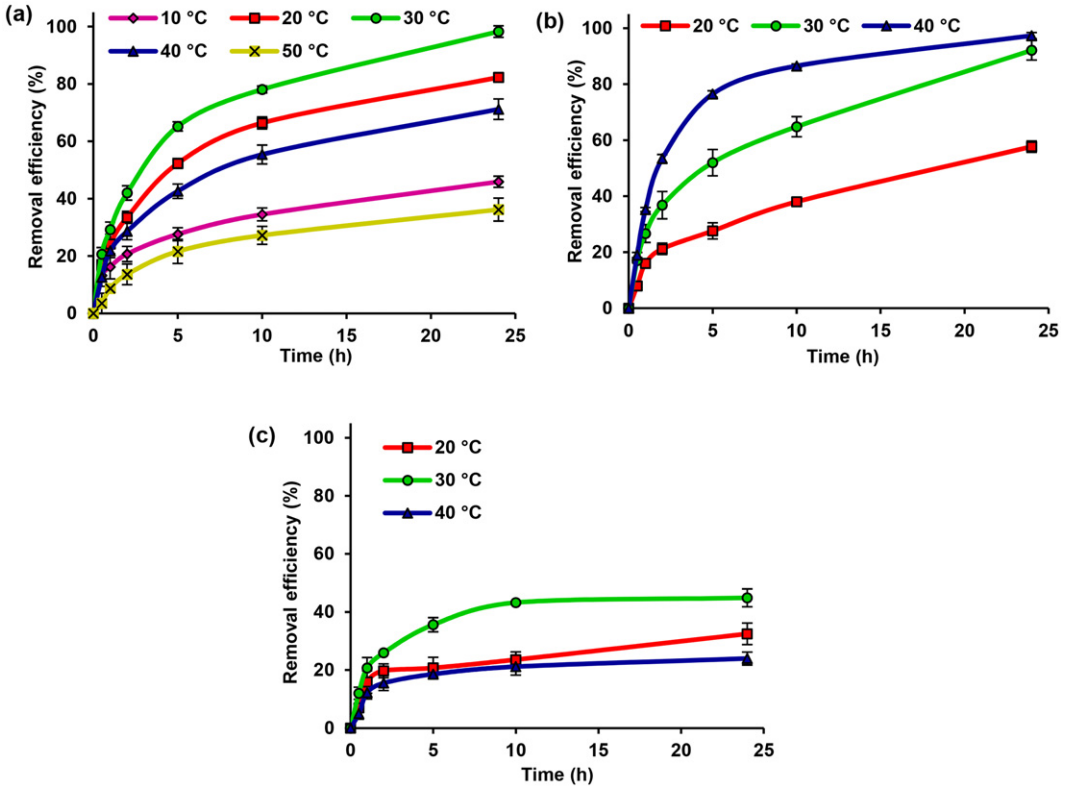

Fig. 5. Effect of temperature on the efficiency of degradation of (a) BPA, (b) BPF and (c) BPS by immobilized laccase.

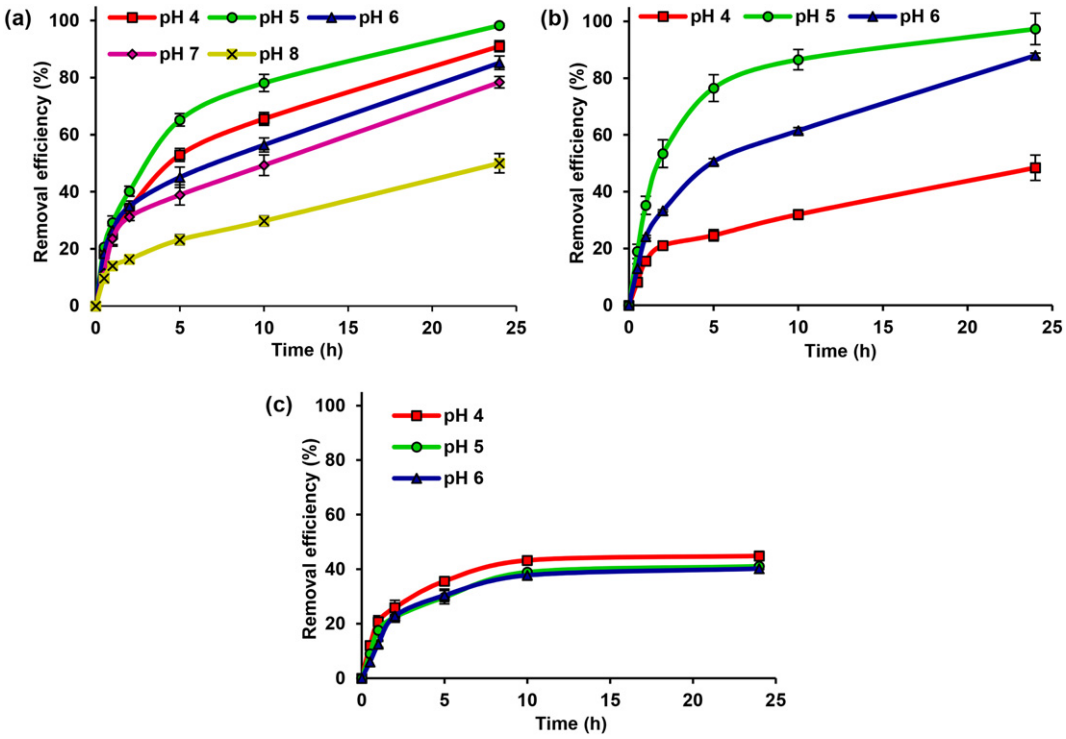

Fig. 6. Effect of pH on the efficiency of degradation of (a) BPA, (b) BPF and (c) BPS by immobilized laccase.

below 40%. The pH of the solution had the least effect on the biodegradation of BPS. Around 40% of BPS was removed over the whole analyzed pH range from 4 to 6.

Strongly acidic as well as even weakly basic pH values negatively affected the structure of the amino acid chains in the enzyme molecule and disturbed their conformation (Kurniawati and Nicell, 2007). In consequence, catalytic activity decreased and lower values of bisphenol removal efficiencies were observed. However, it should be noted that the free laccase removed over 80% of the pollutants only at pH 5, while the obtained biocatalytic system was able to degraded over 80% of BPA and BPF over pH ranges of 4–5 and 5–6 respectively. Thus, the laccase immobilized on *H. communis* spongin demonstrated higher pH

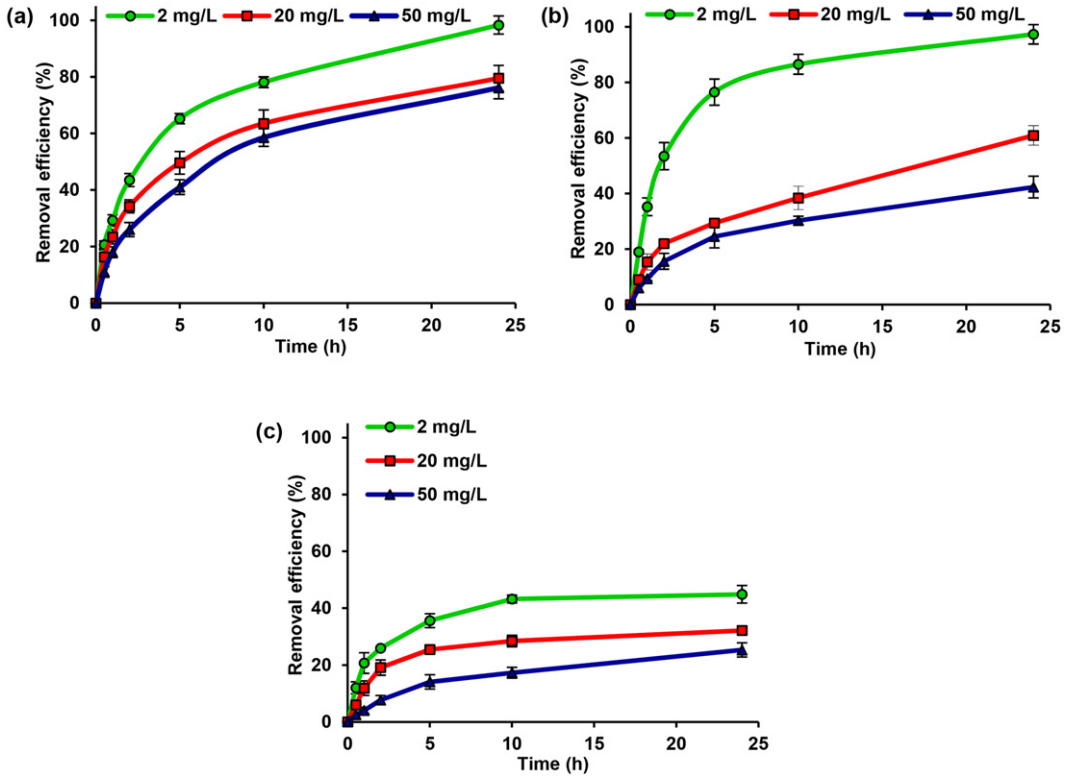

Fig. 7. Effect of bisphenol solution concentration on the removal efficiency of (a) BPA, (b) BPF and (c) BPS by immobilized laccase.

resistance. These observations are in agreement with results on the degradation of BPA and BPF by laccase immobilized on polyacrylonitrile beads. These showed that the free enzyme was able to remove over 80% of BPA and BPF only at pH 5, but when the immobilized enzyme was used, over 80% of BPA and BPF were removed at pH values ranging from 5 to 6 and from 4 to 6 respectively (Nicolucci et al., 2011).

3.3.3. Effect of bisphenol concentration

Figure 7 shows how the removal efficiency of the tested bisphenols is affected by changes in the concentrations of their initial solutions. After 24 h of the process, the highest removal efficiencies were observed for solutions at initial concentration 2 mg/L: 96%, 95% and 53% for BPA, BPF and BPS, respectively. As can be seen from the graphs, the biodegradation efficiencies of BPA, BPF and BPS decreased with increasing initial solution concentration from 2 to 50 mg/L. Regardless of the initial solution concentrations in the tested range, over 70% of BPA was removed. These results are very promising from the point of view of practical applications, since BPA is the most commonly used compound in this group, and thus occurs most abundantly in wastewater. The greatest decrease in the removal efficiency was observed for BPF. The immobilized laccase removed around 60% and <40% of BPF when solutions at initial concentrations of 20 and 50 mg/L respectively were used. According to Gasser et al. (2014) the relatively simple chemical structure of BPF (without additional substituents) caused the creation of oligomeric and polymeric products at high molecular weight. These polymers might blocked active sites of the laccase, reducing the degradation ability of the enzyme. The smallest differences in removal efficiency, around 20%, were recorded for BPS. However, as previously mentioned, this compound is known for its resistance to biodegradation. Nonetheless, over 20% of BPS can be removed by laccase immobilized on *H. communis* sponge skeletons from a solution at a concentration of 50 mg/L. The results clearly showed that the produced biocatalytic systems might be used, with relatively high efficiencies, for the degradation of various bisphenols even from solutions at higher concentrations. By contrast, as reported by Dai et al. (2016), laccase encapsulated in electrospun fibrous membrane was able to remove <60% of BPA from a solution at a concentration of 50 mg/L. Ardao et al. (2015) reported that by using magnetic biotitania nanoparticles with immobilized laccase, over 85% of BPA might be removed from water solutions. However, the concentration of BPA in their study was ten times lower than that analyzed here, which suggests that the biocatalytic system presented in this study offered higher degradation ability.

3.3.4. Degradation of bisphenol in repeated cycles

An important parameter that needs to be considered for the purposes of large-scale practical applications is the reusability of the immobilized laccase. It was tested for degradation of BPA, BPF and BPS over five catalytic cycles (Fig. 8). It has been previously reported that free laccase lost almost all of its catalytic activity after one degradation cycle. Moreover, separation of the water-soluble enzyme from the reaction mixture was extremely difficult (Zdarta and Jesionowski, 2016). As shown in Fig. 8, removal of BPA, BPF and BPS decreased gradually during repeated catalytic cycles. The slowest decrease in biodegradation availability was observed in the case of BSF. This was directly related to its chemical structure and the fact that it has the lowest molecular weight among the tested compounds. Nevertheless, even in the fifth removal cycle, about 30% of BPA, 40% of BPF and 20% of BPS was degraded after 24 h of the process. The results clearly showed that laccase immobilized on *H. communis* spongin scaffolds might be used in repeated degradation cycles of various bisphenols with the retention of relatively high removal efficiencies. This was related to the stabilization of the enzyme structure on immobilization, which made the laccase less sensitive to the denaturation caused by reaction conditions (Arca-Ramos et al., 2016). Meanwhile, the decrease in removal efficiency was related to several factors. One of the most important was the partial inactivation of the immobilized laccase caused by its utilization in repeated cycles. Additionally, the formation of high-molecular-weight products through bisphenol oxidation/polymerization may partially inhibit the enzyme's active sites, which significantly limits the transfer of substrates (Ji et al., 2017). The decrease in the activity of the immobilized laccase was also related to partial enzyme leakage from the matrix. After the first biodegradation cycle, about 10% of the enzyme (10 mg of laccase from 1 g of the matrix) was eluted, while after the fifth cycle about 35% of the immobilized laccase (40 mg of enzyme from 1 g of the matrix) was leaked from the support surface. According to previously published data, laccase covalently immobilized on carbon nanotubes and bimodal mesoporous carbon retained around 80% and 70% respectively of its initial activity (Liu et al., 2012; Xu et al., 2015). However, it should be emphasized that these values were related to the transformation of ABTS (model compound), while in this study water solutions of BPA, BPF and BPS were used to evaluate the degradation ability of the immobilized laccase during repeated catalytic cycles. On the other hand, Koloti et al. (2017) used a polyethersulfone membrane for the immobilization of laccase and removal of BPA. After four repeated degradation cycles this system removed about 40% of the toxic compound. Similar results were reported in the presented study, which proves that the obtained biocatalyst offers good reusability. By contrast, when laccase from *Trametes versicolor* was immobilized on TiO_2 sol-gel coated PVDF membrane and applied in four degradation cycles, after the fourth remediation run the immobilized enzyme removed about 30% of the BPA. Although the final results are similar to those presented in this work, it should be noted that after the second biodegradation cycle < 40% of the BPA was removed (Hou et al., 2014b). By comparison, in this study, over 80% of the BPA was removed after the second reuse, which indicates the better reusability of the presented biocatalytic system.

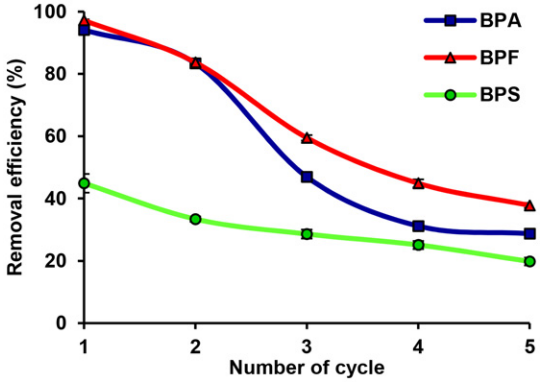

Fig. 8. Reusability of the immobilized laccase for degradation of BPA, BPF and BPS over five removal cycles.

3.4. Identification of degradation products

Laccases are oxidative enzymes that are widely used in many industrial processes and for the removal of a number of phenolic contaminants (Cabana et al., 2007). These properties of laccases were observed in the presented study, as a number of oxidative degradation products were found in the conducted experiments. The structures of the detected degradation products were presented in Fig. 9a. The averaged mass spectra took from the chromatograms showed different intensities of ions reflecting different quantities of compounds present in the samples. For BPA the most abundant ions, at $m/z = 227.1$, 453.6 and 679.9, represented respectively BPA and its dimers and trimers. Low-intensity BPA tetramers (at $m/z = 906.9$) were also observed (this spectrum range is not presented in Fig. 9a). For BPF there were two intensive ions at $m/z = 199.1$ and 397.5, which correspond to BPF and its dimers. The smaller ion at $m/z = 595.7$ representing BPF trimers is also clearly visible in the spectrum. The proposed structures of these

compounds are in accordance with those given in the literature for laccase degradation of BPA (Uchida et al., 2001; Fukuda et al., 2004). As it was reported in those papers, different substitution positions are possible for the linked phenyl rings. Both C—C and C—O bonds between the rings were reported (Galliker et al., 2010). These differently linked structures were also found in the present experiments, and are confirmed by the different HPLC peaks, which elutes one by one for the dimers and trimers of both BPA and BPF (as well as for BPA tetramers). For example, the peaks of BPA trimers (at $m/z = 680.9$) elute at retention times of $t_R = 3.59$, 3.70 and 3.86. Example structures of possible BPA trimers are given in Fig. 9b.

It can be seen that there are four equal positions in the BPA structure, and each of these positions can be linked to another ring by a C—C or a C—O bond. A similar degradation scheme, including coupling of BPA molecules, was reported for another oxidative enzyme – horseradish peroxidase (Huang and Weber, 2005). The less abundant ions visible in the spectra (Fig. 9a) represent oxidative products containing a single phenol ring linked to bisphenols (at $m/z = 319.5$ for BPA and at $m/z =$

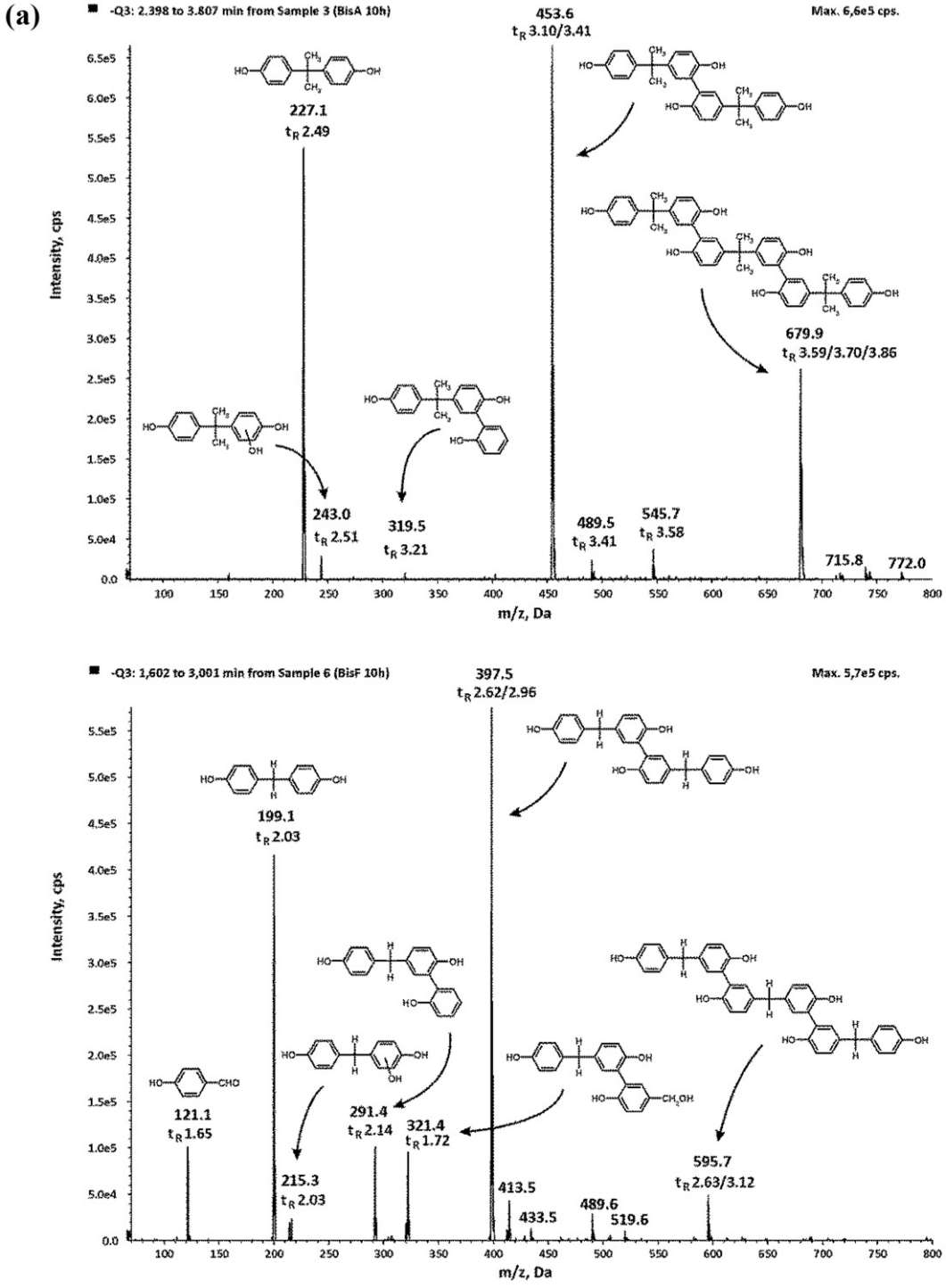

Fig. 9. (a) Mass spectra of bisphenol A, bisphenol F and their degradation products. The peaks are labeled with their m/z values, retention times recorded on chromatograms and proposed structures of degradation products. (b) Example structures of bisphenol A trimers formed during degradation with laccase.

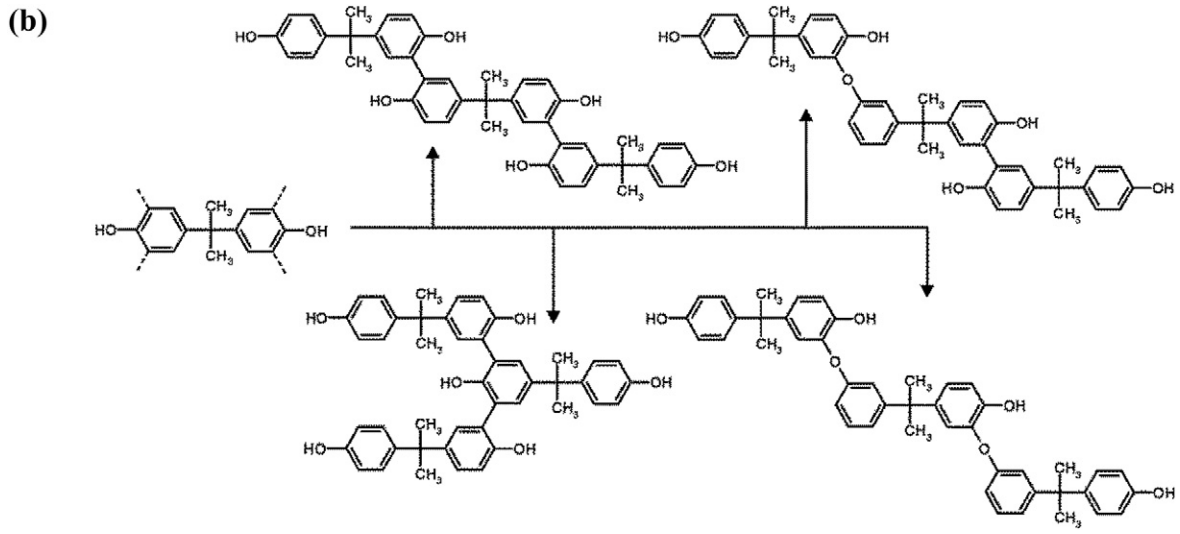

Fig. 9 (*continued*).

291 for BPF) or to their dimers (at $m/z = 545.7$ for BPA dimer and at $m/z = 489.6$ for BPF dimer). Similar products have also been reported for the degradation of BPA (Fukuda et al., 2004). Other oxidative products (of very low abundance) include BPA-catechol (at $m/z = 243.0$) and BPF-catechol (at $m/z = 215.3$). BPA-catechol has also been reported in the literature, but as the main product in the photo-oxidation of BPA (Zhou et al., 2004). Degradation products of BPS were not identified in the present study due to its very low degradation by laccase. The estrogenic activity of the above-mentioned biodegradation products was not tested during this study. Nevertheless, Fukuda et al. (2004) reported that estrogenic activity disappeared when BPA degraded and oligomeric products appeared. Thus, the very high biodegradation of BPA and BPF, and about 40% degradation of BPS, recorded in our study also confirmed the occurrence of oligomeric products formed in tests with BPA and BPF.

4. Conclusions

In this study, for the first time, laccase from *T. versicolor* immobilized on *H. communis* spongin scaffolds was used as an effective catalyst for the biodegradation of bisphenols. Effective deposition of the enzyme was confirmed based on SEM and FTIR results. The effect of various process parameters, as well as the number of repeated catalytic cycles, on the efficiency of degradation of bisphenols was investigated. Under optimal conditions 100% of BPA (pH 5, 30 °C) and BPF (pH 5, 40 °C), as well as over 40% of BPS (pH 4, 30 °C), which is commonly known to be resistant to biodegradation, was removed from a solution with a concentration of 2 mg/mL. Moreover, the immobilized laccase exhibited good reusability: after five repeated biocatalytic cycles over 40% of BPA and BPF was removed from the water solution. The main degradation products for both BPA and BPF were identified. Both of these compounds, in the presence of laccase, form mainly dimers and trimers. Our study provided a proof-in-concept demonstration of the use of laccase immobilized on spongin-based scaffolds as a promising biocatalytic system for the removal of various bisphenols from water solutions under optimized conditions.

Acknowledgements

This work was supported by research grant funds from the National Science Center Poland in accordance with decision no. DEC-2016/20/T/ST8/00391.

References

Abdel-Hamind, A.M., Solbiati, J.O., Cann, I.K.O., 2013. Insight into lignin degradation and its potential industrial applications. Adv. Appl. Microbiol. 82, 1–28.
Arca-Ramos, A., Ammann, E.M., Gasser, C.A., Nastold, P., Eibes, G., Feijoo, G., Lema, J.M., Moreira, M.T., Corvini, P.F.X., 2016. Assessing the use of nanoimmobilized laccases to remove micropollutants from wastewater. Environ. Sci. Pollut. Res. 23, 3217–3228.
Ardao, I., Magnin, D., Agathos, S.N., 2015. Bioinspired production of magnetic laccase-biotitania particles for the removal of endocrine disrupting chemicals. Biotechnol. Bioeng. 112, 1986–1996.
Aydemir, T., Guler, S., 2015. Characterization and immobilization of *Trametes versicolor* laccase on magnetic chitosan-clay composite beads for phenol removal. Artif. Cell. Nanomed. Biotechnol. 43, 425–432.
Ba, S., Kumar, V.V., 2017. Recent developments in the use of tyrosinase and laccase in environmental applications. Crit. Rev. Biotechnol. 23, 1–14.
Bai, X., Gu, H., Chen, W., Shi, H., Yang, B., Huang, X., Zhang, Q., 2014. Immobilized laccase on activated poly(vinyl alcohol) microspheres for enzyme thermistor application. Appl. Biochem. Biotechnol. 173, 1097–1107.
Bilal, M., Iqbal, H.M.N., Shah, S.Z.H., Hu, H., Wang, W., Zhang, X., 2016. Horseradish peroxidase-assisted approach to decolorize and detoxify dye pollutants in a packed bed bioreactor. J. Environ. Manag. 183, 836–842.
Bilal, M., Asgher, M., Iqbal, H.M.N., Hu, H., Zhang, X., 2017a. Bio-based degradation of emerging endocrine-disrupting and dye-based pollutants using cross-linked enzyme aggregates. Environ. Sci. Pollut. Res. 24, 7035–7041.
Bilal, M., Asgher, M., Parra-Saldivar, R., Hu, H., Wang, W., Zhang, X., Iqbal, H.M.N., 2017b. Immobilized ligninolytic enzymes: an innovative and environmental responsive technology to tackle dye-based industrial pollutants – a review. Sci. Total Environ. 576, 646–659.
Bilal, M., Iqbal, H.M.N., Hu, H., Wang, W., Zhang, X., 2017c. Enhanced bio-catalytic performance and dye degradation potential of chitosan-encapsulated horseradish peroxidase in a packed bed reactor system. Sci. Total Environ. 575, 1352–1360.
Bilal, M., Iqbal, H.M.N., Hu, H., Wang, W., Zhang, X., 2017d. Development of horseradish peroxidase-based cross-linked enzyme aggregates and their environmental exploitation for bioremediation purposes. J. Environ. Manag. 188, 137–143.
Bilal, M., Iqbal, H.M.N., Hu, H., Wang, W., Zhang, X., 2017e. Bio-catalytic performance and dye-based industrial pollutants degradation potential of agarose-immobilized MnP using a packed bed reactor system. Int. J. Biol. Macromol. 102, 582–590.
Bradford, M.M., 1976. A rapid and sensitive method for the quantitation of microgram quantities of protein utilizing the principle of protein-dye binding. Anal. Biochem. 72, 248–254.
Bronikowski, A., Hagedoorn, P.L., Koschorreck, K., Urlacher, V.B., 2017. Expression of a new laccase from *Moniliophthora roreri* at high levels in *Pichia pastoris* and its potential application in micropollutant degradation. AMB Express 73, 1–13.
Cabana, H., Jones, J.P., Agathos, S.N., 2007. Elimination of endocrine disrupting chemicals using white rot fungi and their lignin modifying enzymes: a review. Eng. Life Sci. 7, 429–456.
Cabana, H., Alexandre, C., Agathos, S.N., Jones, J.P., 2009. Immobilization of laccase from the white rot fungus *Coriolopsis polyzona* and use of the immobilized biocatalyst for the continuous elimination of endocrine disrupting chemicals. Bioresour. Technol. 100, 3447–3458.
Cha, J., Kim, T., Choi, J., Jang, K., Khaleda, L., Kim, W., Jeon, J., 2017. Fungal laccase-catalyzed oxidation of naturally occurring phenols for enhanced germination and salt tolerance of *Arabidopsis thaliana*: a green route for synthesizing humic-like fertilizers. J. Agric. Food Chem. 65, 1167–1177.

Chatha, S.A.S., Asgher, M., Iqbal, H.M.N., 2017. Enzyme-based solutions for textile processing and dye contaminant biodegradation – a review. Environ. Sci. Pollut. Res. 24, 14005–14018.

Chen, M.-Y., Ike, M., Fujita, M., 2002. Acute toxicity, mutagenicity, and estrogenicity of bisphenol-A and other bisphenols. Environ. Toxicol. 17, 80–86.

Dai, Y., Niu, J., Liu, J., Yin, L., Xu, J., 2010. In situ encapsulation of laccase in microfibers by emulsion electrospinning: preparation, characterization, and application. Bioresour. Technol. 101, 8942–8947.

Dai, Y., Yao, J., Song, Y., Liu, X., Wang, S., Yuan, Y., 2016. Enhanced performance of immobilized laccase in electrospun fibrous membranes by carbon nanotubes modification and its application for bisphenol A removal from water. J. Hazard. Mater. 317, 485–493.

Danzl, E., Sei, K., Soda, S., Ike, M., Fujit, M., 2009. Biodegradation of bisphenol A, bisphenol F and bisphenol S in seawater. Int. J. Environ. Res. Public Health 6, 1472–1484.

Donati, E., Polcaro, C.M., Ciccioli, P., Galli, E., 2015. The comparative study of a laccase-natural clinoptilolite-based catalyst activity and free laccase activity on model compounds. J. Hazard. Mater. 289, 83–90.

Duran, N., Rosa, M.A., D'Annibale, A., Gianfreda, L., 2002. Applications of laccases and tyrosinases (phenoloxidases) immobilized on different supports: a review. Enzym. Microb. Technol. 31, 907–931.

Dwivedi, U.N., Singh, P., Pandey, V.P., Kumar, A., 2011. Structure-function relationship among bacterial, fungal and plant laccases. J. Mol. Catal. B Enzym. 68, 117–128.

EFSA, 2013. Draft Scientific Opinion on the risks to public health related to the presence of bisphenol A (BPA) in foodstuffs – part: Exposure assessment. http://www.efsa.europa.eu/sites/default/files/consultation/130725.pdf, Accessed date: 5 December 2017.

Eladak, S., Grisin, T., Moison, D., Guerquin, M.J., N'Tumba-Byn, T., Pozzi-Gaudin, S., Benachi, A., Livera, G., Rouiller-Fabre, V., Habert, R., 2015. A new chapter in the bisphenol A story: bisphenol S and bisphenol F are not safe alternatives to this compound. Fertil. Steril. 103, 11–21.

Fukuda, T., Uchida, H., Suzuki, M., Miyamoto, H., Morinaga, H., Nawata, H., Uwajima, T., 2004. Transformation products of bisphenol A by a recombinant *Trametes villosa* laccase and their estrogenic activity. J. Chem. Technol. Biotechnol. 79, 1212–1218.

Galliker, P., Hommes, G., Schlosser, D., Corvini, P.F.X., Shahgaldian, P., 2010. Laccase-modified silica nanoparticles efficiently catalyse the transformation of phenolic compounds. J. Colloid Interface Sci. 349, 98–105.

Gasser, C., Yu, L., Svojitka, J., Wintgens, T., Ammann, E., Shahgaldian, P., Corvini, P.X., Hommes, G., 2014. Advanced enzymatic elimination of phenolic contaminants in wastewater: a nano approach at field scale. Appl. Microbiol. Biotechnol. 98, 3305–3316.

Geng, A., Wu, J., Xie, R., Li, X., Chang, F., Sun, J., 2016. Characterization of laccase from wood-feeding termite *Coptotermes formosanus*. Insect Sci. 1, 1–8.

Georgieva, S., Godjevargova, T., Mita, D.G., Diano, N., Menale, C., Carratelli, C.R., Mita, L., Golovinsky, E., 2010. Non-isothermal bioremediation of waters polluted by phenol and some of its derivatives by laccase covalently immobilized on polypropylene membranes. J. Mol. Catal. B Enzym. 66, 210–218.

Grumetto, L., Montesano, D., Seccia, S., Albrizio, S., Barbato, F., 2008. Determination of bisphenol A and bisphenol B residues in canned peeled tomatoes by reversed-phase liquid chromatography. J. Agric. Food Chem. 56, 10633–10637.

Hou, J., Dong, G., Luu, B., Sengpiel, R.G., Ye, Y., Wessling, M., Chen, V., 2014a. Hybrid membrane with TiO_2 based bio-catalytic nanoparticle suspension system for the degradation of bisphenol-A. Bioresour. Technol. 169, 475–483.

Hou, J., Dong, G., Ye, Y., Chen, V., 2014b. Enzymatic degradation of bisphenol-A with immobilized laccase on TiO_2 sol–gel coated PVDF membrane. J. Membr. Sci. 469, 19–30.

Huang, Q., Weber, W.J., 2005. Transformation and removal of bisphenol A from aqueous phase via peroxidase-mediated oxidative coupling reactions: efficacy, products, and pathways. Environ. Sci. Technol. 39, 6029–6036.

Ike, M., Chen, M.Y., Danzl, E., Sei, K., Fujita, M., 2006. Biodegradation of a variety of bisphenols under aerobic and anaerobic conditions. Water Sci. Technol. 53, 153–159.

Jesionowski, T., Zdarta, J., Krajewska, B., 2014. Enzymes immobilization by adsorption: a review. Adsorption 20, 801–821.

Ji, C., Nguyen, L.N., Hou, J., Hai, F.I., Chen, V., 2017. Direct immobilization of laccase on titania nanoparticles from crude enzyme extracts of *P. ostreatus* culture for micropollutant degradation. Sep. Purif. Technol. 178, 215–223.

Jones, S.M., Solomon, E.I., 2015. Electron transfer and reaction mechanism of laccases. Cell. Mol. Life Sci. 72, 869–883.

Jonkers, N., Kohler, H.P.E., Dammshäuser, A., Giger, W., 2009. Mass flows of endocrine disruptors in the Glatt River during varying weather conditions. Environ. Pollut. 157, 714–723.

Kasprzyk-Hordern, B., Dinsdale, R.M., Guwy, A.J., 2008. The occurrence of pharmaceuticals, personal care products, endocrine disruptors and illicit drugs in surface water in South Wales. Water Res. 42, 3498–3518.

Kim, Y.J., Nicell, J.A., 2006. Impact of reaction conditions on the laccase-catalyzed conversion of bisphenol A. Bioresour. Technol. 97, 1431–1442.

Kitamura, S., Suzuki, T., Sanoh, S., Kohta, R., Jinno, N., Sugihara, K., Yoshihara, S., Fujimoto, N., Watanabe, H., Ohta, S., 2005. Comparative study of the endocrine-disrupting activity of bisphenol A and 19 related compounds. Toxicol. Sci. 84, 249–259.

Klecka, G.M., Gonsior, S.J., West, R.J., Goodwin, P.A., Markham, D.A., 2001. Biodegradation of bisphenol A in aquatic environments: river die-away. Environ. Toxicol. Chem. 20, 2725–2735.

Koloti, L.E., Gule, N.P., Arotiba, O.A., Malinga, S.P., 2017. Laccase-immobilized dendritic nanofibrous membranes as a novel approach towards the removal of bisphenol A. Environ. Technol. 1, 1–13.

Krishnan, A.V., Stathis, P., Permuth, S.F., Tokes, L., Feldman, D., 1993. Bisphenol A: an estrogenic substance is released from polycarbonate flasks during autoclaving. Endocrinology 132, 2279–2286.

Kues, U., 2015. Fungal enzymes for environmental management. Curr. Opin. Biotechnol. 33, 268–278.

Kumar, S., Gujjala, L.K.S., Banerjee, R., 2017. Simultaneous pretreatment and saccharification of bamboo for biobutanol production. Ind. Crop. Prod. 101, 21–28.

Kurniawati, S., Nicell, J.A., 2007. Efficacy of mediators for enhancing the laccase-catalyzed oxidation of aqueous phenol. Enzym. Microb. Technol. 41, 353–361.

Landarani-Isfahani, A., Taheri-Kafrani, A., Amini, M., Mirkhani, V., Moghadam, M., Soozanipour, A., Razmjou, A., 2015. Xylanase immobilized on novel multifunctional hyperbranched polyglycerol-grafted magnetic nanoparticles: an efficient and robust biocatalyst. Langmuir 34, 9219–9227.

Le, T.T., Murugesan, K., Lee, C., Vu, C.H., Chang, Y., Jeon, J., 2016. Degradation of synthetic pollutants in real wastewater using laccase encapsulated in core–shell magnetic copper alginate beads. Bioresour. Technol. 216, 203–210.

Liao, C., Kannan, K., 2013. Concentrations and profiles of bisphenol A and other bisphenol analogues in foodstuffs from the United States and their implications for human exposure. J. Agric. Food Chem. 61, 4655–4662.

Liao, C., Liu, F., Guo, Y., Moon, H.B., Nakata, H., Wu, Q., Kannan, K., 2012. Occurrence of eight bisphenol analogues in indoor dust from the United States and several Asian countries: implications for human exposure. Environ. Sci. Technol. 46, 9138–9145.

Lin, J., Liu, Y., Chen, S., Le, X., Zhou, X., Zhao, Z., Ou, Y., Yang, J., 2016. Reversible immobilization of laccase onto metal-ion-chelated magnetic microspheres for bisphenol A removal. Int. J. Biol. Macromol. 84, 189–199.

Liu, Y., Zeng, Z., Zeng, G., Tang, L., Pang, Y., Li, Z., Liu, C., Lei, X., Wu, M., Ren, P., Liu, Z., Chen, M., Xie, G., 2012. Immobilization of laccase on magnetic bimodal mesoporous carbon and the application in the removal of phenolic compounds. Bioresour. Technol. 115, 21–26.

Marco-Urrea, E., Pérez-Trujillo, M., Cruz-Morató, C., Caminal, G., Vicent, T., 2010. Degradation of the drug sodium diclofenac by *Trametes versicolor* pellets and identification of some intermediates by NMR. J. Hazard. Mater. 176, 836–842.

Maryskova, M., Ardao, I., García-González, C.A., Martinova, L., Rotkova, J., Sevcu, A., 2016. Polyamide 6/chitosan nanofibers as support for the immobilization of *Trametes versicolor* laccase for the elimination of endocrine disrupting chemicals. Enzym. Microb. Technol. 89, 31–38.

Mogharabi, M., Faramarzi, M.A., 2014. Laccase and laccase-mediated systems in the synthesis of organic compounds. Adv. Synth. Catal. 356, 897–927.

Narasaki, H., 2002. Determination of bisphenol A in river-waters samples by LC/MS using solid-phase sorbents. Bunseki Kagaku 51, 1027–1035.

Nicolucci, C., Rossi, S., Menale, C., Godjevargova, T., Ivanov, Y., Bianco, M., Mita, L., Bencivenga, U., Mita, D.G., Diano, N., 2011. Biodegradation of bisphenols with immobilized laccase or tyrosinase on polyacrylonitrile beads. Biodegradation 22, 673–683.

Norman, M., Bartczak, P., Zdarta, J., Ehrlich, H., Jesionowski, T., 2016. Anthocyanin dye conjugated with *Hippospongia communis* marine demosponge skeleton and its antiradical activity. Dyes Pigments 134, 541–552.

Rangelov, S., Nicell, J.A., 2015. A model of the transient kinetics of laccase-catalyzed oxidation of phenol at micromolar concentrations. Biochem. Eng. J. 99, 1–15.

Rekuć, A., Bryjak, J., Szymańska, K., Jarzębski, A.B., 2010. Very stable silica-gel-bound laccase biocatalysts for the selective oxidation in continuous systems. Bioresour. Technol. 101, 2076–2083.

Rezg, R., El-Fazaa, S., Gharbi, N., Mornagui, B., 2014. Bisphenol A and human chronic diseases: current evidences, possible mechanisms, and future perspectives. Environ. Int. 64, 83–90.

Rochester, J.R., 2013. Bisphenol A and human health: a review of the literature. Reprod. Toxicol. 42, 132–155.

Singh, G., Bhalla, A., Capalash, N., Sharma, P., 2010. Characterization of immobilized laccase from γ-proteobacterium JB: approach towards the development of biosensor for the detection of phenolic compounds. Indian J. Sci. Technol. 3, 48–53.

Skoronski, E., Souza, D.H., Ely, C., Broilo, F., Fernandes, M., Furigo Junior, A., Ghislandi, M.G., 2017. Immobilization of laccase from *Aspergillus oryzae* on graphene nanosheets. Int. J. Biol. Macromol. 99, 121–127.

Song, S., Ruan, T., Wang, T., Liu, R., Jiang, G., 2012. Distribution and preliminary exposure assessment of bisphenol AF (BPAF) in various environmental matrices around a manufacturing plant in China. Environ. Sci. Technol. 46, 13136–13143.

Staples, C.A., Dorn, P.B., Klecka, G.M., O'Block, S.T., Harris, L.R., 1998. A review of the environmental fate, effects, and exposures of bisphenol A. Chemosphere 36, 2149–2173.

Szatkowski, T., Wysokowski, M., Lota, G., Pęziak, D., Bazhenov, V.V., Nowaczyk, G., Walter, J., Molodtsov, S.L., Stöcker, H., Himcinschi, C., Petrenko, I., Stelling, A.L., Jurga, S., Jesionowski, T., Ehrlich, H., 2015. Novel nanostructured hematite-spongin composite developed using an extreme biomimetic approach. RSC Adv. 5, 79031–79040.

Tiwari, D., Kamble, J., Chilgunde, S., Patil, P., Maru, G., Kawle, D., Bhartiya, U., Joseph, L., Vanage, G., 2012. Clastogenic and mutagenic effects of bisphenol A: an endocrine disruptor. Mutat. Res. 743, 83–90.

Uchida, H., Fukuda, T., Miyamoto, H., Kawabata, T., Suzuki, M., Uwajima, T., 2001. Polymerization of bisphenol A by purified laccase from *Trametes villosa*. Biochem. Biophys. Res. Commun. 287, 355–358.

Uhnakova, B., Petrícková, A., Biedermann, D., Homolka, L., Vejvoda, V., Bednár, P., Papousková, B., Sulc, M., Martínková, L., 2009. Biodegradation of brominated aromatics by cultures and laccase of *Trametes versicolor*. Chemosphere 76, 826–832.

Wong, P.T.T., Nong, R.K., Caputo, T.A., Godwin, T.A., Rigas, B., 1991. Infrared spectroscopy of exfoliated human cervical cells: evidence of extensive structural changes during carcinogenesis. Proc. Natl. Acad. Sci. 88, 10988–10992.

Xu, R., Chi, C., Li, F., Zhang, B., 2013. Laccase–polyacrylonitrile nanofibrous membrane: highly immobilized, stable, reusable, and efficacious for 2,4,6-trichlorophenol removal. ACS Appl. Mater. Interfaces 5, 12554–12560.
Xu, R., Tang, R., Zhou, Q., Li, F., Zhang, B., 2015. Enhancement of catalytic activity of immobilized laccase for diclofenac biodegradation by carbon nanotubes. Chem. Eng. J. 262, 88–95.
Yadav, M., Yadav, H.S., 2015. Application of lignolytic enzymes to pollutants, wastewater, dyes, soil, coal, paper and polymers. Environ. Chem. Lett. 13, 309–318.
Yang, Y., Guan, J., Yin, J., Shao, B., Li, H., 2014. Urinary levels of bisphenol analogues in residents living near a manufacturing plant in south China. Chemosphere 112, 481–486.
Zdarta, J., Jesionowski, T., 2016. *Luffa cylindrica* sponges as a thermally and chemically stable support for *Aspergillus niger* lipase. Biotechnol. Prog. 32, 657–665.
Zdarta, J., Norman, M., Smułek, W., Moszyński, D., Kaczorek, E., Stelling, A.L., Ehrlich, H., Jesionowski, T., 2017. Spongin-based scaffolds from *Hippospongia communis* demosponge as an effective support for lipase immobilization. Catalysts 7, 147–168.
Zeeb, B., Fisher, L., Weiss, J., 2014. Stabilization of food dispersion by enzymes. Food Funct. 5, 198–213.
Zhou, D., Wu, F., Deng, N., Xiang, W., 2004. Photooxidation of bisphenol A (BPA) in water in the presence of ferric and carboxylate salts. Water Res. 38, 4107–4116.